

INTERNATIONAL ATOMIC ENERGY AGENCY

INDC(NDS)-453

Distr.: RS

I N D C **INTERNATIONAL NUCLEAR DATA COMMITTEE**

Summary Report
of the Second Research Co-ordination Meeting on
Improvement of the Standard Cross Sections for Light Elements

National Institute of Standards and Technology
Gaithersburg, MD, USA

13 - 17 October 2003

Prepared by
A.D. Carlson, G.M. Hale and V.G. Pronyaev

March 2004

IAEA NUCLEAR DATA SECTION, WAGRAMER STRASSE 5, A-1400 VIENNA

Produced by the IAEA in Austria
March 2004

Summary Report
of the Second Research Co-ordination Meeting on
Improvement of the Standard Cross Sections for Light Elements

National Institute of Standards and Technology
Gaithersburg, MD, USA

13 - 17 October 2003

Prepared by
A.D. Carlson, G.M. Hale and V.G. Pronyaev

Abstract

Results are presented following one and a half years of work under the Coordinated Research Project (CRP) on Improvement of the Standard Cross Sections for Light Elements. They include the use of the refined resonating group model for the theoretical prediction of the R-matrix poles and preliminary R-matrix model fits of the full experimental database for the ${}^6\text{Li}+n$ system obtained with different codes. Significant attention was paid to the exclusion of the bias in the evaluated data caused by the possible presence of Pelle's Pertinent Puzzle effect in the experimental data. Updates were also presented of the experimental database for light and heavy element standards including fission cross sections up to 200 MeV. First results and observed trends for all standard reactions are given, including the preliminary results of combining the model (for light elements) and non-model fits. The timetable for further work was agreed, which should lead to new reaction cross section standards for light and heavy elements by the end 2004.

March 2004

CONTENTS

1. Summary of Meeting.....	7
2. Action list.....	15
3. Contents of the final report of the CRP (IAEA TECDOC report series).....	18
4. Annexes.....	21
Annex 1. Agenda and time schedule.....	21
Annex 2. List of participants.....	27
Annex 3. Participants' presentations, working papers and consultants' reports submitted for inclusion in the summary report.....	29
<i>H.M. Hofmann, Calculations of R-matrix poles in the refined resonating group model.....</i>	31
<i>N. Larson, Some thoughts on the data analysis process.....</i>	47
<i>N. Larson, On equivalence of using the normalization as a fitting parameter, vs. generating the off-diagonal data covariance matrix.....</i>	97
<i>CHEN Zhenpeng and SUN Yeying, Progress report on analysis of ⁷Li system with RAC.....</i>	119
<i>CHEN Zhenpeng and SUN Yeying, Progress report on analysis of ¹¹B system with RAC.....</i>	127
<i>E.V. Gai, S.A. Badikov, Once again on the Peelle's puzzle.....</i>	139
<i>Soo-Youl Oh, On the applicability of the law of error propagation with the first order approximation to a response variable in the quotient form.....</i>	143
<i>A.D. Carlson, Status of the experimental data for the international standards evaluation.....</i>	153
<i>A.D. Carlson, Status of the database for the new international evaluation of the neutron cross section standards.....</i>	165
<i>F.-J. Hamsch, Status of the 10B measurements at IRMM.....</i>	195

<i>S.A. Badikov, E.V. Gai, The results of polynomial and rational least squares fits for the ${}^6\text{Li}(n,t)$ reaction cross section.....</i>	207
<i>F.-J. Hambsch, New evaluation of the fission cross section of ${}^{235}\text{U}$.....</i>	221
<i>V.G. Pronyaev, GMA database updating, evaluating procedures and trends in new standards evaluation.....</i>	239
<i>V.G. Pronyaev, Subjective judgment on measure of data uncertainty.....</i>	327
<i>D.L. Smith and V.G. Pronyaev, Update of GMA code to solve the PPP problem (technically).....</i>	333
<i>D.L. Smith and V.G. Pronyaev, "GMA" - "GMAP" inter-comparison for the full GMA database combined with the RAC result for ${}^6\text{Li}(n,t)$.....</i>	343
<i>E.V. Gai, The least square method formulation with account of systematic errors.....</i>	359
<i>Chen Zhenpeng, The approach for processing of the data uncertainty in the R-Matrix fitting.....</i>	363

1. Summary of Meeting

The meeting was hosted by the National Institute of Standards and Technology (NIST), Gaithersburg, MD, USA. David Gilliam, Neutron Interactions and Dosimetry Group Leader, Ionizing Radiation Division, NIST, welcomed the participants and expressed his interest, strong support and a desire to continue contributions from NIST to the finalization of the new standards. NIST is a non-regulatory federal agency that provides standards, including nuclear, for US industry.

Vladimir Pronyaev, the Scientific Secretary, informed the participants that due to visa problems, that could not be overcome even with appreciable help from the local organizers, one CRP participant (Chen Zhenpeng from China) could not participate in the meeting.

Allan Carlson was elected as Chairman and Gerry Hale as Rapporteur of the meeting. The Agenda was adopted with small corrections, and is given in Appendix 1.

Session 1 was devoted to the participants' presentations of their work during the last year. Hartmut Hofmann presented the results of direct calculations of the R-matrix poles in the refined resonating group model. It is shown that the use of effective NN-potentials and the expansion of all radial functions in terms of Gaussians allows to calculate in good approximation the position of the low-lying poles and the general energy dependence of the phase shifts observed in experiment. The results depend sensitively on the number of Gaussians used in the expansion and the maximum value of the channel radius. But the value of the channel radius and the number of Gaussians can be optimised for a comparison with the R-matrix fit to the data (except for the distant poles).

Gerry Hale described the results of a coulomb-corrected, charge-independent, relativistic R-matrix analysis of the nucleon-nucleon system at incident energies up to 30 MeV in the laboratory frame system. R-matrix treatment of photon channels was incorporated. The fitted cross sections were p-p and n-p scattering, n+p capture and γ +d disintegration. Total chi-square per degree of freedom was equal to 1.02 and near one for each reaction. The largest difference of ~1%, compared with the results of the ENDF/B-VI evaluation for the n-p total cross section was observed near 10 MeV. The capture cross section at astrophysical energies is a few percent below the ENDF/B-VI values and has an uncertainty not larger than 2.5%.

Gerry Hale also presented results from a new R-matrix analysis of the ${}^7\text{Li}$ system. The fitted n+ ${}^6\text{Li}$ experimental data covered the neutron energy up to 4 MeV and even higher energies were used for t+ ${}^4\text{He}$ measurements. The total chi-square per degree of freedom (4.56) is rather high with the largest contribution coming from the charged particle data. The experimental database is discrepant, especially for charged particle data. The difference compared with the old standards (ENDF/B-VI) is between -0.2 and +1.2% ($E_n < 100$ keV), and is larger at higher energies compared with a previous R-matrix fit.

Nancy Larson gave a presentation entitled "Thoughts on the Data Analysis Process", which included three topics. The first (and most extensively covered) topic, "Peelle's Pertinent Puzzle/Paradox (PPP)", was based on the premise that the goal of a least-squares or Bayesian analysis utilizing a full off-diagonal experimental data covariance matrix (EDCM) should be to obtain the same results as an analysis which includes the data-reduction procedure in the theory (and thus involves a fit to uncorrelated experimental data). This goal would only be obtained if the EDCM is generated from the theoretical (not experimental)

values of the fitting parameters; if this is true, PPP does not exist, because the numbers in Peelle's original covariance matrix would have different values. The second topic was "Implicit Data Covariance Methodology", in which a method was described for using the information contained in an EDCM without generating, storing, or inverting the entire EDCM. This method provides significant savings in array space and computation time, and has the added bonus of increasing the accuracy of the calculations. The third topic was "Transformation of Variables", which suggested that the implications of the non-Gaussian nature of the distributions of fitting parameters might be important and should be given consideration.

The reports prepared by Chen Zhenpeng on analysis of ${}^7\text{Li}$ and ${}^{11}\text{B}$ systems with R-matrix code RAC were presented and discussed. Most experimental data on neutron-induced reactions (total, elastic, (n,t) for ${}^7\text{Li}$, and (n, α_0) and (n, α_1) for ${}^{11}\text{B}$) which were available in the GMA database were included in the RAC fit. The data on the ratio of the ${}^6\text{Li}(n,t)$ to the ${}^{10}\text{B}+n$ cross sections were also included in the combined fit. The charged-particle data for reactions leading to the ${}^{11}\text{B}$ compound nucleus, as taken from the experimental database EXFOR, were not complete and will be updated. The difference compared with the old standards (ENDF/B-VI) for the ${}^6\text{Li}(n,t)$ reaction is at the level of 2% near the 0.245 MeV resonance and less below 0.1 MeV.(note-it is used as a standard up to 1 MeV!!) The uncertainty of the ${}^6\text{Li}(n,t)$ RAC fit is 0.4% at 10 keV and below, and increases to 0.6% at 100 keV and 1.2% at 1 MeV. Similar differences and uncertainties are obtained for the ${}^{10}\text{B}(n,\alpha_1)$ and ${}^{10}\text{B}(n,\alpha_0+\alpha_1)$ reactions. The elements of the covariance matrices of the uncertainties of the evaluated data (as well as the correlation coefficients) obtained with the RAC fit implementing the full scale error propagation law, that are far from the diagonal, are rather large. The RAC fit generally follows the trend obtained in the non-model generalized least-squares fit of these reactions.

Sergei Badikov presented a paper considering the case of an exactly solvable model of 2 measurements and a non-constant evaluated function, for which a generalized inequality was derived, which, if fulfilled, will guarantee the absence of PPP. This generalized inequality imposes restriction on the relative uncertainties. At the same time this generalized equality for an exactly solvable model of three measurements with a constant function gives only a necessary (and not sufficient) condition for the absence of the PPP.

Soo-Youl Oh gave a paper in which the accuracy with which the least-squares method can be applied to data fitting had been studied. For this, the semi-analytical approach was used, which works directly with probability distribution functions (PDF). It was shown that in first order approximation for the non-linear models (e.g. ratio of two observables, each having normal PDF and no correlations between them) the resulting PDF is non-normal and skewed to the low values. The maximum of this PDF is below the average (evaluated) value obtained with the error propagation law, and the same is true for the standard deviations. The higher order approximations can improve consistency for the standard deviations but not for the average (evaluated) values. Applying this approach to the original Peelle example gave a rigorous solution of 1.207 ± 0.297 (for a skewed evaluated PDF with a most probable value of 1.072), which is close to 1.21 ± 0.3 as estimated by Donald Smith numerically (method 1 on p. 206 of Smith's monograph). This value can be compared with the value 0.882 ± 0.218 obtained by Peelle and considered a puzzle, 1.154 ± 0.245 (method 4 on p. 207 of Smith's monograph) obtained by Zhao-Perey and later by Larson using a raw data fit approach, 1.225 ± 0.265 (method 2 on p. 206 of Smith's monograph) obtained by Oh for Box-Cox solution (logarithm transformation in this case) and 1.250 ± 0.265 (method 7 on p. 207 of

monograph by D.L. Smith, "Probability, Statistics, and Data Uncertainties in Nuclear Science and Technology", ANS, 1991) obtained by Chiba-Smith for the approach where percent uncertainties (but not absolute uncertainties) are used. The difference between 1.154 ± 0.245 (Zhao-Perey and Larson value) and 1.250 ± 0.265 (Chiba-Smith value) arises from taking into account the mini-PPP effect in the Chiba-Smith approach.

Herbert Vonach reported on the modification of the Bayesian least squares code GLUCS to remove the effects of the PPP. The revision is based on the prescription of equalizing the weighting of experimental data situated below and above the "true" value. The results obtained with the code in fitting the TEST1 data showed good consistency with the results of other codes using the same approach (GMAJ by Satoshi Chiba).

Soo-Youl Oh presented the Monte-Carlo simulation of the PPP problem in space of four variables. The importance of this approach was stressed for testing the PPP solutions obtained with empirical and semi-analytical methods and its extension to spaces of larger numbers of variables.

The Box-Cox transformation can be used for resolving PPP, and was presented by Soo-Youl Oh for the original Peelle example and for the TEST1 case. For the original Peelle example, the optimal λ parameter of the Box-Cox transformation was equal to 0 and transformed into an ordinary logarithm transformation. For the TEST1 case, $\lambda = -0.07$ was optimal, and the fit with the Box-Cox transformation gave evaluated values that are an average of 1% higher than those obtained with the logarithm transformation. Considering the errors of the evaluated data, the result is consistent with that obtained with the Chiba-Smith approach.

The status of the experimental data for the international standards evaluation was reported by Allan Carlson. The results of many new experiments completed after 1987 were introduced in the standards database, including 36 data sets in 2003. The cutoff date for input of the latest experimental data, analysis of which is still not completed, was set as early spring of 2004. The most important extension of the database is the inclusion of the data for the ^{235}U , ^{238}U and ^{239}Pu fission cross sections up to an energy of 200 MeV. This allows low- and high-energy fission cross section standards to be merged into one consistent set of evaluated data. The latest data, which resolve old discrepancies and can strongly impact on the new standards, include: absolute H(n,n) differential cross section measurements with 1% level precision at 200 MeV from Indiana University, and at 10 MeV through an NIST-Ohio University-LANL collaboration; $^{10}\text{B}(n,\alpha)$ and $^{10}\text{B}(n,\alpha_1)$ measurements with Frisch-gridded ionization chambers made at IRMM by experimental groups at the Linac and Van de Graaff facilities providing both branching ratio and cross section data; ^{10}B total cross section measurements at the IRMM Linac facility, at the IRMM Van de Graaff facility and at the ORELA facility by an NIST-ORNL collaboration; and high-precision measurements of high-energy neutron fission cross sections for ^{235}U and ^{238}U at WNR and the GNEIS facilities.

The status of the ^{10}B measurements at IRMM was reported on by Franz-Josef Hamsch. Measurements of the branching ratio of the $^{10}\text{B}(n,\alpha_0)$ to $^{10}\text{B}(n,\alpha_1)$ cross sections were undertaken with a double Frisch-gridded ionization chamber. Two-dimensional analysis (particle-emission angle vs anode pulse amplitude) using fast digitization techniques can provide information on the particle leaking effect, which is a large effect, that can lead to a large underestimation of the cross sections measured with ionization chambers. Data measured earlier using ionization chambers should be re-analyzed and corrected for this effect, which depends on the geometry of the chamber and the angular distribution of the

alpha particles for given neutron energy. The correction can be calculated and possibly introduced in old data. For these calculations, the angular distributions of alpha particles and residual nuclei calculated with the R-matrix can be used. The IRMM linac data can be corrected for the particle leaking effect and the contribution resulting from epithermal neutrons, and will be an important part of the standards database.

Sergei Badikov presented a paper in which the experimental data set selected for the TEST1 case was fitted with a seven- or nine-parameter polynomial and a ten-parameter rational model expansion. The quality of the fit with the polynomial model was very poor, because the model clearly is not “natural” for the presentation of shape of data with a resonance. Increasing the number of parameters from 7 to 9 does not improve the quality of the fit. A strong reduction (bias) in the fit relative to the experimental data is observed when experimental data are fitted using their (positive) correlations. When correlations between the points of the experimental data set are set to 0, there is no visible bias. This is clear evidence of PPP in the model fit of strongly correlated data, which cannot be reproduced by any choice of parameters. At the same time, the model fit with the rational function, which is natural for presentation of TEST1 data, gives an excellent fit with very low chi-square and no bias (no PPP) even when the experimental data have a very high level of correlation. The situation will be more complex when several experimental data sets, each having different shape (strong correlations), are fitted with the physical model, which is the most natural presentation for this type of experimental data. The inequality introduces the physical limit of correlations between points, and should be used in this case. It was shown that the sum of the elements of the covariance matrix of uncertainties of evaluated data can be considered as the global measure of the quality of the fit.

Franz-Josef Hamsch presented the results of a nuclear model evaluation of the $^{235}\text{U}(n,f)$ cross section in the energy range 1 keV – 6 MeV (up to the threshold for second-chance fission). Statistical theory was used, taking into account sub-barrier effects and multimodal fission in the double humped barrier model for the evaluation of the fission cross section. The direct reaction mechanism was taken into account for neutron channels to give a better determination of the compound reaction cross section. The nuclear model parameters were adjusted from a best fit of total, elastic and inelastic scattering, capture and fission cross-sections. Experimental data such as the mass distribution of fission fragments were used to determine of the contributions of the different modes to fission and the parameters of the fission barriers for each mode. Because the different modes have different energy dependence, this procedure gives a better description of the total fission cross section observed in the experiment.

Vladimir Pronyaev presented the results of the standards database updating, discussed the procedures which can be used to treat the discrepant data and PPP, showed preliminary results of combining the R-matrix evaluations for light elements with generalized least-squares data fit for the light and heavy elements, and showed the resulting trends in the new standards evaluation based on this work. 25 data sets have been added to the database, which now includes 422 data sets as of September 2003. High-energy fission data were also added to the database to allow a joint evaluation of high- and low-energy standards. In general, the new experimental data exhibited good consistency with the results of the posterior evaluation. Evaluation procedures included a test of the database for the presence of the PPP; determination of the discrepant data (outliers) and revision of uncertainties assigned to these data; combining data by direct use of the cross sections and covariance matrices of their uncertainties, for light elements evaluated in an R-matrix model, as data sets in the generalized least squares fit of light and heavy element standards. The new standards are

generally higher than the old standards with the largest differences occurring for the fission cross sections above 14 MeV.

Vladimir Pronyaev considered integral parameters, which can be derived from the covariance matrix of the uncertainties and can serve as a general measure of uncertainties in comparisons of different fits. Using realistic examples and simple data model fits with a variable number of parameters, he was able to show that the sum of all elements of the covariance matrix is a best general measure for characterizing and comparing uncertainties obtained in different model and non-model fits. Discussions also included the problem of non-positive definiteness of the covariance matrix of the uncertainty of the cross sections obtained from the covariance matrix of the uncertainty of the parameters in cases where the number of parameters is less than number of cross section points. As a consequence of the numerical inaccuracy of the calculations that are always many orders larger than the presentation of the machine zero, it was concluded that the calculated eigenvalues of semi-positive definite matrices have no machine zeros. These covariance matrices can be inverted when they are used in the error propagation equations. So the procedure for transformation of the semi-positive definite matrices to positive ones by introducing minimal changes into the matrix (changes that are equivalent to introducing additional non-informative parameters in the model) is generally not needed. But caution should be observed, because there can be cases where uncertainties can be unphysical, e.g. integral parameters estimated with formally non-positive-definite covariance matrices.

Session 2 was devoted to discussions on key topics, and was guided by each of the moderators.

Brief notes on each topic are given below:

1. (Moderator: Hartmut Hofmann). **Distant R-matrix poles in RRGM.** High-lying poles are strongly dependent on the channel radii, and in particular, seem to be determined by the largest channel radius. Herbert Vonach asked why all channel radii cannot be taken to be the same. Hale explained that the sizes of the bound clusters in the different arrangement channels differ, giving as an example the 5-nucleon system, in which the alpha particle is much more tightly bound than either the deuteron or triton, and therefore the n-alpha channel radius (~3 fm) is smaller than the d-t radius (~5 fm). There was also a discussion of the connection of R-matrix poles to S-matrix poles and resonances, and of the importance of the higher-lying poles for describing the low-energy data. Information about these poles is beginning to emerge from RRGM calculations.
2. (Moderator Gerry Hale). **Further intercomparisons of the R-matrix codes; reduction of uncertainties in the model fits.** Because the data included in Chen's RAC analyses are not precisely known, nor what (if any) modifications to the original data covariance matrices and/or uncertainties he included, no conclusions can be drawn from the apparent differences between the RAC and the EDA covariance matrices for the cross sections as calculated from the fitted parameters. It is necessary to compare exactly the same calculations. Detailed comparisons will be made of analyses by the three codes (RAC, EDA, and SAMMY) using exactly the same experimental data set (one set only, at first), with exactly the same normalization uncertainty (treated via the data covariance matrix in RAC, as a fitting parameter in EDA, and by both methods in SAMMY), and using non-relativistic kinematics (since only EDA is capable of relativistic kinematics). Only random and normalization

uncertainties will be used in these analyses.

3. (Moderator Vladimir Pronyaev). **Semi-positive definiteness of output covariance matrices from R-matrix (or other model) codes – is there a problem constructing errors on integral quantities?** Badikov gave his numerical prescription for converting such matrices to positive-definite form without altering the content significantly.
4. (Moderator Soo-Youl Oh). **PPP manifestation in GMA database.** Oh showed GMA residuals for a fit including just the Friesenhahn and Lamaze data that clearly indicated the presence of the PPP effect. A discussion followed about a specific proposal for identifying PPP effects in data fits. An action is proposed, - three different (but similar) prescriptions (Vonach, Oh, and Chen) for “removing” PPP effects should be tested on the same limited GMA data set (Au and ^{238}U capture), and the results compared. Pronyaev described a time-consuming iterative process used by the Bayesian GLUCS code for input of many data sets that could be automated using a script. A computer specialist working at the NDS could be enlisted to write this script. He also will look at modifications to GMA to generate covariances in a form that can be used by the other codes (GLUCS, GMAJ).
5. (Moderator Gerry Hale). **Databases for ^7Li and ^{11}B systems.** Some neutron data in the GMA database are not yet in the EDA analysis. Charged-particle data for both systems are fairly complete and have been shared by Hale and Chen. Angular distributions for neutron reactions on ^6Li and ^{10}B have been measured by Zhang, but there may be large leakage corrections needed for these data at angles near 0 degree. We look forward to new measurements for $n+^{10}\text{B}$ from Geel.
6. (Moderator Nancy Larson). **Data reduction for R-matrix fits of resonance reactions.** How to remove resolution effects from cross sections for GMA fitting? Should cross sections evaluated in R-matrix for joint fit with GMA data be binned? Output from R-matrix fitting should be resolution-broadened in order to be combined with GMA. How to do this? Finally, it was decided not to include poor-resolution data (like ratio measurements) in the database for R-matrix fitting. Carlson and Hale will explore these (resolution/binning) effects for $n+^6\text{Li}$ data. It is also recommended to increase relative errors on $t+^4\text{He}$ data (factor of 1.5-2.0).
7. (Moderator Vladimir Pronyaev). **Combining R-matrix and GMA results.** Vonach proposed using R-matrix analyses for the ^{10}B and ^6Li cross section data, using GMA for all others and combining them using GMA. The result would not be smooth, but could be put back into the R-matrix code (as was done for ENDF/B VI) for this purpose. The process could be iterated, and hopefully would converge quickly. Larson suggests using other methods and comparing the final outcomes.
8. (Moderator Alan Carlson). **Status of GMA database.** Pronyaev solicited help from experimentalists with the task of looking through the GMA database (465 data sets) to see if his identification of outlying points is reasonable. He described a procedure to make outliers consistent with the assumed prior by increasing the medium-range correlated error, so that the overall chi-square per datum of the fit went from about 3 to 0.8. An action was proposed: Carlson, Vonach, and Hamsch agreed to look at the

data base - Habsch will look at $n+^{10}\text{B}$ measurements; Carlson at fission measurements, Vonach will consider capture on Au and ^{238}U and $n+^6\text{Li}$ data will be looked at by Carlson and Hale. Discussions about specific fission cross-section ratios followed. Some of the data deviate strongly from the expectation that these ratios should be close to unity at high energies. Particular concern was expressed about the data of Sherbakov and of Staples relative to those of Lisowski.

9. (Moderator Herbert Vonach). **Procedures to deal with discrepant data.** This had been already discussed to some degree. The basic idea is to scale up the errors on outlying points such that the chi-square contribution is unity, and throw out points that are more than 3 standard deviations away from the assumed prior. This would involve investigating various prescriptions for generating the “prior” (e.g. a previous evaluation, or an unweighted average of the data points). Badikov will send results from his procedure for identifying outliers in the GMA database to Pronyaev.
10. (Moderator Vladimir Pronyaev). **Preliminary results of the standards evaluation obtained with the updated GMA database.** Aspects of these results were already discussed and documented in a significant publication by Pronyaev. They can be shown at the CSEWG meeting as preliminary results. A discussion followed about how to deal with the structure in low-energy fission cross sections. Some may be real, and some an artifact of combining the data. Some theoretical calculations indicate the cross sections should be smooth in this region, but they may not contain all resonant mechanisms. A smoothing process should be used, either by binning or by spline fitting. Probably there will be a spline fit to the cross sections and binning of the covariances. Vonach estimated that the cross sections and covariances for all the standards should be represented by something like 500 points. This would result in not having to deal with inordinately large matrices. Pronyaev pointed out that not all reactions will be coupled, so the covariance matrix will contain blocks of off-diagonal zeroes that do not have to be tabulated.
11. (Moderator Herbert Vonach). **Uncertainty introduced by smoothing.** Vonach proposed that after smoothing, one should use the original errors of the experimental data if no more than 1/3 of the points lie outside the smooth curve. Carlson also suggested the use of model shapes to do the smoothing or give information on how to smooth the data.
12. (Moderator Nancy Larson). **Different chi-square expressions.** It was shown that when using normalization as a fitting parameter with the prior uncertainty specified via Bayes’ equations (as is done in EDA), the equations for the other fitting parameters (e.g. the R-matrix parameters) are almost identical to what is used in the least-squares equations when the normalization uncertainty is incorporated into the data covariance matrix (the method used in RAC). “Almost” is due to the use of the theoretical cross-section values used in the EDA/Bayes approach, and the use of the experimental values in the RAC/least-squares approach. Larson will extend her study of this matter to include other data-reduction parameters in addition to normalizations (backgrounds, energy-dependent normalizations and backgrounds, resolution functions, etc.).
13. (Moderator Herbert Vonach). **Representation of evaluated covariances in the file.**

Vonach feels that the original covariance matrix should be tabulated, and used to create collapsed matrices for broader group structure.

14. (Moderator Sergei Badikov). **Requirements for covariance matrices.** Obvious requirements were noted, such as the magnitude of the correlation coefficients must not exceed unity. In addition, there are restrictions on the sizes of the off-diagonal elements in order to avoid PPP problems. These are not generally known, but have been worked out in specific cases by Badikov and Gai. Vonach also presented a relation involving the relative uncertainties of the points i and j that could limit $\rho_{ij}(max)$ to a physical possible maximum. This condition would be useful for testing covariance matrices that are not constructed from components. Pronyaev added a third condition that the magnitude of an off-diagonal covariance element should not exceed either of the diagonal elements, which is the condition of Chiba and Smith for avoiding PPP. Vonach argued that the second condition often gives the third one.

Session 3 was devoted to preparing the actions, recommendations and conclusions.

The action list of the first Research Co-ordination Meeting was reviewed. Completed items were deleted, other items were revised with later dates, and new items were added (see Appendix 2). The draft minutes of the meeting were reviewed in order to add action items listed there not already included. Speakers were asked to send single-paragraph summaries (in Word) of their presentations within a week. Presentations can be sent (in PDF format) electronically for publication on the IAEA website.

Topics for the TECDOC were identified and discussed (see Appendix 3). The title agreed upon was "An International Evaluation of the Neutron Standard Cross Sections".

Several topics from the CRP were proposed to be presented at ND2004, hopefully some of which will be invited presentations. Carlson proposed having a satellite meeting on the Standards RCM at the Santa Fe conference.

Proposed dates for the next RCM in Vienna (18-22 October 2004) were agreed by the group.

Conclusions and recommendations were not discussed in detail. Generally, the recommendations are contained in the revised action list.

Pronyaev raised a question about the uncertainties quoted on the criticality eigenvalue calculation for Godiva using the CRP preliminary $^{235}\text{U}(n,f)$ cross section. He pointed out that the prompt neutron spectrum is very uncertain, and wondered about its effect on the final value and uncertainty of the eigenvalue. Carlson and Hale will ask those in T-16 who did the calculation.

Carlson asked what to present at the upcoming CSEWG meeting, and some the positive accomplishments were reviewed. The main negative aspect is a delay in some of the desired accomplishments.

2. Action list

1. Input from Resonating Group Microscopic Nuclear Model (RGM) predictions to the R-Matrix (RM) Phenomenological Model Fit

No.	Action	Participant(s)	Terms
1.1.	Fix the approach for conversion of the RGM parameters in the parameters of the R-matrix model.	H. Hofmann	February 2004
1.2	Undertake RGM calculations which account for all channels contributing in the energy range of interest for the standards for the system with A=11 through poles located in this energy range or through distant poles. Prepare the information on R-Matrix poles.	H. Hofmann	June 2004

2. R-Matrix codes inter-comparison and data evaluation: testing of different approaches to the implementation of the error propagation law in codes EDA, SAMMY and RAC, testing of the convergence in the parameters search, testing in the cases where strong non-linearity in parameters/cross section exists; comparison of the results of the R-matrix model with non-model fit based on the same sets of experimental data

No.	Action	Participant(s)	Terms
2.1.	Prepare specifications for R-Matrix codes search and covariance matrix inter-comparison exercise with realistic data, that can be used for fits with EDA, RAC and SAMMY.	G.Hale	February 2004
2.2	Run EDA, RAC and SAMMY with data prepared for inter-comparison exercise, to analyze the differences in the central values and covariance matrices of uncertainties of evaluated data.	G.Hale, Chen Zhenpeng, N.Larson	July 2004
2.3.	Test to what extent the linear approximation for presentation of sensitivity coefficients is good for the case of R-Matrix fits for the ${}^6\text{Li}(n,t)$ reaction. To test the accuracies of numerical versus analytical determination of sensitivity coefficients applied in different R-matrix codes.	G.Hale, Chen Zhenpeng, N.Larson	July 2004
2.4.	Inter-compare the results of least-squares fits with the R-Matrix codes EDA, RAC and SAMMY and the model code PADE2 versus non-model codes GLUCS and GMA of the same experimental data. Demonstrate the factors leading to the reduction of the variances in the R-Matrix model fits: unitarity following from the relations between total and partial channels, and intrinsic medium and long energy range correlations induced by the model through predetermined functional shape.	G.Hale, Chen Zhenpeng, N.Larson, S.Tagesen, V.Pronyaev, Soo-Youl Oh, S.Badikov, E.Gai	July 2004
2.5.	Obtain final consistent evaluation of ${}^6\text{Li}(n,t)$ and ${}^{10}\text{B}(n,\alpha)$ reactions in R-Matrix model fits with EDA, RAC and SAMMY codes.	G.Hale, Chen Zhenpeng, N.Larson	August 2004

3. GMA database of experimental cross sections for standards evaluation and evaluation of data with GMA.

No.	Action	Participant(s)	Terms
3.1.	Revise the list of experimental data not included in the GMA database (as of December 2003) for standards; obtain these data from experimentalists and introduce them in GMA database.	A. Carlson, V. Pronyaev	May 2004
3.2.	Explore the possibility of re-evaluation of thermal cross sections needed for standards evaluations.	A. Carlson	June 2004
3.3.	Analyze and validate the full GMA database by splitting responsibilities for: ${}^6\text{Li}(n,t)$, ${}^{10}\text{B}(n,\alpha)$ by F.-J. Hambsch, $\text{Au}(n,\gamma)$, ${}^{238}\text{U}(n,\gamma)$ by H. Vonach, ${}^{235}\text{U}(n,f)$, ${}^{238}\text{U}(n,f)$, ${}^{239}\text{Pu}(n,f)$ by A. Carlson.	F. J. Hambsch, H. Vonach, A. Carlson	July 2004
3.4.	Correspond with the authors of the experimental works on measurement of the fission cross sections at high energies ($E_n > 20$ MeV) on the problem of resolution of discrepancies between the data.	A. Carlson, V. Pronyaev	February 2004

4. Study of Peelle's Pertinent Puzzle (PPP) and improvement of GMA and other general least-squares codes to exclude bias of evaluated data caused by the PPP.

No.	Action	Participant(s)	Terms
4.1.	Study the possibility of implementing Chiba-Smith approach in the GMA for exclusion of the PPP. Run test case prepared under 4.2., to demonstrate exclusion of PPP and for comparison with logarithm transformation approach.	Soo-Youl Oh, V. Pronyaev	February 2004
4.2.	Send $\text{Au}(n,\gamma)$ and ${}^{238}\text{U}(n,\gamma)$ coupled subsets of data to H. Vonach and Soo-Youl Oh for testing and comparison of different approaches to exclude the PPP.	V. Pronyaev	February 2004
4.3.	Introduce Box-Cox (or logarithm) transformation of data in the GMA code.	Soo-Youl Oh	July 2004
4.4.	Study the justification for the general measure of uncertainty (sum of elements of covariance matrix of uncertainties, or similar practically conserving measure) for the data evaluated with different least-square approaches.	N. Larson, E. Gai, S. Badikov	July 2004
4.5.	Study $\text{Au}(n,\gamma)$ and ${}^{238}\text{U}(n,\gamma)$ coupled subsets of data for the presence of PPP and compare different approaches to exclude the PPP	S. Tagesen, Soo-Youl Oh V. Pronyaev	July 2004
4.6.	Monte Carlo simulation with known data to study the PPP.	Soo-Youl Oh	August 2004

5. Combining of the results of R-Matrix model fits for $^{10}\text{B}(n,\alpha)$ and $^6\text{Li}(n,t)$ reaction cross sections with general least-squares non-model evaluations of heavy elements.

No.	Action	Participant(s)	Terms
5.1.	Study an option where data for all constraint reactions (total, elastic) from the GMA database are transferred to the R-matrix fit so the only lithium and boron cross sections used in the GMA fit are the standard reactions.	V.Pronyaev, Chen Zhenpeng, Soo-Youl Oh	March 2004
5.2.	Study an option where light-element standard cross sections evaluated in the R-Matrix model are introduced as cross-reaction correlated data sets ($^{10}\text{B}(n,\alpha_0)$ and $^{10}\text{B}(n,\alpha_1)$) with their evaluated covariance matrix in the final combined GMA fit.	V.Pronyaev, Chen Zhenpeng, Soo-Youl Oh	May 2004
5.3.	Develop a method for converting the non-positive covariance matrix of the uncertainties of the cross sections obtained in R-matrix fits to positive definite with minimal changes of the matrix.	S.Badikov, E.Gai, V.Pronyaev	July 2004
5.4	Obtain the results for combined R-matrix and GMA evaluations.	All	August 2004

6. Other important topics.

No.	Action	Participant(s)	Terms
6.1.	Prepare CRP Web site, and introduce information which can be useful to participants.	V. Pronyaev	August 2004
6.2.	Make best estimation of the numerical uncertainties introduced by different methods of solution and numerical procedures used (GLUCS versus GMA) for realistic subset of data ($\text{Au}(n,\gamma)$, $^{238}\text{U}(n,\gamma)$).	S.Tagesen, Soo-Youl Oh, V.Pronyaev	July 2004
6.3.	Prepare a paper for the ND2004 conference with a description of the methodology and preliminary results for the new standards evaluation.	All	August 2004
6.4.	Develop the simplest smoothing procedure, which will preserve the physical variations of the cross sections and remove the “noise” obtained in least-squares fitting, and use for smoothing.	Soo-Youl Oh, V.Pronyaev	September 2004
6.5.	Prepare ENDF-7 formatted standards cross sections and covariance matrices of uncertainties.	S.Tagesen, H.Vonach, V.Pronyaev	October 2004

3. Contents of the final report of the CRP (IAEA TECDOC report series)

The title of the report describing the final results obtained by the CRP will be “An International Evaluation of the Neutron Cross Section Standards” (agreed between the participants). The report will include the following chapters:

1. Introduction (brief review of the approach used for the previous standards evaluation (called “old standards” below), unresolved problems in the old standards evaluation, main objectives in the new standards evaluation).

2. Methodology of the evaluation and codes (justification of the old Poenitz methodology for the new standards, improvement of the methodology (brief summary), work with uncertainties of discrepant data, physical and technical fixes to avoid PPP, joining of the low- and high-energy standards in one fit, procedure for combining the light and heavy element standards; brief description of the codes used in evaluation: EDA, RAC, SAMMY, GLUCS, GMA, and their intercomparisons and tests).

3. Experimental database improvement (W. Poenitz (1987) experimental database with 1997 updates, discrepancies between experimental data, 2003-2004 update, joining of low-energy ($E_n < 20$ MeV) and high-energy ($E_n > 20$ MeV) standards databases, corrections for particle leaking to the results obtained with Frisch-gridded ionization chambers, and revision of the uncertainties of some data recommended by the experts).

4. Microscopic nuclear models and light element standard cross sections (ambiguities in R-matrix parameterization of wide and distant poles, RGM, RRGGM results for ${}^6\text{Li}+n$ and ${}^{10}\text{B}+n$ systems).

5. R-matrix theory and evaluation of light element standards (experimental database, EDA and RAC results for ${}^7\text{Li}$ and ${}^{11}\text{B}$ systems, their consistency, uncertainties of the evaluated data in the R-matrix model fits, problems with positive definiteness of the covariance matrix of the uncertainties of the evaluated data derived from the covariance matrix of the parameters if $N < M$).

6. PPP and its exclusion (PPP history, reasons for PPP, PPP manifestation in fits of realistic multi-point data sets including subsets of data from the GMA database and the full GMA database, physical and technical fixes for PPP, updating of the codes used for standards evaluation to minimize PPP, demonstration that different technical fixes produce consistent results).

7. Evaluation of standards for heavy and light element standards, combination procedure (GMA fit of heavy and light element standards with a combining procedure using the R-matrix light element standards evaluations treated as data sets in the GMA fit along with all data for heavy element standards and ratios between light and heavy element standards, results of the evaluation, - central values, uncertainties, cross-energy and cross-reaction correlations, additional components of the uncertainties which were added – as numerical solution uncertainty and uncertainty of the technical fix used to avoid PPP, how to compare the uncertainty presented through covariance matrices with experts’ estimation of percent uncertainties).

8. Data presentation for standards (original results produced by GMA; smoothed point-wise evaluated data with increased uncertainties (if needed due to smoothing) and deleted cross-reaction correlation blocks of the total covariance matrix having levels of correlations below a few percent – as table (human-readable) and ENDF-7 formats;

covariance matrix of uncertainties of evaluated data in a wide-group structure in user-friendly tables and ENDF-7 format.

Annex 1

Agenda and time schedule

International Atomic Energy Agency
Second Research Co-ordination Meeting on
Improvement of the Standard Cross Sections for Light Elements
National Institute of Standards and Technology
Gaithersburg, MD, United States of America
13 – 17 October 2003

Monday, 13 October

09:00 - 09:20 Registration (NIST Main Gate, NIST, Gaithersburg)

09:30 – 9:40 Opening Session:

- Welcome Address from the NIST
- Election of Chairman and Rapporteur
- Adoption of Agenda (Chairman)

9:40 - 12:20 Session 1: Presentations by Participants

[Break when appropriate]

(max. 40 minutes for each presentation and discussion):

1. *Direct Calculation of R-Matrix Poles in the Refined Resonating Group Model*
Hartmut M. Hofmann, Universität Erlangen-Nürnberg, Erlangen, Germany.
2. *n+p Cross Sections and Uncertainties from the N-N R-matrix Analysis*
Gerry M. Hale, Los Alamos National Laboratory, USA.
3. *n+⁶Li cross sections from a new analysis of ⁷Li system data*
Gerry M. Hale, Los Alamos National Laboratory, USA.
4. *Some thoughts on data analysis problems*
Ms. Nancy M. Larson, Oak Ridge National Laboratory, USA.

12:20 - 14:00 IAEA&NIST Welcome Lunch and Administrative/Financial Matters

14:00 - 17:00

Session 1: Presentations by Participants (cont.)

[Coffee break when appropriate]

5. *Progress Report on analysis of ⁷Li system with RAC*
Chen Zhenpeng, Tsinghua University, Beijing, China.
6. *Progress Report on analysis of ¹¹B system with RAC*
Chen Zhenpeng, Tsinghua University, Beijing, China.
7. *Once Again on the Peelle's Puzzle*
Sergei A. Badikov, Institute of Physics and Power Engineering, Obninsk, Russia.

8. *On the evaluation of the quantity formulated with raw data in quotient form*
Soo Youl Oh, KAERI, Republic of Korea.
9. *GLUCS code modification to remove the effects of PPP*
Herbert Vonach, Siegfried Tagesen
Institut für Isotopenforschung und Kernphysik der Universität Wien,
Vienna, Austria.
10. *Box-Cox Transformation for Resolving PPP*
Soo Youl Oh, KAERI, Republic of Korea.
11. *Status of the Experimental Data for International Standards Evaluation*
Allan D. Carlson, National Institute of Standards and Technology,
Gaithersburg, USA.

Tuesday, 14 October

9:00 - 12:30 Session 1: Presentations by Participants (contd.)

[Coffee break when appropriate]

12. *The Latest Results on the $^{10}\text{B}(n,\alpha)$ Measurements at IRMM*
Franz-Josef Hambsch, Institute for Reference Materials
and Measurements, Geel, Belgium.
13. *The Results of Polynomial and Rational Least Squares Fits for the $6\text{Li}(n,t)$
reaction cross section*
Sergei A. Badikov, Institute of Physics and Power Engineering, Obninsk,
Russia.
14. *New Evaluation of the Fission Cross Section of ^{235}U*
Franz-Josef Hambsch, Institute for Reference Materials
and Measurements, Geel, Belgium.
15. *Updating of GMA Data Base and Trends in New Standards Evaluation*
Vladimir G. Pronyaev, International Atomic Energy Agency, Vienna,
Austria.
16. *Subjective Judgment about Uncertainty Measure*
Vladimir G. Pronyaev, International Atomic Energy Agency, Vienna, `Austria.

12:30 - 14:00 Lunch

14:00 - 17:30 Session 2: Discussions on key topics (name of moderator is given in brackets)

[Coffee break when appropriate]

- Use of the poles characteristics predicted in the theoretical model approaches for the R-matrix fit of Li^{6+n} and B^{10+n} reactions: remote wide resonances (*Hartmut M. Hofmann*)

- Further intercomparison of the R-matrix codes: test of error propagation (*G.M. Hale, N.M. Larson, Chen Zhenpeng*)

- Reduction of the uncertainties in the model fits: least square fits with separated contribution of normalization and statistical uncertainty in chi-square versus fits with full covariance matrices (*G.M. Hale, Chen Zhenpeng*)

- Semi-positive definiteness of the covariance matrices of uncertainties of the cross sections reconstructed in n points from covariance matrix of m ($m < n$) resonance parameters: how bad is this, practical impact at the data processing, conversion it to positive definite without substantial changes (*V.G. Pronyaev, S.A. Badikov*)

- PPP: is there the PPP manifestation in the GMA database and how to deal with ? (*Soo Youl Oh, S.A. Badikov*)

- Database for R-matrix fit of $\text{Li}6+n$ and $\text{B}10+n$ reactions: completeness (*G.M. Hale, Chen Zhenpeng*)

- Data reduction for R-matrix resonance fit of ${}^6\text{Li}+n$ and ${}^{10}\text{B}+n$ reactions: is it needed to correct data in some channels for experimental resolution and how it can be done? (*N.M. Larson*)

- Combining the R-matrix and GMA results: using GMA, other options (*V.G. Pronyaev*)

- Status of the GMA database: new data, data which still should be analysed and corrected if needed (*A.D. Carlson, F.-J. Hambsch*)

- Procedures to work with the discrepant data: how to resolve discrepancies and reduce chi-square of fit to the level of 1 (*H. Vonach, S.A. Badikov*)

- Review of the preliminary results of the standards evaluation obtained with the updated GMA database (*V.G. Pronyaev*)

- Smoothing of the data evaluated with GMA, uncertainty introduced by smoothing

- Presentation of evaluated covariance matrices in the evaluated data files: reducing to more wide group structure?

Tuesday, 15 October

9:00 - 12:30 Session 2: Discussions on key topics (continued)

[Coffee break when appropriate]

12:30 - 14:00 Lunch

14:00 - 17:30 Session 2: Discussions on key topics (continued)

[Coffee break when appropriate]

Tuesday, 16 October

9:00 - 12:30 Session 2: Discussions on key topics (continued)

[Coffee break when appropriate]

12:30 - 14:00 Lunch

14:00 - 17:30 Session 3: Recommendations and conclusions

[Coffee break when appropriate]

- Reviewing of the actions of the RCM-1 and preparing new action list

- Preparing of the meeting summary and conclusions

- Distribution of the work aimed at the preparation of the IAEA TECDOC report with the CRP results

- Preparing the abstracts of papers to be submitted at the ND2004 Conference with the results obtained in the CRP frameworks

- Date and place of RCM-3 (proposal is IAEA Headquarter, 18-22 October 2004)

Tuesday, 17 October

9:00 - 12:30 **Session 3: Recommendations and conclusions (continued)**

[Coffee break when appropriate]

12:30 - 14:00 **Lunch**

14:00 - 16:00 **Session 3: Recommendations and conclusions (continued)**

[Coffee break when appropriate]

Annex 2

LIST OF PARTICIPANTS

CRP PARTICIPANTS

AUSTRIA

Mr. Herbert K. VONACH
Institut für Isotopenforschung und
Kernphysik der Universität Wien
Boltzmannngasse 3
A-1090 Vienna

Res. Agreement No. 12021

Phone: +43 1 3177205
Fax: +43 1 4277 51752
E-mail: Herbert.Vonach@utanet.at

GERMANY

Mr. Hartmut M. HOFMANN
Room No. 02.534, Building B2
Institut für Theoretische Physik III
Universität Erlangen-Nürnberg
Staudtstrasse 7
D-91058 Erlangen

Res. Agreement No. 12023

Phone: +49 9131 852 8470
Fax: +49 9131 852 7704
E-mail:
HMH@theorie3.physik.uni-erlangen.de

KOREA, Republic of

Mr. Soo-Youl OH
HANARO Center
Korea Atomic Energy Research Institute
P.O. Box 105
Yuseong, Daejeon, 305-600

Res. Contract No. 12025

Phone: +82 42 868 2961
Fax: +82 42 868 8341
E-mail: SYOh@kaeri.re.kr

RUSSIA

Mr. Sergei A. BADIKOV
Institute of Physics and Power Engineering
Bondarenko Sq. 1
249 033 Obninsk, Kaluga Region

Res. Contract No. 12026

Phone: +7 08439 98847
Fax: +7 095 230 2326
E-mail: Badikov@ippe.obninsk.ru

UNITED STATES OF AMERICA

Mr. Allan D. CARLSON
Building 245, Room C308
National Institute
of Standards and Technology (NIST)
100 Bureau Drive Stop 8463
Gaithersburg, MD 20899-8463

Res. Agreement No. 12029

Phone: +1 301 975 5570
Fax: +1 301 975 4766
Fax: +1 301 869 7682 (for larger jobs)
E-mail: Carlson@nist.gov
E-mail: Allan.Carlson@nist.gov

Mr. Gerald M. HALE
Group T-16, MS B-243
Los Alamos National Laboratory
Los Alamos, NM 87545

Res. Agreement No. 12028

Phone: +1 505 667 7738
Fax: +1 505 667 9671
E-mail: GHale@lanl.gov

Ms. Nancy M. LARSON
Bldg 6011, Rm 118, MS 6370
Oak Ridge National Laboratory
P.O. Box 2008
Oak Ridge, TN 37831-6370

Res. Agreement No. 12027

Phone: +1 865 574 4659
Fax: +1 865 574 8727
E-mail: LarsonNM@ornl.gov

OBSERVER OF AN INTERNATIONAL ORGANIZATION

BELGIUM

Mr. Franz-Josef HAMBSCHE
Neutron Physics Unit
Van de Graaff Laboratory
EC-JRC-Institute for Reference Materials
and Measurements (IRMM)
Retieseweg
B-2440 Geel

Phone: +32 14 571 351
Fax: +32 14 571 376
E-mail: Franz-Josef.Hambsch@irmm.jrc.be
E-mail: Hambsch@irmm.jrc.be

IAEA, Vienna, AUSTRIA

Mr. Vladimir G. PRONYAEV
(Scientific Secretary of the Meeting)
IAEA Nuclear Data Section
Wagramer Strasse 5
P.O. Box 100
A-1400 Vienna

Phone: +43 1 2600 21717
Fax: +43 1 26007
E-mail: V.Pronyaev@iaea.org

Annex 3. Participants' presentations, working papers and consultants reports submitted for inclusion in the summary report

Calculation of R-matrix Poles in the Refined Resonating Group Model

Hartmut M. Hofmann
Institut für Theoretische Physik III
Universität Erlangen-Nürnberg

October 13 2003

RRGM primer
R-matrix primer

Comparison of methods
Example ${}^7\text{Li}$ - system
Interpretation
Sensitivity

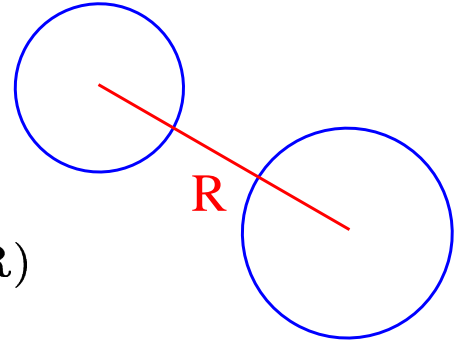
Dependencies

Scattering lengths of neutrons off ${}^3\text{He}$

Effective NN-potential versus realistic nuclear interaction

Refined Resonating Group Model Basics

Composite system



$$\text{RGM Ansatz } \Psi_l = \sum_{k=1}^{chan} \psi_{chan}^k \cdot \chi_{rel}^{lk}(\mathbf{R})$$

$$\text{Variation } \langle \delta \Psi_l \mathcal{A} | H - E | \Psi_l \rangle = 0$$

$$\text{Channel function } \psi_{chan} = [Y_L(\hat{\mathbf{R}}) \otimes [\phi_1^{j_1} \otimes \phi_2^{j_2}]^{S_c}]^J$$

$$\text{Ansatz } \psi = \psi_{chan}(\sum_i b_i \cdot \text{Gaussian}) \quad (\text{bound state})$$

$$\text{or } \chi_{rel}^{lk}(R) = \delta_{lk} \cdot F_k(R) + a_{lk} \cdot \tilde{G}_k(R) + \sum_i b_{lki} \cdot \text{Gaussian} \\ (\text{scattering state})$$

Variational parameters a_{lk} and $b_{(lk)i}$

Decompose Hamiltonian

$$\begin{aligned} H - E &= H_1 - E_1 + H_2 - E_2 + \\ &\sum_{\substack{i \in 1 \\ j \in 2}} V_{ij} - V_{Coul} + \\ &T_R + V_{Coul} - (E - E_1 - E_2) = \\ &H_1 - E_1 + H_2 - E_2 + V_{short} + H_R - \tilde{E} \end{aligned}$$

$$\text{with } \mathcal{A} \cdot (H_i - E_i) \phi_i = 0 \text{ and } (H_R - \tilde{E}) F/G = 0$$

\Rightarrow All integrals shortranged

Note: Relative thresholds fixed by \tilde{E}

Refined Resonating Group Model Variation

⇒ Expand all functions including F and G

- in terms of Gaussians
- times solid spherical harmonics

⇒ All individual integrals analytically calculable,
provided potential is of Gaussian form including differential operators
All operators allowed which occur in Argonne and Bonn (r-space)
potentials and in Urbana IX NNN-force

Variational equations complicated matrix equations

Diagonalize hamiltonian and norm matrix in Gaussian function space
yielding Γ_μ with

$$\langle \Gamma_\nu | \mathcal{A} \Gamma_\mu \rangle = \delta_{\nu\mu} \text{ and}$$

$$\langle \Gamma_\nu | H' | \mathcal{A} \Gamma_\mu \rangle = \epsilon_\nu \delta_{\nu\mu}$$

Refined Resonating Group Model

Variation continued

New Ansatz

$$\Psi_l(R) = \mathcal{A} \left(\sum_k (\delta_{lk} \cdot f_k(R) + a_{lk} \cdot \tilde{g}_k(R)) + \sum_\nu d_{l\nu} \cdot \Gamma_\nu \right)$$

Variation $\langle \delta \Psi_l | \underbrace{H - E}_{\hat{H}} | \mathcal{A} \Psi_l \rangle = 0$

Variational equations

$$\langle g_k | \hat{H} | \mathcal{A} f_l \rangle + \sum_{k'} \langle g_k | \hat{H} | \mathcal{A} g_{k'} \rangle a_{lk'} + \sum_\nu \langle g_k | \hat{H} | \mathcal{A} \Gamma_\nu \rangle d_{l\nu} = 0$$

and

$$\langle \Gamma_\nu | \hat{H} | \mathcal{A} f_l \rangle + \sum_{k'} \langle \Gamma_\nu | \hat{H} | \mathcal{A} g_{k'} \rangle a_{lk'} + \sum_{\nu'} \underbrace{\langle \Gamma_\nu | \hat{H} | \mathcal{A} \Gamma_{\nu'} \rangle}_{(\epsilon_\nu - E) \delta_{\nu\nu'}} d_{l\nu'} = 0$$

Solve for $d_{l\nu}$ and define $\tilde{H} = \hat{H} - \sum_\nu \frac{\hat{H} | \mathcal{A} \Gamma_\nu \rangle \langle \Gamma_\nu | \hat{H}}{\epsilon_\nu - E}$

then in matrix notation

$$a = -\langle G | \tilde{H} | F \rangle^T \langle G | \tilde{H} | G \rangle^{-1}$$

This is the basic expression, it can be improved, rewritten in other scattering matrices, etc.

How to choose the Gaussians?

Choose a large number N of Gaussians to

Cover the interaction region

Reproduce the oscillating scattering wave functions in a large region

Choose a small number N of Gaussians to

Blackuce the computational effort growing with N^2

Avoid numerical linear dependence in diagonalization procedure

Compromise

15 to 25 Gaussians centered at the origin per partial wave channel

Width parameters ranging between 100 fm^{-2} to 0.0001 fm^{-2}

nearly geometrical progression

depending on force used

realistic forces need larger width parameters to account for core

Eigenvalues ϵ_ν of the hamiltonian matrix below the LOWEST threshold are variational approximations to bound state energies

Corresponding Γ_ν approximate the bound state wave function

All other eigenvalues have no physical significance!

They accumulate just above the thresholds, becoming scarce with increasing energy and reaching up to 1000 MeV

R-matrix Approach

Separate configuration space by channel radius a_c into interaction region and asymptotic region (at most Coulomb)

Hamiltonian not hermitian when restricted to interaction region
Need Bloch operator \mathcal{L} defined on the channel surface

Following D.Baye et al. PRC 59(1999)817
the poles of the R-matrix are at the eigenvalues of $\tilde{H} + \mathcal{L} - E\tilde{N}$ restricted to the interaction region

The matrix elements can be calculated by integration over all space (antisymmetrized) minus integration over the asymptotic region (direct terms only)

Assuming antisymmetrization unnecessary beyond a_c

For Gaussians centered at the origin the integration over the asymptotic region yields incomplete gamma functions

Aim for small a_c to create only few poles in energy region considered

Since fitting data, one wants as few parameters as possible

Can we use the matrix elements calculated with the RRGM?

Yes and No

Comparison of Methods

RRGM: Reproduce oscillating scattering wave for arbitrary energy in large region \Rightarrow many Gaussians necessary

R-matrix: Need integrals only within channel radius a_c
 \Rightarrow functions have to be different in interaction region
no antisymmetrization beyond a_c
 \Rightarrow no small width parameters allowed

Restricted norm matrix no more positive definite!

Recipe: Take RRGM scattering calculation

Calculate asymptotic part of norm and hamilton matrix

Subtract from RRGM matrices

Delete small width parameter functions till norm is positive definite
(Delete also next smallest width parameter to avoid tiny norm eigenvalues)

Determine energy eigenvalues

Finding

Most eigenvalues very sensitive to chosen a_c
lowest rather stable

Example ${}^7\text{Li}$

Properties

Two particle bound states

Well developed (narrow) resonances

Many thresholds and channels

α – triton, 0 MeV

${}^6\text{Li}$ – neutron, 4.78 MeV

${}^6\text{Li}(3^+)$ – neutron, 6.97 MeV

${}^5\text{He}$ – deuteron, 7.06 MeV

${}^6\text{He}$ – proton, 7.51 MeV

${}^6\text{Li}(0^+, 1)$ – neutron, 8.34 MeV

${}^6\text{Li}(2^+)$ – neutron, 9.09 MeV

${}^6\text{Li}(2^+, 1)$ – neutron, 10.15 MeV

${}^6\text{Li}(1^{+*})$ – neutron, 10.43 MeV

Old RRGM calculation yields results rather close to R-matrix analysis

NPA 410(1983)208-236 and NPA 416(1984) 363c

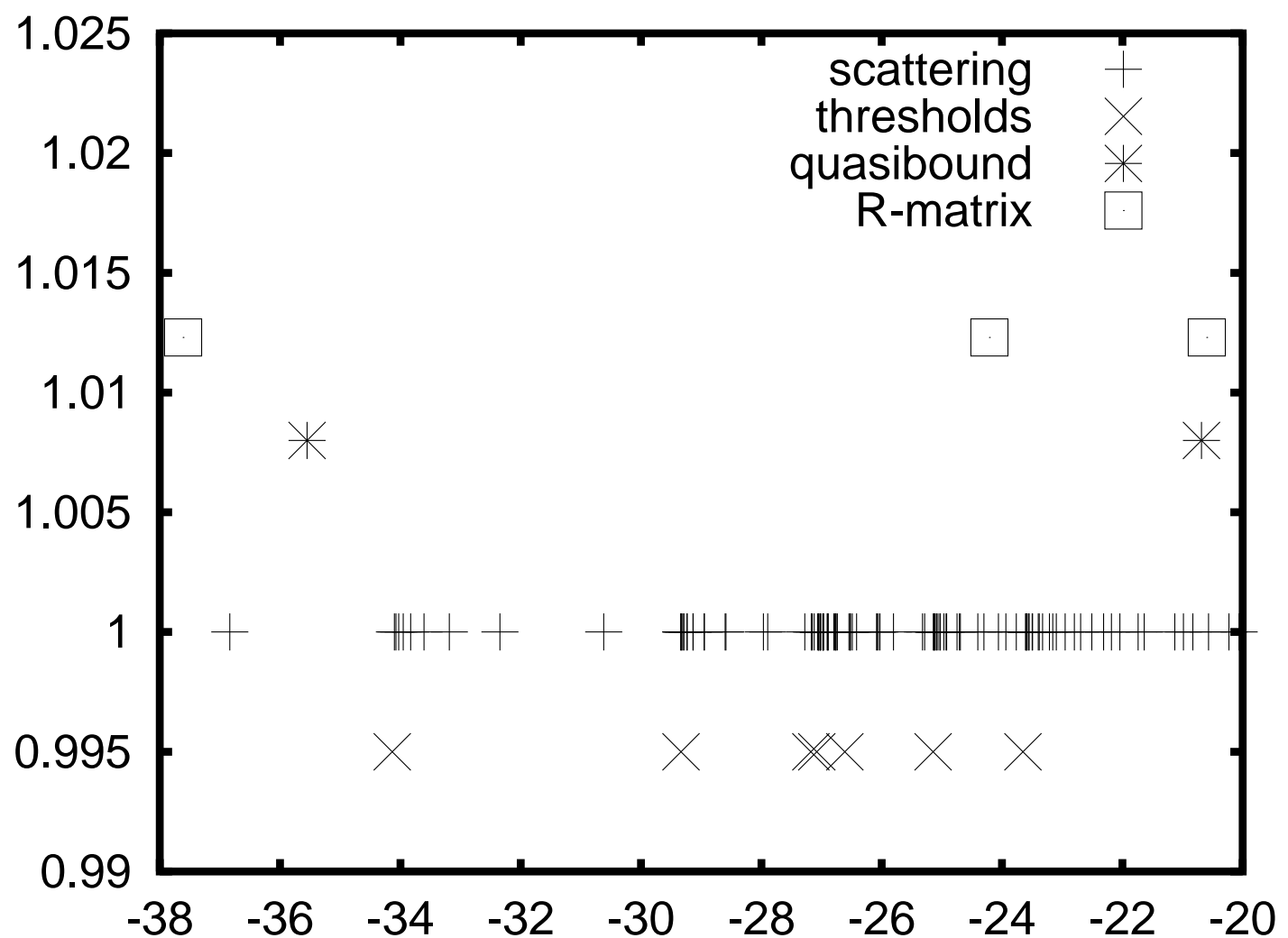
Comparison of the eigenvalues for various partial waves from

the full scattering calculation

restricted to larger width parameters 'quasi bound'

restricted to the internal region 'R-matrix'

$3/2^-$ partial waves

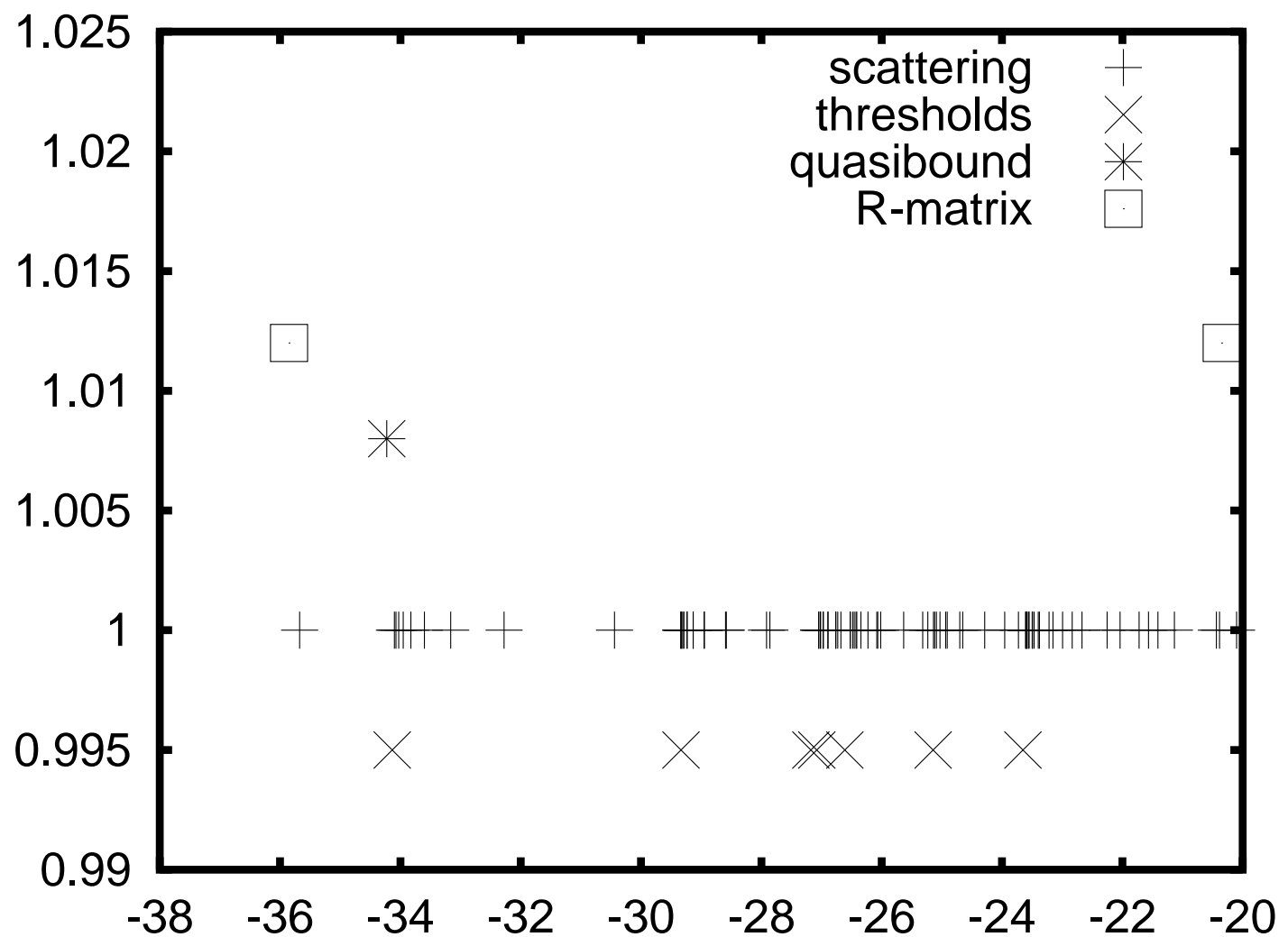


Scattering calculation yields one bound state
eigenvalues accumulate at all thresholds

Quasibound calculation yields bound state
and one additional eigenvalue

R-matrix yields bound state
and two high lying eigenvalues

$1/2^-$ partial waves

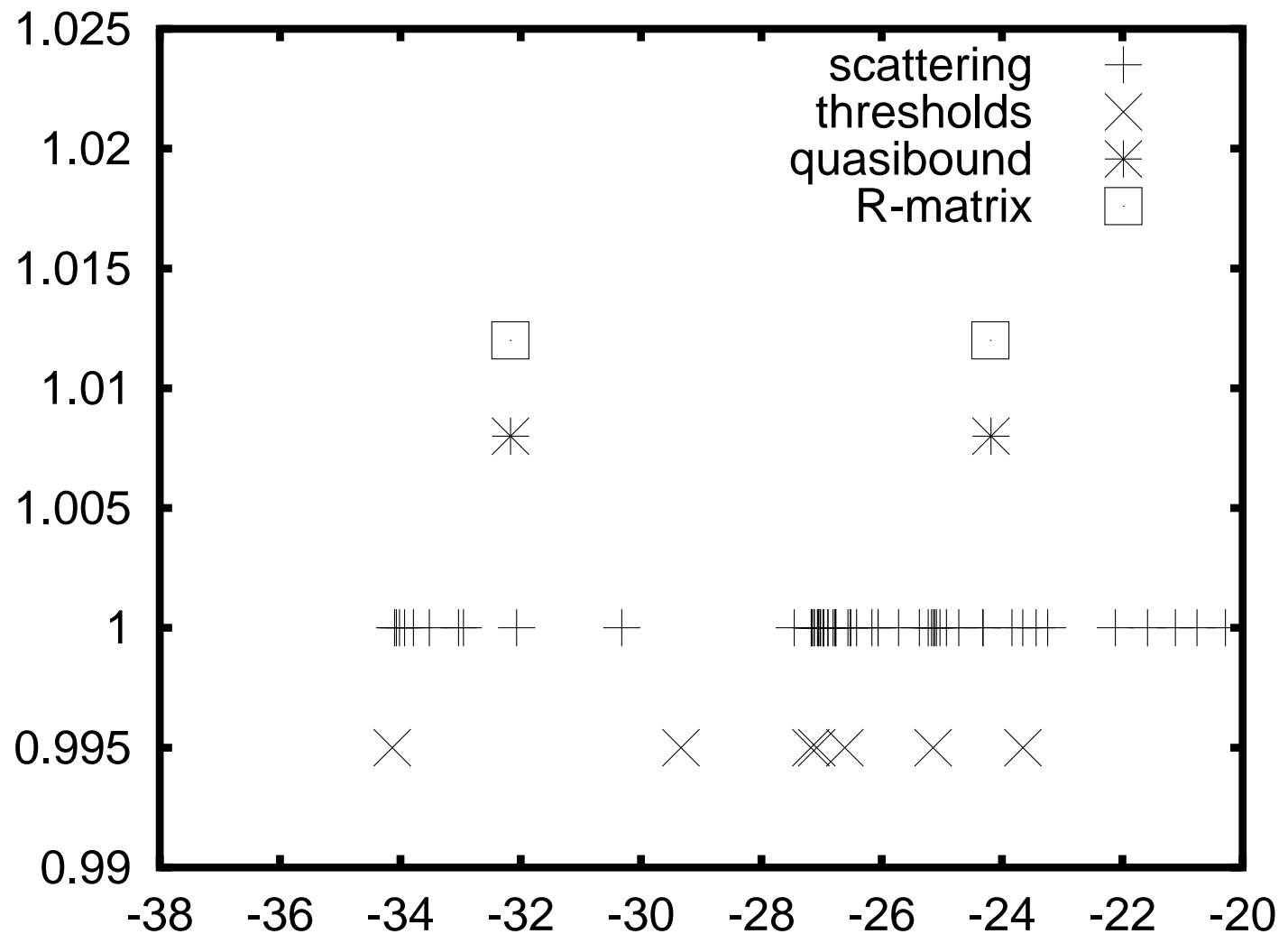


Scattering calculation yields one bound state
eigenvalues accumulate at all thresholds

Quasibound calculation yields state close to lowest
threshold, bound?

R-matrix yields bound state
and one high lying eigenvalue

$7/2^-$ partial waves

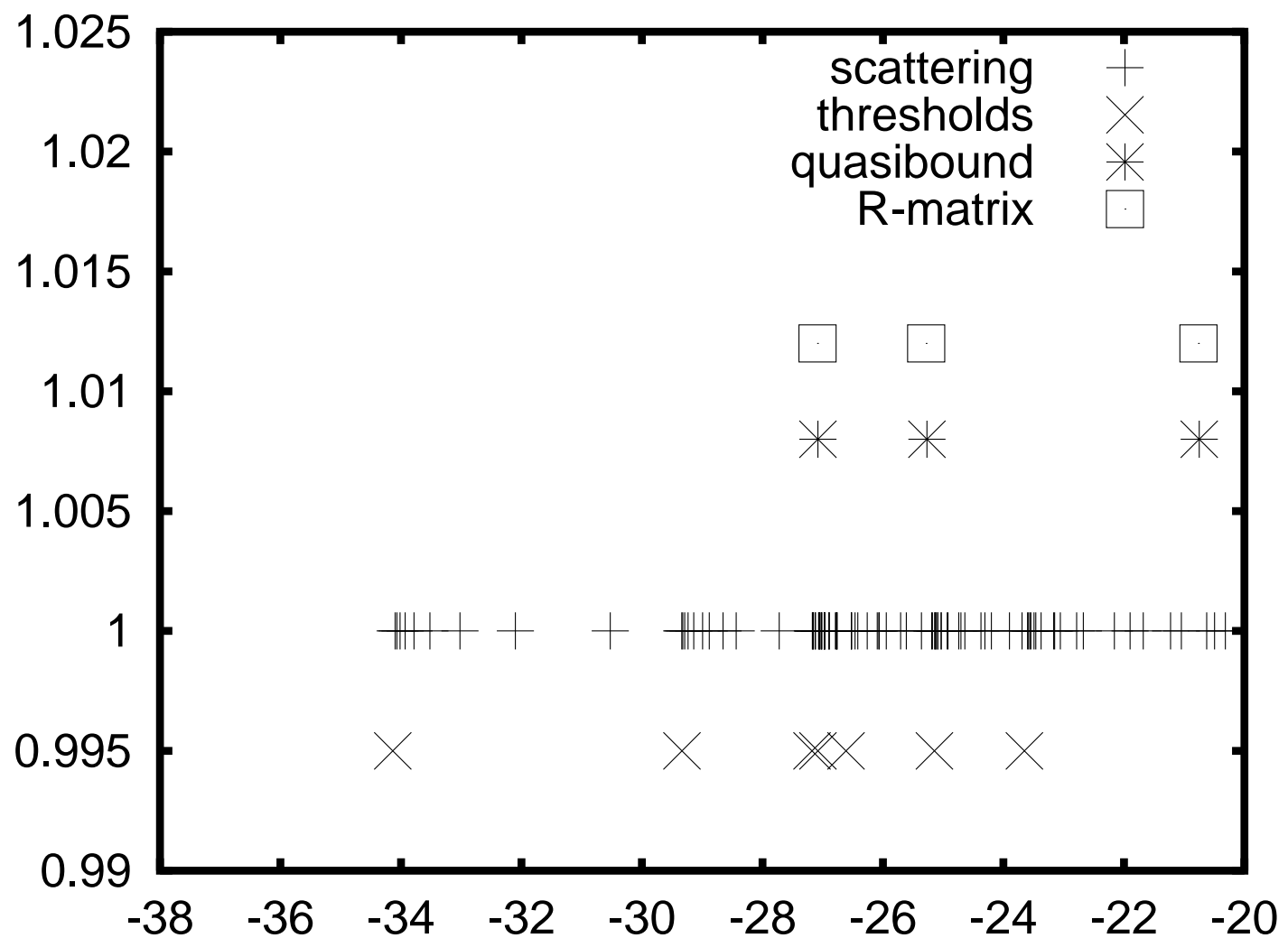


Scattering calculation yields no bound state eigenvalues accumulate at all thresholds

Quasibound calculation yields two well separated states

R-matrix yields two well separated states very close to quasibound positions

$5/2^-$ partial waves

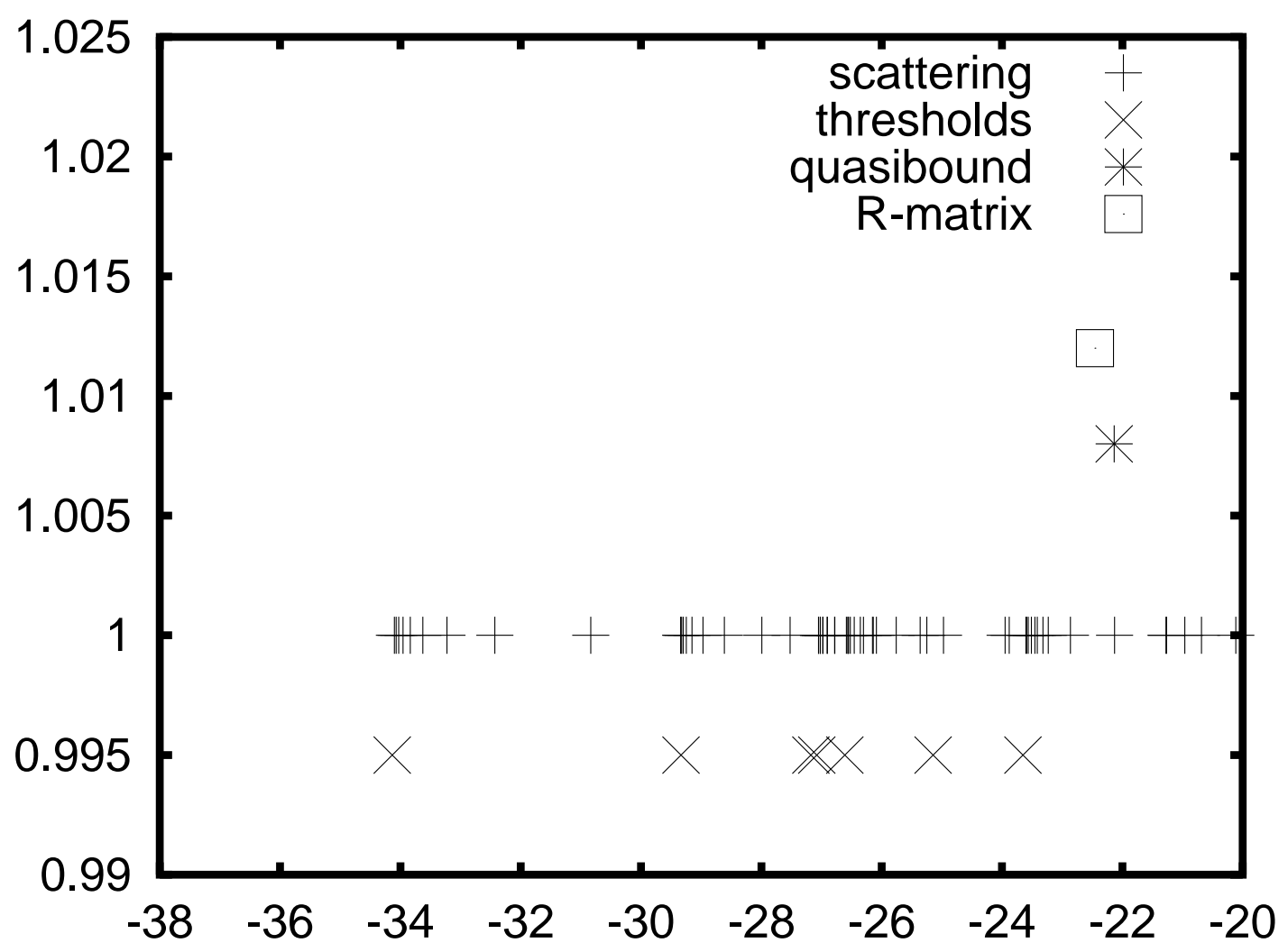


Scattering calculation yields no bound state eigenvalues accumulate at all thresholds

Quasibound calculation yields two close states and another highlying one

R-matrix yields two close states and another highlying one very close to quasibound positions

$1/2^+$ partial waves

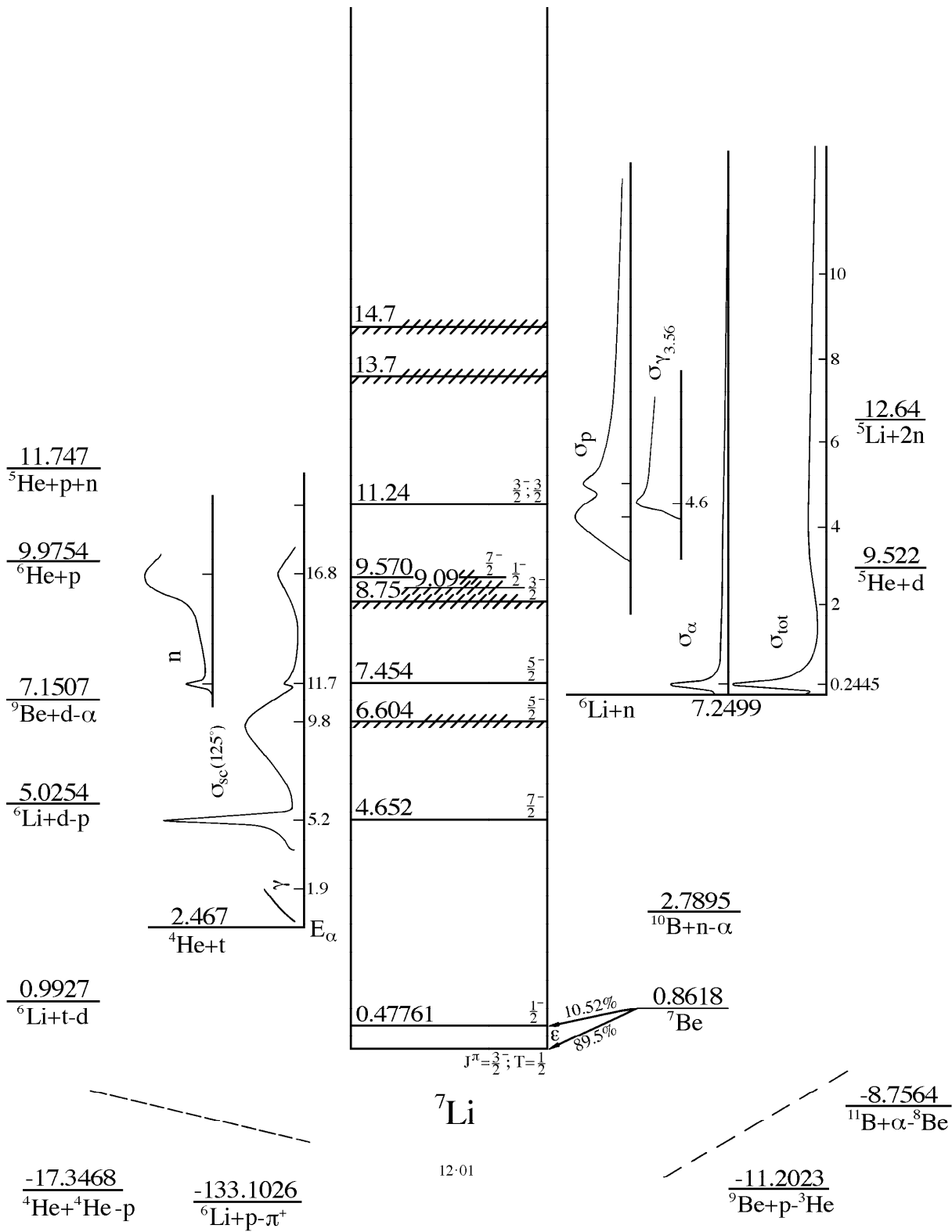


Scattering calculation yields no bound state eigenvalues accumulate at all thresholds

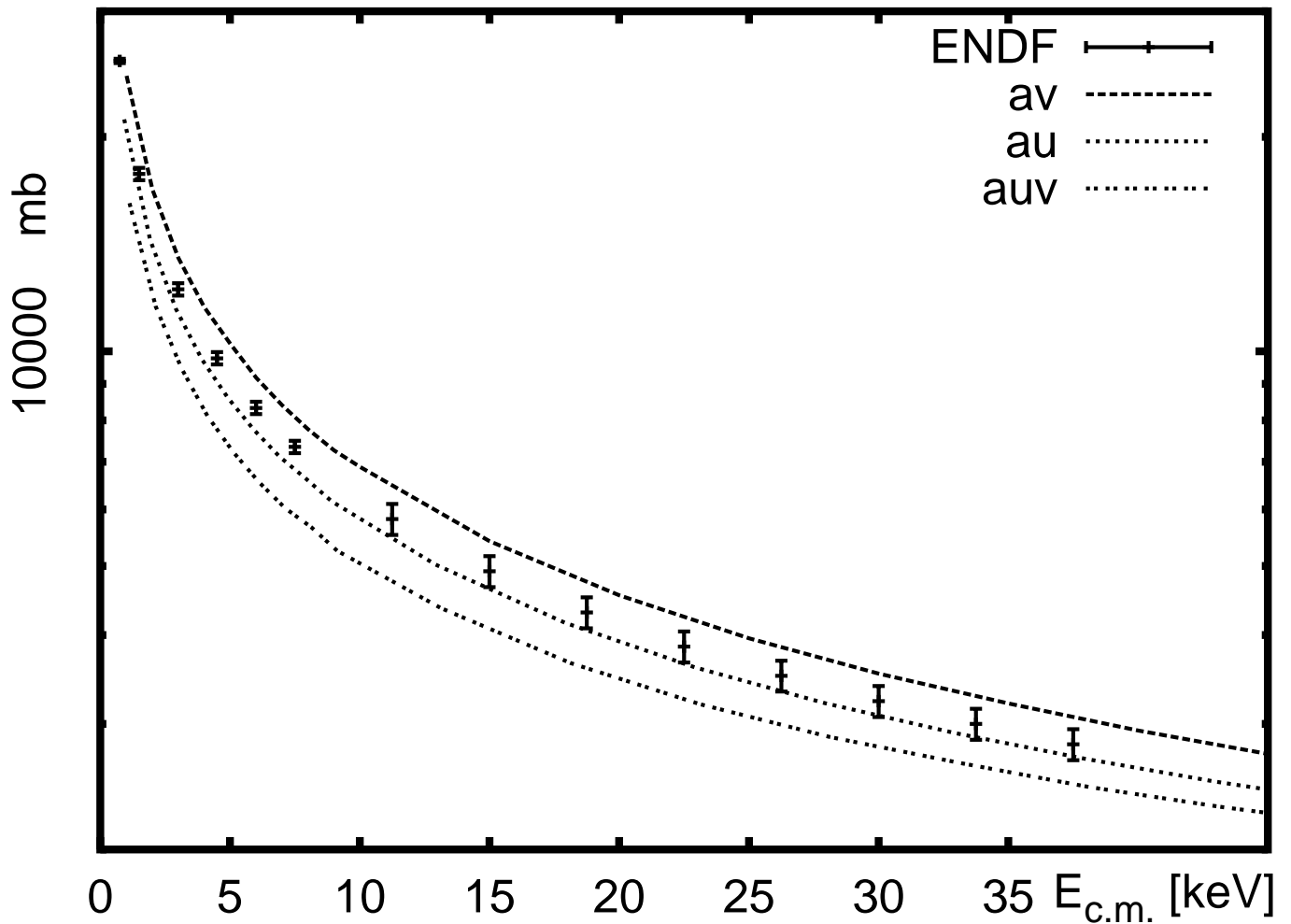
Quasibound calculation yields one high lying state

R-matrix yields one high lying state

${}^7\text{Li}$ level scheme



Standard cross section ${}^3\text{He}(n,p)$



Dominant contribution 1S_0 , P-wave 0.2 ... 7 %, 3S_1 0.7 ... 0.5 %

Spin dependent complex scattering lengths

potential	a_0		a_1	
	\Re	\Im	\Re	\Im
AV18	7.790(4)	-4.984(10)	3.448(2)	-0.0066(1)
... + UIX	7.629(2)	-4.053(3)	3.311(1)	-0.0051(1)
... + V_3^*	7.632(2)	-3.423(1)	3.310(1)	-0.0049(1)
R-matrix	7.400(3)	-4.449(1)	3.286(6)	-0.0012(2)
exp.	7.370(58)	-4.448(5)	3.278(53)	-0.001(2)

Effective NN-potentials versus realistic nuclear interactions

Effective NN-potentials allow for

simple wave functions of light nuclei

(S-waves only, cluster structure corresponds to lowest shell model configuration)

fast calculations, standard PC enough

various potentials readily available

systems up to $A=12$, or higher feasible

Increasing model space might overbind

too large model spaces might yield nonsense results

additional parameters required

different scattering channels non-orthogonal?

difficult (impossible) to reproduce threshold energies and interaction radius simultaneously

Realistic nuclear interactions need

very complicated wave functions already for triton etc.

huge computer resources

($A=4$ system: typically 50 000 CPU hours, 500 GB storage)

careful study of wave functions necessary

very few realistic interactions exist

Calculations restricted at the moment to $A \leq 5(6?)$

increasing model spaces improve calculation

no adjustable parameter

calculation must reproduce data, otherwise new interaction needed

Quasi-bound calculation do not care for non-orthogonality!

Some Thoughts on the Data Analysis Process

Nancy Larson

**Second Research Co-ordination Meeting on
Improvement of the Standard Cross Sections for
Light Elements**

**13-17 October 2003
NIST, Gaithersburg, MD, USA**

Topics to be ~~covered~~ touched on

- **Peelle's Pertinent Puzzle/Paradox**
- **Implicit data covariance (IDC) methodology**
- **Transformation of variables**

What is an appropriate goal of data analysis?

- If we make the (rash) assumption that the measured quantities¹ (the raw data) obey Gaussian statistics, then fitting to the measured quantities should give the correct result (“Truth”).
- The goal of an analysis which fits to derived quantities² is then to obtain the same value of “Truth” (or as close to it as possible) .

¹In a time-of-flight (tof) measurement this might be counts per time channel.

²Cross section per energy, in a tof measurement.

References for PPP

- **Zhao and Perey**
 - “The Covariance Matrix of Derived Quantities and Their Combination”
 - ORNL/TM-12106 (1992)

- **Chiba and Smith**
 - “Some comments on Peelle’s Pertinent Puzzle”
 - JAERI-M 94-068 page 5-12 (1994)

Solution to PPP ?

- **Least-squares equations*** are a linear expansion of a non-linear problem
 - Everywhere throughout the equations, the expansion must be made with respect to the same estimate of the value of any given parameter
 - Data covariance matrix is generally derived assuming different estimates for the same parameter 

* or Bayes' Equations

A trivial example

- Suppose the function Y is given by the product of two other (nonlinear) functions, f and g

$$Y(x) = f(x) g(x)$$

- Suppose further that, when f was measured, the value of x was known to be approximately a . Therefore, for $x \approx a$, f can be expanded in a Taylor series to give

$$f(x) \approx f(a) + f_x (x-a)$$

A trivial example, cont. ($Y = f g$)

- Suppose also that, when g was measured, the value of x was known to be $\approx b$. Hence, for x close to b , g can be expanded as

$$g(x) \approx g(b) + g_x(x-b)$$

- Therefore Y might be written

$$Y(x) = f(x) g(x) \approx [f(a) + f_x(x-a)] [g(b) + g_x(x-b)]$$

- Where is this equation valid?

– For $x \approx a$?

– For $x \approx b$?

No where! unless $a \approx b$

How does this apply to PPP ?

- Let d_1 and d_2 represent two (uncorrelated) measurements of the same quantity, with uncertainties Δd_1 and Δd_2 respectively.
- Let n represent the normalization (identical for the two measurements), and Δn its uncertainty.
- Let P represent the parameter of interest; P is related to the measured quantity via $P = d/n$.

PPP, continued

- To fit to the raw data, one way to formulate Bayes' Equations is

$$\begin{bmatrix} P' \\ n' \end{bmatrix} = \begin{bmatrix} P \\ n \end{bmatrix} - M' G^t V^{-1} \begin{bmatrix} nP - d_1 \\ nP - d_2 \end{bmatrix}$$

where the partial derivative matrix G and data covariance matrix V are given by

$$G = \begin{bmatrix} n & P \\ n & P \end{bmatrix}$$

$$V = \begin{bmatrix} \Delta^2 d_1 & 0 \\ 0 & \Delta^2 d_2 \end{bmatrix}$$

PPP, continued (fit raw data)

The (final) parameter covariance matrix M' is found from

$$M' = (M^{-1} + W)^{-1}$$

with W defined by $W = G^t V^{-1} G$

and the (initial) parameter covariance matrix M by

$$M = \begin{bmatrix} \Delta^2 P & 0 \\ 0 & \Delta^2 n \end{bmatrix} = \begin{bmatrix} \infty & 0 \\ 0 & \Delta^2 n \end{bmatrix} \quad \text{so} \quad M^{-1} = \begin{bmatrix} 0 & 0 \\ 0 & \Delta^{-2} n \end{bmatrix}$$

$$\begin{bmatrix} P' \\ n' \end{bmatrix} = \begin{bmatrix} P \\ n \end{bmatrix} - M'Y \quad Y = G'V^{-1} \begin{bmatrix} nP - d_1 \\ nP - d_2 \end{bmatrix} \quad M^{-1} = \begin{bmatrix} 0 & 0 \\ 0 & \Delta^{-2}n \end{bmatrix} \quad G = \begin{bmatrix} n & P \\ n & P \end{bmatrix} \quad V = \begin{bmatrix} \Delta^2 d_1 & 0 \\ 0 & \Delta^2 d_2 \end{bmatrix}$$

$$G'V^{-1} = \begin{bmatrix} n & n \\ P & P \end{bmatrix} \begin{bmatrix} \Delta^{-2}d_1 & 0 \\ 0 & \Delta^{-2}d_2 \end{bmatrix} = \begin{bmatrix} n\Delta^{-2}d_1 & n\Delta^{-2}d_2 \\ P\Delta^{-2}d_1 & P\Delta^{-2}d_2 \end{bmatrix}$$

$$Y = G'V^{-1} \begin{bmatrix} nP - d_1 \\ nP - d_2 \end{bmatrix} = \begin{bmatrix} n\Delta^{-2}d_1 & n\Delta^{-2}d_2 \\ P\Delta^{-2}d_1 & P\Delta^{-2}d_2 \end{bmatrix} \begin{bmatrix} nP - d_1 \\ nP - d_2 \end{bmatrix} = \begin{bmatrix} n^2P(\Delta^{-2}d_1 + \Delta^{-2}d_2) - n(d_1\Delta^{-2}d_1 + d_2\Delta^{-2}d_2) \\ nP^2(\Delta^{-2}d_1 + \Delta^{-2}d_2) - P(d_1\Delta^{-2}d_1 + d_2\Delta^{-2}d_2) \end{bmatrix} = \begin{bmatrix} n(nPQ - R) \\ P(nPQ - R) \end{bmatrix}$$

$$W = G'V^{-1}G = \begin{bmatrix} n\Delta^{-2}d_1 & n\Delta^{-2}d_2 \\ P\Delta^{-2}d_1 & P\Delta^{-2}d_2 \end{bmatrix} \begin{bmatrix} n & P \\ n & P \end{bmatrix} = \begin{bmatrix} n^2(\Delta^{-2}d_1 + \Delta^{-2}d_2) & nP(\Delta^{-2}d_1 + \Delta^{-2}d_2) \\ nP(\Delta^{-2}d_1 + \Delta^{-2}d_2) & P^2(\Delta^{-2}d_1 + \Delta^{-2}d_2) \end{bmatrix}$$

$$M^{-1} + W = \begin{bmatrix} n^2(\Delta^{-2}d_1 + \Delta^{-2}d_2) & nP(\Delta^{-2}d_1 + \Delta^{-2}d_2) \\ nP(\Delta^{-2}d_1 + \Delta^{-2}d_2) & P^2(\Delta^{-2}d_1 + \Delta^{-2}d_2) + \Delta^{-2}n \end{bmatrix} = \begin{bmatrix} n^2Q & nPQ \\ nPQ & P^2Q + \Delta^{-2}n \end{bmatrix}$$

$$\begin{aligned} Q &= \Delta^{-2}d_1 + \Delta^{-2}d_2 \\ R &= d_1\Delta^{-2}d_1 + d_2\Delta^{-2}d_2 \end{aligned}$$

$$M' = (M^{-1} + W)^{-1} = (n^2Q\Delta^{-2}n)^{-1} \begin{bmatrix} P^2Q + \Delta^{-2}n & -nPQ \\ -nPQ & n^2Q \end{bmatrix} = \begin{bmatrix} \frac{P^2}{n^2}\Delta^2n + \frac{1}{n^2Q} & -\frac{P}{n}\Delta^2n \\ -\frac{P}{n}\Delta^2n & \Delta^2n \end{bmatrix}$$

$$\begin{bmatrix} P' \\ n' \end{bmatrix} = \begin{bmatrix} P \\ n \end{bmatrix} - (n^2Q\Delta^{-2}n)^{-1} \begin{bmatrix} P^2Q + \Delta^{-2}n & -nPQ \\ -nPQ & n^2Q \end{bmatrix} \begin{bmatrix} n(nPQ - R) \\ P(nPQ - R) \end{bmatrix} =$$

$$(n^2Q\Delta^{-2}n)^{-1} \begin{bmatrix} n^2PQ\Delta^{-2}n - nP^2Q(nPQ - R) - n\Delta^{-2}n(nPQ - R) + nP^2Q(nPQ - R) \\ n^3Q\Delta^{-2}n + n^2PQ(nPQ - R) - n^2PQ(nPQ - R) \end{bmatrix} = \begin{bmatrix} R/(n^2Q) \\ n \end{bmatrix}$$

PPP, continued (fit raw data)

- After a bit of algebra, results are

$$P' = \frac{\left(\frac{d_1}{\Delta^2 d_1} + \frac{d_2}{\Delta^2 d_2} \right)}{n \left(\frac{1}{\Delta^2 d_1} + \frac{1}{\Delta^2 d_2} \right)} \quad \text{(as expected)}$$

and

$$n' = n$$

PPP, continued (fit raw data)

- New parameter covariance matrix is

$$M' = \begin{bmatrix} \frac{1}{n^2} \left(\frac{1}{\Delta^2 d_1} + \frac{1}{\Delta^2 d_2} \right)^{-1} + \frac{P^2}{n^2} \Delta^2 n & -\frac{P}{n} \Delta^2 n \\ -\frac{P}{n} \Delta^2 n & \Delta^2 n \end{bmatrix}$$

$\Delta^2 P'$

- Note that the updated parameter value P' does not depend on starting value P , but uncertainty does depend on P .

Therefore we would iterate, and the result would be to write $\Delta P'$ in terms of P' rather than P

- (Both value and uncertainty depend upon n .)

Results for fitting to raw data -

$$P' = \frac{\left(\frac{d_1}{\Delta^2 d_1} + \frac{d_2}{\Delta^2 d_2} \right)}{n \left(\frac{1}{\Delta^2 d_1} + \frac{1}{\Delta^2 d_2} \right)}$$

“Truth”

$$\Delta^2 P' = \frac{1}{n^2} \left(\frac{1}{\Delta^2 d_1} + \frac{1}{\Delta^2 d_2} \right)^{-1} + \frac{P'^2}{n^2} \Delta^2 n$$

PPP, continued

- **So much for fitting to raw data**
- **Usually we must fit to reduced data**
 - **So how do the equations change ?**

PPP, continued

- To fit to the **reduced** data, set $D_i = d_i/n$.
- Bayes' Equations then take the form

$$[P'] = [P] - M' G^t V^{-1} \begin{bmatrix} P - D_1 \\ P - D_2 \end{bmatrix}$$

where the usual expressions for V and G are

$$V = \begin{bmatrix} \frac{\Delta^2 d_1}{n^2} + \frac{d_1^2 \Delta^2 n}{n^2 n^2} & \frac{d_1 d_2 \Delta^2 n}{n^2 n^2} \\ \frac{d_1 d_2 \Delta^2 n}{n^2 n^2} & \frac{\Delta^2 d_2}{n^2} + \frac{d_2^2 \Delta^2 n}{n^2 n^2} \end{bmatrix}$$

statistical
 $G = [1 \ 1]$
systematic
(common)

PPP, continued (fit reduced data, usual method)

The (final) parameter covariance matrix M' is found from

$$M' = (M^{-1} + W)^{-1}$$

with W defined by $W = G^t V^{-1} G$

and the (initial) parameter covariance matrix M by

$$M = [\Delta^2 P] = [\infty] \quad \text{so} \quad M^{-1} = [0]$$

$$[P'] = [P] - M'Y \quad Y = G'V^{-1} \begin{bmatrix} P - d_1/n \\ P - d_2/n \end{bmatrix} \quad G = \begin{bmatrix} 1 \\ 1 \end{bmatrix} \quad V = \begin{bmatrix} a^2 + x^2q & xyq \\ xyq & b^2 + y^2q \end{bmatrix} \quad q = \Delta^2 n / n^2$$

$$\begin{aligned} a^2 &= \Delta^2 d_1 / n^2 \\ x &= d_1 / n \\ b^2 &= \Delta^2 d_2 / n^2 \\ y &= d_2 / n \end{aligned}$$

$$G'V^{-1} = \begin{bmatrix} 1 & 1 \\ b^2 + y^2q & -xyq \\ -xyq & a^2 + x^2q \end{bmatrix} \quad Z = \begin{bmatrix} (b^2 + y^2q - xyq) & (a^2 + x^2q - xyq) \end{bmatrix} \quad Z = (a^2b^2 + (a^2y^2 + b^2x^2)q)^{-1}$$

$$Y = G'V^{-1} \begin{bmatrix} P - d_1/n \\ P - d_2/n \end{bmatrix} = Z \begin{bmatrix} b^2 + y^2q - xyq & a^2 + x^2q + xyq \end{bmatrix} \begin{bmatrix} P - x \\ P - y \end{bmatrix} = Z \begin{bmatrix} P(a^2 + b^2 + (x^2 - 2xy + y^2)q) \\ \dots - x(b^2 + (y^2 - xy)q) - y(a^2 + (x^2 - xy)q) \end{bmatrix}$$

$$W = G'V^{-1}G = [a^2 + b^2 + (x - y)^2q]Z$$

$$M' = W^{-1} = [a^2 + b^2 + (x - y)^2q]^{-1} Z^{-1} = \frac{a^2b^2 + (a^2y^2 + b^2x^2)q}{a^2 + b^2 + (x - y)^2q} = \frac{1 + \left(\frac{x^2}{a^2} + \frac{y^2}{b^2}\right)q}{\frac{1}{a^2} + \frac{1}{b^2} + \frac{(x - y)^2}{a^2b^2}q}$$

$$\begin{aligned} P' &= P - M'Y = P - \{a^2 + b^2 + (x^2 - 2xy + y^2)q\}^{-1} Z^{-1}Z \{P(a^2 + b^2 + (x^2 - 2xy + y^2)q) - x(b^2 + (y^2 - xy)q) - y(a^2 + (x^2 - xy)q)\} \\ &= \{a^2 + b^2 + (x^2 - 2xy + y^2)q\}^{-1} \left(P\{[a^2 + b^2 + (x^2 - 2xy + y^2)q] - [a^2 + b^2 + (x^2 - 2xy + y^2)q]\} \right. \\ &\quad \left. + xb^2 + ya^2 + xq\{y^2 - x^2y + x^2y - xy^2\} \right) \\ &= \{a^2 + b^2 + (x^2 - 2xy + y^2)q\}^{-1} (x/a^2 + y/b^2)a^2b^2 \\ &= \{\Delta^2 d_1 + \Delta^2 d_2 + (d_1 - d_2)^2 \Delta^2 n / n^2\}^{-1} (d_1 / \Delta^2 d_1 + d_2 / \Delta^2 d_2) \Delta^2 d_1 \Delta^2 d_2 / n \\ &= \{Q + (d_1 - d_2)^2 \Delta^2 n / (n^2 \Delta^2 d_1 \Delta^2 d_2)\}^{-1} R / n \end{aligned}$$

$$\begin{aligned} Q &= \Delta^{-2} d_1 + \Delta^{-2} d_2 \\ R &= d_1 \Delta^{-2} d_1 + d_2 \Delta^{-2} d_2 \end{aligned}$$

PPP, continued (fit reduced data, usual method)

- After doing all the algebra, we find the result for P' & $\Delta^2 P'$

$$P' = \frac{\left(\frac{d_1}{\Delta^2 d_1} + \frac{d_2}{\Delta^2 d_2} \right)}{n \left(\frac{1}{\Delta^2 d_1} + \frac{1}{\Delta^2 d_2} \right) + n \frac{(d_2 - d_1)^2}{\Delta^2 d_1 \Delta^2 d_2} \Delta^2 n}$$

$$\Delta^2 P' = \frac{\left\{ \frac{1}{n^2} \left(\frac{1}{\Delta^2 d_1} + \frac{1}{\Delta^2 d_2} \right)^{-1} + \frac{1}{n^4} \left(\frac{d_1^2}{\Delta^2 d_1} + \frac{d_2^2}{\Delta^2 d_2} \right) \left(\frac{1}{\Delta^2 d_1} + \frac{1}{\Delta^2 d_2} \right)^{-1} \Delta^2 n \right\}}{\left\{ 1 + \frac{(d_2 - d_1)^2}{\Delta^2 d_1 \Delta^2 d_2} \left(\frac{1}{\Delta^2 d_1} + \frac{1}{\Delta^2 d_2} \right)^{-1} \frac{\Delta^2 n}{n^2} \right\}}$$

PPP, continued (fit reduced data, usual method)

- **Reproduce PPP's original numbers?**

- **Set $d_1 = 1.5$, $\Delta d_1 = 0.15$, $d_2 = 1.0$, $\Delta d_2 = 0.1$, $n = 1.0$, $\Delta n = 0.2$**

$$V = \begin{bmatrix} 0.15^2 + 1.5^2 0.2^2 & (1.5)(1.0)0.2^2 \\ (1.5)(1.0)0.2^2 & 0.10^2 + 1.0^2 0.2^2 \end{bmatrix} = \begin{bmatrix} 0.1125 & 0.06 \\ 0.06 & 0.05 \end{bmatrix}$$

$$P' = \frac{\left(\frac{1.5}{0.15^2} + \frac{1.0}{0.10^2} \right)}{1.0 \left(\frac{1}{0.15^2} + \frac{1}{0.10^2} \right) + \frac{(1.5-1.0)^2}{0.15^2 0.10^2} 0.20^2} = \frac{15}{17} = 0.8823529\dots$$

$$\Delta^2 P' = \frac{\left\{ \frac{1}{1.0^2} \left(\frac{1}{0.15^2} + \frac{1}{0.10^2} \right)^{-1} + \frac{1}{1.0^4} \left(\frac{1.5^2}{0.15^2} + \frac{1.0^2}{0.10^2} \right) \left(\frac{1}{0.15^2} + \frac{1}{0.10^2} \right)^{-1} 0.2^2 \right\}}{\left\{ 1 + \frac{(1.5-1.0)^2}{0.15^2 0.10^2} \left(\frac{1}{0.15^2} + \frac{1}{0.10^2} \right)^{-1} \frac{0.2^2}{1.0^2} \right\}} = (0.21828206\dots)^2$$

PPP, continued (fit reduced data, usual method)

- Result for P' is the same result as in the fit-to-raw-data case **only if $d_2 \rightarrow d_1$ or $\Delta^2 n \rightarrow 0$.**

$$P' = \frac{\left(\frac{d_1}{\Delta^2 d_1} + \frac{d_2}{\Delta^2 d_2} \right)}{n \left(\frac{1}{\Delta^2 d_1} + \frac{1}{\Delta^2 d_2} \right) + n \frac{(d_2 - d_1)^2}{\Delta^2 d_1 \Delta^2 d_2} \Delta^2 n}$$

PPP, continued (fit reduced data, usual method)

Result for M' $(\Delta P')$ ² is equal to Truth **only in the limit**
as $d_2 \rightarrow d_1$ or $\Delta^2 n \rightarrow 0$...

$$\Delta^2 P' = \frac{\left\{ \frac{1}{n^2} \left(\frac{1}{\Delta^2 d_1} + \frac{1}{\Delta^2 d_2} \right)^{-1} + \frac{1}{n^4} \left(\frac{d_1^2}{\Delta^2 d_1} + \frac{d_2^2}{\Delta^2 d_2} \right) \left(\frac{1}{\Delta^2 d_1} + \frac{1}{\Delta^2 d_2} \right)^{-1} \Delta^2 n \right\}}{\left\{ 1 + \frac{(d_2 - d_1)^2}{\Delta^2 d_1 \Delta^2 d_2} \left(\frac{1}{\Delta^2 d_1} + \frac{1}{\Delta^2 d_2} \right)^{-1} \frac{\Delta^2 n}{n^2} \right\}}$$
$$= \frac{a+b}{1+c} \Rightarrow a + (b - ac)$$

$$M' = \frac{1 + \left(\frac{x^2}{a^2} + \frac{y^2}{b^2} \right) q}{\frac{1}{a^2} + \frac{1}{b^2} + \frac{(x-y)^2}{a^2 b^2} q} \rightarrow \text{what?}$$

$$M' = \frac{F + G}{1 + H} \rightarrow F + G - FH$$

$$F = \frac{1}{\frac{1}{a^2} + \frac{1}{b^2}} \quad G = \left(\frac{x^2}{a^2} + \frac{y^2}{b^2} \right) qF \quad H = \frac{(x-y)^2}{a^2 b^2} qF$$

$$\begin{aligned} \Rightarrow G - FH &= Fq \left\{ \frac{x^2}{a^2} + \frac{y^2}{b^2} - \frac{(x-y)^2}{a^2 b^2} \frac{a^2 b^2}{a^2 + b^2} \right\} = Fq \left\{ x^2 b^2 (a^2 + b^2) + y^2 a^2 (a^2 + b^2) - (x-y)^2 a^2 b^2 \right\} \frac{1}{(a^2 + b^2) a^2 b^2} \\ &= Fq \left\{ x^2 (a^2 b^2 + b^4 - a^2 b^2) + y^2 (a^4 + a^2 b^2 - a^2 b^2) + 2xy a^2 b^2 \right\} \frac{1}{(a^2 + b^2) a^2 b^2} \\ &= Fq \left\{ x^2 b^4 + y^2 a^4 + 2xy a^2 b^2 \right\} \frac{1}{(a^2 + b^2) a^2 b^2} \\ &= Fq \left\{ \frac{x}{a^2} + \frac{y}{b^2} \right\}^2 \frac{a^2 b^2}{(a^2 + b^2)} = F^2 \left\{ \frac{x}{a^2} + \frac{y}{b^2} \right\}^2 q = \frac{P^2}{n^2} \Delta^2 n \end{aligned}$$

PPP, continued (fit reduced data, usual method)

In the limit...

$$\begin{aligned}\Delta^2 P' &\rightarrow \frac{1}{n^2} \left(\frac{1}{\Delta^2 d_1} + \frac{1}{\Delta^2 d_2} \right)^{-1} + \frac{1}{n^4} \left(\frac{d_1}{\Delta^2 d_1} + \frac{d_2}{\Delta^2 d_2} \right)^2 \left(\frac{1}{\Delta^2 d_1} + \frac{1}{\Delta^2 d_2} \right)^{-2} \Delta^2 n \\ &= \frac{1}{n^2} \left(\frac{1}{\Delta^2 d_1} + \frac{1}{\Delta^2 d_2} \right)^{-1} + \frac{P'^2}{n^2} \Delta^2 n\end{aligned}$$

PPP, continued (fit reduced data)

- So what's causing the problem? It's in the definition of V –

$$V = \begin{bmatrix} \frac{\Delta^2 d_1}{n^2} + \frac{d_1^2}{n^2} \frac{\Delta^2 n}{n^2} & \frac{d_1 d_2}{n^2} \frac{\Delta^2 n}{n^2} \\ \frac{d_1 d_2}{n^2} \frac{\Delta^2 n}{n^2} & \frac{\Delta^2 d_2}{n^2} + \frac{d_2^2}{n^2} \frac{\Delta^2 n}{n^2} \end{bmatrix}$$

Comes from linear expansion
valid only near $D = d_1/n$

Comes from linear expansion
valid only near $D = d_2/n$

PPP, continued (fit reduced data)

- **Solution? Expand around $D = P$.**

$$V = \begin{bmatrix} \frac{\Delta^2 d_1}{n^2} + P^2 \frac{\Delta^2 n}{n^2} & P^2 \frac{\Delta^2 n}{n^2} \\ P^2 \frac{\Delta^2 n}{n^2} & \frac{\Delta^2 d_2}{n^2} + P^2 \frac{\Delta^2 n}{n^2} \end{bmatrix}$$

- **In this case, results for P' and $\Delta P'$ are the same in the fit-to-raw-data case as in the fit-to-reduced-data**

$$[P'] = [P] - M'Y \quad Y = G'V^{-1} \begin{bmatrix} P - d_1/n \\ P - d_2/n \end{bmatrix} \quad G = \begin{bmatrix} 1 \\ 1 \end{bmatrix} \quad V = \begin{bmatrix} a^2 + P^2q & Pq \\ P^2q & b^2 + P^2q \end{bmatrix} \quad q = \Delta^2 n / n^2$$

$$\begin{aligned} a^2 &= \Delta^2 d_1 / n^2 \\ x &= d_1 / n \\ b^2 &= \Delta^2 d_2 / n^2 \\ y &= d_2 / n \end{aligned}$$

$$G'V^{-1} = \begin{bmatrix} 1 & 1 \end{bmatrix} \begin{bmatrix} b^2 + P^2q & -P^2q \\ -P^2q & a^2 + P^2q \end{bmatrix} Z = \begin{bmatrix} b^2 & a^2 \end{bmatrix} Z \quad Z = (a^2b^2 + (a^2 + b^2)P^2q)^{-1}$$

$$Y = G'V^{-1} \begin{bmatrix} P - d_1/n \\ P - d_2/n \end{bmatrix} = Z \begin{bmatrix} b^2 & a^2 \end{bmatrix} \begin{bmatrix} P - x \\ P - y \end{bmatrix} = Z [P(a^2 + b^2) - xb^2 - ya^2]$$

$$W = G'V^{-1}G = [a^2 + b^2]Z$$

$$M' = W^{-1} = [a^2 + b^2]^{-1} Z^{-1} = \frac{a^2b^2 + (a^2 + b^2)P^2q}{a^2 + b^2} = \frac{a^2b^2}{a^2 + b^2} + P^2q = \frac{1}{n^2} \left(\frac{1}{\Delta^2 d_1} + \frac{1}{\Delta^2 d_2} \right)^{-1} + P^2 \frac{\Delta^2 n}{n^2}$$

$$P' = P - M'Y = P - \{a^2 + b^2\}^{-1} Z^{-1} Z \{P(a^2 + b^2) - xb^2 - ya^2\} = P - P + \frac{xb^2 + ya^2}{(a^2 + b^2)} = \frac{\frac{x}{a^2} + \frac{y}{b^2}}{\frac{1}{a^2} + \frac{1}{b^2}} = \frac{1}{n} \frac{\frac{d_1}{\Delta^2 d_1} + \frac{d_2}{\Delta^2 d_2}}{\frac{1}{\Delta^2 d_1} + \frac{1}{\Delta^2 d_2}}$$

Results for fitting to reduced data with the correct data covariance matrix–

$$P' = \frac{\left(\frac{d_1}{\Delta^2 d_1} + \frac{d_2}{\Delta^2 d_2} \right)}{n \left(\frac{1}{\Delta^2 d_1} + \frac{1}{\Delta^2 d_2} \right)} = \frac{\left(\frac{1.5}{0.15^2} + \frac{1.0}{0.10^2} \right)}{1.0 \left(\frac{1}{0.15^2} + \frac{1}{0.10^2} \right)} = \frac{15}{13} = 1.153846\dots$$

$$\begin{aligned} \Delta^2 P' &= \frac{1}{n^2} \left(\frac{1}{\Delta^2 d_1} + \frac{1}{\Delta^2 d_2} \right)^{-1} + \frac{P'^2}{n^2} \Delta^2 n \\ &= \frac{1}{1.0} \left(\frac{1}{1.5^2} + \frac{1}{1.5^2} \right)^{-1} + \frac{\left(\frac{15}{13} \right)^2}{1.0^2} (0.2)^2 = (0.245311057\dots)^2 \end{aligned}$$

Practical application?

- **Years ago I added capability to use “implicit data covariance matrix” in SAMMY**
 - **First, using wrong V (the one derived from data D)**
 - **Runs kept misbehaving, numerical problems etc.**
 - **So switched from using D (measured data) in generating V , to using T (theoretical values)**
 - **Numerical problems disappeared.**
- **I got it right by accident!**

Observation and Question concerning this example

- **Observation**

- **When fitting reduced data, if systematic uncertainties are completely ignored, then**
 - **Parameter value P' is correct**
 - **Uncertainty $\Delta P'$ can be found by adding systematic uncertainty in quadrature**

- **Question**

- **Can this be generalized?**
 - **Multivariate?**
 - **Non-linear?**

O&Q

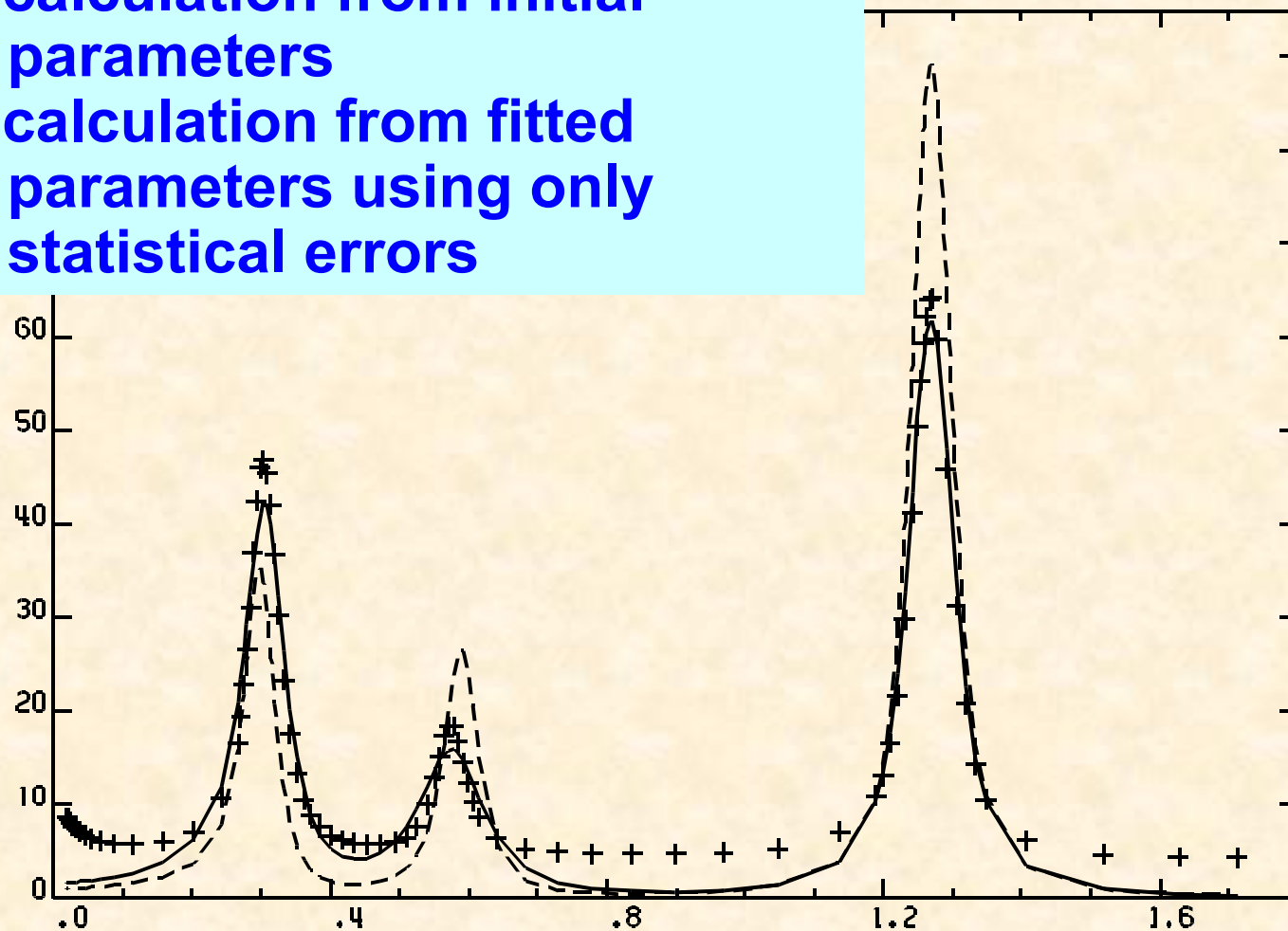
- **My expectation is “Not easily”**
 - **Example: R-matrix analysis of fission cross section with obviously-wrong background produces obviously-wrong resonance parameters ...**

^{241}Am fission cross section

cross = "experiment"

dash = calculation from initial parameters

solid = calculation from fitted parameters using only statistical errors



(end of PPP
discussion)

Topics to be ~~covered~~ touched on

- **Peelle's Pertinent Puzzle/Paradox**
- **Implicit data covariance (IDC) methodology**
- **Transformation of variables**

Implicit Data Covariance Method

Complete data covariance matrix is

$$V = v + X Q X^t$$

where

- **V is the data covariance**
- **v represents the statistical uncertainties**
- **X is the sensitivity matrix (partial derivative of data with respect to data-reduction parameters) [evaluated at current values of fitting parameters to avoid PPP-type difficulties]**
- **Q is the covariance matrix for the data-reduction parameters**

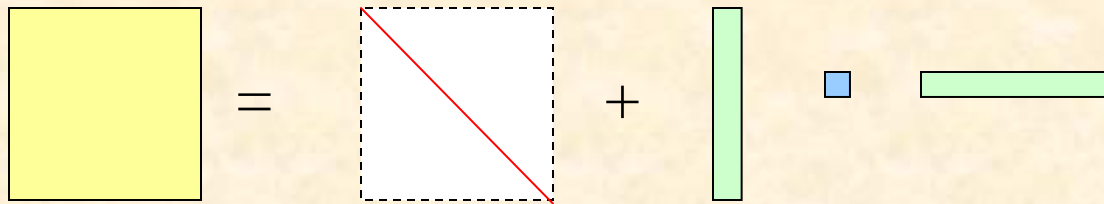
(what are these data reduction parameters?)

- **used for describing experimental conditions**
 - normalization, background
 - burst width
 - isotopic abundance
 - etc.

- **can be used in two ways**
 - **used to generate data covariance matrix**
 - **included as varied parameters in fitting procedure**
 - mathematically equivalent to using data-covariance matrix
 - numerically more stable
 - **bonus: values of data-reduction parameters are updated**

Data Covariance Matrix, symbolically

$$V = v + X Q X^t$$

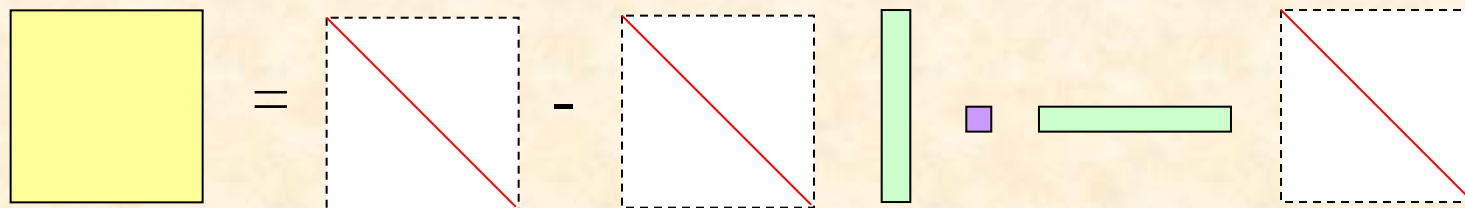


where

- size of box may be considered to be logarithmic
 - large ~ thousands (or 10 K or 100 K)
 - small ~ very few (5? 10?)
- dashed box with diagonal line indicates diagonal matrix
- solid box indicates non-diagonal matrix

Inverse of Data Covariance Matrix, symbolically

$$\begin{aligned}
 \mathbf{V}^{-1} &= (\mathbf{v} + \mathbf{X} \mathbf{Q} \mathbf{X}^t)^{-1} \\
 &= \mathbf{v}^{-1} - \mathbf{v}^{-1} \mathbf{X} (\mathbf{Q}^{-1} + \mathbf{X}^t \mathbf{v}^{-1} \mathbf{X})^{-1} \mathbf{X}^t \mathbf{v}^{-1} \\
 &= \mathbf{v}^{-1} - \mathbf{v}^{-1} \mathbf{X} \mathbf{Z}^{-1} \mathbf{X}^t \mathbf{v}^{-1}
 \end{aligned}$$



where

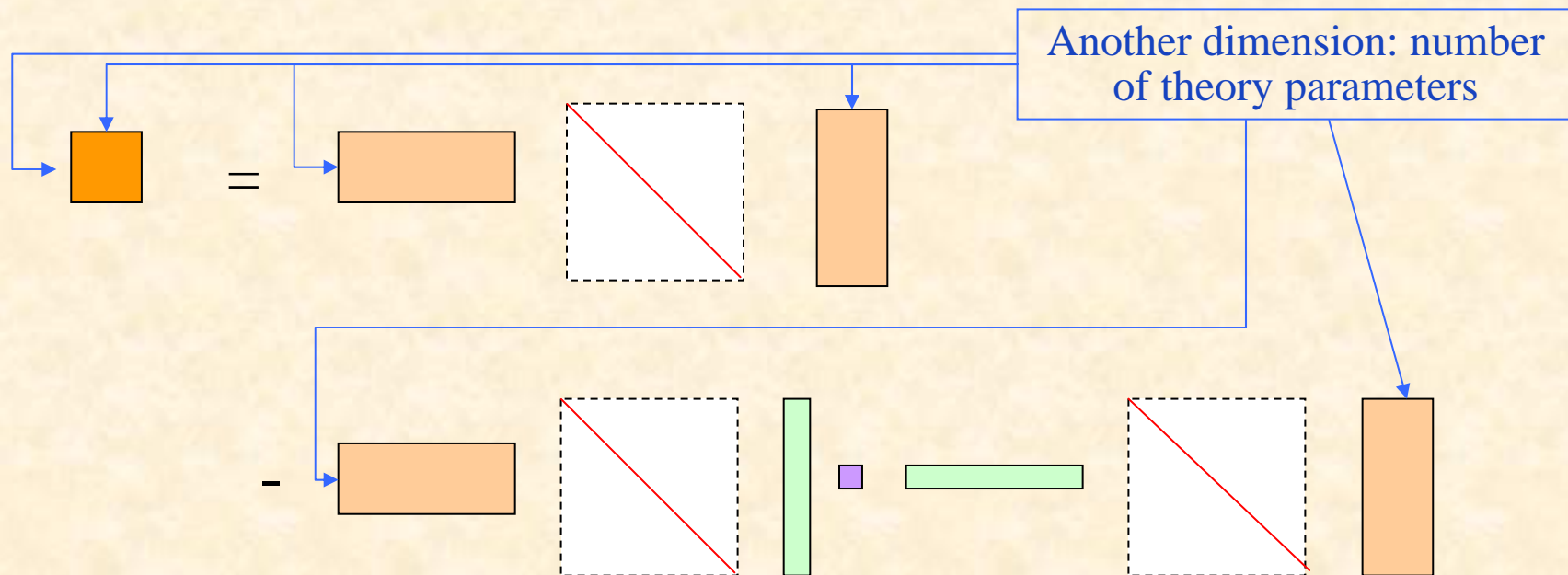
$$\mathbf{Z} = \mathbf{Q}^{-1} + \mathbf{X}^t \mathbf{v}^{-1} \mathbf{X}$$

The diagram illustrates the definition of \mathbf{Z} . It shows a purple square representing \mathbf{Z} on the left. This is followed by an equals sign and a sequence of terms: a blue square representing \mathbf{Q}^{-1} , a plus sign, a horizontal green bar representing $\mathbf{X}^t \mathbf{v}^{-1} \mathbf{X}$, a dashed square with a red diagonal representing \mathbf{Q}^{-1} , and a vertical green bar representing $\mathbf{X}^t \mathbf{v}^{-1} \mathbf{X}$.

Quantities needed in Bayes' equations: W

$$W = G^t V^{-1} G$$

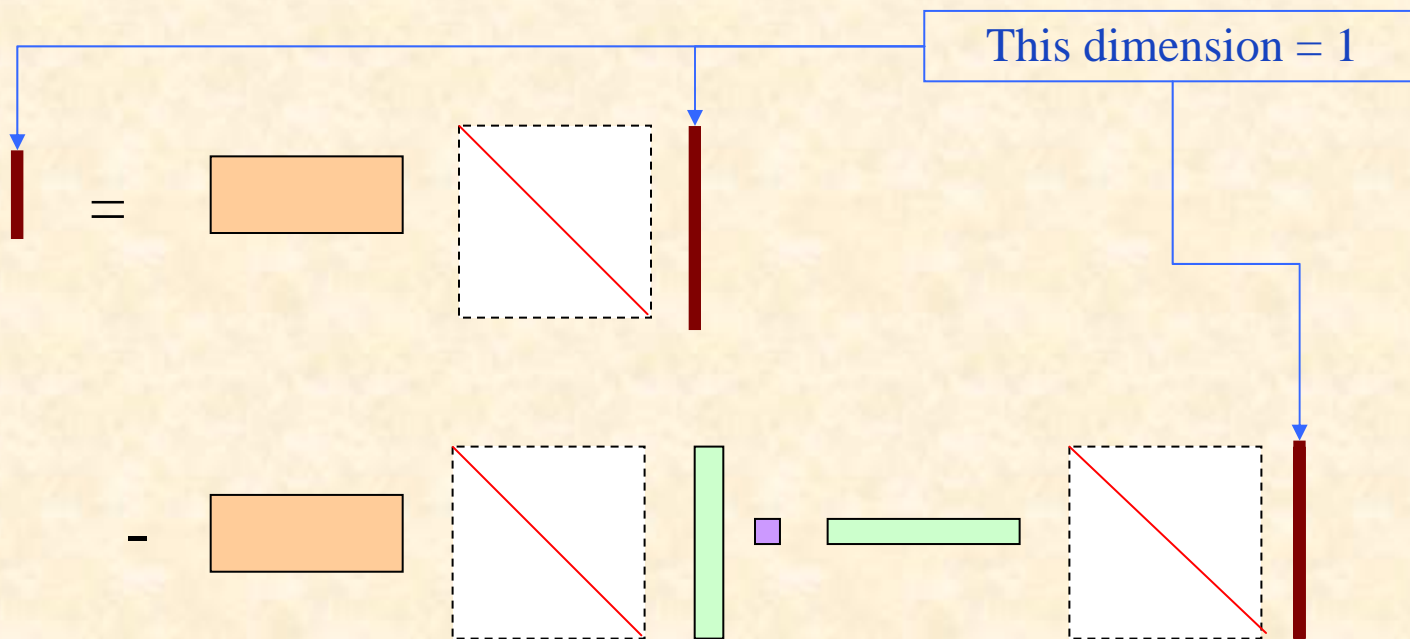
$$= G^t v^{-1} G - G^t v^{-1} X Z^{-1} X^t v^{-1} G$$



Quantities needed in Bayes' equations: Y

$$Y = G^t V^{-1} (D - T)$$

$$= G^t v^{-1} (D - T) - G^t v^{-1} X Z^{-1} X^t v^{-1} (D - T)$$



Why bother with all these arrays?

Matrices in W and Y are easier to invert than V –

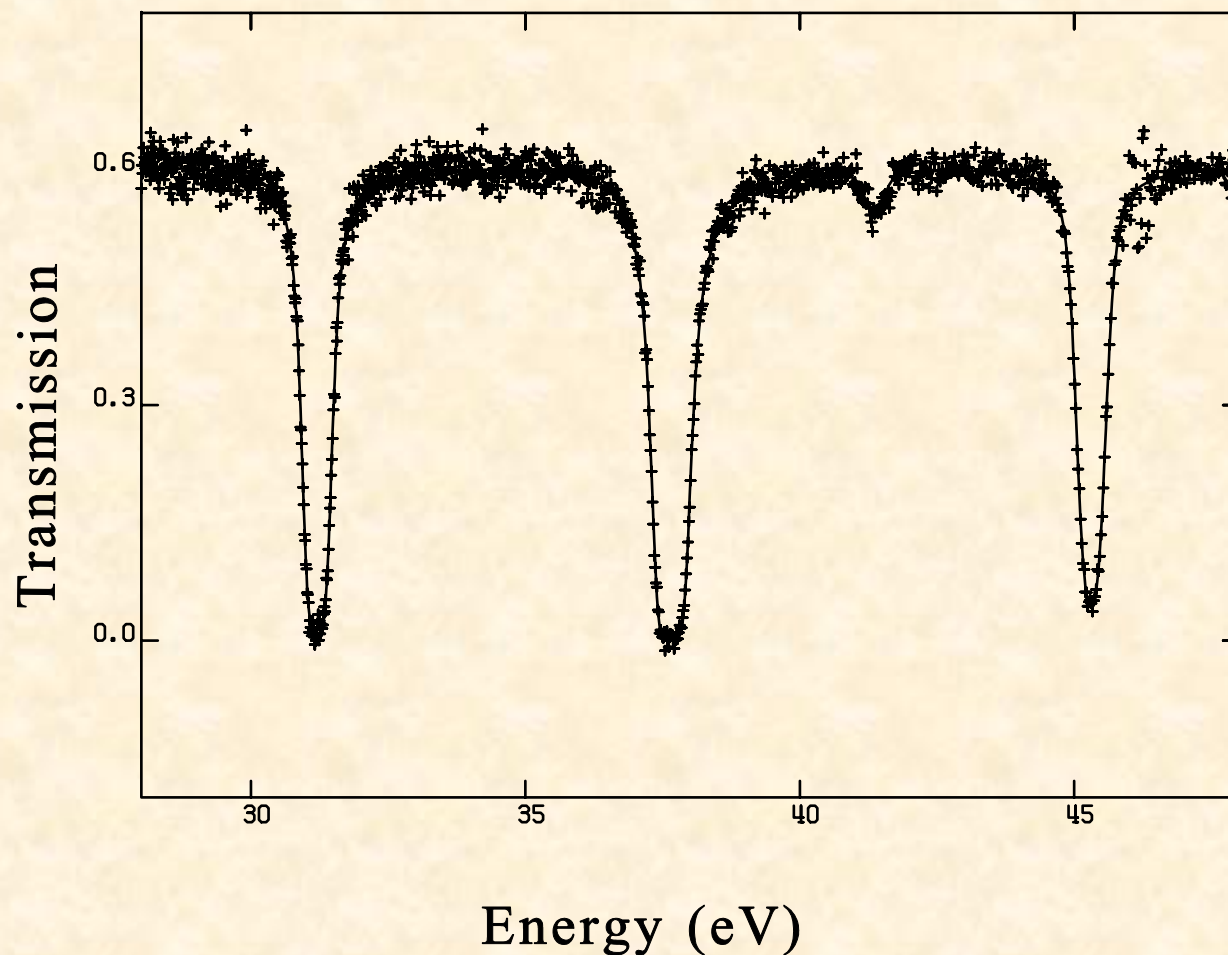
- v is large but **diagonal**
 - (size ~ thousands of data points)
 - Q is **small** and often diagonal
 - (size ~ tens of data-reduction parameters)
 - Z is off-diagonal but **small**
 - (size ~ tens)
- which leads to savings in**
- computation **time** (never calculate V or V^{-1})
 - computer **memory** (never store V or V^{-1})
 - numerical **accuracy** and stability (fewer round-off problems)

In SAMMY, implicit data covariance (IDC) matrices can be used for

- normalization
- background correction factors
- user-supplied implicit data covariance new
 - external code can be used to generate pieces (X and Q)

Example from SAMMY Test Case tr140: ^{129}I transmission data

Geel data
provided
by Gilles
Noguere,
Cadarache



Example, continued

1245 experimental data points;

[full data set has 32660 data points]

9 data-reduction parameters;

655 resonances; 9 varied parameters

Description of data covariance treatment for this run	Cpu time for Bayes solver (sec)	Total cpu time (sec)	Array size
a only statistical errors	0.03	14	254 K
b statistical plus systematic, only on diagonal	0.03	14	254 K
c explicit data cov matrix	16.46	59	1800 K
d IDC matrix	0.06	14	267 K

Note: c & d give essentially the same results

For more on covariance matrices and IDC –

“Practical Alternatives to Explicitly Generating and Inverting Data Covariance Matrices”

N. M. Larson

*Nuclear Mathematical and Computational Sciences:
A Century in Review, A Century Anew*

Gatlinburg, Tennessee, April 6-11, 2003

On CD-ROM

American Nuclear Society, LaGrange Park, IL (2003)

Suppose we want to make use of uncertainties for non-varied parameters ?

(e.g., resolution-function parameters)

Add a third option for parameter flag in SAMMY:

- 0 = do not vary
- 1 = vary
- 3 = calculate partial derivatives, propagate uncertainties
 - to be treated in similar fashion to IDC

current SAMMY options

to be implemented soon

(end of IDC discussion)

Topics to be ~~covered~~ touched on

- **Peelle's Pertinent Puzzle/Paradox**
- **Implicit data covariance (IDC) methodology**
- **Transformation of variables**

Transformation of variables

- **Least-squares equations (and/or Bayes' equations) are based on the implicit assumption that the parameters obey Gaussian statistics.**
- **Transformation (via *log*, or *sqrt*, or whatever) will introduce a new variable which obeys another statistic.**
- **Results obtained with the new variable will therefore be different from results obtained with the original.**
- **Which result is “correct” depends at least in part on which variable obeys the appropriate (Gaussian) statistic.**

Transformation of variables

- **Least-squares equations (and/or Bayes' equations) are based on the implicit assumption that the parameters obey Gaussian statistics.**
- **Transformation (via *log*, or *sqrt*, or whatever) will introduce a new variable which obeys another statistic.**
- **Results obtained with the new variable will therefore be different from results obtained with the original.**
- **Which result is “correct” depends at least in part on which variable obeys the appropriate (Gaussian) statistic.**

THE END

The End

On the equivalence of using the normalization as a fitting parameter, vs. generating the off-diagonal data covariance matrix

Nancy Larson

Afterthoughts on the Second Research Coordination Meeting on Improvement of the Standard Cross Sections for Light Elements

**13-17 October 2003
NIST, Gaithersburg, MD, USA**

Hypothesis:

- **Assuming Bayes' Equations (and Least-Squares) are correct for the types of parameters being considered, the following two procedures are effectively identical:**
 - **Generate the off-diagonal data covariance matrix by using the measured uncertainty on the normalization for the systematic portion**
 - **Treat the normalization as a fitting parameter with the measured uncertainty squared taken for the prior variance**

Definitions of terms:

- **P = theory parameters**
 - (R-matrix widths etc)
- **n = normalization**
- **D = experimental cross section**
- **d = measured quantity**
 - $D = d/n$
- **T = theory corresponding to cross section**
- **t = theory corresponding to measured quantity**
 - $T = t/n$

Definitions of terms, continued:

- Initial (measured) uncertainty on n is Δn .
 - For simplicity, set $N = \Delta^2 n$
- Initial uncertainty on parameters P is zero
- Covariance matrix for d is v .
 - Presumably, v is diagonal.
- g = partial derivative of theory t with respect to theory parameters P
- G = partial derivative of theory T with respect to theory parameters P
 - $G = g/n$
- Partial derivative of theory t with respect to normalization n is T
 - $t = nT \rightarrow \partial t / \partial n = T$

Bayes' Equations, in general:

$$\mathcal{P}' = \mathcal{P} + \mathcal{M}'\mathcal{Y} \quad \mathcal{M}' = (\mathcal{M}^{-1} + \mathcal{W})^{-1}$$

$$\mathcal{Y} = \mathcal{G}^t \mathcal{V}^{-1}(\mathcal{D} - \mathcal{T}) \quad \mathcal{W} = \mathcal{G}^t \mathcal{V}^{-1} \mathcal{G}$$

where \mathcal{P} represents all parameters, \mathcal{M} the full covariance matrix for all parameters, \mathcal{D} the measured data, \mathcal{T} the corresponding theoretical calculation, \mathcal{G} the partial derivative of \mathcal{T} with respect to \mathcal{P} , and \mathcal{V} the data covariance matrix. Primes represent updated values for \mathcal{P} and \mathcal{M} . (Superscript t indicates matrix transpose.)

Note that these equations define \mathcal{Y} and \mathcal{W} .

Equations for first method (off-diagonal data covariance matrix):

- In Bayes' equations on page 5, substitute

$\mathcal{P} \rightarrow \mathbf{P}$, $\mathcal{M} \rightarrow \mathbf{M}$, $\mathcal{D} \rightarrow \mathbf{D}$, $\mathcal{T} \rightarrow \mathbf{T}$, $\mathcal{G} \rightarrow \mathbf{G}$, $\mathcal{V} \rightarrow \mathbf{V}$ where \mathbf{V} is given by

$$V_{ij} = \frac{v_i \delta_{ij}}{n^2} + \frac{d_i d_j}{n^2} \frac{\Delta^2 n}{n^2} = \frac{v_i \delta_{ij}}{n^2} + \mathbf{D}_i \mathbf{D}_j \frac{\Delta^2 n}{n^2}$$

- Also note that M is infinite. Bayes' Equations therefore become

$$\mathcal{P}' \rightarrow \mathbf{P}' = \mathbf{P} + \mathbf{M}' \mathbf{Y} \quad \mathcal{M}' \rightarrow \mathbf{M}' = (\mathbf{0} + \mathbf{W})^{-1}$$

$$\mathcal{Y} \rightarrow \mathbf{Y} = \mathbf{G}^t \mathbf{V}^{-1} (\mathbf{D} - \mathbf{T}) \quad \mathcal{W} \rightarrow \mathbf{W} = \mathbf{G}^t \mathbf{V}^{-1} \mathbf{G}$$

Equations for the second method (normalization = fitting parameter):

- In Bayes' equations on page 5, substitute

$\mathcal{D} = d = nD$ and $\mathcal{T} = t = nT$, and $\mathcal{V} = v$. Also

$$\mathcal{P} = \begin{bmatrix} \mathbf{P} \\ \mathbf{n} \end{bmatrix} \quad \mathcal{M} = \begin{bmatrix} \infty & \mathbf{0} \\ \mathbf{0} & \Delta^2 \mathbf{n} \end{bmatrix} \quad \mathcal{G} = \begin{bmatrix} n\mathbf{G} & \mathbf{T} \end{bmatrix}$$

Note that the inverse of \mathcal{M} is $\mathcal{M}^{-1} = \begin{bmatrix} \mathbf{0} & \mathbf{0} \\ \mathbf{0} & \Delta^{-2} \mathbf{n} \end{bmatrix}$

Equations for the second method, continued:

$\mathcal{W} = \mathcal{G}^t \mathcal{V}^{-1} \mathcal{G}$ is therefore found from

$$\mathcal{G}^t \mathcal{V}^{-1} = \begin{bmatrix} n\mathbf{G}^t \mathbf{v}^{-1} \\ \mathbf{T}^t \mathbf{v}^{-1} \end{bmatrix}; \quad \mathcal{G}^t \mathcal{V}^{-1} \mathcal{G} = \begin{bmatrix} n\mathbf{G}^t \mathbf{v}^{-1} \mathbf{G} \mathbf{n} & n\mathbf{G}^t \mathbf{v}^{-1} \mathbf{T} \\ \mathbf{T}^t \mathbf{v}^{-1} \mathbf{G} \mathbf{n} & \mathbf{T}^t \mathbf{v}^{-1} \mathbf{T} \end{bmatrix}$$

So that $(\mathcal{M}')^{-1}$ becomes

$$(\mathcal{M}')^{-1} = \mathcal{G}^t \mathcal{V}^{-1} \mathcal{G} + \mathcal{M} = \begin{bmatrix} n\mathbf{G}^t \mathbf{v}^{-1} \mathbf{G} \mathbf{n} & n\mathbf{G}^t \mathbf{v}^{-1} \mathbf{T} \\ \mathbf{T}^t \mathbf{v}^{-1} \mathbf{G} \mathbf{n} & \mathbf{T}^t \mathbf{v}^{-1} \mathbf{T} + \Delta^{-2} \mathbf{n} \end{bmatrix}$$

Is second method equivalent to first?

\mathcal{M}' is found by inverting that equation. For arbitrary X (in particular for $X = (\mathcal{M}')^{-1}$) we find

$$X = \begin{bmatrix} A & C^t \\ C & B \end{bmatrix} \Rightarrow X^{-1} = \begin{bmatrix} (A - C^t B^{-1} C)^{-1} & -(A - C^t B^{-1} C)^{-1} C^t B^{-1} \\ -(B - C A^{-1} C^t)^{-1} C A^{-1} & (B - C A^{-1} C^t)^{-1} \end{bmatrix}$$

Check:
$$\begin{bmatrix} (A - C^t B^{-1} C)^{-1} & -(A - C^t B^{-1} C)^{-1} C^t B^{-1} \\ -(B - C A^{-1} C^t)^{-1} C A^{-1} & (B - C A^{-1} C^t)^{-1} \end{bmatrix} \begin{bmatrix} A & C^t \\ C & B \end{bmatrix}$$
$$= \begin{bmatrix} (A - C^t B^{-1} C)^{-1} (A - C^t B^{-1} C) & (A - C^t B^{-1} C)^{-1} (C^t - C^t B^{-1} B) \\ (B - C A^{-1} C^t)^{-1} (-C A^{-1} A + C) & (B - C A^{-1} C^t)^{-1} (-C A^{-1} C^t + B) \end{bmatrix} = \begin{bmatrix} 1 & 0 \\ 0 & 1 \end{bmatrix}$$

#2 =? #1, cont.

A little more algebra, just to be sure we know what we're doing –

$$\begin{aligned}(A - C^t B^{-1} C)^{-1} C^t B^{-1} &= ? = A^{-1} C^t (B - C A^{-1} C^t)^{-1} \\(A - C^t B^{-1} C)^{-1} C^t B^{-1} &= (A - C^t B^{-1} C)^{-1} C^t B^{-1} (B - C A^{-1} C^t) (B - C A^{-1} C^t)^{-1} \\&= (A - C^t B^{-1} C)^{-1} C^t B^{-1} B (B - C A^{-1} C^t)^{-1} - (A - C^t B^{-1} C)^{-1} C^t B^{-1} (C A^{-1} C^t) (B - C A^{-1} C^t)^{-1} \\&= (A - C^t B^{-1} C)^{-1} C^t (B - C A^{-1} C^t)^{-1} + (A - C^t B^{-1} C)^{-1} (-C^t B^{-1} C) A^{-1} C^t (B - C A^{-1} C^t)^{-1} \\&= (A - C^t B^{-1} C)^{-1} C^t (B - C A^{-1} C^t)^{-1} + (A - C^t B^{-1} C)^{-1} (A - C^t B^{-1} C - A) A^{-1} C^t (B - C A^{-1} C^t)^{-1} \\&= (A - C^t B^{-1} C)^{-1} C^t (B - C A^{-1} C^t)^{-1} + (A - C^t B^{-1} C)^{-1} (A - C^t B^{-1} C) A^{-1} C^t (B - C A^{-1} C^t)^{-1} \\&\quad + (A - C^t B^{-1} C)^{-1} (-A) A^{-1} C^t (B - C A^{-1} C^t)^{-1} \\&= (A - C^t B^{-1} C)^{-1} C^t (B - C A^{-1} C^t)^{-1} + A^{-1} C^t (B - C A^{-1} C^t)^{-1} + (A - C^t B^{-1} C)^{-1} C^t (B - C A^{-1} C^t)^{-1} \\&= A^{-1} C^t (B - C A^{-1} C^t)^{-1}\end{aligned}$$

#2 =? #1, cont.

Substituting from page 8 for $X = (\mathcal{M}')^{-1}$, we find that the first term in $X^{-1} = \mathcal{M}'$ has the form

$$\begin{aligned} A - C^t B^{-1} C &= nG^t v^{-1} Gn - nG^t v^{-1} T (T^t v^{-1} T + \Delta^{-2} n)^{-1} T^t v^{-1} Gn \\ &= nG^t \left\{ v^{-1} - v^{-1} T (T^t v^{-1} T + \Delta^{-2} n)^{-1} T^t v^{-1} \right\} Gn \\ &= nG^t \left(v + T \Delta^2 n T^t \right)^{-1} Gn \end{aligned}$$

#2 =? #1, cont.

Testing to be sure we believe that last line...

$$\begin{aligned} & v^{-1} - v^{-1}T(T^t v^{-1}T + Q^{-1})^{-1}T^t v^{-1} \\ &= v^{-1} - v^{-1}T(T^t v^{-1}T + Q^{-1})^{-1}T^t v^{-1}(TQT^t + v)(TQT^t + v)^{-1} \\ &= v^{-1} - v^{-1}T(T^t v^{-1}T + Q^{-1})^{-1}(T^t v^{-1}TQT^t + T^t v^{-1}v)(TQT^t + v)^{-1} \\ &= v^{-1} - v^{-1}T(T^t v^{-1}T + Q^{-1})^{-1}((T^t v^{-1}T + Q^{-1} - Q^{-1})QT^t + T^t)(TQT^t + v)^{-1} \\ &= v^{-1} - v^{-1}T(T^t v^{-1}T + Q^{-1})^{-1}((T^t v^{-1}T + Q^{-1})QT^t - Q^{-1}QT^t + T^t)(TQT^t + v)^{-1} \\ &= v^{-1} - v^{-1}T(T^t v^{-1}T + Q^{-1})^{-1}(T^t v^{-1}T + Q^{-1})QT^t(TQT^t + v)^{-1} \\ &= v^{-1} - v^{-1}TQT^t(TQT^t + v)^{-1} \\ &= v^{-1} - v^{-1}(TQT^t + v - v)(TQT^t + v)^{-1} \\ &= v^{-1} - v^{-1}(TQT^t + v)(TQT^t + v)^{-1} + v^{-1}v(TQT^t + v)^{-1} \\ &= v^{-1} - v^{-1} + (TQT^t + v)^{-1} \\ &= (TQT^t + v)^{-1} \end{aligned}$$

QED

#2 =? #1, cont.

Continuing from page 11. Define F via $F = v + T \Delta^2 n T^t$

Then $A - C^t B^{-1} C = n G^t \left(v + T \Delta^2 n T^t \right)^{-1} G n = n G^t F^{-1} G n$

Similarly define S via $S = \Delta^2 n + n G v G^t n$

Then $B - C A^{-1} C^t = T^t \left(\Delta^2 n + n G v G^t n \right)^{-1} T = T^t S^{-1} T$

Also, since $B = T^t v^{-1} T + \Delta^{-2} n$

Then $B^{-1} = \Delta^2 n - \Delta^2 n T^t F^{-1} T \Delta^2 n$

#2 =? #1, cont.

- Making all these substitutions into equation for X^{-1} on page 9 gives this for \mathcal{M}' :

$$\mathcal{M}' = \begin{bmatrix} (nG^t F^{-1} Gn)^{-1} & - (nG^t F^{-1} Gn)^{-1} nG^t T (\Delta^2 n - \Delta^2 n T^t F^{-1} T \Delta^2 n) \\ - (T^t S^{-1} T)^{-1} T^t v^{-1} Gn (nG^t F^{-1} Gn)^{-1} & (T^t S^{-1} T)^{-1} \end{bmatrix}$$

#2 =? #1, cont.

- Similarly, for $\mathcal{Y} = \mathcal{G}^t \mathcal{V}^{-1} (\mathcal{D}-\mathcal{T})$ we find $\mathcal{Y} = \begin{bmatrix} nG^t v^{-1} (d-t) \\ T^t v^{-1} (d-t) \end{bmatrix}$

which leads to

$$\begin{bmatrix} P'-P \\ n'-n \end{bmatrix} = \begin{bmatrix} (nG^t F^{-1} Gn)^{-1} nG^t v^{-1} (d-t) - (nG^t F^{-1} Gn)^{-1} nG^t v^{-1} T (\Delta^2 n - \Delta^2 n T^t F^{-1} T \Delta^2 n) T^t v^{-1} (d-t) \\ -(T^t S^{-1} T)^{-1} T^t v^{-1} Gn (nG^t F^{-1} Gn)^{-1} nG^t v^{-1} (d-t) + (T^t S^{-1} T)^{-1} T^t v^{-1} (d-t) \end{bmatrix}$$

$$= \begin{bmatrix} (nG^t F^{-1} Gn)^{-1} nG^t v^{-1} \{ 1 - T (\Delta^2 n - \Delta^2 n T^t F^{-1} T \Delta^2 n) T^t v^{-1} \} (d-t) \\ (T^t S^{-1} T)^{-1} T^t v^{-1} \{ -Gn (nG^t F^{-1} Gn)^{-1} nG^t v^{-1} + 1 \} (d-t) \end{bmatrix}$$

#2 =? #1, cont.

- **Rewriting**

$$\begin{aligned} \begin{bmatrix} P'-P \\ n'-n \end{bmatrix} &= \begin{bmatrix} (nG^t F^{-1} Gn)^{-1} nG^t v^{-1} \{v - T\Delta^2 nT^t + T\Delta^2 n T^t F^{-1} T\Delta^2 nT^t\} v^{-1} (d-t) \\ (T^t S^{-1} T)^{-1} T^t v^{-1} \{-Gn(nG^t F^{-1} Gn)^{-1} nG^t + v\} v^{-1} (d-t) \end{bmatrix} \\ &= \begin{bmatrix} (nG^t F^{-1} Gn)^{-1} nG^t v^{-1} \{v - T\Delta^2 nT^t + T\Delta^2 n T^t F^{-1} (T\Delta^2 nT^t + v - v)\} v^{-1} (d-t) \\ (T^t S^{-1} T)^{-1} T^t v^{-1} \{-Gn(nG^t F^{-1} Gn)^{-1} nG^t v^{-1} + 1\} (d-t) \end{bmatrix} \\ &= \begin{bmatrix} (nG^t F^{-1} Gn)^{-1} nG^t v^{-1} \{v - T\Delta^2 nT^t + T\Delta^2 n T^t F^{-1} (F - v)\} v^{-1} (d-t) \\ (T^t S^{-1} T)^{-1} T^t v^{-1} \{-Gn(nG^t F^{-1} Gn)^{-1} nG^t v^{-1} (GnZnG^t)(GnZnG^t)^{-1} + 1\} (d-t) \end{bmatrix} \end{aligned}$$

where Z is essentially arbitrary

#2 =? #1, cont.

- More arithmetic ...

$$\begin{aligned}
 \begin{bmatrix} P'-P \\ n'-n \end{bmatrix} &= \begin{bmatrix} (nG^t F^{-1} Gn)^{-1} nG^t v^{-1} \{v - T\Delta^2 n T^t + T\Delta^2 n T^t - T\Delta^2 n T^t F^{-1} v\} v^{-1} (d-t) \\ (T^t S^{-1} T)^{-1} T^t v^{-1} \left\{ -Gn(nG^t F^{-1} Gn)^{-1} (nG^t v^{-1} Gn) ZnG^t (GnZnG^t)^{-1} + 1 \right\} (d-t) \end{bmatrix} \\
 &= \begin{bmatrix} (nG^t F^{-1} Gn)^{-1} nG^t v^{-1} \{v - (T\Delta^2 n T^t + v - v)F^{-1} v\} v^{-1} (d-t) \\ (T^t S^{-1} T)^{-1} T^t v^{-1} \left\{ -GnZnG^t (GnZnG^t)^{-1} + 1 \right\} (d-t) \end{bmatrix} \\
 &= \begin{bmatrix} (nG^t F^{-1} Gn)^{-1} nG^t v^{-1} \{v - (F - v)F^{-1} v\} v^{-1} (d-t) \\ (T^t S^{-1} T)^{-1} T^t v^{-1} \{-1 + 1\} (d-t) \end{bmatrix} \\
 &= \begin{bmatrix} (nG^t F^{-1} Gn)^{-1} nG^t v^{-1} \{v - v + vF^{-1} v\} v^{-1} (d-t) \\ (T^t S^{-1} T)^{-1} T^t v^{-1} \{-1 + 1\} (d-t) \end{bmatrix} = \begin{bmatrix} (nG^t F^{-1} Gn)^{-1} nG^t F^{-1} (d-t) \\ 0 \end{bmatrix}
 \end{aligned}$$

#2 =? #1, cont.

- Consider now the results for P' and the associated covariance matrix (which we'll call m')...

$$P' - P = m' n G^t F^{-1} (d - t) \quad \text{with} \quad m' = \left(n G^t F^{-1} G n \right)^{-1}$$

- Remember that F is given by $F = v + T \Delta^2 n T^t$
- Define $U = F/n^2$. Note that U is similar to V of Method 1 (see page 6):

$$U_{ij} = \frac{v_i \delta_{ij}}{n^2} + T_i T_j \frac{\Delta^2 n}{n^2} \quad \text{and} \quad V_{ij} = \frac{v_i \delta_{ij}}{n^2} + D_i D_j \frac{\Delta^2 n}{n^2}$$

#2 =? #1, cont.

- **Rearranging the equations for P' and m' gives**

$$P' - P = m' G^t n F^{-1} n \begin{pmatrix} d \\ n \end{pmatrix} - \frac{t}{n} \quad \text{and} \quad m' = \left(G^t n F^{-1} n G \right)^{-1}; \quad \text{or}$$

$$P' - P = m' G^t U^{-1} (D - T) \quad \text{and} \quad m' = \left(G^t U G \right)^{-1}$$

- **Conclusion? Method #2 = Method # 1 only if $D = T$.**

Conclusion:

- **Assuming Bayes' Equations (and Least-Squares) are correct for the types of parameters being considered, these two procedures are almost identical:**
 - **Generate the off-diagonal data covariance matrix by using the measured uncertainty on the normalization for the systematic portion**
 - **Treat the normalization as a fitting parameter with the measured uncertainty squared taken for the prior variance**

Conclusion:

- **Assuming Bayes' Equations (and Least-Squares) are correct for the types of parameters being considered, these two procedures are exactly identical:**
 - **Generate the off-diagonal data covariance matrix by using the measured uncertainty on the normalization for the systematic portion, taking care to use the theoretical cross section, not the measured data, in generating the systematic portion**
 - **Treat the normalization as a fitting parameter with the measured uncertainty squared taken for the prior variance**

The End

Progress Report on analysis of ^7Li system with RAC

CHEN Zhenpeng SUN Yeying
Tsinghua University, Beijing 100084, China;
(2003/12/13)

The analysis of ^7Li system has been done with RAC. In this simultaneous analysis the most of 'good' data about ^7Li compound system have been included. The evaluated cross section of ^6Li (n, t) ^4He seems good. The standard deviation (STD(%)) of ^6Li (n, t) ^4He seems reasonable.

1. Data base

The experimental data involve all open reaction channels and reaction types in the energy range considered for ^7Li system. The reaction channels are (n, ^6Li) and (t, α); the data types include neutron total cross section σ_t , all kinds of integral reaction cross section and differential cross section, polarization of elastic scattering particle.

The data-base used is shown in Table 1. The most of integrated cross sections are taken from the original GMA-data base. The different cross sections are taken from EXFOR or EDA-data base. The total data points is 2734.

Table 1 Information of data-base used in RAC fit

Reaction	Norm. Fac.		Chi Square		
$^6\text{Li}+\text{n}$, (total)					
'NTOTgoul'	0.990000	' ' 2.000	1.000	0.276	
'NTOTguen'	1.000000	' ' 2.000	1.200	1.623	
'NTOTmead'	1.000000	' ' 2.000	1.000	0.554	
'NTOThar1'	1.000000	' ' 2.000	2.000	4.724	
'NTOTkmit'	1.000000	' ' 2.000	2.200	6.698	
'NTOTtutly'	1.000000	' ' 2.000	1.000	1.000	
^6Li (n, n) ^6Li					
'NNCSkmit'	1.020000	' ' 2.000	1.100	1.302	integrated
'NNDAlan1'	1.020000	' ' 2.000	3.500	4.930	Dif.
'NNDAlan2'	1.020000	' ' 2.000	2.000	0.495	Dif.
'NNDAsmit'	1.010000	' ' 2.000	2.500	1.614	Dif.
'NNAYlane'	1.000000	' ' 2.000	5.500	6.603	polarization
^6Li (n, t) ^4He					
'NTCSmead'	1.000000	' ' 2.000	1.000	0.118	
'NTCSslem'	1.010000	' ' 2.000	1.000	0.815	
'NTCSslen'	1.000000	' ' 2.000	1.000	0.709	
'NTCScoat'	1.010000	' ' 2.000	1.000	0.632	
'NTCSren1'	1.000000	' ' 2.000	1.000	1.062	
'NTCSren2'	1.000000	' ' 2.000	1.000	0.033	
'NTCSlama'	1.000000	' ' 2.000	1.000	0.789	
'NTCSfor1'	1.009000	' ' 2.000	1.000	0.530	
'NTCSfor2'	1.014000	' ' 2.000	1.000	1.030	
'NTCSfor3'	0.980000	' ' 2.000	1.400	1.927	
'NTCSfor4'	1.000000	' ' 2.000	1.000	0.550	
'NTCSpoen'	0.988000	' ' 2.000	1.300	1.675	
'NTCSgayt'	0.970000	' ' 2.000	2.200	5.621	
'NTDAover'	0.980000	' ' 2.000	4.633	1.010	Dif.
'NTDAove1'	0.980000	' ' 2.000	4.042	1.036	Dif.
'NTDAbrow'	1.000000	' ' 2.000	6.708	1.702	Dif.

'NTDAknox'	1.000000	' ' 2.000	2.026	1.000	Dif.
${}^6\text{Li}(\text{n}, \text{t}) / {}^{10}\text{B}(\text{n}, \alpha 0)$ or ${}^6\text{Li}(\text{n}, \text{t}) / {}^{10}\text{B}(\text{n}, \alpha 1)$					
'RLI-Bso2'	1.000000	'F' 2.000	1.000	0.462	
'RLI-Bso1'	1.000000	'F' 2.000	1.000	0.195	
'RLI-Bbas'	1.000000	'F' 2.000	1.000	0.767	
'RLI-Bcar'	1.000000	'F' 2.000	1.000	0.293	
${}^4\text{He}(\text{t}, \text{t}) {}^4\text{He}$					
'TTDAjar1'	1.000000	' ' 2.000	8.734	3.210	
'TTDAspig'	0.688000	' ' 2.000	5.430	5.342	
'TTAYjar1'	1.000000	' ' 2.000	8.138	11.959	Analyzing power
${}^4\text{He}(\text{t}, \text{n}) {}^6\text{Li}$					
'TNDAdros'	1.030000	' ' 2.000	1.004	0.013	
'TNDAdro1'	0.907000	' ' 2.000	3.194	3.358	

2. R-matrix parameters

2 channel

	Radii of channel		L_{max}	
'N, 6Li'	4.4701420279832	' ' 0.4	2	0.000000
'T, 4HE'	3.8297967468919	' ' 0.4	5	4.783959

- 10 evels with different total spin or parity from +1/2 to -9/2
- 26 adjusted reduced width magnitudes
- 6 adjusted energies of levels
- 32 normalizing factors of data

3. Calculated result of ${}^6\text{Li}(\text{n}, \text{t}) {}^4\text{He}$

Refer to Table 2. and Fig. 1.

It is hard to make comment about RAC2003 and ENDF/b6 by comparison of them with experimental data. Both look very good. But the ratio of RAC2003 to ENDF/B6 will display some problem.

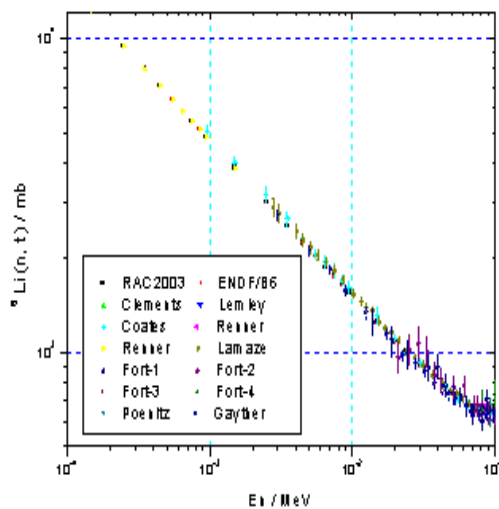


Fig.1-a Comparison of RAC2003 and experimental data for ${}^6\text{Li}(\text{n}, \text{t}) {}^4\text{He}$

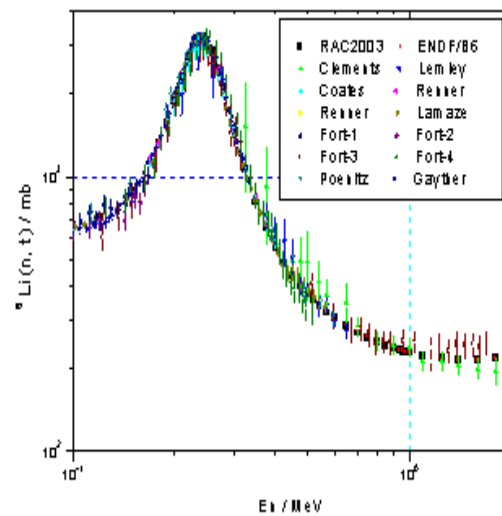


Fig.1-b Comparison of RAC2003 and experimental data for ${}^6\text{Li}(\text{n}, \text{t}) {}^4\text{He}$

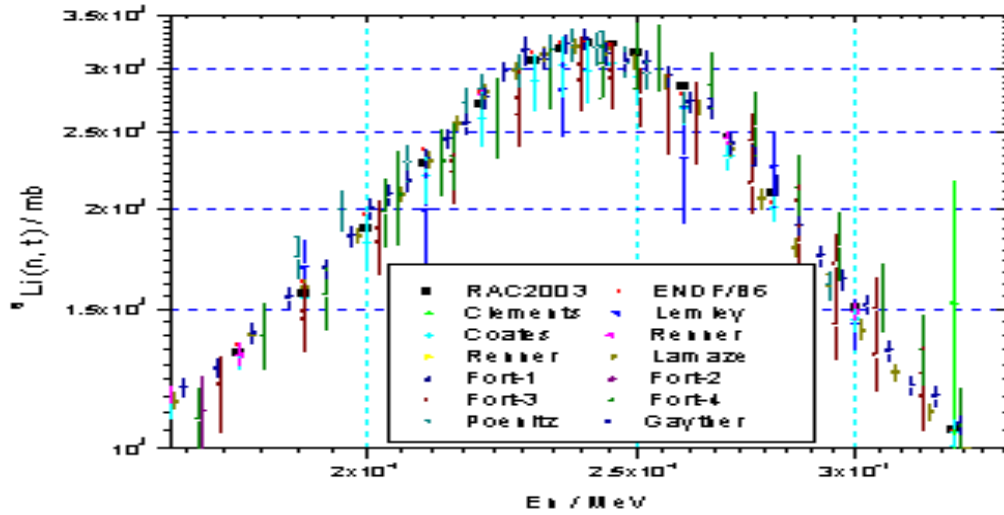


Fig.1-c Comparison of RAC2003 and experimental data for ${}^6\text{Li}(n,t){}^4\text{He}$

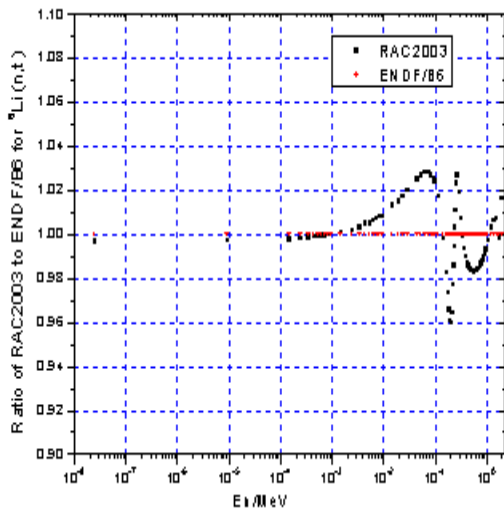


Fig. 2-a The ratio of RAC2003 to ENDF/B6 for ${}^6\text{Li}(n,t){}^4\text{He}$

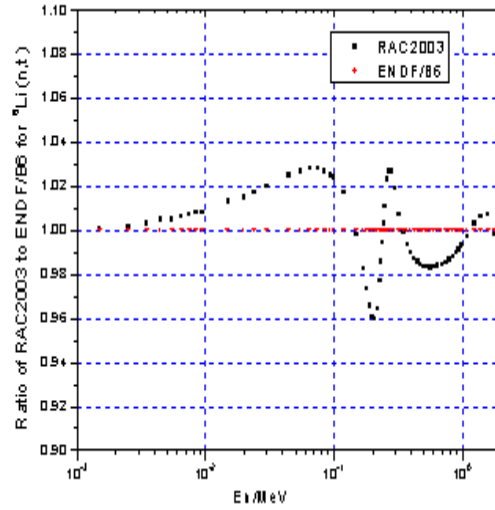


Fig. 2-b The ratio of RAC2003 to ENDF/B6 for ${}^6\text{Li}(n,t){}^4\text{He}$

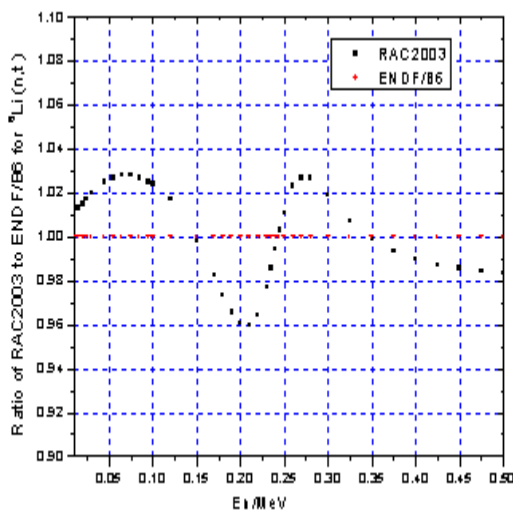


Fig. 2-c The ratio of RAC2003 to ENDF/B6 for ${}^6\text{Li}(n,t){}^4\text{He}$

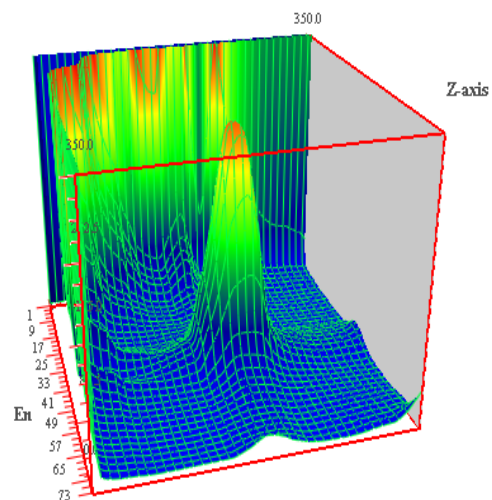


Fig. 3 The covariance for ${}^6\text{Li}(n,t){}^4\text{He}$

Near the $E_n=0.075$ MeV, the difference is rather large; the discrepancy of data is relative larger around this energy.

Near the $E_n=0.200$ MeV, the difference is rather large; the discrepancy of data is relative larger around this energy.

The difference of position of peak (-5/2) is about 0.003 MeV; less than that of ENDF/B6.

The width of peak (-5/2) seems broader than that of ENDF/B6.

The ${}^6\text{Li}$ (n, t) data of W. GAYTHER (EXFOR SUBENT 20862003) may produce some difference; It has not been find by me in GMA-data base.

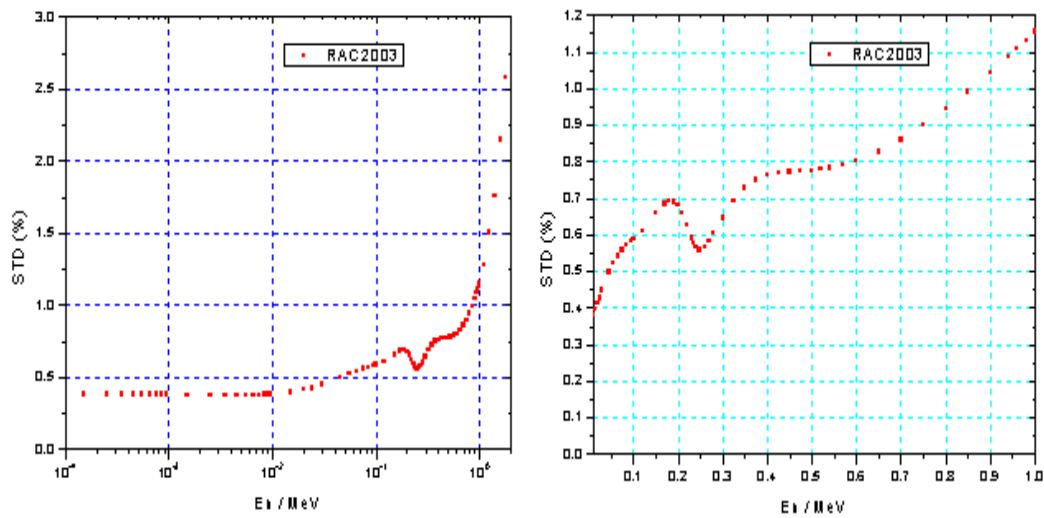


Fig. 4 The standard deviation (STD%) in percent of RAC2003 for ${}^6\text{Li}$ (n, t) ${}^4\text{He}$

The standard deviation (STD%) is calculated by error propagation formula with final R-matrix parameter. The errors of some different cross sections were increased to make it's correspond chi-square/freedom near 1.0 .

The covariance is calculated by error propagation formula with final R-matrix parameter. The errors of some different cross sections were increased to make it's correspond chi-square/freedom near 1.0 . Fig. 3.

4. Comparison of RAC2003 and other integrated experimental data

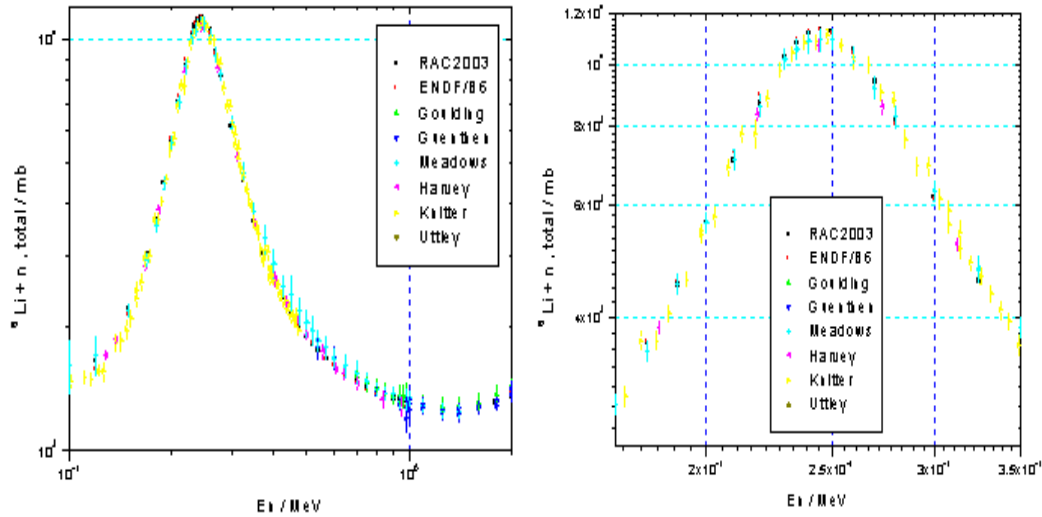


Fig. 5 Comparison of RAC2003 and experimental data for ${}^6\text{Li} + n$ total cross section

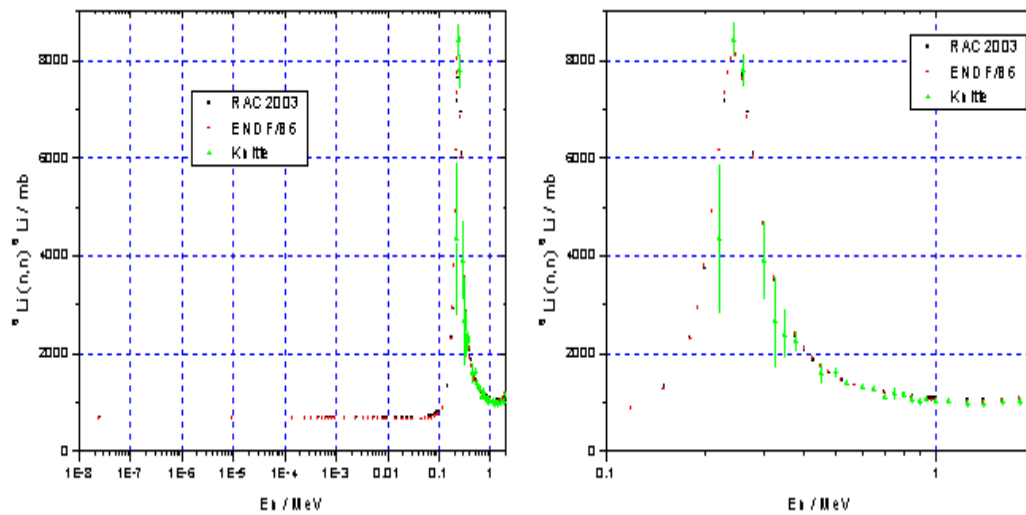


Fig. 6 is the comparison of RAC2003 and experimental cross section of ${}^6\text{Li}(n, n){}^6\text{Li}$

5. Comparison of RAC2003 and other different experimental data

Fig. 7 Comparison of RAC2003 and experimental elastic scattering neutron polarization P.

Fig. 8 Comparison of RAC2003 and experimental different cross section of ${}^6\text{Li}(n, n){}^6\text{Li}$.

Fig. 9 Comparison of RAC2003 and experimental different cross section of ${}^6\text{Li}(n, t){}^4\text{He}$.

Fig. 10 Comparison of RAC2003 and experimental analyzing power of ${}^4\text{He}(t, t){}^4\text{He}$.

Fig. 11 Comparison of RAC2003 and experimental different cross section of ${}^4\text{He}(t, t){}^4\text{He}$.

Fig. 12 Comparison of RAC2003 and experimental different cross section of ${}^4\text{He}(t, n){}^6\text{Li}$.

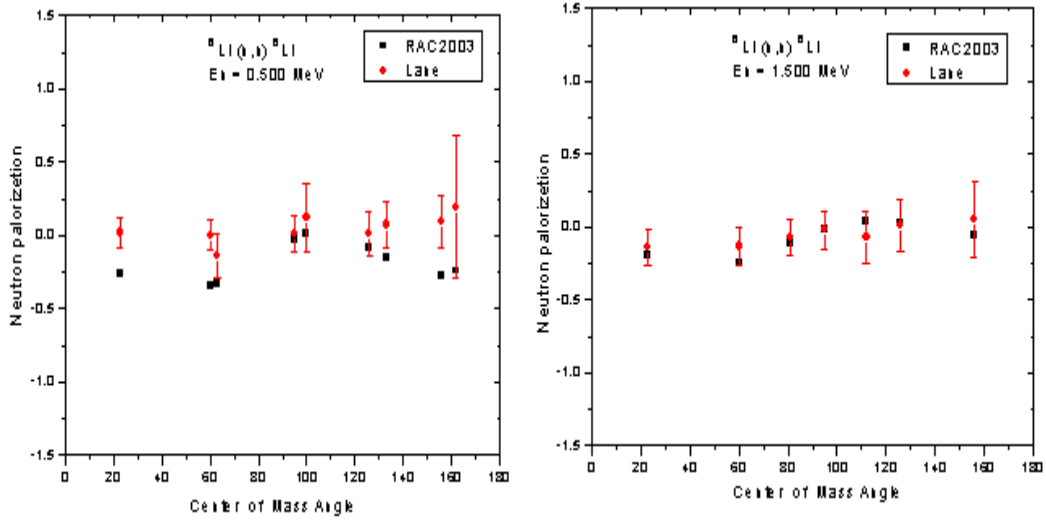


Fig. 7 Comparison of RAC2003 and experimental elastic scattering neutron polarization P .

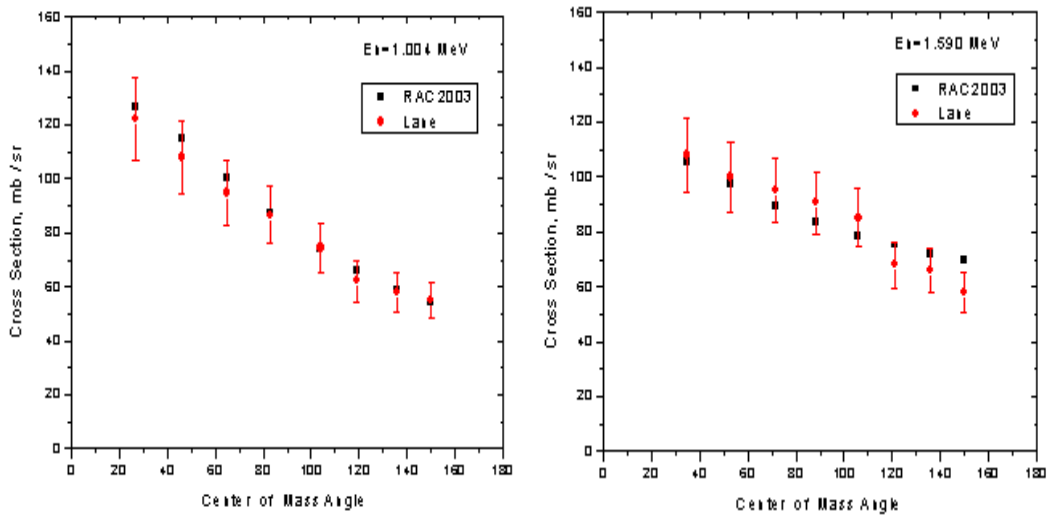


Fig. 8 Comparison of RAC2003 and experimental differential cross section of ${}^6\text{Li}(n,n){}^6\text{Li}$

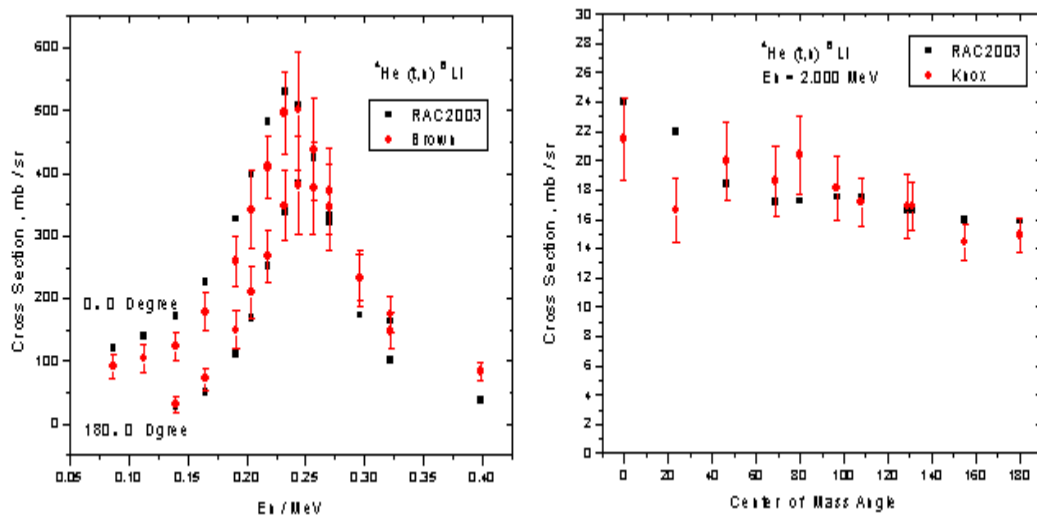


Fig. 9 Comparison of RAC2003 and experimental differential cross section of ${}^6\text{Li}(n,t){}^4\text{He}$

It was found that the different cross sections ${}^6\text{Li}(n,t)$ of Knox play very important role for determining the cross section of ${}^6\text{Li}(n,t)$ on the higher energy region.

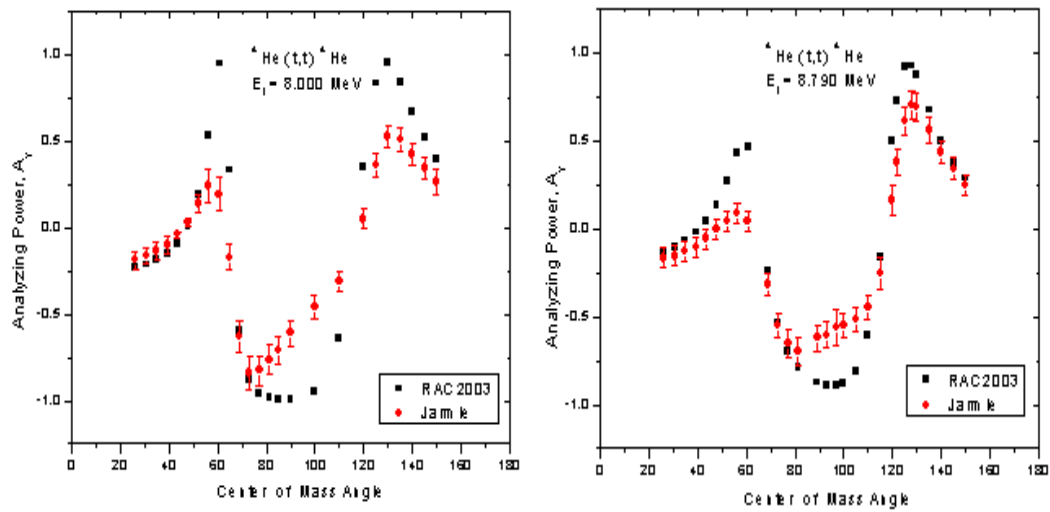


Fig. 10 Comparison of RAC2003 and experimental analyzing power of ${}^4\text{He}(t,t){}^4\text{He}$

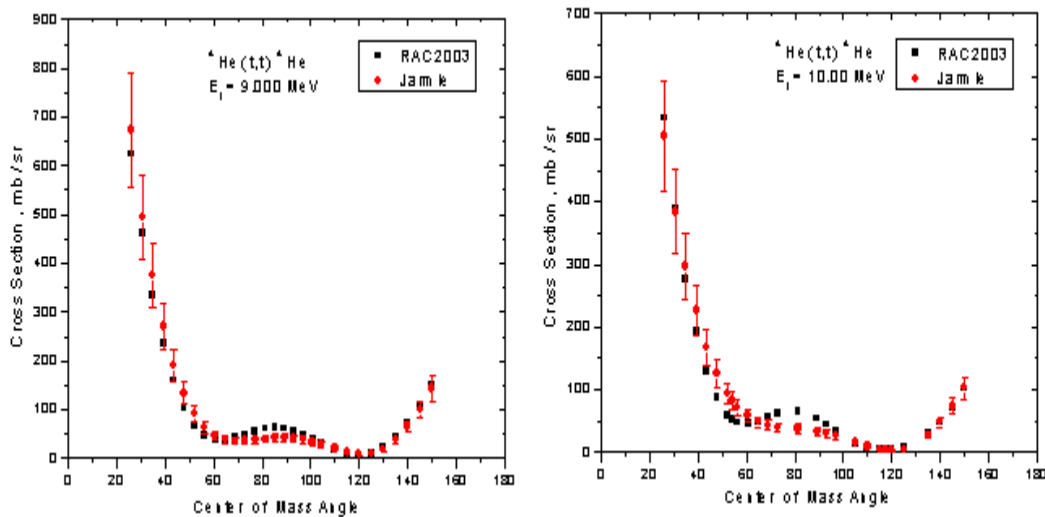


Fig. 11 Comparison of RAC2003 and experimental different cross section of ${}^4\text{He}(t,t){}^4\text{He}$

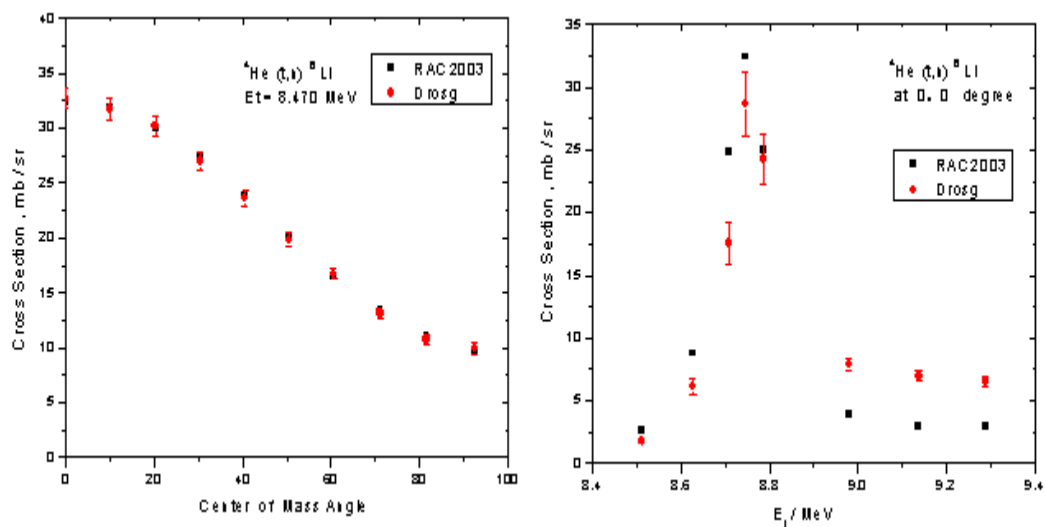


Fig. 12 Comparison of RAC2003 and experimental different cross section of ${}^4\text{He}(t,n){}^6\text{Li}$.

6. Test of positive definiteness

The covariance of R-matrix parameter is positive definite, the covariance of ${}^6\text{Li} (n, t) {}^4\text{He}$ is semi-positive definite.

7. Problem

The problem includes:

- a. At $E_n=0.2530\text{E-}07$ MeV the cross section of ${}^6\text{Li} (n, t)$ is $0.93799\text{E+}06$ mb; if Friesenhahn's data is included the value will prefer $0.910\text{E+}06$ mb.
- b. The center position of peak (-5/2) is about 0.003 MeV less than that of ENDF/B6.
- c. The width of peak (-5/2) seems broader than that of ENDF/B6.
- d. The ${}^6\text{Li} (n, t)$ data of W. GAYTHER (EXFOR SUBENT 20862003) may produce some problem; I has not found it in the GMA-data base.
- e. All the covariance of experimental data is positive definite; the covariance of R-matrix parameter is positive definite; but the covariance of ${}^6\text{Li} (n, t) {}^4\text{He}$ is half positive definite.
- f. The given errors of some charged particle data look too lower; it is increased a lot.
- g. The correlation is much stronger than that in GMA-fit.

Progress Report on Analysis of ^{11}B System with RAC

CHEN Zhenpeng SUN Yeying
Tsinghua University, Beijing 100084, China;
(2003/10/13)

The analysis of ^{11}B compound system has been done with RAC. In this simultaneous analysis the most of 'good' data about ^{11}B compound system have been included. The evaluated cross section of $^{10}\text{B}(n, \alpha 1)$ and $^{10}\text{B}(n, \alpha 0 + \alpha 1)$ seems good. The standard deviation (STD(%)) $^{10}\text{B}(n, \alpha 1)$ and $^{10}\text{B}(n, \alpha 0 + \alpha 1)$ seems reasonable.

1. Data base

The data-base used is shown in Table 1.

Experimental data involve all open reaction channels and reaction types in the energy range considered for ^{11}B system. The reaction channels are $(n, ^{10}\text{B})$, $(\alpha 0, ^7\text{Li})$ and $(\alpha 1, ^7\text{Li}^*)$; the data types include neutron total cross section σ_t , all kinds of integral reaction cross section and differential cross section, polarization of elastic scattering particle.

The data-base used is shown in Table 1. The most of integrated cross sections are taken from the original GMA-data base. The different cross sections are taken from EXFOR. The total number of data points is 3011.

Table 1 Information of data-base used in RAC fit

J	Auth	No	Ava-ch	Ori-rel	Cal-rel	Ratio
$^{10}\text{B} + n$, (total)						
2	NTOTbock	80	0.246	11.73	0.91621	0.0781
3	NTOTsaff	10	1.143	0.38	0.22448	0.5912
4	NTOTschm	82	0.009	14.81	0.22448	0.0152
5	NTOTthugh	49	0.372	5.56	0.25039	0.0450
6	NTOTspe1	52	0.173	7.76	0.89353	0.1151
7	NTOTspe2	57	0.154	7.66	0.88836	0.1159
8	NTOTdim1	14	0.121	6.28	0.46085	0.0734
9	NTOTdim2	52	0.091	6.21	0.31116	0.0501
$^{10}\text{B}(n, n)^{10}\text{B}$						
12	NNCSmoor	53	0.365	6.36	1.17206	0.1842
13	NNCSasam	30	0.017	17.97	1.48207	0.0825
14	NNCSlane	45	0.982	9.26	1.11835	0.1208
15	NNDAAlan1	100	1.124	4.66	1.13573	0.2438
16	NNDAAlan2	130	25.567	8.07	1.22956	0.1524
$^{10}\text{B}(n, \alpha 0)^7\text{Li}$						
18	NA0Cmack	16	3.090	5.74	1.14920	0.2002
19	NA0Cseal	71	0.272	9.51	1.18314	0.1244
20	NA0Colso	54	0.470	5.46	1.19970	0.2195
21	NA0Cgibb	11	0.625	8.45	1.25341	0.1484
22	NA0Cover	21	0.001	1096.10	1.22274	0.0011 no informative

23 NA0DAse1 56 0.449 76.71 1.73636 0.0226
 24 NA0DAse2 112 0.498 60.24 2.44563 0.0406

$^{10}\text{B}(\text{n}, \alpha 1) ^7\text{Li}^*$

26 NA1Cchr 36 0.976 3.15 0.58087 0.1844
 27 NA1Cfrie 56 0.992 6.01 0.60210 0.1003
 28 NA1Cvie1 7 0.410 8.03 0.86918 0.1082
 29 NA1Cvie2 11 0.451 7.21 1.35280 0.1876
 30 NA1Cvie3 9 0.946 7.26 1.53711 0.2117
 31 NA1Ccoat 95 0.443 5.86 0.36174 0.0617

$^{10}\text{B}(\text{n}, \alpha 0 + \alpha 1) ^7\text{Li}$

33 NATOmead 2 0.013 0.71 0.22461 0.3176
 34 NATObich 57 0.154 22.36 1.11540 0.0499
 35 NATOboga 27 0.465 13.28 0.56824 0.0428
 36 NATOcoxf 12 0.604 10.16 0.44899 0.0442

$^{10}\text{B}(\text{n}, \alpha 0) ^7\text{Li} / ^{10}\text{B}(\text{n}, \alpha 1) ^7\text{Li}^*$

39 NARAtthem 2 0.013 0.98 0.43243 0.4408
 40 NARATwes 24 1.174 30.80 1.42326 0.0462
 41 NARAstel 3 0.497 3.39 0.52164 0.1539
 42 NARAdavi 22 1.264 19.50 2.08650 0.1070
 43 NARAMac1 8 0.418 14.35 1.12731 0.0786
 44 NARAMac2 9 0.864 24.30 1.17708 0.0484
 45 NARAsow1 23 0.483 19.40 0.62851 0.0324
 46 NARAsow2 20 0.517 16.94 0.97832 0.0577
 47 NARApet1 9 0.769 22.63 1.66520 0.0736
 48 NARApet2 3 0.577 24.05 3.09302 0.1286

$^6\text{Li}(\text{n}, \alpha) / ^{10}\text{B}(\text{n}, \alpha 0 + \alpha 1) \text{ or } ^6\text{Li}(\text{n}, \alpha) / (^{10}\text{B}(\text{n}, \alpha 1))$

49 RLI-Bso2 24 0.573 1.25 0.24342 0.1948
 50 RLI-Bso1 9 0.080 1.71 0.22146 0.1298
 51 RLI-Bbas 47 0.955 8.10 0.44857 0.0554
 52 RLI-Bcar 5 0.785 1.17 0.22186 0.1893
 53 NA1DAse1 56 1.269 47.05 1.38050 0.0293
 54 NA1DAse2 120 1.813 19.32 1.90521 0.0986

$^7\text{Li}(\alpha, \alpha) ^7\text{Li}$

55 AA0DAcus 137 26.677 8.60 0.95354 0.1109
 56 AA0DAcut 172 24.493 7.57 1.51442 0.2001

$^7\text{Li}(\alpha, \alpha 1) ^7\text{Li}^*$

57 AA1DAcus 143 3.862 29.29 4.49249 0.1534

$^7\text{Li}(\alpha, \text{n}) ^{10}\text{B}$

58 ANCSseal 71 0.098 26.57 1.17069 0.0441
 59 ANDAvan1 65 0.973 37.11 1.75533 0.0473
 60 ANDAvan2 77 0.946 40.87 4.48816 0.1098

61 ANDAseal 51 2.291 10.75 1.70150 0.1582
62 ANDAsea0 64 0.083 53.20 2.63991 0.0496

2. R-matrix parameter

Table 2 shows the R-matrix parameter.

Table 2. R-matrix parameter

	Radii of channel		L_{\max}		
'N, 10B '	0.41160042492225E+01	''	1.0	2	0.000000
'4HE,7Li '	0.39731752178801E+01	''	1.0	5	2.789800
'4HE,7Li*'	0.61340200554819E+01	''	1.0	5	2.312100

11 levels with different total spin or parity from +1/2 to +11/2
34 Adjusted reduced width magnitudes
3 Adjusted energies of levels
31 Adjusted normalizing factors of data

3. Calculated results for $^{10}\text{B} (n, \alpha 1)$ and $^{10}\text{B} (n, \alpha 0 + \alpha 1)$

Refer to Fig. 1. for $^{10}\text{B} (n, \alpha 0)$; Fig. 2. for $^{10}\text{B} (n, \alpha 1)$; Fig. 3. for $^{10}\text{B} (n, \alpha 0 + \alpha 1)$

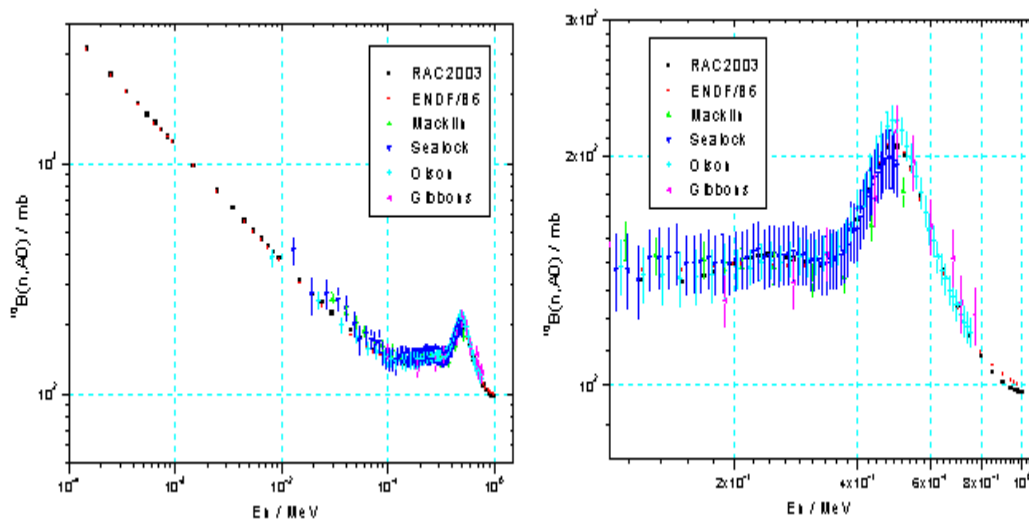


Fig.1 Comparison of RAC2003 and experimental data for $^{10}\text{B} (n, \alpha 0) ^7\text{Li}$

From $E_n=0.1$ to 0.2 MeV, the experimental cross section of $^{10}\text{B} (n, \alpha 0) ^7\text{Li}$ changed smoothly. This looks strange and is very difficult to get good fit with R-matrix model.

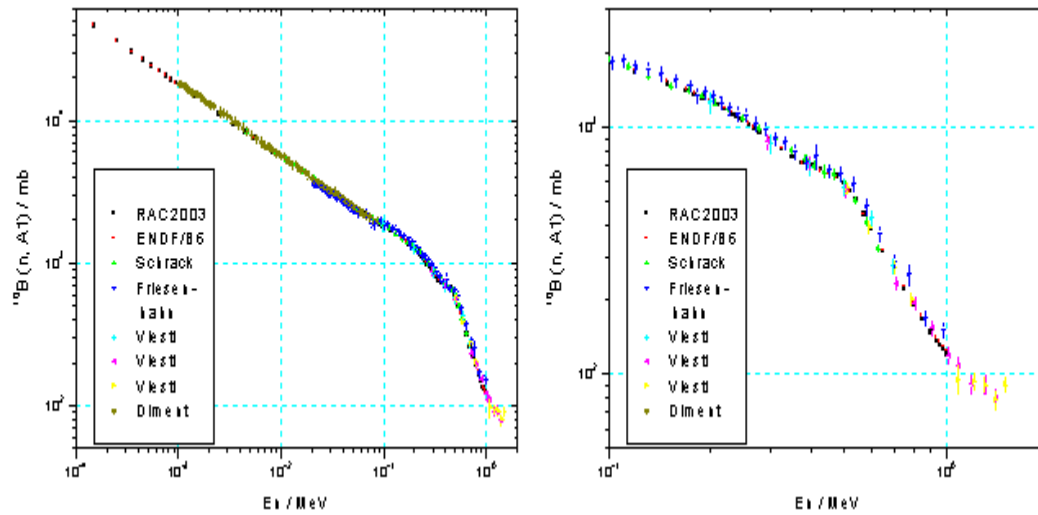


Fig.2 Comparison of RAC2003 and experimental data of $^{10}\text{B}(n, \alpha 1) ^7\text{Li}^*$

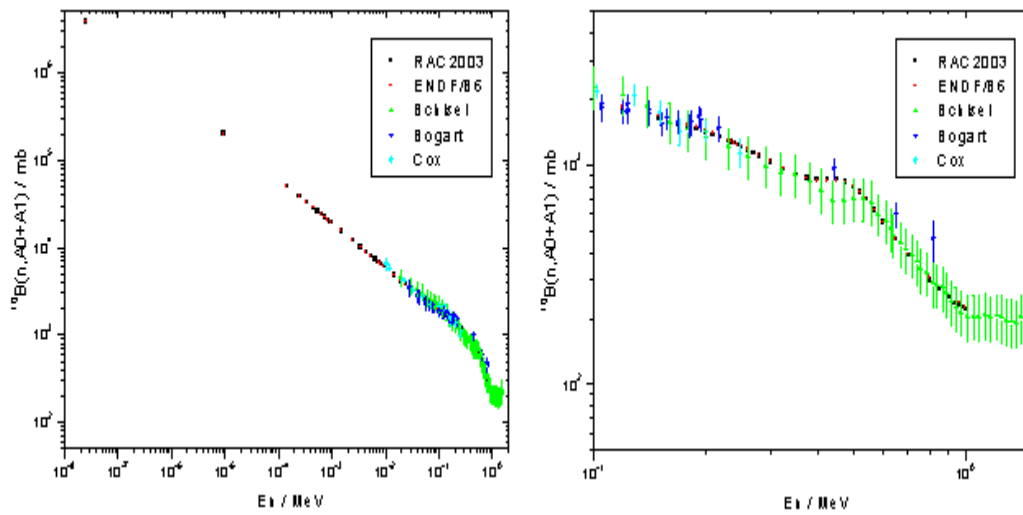


Fig.3 Comparison of RAC2003 and experimental data for $^{10}\text{B}(n, \alpha 0+\alpha 1) ^7\text{Li}$

The comparisons of RAC2003 and ENDF/b6 with experimental data look very good. **But the ratio of RAC2003 to ENDF/B6 will display some problem.**

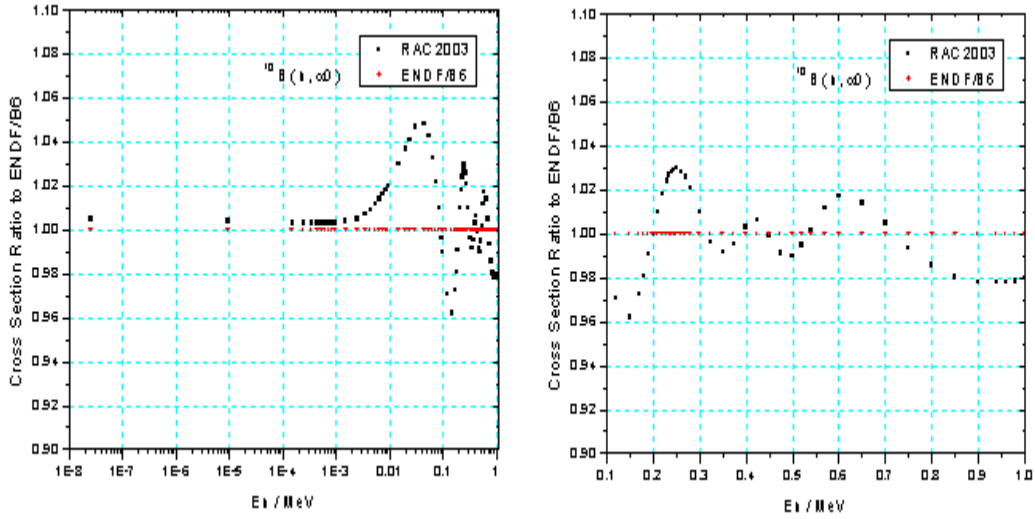


Fig. 4 The ratio of RAC2003 to ENDF/B6 for $^{10}\text{B} (n, \alpha 0)$

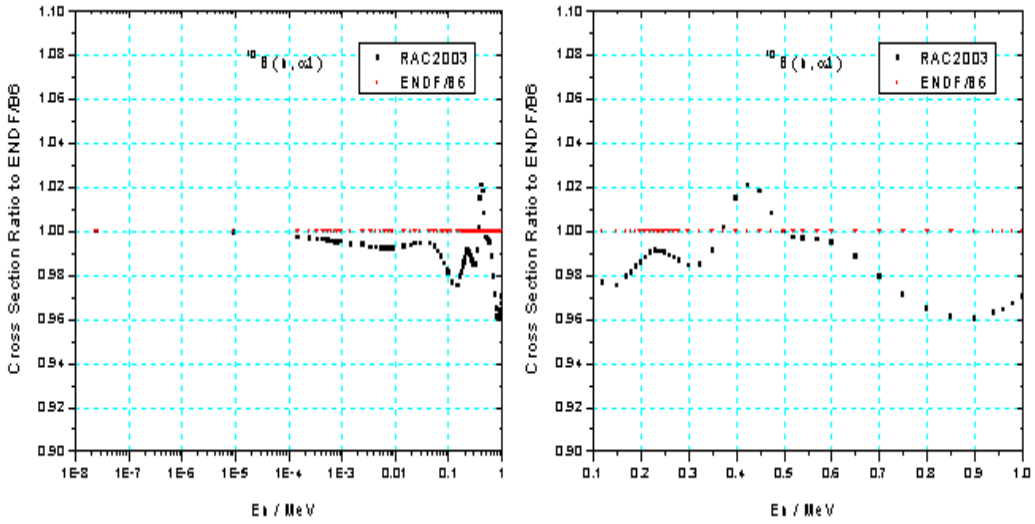


Fig. 5 The ratio of RAC2003 to ENDF/B6 for $^{10}\text{B} (n, \alpha 1)$

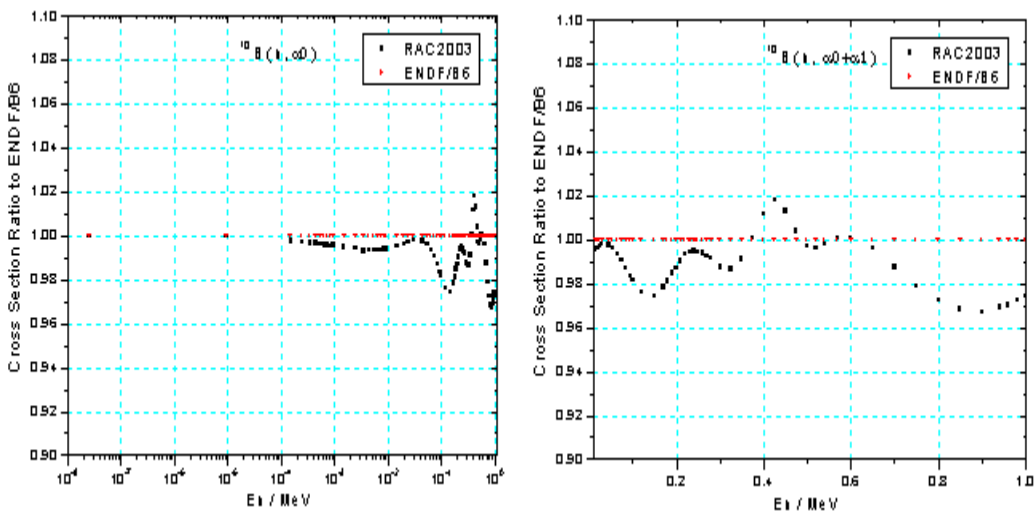


Fig. 6 The ratio of RAC2003 to ENDF/B6 for $^{10}\text{B} (n, \alpha 0 + \alpha 1)$

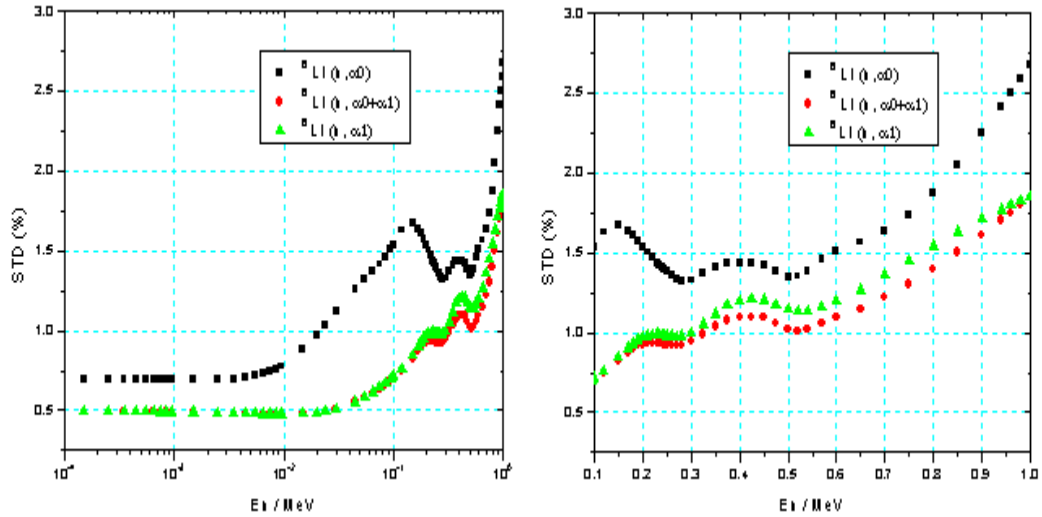


Fig. 7 The standard deviation (STD%) in percent of RAC2003 for $^{10}\text{B} (n, \alpha)$

The standard deviation (STD%) is calculated by full error propagation formula. **Some errors were increased to make it's correspond chi-square/freedom is near 1.0 .**

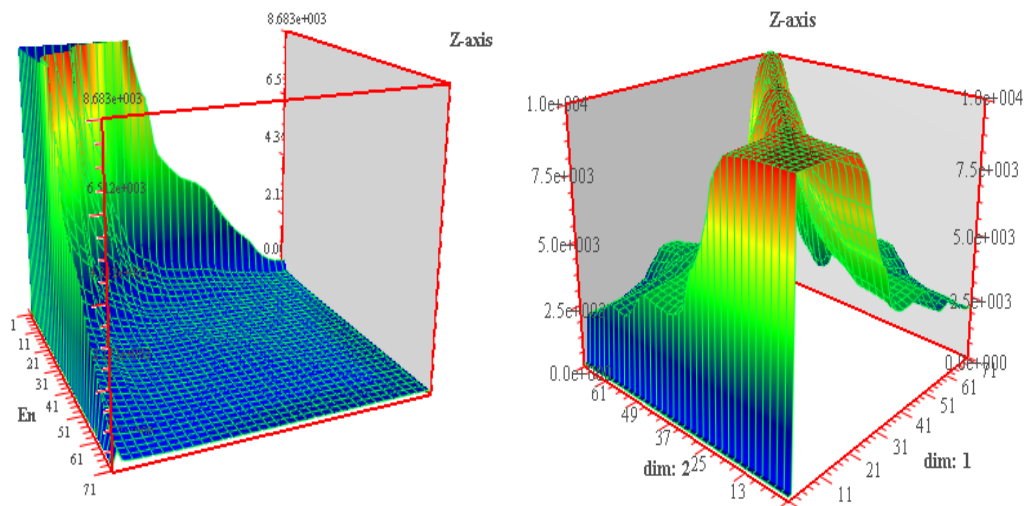


Fig. 8 The covariance of RAC2003 for $^{10}\text{B} (n, \alpha 1)$

The covariance is calculated by error propagation formula with final R-matrix parameter. some errors were increased to make it's correspond chi-square/freedom near 1.0 .

4. Comparison of RAC2003 and other integrated experimental data

Fig. 9 is about $^{10}\text{B} (n, n)$ ^{10}B ; Fig. 10 iabout $^{10}\text{B} +n$ total cross section.; Fig. 11 is about $^{10}\text{B} (n, \alpha 0)$ $^7\text{Li} / ^{10}\text{B} (n, \alpha 1)$ $^7\text{Li}^*$. All seem very good.

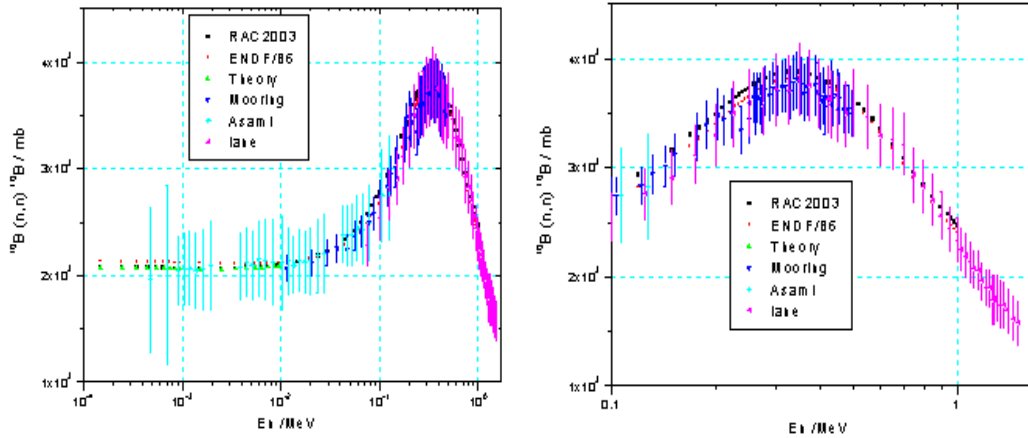


Fig. 9 Comparison of RAC2003 and experimental data for neutron elastic scattering cross section

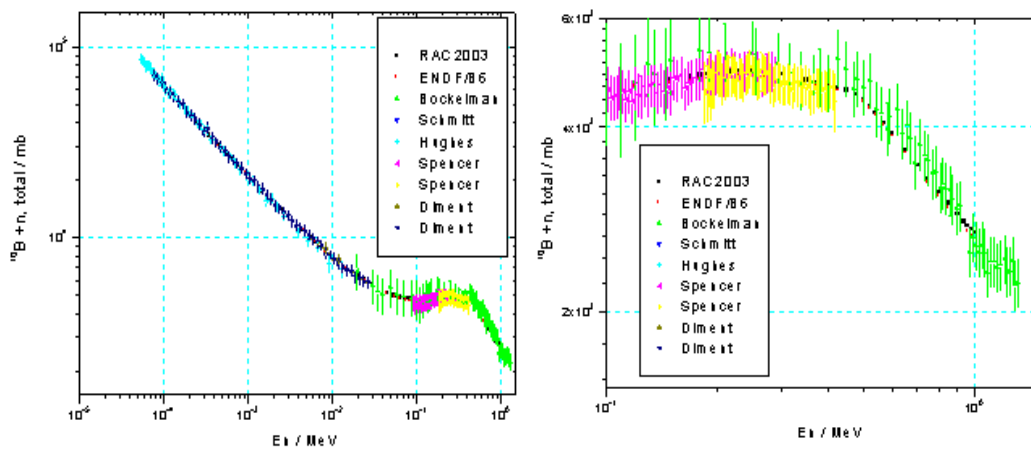


Fig. 10 Comparison of RAC2003 and experimental data for ${}^6\text{Li} + n$ total cross section

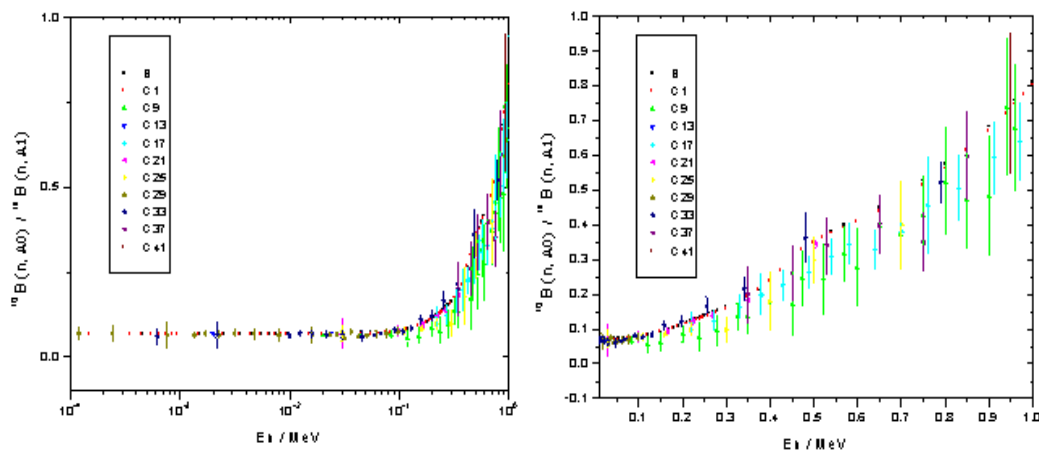


Fig. 11 Comparison of RAC2003 and experimental ${}^{10}\text{B}(n, \alpha 0) {}^7\text{Li} / {}^{10}\text{B}(n, \alpha 1) {}^7\text{Li}^*$

5. Comparison of RAC2003 and other different experimental data

Fig. 12 is about ${}^{10}\text{B}(n, n) {}^{10}\text{B}$; Fig. 13 is about ${}^{10}\text{B}(n, \alpha 0) {}^7\text{Li}$; Fig. 14 is about ${}^{10}\text{B}(n, \alpha 1) {}^7\text{Li}^*$. It looks not good for the fit of ${}^{10}\text{B}(n, \alpha 0) {}^7\text{Li}$ and ${}^{10}\text{B}(n, \alpha 1) {}^7\text{Li}^*$.

'NAODase1' 1.050000 ' 2.000 2.500 1.085 Dif.

'NA0DAse2'	1.060000	' 2.000	2.500	1.098	Dif.
'NA1DAse1'	1.050000	' 2.000	4.500	1.288	Dif.
'NA1DAse2'	1.060000	' 2.000	6.000	1.298	Dif.

The data $^{10}\text{B} (n, \alpha 0) ^7\text{Li}^{10}$ and $\text{B} (n, \alpha 1) ^7\text{Li}^*$ of Sealock are systematically 5% to 20% lower; the shape of their integrated cross sections are different with other data sets very much. It has to be make normalization by he factor larger then 5%. The error have to be increased 2.5 to 6 times.

Fig. 15 is about $^7\text{Li} (\alpha , \alpha 0) ^7\text{Li}$; Fig. 16 is about $^7\text{Li} (\alpha , \alpha 1) ^7\text{Li}^*$; Fig. 17 is about $^7\text{Li} (\alpha , n) ^{10}\text{B}$. Rather larger discrepancy exist in those data.

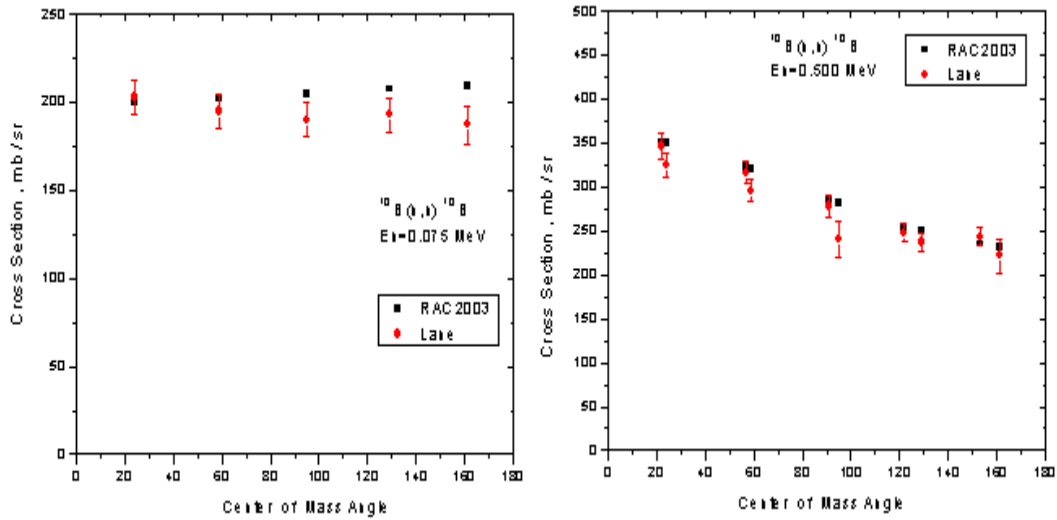


Fig. 12 Comparison of RAC2003 and experimental different cross section of $^{10}\text{B} (n, n) ^{10}\text{B}$

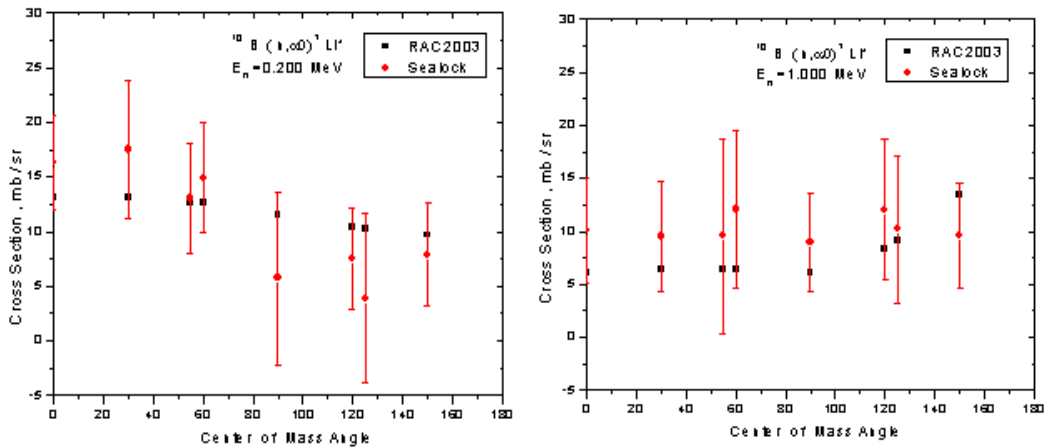


Fig. 13 Comparison of RAC2003 and experimental different cross section of $^{10}\text{B} (n, \alpha 0) ^7\text{Li}$

It looks not good for the fit of $^{10}\text{B} (n, \alpha 0) ^7\text{Li}$.

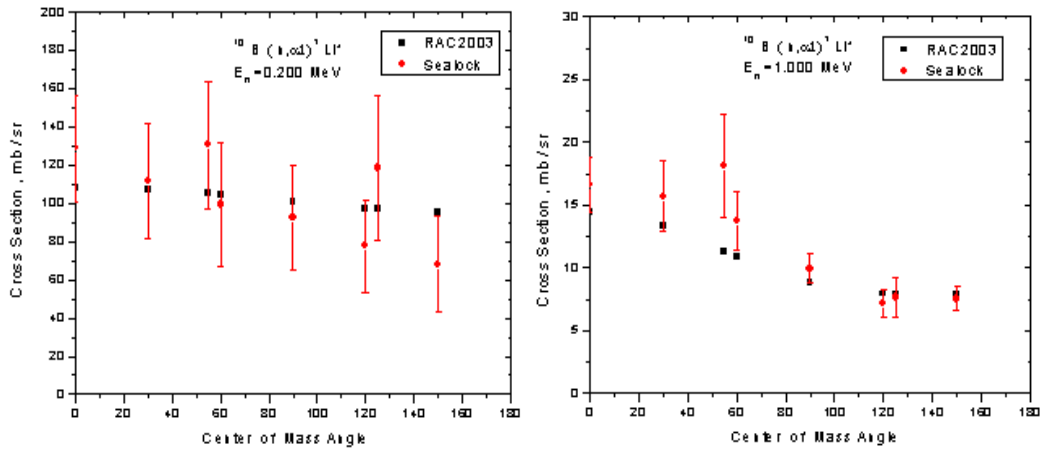


Fig. 14 Comparison of RAC2003 and experimental different $^{10}\text{B}(n, \alpha)^7\text{Li}^*$

It looks not good for the fit of $\text{B}(n, \alpha)^7\text{Li}^*$.

In the fit procedure the data have been corrected as follow:

'NA0Dase1'	1.050000	''	2.000	2.500	1.085	Dif.
'NA0Dase2'	1.060000	''	2.000	2.500	1.098	Dif.
'NA1Dase1'	1.050000	''	2.000	4.500	1.288	Dif.
'NA1Dase2'	1.060000	''	2.000	6.000	1.298	Dif.

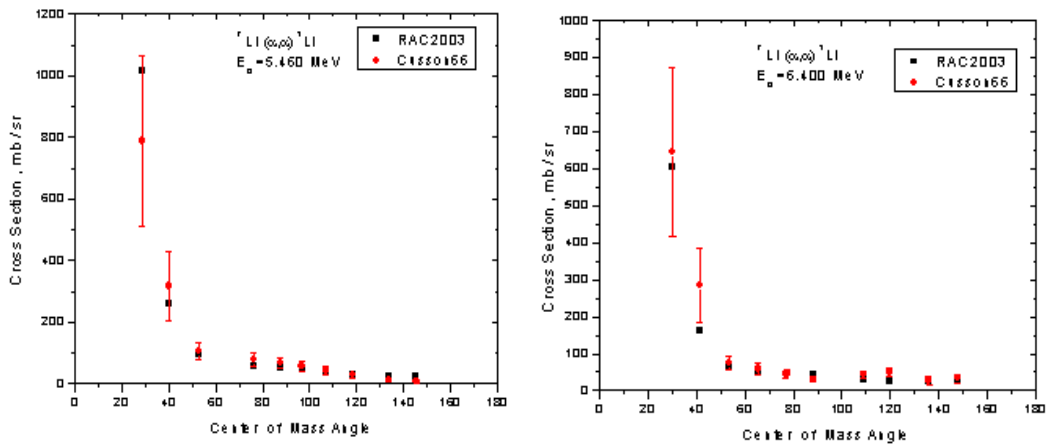


Fig. 15 Comparison of RAC2003 and experimental different $^7\text{Li}(\alpha, \alpha)^7\text{Li}$

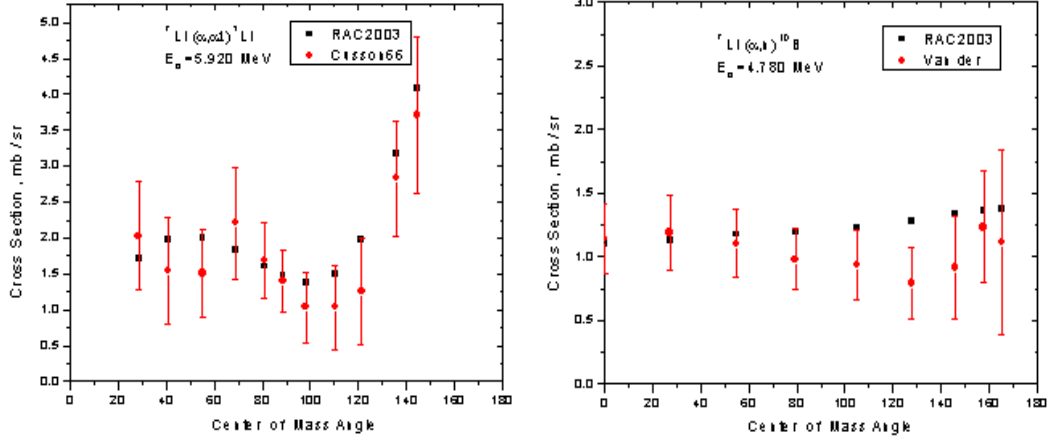


Fig. 16 Comparison of RAC2003 and experimental different ${}^7\text{Li}(\alpha, \alpha) {}^7\text{Li}^*$

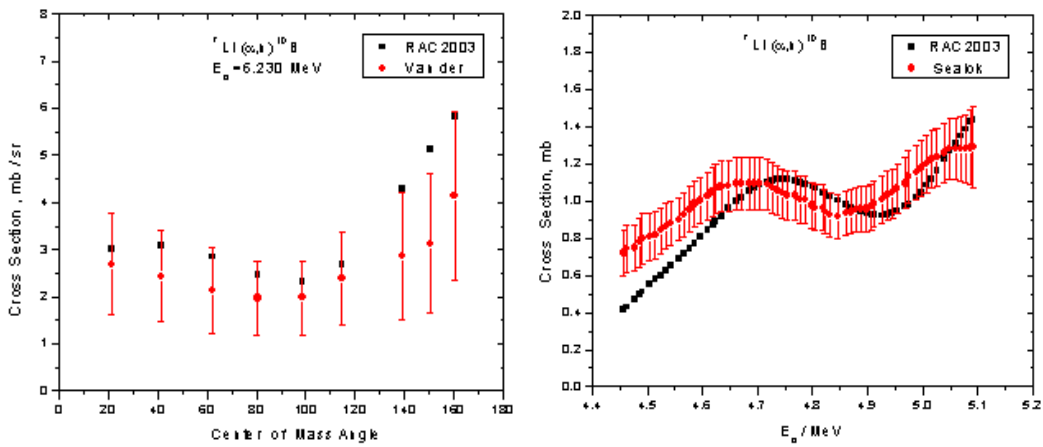


Fig. 17 Comparison of RAC2003 and experimental different ${}^7\text{Li}(\alpha, n) {}^{10}\text{B}$

6. Test of positive definiteness

The R-matrix parameters is positive definite, the cross section is half-positive definite.

Table 4. Test of positive definiteness for R-matrix parameters

EIGENVALUES

1.7088D+02 1.1477D+01 5.6932D+00 7.8182D-01 4.6911D-01 3.4366D-01
 1.7549D-01 1.5896D-01 1.1697D-01 9.8444D-02 9.5270D-02 7.5945D-02
 7.0883D-02 6.8232D-02 4.7776D-02 4.4528D-02 3.5929D-02 3.5324D-02
 2.5940D-02 2.2487D-02 1.5468D-02 1.4266D-02 7.7834D-03 5.7479D-03
 5.5201D-03 5.0117D-03 4.7907D-03 4.5811D-03 4.4718D-03 4.3501D-03
 4.3035D-03 4.2292D-03 4.1916D-03 3.8503D-03 3.5550D-03 3.4212D-03
 3.0101D-03 2.9366D-03 2.7737D-03 2.5832D-03 2.5438D-03 2.4033D-03
 2.3599D-03 2.1100D-03 1.6917D-03 1.6465D-03 1.4882D-03 1.2616D-03
 1.1376D-03 1.0869D-03 1.0646D-03 7.6487D-04 7.3706D-04 6.3586D-04
 4.8973D-04 3.2338D-04 3.1407D-04 2.5110D-04 2.1353D-04 1.8549D-04
 1.4695D-04 1.0208D-04 8.3622D-05 7.3143D-05 6.0679D-05 3.7575D-05
 3.4051D-05 1.7855D-05 1.5339D-05 1.2309D-05 8.1286D-06 2.4466D-06
 1.3439D-06 7.8177D-07 6.9544D-07 4.5289D-07 1.9549D-07 5.9899D-08
 NUMBER OF POSITIVE EIGENVALUES: 78
 NUMBER OF ZERO EIGENVALUES: 0
 NUMBER OF NEGATIVE EIGENVALUES: 0

Table 5. Test of positive definiteness for ${}^{10}\text{B}(n, \alpha) {}^7\text{Li}^*$

EIGENVALUES

3.3218D+08 2.5451D+03 9.3115D+02 4.6108D+02 3.3696D+02 1.6017D+02
 1.2856D+02 7.8193D+01 6.2112D+01 2.7271D+01 1.2452D+01 9.5432D+00
 7.7396D+00 3.7468D+00 3.1200D+00 2.7226D+00 1.8944D+00 1.0788D+00
 9.6616D-01 7.5306D-01 4.9016D-01 3.1696D-01 2.2183D-01 1.7127D-01
 1.6282D-01 1.5431D-01 1.2163D-01 1.0871D-01 7.8020D-02 6.1958D-02
 3.5226D-02 2.9348D-02 2.0856D-02 1.7573D-02 1.4686D-02 1.2163D-02
 8.1293D-03 4.9430D-03 3.0573D-03 7.5127D-04 5.4780D-04 1.3150D-04
 -8.5660D-04 -2.3817D-03 -4.9977D-03 -6.3473D-03 -1.0008D-02 -1.1825D-02
 -1.4268D-02 -1.6392D-02 -2.5166D-02 -3.0390D-02 -4.6974D-02 -5.7062D-02
 -7.2580D-02 -8.2581D-02 -9.2935D-02 -1.0820D-01 -1.1959D-01 -1.4317D-01
 -2.5439D-01 -3.0062D-01 -4.1794D-01 -7.6719D-01 -9.0686D-01 -2.2572D+00
 -8.3052D+00 -9.0033D+00 -1.5365D+01 -7.6230D+01
 NUMBER OF POSITIVE EIGENVALUES: 42
 NUMBER OF ZERO EIGENVALUES: 0
 NUMBER OF NEGATIVE EIGENVALUES: 28

7. Sensitive coefficient

Fig. 18, Fig. 19 and Fig. 19 show the sensitive coefficient about $^{10}\text{B} (n, \alpha 1) ^7\text{Li}^*$.

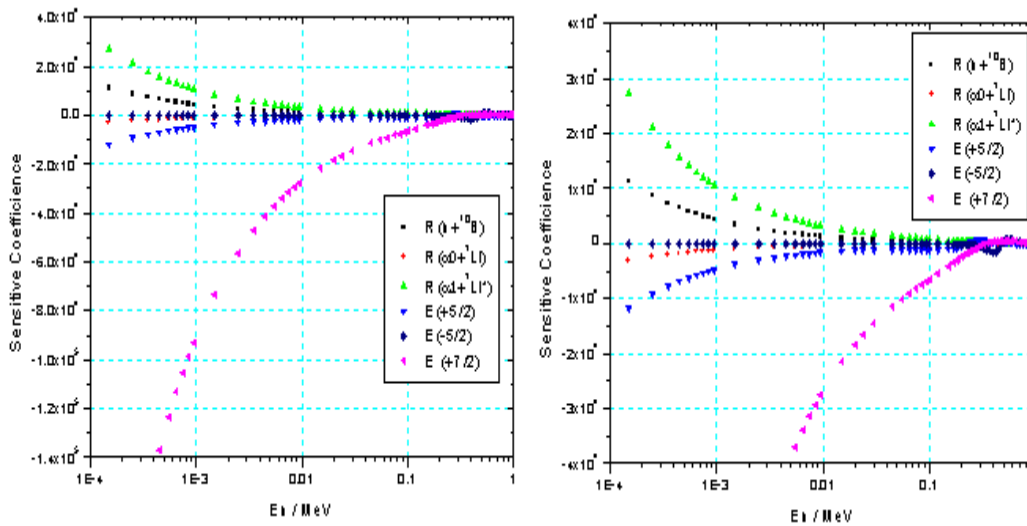


Fig. 18 The sensitive coefficient relative to R-matrix parameters for $^{10}\text{B} (n, \alpha 1) ^7\text{Li}^*$. The parameters are channel ratio R and position of energy levels E.

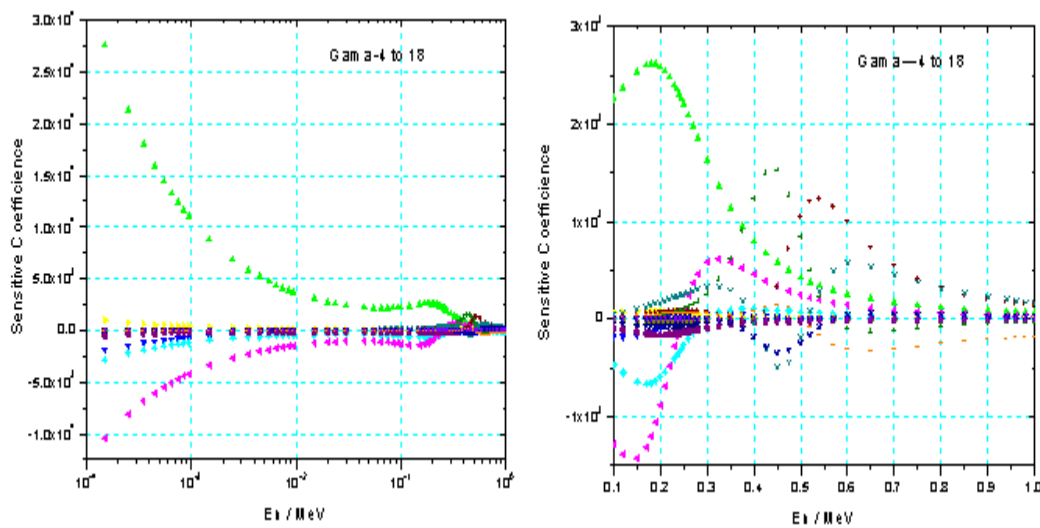


Fig. 19 The sensitive coefficient relative to R-matrix parameters for $^{10}\text{B} (n, \alpha 1) ^7\text{Li}^*$. The parameters are the reduced width magnitude no. 4 to no.18.

8. Problems

The problem includes:

- a. The discrepancy of experimental integrated $^{10}\text{B} (n, \alpha 0) ^7\text{Li}^{10}$ is rather larger.
- b. From $E_n=0.1$ to 0.2 MeV, the experimental cross section of $^{10}\text{B} (n, \alpha 0) ^7\text{Li}$ changed smoothly. This looks strange and is very difficult to get good fit with R-matrix model.
- c. The different cross section $^{10}\text{B} (n, \alpha 0) ^7\text{Li}^{10}$ and $\text{B} (n, \alpha 1) ^7\text{Li}^*$ of Sealcock are systematically 5% to 20% lower; the shape of their integrated cross sections are different with other data sets very much. It has to be normalized by the factor larger than 5%. The errors have to be increased about 2.5 to 6 times. Otherwise, the calculated $^{10}\text{B} (n, \alpha 0) ^7\text{Li}^{10}$ and $\text{B} (n, \alpha 1) ^7\text{Li}^*$ will be much lower systematically.
- d. The covariance of experimental data is positive definite; the covariance of R-matrix parameter is positive definite; but the covariance of calculated cross sections is half positive definite.

ONCE AGAIN ON THE PEELLE'S PUZZLE

E.V.Gai, S.A.Badikov
Institute of Physics and Power Engineering,
249033 Obninsk, Kaluga region, Russia

Abstract

The features identifying the Peelle's Pertinent Puzzle in known model [1] with 2 measurements and constant estimated function are studied in more complicated exactly solved models. The *generalized* inequality which signals on the absence of the Peelle's Puzzle is deduced in model with non-constant model function and 2 measurements. The *generalized* inequality imposes restriction on *relative* (to approximant's value) uncertainties. It is transformed in already known inequality in case constant estimated function.

It is shown in the model with 3 measurements and constant estimated function that *generalized* inequality provides necessary (not sufficient) condition for absence of the Peelle's Puzzle.

Introduction

An anomaly known as the Peelle's Pertinent Puzzle is characterized by a systematic bias of estimated values relative to measurements in general least squares fits [2]. As shown within exactly solved model with 2 measurements [1], the anomaly does not exist if

$$\rho_{ij} < \sigma_i / \sigma_j, \quad \text{if } \sigma_i < \sigma_j, \quad (1)$$

where σ_i and σ_j – uncertainties of experimental errors ε_i and ε_j , ρ_{ij} – correlation between ε_i and ε_j . It was demonstrated within the same model with 2 measurements that starting from some value of the correlation a variance of the estimate falls into unphysical range; this value $\rho_0 = \sigma_i / \sigma_j$ can be defined as a *limit correlation*: [3]. Thus, in the simplest model there are 2 features – the systematic bias and inequality (1) – identifying the Peelle's Puzzle effects. These features must be tested in more complicated models (with number of measurements exceeding 2 and non-constant model function) before their application in routine evaluation work. So, a consideration of new models for testing features mentioned above is of prime interest.

Model with non-constant estimated function

Simplest of non-constant model functions is one-parametric stepwise function. Consider 2 measurements y_1 and y_2 of the stepwise function $y(x_1)=z$ and $y(x_2)=rz$ with unknown parameter z . The uncertainties of the measurements are σ_1 and σ_2 . A variance $V(z)$ of the LSM – estimate for z can be written as

$$V(z) = (1 - \rho^2) \frac{\sigma_1^2 \sigma_2^2}{r^2 \sigma_1^2 - 2\rho r \sigma_1 \sigma_2 + \sigma_2^2}. \quad (2)$$

The deviations of the estimate from the measurements are

$$\tilde{z} - y_1 = \frac{\rho\sigma_1\sigma_2 - r\sigma_1^2}{r^2\sigma_1^2 - 2\rho r\sigma_1\sigma_2 + \sigma_2^2} (ry_1 - y_2), \quad (3)$$

$$r\tilde{z} - y_2 = \frac{\sigma_2^2 - \rho r\sigma_1\sigma_2}{r^2\sigma_1^2 - 2\rho r\sigma_1\sigma_2 + \sigma_2^2} (ry_1 - y_2), \quad (4)$$

χ^2 - value:

$$\chi^2 = \frac{(ry_1 - y_2)^2}{r^2\sigma_1^2 - 2\rho r\sigma_1\sigma_2 + \sigma_2^2} \quad (5)$$

Define ratios $r = y(x_2)/y(x_1)$, σ_2 / σ_1 as parameters of the shape for stepwise function and uncertainties respectively. In Fig.1 the *limit correlation* is given in dependence on ratio of shape's parameters.

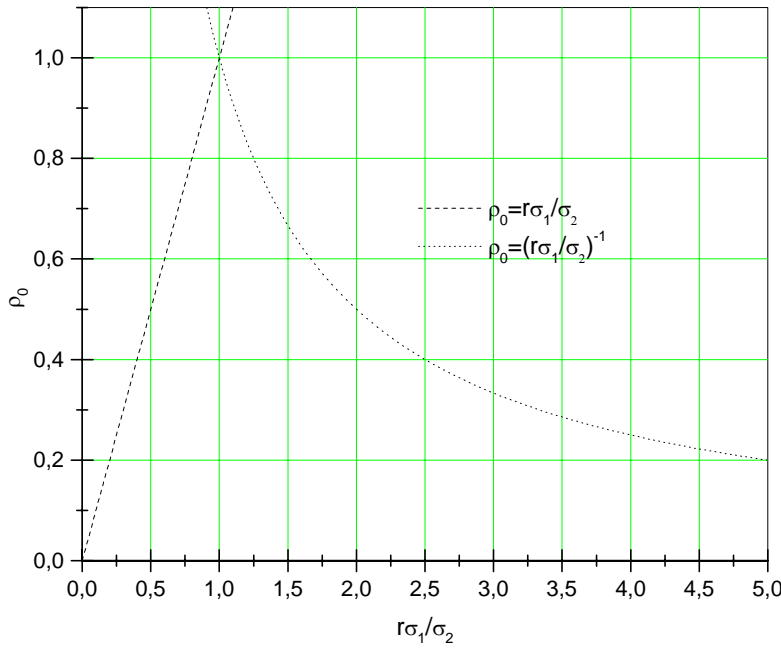


Fig.1 *Limit correlation* in dependence on ratio of shape's parameters of stepwise function ($r = y(x_2)/y(x_1)$) and experimental uncertainties (σ_2 / σ_1) in case $\sigma_2 > \sigma_1$.

As seen, Peelle's Puzzle is not observable at

$$\rho < \rho_0 = (y(x_2)/y(x_1)) / (\sigma_2 / \sigma_1) \quad (6)$$

The Peelle's Puzzle doesn't exist only in case when shape's parameters equal each other ($r / (\sigma_2 / \sigma_1) = 1$).

Note that last inequality is transformed into restriction (1) if model function is a constant. So, inequality (6) is a generalized one.

The inequality (6) can be rewritten in following form

$$\rho < \rho_0 = (\sigma_1 / y(x_1)) / (\sigma_2 / y(x_2)) \quad (7)$$

Thus, the inequality (6) imposes restriction on the experimental uncertainties in relative units whereas the inequality (1) – on the uncertainties in absolute units. As follows from the expression (7) the Peelle's Puzzle is absent in processing measurements with constant relative (to approximant's value) uncertainties.

Model with constant estimated function and 3 measurements

Consider exactly solved model with constant function estimated on the basis of 3 measurements. Similar model with 2 measurements is rather simple. Adding even 1 measurement complicates model essentially, since an estimate and their statistical characteristics are functions of several variables.

Let y_1, y_2, y_3 – three measurements of unknown mean. A covariance matrix of experimental errors has following form

$$V(\rho_1, \rho_2, \rho_3) = \begin{pmatrix} \sigma_1^2 & \rho_1 \sigma_1 \sigma_2 & \rho_3 \sigma_1 \sigma_3 \\ \rho_1 \sigma_1 \sigma_2 & \sigma_2^2 & \rho_2 \sigma_2 \sigma_3 \\ \rho_3 \sigma_1 \sigma_3 & \rho_2 \sigma_2 \sigma_3 & \sigma_3^2 \end{pmatrix} \quad (8)$$

Its inverse matrix is

$$V^{-1}(\rho_1, \rho_2, \rho_3) = \frac{1}{F} \begin{pmatrix} \frac{1 - \rho_2^2}{\sigma_1^2} & \frac{\rho_2 \rho_3 - \rho_1}{\sigma_1 \sigma_2} & \frac{\rho_1 \rho_2 - \rho_3}{\sigma_1 \sigma_3} \\ \frac{\rho_2 \rho_3 - \rho_1}{\sigma_1 \sigma_2} & \frac{1 - \rho_3^2}{\sigma_2^2} & \frac{\rho_1 \rho_3 - \rho_2}{\sigma_2 \sigma_3} \\ \frac{\rho_1 \rho_2 - \rho_3}{\sigma_1 \sigma_3} & \frac{\rho_1 \rho_3 - \rho_2}{\sigma_2 \sigma_3} & \frac{1 - \rho_1^2}{\sigma_3^2} \end{pmatrix} \quad (9)$$

where $F = 1 - \rho_1^2 - \rho_2^2 - \rho_3^2 + 2\rho_1\rho_2\rho_3$.

An informational matrix can be written as

$$I = \sum_{i,j} (V^{-1})_{ij} = \frac{1}{F} \left[\frac{1 - \rho_2^2}{\sigma_1^2} + \frac{1 - \rho_3^2}{\sigma_2^2} + \frac{1 - \rho_1^2}{\sigma_3^2} + 2 \left(\frac{\rho_2 \rho_3 - \rho_1}{\sigma_1 \sigma_2} + \frac{\rho_1 \rho_2 - \rho_3}{\sigma_1 \sigma_3} + \frac{\rho_1 \rho_3 - \rho_2}{\sigma_2 \sigma_3} \right) \right] = \frac{G}{F} \quad (10)$$

Correspondingly, a variance of the estimate θ equals to

$$W(\theta, \rho_1, \rho_2, \rho_3) = \frac{F}{G} \quad (11)$$

The derivatives of W relative to the correlations are rather cumbersome. So, we present an expression only for the derivative of W relative to ρ_1 :

$$\frac{\partial W}{\partial \rho_1} = (-\rho_1 + \rho_2 \rho_3)G - \left(-\frac{\rho_1}{\sigma_3^2} - \frac{1}{\sigma_1 \sigma_2} + \frac{\rho_2}{\sigma_1 \sigma_3} + \frac{\rho_3}{\sigma_2 \sigma_3} \right) F \quad (12)$$

Let $\sigma_1 < \sigma_2 < \sigma_3$. Substituting the values of correlations $\tilde{\rho}_1 = \sigma_1 / \sigma_2$, $\tilde{\rho}_2 = \sigma_2 / \sigma_3$,

$\tilde{\rho}_3 = \sigma_1 / \sigma_3$ in the derivatives $\frac{\partial W}{\partial \rho_i}, i=1,2,3$ check directly that the derivatives equal to 0.

Thus, set of correlations $(\tilde{\rho}_1, \tilde{\rho}_2, \tilde{\rho}_3)$ provides maximum value for the variance of the estimate. Sets of correlations with values lower than $(\tilde{\rho}_1, \tilde{\rho}_2, \tilde{\rho}_3)$ exclude an existence of the Peelle's Puzzle. Note, that inverse statement is not correct.

Summary

1. The *generalized* inequality which signals on the absence of the Peelle's Puzzle is deduced in model with non-constant model function and 2 measurements. The *generalized* inequality imposes restriction on *relative* (to approximant's value) uncertainties. It is transformed in already known inequality in case constant estimated function.
2. It is shown in the model with 3 measurements and constant estimated function that *generalized* inequality provides necessary (not sufficient) condition for absence of the Peelle's Puzzle.

References

1. S.Chiba, D.L.Smith, "A Suggested Procedure for Resolving an Anomaly in Least Squares Data Analysis Known as Peelle's Pertinent Puzzle and the General Implications for Nuclear Data Evaluation", ANL/NDM-121, ANL, USA, 1991.
2. R.W.Peelle, "Peelle's Pertinent Puzzle", Informal memorandum dated October 13, 1987, Oak Ridge National Laboratory, Oak Ridge, USA, 1987.
3. S.A.Badikov, E.V.Gai, "Some Sources of the Underestimation of Evaluated Cross Section Uncertainties", Summary Report of the First Research Co-ordination Meeting on Improvement of the Standard Cross Sections for Light Elements, Prepared by A.D.Carlson, G.M.Hale and V.G.Pronyaev, p.117, Report INDC(NDS)-438, IAEA, 2003.

On the evaluation of a quantity formulated with raw data in quotient form

Soo-Youl Oh
February 2004

Abstract

This note presents the analytical posterior probability density function (pdf) for a derived quantity that is formulated in quotient form with independent random variables such that $Z=X/Y$ with raw, random data X and Y . It is shown, even though not surprising, that the mean of Z as well as its variance computed with the pdf differs from the estimates from the law of error propagation. For resolving the Peelle's Pertinent Puzzle, as Froehner pointed out, it is suggested to begin the evaluation with the joint pdf for raw data, instead of dealing with the derived quantity. However, a task remains how to retrieve or guess the information lost during the data reduction. On the other hand, proposed is a Monte-Carlo method that might be useful for evaluating a derived quantity for which the pdf is not or hardly derived analytically from the joint pdf for raw data.

1. Introduction

Among several methods for resolving the Peelle's Pertinent Puzzle (PPP), the method dealing with the probability density function (pdf) seems to have the firmest theoretical basis. Smith's Bayesian approach[1] and Froehner's interpretation such that the PPP is due to non-linearity[2] begins, respectively, with the joint pdf for the raw variables a and c , where there are two independent measured data a_1 ($=1.5\pm 0.15$) and a_2 ($=1.0\pm 0.10$) and one common normalization factor c_0 ($=1.0\pm 0.20$). Even though their estimates are different from each other (Smith's 1.21 ± 0.29 vs. Froehner's 1.15 ± 0.25), the basic idea in both approaches is exactly the same. The difference stems from the form of the normalization, *i.e.* Smith's quantity under evaluation is $z = a/c$ while Froehner's is $z = a \times c$.

This note is intended to demonstrate an evaluation with a rather explicit pdf for a derived (or "reduced" in other word) quantity in the quotient form, $Z=X/Y$. The posterior pdf, $p(z)$, for the derived quantity has been analytically derived which the mean and standard deviation of Z are computed by weighting with. Actually, utilizing the analytical pdf to the PPP just reproduces the Smith's Bayesian result, and the argument on the limited applicability of the law of error propagation of the first order is neither new nor surprising. The argument, however, reminds the importance of dealing with the raw data. It might be the clue for an answer to the question: Is it valuable enough to try to retrieve some lost information during the data reduction or will we treat the derived quantity as it is?

On the other hand, this note provides an idea of the Monte-Carlo evaluation for a derived quantity for which the pdf is not or hardly derived analytically from the joint pdf for raw data. Some numerical results for several nonlinear functions suggest the feasibility.

2. Posterior pdf of Z, Z=X/Y

Problem

The problem we are dealing with is: Estimate the mean and standard deviation of Z, $Z = X/Y$, where X and Y are the mutually independent random samples from the normal distribution

$$X \sim N(\mu_x, \sigma_x^2) \text{ and } Y \sim N(\mu_y, \sigma_y^2).$$

Note that, from the information theory, the normal distribution is the most objective choice as the pdf when the available knowledge includes both the mean value and its uncertainty.

Derivation of the pdf, p(z)

The joint pdf for mutually independent X and Y is written as

$$p(x, y) = p(x)p(y) = \frac{1}{2\pi \sigma_x \sigma_y} \exp\left\{-\frac{(x - \mu_x)^2}{2\sigma_x^2} - \frac{(y - \mu_y)^2}{2\sigma_y^2}\right\}. \quad (1)$$

We introduce an additional parameter W, that will disappear later, such that $W = Y$. For the variable transformation from (x,y) to (z,w), the Jacobian J is obtained as

$$J = \begin{vmatrix} \partial z/\partial x & \partial z/\partial y \\ \partial w/\partial x & \partial w/\partial y \end{vmatrix} = \begin{vmatrix} \frac{1}{y} & -\frac{x}{y^2} \\ 0 & 1 \end{vmatrix} = \frac{1}{y}. \quad (2)$$

With x and y which are replaced by zw and w, respectively, $p(z,w)$ is represented as

$$p(z, w) = \frac{p(x, y)}{|J|} = |y| p(x, y) = |w| \frac{1}{2\pi \sigma_x \sigma_y} \exp\left\{-\frac{(zw - \mu_x)^2}{2\sigma_x^2} - \frac{(w - \mu_y)^2}{2\sigma_y^2}\right\}.$$

Then $p(z)$ as a marginal pdf is obtained by

$$\begin{aligned} p(z) &= \int_{-\infty}^{\infty} p(z, w) dw \\ &= \frac{e^{-C}}{2\pi \sigma_x \sigma_y A} \left\{ 1 + B \sqrt{\frac{\pi}{A}} e^{\frac{B^2}{A}} \operatorname{erf}\left(\frac{B}{\sqrt{A}}\right) \right\} \end{aligned}$$

where

$$A = \frac{1}{2} \left(\frac{z^2}{\sigma_x^2} + \frac{1}{\sigma_y^2} \right), \quad B = \frac{1}{2} \left(\frac{z\mu_x}{\sigma_x^2} + \frac{\mu_y}{\sigma_y^2} \right), \text{ and } C = \frac{1}{2} \left(\frac{\mu_x^2}{\sigma_x^2} + \frac{\mu_y^2}{\sigma_y^2} \right). \quad (3)$$

With a large C (e.g. with small fractional standard deviations σ_x/μ_x and/or σ_y/μ_y), following form is better for the numerical computation:

$$p(z) = \frac{e^{-C}}{2\pi \sigma_x \sigma_y A} + \frac{B}{2\pi \sigma_x \sigma_y A} \sqrt{\frac{\pi}{A}} e^{-C + \frac{B^2}{A}} \operatorname{erf}\left(\frac{B}{\sqrt{A}}\right). \quad (4)$$

A special case (Cauchy pdf)

For $X \sim N(0,1)$ and $Y \sim N(0,1)$, $A = (z^2 + 1)/2$ and $B = C = 0$. Then

$$p(z) = \frac{1}{\pi(z^2 + 1)}$$

that is the Cauchy distribution.

A numerical example

Suppose $X \sim N(1.5, 0.15^2)$ and $Y \sim N(1.0, 0.2^2)$. Then, the pdf of $Z = X/Y$ is shown in solid curve in Fig. 1. The dotted line is the Gaussian pdf of $N(1.50, 0.335^2)$.

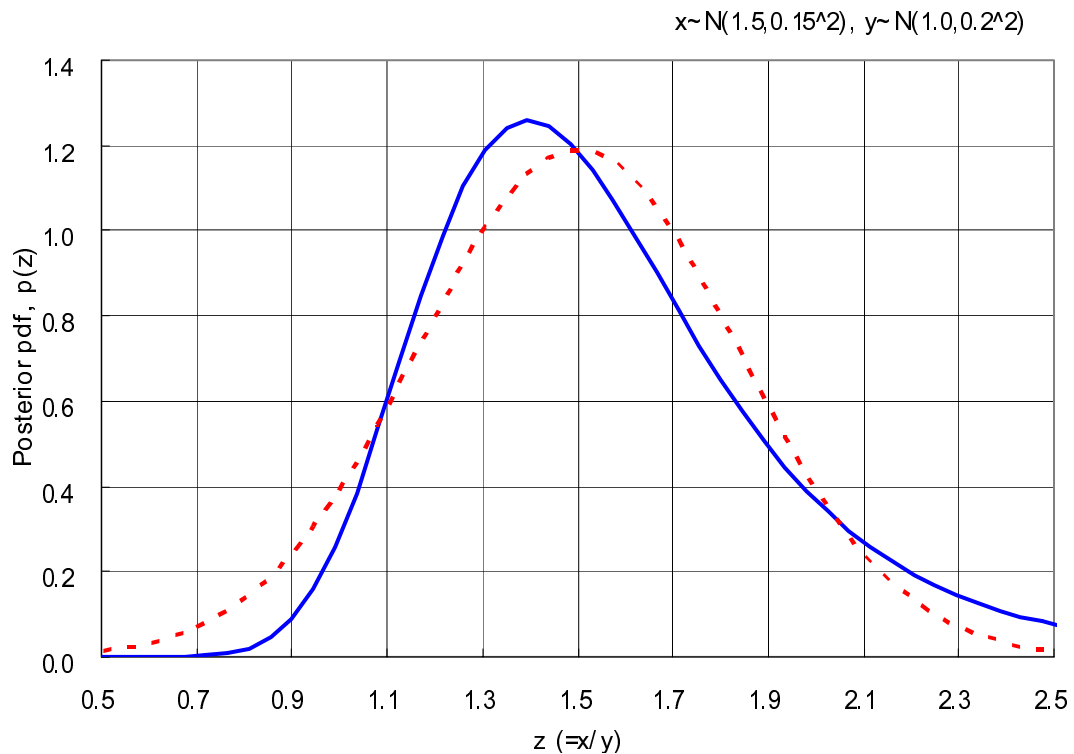


Fig. 1. The probability density function of $Z, Z=X/Y$

It is observed that the pdf is skewed toward smaller z . The mean value of z and its standard deviation are obtained from numerical integrations:

$$\langle z \rangle = \int_0^{10} z p(z) dz = 1.569 \quad \text{and} \quad \sigma_z^2 = \int_0^{10} z^2 p(z) dz - \langle z \rangle^2 = 0.403^2 \quad \text{with} \quad \int_0^{10} p(z) dz = 1.000.$$

These are different from the usual estimates from the law of error propagation with the first order approximation such that

$$\langle z \rangle = \mu_x / \mu_y = 1.500 \quad \text{and} \quad \sigma_z^2 = \langle z \rangle^2 \left(\frac{\sigma_x^2}{\mu_x^2} + \frac{\sigma_y^2}{\mu_y^2} \right) = 0.335^2.$$

Concerning the mean value, even a second or higher order approximation may not result in an estimate close to that of semi-analytic (*i.e.*, analytical $p(z)$), but numerical integration for the mean and standard deviation of z) since the law of error propagation supposes

$$\mu_y = f(\mu_1, \mu_2, \dots, \mu_n)$$

for an arbitrary function Y , $Y = f(X_1, X_2, \dots, X_n)$, of independent random variables X_i 's of which mean values are μ_i 's.

It is also noticed that the semi-analytical standard deviation σ_z is larger than that from the first order law of error propagation.

Meanwhile, Table 1 below shows how the standard deviations σ_x and σ_y affect the values of $\langle z \rangle$ and σ_z . The $\langle z \rangle$ from the semi-analytical estimation is affected by σ_y , but not by σ_x .¹

Table 1. The mean and standard deviation of Z , $Z=X/Y$

μ_x	μ_y	σ_x	σ_y	Semi-Analytical		Law of error propagation, 1 st order	
				$\langle z \rangle$	σ_z	$\langle z \rangle$	σ_z
1.50	1.00	0.15	0.20	1.569	0.403	1.500	0.335
		0.015	0.20	1.569	0.369	1.500	0.300
		0.15	0.10	1.516	0.218	1.500	0.212
		0.015	0.10	1.516	0.157	1.500	0.151
		0.15	0.01	1.500	0.151	1.500	0.151
		0.015	0.01	1.500	0.021	1.500	0.021

In fact, it is neither new nor surprising that the result with an explicit pdf differs from that from the law error propagation of the first order. It is discussed in, for instance, Arras' report[3] under what conditions the law is good one. The point is as follows. In a non-linear data reduction from raw data, the law of error propagation may not be appropriate if the uncertainties of raw data that cause the non-linearity (the raw data Y in the above example) are large. This point is well described in Section XII of Ref. 2.

3. Pdf of the quantity in the Peelle's Puzzle

There are two independent measurements of a , namely, $a_1 \pm \sigma_1$ and $a_2 \pm \sigma_2$. On the other hand, c has been measured only once, with the result of $c_0 \pm \sigma_0$. The task is to find a best estimate of z , $z = a/c$.

From the Bayes' theorem, the posterior pdf is obtained as

$$p(a, c | a_1, \sigma_1, a_2, \sigma_2, c_0, \sigma_0) \propto \exp \left\{ -\frac{(a - a_1)^2}{2\sigma_1^2} - \frac{(a - a_2)^2}{2\sigma_2^2} - \frac{(c - c_0)^2}{2\sigma_0^2} \right\}.$$

Re-arranging the argument of the exponential term results in

¹ For $Z=X/Y$, where X and Y obeys the normal distribution, respectively, the mean value is approximated as

$$\langle z \rangle = \langle x \rangle \cdot \left\langle \frac{1}{y} \right\rangle \approx \frac{\langle x \rangle}{\langle y \rangle} \left(1 + \frac{\sigma_y^2}{\langle y \rangle^2} \right)$$

for a small fractional standard deviation[4].

$$p(a, c | \bar{a}, \sigma_a, c_0, \sigma_0) = K' \exp \left\{ -\frac{(a - \bar{a})^2}{2\sigma_a^2} - \frac{(c - c_0)^2}{2\sigma_0^2} \right\},$$

where

$$\bar{a} = \frac{(a_1/\sigma_1^2 + a_2/\sigma_2^2)}{(1/\sigma_1^2 + 1/\sigma_2^2)} \quad \text{and} \quad \sigma_a^2 = \frac{1}{(1/\sigma_1^2 + 1/\sigma_2^2)}.$$

What we want is $p(z | \bar{a}, \sigma_a, c_0, \sigma_0) \equiv p(z | D)$, and it is readily obtained from Eq. (4):

$$p(z | D) = \frac{K' e^{-C'}}{A'} + \frac{K' B'}{A'} \sqrt{\frac{\pi}{A'}} e^{-C' + \frac{B'^2}{A'}} \operatorname{erf} \left(\frac{B'}{\sqrt{A'}} \right), \quad (4')$$

where

$$A' = \frac{1}{2} \left(\frac{z^2}{\sigma_a^2} + \frac{1}{\sigma_0^2} \right), \quad B' = \frac{1}{2} \left(\frac{\bar{a}z}{\sigma_a^2} + \frac{c_0}{\sigma_0^2} \right), \quad C' = \frac{1}{2} \left(\frac{\bar{a}^2}{\sigma_a^2} + \frac{c_0^2}{\sigma_0^2} \right),$$

and the normalization constant

$$K' = 1 / 2\pi\sigma_a\sigma_0.$$

The pdf in Eq.(4') is quite different from the posterior pdf for reduced data that is the Gaussian distribution as the most objective choice[2, Eq.(96)].

With the values $a_1 = 1.5 \pm 0.15$, $a_2 = 1.0 \pm 0.10$ (thus $\bar{a} = 1.154 \pm 0.083$), and $c_0 = 1.0 \pm 0.2$, the mean value of z and its standard deviation are numerically computed and the results are

$$\langle z \rangle = 1.207 \pm 0.297.$$

This is regarded as the rigorous solution to the PPP[1]. Similar to Fig. 1 already shown, the pdf $p(z|D)$ is skewed toward smaller z , thus the most probable value of 1.072 is smaller than the mean value.

Froehner's solution to the PPP[2] is 1.15 ± 0.25 , but his solution is for z such that $z = a \times c$. The difference between the results of Smith and of Froehner is due to the form of the normalization, which is not clearly revealed in the description of the Puzzle. However, their main points are the same: Dealing with the raw data and their proper pdf's, instead of the data derived (or "reduced" in Froehner's term) from the raw data, is the most rigorous and promising way for resolving the PPP.

4. Monte Carlo simulation of the PPP

Suppose that we are given some information on the raw data but the derived quantity is so complex that no analytical pdf for the derived quantity is available. The Monte Carlo evaluation proposed below might be a useful tool for constructing the pdf numerically.

A primitive computer program was written for the Monte Carlo simulation searching for the solution to the PPP as well as for estimates of some quantities formulated with independent variable(s). The algorithm in the program is as follows.

- 1) Sample a pair of random numbers r and r' from the normal distribution $N(0,1^2)$, respectively, and compute so that $r_1 \leftarrow \bar{a} + r \times \sigma_a$ and $r_2 \leftarrow c_0 + r' \times \sigma_0$.
- 2) Score $z \leftarrow z + r_1/r_2$ and $s \leftarrow s + (r_1/r_2)^2$ for the PPP simulation, or
- 2') Score $z \leftarrow z + f(r_1, r_2)$ and $s \leftarrow s + f^2(r_1, r_2)$ for a derived quantity by the function f .
- 3) Repeat steps 1) and 2) until enough number of sample pairs accumulates.
- 4) Compute $\langle z \rangle \leftarrow z / N_p$ and $\sigma_z^2 \leftarrow s / N_p - \langle z \rangle^2$, where N_p is the number of sample pairs.

With up to 10 million random sample pairs, this MC simulation resulted in the mean and its standard deviation that are same to those in the previous section in five effective digits. In addition, the pdf for z that is constructed in the second step by categorizing per the magnitude of the ratio r_1/r_2 is identical to the analytical pdf.

Meanwhile, the scoring such that $z \leftarrow z + r_1 \times r_2$ reproduced the Froehner's mean and variance, too. Table 2 compares MC estimates, which are regarded as rigorous by utilizing proper pdf's, with those from the first order law of error propagation. In cases of the multiplication ($Z=X*Y$) or addition ($Z=X\pm Y$), the rigorous estimates are same to those from the law of error propagation of the first order.

Table 2. The mean and standard deviation for various derived quantities

Z	Raw data	Monte Carlo estimates	Law of error propagation, 1 st order
1/X	$X \sim N(1.5, 0.15^2)$	0.674 ± 0.070	0.667 ± 0.067
	$X \sim N(1.5, 0.015^2)$	0.667 ± 0.007	0.667 ± 0.007
ln X	$X \sim N(1.5, 0.15^2)$	0.401 ± 0.101	0.406 ± 0.100
	$X \sim N(1.5, 0.015^2)$	0.405 ± 0.010	0.406 ± 0.010
$X*Y$	$X \sim N(1.5, 0.15^2)$ $Y \sim N(1.0, 0.20^2)$	1.500 ± 0.336	1.500 ± 0.335
X/Y	$X \sim N(1.5, 0.15^2)$ $Y \sim N(1.0, 0.20^2)$	1.569 ± 0.403	1.500 ± 0.335

This MC approach does not need any analytical pdf for a derived (reduced) quantity. In spite of its disadvantage such that some information (or guess) on the “raw” data is required, the approach seems to be valuable to explore more.

5. Summary and remark

In this note, presented are

- an analytical probability density function for a derived (or reduced) quantity Z in quotient form of independent raw data X and Y such that $Z = X/Y$,
- reproduction of a numerical solution to the PPP utilizing the pdf and discussion on the limited applicability of the law of error propagation, and
- an idea of Monte Carlo evaluation.

Still a question remains. When we face correlated data under the evaluation, it is seldom identified explicitly the origin(s) of the correlation such as, for instance, the normalization in quotient form. In this case, shall we guess the origin of the correlation and then deal with reconstructed raw data, or shall we directly deal with the reduced data while accepting the danger of the PPP? Then, if we take the former option, how we can do it?

If we can find out a ‘proper’ covariance matrix \mathbf{V}_z for the derived (reduced) variable, with which the Gaussian pdf results in the same estimates to those with the (skewed) pdf derived from the joint pdf’s for raw data, we may deal with derived data.² Usually we compute \mathbf{V}_z using the law of error propagation, but it has been shown that such a covariance matrix causes the PPP[for instance, 2].

References

1. D. L. Smith, Probability, Statistics, and Data Uncertainties in Nuclear Science and Technology, OECD NEA, Published by American Nuclear Society, Inc., p.206 (1991).
2. F. H. Froehner, “Assigning Uncertainties to Scientific Data,” *Nucl. Sci. Eng.*, **126**, 1 (1997).
3. K. O. Arras, “An Introduction to Error Propagation: Derivation, Meaning and Examples of Equation $C_Y = F_X C_X F_X^T$,” EPFL-ASL-TR-98-01 R3, Swiss Federal Institute of Technology Lausanne (EPFL) (1998).
4. F. H. Froehner, private communication, Forschungszentrum Karlsruhe (Feb. 2004).

² In the case of the PPP, the maximum entropy posterior pdf (for uniform prior) is the Gaussian such that

$$p(z | z_1, z_2, \mathbf{V}_z) \propto \exp \left\{ -\frac{1}{2} \begin{pmatrix} z_1 - z \\ z_2 - z \end{pmatrix}^t \cdot \mathbf{V}_z^{-1} \cdot \begin{pmatrix} z_1 - z \\ z_2 - z \end{pmatrix} \right\},$$

where $z_1 = a_1/c_0$ and $z_2 = a_2/c_0$. The estimates with the above and with the pdf in Eq.(4') shall be the same with a proper \mathbf{V}_z (if any).

Attachment:

Multiple Linear Regression Specification:

Given a sample of T observations, the specification can be expressed as

$$\mathbf{y} = \mathbf{X}\boldsymbol{\beta} + \mathbf{e}(\boldsymbol{\beta}), \quad (1)$$

where $\boldsymbol{\beta} = (\beta_1 \beta_2 \cdots \beta_k)'$ is the vector of unknown parameters, \mathbf{y} and \mathbf{X} contains all the observations of the dependent and explanatory variables, i.e.,

$$\mathbf{y} = \begin{bmatrix} y_1 \\ y_2 \\ \vdots \\ y_T \end{bmatrix}, \quad \mathbf{X} = \begin{bmatrix} x_{11} & x_{12} & \cdots & x_{1k} \\ x_{21} & x_{22} & \cdots & x_{2k} \\ \vdots & \vdots & \ddots & \vdots \\ x_{T1} & x_{T2} & \cdots & x_{Tk} \end{bmatrix}$$

where each column of \mathbf{X} contains T observations of an explanatory variable, and $\mathbf{e}(\boldsymbol{\beta})$ is the vector of errors.

Ordinary Least Squares (OLS) estimator:

$$\hat{\boldsymbol{\beta}}_{OLS} = (\mathbf{X}'\mathbf{X})^{-1} \mathbf{X}' \mathbf{y}$$
$$\text{var}(\hat{\boldsymbol{\beta}}_{OLS}) = \sigma_0^2 (\mathbf{X}'\mathbf{X})^{-1}$$

Generalized Least Squares (GLS) estimator:

$$\hat{\boldsymbol{\beta}}_{GLS} = (\mathbf{X}'\mathbf{V}_y^{-1}\mathbf{X})^{-1} \mathbf{X}' \mathbf{V}_y^{-1} \mathbf{y}$$
$$\text{var}(\hat{\boldsymbol{\beta}}_{GLS}) = (\mathbf{X}'\mathbf{V}_y^{-1}\mathbf{X})^{-1}$$

Feasible Generalized Least Squares (FGLS) estimator:

Usually \mathbf{V}_y is unknown, so substituting an estimator $\hat{\mathbf{V}}_T$ for \mathbf{V}_y yields

$$\hat{\boldsymbol{\beta}}_{FGLS} = (\mathbf{X}'\hat{\mathbf{V}}_T^{-1}\mathbf{X})^{-1} \mathbf{X}' \hat{\mathbf{V}}_T^{-1} \mathbf{y}$$

Conditions on data:

[A1] \mathbf{X} is non-stochastic.

[A2] \mathbf{y} is a random vector such that

- (i) $E\{\mathbf{y}\} = \mathbf{X}\boldsymbol{\beta}_0$ for some $\boldsymbol{\beta}_0$;
- (ii) $\text{var}(\mathbf{y}) = \sigma_0^2 \mathbf{I}_T$ for some $\sigma_0^2 > 0$.

[A3] \mathbf{y} is a random vector such that $\mathbf{y} \sim N(\mathbf{X}\boldsymbol{\beta}_0, \sigma_0^2 \mathbf{I}_T)$ for some $\boldsymbol{\beta}_0$ and $\sigma_0^2 > 0$.

[A3'] \mathbf{y} is a random vector such that $\mathbf{y} \sim N(\mathbf{X}\boldsymbol{\beta}_0, \mathbf{V}_y)$, where \mathbf{V}_y is a positive definite matrix.

Gauss-Markov Theorem:

Given the linear specification (1), suppose that [A1] and [A2] hold. Then the OLS estimator $\hat{\beta}_{OLS}$ is the best linear unbiased estimator (BLUE) for β_0 .

Aitken Theorem:

Given the linear specification (1), suppose that [A1] and [A2](i) hold and that $\text{var}(\mathbf{y}) = \mathbf{V}_y$ is a positive definite matrix. Then the GLS estimator $\hat{\beta}_{GLS}$ is the BLUE for β_0 with the variance-covariance matrix $(\mathbf{X}'\mathbf{V}_y^{-1}\mathbf{X})^{-1}$.

Theorem

Given the specification (1), suppose that [A1] and [A3'] hold. Then $\hat{\beta}_{GLS}$ is the BUE for β_0 and $\hat{\beta}_{GLS} \sim N(\beta_0, (\mathbf{X}'\mathbf{V}_y^{-1}\mathbf{X})^{-1})$.

Status of the Experimental Data for the International Standards Evaluation

Second RCM

A.D. Carlson

13 October 2003

Introduction

The database for the ENDF/B-VI standards evaluation was defined in September of 1987. Since that time, many experiments relevant to a new evaluation of the standards have been completed. There are also a large number of experiments that are not finished since data taking is still underway or experimental data are under analysis. Also some of the measurements that were used in the ENDF/B-VI evaluation have been found to need additional corrections, or errors have been found. All of these data can be used to define the changes in the database for the new international evaluation of the neutron cross section standards. The original cutoff date for data that would be used in the evaluation has passed. Unfortunately there are still many experiments that could have an impact on the evaluation that are not completed. Once the process for doing the complete evaluation is established, it should be relatively easy to add additional data sets and re-do the evaluation. Thus since the evaluation is expected to be completed next year, we should be able to accept additional data sets early into 2004. Thus the cutoff date will be extended to early spring of 2004.

Table 1. Neutron Cross Section Standards

Reaction	Proposed energy range
H(n,n)	1 keV to 200 MeV
$^3\text{He}(n,p)$ †	0.0253 eV to 50 keV
$^6\text{Li}(n,t)$	0.0253 eV to 1 MeV
$^{10}\text{B}(n,\alpha)$	0.0253 eV to 1 MeV
$^{10}\text{B}(n,\alpha_1\gamma)$	0.0253 eV to 1 MeV
C(n,n)*	0.0253 eV to 1.8 MeV
Au(n, γ)	0.0253 eV, 0.2 to 2.5 MeV
$^{235}\text{U}(n,f)$	0.0253 eV, 0.15 to 200 MeV
$^{238}\text{U}(n,f)$ ††	Threshold to 200 MeV

In Table 1, the cross section standards to be evaluated are listed. The database also includes data involving the $^{238}\text{U}(n,\gamma)$ and $^{239}\text{Pu}(n,f)$ cross sections. There are many very accurate measurements of these cross sections. The use of these additional data improves the database as a result of ratio measurements of those cross sections to the traditional standards. Also scattering and total cross section data have been included for ^6Li and ^{10}B since they provide information on the standard cross sections. There is a significant increase in the energy range of the database for the standards compared with previous evaluations. No evaluation of the C(n,n) cross section is planned since very little new data have been obtained since the last evaluation and what was obtained is in good agreement with that evaluation.

Database Studies

Work continues on the encouraging, motivating and coordinating of measurements that can be used in the evaluation. Studies of possible experiments for the standards database continues. For each experiment a process is followed that includes checking the documentation for corrections that may need to be made and looking for possible errors or missing information. Poor documentation is a very frequent problem! The investigative procedure can lead to improved estimates of the uncertainties within an experiment and correlations with other experiments. This information is used to assist in forming covariance matrices for the measurements so that a proper analysis can be performed for the evaluation. Additional experiments will to be added as they are found in the literature searches that are underway. Also corrections to new or old experiments will be incorporated in the experimental results. Recently documentation was received from W.P. Poenitz containing corrections and comments concerning experiments used for the GMA database in the ENDF/B-VI standards evaluation. Some effort has been and will be spent looking at that documentation. There is concern about certain experiments used in the ENDF/B-VI evaluation process that had large weight in the evaluation. Investigations are being made of those experiments.

Table 2 lists standards related experiments that have been investigated, at least to some degree. Additional experimental work will be added to this list as they become available. Recent measurements that should have important impact on the evaluations have been done on the H(n,n), ^3He total, $^6\text{Li}(n,t)$, $^{10}\text{B}(n,\alpha)$, $^{235}\text{U}(n,f)$, $^{238}\text{U}(n,f)$ and $^{239}\text{Pu}(n,f)$ cross sections.

Hydrogen Scattering

The most recent measurements of the hydrogen scattering angular distribution are those of Vigdor et al. Since these data have been obtained with high accuracy and are absolute, they can make an important contribution with respect to both the shape and normalization of the hydrogen scattering cross section thereby providing needed information for understanding a discrepancy at back angles. This discrepancy is present at 90 and 162 MeV in measurements by the Uppsala group of the differential H(n,n) cross section that disagree with the evaluated shape given by the Arndt VL40 phase-shift solution. The Arndt evaluation was accepted by the NEANDC/INDC as a primary standard for cross section measurements in the 20 MeV to 350 MeV range. The Uppsala data have a steeper angular shape at back angles by as much as 10% compared with the VL40 results. This discrepancy has led to large increases in the uncertainty associated with this cross section. The Vigdor et al. data are high accuracy absolute H(n,n) measurements at 200 MeV that ultimately should have about 1% accuracy. They were obtained at Indiana University using tagged neutrons. Some of the experimental data have been analyzed by Sarsour, so that results at about the 5% level are available. The preliminary results suggest better agreement with the Bonner data (and the VL40 solution) than the Uppsala data at back angles. Complicating the issue are the PSI data of Franz et al. at somewhat higher energies that tend to support the Uppsala work. The analysis of the remainder of the Indiana data continues. Final results are expected by the end of this year.

The NIST-Ohio University-LANL collaboration on measurements of the hydrogen scattering angular distribution has begun diagnostic work leading to measurements at 15 MeV neutron energy. It is hoped that these data will be available in time for the

present international evaluation. These data are needed as a result of the reduction in the quality of the database at ~14 MeV since our studies have shown that the measurements of Nakamura, and Shirato near 14 MeV, which had small reported uncertainties, required expanded uncertainties. This NIST-Ohio University-LANL collaboration led to H(n,n) measurements with an average uncertainty of less than 1% at 10 MeV neutron energy (Boukharouba et al.) that resolved a problem with the shape of the angular distribution given by evaluations of this cross section.

³He

Measurements were made by Keith et al. of the ³He total neutron cross with uncertainties of less than 1% for the energy region from 0.1 to 500 eV. They are the most precise measurements of this cross section. The results are in excellent agreement with those of Als-Nielsen & Dietrich (1964) that had very high weight in previous evaluations of the ³He(n,p) standard cross section. The results suggest that the data of Borzakov (1982) that have a reported uncertainty of about 1%, but are lower than the Keith results by about 8%, are in error.

⁶Li(n,t)

Zhang et al. have made the latest measurements of this cross section. The most recent being published in 2003. In separate experiments, data were obtained at 3.67 MeV and 4.42 MeV; and at 1.85 and 2.67 MeV. The data were all obtained with a gridded ionization chamber. Angular distribution measurements were obtained with this detector. The distributions have gaps near 90 degrees in the CMS which require fitting to get the integrated cross section. Corrections must be made to these data to account for the “particle leaking” effect. Particle leaking results when both reaction products are emitted in the forward direction. The particle identification feature which is possible with the gridded chamber treats this as a quasi ⁷Li+α particle. It appears in the pile-up portion of the spectrum and is rejected. Data taken without taking this into account are correct over only a limited angular range. Since particles are lost, the integrated cross section will be lower than the correct value. The magnitude of this correction is not known for the Zhang et al. data.

¹⁰B Standards

The relatively poor ¹⁰B database caused problems with the ENDF/B-VI standards evaluation process. These problems led to appreciable experimental activity on the ¹⁰B(n,α) and ¹⁰B(n,α₁γ) standards since the completion of the ENDF/B-VI standards evaluation. Work was done on the differential cross section for the ¹⁰B(n,α)⁷Li reaction, the branching ratio, the ¹⁰B(n,α₁γ) cross section, the total neutron cross section, and the ¹⁰Be(p,n) reaction. The use of the R-matrix allows all these types of data to be used in helping to define the ¹⁰B(n,α) cross sections.

Differential cross section measurements in the MeV energy region have recently been made by Zhang et al., and Giorganis and Khriachkov using Frisch-gridded ionization chambers. The Zhang et al. data are significantly lower than those of Giorganis and Khriachkov. This is a result of the previously noted “particle leaking” effect. Since particles are lost, the integrated cross section is lower than the correct value. This agrees with the comparison between the Giorganis and Khriachkov, and Zhang et al. data sets. Zhang et al. have decided they can not correct for this effect. They are

planning to re-measure the cross section using a more sophisticated data taking method.

Measurements by Weston and Todd of the branching ratio, (the $^{10}\text{B}(n,\alpha_0\gamma)$ cross section/the $^{10}\text{B}(n,\alpha_1\gamma)$ cross section), are 10 % to 30 % low in the 100 keV to 600 keV energy region compared with the ratios calculated from the ENDF/B-VI cross sections. The data agree with ENDF/B-VI at the lowest and highest energies of the experiment. To check these data, measurements of this ratio have been measured in this energy region by Hamsch and Bax. The measurements of Hamsch and Bax are in better agreement with ENDF/B-VI than the Weston and Todd measurements. Higher values were obtained by Hamsch and Bax in the hundred keV energy region that are expected to be a result of backgrounds which have not been subtracted yet. These data were obtained with a Frisch-gridded ionization chamber and require the particle leaking correction referred to previously. However the ratio should depend only weakly on particle leaking. Also the leaking correction is less at lower neutron energies.

In an NIST/ORNL collaboration, Schrack et al. have made measurements of the shape of the $^{10}\text{B}(n,\alpha_1\gamma)$ cross section from 0.3 MeV to 4.0 MeV neutron energy. The cross sections obtained from this investigation, normalized to the ENDF/B-VI evaluation over the region from 0.2 MeV to 1 MeV, agree with the ENDF/B-VI evaluation below 1.5 MeV. The measured cross sections differ as much as 40 % with the ENDF/B-VI evaluation for neutron energies greater than 1.5 MeV. An additional measurement by this collaboration extended the cross section to lower energies so that better normalization of shape measurements could be made. The measurement covered the neutron energy range from 10 keV to 1 MeV. These data are lower than the ENDF/B-VI shape by about 5 % in the region above 100 keV.

Measurements of the ^{10}B total cross section have been made at the IRMM linac and Van de Graaff facilities. The linac work extends to 730 keV neutron energy. The present results of this work are approximate agreement with ENDF/B-VI below 10 keV, a maximum deviation above ENDF/B-VI of 5% at 100 keV and a maximum deviation below ENDF/B-VI of 7% at 700 keV. These data are under final analysis. The Van de Graaff facility data are lower than ENDF/B-VI by 3-4% at 0.3 and 0.4 MeV, and by 6 to 9% from 0.6 to 1.3 MeV. They agree with that evaluation at 1.7 and 1.9 MeV. These data are expected to be finalized later this year. Wasson et al., in an NIST-ORNL collaboration have also made measurements of the ^{10}B total cross section. These data extend from about 20 keV to 20 MeV using two different flight paths at the ORELA facility. The results of these experiments agree with the ENDF/B-VI evaluation for neutron energies greater than about 2 MeV, but are lower by as much as 4 % between 600 keV and 2 MeV, and are greater by as much as about 5 % below 600 keV. There is generally good agreement among the IRMM linac, IRMM Van de Graaff and NIST-ORNL measurements within the uncertainties. The data sets are still undergoing checks and corrections which are expected to improve the agreement.

Though many of the experiments are preliminary, the lower $^{10}\text{B}(n,\alpha_1\gamma)$ cross sections of Schrack et al., and the higher total cross section work suggest that the Weston and Todd branching ratio data are in error in the hundred keV energy region. The

preliminary branching ratio work of Hamsch and Bax appear to be more consistent with those measurements.

$^{235}\text{U}(\text{n},\text{f})$

The most recent measurements of the $^{235}\text{U}(\text{n},\text{f})$ cross section below 20 MeV are those of Carlson et al., Lisowski et al., and Alkharov et al. These measurements suggest a cross section as much as 5% larger than the ENDF/B-VI evaluation above 14 MeV neutron energy. For the energy region above 20 MeV, very few measurements have been made. The recent work by Nolte et al. is an important contribution since these are the only data other than those of Lisowski et al. in this energy region that have relatively small uncertainties. Except for a data point at 96 MeV, which Nolte et al. suggest may be a normalization problem, there is agreement within the uncertainties with the Lisowski et al. data. Since so many cross sections are being measured relative to the $^{235}\text{U}(\text{n},\text{f})$ cross section, additional corroborative measurements of this important standard should be made.

$^{238}\text{U}(\text{n},\text{f})$

The most recent measurements of the $^{238}\text{U}(\text{n},\text{f})$ cross section in the 10 to 20 MeV energy region, those of Lisowski et al., Merla et al. and Winkler et al., indicate the ENDF/B-VI evaluation is low an average of a few percent from 15 to 20 MeV. Above 20 MeV, the most recent measurements are those of Nolte et al., Shcherbakov et al. and Lisowski et al. The measurements reported by Newhauser et al. required revision. The corrected results from that work have been incorporated into the Nolte work. The Nolte et al. values are consistently higher by as much as 10% than the other measurements between 30 and 100 MeV; but agree at about 14 MeV where the cross section is thought to be well defined. These measurements are being reexamined and possibly new data will be taken to help understand these measurements. There is a difference between the Shcherbakov et al and the Lisowski et al. measurements that is a couple of percent at the lowest energies but becomes more than 5% at the highest energies. Preliminary measurements have been made by Eismont et al. at 22 and 75 MeV neutron energy. These data are low compared with the Lisowski et al. However, they are generally in good agreement with the Lisowski et al. data, within the rather large uncertainties of the Eismont et al. measurements. It may not be possible to reduce the uncertainties on the Eismont et al. data due to the uncertainties in the neutron fluence.

$^{239}\text{Pu}(\text{n},\text{f})$

The most recent measurements of the $^{239}\text{Pu}(\text{n},\text{f})/^{235}\text{U}(\text{n},\text{f})$ cross section ratio are those of Lisowski et al, Staples and Morley, and Shcherbakov et al. The three data sets agree very well up to about 20 MeV neutron energy. Between 20 MeV and 60 MeV neutron energy, the Staples and Morley data are about 4% higher than the Lisowski et al. data. In that same interval the Shcherbakov et al. data increase from 0% to about 2% higher than the Lisowski et al. data. Above 60 MeV neutron energy, the disagreement increases between the Shcherbakov et al. and Lisowski et al. data sets with the Shcherbakov et al. data being almost 10% higher than the Lisowski et al. data set at 200 MeV.

Conclusion

Better measurements and improved methods to handle discrepant data are needed. But working with what is available, the database continues to be prepared for use in the new international evaluation of the neutron cross section standards.

Table 2. New Experiments for the Standards Database

⁺⁺ means the data have been reviewed and are in the library

⁺ means the data are available and the review process is underway

no superscript means that final data are not available

H(n,n)

⁺⁺Nakamura, J. Phys. Soc. Japan 15 (1960) 1359, 14.1 MeV; error in transformation from laboratory to CMS angles; needs correction for proton scattering, an estimate of error associated with neglecting these corrections was made; tail problems; note Table II uncertainty is statistical only (mb/sr).

⁺⁺Shirato, J. Phys. Soc. Japan 36 (1974) 331, 14.1 MeV, needs correction for proton scattering; tail problems.

⁺Ryves, 14.5 MeV, $\sigma(180^\circ)/\sigma(90^\circ)$, Ann. Nucl. Energy 17, 657 (1990).

⁺⁺Buerkle, 14.1 MeV, angular distribution from 89.7° to 155.7°, Few-Body Systems 22, 11 (1997). The angular range is too limited.

⁺⁺Boukharouba, Phys Rev C 65, 014004, 10 MeV, angular distribution from 60° to 180°, additional work planned for 15 MeV.

Uppsala data:

⁺Rönnqvist, Phys Rev C45, R496 (1992), 96 MeV angular distribution from 116° to 180°

⁺Rahm, Phys. Rev. C57, 1077 (1998) 162 MeV, angular distribution from 72° to 180°,

⁺Benck, (Louvain la Neuve), Nucl. Phys. A615, 222 (1997) and Proc. Conf. on NDST, Trieste (1997) p.1265, 28-75 MeV, angular distribution from 40° to 140°. Angular range is too limited.

Vigdor (IUCF) 185-200 MeV, angular distribution from 90° to 180°. Data have been obtained. Sarsour is analyzing the data and has preliminary data at 200 MeV, Private Comm.

³He(n,p)

⁺⁺Borzakov, 0.26 keV to 142 keV, relative to ⁶Li(n,t), Sov. J. Nucl. Phys. 35, 307 (1982). OK

³He total cross section

⁺⁺Keith, 0.1 to 500 eV, BAPS DNP Oct 1997 paper IG.03 and thesis of D. Rich, U of Indiana. OK.

⁶Li(n,t)

⁺NIST collaboration, thermal measurement with high accuracy using cryogenic calorimeter, Private Comm. OK

⁺⁺Knitter, (1983) NS&E 83, 229; ${}^6\text{Li}(n,t){}^4\text{He}$ angular distribution, 0.035-325 keV, new corrections required for particle leaking effect. Giorganis is investigating

⁺⁺Drosg, 0.50 MeV to 4.1 MeV, NIM B94, p.319 (1994), using concept based on the two groups from the source reaction. Set 1011. OK

Bartle, 2 to 14 MeV, angular distribution, Proc. Conf on Nuclear Data for Basic and Applied Science, Sante Fe (1985), p. 1337 (questionable value, due to energy range and information not available).

Schwarz, 1 to 600 keV, NP 63, p.593, some based on hydrogen scattering cross section. Assumptions need study!

Koehler, 1 keV to 2.5 MeV, angular distribution data (ratio of forward and backward hemispheres responses), private comm.

Yu Gledenov, .025 eV, 87KIEV 2 237 (1988) no data given

⁺Guohui Zhang, 3.67 and 4.42 MeV, angular distribution, Comm. Of Nuclear Data Progress No.21 (1999) China Nuclear Data Center, also NSE 134, 312 (2000). Also 1.85 MeV and 2.67 MeV, NSE 143, 86 (2003). Has "particle leaking" effect.

¹⁰**B(n, α γ)**

Maerten, 320 keV to 2.8 MeV, GELINA linac, relative to ${}^{235}\text{U}(n,f)$ and carbon standards, private comm. from H. Weigmann. Not enough information on uncertainties is available.

⁺⁺Schrack, 0.2 MeV to 4 MeV, shape data relative to Black Detector (at ORNL), NSE 114, 352 (1993). Set 113. OK

⁺Schrack, 10 keV to 1 MeV, shape data relative to H(n,n) prop ctr (at ORNL), Proc. Conf. on NDST, Gatlinburg (1994)p. 43. Set 1034 OK

⁺Schrack, .3 MeV to 10 MeV, relative to ${}^{235}\text{U}(n,f)$ ion chamber (at LANL), Private comm. Set 1033 OK

¹⁰**B(n, α) Branching Ratio**

⁺⁺Weston, 0.02 MeV to 1 MeV, Solid State detectors, NSE 109, 113 (1991). Set 1024. May have systematic errors.

⁺⁺Hamsch and Bax, ND2001, 0.04 MeV to 1.0 MeV, Frisch gridded ion chamber, in progress. Set 1015. Background problems

¹⁰**B(n, α)**

Haight, 1 MeV to 6 MeV, angular distribution at 30°, 60°, 90° and 135°, private comm.

Hambusch and Bax, ND2001, keV to MeV, angular distribution, Frisch gridded ion chamber, in progress.

Giorginis and Khriachkov, MeV energies, angular distribution, VdG data. The integrated cross sections are available. Private communication (2003). OK

+Guohui Zhang, 4.17, 5.02, 5.74, 6.52 MeV angular distribution, submitted for publication to NSE. Problems with particle leaking.

¹⁰B total cross section

+Wasson, 0.02 MeV to 20 MeV, NE-110 detector, Proc. Conf. on NDST, Gatlinburg (1994), p. 50. OK

Wattecamps, Van de Graaff, 1 to 18 MeV, large statistical uncertainty, NE-213 detector, Proc. Conf. on NDST, Gatlinburg (1994), p. 47. OK

Plompen, Van de Graaff, 0.3 MeV to 1.9 MeV, NE-213 detector, 3 independent monitors, Proc. Conf. on NDST, Trieste (1997), p. 1283. OK

Brusegan, Linac data, 80 eV to 730 keV, Li-glass detector, Proc. Conf. on NDST, Gatlinburg (1994)p. 47, Proc. Conf. on NDST, Trieste (1997)p. 1283 and private comm. OK

¹⁰Be(p,n) ¹⁰B

Massey, E_p from 1.5 MeV to 4 MeV, data at 0°, private comm. New measurements to be made at lower energies (~.5 MeV). Also possibly ¹⁰Be (p,α). No final data.

C total cross section

+Schmiedmayer and M. C. Moxon, Proc. Conf. Nuclear Data for Science and Technology Mito, Japan, May 30 June 3, 1988, p. 165, 50 eV to 100 keV, linac, excellent agreement with ENDF/B-VI.

+Kirilyuk, *et al.*, Proc. of the Int. Conf. on Neutron Physics, Kiev, 1987, vol. 2, p. 298, filtered beam measurement at 2 keV, very good agreement with ENDF/B-VI.

Au(n,γ)

+Yamamoto, thermal, linac, NEANDC(J)-155,59,9008, 1990. Little impact due to high accuracy of evaluated cross section.

++Tolstikov, 0.49 to 0.69 MeV, Van de Graaff, relative to ²³⁵U(n,f), Yad Konstany,4, 46 (1994). Set 1020. OK.

++Sakamoto, 23 keV and 967 keV, photoneutron source, activation experiment, NSE 109,215 (1991). Set 452. May have systematic error.

++Davletshin, .16 MeV to 1.1 MeV, relative to H(n,n), Sov. J. At. Energy 65, 91 (1988), (Corrected data from Sov. J. At. Energ. 58, 183 (1985)). Two sets 347 & 348. OK

++Davletshin, .62 MeV to .78 MeV, relative to ²³⁵U(n,f), Sov. J. At. Energy 65, 91 (1988). Set 349. OK

⁺⁺Davletshin, .813 MeV to 2.435 MeV, relative to ²³⁵U(n,f) YK,(1), 41 (1992). Set 1018. OK

⁺⁺Davletshin, .37 MeV to 1.0 MeV, relative to ²³⁵U(n,f), YK,(1), 13 (1993). Set 1019 OK

⁺⁺Kazakov, Yad Konstany, 44, 85 (1985); AE,64,(2),152,1988, Van de Graaff, relative to ⁶Li(n,t) .0035 to .105 MeV. Set 1021. OK

⁺⁺Kazakov, Yad Konstany, 44, 85 (1985); AE,64,(2),152,1988, Van de Graaff, relative to ¹⁰B(n, α_1) .115 to .41 MeV set 1022. May have systematic errors

⁺Demekhin, 2.7 MeV, Proc. 36th All Union Conf. on Nuclear Data, p. 94 (1986). No data

⁺⁺Voignier, ~.5 MeV to ~3 MeV, NSE, 93, 43 (1986), long counter, capture gamma spectrometer, private comm. Set 1016. OK

²³⁵U(n,f)

⁺⁺Carlson, 2 MeV to 30 MeV, relative to H(n,n), Proc. Spec. Meeting on Neutron Cross Section Standards for the Energy Region above 20 MeV, Uppsala, Sweden, 1991, Report NEANDC-305, "U", p. 165. Set 524 OK

⁺⁺Merla, ⁺2.6, ⁺4.45, ⁺8.46, ⁺14.7, ⁺18.8 MeV ?, associated particle, Proc. Conf. on NDST Juelich (1991) p.510. Sets 591, 590, 592, 593, 587. OK

⁺⁺Lisowski, 3 MeV to 200 MeV, relative to H(n,n), Proc. Spec. Meeting on Neutron Cross Section Standards for the Energy Region above 20 MeV, Uppsala, Sweden, 1991, Report NEANDC-305, "U", p. 177, and private communication. Set 1028 OK

⁺Nolte, 14 to 150 MeV, ND2001, and Private Comm. to increase energy range, Preliminary data. Concerns about 96 MeV point. Additional work underway

⁺⁺Buleeva, 0.624 MeV to 0.785 MeV, relative to H(n,n), Sov. J. Atomic Energy 65, 930 (1988). Set 522. OK

Grundl comment, ²⁵²Cf spontaneous fission spectrum averaged cross section. NOTE; only the last NIST measurement (Schroder) should be used in the evaluation. The earlier data are improved upon with each new measurement.

⁺⁺Kalinin, 1.88 MeV, 2.37 MeV CCW, associated particle, Sov. J. Atomic Energy 71,(2),181,1988 Set 1026 OK

⁺⁺Carlson, 0.3 MeV to 3 MeV, absolute fluence from black detector, Proc. IAEA Advisory Group Meeting on Nuclear Standard Reference Data, Geel Belgium, p.163, IAEA-TECDOC-335 (1985). Set 523. OK

⁺⁺Johnson, 1 MeV to 6 MeV, absolute fluence from a dual thin scintillator, Proc. Conf. on NDST Mito (1988) p.1037. Set 1025 OK

⁺⁺Iwasaki, 14 MeV (13.5 to 14.9 MeV), relative to H(n,n) and associated particle, Proc. Conf. on NDST Mito (1988) p. 87. Set 1027 OK

⁺⁺Weston and Todd, NSE 111, 415 (1992), relative to ¹⁰B(n,α), 0.15 keV to 1.5 keV. Set 1023 OK

²³⁸U(n,f)

⁺⁺Merla, 5 MeV +, associated particle, Proc. Conf. on NDST Juelich (1991) p.510. Set 810. OK

⁺⁺Winkler, 14.5 MeV, relative to Al(n,α) & ⁵⁶Fe(n,p), Proc. Conf. on NDST Juelich (1991), p.514. Set 809. OK

⁺⁺Lisowski, 0.8 MeV to 357 MeV, relative to H(n,n), Proc. Spec. Meeting on Neutron Cross Section Standards for the Energy Region above 20 MeV, Uppsala, Sweden, 1991, Report NEANDC-305, "U", p. 177, and private communication. Set 1030. OK, possible problems at highest energies compared with Shcherbakov

⁺Nolte, 14 to 150 MeV, ND2001, and Private Comm. to increase energy range, Preliminary data. Concerns about data from 30 MeV to 100 MeV

⁺Newhauser, 34, 46, and 61 MeV MeV, absolute, Proc. Conf. on NDST Juelich (1991), *removed from database*.

⁺Meadows, 14.74 MeV, CCW, ANE,15,421 (1988), relative to ²³⁵U(n,f).

⁺⁺Baba, 4.6 MeV to 6 MeV, Van de Graaff relative to ²³⁵U(n,f), J. Nucl. Sci. & Techn.,26,11 (1989). Set 1035

⁺⁺Shcherbakov, 1-196 MeV, relative to ²³⁵U(n,f), ISTC 609-97, see also Fomichev, 0.7 MeV to 200 MeV, relative to ²³⁵U(n,f), Proc. Conf. on NDST, Trieste (1997), p.1283, also ND2001 set 1013. OK except possibly at the highest energies (inconsistent with Lisowski there)

⁺Li Jingwen, 14.7 MeV, CCW, ratio to ²³⁵U(n,f) CNP,11,(3),17,89.

Eismont, Trieste conf, p.494, 33.7, 46 and 60.6 MeV, relative to hydrogen scattering cross section. See also Gatlinburg conference results at 135 and 160 MeV. Data not finalized. They have concerns about neutron fluence determination for getting smaller uncertainty.

⁺Garlea, 14.7 MeV, relative to ²³⁵U(n,f) cross section, RRP,37,(1),19,92.

²³⁸U(n,γ)

⁺Corvi. Thermal range, linac, Mito conf (1988).

⁺Macklin, linac, 1 to 100 keV, ANE,18,567,91, relative to ⁶Li(n,t) cross section.

⁺Kazakov, Yad Konstany, 37, (1986); Van de Graaff, 4-440 keV, liquid scintillator, VDG.

⁺⁺Kobayashi, 0.024 MeV, 0.055 MeV, 0.146 MeV, relative to $^{10}\text{B}(n,\alpha_1\gamma)$, Proc. Conf. on NDST Juelich (1991), p. 65. Set 448 OK

⁺⁺Quang, 23 keV and 964 keV, photoneutron source, activation experiment, NSE 110, 282 (1992). Set 453 OK except point at 964 may have systematic error.

⁺⁺Adamchuck, 150 eV to 45 keV, relative to $^{10}\text{B}(n,\alpha_1\gamma)$, J. Atomic Energy, 65, 920 (1989). Set 446 OK

⁺⁺Buleeva (Davletshin), 0.34 MeV to 1.39 MeV, relative to H(n,n), Sov. J. Atomic Energy, 65, 930 (1989). Set 436 OK except possible systematic errors at highest energies. Also 0.62 MeV and 0.78 MeV relative to Au(n, γ) Set 437 OK

⁺⁺Voignier, ~0.5 to 1.1 MeV, NSE,93,43 (1986), capture gamma spectrometer, long counter, Van de Graaff. Set 1017 Method gives large uncertainties.

²³⁹Pu(n,f)

⁺⁺Weston, linac, 0.15 keV to 15 keV, fission chamber, $^{10}\text{B}(n,\alpha)$ standard, NSE 111,415 (1992). Set 1024 OK

⁺⁺Merla, 4.9, 8.65, 14.7 and 18.8 MeV, associated particle, Proc. Conf. on NDST Juelich (1991) p.510; see also Alkhazov, YK,1986,(4),19,198612. Sets 611, 617, 615, and 616. OK

⁺Meadows, 14.74 MeV, CCW, ANE,15,421,8808, relative to $^{235}\text{U}(n,f)$.

⁺Shcherbakov, 0.6-196 MeV, relative to $^{235}\text{U}(n,f)$, ISTC 609-97 (2000). Set 1012. OK but problems at high energy compared with Lisowski.

⁺Staples, 0.8 MeV to 62 MeV, relative to $^{235}\text{U}(n,f)$, NSE 129, 149 (1998). Set 1014. OK except differences compared with Lisowski and Shcherbakov at highest energies.

⁺Lisowski, 0.5 MeV to 256 MeV, relative to H(n,n) and $^{235}\text{U}(n,f)$, Proc. Spec. Meeting on Neutron Cross Section Standards for the Energy Region above 20 MeV, Uppsala, Sweden, 1991, Report NEANDC-305, "U". Set 1029 OK problems at highest energies compared with Shcherbakov

⁺⁺Garlea, 14.7 MeV, relative to $^{235}\text{U}(n,f)$ cross section, RRP,37,(1),19,92. Set 633 Value is high

**STATUS OF THE DATABASE
FOR THE
NEW INTERNATIONAL EVALUATION
OF THE
NEUTRON CROSS SECTION STANDARDS**

**Allan D. Carlson
Ionizing Radiation Division
National Institute of Standards and Technology**

**Presented at the
Second Research Coordination Meeting
on
Improvement of the Standard Cross Sections**

**NIST
Gaithersburg, MD
October 13-17, 2003**



**If an experiment requires statistical analysis
to establish a result,
Then one should do a better experiment.**

Ernest Rutherford (1871-1937)

English Physicist

Nobel prize for chemistry, 1908

Table 1. Neutron Cross Section Standards

Reaction	Proposed energy range
H(n,n)	1 keV to 200 MeV
$^3\text{He}(n,p)^\dagger$	0.0253 eV to 50 keV
$^6\text{Li}(n,t)$	0.0253 eV to 1 MeV
$^{10}\text{B}(n,\alpha)$	0.0253 eV to 1 MeV
$^{10}\text{B}(n,\alpha_1\gamma)$	0.0253 eV to 1 MeV
$\text{C}(n,n)^*$	0.0253 eV to 1.8 MeV
$\text{Au}(n,\gamma)$	0.0253 eV, 0.2 to 2.5 MeV
$^{235}\text{U}(n,f)$	0.0253 eV, 0.15 to 200 MeV
$^{238}\text{U}(n,f)^\dagger\dagger$	Threshold to 200 MeV

H(n,n)

⁺⁺Nakamura, J. Phys. Soc. Japan 15 (1960) 1359, 14.1 MeV; error in transformation from laboratory to CMS angles; needs correction for proton scattering, an estimate of error associated with neglecting these corrections was made; tail problems; note Table II uncertainty is statistical only (mb/sr).

⁺⁺Shirato, J. Phys. Soc. Japan 36 (1974) 331, 14.1 MeV, needs correction for proton scattering; tail problems.

⁺Ryves, 14.5 MeV, $\sigma(180^\circ)/\sigma(90^\circ)$, Ann. Nucl. Energy 17, 657 (1990).

⁺⁺Buerkle, 14.1 MeV, angular distribution from 89.7° to 155.7° , Few-Body Systems 22, 11 (1997).

The angular range is too limited.

⁺⁺Boukharouba, Phys Rev C 65, 014004, 10 MeV, angular distribution from 60° to 180° , additional work planned for 15 MeV.

Uppsala data:

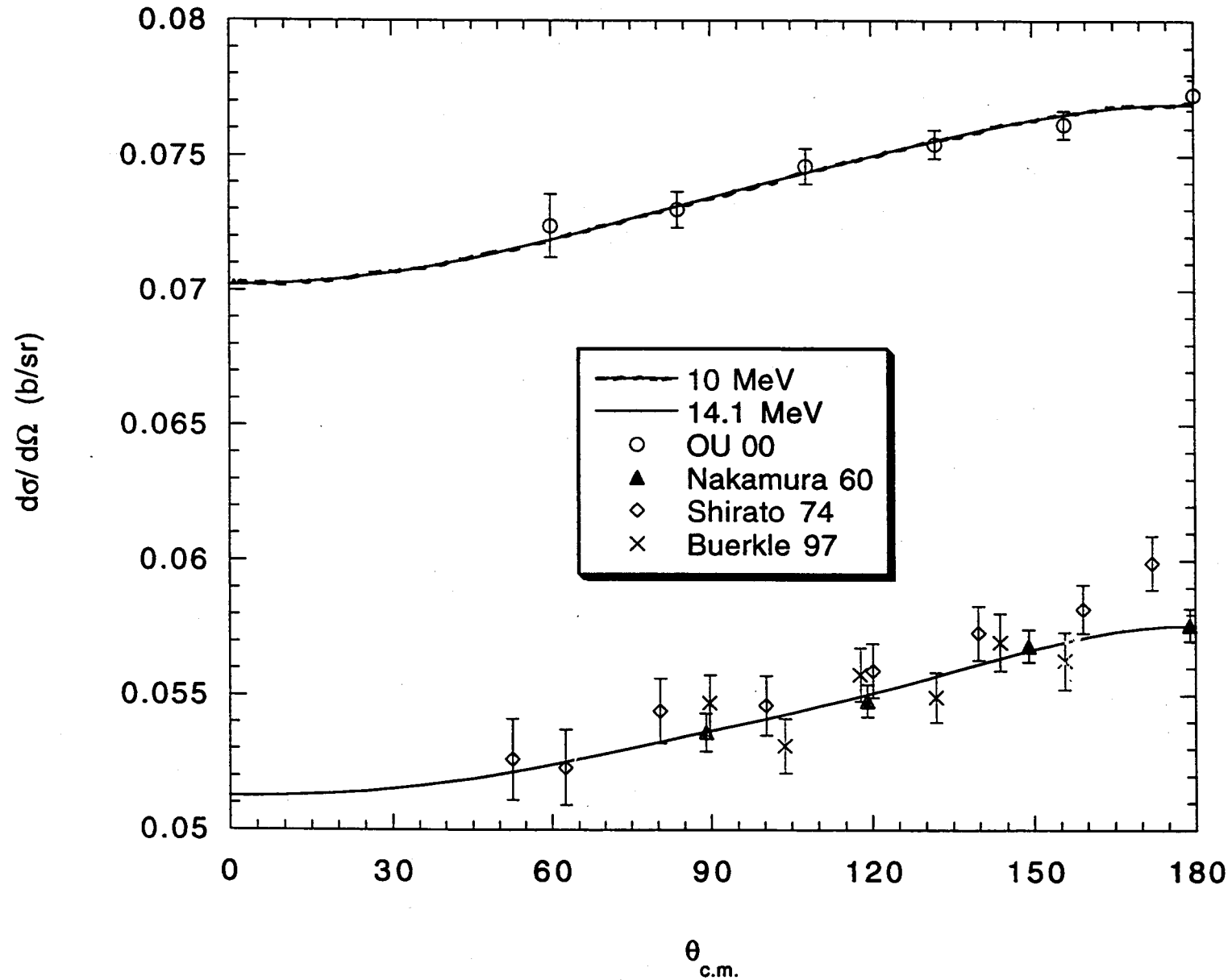
⁺Rönnqvist, Phys Rev C45, R496 (1992), 96 MeV angular distribution from 116° to 180°

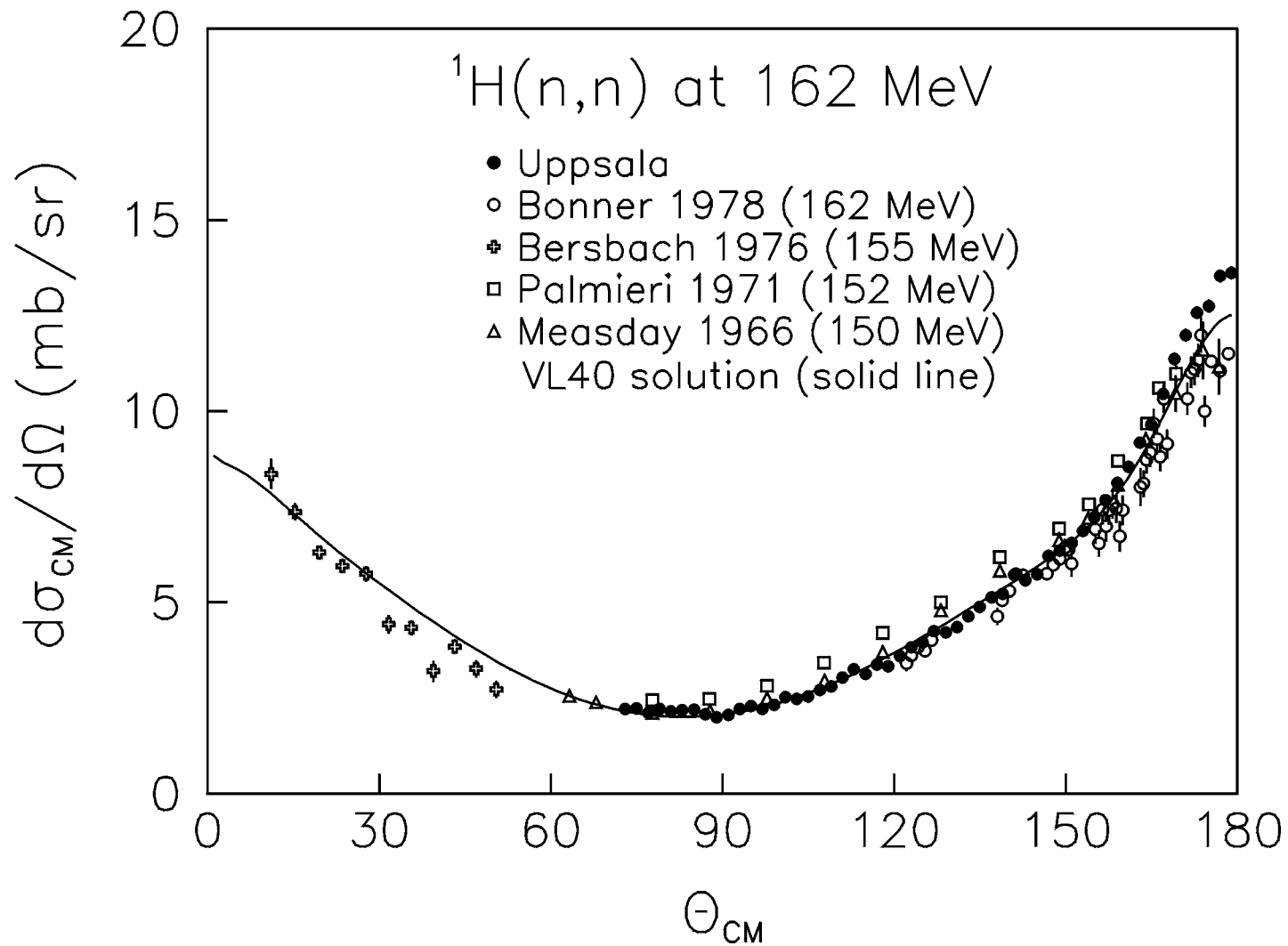
⁺Rahm, Phys. Rev. C57, 1077 (1998) 162 MeV, angular distribution from 72° to 180° ,

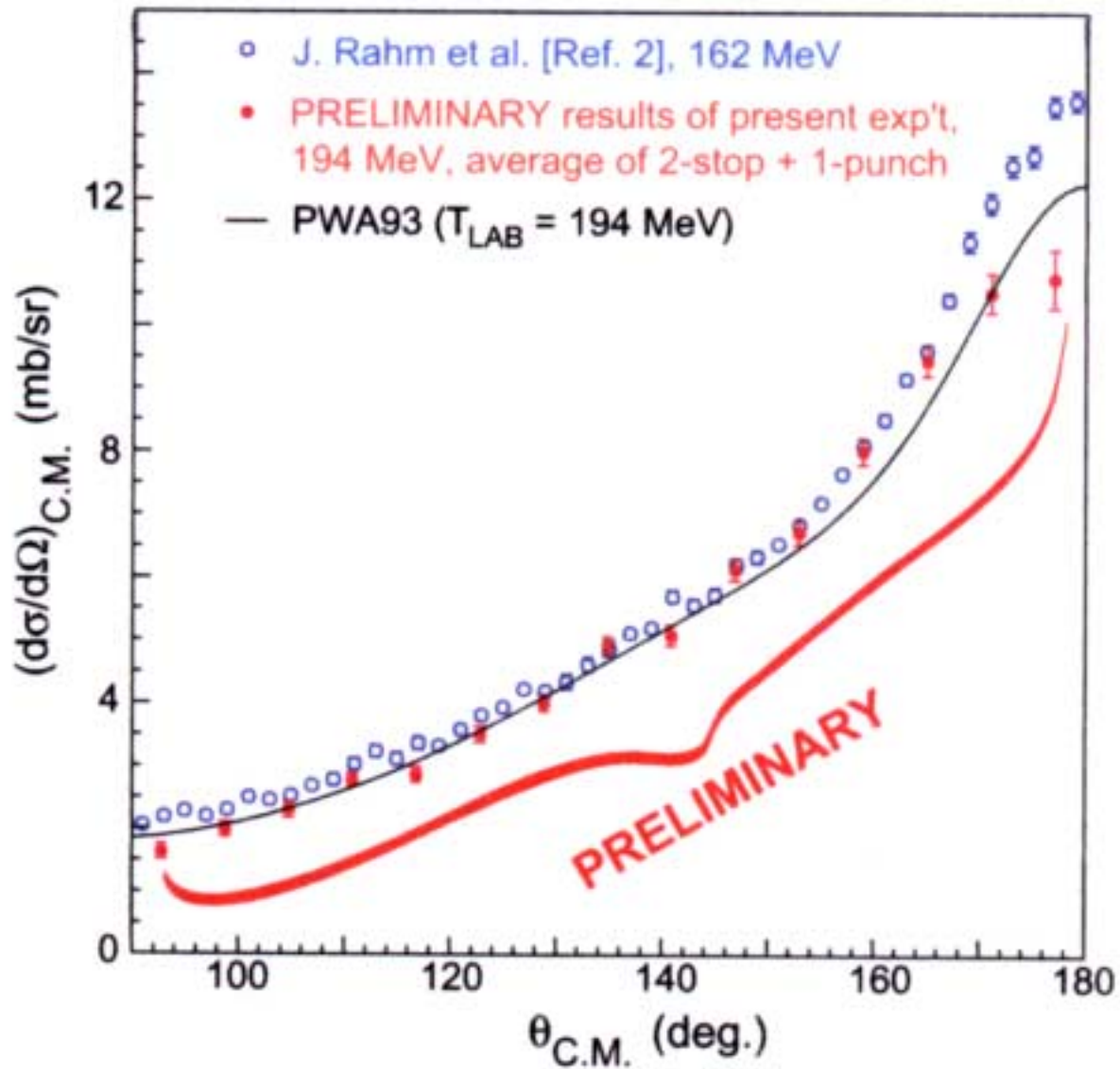
⁺Benck, (Louvain la Neuve), Nucl. Phys. A615, 222 (1997) and Proc. Conf. on NDST, Trieste (1997) p.1265, 28-75 MeV, angular distribution from 40° to 140° . Angular range is too limited.

Vigdor (IUCF) 185-200 MeV, angular distribution from 90° to 180° . Data have been obtained. Sarsour is analyzing the data and has preliminary data at 200 MeV, Private Comm.

n-p Differential Cross Section







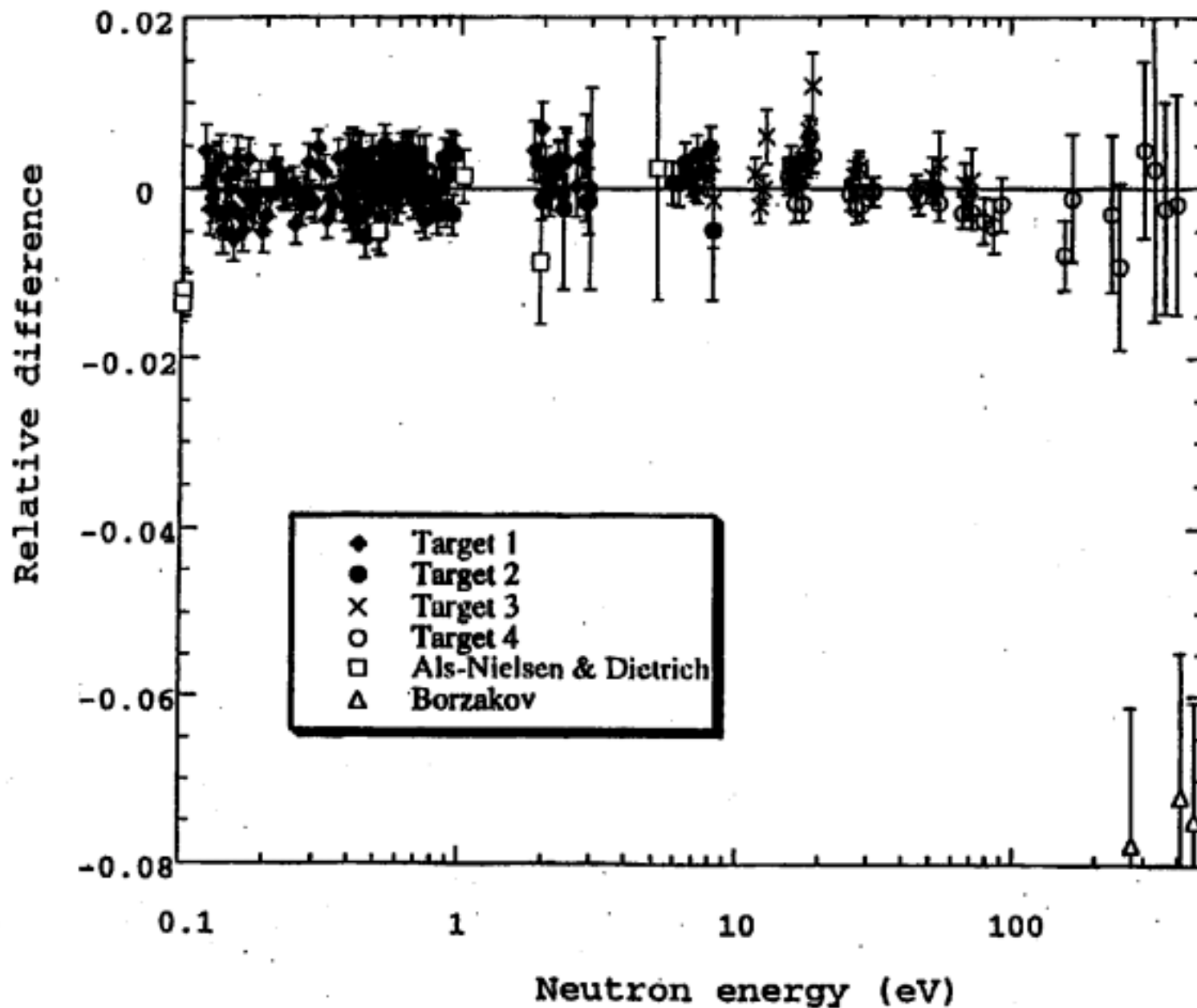
Indiana University Preliminary H(n,n) Results

$^3\text{He}(n,p)$

⁺⁺Borzakov, 0.26 keV to 142 keV, relative to $^6\text{Li}(n,t)$, Sov. J. Nucl. Phys. 35, 307 (1982). OK

^3He total cross section

⁺⁺Keith, 0.1 to 500 eV, BAPS DNP Oct 1997 paper IG.03 and thesis of D. Rich, U of Indiana. OK.



Relative difference between the data of Keith et al., using 4 different sample thicknesses, and a $1/v$ fit to the cross section. Also shown is a sampling of the data of Als-Nielsen & Dietrich, and Borzakov.

${}^6\text{Li}(n,t)$

+NIST collaboration, thermal measurement with high accuracy using cryogenic calorimeter, Private Comm. OK

++Knitter, (1983) NS&E 83, 229; ${}^6\text{Li}(n,t){}^4\text{He}$ angular distribution, 0.035-325 keV, new corrections required for particle leaking effect. Giorginis is investigating

++Drosg, 0.50 MeV to 4.1 MeV, NIM B94, p.319 (1994), using concept based on the two groups from the source reaction. Set 1011. OK

Bartle, 2 to 14 MeV, angular distribution, Proc. Conf on Nuclear Data for Basic and Applied Science, Sante Fe (1985), p. 1337 (questionable value, due to energy range and information not available).

Schwarz, 1 to 600 keV, NP 63, p.593, some based on hydrogen scattering cross section. Assumptions need study!

Koehler, 1 keV to 2.5 MeV, angular distribution data (ratio of forward and backward hemispheres responses), private comm.

Yu Gledenov, .025 eV, 87KIEV 2 237 (1988) no data given

+Guohui Zhang, 3.67 and 4.42 MeV, angular distribution, Comm. Of Nuclear Data Progress No.21 (1999) China Nuclear Data Center, also NSE 134, 312 (2000).

Also 1.85 MeV and 2.67 MeV, NSE 143, 86 (2003). Has “particle leaking” effect.

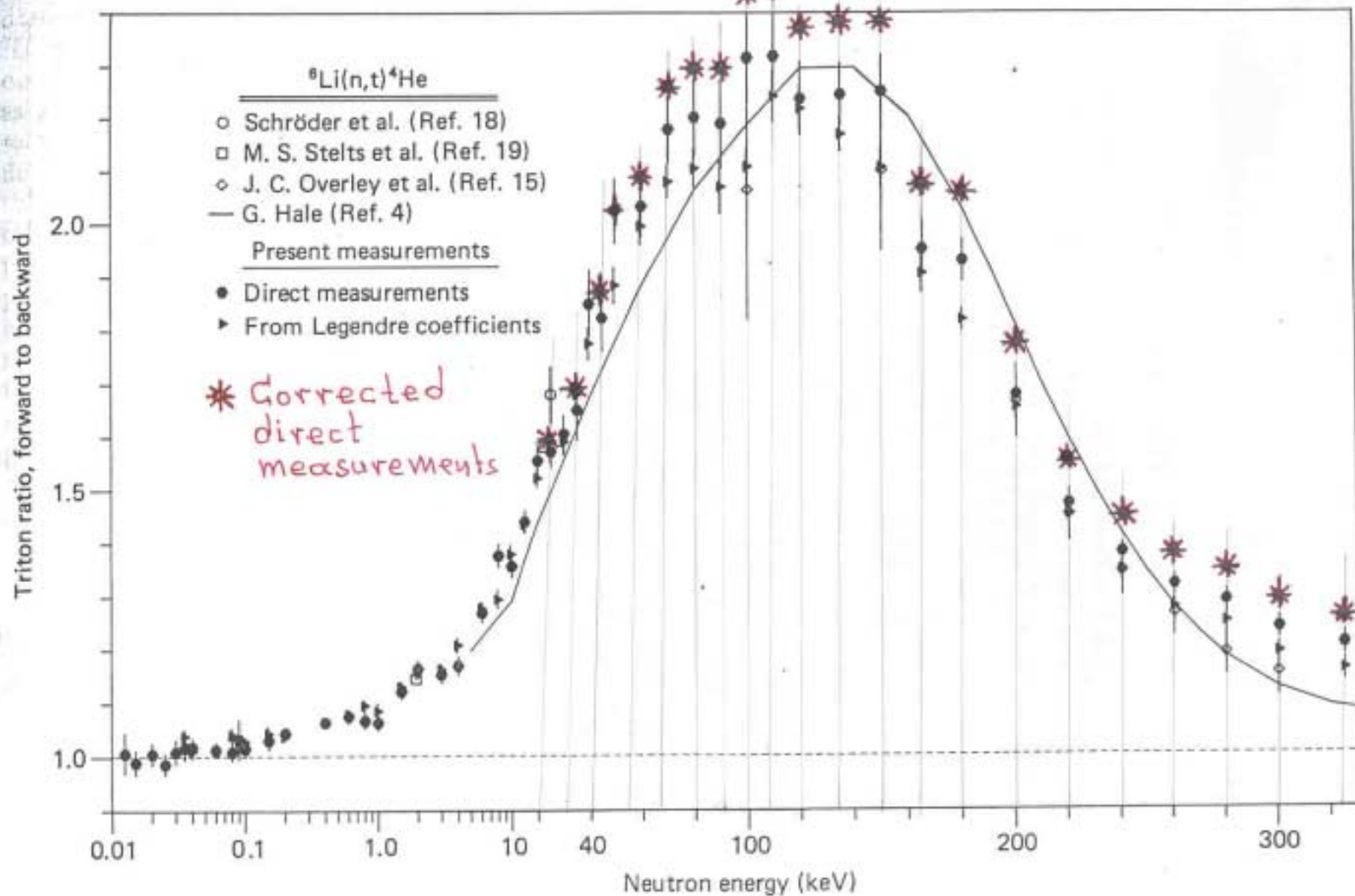


Fig. 8. The triton emission ratio of the reaction ${}^6\text{Li}(n,t){}^4\text{He}$ into the forward and backward hemispheres of the laboratory reference system is plotted versus the incident laboratory neutron energy.

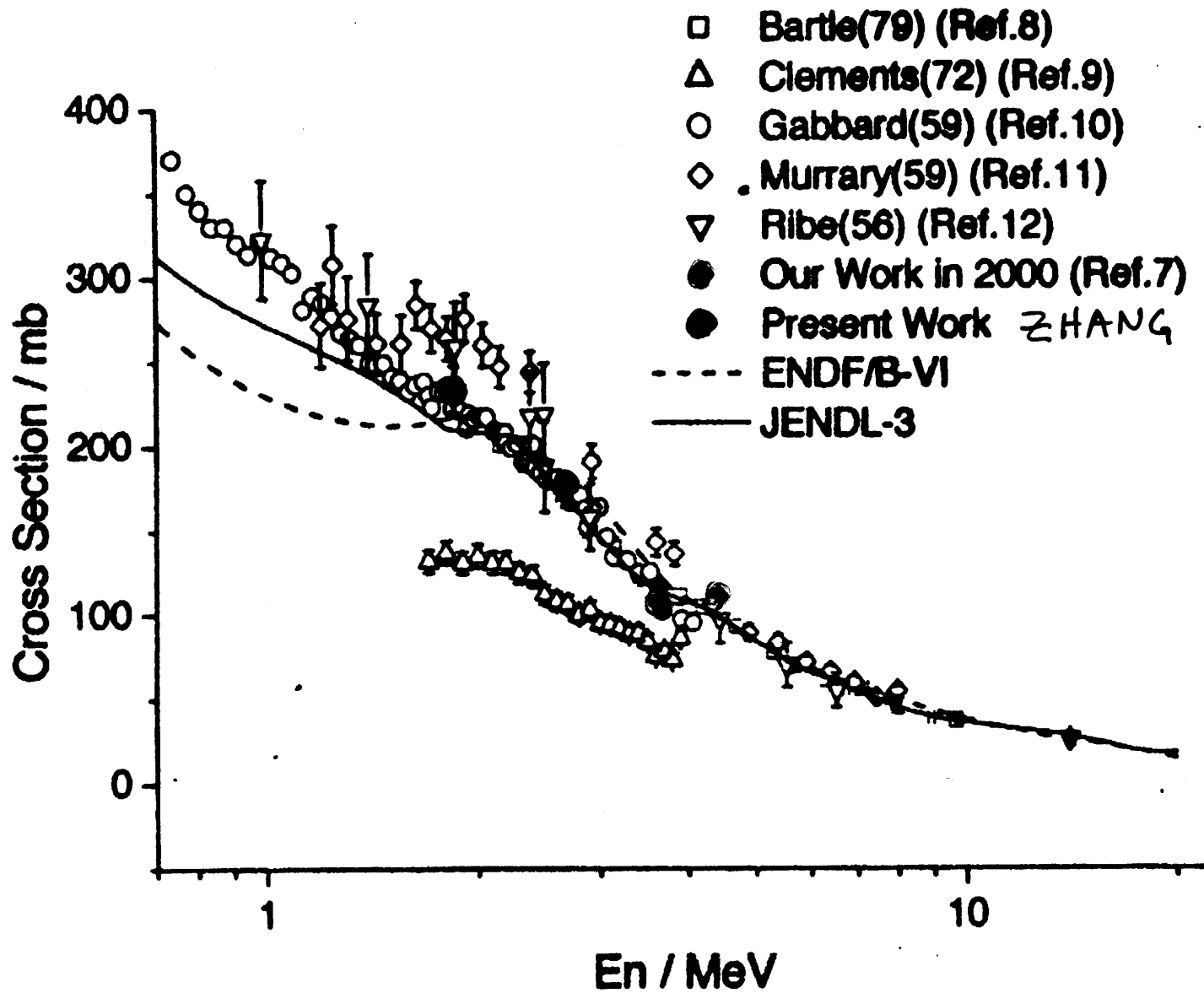


Fig. 5. The present results for the ${}^6\text{Li}(n, t){}^4\text{He}$ reaction cross section compared with existing data.

${}^6\text{Li}(n,t)$ Thermal Data

<u>Author</u>	<u>Cross Section</u>	<u>(b) Comment</u>
Silk et al.	943.8 ± 2.8	Used in V-6 Simult. Eval.
Meadows	936 ± 4	Used in V-6 R-matrix Eval.
Becker et al.	944 ± 19	Used in V-6 Simult. Eval.
Average	941.3 ± 2.3	
ENDF/B-VI	$941. \pm 1.3$	Combination of Simult. Eval and R-matrix Eval.
Simult. Eval. (ENDF/B-VI)	$941. \pm 1.7$	
interim Eval.	937.9 ± 1.6	Does not include the Chowdhuri (NIST) data, but is close to the value from that experiment
ENDF/B-V	935.9 ± 3.7	

$^{10}\text{B}(n,\alpha)$ Branching Ratio

⁺⁺Weston, 0.02 MeV to 1 MeV, Solid State detectors, NSE 109, 113 (1991). Set 1024. May have systematic errors.

⁺⁺Hambsch and Bax, ND2001, 0.04 MeV to 1.0 MeV, Frisch gridded ion chamber, in progress. Set 1015. Background problems

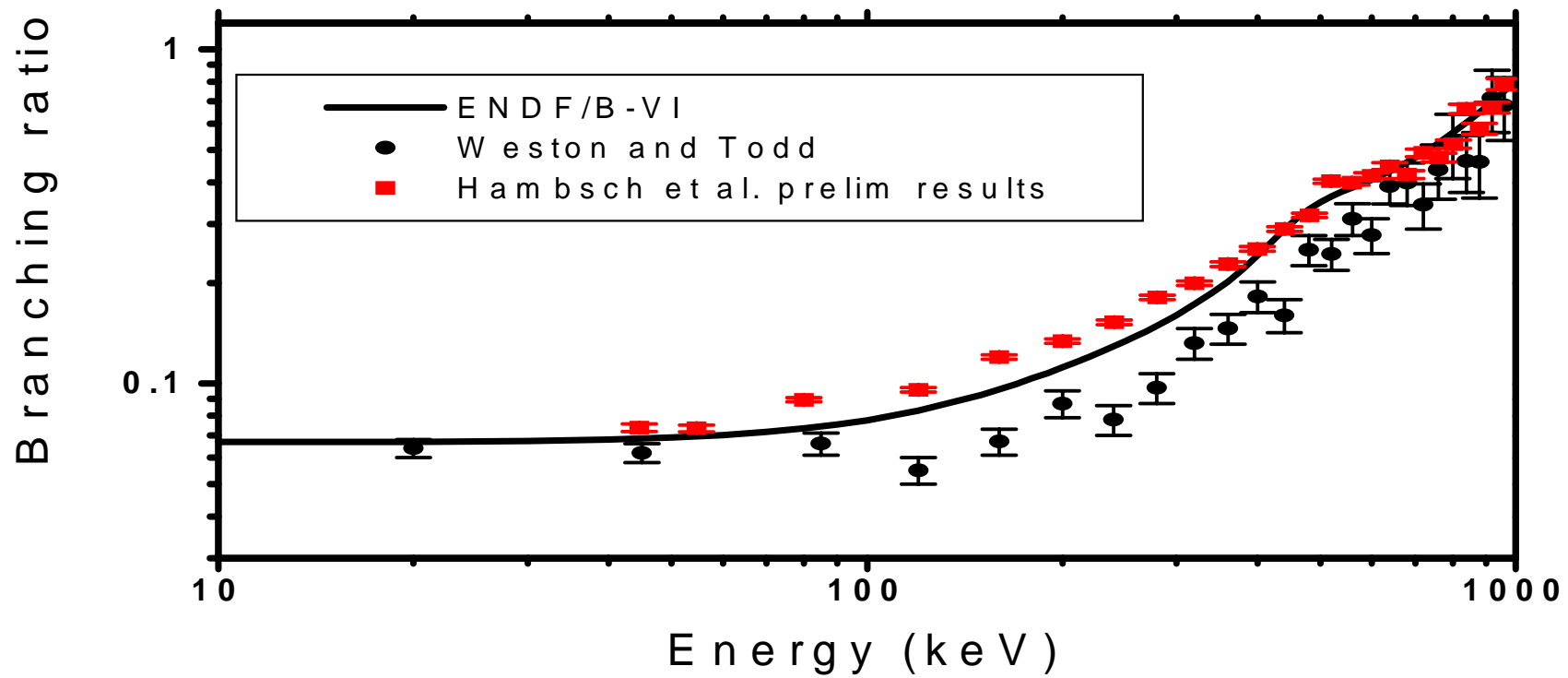
$^{10}\text{B}(n,\alpha)$

Haight, 1 MeV to 6 MeV, angular distribution at 30°, 60°, 90° and 135°, private comm.

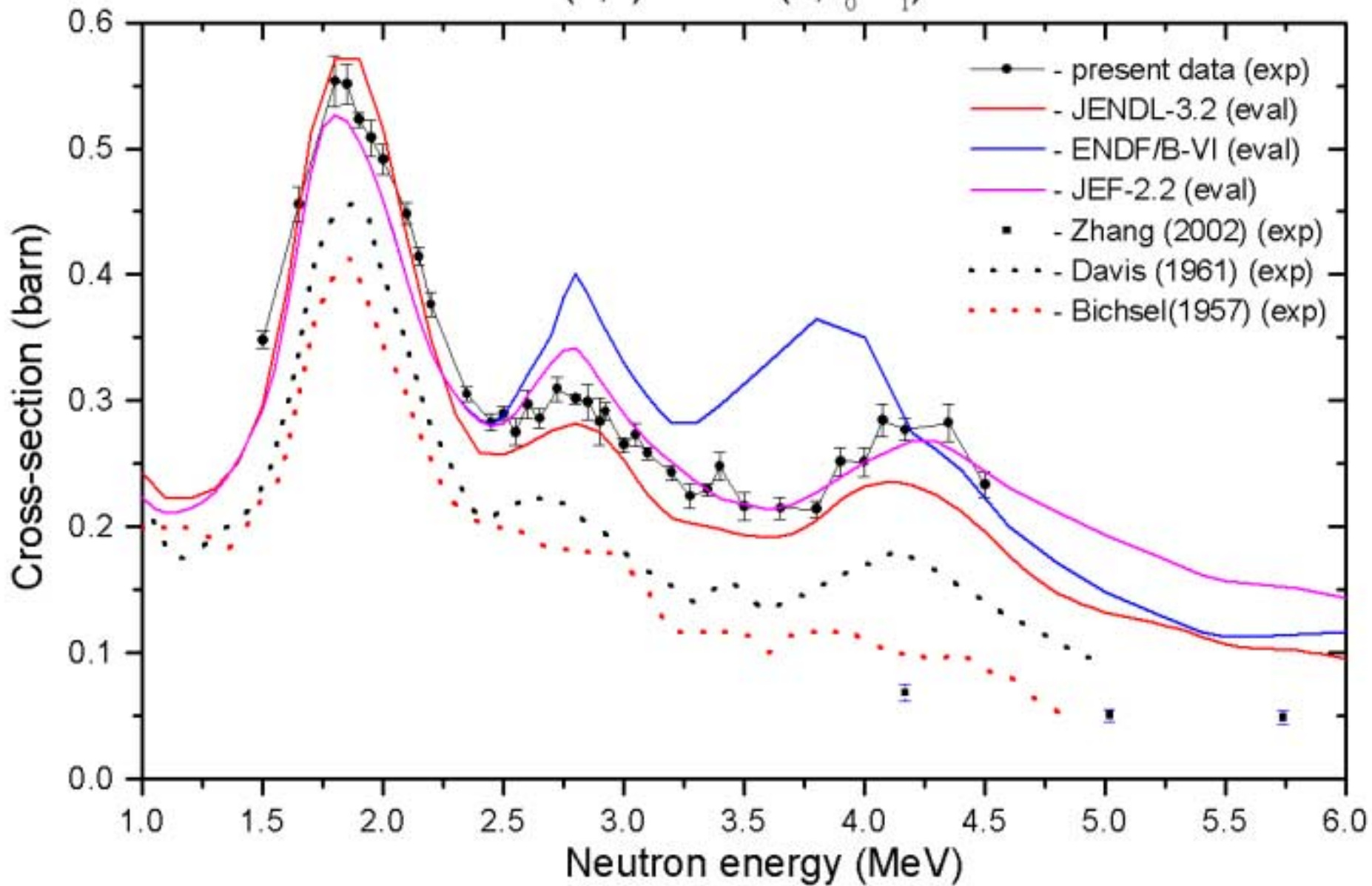
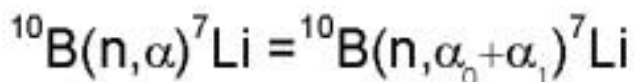
Hambsch and Bax, ND2001, keV to MeV, angular distribution, Frisch gridded ion chamber, in progress.

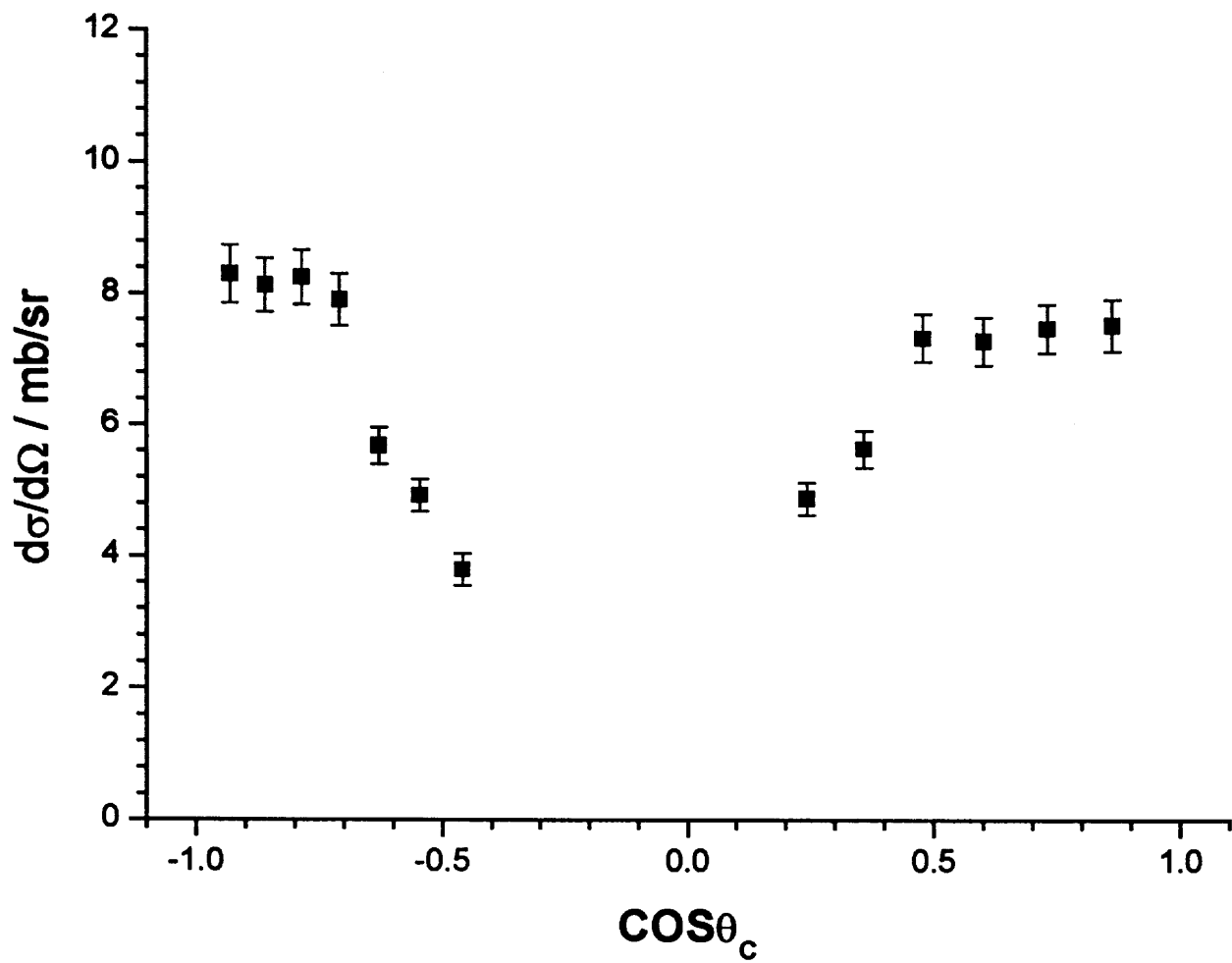
Giorginis and Khriachkov, MeV energies, angular distribution, VdG data. The integrated cross sections are available. Private communication (2003). OK

⁺Guohui Zhang, 4.17, 5.02, 5.74, 6.52 MeV angular distribution, submitted for publication to NSE. Problems with particle leaking.



Present data: G. Giorginis and V. Khriatchkov, IRMM, June 2003





Differential cross section for the $^{10}\text{B}(n,\alpha)^7\text{Li}$ reaction at 4.17 MeV by Zhang et al.

$^{10}\text{B}(n,\alpha_1\gamma)$

Maerten, 320 keV to 2.8 MeV, GELINA linac, relative to $^{235}\text{U}(n,f)$ and carbon standards, private comm. from H. Weigmann. Not enough information on uncertainties is available.

++Schrack, 0.2 MeV to 4 MeV, shape data relative to Black Detector (at ORNL), NSE 114, 352 (1993). Set 113. OK

+Schrack, 10 keV to 1 MeV, shape data relative to H(n,n) prop ctr (at ORNL), Proc. Conf. on NDST, Gatlinburg (1994)p. 43. Set 1034 OK

+Schrack, .3 MeV to 10 MeV, relative to $^{235}\text{U}(n,f)$ ion chamber (at LANL), Private comm. Set 1033 OK

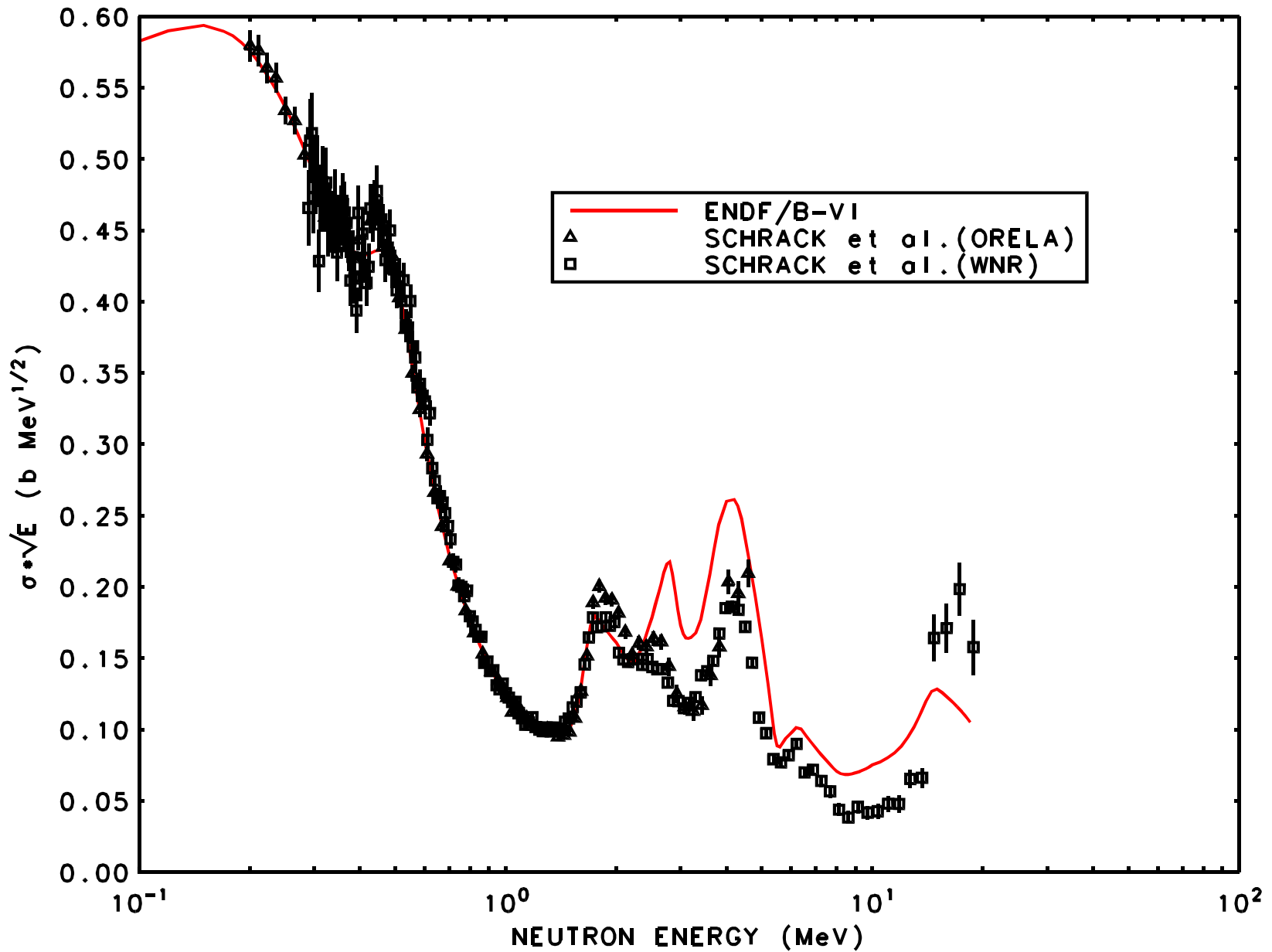


Fig. 15 Comparison of the $^{10}\text{B}(n, \alpha, \gamma)$ cross section measurements of Schrack et al. at ORELA (BD mon) and WNR (FC mon) with ENDF/B-VI

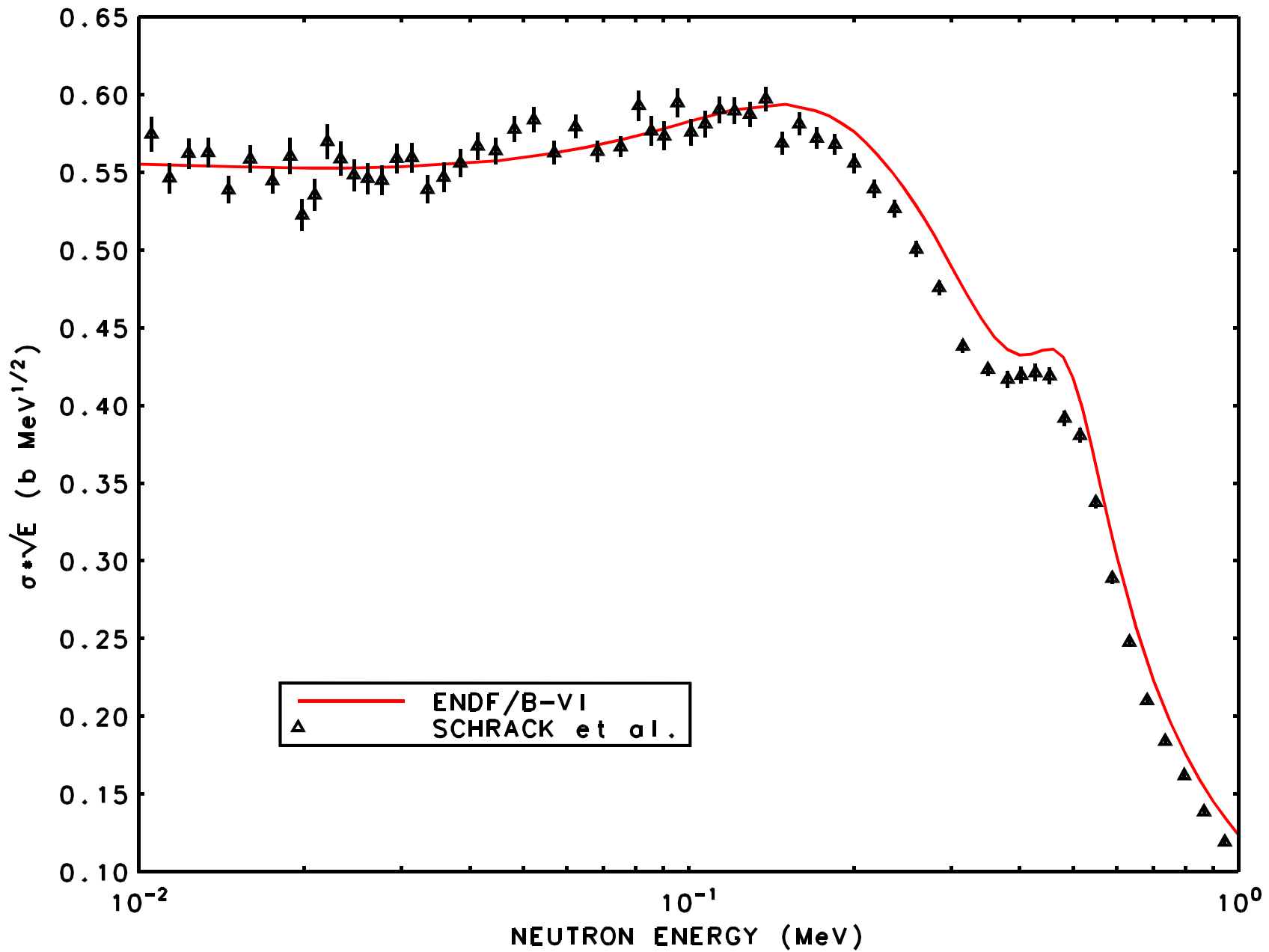


Fig. 14 $^{10}\text{B}(n,\alpha,\gamma)$ cross section measurements by Schrack et al at ORELA (PC mon)

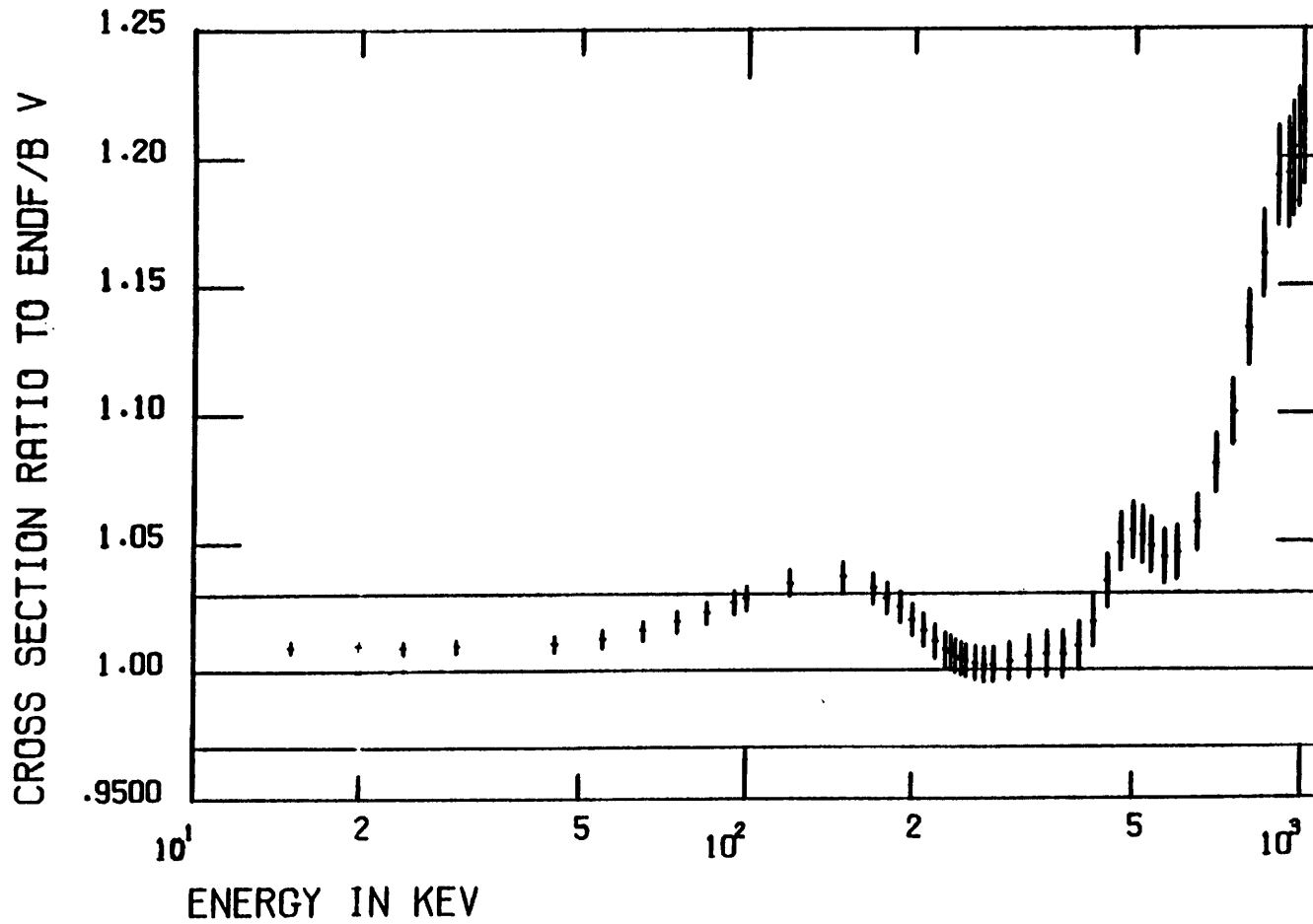
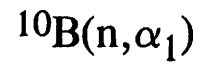


Fig. 28 Ratio of the result of this evaluation process to that of ENDF/B-V for the $^{10}\text{B}(n,\alpha_1)$ reaction from about 10 keV to 1 MeV. The lines at ratios of 0.97 and 1.03 are guides to the eye.

$^{235}\text{U}(\text{n},\text{f})$

++Carlson, 2 MeV to 30 MeV, relative to H(n,n), Proc. Spec. Meeting on Neutron Cross Section Standards for the Energy Region above 20 MeV, Uppsala, Sweden, 1991, Report NEANDC-305, “U”, p. 165. Set 524 OK

++Merla, +2.6, +4.45, +8.46, +14.7, +18.8 MeV ?, associated particle, Proc. Conf. on NDST Juelich (1991) p.510. Sets 591, 590, 592, 593, 587. OK

++Lisowski, 3 MeV to 200 MeV, relative to H(n,n), Proc. Spec. Meeting on Neutron Cross Section Standards for the Energy Region above 20 MeV, Uppsala, Sweden, 1991, Report NEANDC-305, “U”, p. 177, and private communication. Set 1028 OK

+Nolte, 14 to 150 MeV, ND2001, and Private Comm. to increase energy range, Preliminary data. Concerns about 96 MeV point. Additional work underway

++Buleeva, 0.624 MeV to 0.785 MeV, relative to H(n,n), Sov. J. Atomic Energy 65, 930 (1988). Set 522. OK
Grundl comment, ^{252}Cf spontaneous fission spectrum averaged cross section. NOTE; only the last NIST measurement (Schroder) should be used in the evaluation.

++Kalinin, 1.88 MeV, 2.37 MeV CCW, assoc. particle, Sov. J. Atomic Energy 71,(2),181,1988 Set 1026 OK

++Carlson, 0.3 MeV to 3 MeV, absolute fluence from black detector, Proc. IAEA Advisory Group Meeting on Nuclear Standard Reference Data, Geel Belgium, p.163, IAEA-TECDOC-335 (1985). Set 523. OK

++Johnson, 1 MeV to 6 MeV, absolute fluence from a dual thin scintillator, Proc. Conf. on NDST Mito (1988) p.1037. Set 1025 OK

++Iwasaki, 14 MeV (13.5 to 14.9 MeV), relative to H(n,n) and assoc. particle, Proc. Conf. on NDST Mito (1988) p. 87. Set 1027 OK

++Weston and Todd, NSE 111, 415 (1992), relative to $^{10}\text{B}(\text{n},\alpha)$, 0.15 keV to 1.5 keV. Set 1023 OK

Using the CSEWG Godiva specifications, three runs were made to test the IAEA set with context:

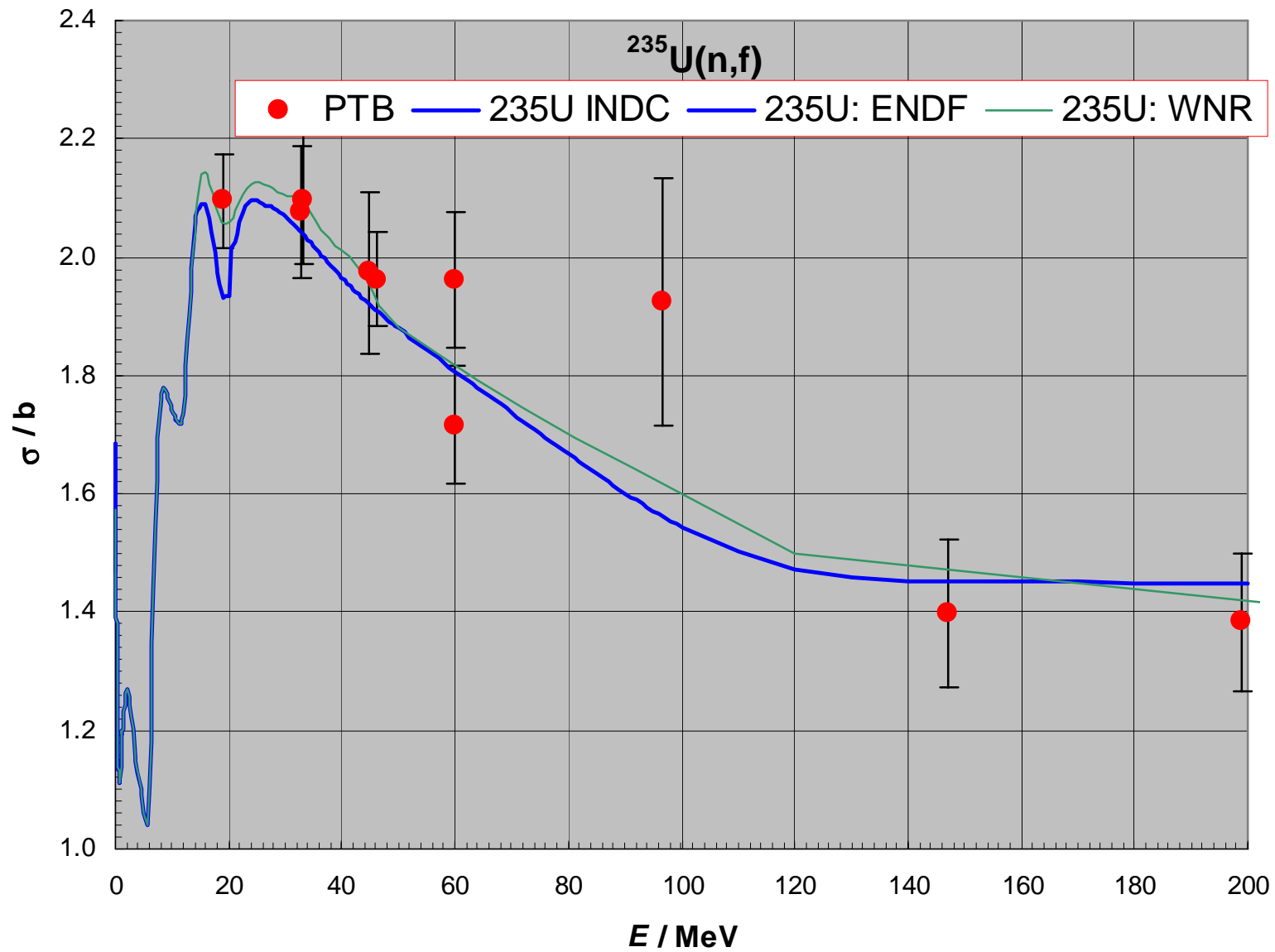
regular "I" materials .99941+/-0.00020 [Using the previously released pre-VII materials from T-16]

replace with u235la1 1b .99893+/-0.00021 [IAEA]

replace with u235e .99628+/-0.00021 [Rel.5]

It wouldn't take much change in nubar to make it prettier!
And it didn't go back anywhere close to the old Rel.5 result.

Bob



$^{238}\text{U}(\text{n},\text{f})$

++Merla, 5 MeV +, assoc. particle, Proc. Conf. on NDST Juelich (1991) p.510. Set 810. OK

++Winkler, 14.5 MeV, rel.to Al(n, α) & $^{56}\text{Fe}(\text{n},\text{p})$, Proc. Conf. on NDST Juelich (1991), p.514. Set 809. OK

++Lisowski, 0.8 MeV to 357 MeV, relative to H(n,n), Proc. Spec. Meeting on Neutron Cross Section Standards for the Energy Region above 20 MeV, Uppsala, Sweden, 1991, Report NEANDC-305, "U", p. 177, and private communication. Set 1030. OK, possible problems at highest energies compared with Shcherbakov

+Nolte, 14 to 150 MeV, ND2001, and Private Comm. to increase energy range, Preliminary data.

+Newhauser, 34, 46, and 61 MeV MeV, absolute, Proc. Conf. on NDST Juelich (1991),
removed from database.

+Meadows, 14.74 MeV, CCW, ANE,15,421 (1988), relative to $^{235}\text{U}(\text{n},\text{f})$.

++Baba, 4.6 MeV to 6 MeV, Van de Graaff relative to $^{235}\text{U}(\text{n},\text{f})$, J. Nucl. Sci. & Techn.,26,11 (1989). Set 1035

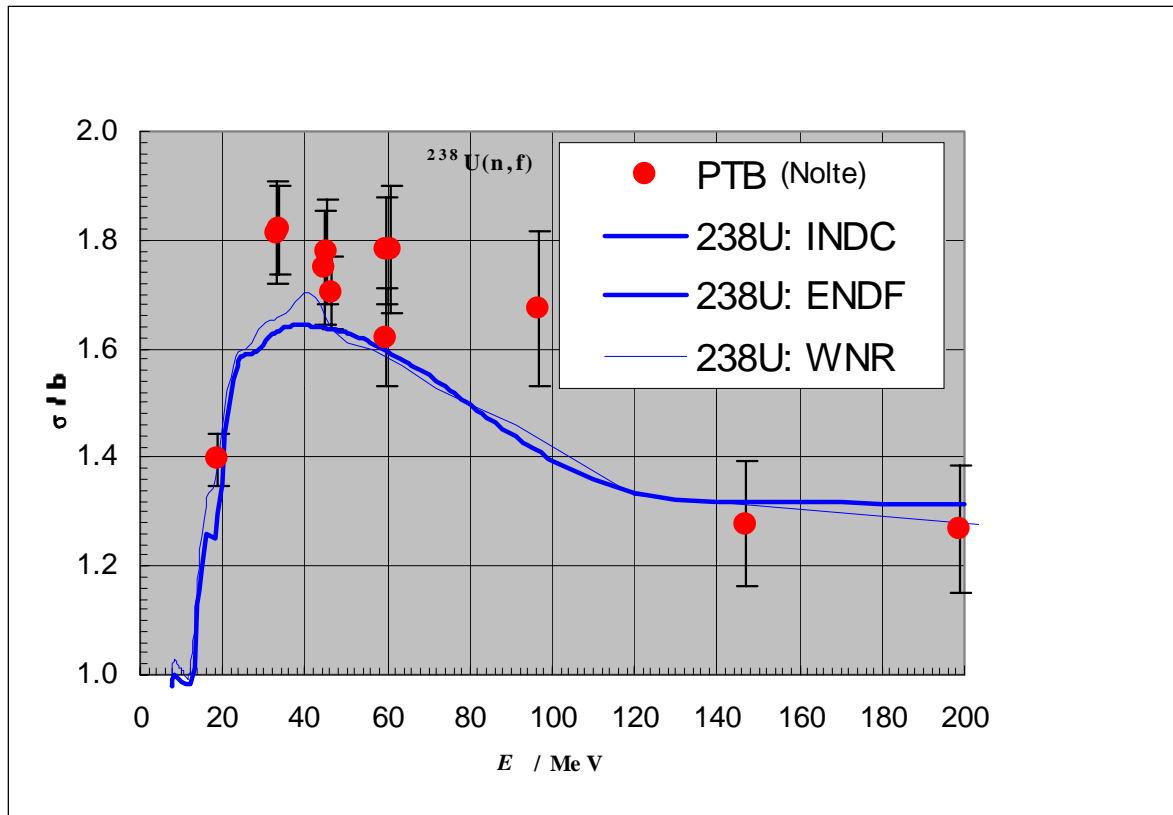
++Shcherbakov, 1-196 MeV, relative to $^{235}\text{U}(\text{n},\text{f})$, ISTC 609-97, see also Fomichev, 0.7 MeV to 200 MeV, relative to $^{235}\text{U}(\text{n},\text{f})$, Proc. Conf. on NDST, Trieste (1997), p.1283, also ND2001 set 1013.

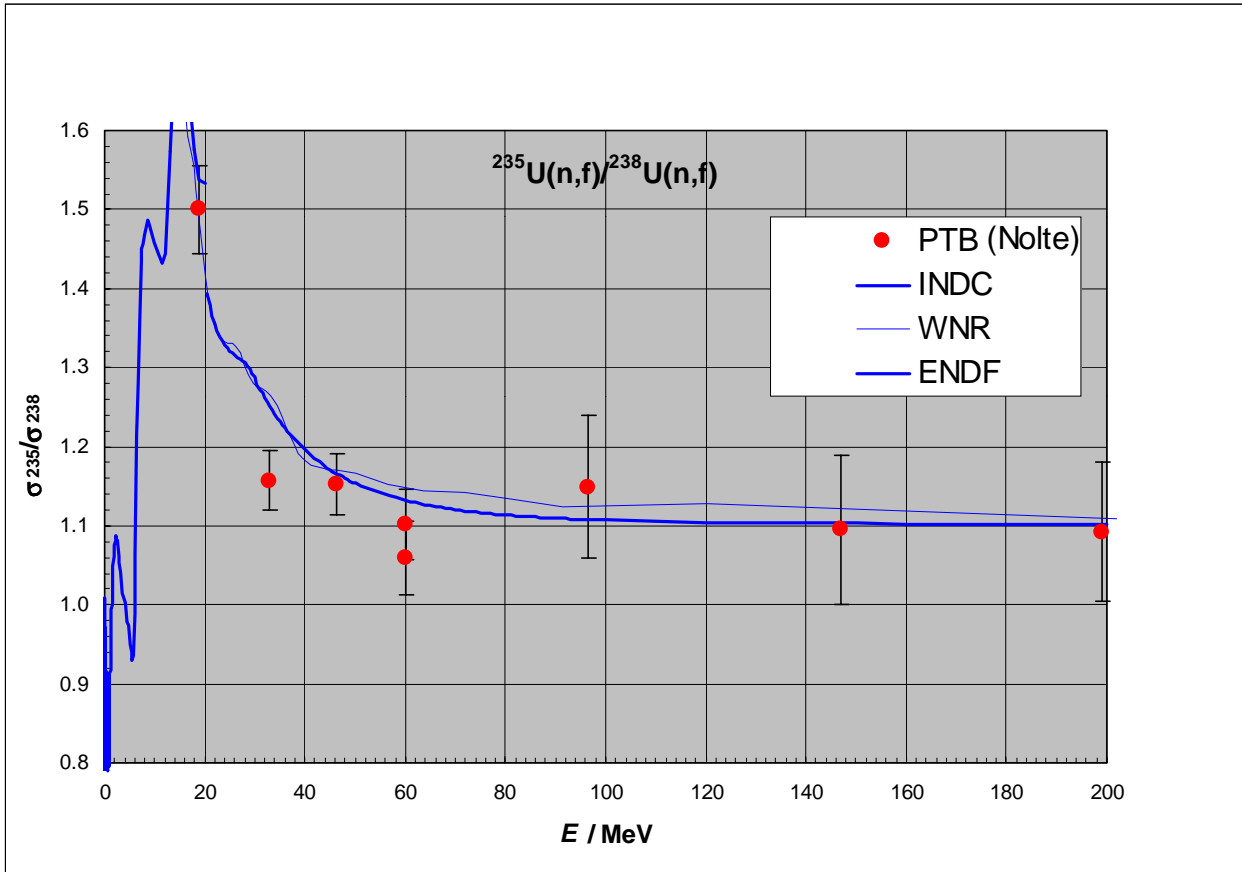
OK except possibly at the highest energies (inconsistent with Lisowski there)

+Li Jingwen, 14.7 MeV, CCW, ratio to $^{235}\text{U}(\text{n},\text{f})$ CNP,11,(3),17,89.

Eismont, Trieste conf, p.494, 33.7, 46 and 60.6 MeV, relative to hydrogen scattering cross section. See also Gatlinburg conference results at 135 and 160 MeV. Data not finalized. They have concerns about neutron fluence determination for getting smaller uncertainty.

+Garlea, 14.7 MeV, relative to $^{235}\text{U}(\text{n},\text{f})$ cross section, RRP,37,(1),19,92.





$^{239}\text{Pu}(n,f)$

++Weston, linac, 0.15 keV to 15 keV, fission chamber,
 $^{10}\text{B}(n,\alpha)$ standard, NSE 111,415 (1992). Set 1024 OK

++Merla, 4.9, 8.65, 14.7 and 18.8 MeV, associated particle, Proc. Conf. on NDST
Juelich (1991) p.510; see also Alkhazov, YK,1986,(4),19,198612.
Sets 611, 617, 615, and 616. OK

+Meadows, 14.74 MeV, CCW, ANE,15,421,8808, relative to $^{235}\text{U}(n,f)$.

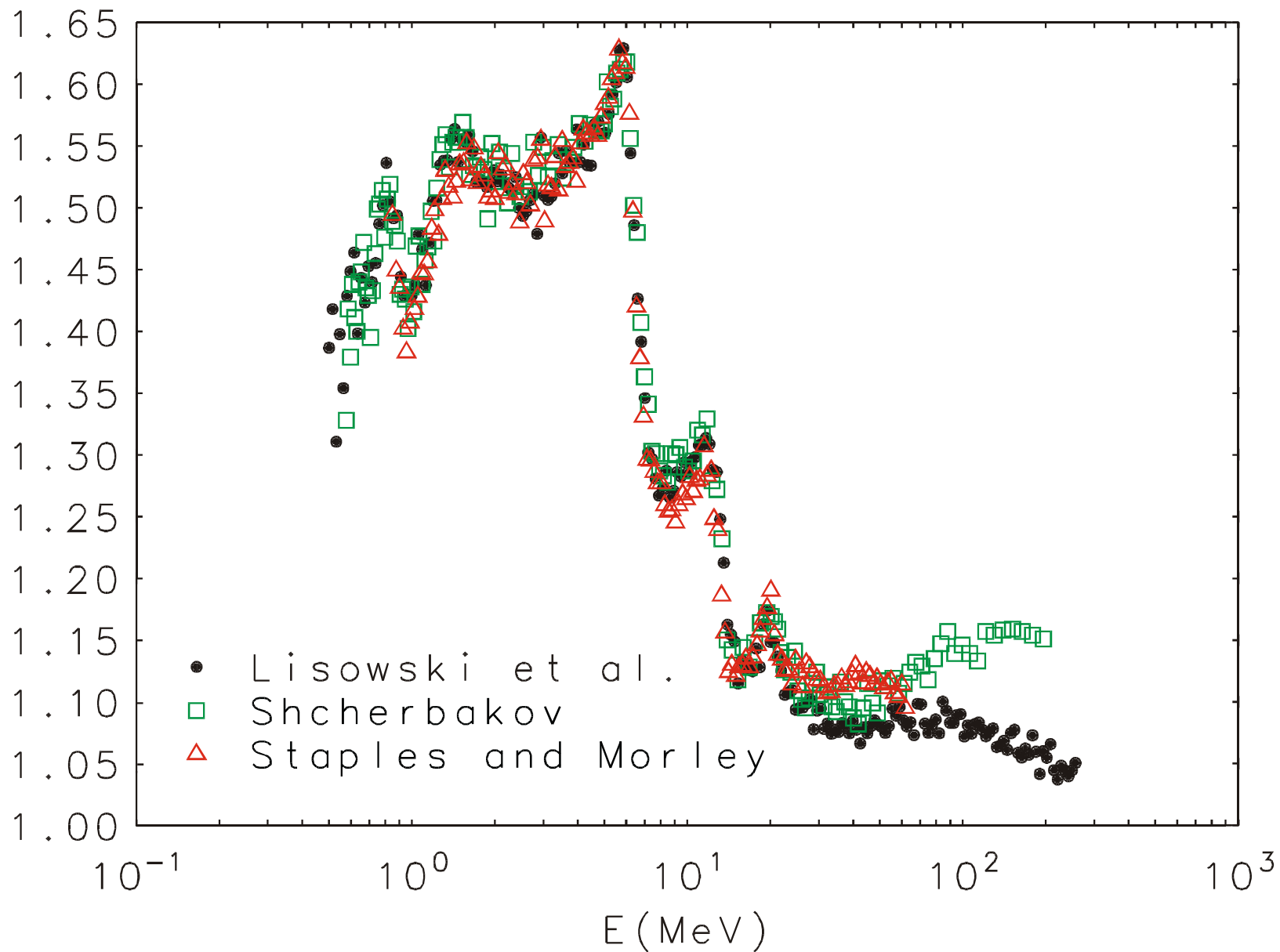
+Shcherbakov, 0.6-196 MeV, relative to $^{235}\text{U}(n,f)$, ISTC 609-97 (2000). Set 1012.
OK but problems at high energy compared with Lisowski.

+Staples, 0.8 MeV to 62 MeV, relative to $^{235}\text{U}(n,f)$, NSE 129, 149 (1998). Set 1014.
OK except differences compared with Lisowski and Shcherbakov at highest energies.

+Lisowski, 0.5 MeV to 256 MeV, relative to $\text{H}(n,n)$ and $^{235}\text{U}(n,f)$,
Proc. Spec. Meeting on Neutron Cross Section Standards for the Energy Region above
20 MeV, Uppsala, Sweden, 1991, Report NEANDC-305, "U". Set 1029 OK
problems at highest energies compared with Shcherbakov

++Garlea, 14.7 MeV, relative to $^{235}\text{U}(n,f)$ cross section, RRP,37,(1),19,92. Set 633 Value is high

Ratio of the $^{239}\text{Pu}(n,f)$ to $^{235}\text{U}(n,f)$ Cross Sections



Conclusion

Better measurements and improved methods to handle discrepant data are needed. But working with what is available, the database continues to be prepared for use in the new international evaluation of the neutron cross section standards.



Status of the ^{10}B measurements at IRMM

F.-J. Hamsch

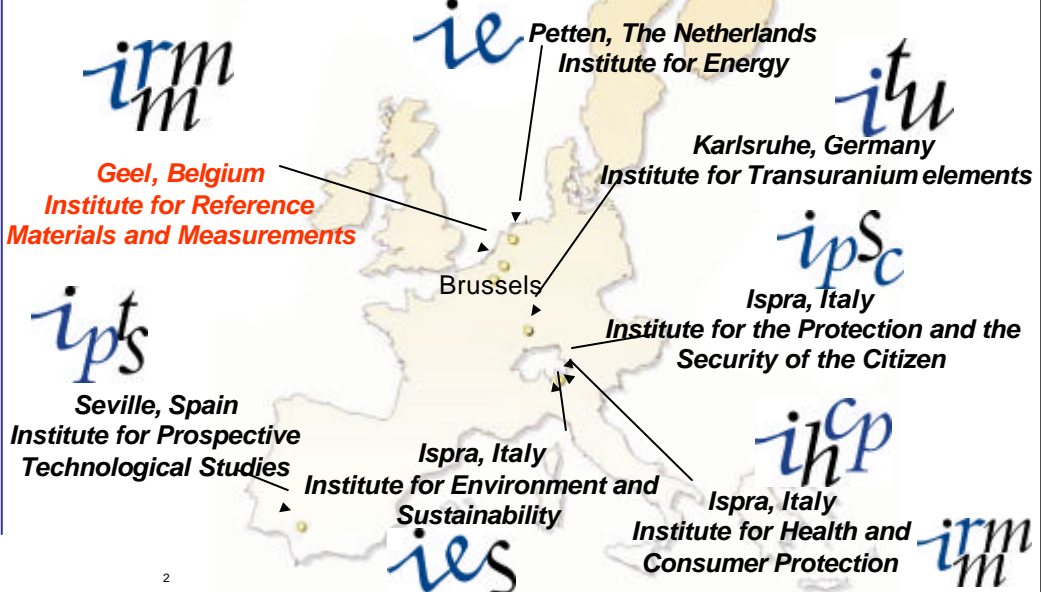
*Institute for Reference Materials and
Measurements (IRMM)
Geel, Belgium*

<http://www.irmm.jrc.be>
<http://www.jrc.cec.eu.int>

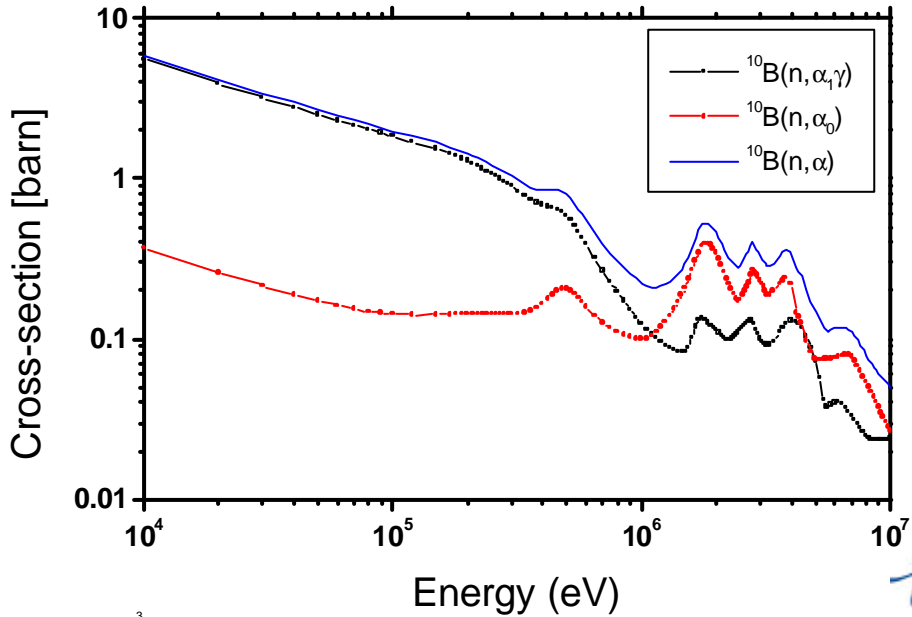


Organization of the JRC, a DG of the European Commission

7 Institutes in 5 Member States:



Evaluated cross section

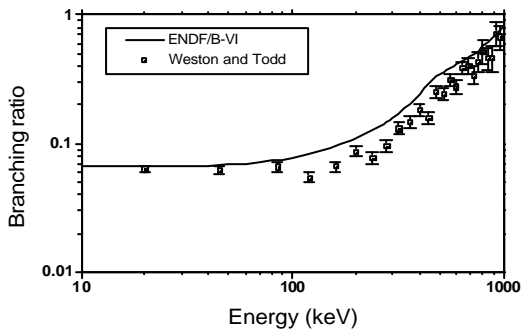


3



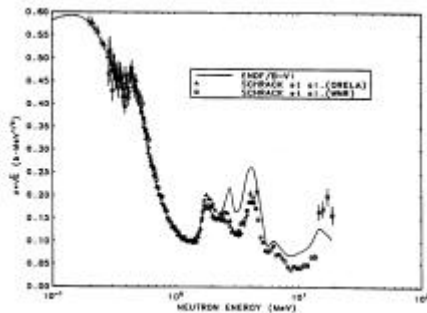
Problems

Branching ratio $\sigma(\alpha_0)/\sigma(\alpha_1)$



Up to 30% difference

$^{10}\text{B}(n, \alpha_1 \gamma)^7\text{Li}$ cross section



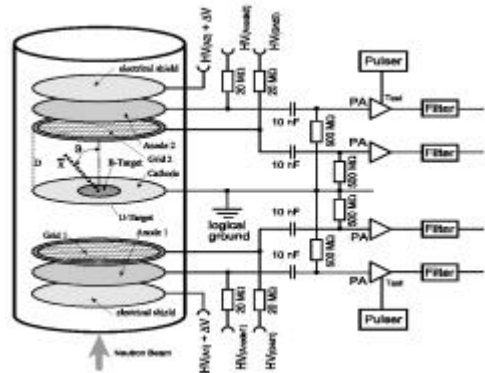
Above 2 MeV lower $^{10}\text{B}(n, \alpha_1 \gamma)^7\text{Li}$

4



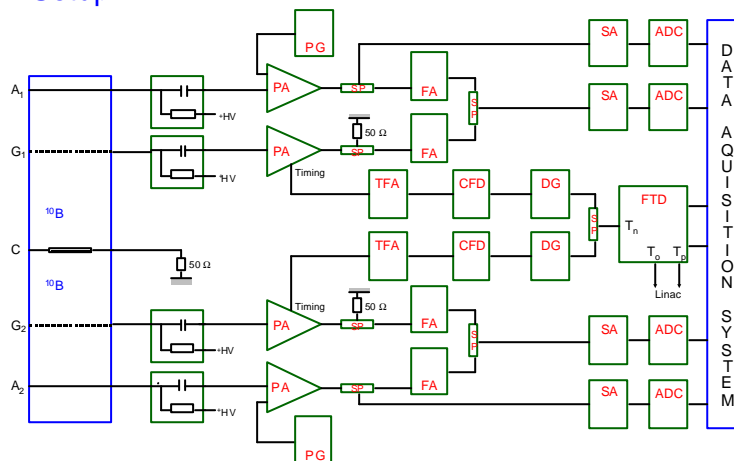
Experimental set-up at GELINA

- Double Frisch gridded ionization chamber (IC).
- ^{10}B samples ($30 \text{ mg/cm}^2, 7 \text{ cm } \text{\AA}$) in back to back geometry (IRMM-SP).
- IC covered with Cd.
- Counting gas: continuous flow 95%Ar+5%CO₂.
- Time of flight: 28.241 m.



Electronic scheme GELINA

^{10}B Setup



PA = Pre-amplifier
FA = Fast Amplifier
SA = Spectroscopy Amplifier

SP = Splitter
TFA = Timing Filter Amplifier
CFD = Constant Fraction Discriminator

DG = Delay Generator
PG = Pulse Generator
FTD = Fast Time Digitizer

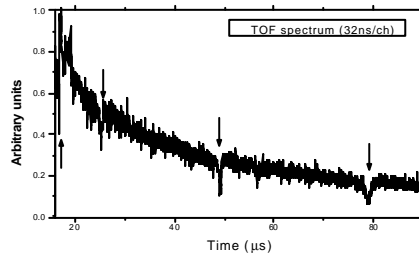
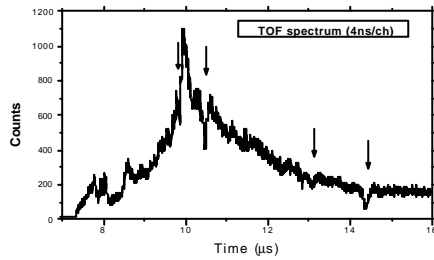


Difficulties

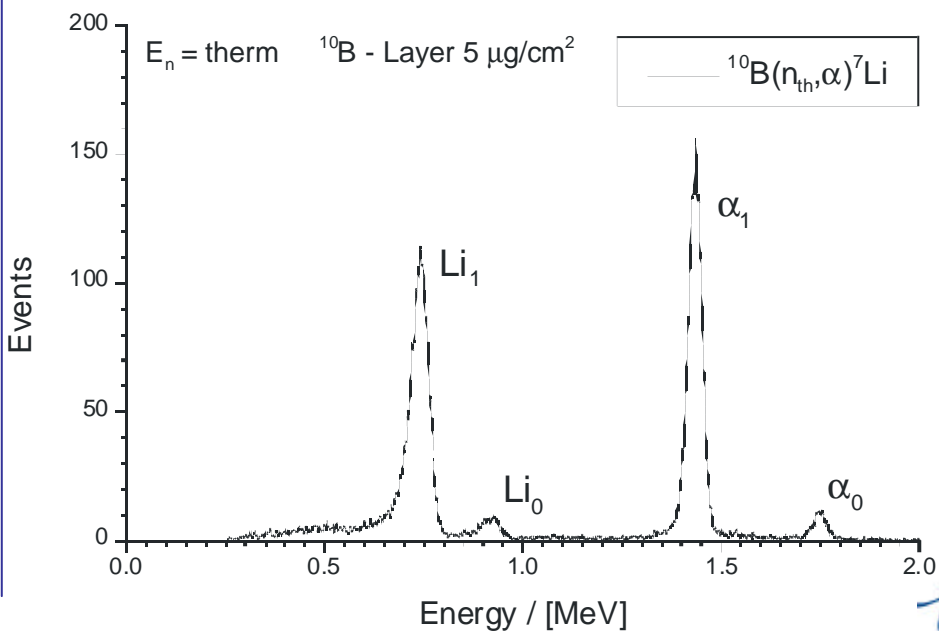
- Very thin samples ($<30 \text{ mg/cm}^2$) because of resolution degradation due to energy loss, hence low count rate.
- Low energy of α -particles:
 - $E(\alpha_0) = 1.7891 \text{ MeV}$, $E(\alpha_1) = 1.4832 \text{ MeV}$.
- g-flash at LINAC, noise level at VdG.
- Kinematics of the reaction leads to overlapping α -peaks at higher incident neutron energy.

Energy calibration

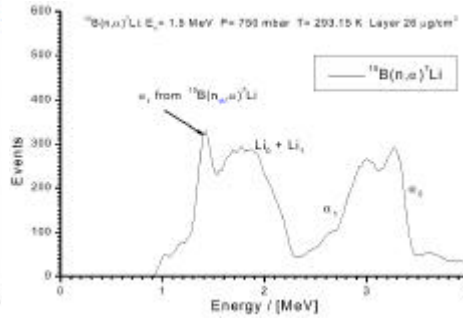
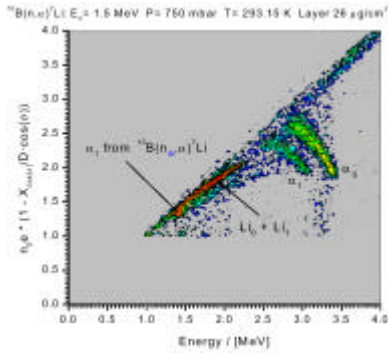
- Use of filtered beams:
 - Pb, Bi.
- Via known resonance energies determine incident neutron energy.
- Used resonances (keV):
 - Pb (41.3,78.2,115.2,354.1,510)
 - Bi (0.8,2.31,15.5,33.3).



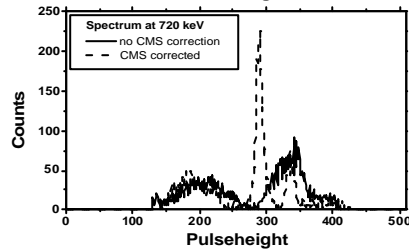
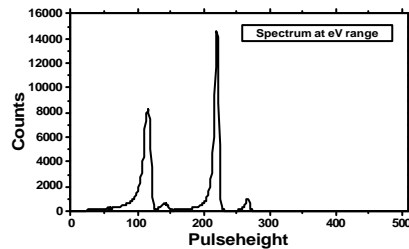
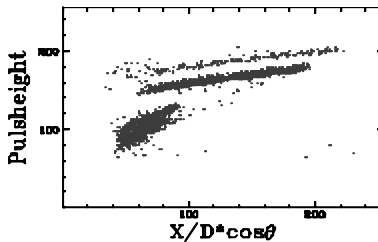
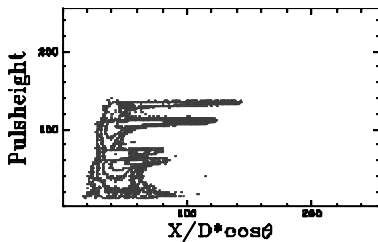
¹⁰B-spectrum at thermal energy



1.5 MeV neutrons

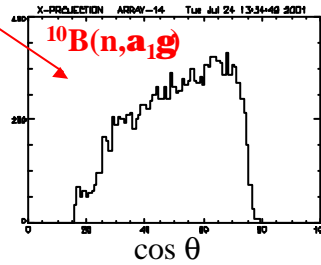
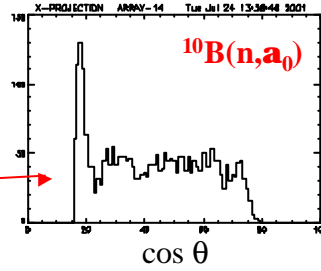
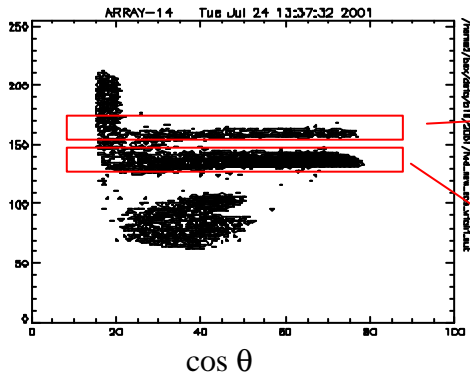


Importance of multi-dim. data analysis



Angular distribution in CMS at $E_n = 520\text{keV}$

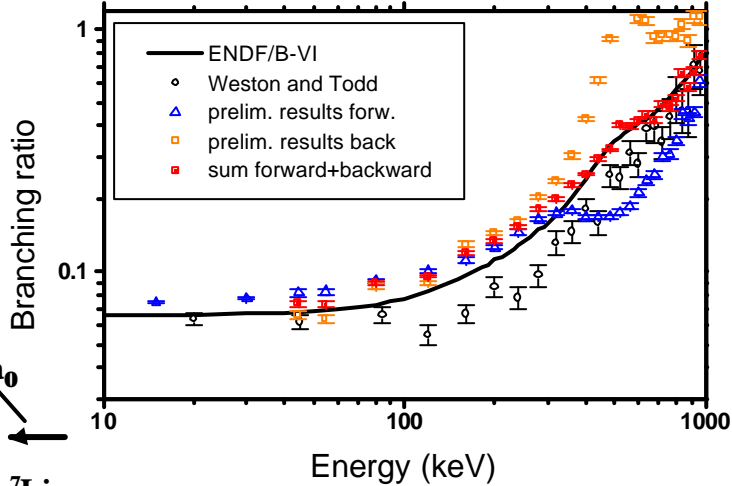
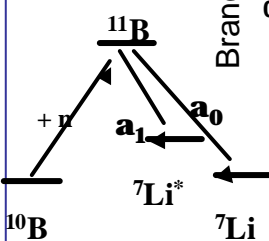
Joint Research Centre



Strong anisotropy observed for a_1 transition and isotropy for a_0

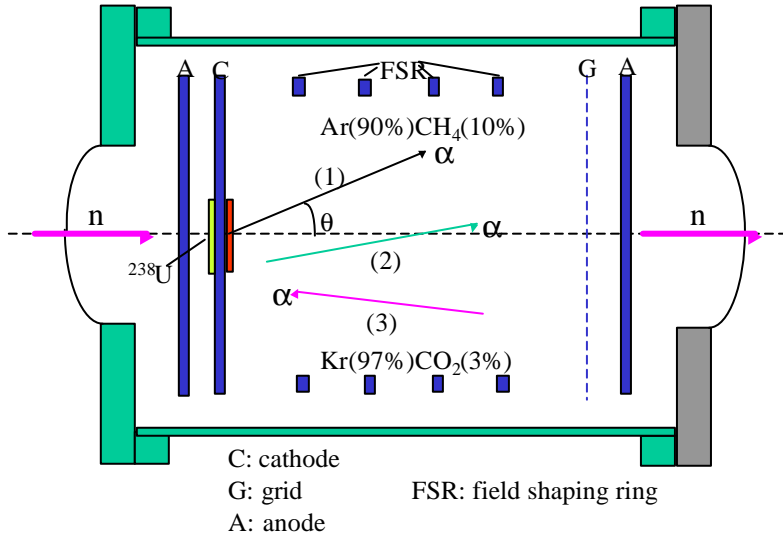
Branching ratio $^{10}\text{B}(n, a_0)/^{10}\text{B}(n, a_1)$

Joint Research Centre



Above $\sim 300\text{keV}$ strong anisotropic angular distribution observed in forward and backward direction

Experimental arrangement at VdG

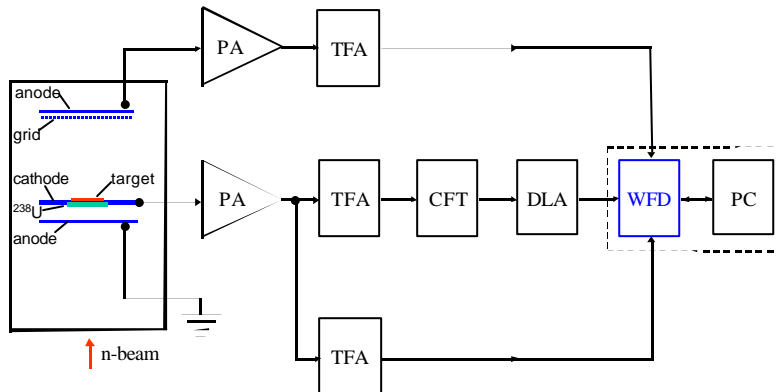


15



Digitization technique

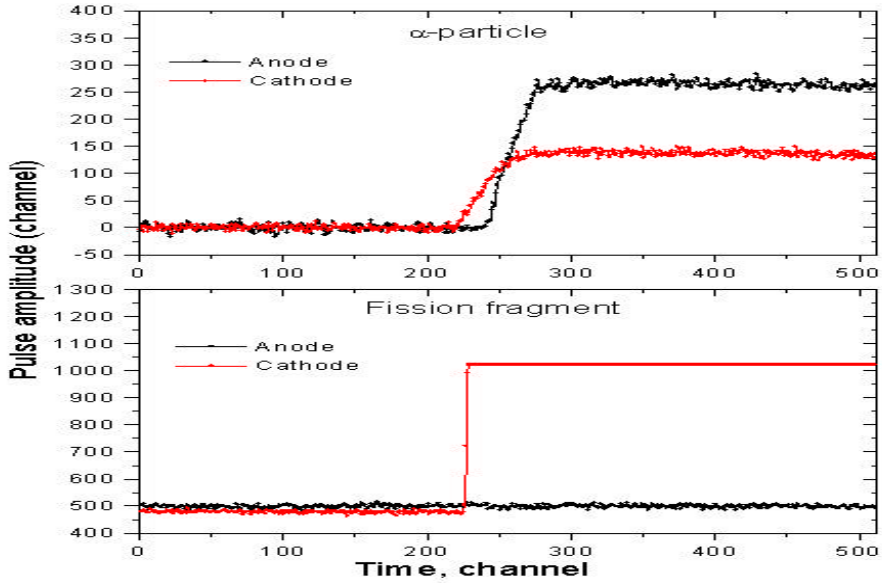
Block diagramme for PDA12A (WFD) in external-pretrigger mode



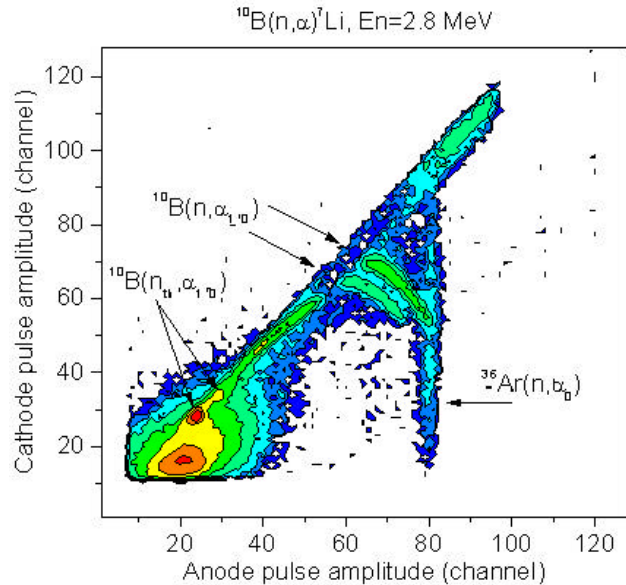
16



Typical digitizer signals

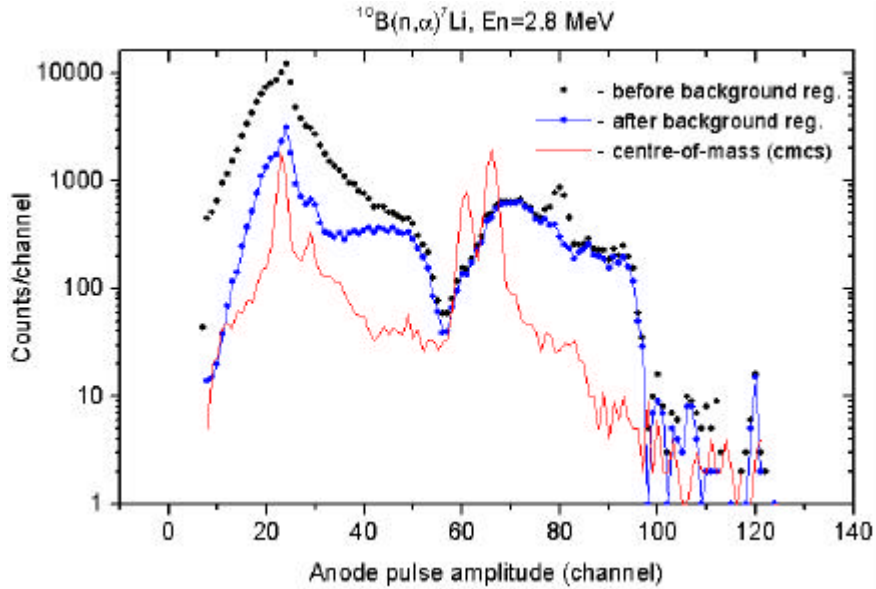


Background problems



(a)

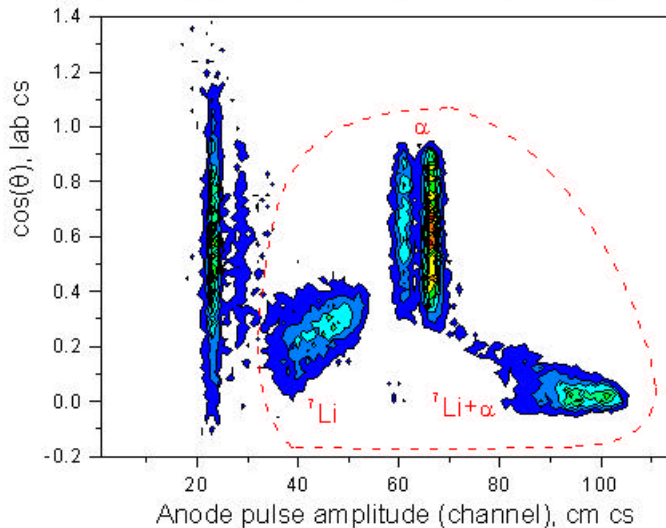
Correction of background



19



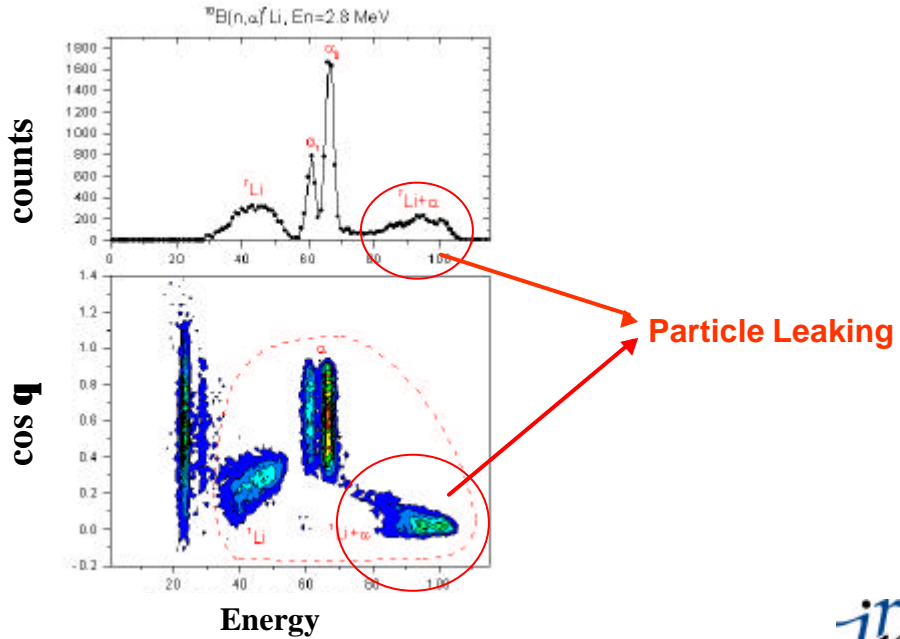
Importance of 2-dim analysis



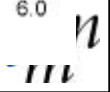
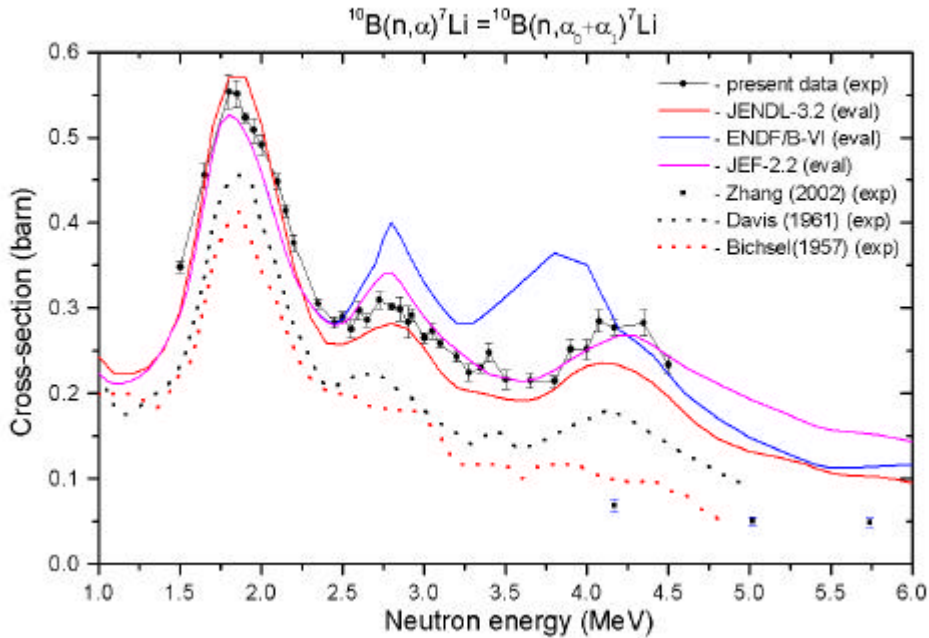
20



Effect of Particle Leaking



Present data: G. Giorginis and V. Khriatchkov, IRMM, June 2003



THE RESULTS OF POLYNOMIAL AND RATIONAL LEAST SQUARES FITS FOR THE ${}^6\text{Li}(n,t)$ REACTION CROSS-SECTION

S.A.Badikov, E.V.Gai
Institute of Physics and Power Engineering,
249033 Obninsk, Kaluga region, Russia

Abstract

The results of polynomial and rational approximation for the ${}^6\text{Li}(n,t)$ reaction cross-section are presented. The polynomial least squares fits fail because of the Peelle's Puzzle effects. A comparison between model and "non-model" least squares fits is carried out. The rational approximants agree with the R-matrix model calculations with the RAC code. The "non-model" fit (GMA code) is systematically lower the RAC curve, rational approximant and the main bulk of the experimental data. The bias is also caused by the Peelle's Puzzle effects.

A validity and performance of "generalized measure of uncertainty" proposed in [2] is studied. In considered cases *generalized measures of uncertainty* calculated for model and "non-model" least squares fits are in good agreement. Together with other statistical criteria (as determinant of covariance matrix) the *generalized measure of uncertainty* can be used for analysis of the quality of the evaluations.

Introduction

Preparation of the TEST1 have pursued two objects [1]: a) to check the performance and consistency of the GMA and GLUCS codes realizing "non-model" fits to the experimental data; b) to compare the results of model and "non-model" least squares fits. Of the model fits only the results of R-matrix fit with RAC code have been presented and published [1-3]. Present work describes the polynomial and rational fits for TEST1 and, thus, expands the base for the comparison of model and "non-model" least squares fits.

Besides, a new generalized measure of uncertainty for comparison of different least squares fits was proposed [2] and its use for analysis of model and "non-model" least squares fits of the ${}^6\text{Li}(n,t)$ reaction cross-section was considered. In this connection an application of the generalized measure of uncertainty for analysis of new "object" – rational least squares fits – is of special interest.

Input data

Input data for TEST1 include 5 experimental data sets for the ${}^6\text{Li}(n,t)$ reaction cross-section in the neutron energy range 2.5 – 800 KeV. The cross-sections and their uncertainties were extracted from the database used for the ENDF/B-VI neutron standards [1] whereas correlations were calculated anew. Unlike the procedure used by Poenitz [4] the correlations were prepared on the basis of two components of the total uncertainty: long

energy range (LERC) and statistical (SERC) [1]. All the numerical values and corresponding references for the input data are given in Annex 4 of the Report IAEA INDC(NDS)-438.

Results

We omit a description of straightforward and well known procedure for getting exact LSM-solution in case of polynomial approximation. Corresponding procedure for rational approximation is much more complicated since least squares problem is non-linear. This procedure was outlined in [5].

The results of polynomial approximations for TEST1 are presented in Fig.1. A polynomial least squares fit with 7 parameters provides best approximant for the experimental data set Lamaze 78 with measurements processed as independent. The parameters of the polynomial are given in Table 1. The value of minimized functional

$$S_1 = \sqrt{\frac{1}{N-L} \sum_{i=1}^N \frac{(y_i - f_i)^2}{\sigma_i^2}} \quad (1)$$

is 11.1. In (1) N – number of measurements, L – number of parameters, y_i and f_i – experimental and approximant's values correspondingly, σ_i – uncertainty of measurement. As seen from Fig.1 the polynomial doesn't reproduce even the shape of the experimental data. Increasing the number of polynomial's parameters (from 7 to 9 with S_1 equal to 11.2) didn't result in improvement consistency between the approximant and the experimental data. Inclusion the correlations between experimental errors in calculations leads to strong shift of the polynomial approximant down relative to measurements. As a result there is a large gap between the most low of the measurements Lamaze 78 and the best polynomial of the 6-th degree (see Fig.1). This is an effect of the Peelle's Puzzle type [6,7]. Actually, 474 of 1275 correlations between experimental errors ε_i and ε_j don't satisfy restriction

$$\text{cor}(\varepsilon_i, \varepsilon_j) \leq (\sigma_i / f_i) / (\sigma_j / f_j) \quad (2)$$

which ensures the absence of the effects of the Peelle's Puzzle type [8]. The value of minimized functional

$$S_2 = \sqrt{\frac{1}{N-L} \sum_{i=1}^N \sum_{j=1}^N (y_i - f_i)(V^{-1})_{ij}(y_j - f_j)} \quad (3)$$

equals to $S_2=8.25$. Here V – covariance matrix for experimental errors. The parameters of the polynomial are given in Table 1. Again increasing the number of polynomial's parameters (from 7 to 9 with S_2 equal to 8.37) didn't improve agreement between the polynomial and the experimental data. Thus, the polynomial fits fail in case of the ${}^6\text{Li}(n,t)$ reaction cross-section approximation.

Unlike the polynomials the rational approximants demonstrate very good agreement with the experimental data in both cases (with correlations included in and excluded from calculations). In Fig.2 the rational approximants with 10 parameters are given in comparison with the experimental data Lamaze 78. The values of functional are $S_1=0.530$ and $S_2=0.753$ respectively. The parameters of the rational approximants are given in Table 2 in pole representation

$$f^{[M_1, M_2]}(E, \theta) \equiv c + \sum_{k=1}^K \frac{a_k}{E - r_k} + \sum_{j=1}^J \frac{\alpha_j (E - \varepsilon_j) + \beta_j}{(E - \varepsilon_j)^2 + \gamma_j^2} \quad (4)$$

($L = 2K + 4J + 1$ when $M_1 = M_2$ and $L = 2K + 4J$ when $M_1 = M_2 - 1$, M_1 and M_2 – degrees of numerator and denominator of the rational function). As seen from Fig.2 and Tables 3 and 4 the rational approximant agrees also with RAC calculations [2,3]. The results of the least squares fits with the RAC and PADE2 code have reasonable and clear justification. As follows from Table 3 lower limit of the estimated cross-section uncertainty is a little higher than 1.6% - value of long-range (100% correlated) component of total experimental uncertainty for measurements Lamaze 78. As expected, a statistical component of the uncertainty decreased essentially after processing while the long-range component of the uncertainty remained unchanged since only one experimental data set was available for processing.

Before interpretation of numerical values from Table 4 and application of *generalized measure of uncertainty* for their analysis let's consider a performance of the *measure* in case of simple exactly solved model. Let N measurements of the same mean are carried out with uncertainties $\sigma_i = \sigma$; errors of the measurements correlate with the same coefficient ρ . The *generalized measure of uncertainty* is defined as a sum of experimental or estimated covariances at points of measurements, divided by the number of elements in the matrix [2]. In considered model the sum of experimental covariances T_{ex} equals to:

$$T_{ex} = \sigma^2 (1-\rho)/N + \rho\sigma^2 = \varepsilon^2/N + \omega^2,$$

where ε^2 , ω^2 – variances of statistical and systematic experimental errors, respectively. All the estimated covariances are the same and, correspondingly, $T_{ev} = \varepsilon^2/N + \omega^2$. Thus, *generalized measure of uncertainty* preserved during statistical processing - $T_{ex} = T_{ev}$ (all the $N-1$ covariances in the row increased by value which is $(N-1)$ times lower the magnitude corresponding decreasing the variance – preserving average matrix element). The result changes in case of measurements with different uncertainties regardless of value of the correlation. For independent measurements $T_{ex} = \sum_{i=1}^N \sigma_i^2 / N$, $T_{ev} = (\sum_{i=1}^N \frac{1}{\sigma_i^2})^{-1}$ and $T_{ev} < T_{ex}$.

For example, at $(\sigma_i)^2 = k^{i-1} \sigma^2$, $i = 1, \dots, N$

$$T_{ex} / T_{ev} = \frac{(1 - k^N)^2}{N^2 (1 - k)^2 k^{N-1}}.$$

And at $N=3$, $k=1.5$ $T_{ex} / T_{ev} \approx 1.11$. So, in case of measurements with different uncertainties we should expect decreasing the *generalized measure of uncertainty*.

Table 4 includes the experimental and evaluated cross-section covariances from the rows 1 and 25. The experimental covariances are in reasonable agreement with estimated ones calculated with the RAC and PADE2 codes. This result can be interpreted in following manner. The experimental covariances are determined by systematic uncertainties while estimated covariances are induced by two components: 1) a rigidity of the model curve and 2) systematic uncertainties. A contribution from the first component can be approximately calculated in rational fit of the experimental data with measurements processed as independent. In this case estimated covariances are determined by the rigidity of the model curve only. In Table 5 the estimated covariances calculated in assumption of independent and correlated measurements are presented. As seen, a contribution to the total estimated

covariances from the covariances induced by the rigidity of the model curve is negligible at most of points. Thus, in rows with the same numbers the experimental and estimated covariances equal each other approximately except for variances. A difference in variances is caused by reduction of the statistical component of total experimental uncertainty after processing. Correspondingly, the sums of the experimental and estimated covariances (over row) differ from each other by very small value. To make a rough estimate let's accept, that variance and covariances contribute to the sum in equal degree approximately (about $1/n$, n – number of elements in the row). Then decreasing the variance in k times results in decreasing the sum in $nk/(1+k(n-1))$ times. After processing with the rational function as a model one the statistical part of the variance decreased in $k = N/L = 51/10 \approx 5.1$ times. In correspondence with the rough estimate it results in decreasing the sum in 1.016 times. Thus, the sums of experimental and estimated covariances must differ within few percent – in good agreement with the data from the Table 4.

The results of rational approximation for 5 experimental data sets are given in Fig.3 and Tables 6 and 7. As follows from Fig.3 and Table 6 the rational approximant (PADE2) is in good agreement with the RAC curve. The GMA approximant is systematically lower the RAC and PADE2 curves and the main bulk of the experimental data. The shift is probably induced by unrealistic correlations between experimental errors: For example, for the experimental data Lamaze 78 657 of 1275 correlations don't satisfy restriction (2), which excludes, probably, the Peelle's Puzzle effects.

In Table 7 estimated covariances calculated in “non-model” (GMA) and model (PADE2, RAC) least squares fits are compared. As follows from the Table 7 “non-model” and model fits treat the systematic uncertainty in similar manner. And difference in the sums of the covariances (over row) is caused by a degree of decreasing the statistical experimental uncertainty.

The *generalized measure of uncertainty* ($varU$ [2]) can be considered as universal measure of uncertainty of data sets, both experimental and evaluated ones. In case TEST1 this measure does not differ essentially for experimental data and for results of model and “non-model” evaluations. It can be shown that such a stability takes place in many other practical problems, especially if the variation of corresponding experimental and evaluated values with energy is comparatively small (times, not orders), even in case of simultaneous fit of many experimental data sets. This measure is, by the definition, variance of mean value of some data, and in mean value statistical fluctuations are compensated in the same degree as in estimated data. It permits to use $varU$ for comparison of quality of different data sets even without their analysis and evaluation of model dependence. But for comparison of quality of different model and non-model fits we propose to use it simultaneously with mean

dispersion (variation) of fit, $\sigma = \frac{1}{N} \sum_i \sigma_i$ (mean uncertainty), taken in the same points for all fits. In our understanding the best fit is one with narrowest corridor of errors and their full correlations, i.e. with covariances $\sigma_i \sigma_k$ and $\sigma^2 = varU$. In dependence on quality of the fit the value of σ^2 can vary between σ_{exp}^2 (upper boundary) and $varU$ (lower boundary), and it is possible to use $q = (\sigma_{exp}^2 - \sigma^2) / (\sigma_{exp}^2 - varU)$ as quantitative measure of fit's statistical quality. Note that value $q=1$ may be not accessible with use of physical model fits.

Summary

1. The polynomial least squares fits of the experimental data for the ${}^6\text{Li}(n,t)$ reaction cross-section fail because of the Peelle's Puzzle effects.
2. The results of rational approximation for the ${}^6\text{Li}(n,t)$ reaction cross-section agree with the R-matrix model calculations with the RAC code. The "non-model" fit (GMA code) is systematically lower the RAC curve, rational approximant and the main bulk of the experimental data. The shift is probably caused by the Peelle's Puzzle effects.
3. Validity and performance of "generalized measure of uncertainty" proposed in [2] was studied. In considered cases *generalized measures of uncertainty* calculated for model and "non-model" least squares fits are in good agreement. Together with other statistical criteria (as determinant of covariance matrix) the *generalized measure of uncertainty* can be used for analysis of the quality of the evaluations.

References

1. V.G.Pronyaev, "Test and Intercomparisons of Data Fitting with General Least Squares Code GMA versus Bayesian Code GLUCS", Summary Report of the First Research Co-ordination Meeting on Improvement of the Standard Cross Sections for Light Elements, Prepared by A.D.Carlson, G.M.Hale and V.G.Pronyaev, p.159, Report INDC(NDS)-438, IAEA, 2003.
2. V.G.Pronyaev, "Does Model Fit Decrease the Uncertainty of the Data in Comparison with a General Non-Model Least Squares Fit", Summary Report of the First Research Co-ordination Meeting on Improvement of the Standard Cross Sections for Light Elements, Prepared by A.D.Carlson, G.M.Hale and V.G.Pronyaev, p.172, Report INDC(NDS)-438, IAEA, 2003.
3. Chen Zhenpeng, SUN Yeying, "Progress Report on Calculation of ${}^6\text{Li}(n,t)$ with RAC", Summary Report of the First Research Co-ordination Meeting on Improvement of the Standard Cross Sections for Light Elements, Prepared by A.D.Carlson, G.M.Hale and V.G.Pronyaev, p.65, Report INDC(NDS)-438, IAEA, 2003.
4. W.P.Poenitz, S.E.Aumeier, "The Simultaneous Evaluation of the Standards and Other Cross Sections of Importance for Technology", p.16, Report ANL/NDM-139, ANL, USA, 1997.
5. S.A.Badikov, E.V.Gai, M.A.Guseynov, N.S.Rabotnov, "Nuclear Data Processing, Analysis, Transformation and Storage with Pade-approximants", Proceedings of International Conference "Nuclear Data for Science and Technology", 13-17 May 1991, Julich, Germany, p.182, Springer-Verlag, 1992.
6. R.W.Peelle, "Peelle's Pertinent Puzzle", Informal memorandum dated October 13, 1987, Oak Ridge National Laboratory, Oak Ridge, Tennessee, USA, 1987.
7. S.Chiba, D.L.Smith, "A Suggested Procedure for Resolving an Anomaly in Least Squares Data Analysis Known as Peelle's Pertinent Puzzle and the General Implications for Nuclear Data Evaluation", ANL/NDM-121, ANL, USA, 1991.
8. E.V.Gai, S.A.Badikov, "Once Again on the Peelle's Puzzle", Summary Report of the Second Research Coordination Meeting on Improvement of the Standard Cross Sections for Light Elements, to be published.

Table 1. Parameters of the polynomial least squares fits for the experimental data Lamaze 78 (${}^6\text{Li}(n,t)$ reaction cross-section) processed as non-correlated (I) and correlated (II) measurements (energy in MeV).

Degree of variable E	Parameters	
	I	II
0	2.193132+00	5.496052-01
1	-5.787103+01	-1.489736+01
2	6.727443+02	1.724215+02
3	-3.013504+03	-7.695846+02
4	6.251769+03	1.591357+03
5	-6.108457+03	-1.549776+03
6	2.279770+03	5.764785+02

Table 2. Parameters (in representation (4)) of the rational least squares fits for the experimental data Lamaze 78 (${}^6\text{Li}(n,t)$ reaction cross-section) processed as non-correlated (I) and correlated (II) measurements (energy in MeV).

	Parameters	
	I	II
α_1	1.490599-02	1.441790-02
β_1	5.884416-03	5.812856-03
ε_1	2.371290-01	2.372534-01
γ_1	4.518541-02	4.489927-02
a_1	3.533810-01	3.757729-01
r_1	-1.241763-00	-1.388811-00
a_2	1.855675-02	1.805139-02
r_2	-1.276004-02	-1.997368-02
a_3	4.502873-03	7.137620-03
r_3	-5.016321-04	-1.205583-03
c	0.0	

Table 3. Comparison of the experimental data Lamaze 78 (${}^6\text{Li}(n,t)$ reaction cross-section) with their model (RAC, PADE2) fits.

Energy, MeV	Experimenta l X-section,b	Estimated X-section (RAC),b	Estimated X-section (PADE2),b	Experimenta l error, %	Estimated error (RAC), %	Estimated error (PADE2), %
0.2500-02	3.0420+00	3.0559+00	3.0420+00	6.9957	2.2686	6.0855
0.3500-02	2.5700+00	2.5828+00	2.5989+00	6.6189	2.1389	3.2379
0.4500-02	2.3020+00	2.2786+00	2.3020+00	4.7697	2.0451	2.4916
0.5500-02	2.0780+00	2.0622+00	2.0869+00	3.6797	1.9751	2.2541
0.6500-02	1.9340+00	1.8983+00	1.9224+00	3.5651	1.9216	2.1099
0.7500-02	1.8210+00	1.7687+00	1.7917+00	3.3466	1.8805	2.0056
0.8500-02	1.7200+00	1.6630+00	1.6846+00	3.0901	1.8485	1.9394
0.9500-02	1.5850+00	1.5747+00	1.5948+00	2.5673	1.8236	1.9058
0.1500-01	1.2750+00	1.2621+00	1.2750+00	2.4534	1.7584	1.9133
0.2000-01	1.1300+00	1.1018+00	1.1094+00	2.4823	1.7445	1.8829
0.2400-01	1.0030+00	1.0131+00	1.0173+00	2.6829	1.7420	1.8430
0.3000-01	9.2170-01	9.1723-01	9.1761-01	2.4000	1.7401	1.8068
0.4500-01	7.7240-01	7.7713-01	7.7240-01	2.3537	1.7244	1.7949
0.5500-01	7.2400-01	7.2446-01	7.1843-01	2.2694	1.7086	1.7764
0.6500-01	6.9080-01	6.9022-01	6.8379-01	2.4724	1.6948	1.7462
0.7500-01	6.5160-01	6.6929-01	6.6299-01	2.3956	1.6858	1.7194
0.8500-01	6.5780-01	6.5910-01	6.5330-01	2.1861	1.6822	1.7046
0.9500-01	6.6190-01	6.5855-01	6.5350-01	2.3962	1.6828	1.7024
0.1000-00	6.5140-01	6.6180-01	6.5723-01	2.1048	1.6841	1.7047
0.1200-00	6.9840-01	7.0032-01	6.9840-01	1.9945	1.6910	1.7203
0.1500-00	8.6130-01	8.6362-01	8.7063-01	1.9540	1.6964	1.7200
0.1700-00	1.1400+00	1.0968+00	1.1184+00	2.1799	1.6981	1.7101
0.1800-00	1.3410+00	1.2772+00	1.3113+00	2.1074	1.6978	1.7059
0.1900-00	1.5970+00	1.5178+00	1.5691+00	2.1239	1.6956	1.7007
0.2000-00	1.8970+00	1.8314+00	1.9040+00	2.1239	1.6919	1.6935
0.2100-00	2.2750+00	2.2194+00	2.3120+00	1.8839	1.6897	1.6869
0.2200-00	2.7700+00	2.6487+00	2.7460+00	1.8841	1.6929	1.6877
0.2300-00	3.1070+00	3.0272+00	3.0948+00	1.9925	1.7003	1.6977
0.2400-00	3.2220+00	3.2197+00	3.2220+00	2.1840	1.7034	1.7078
0.2450-00	3.1810+00	3.2154+00	3.1810+00	2.1838	1.7019	1.7106
0.2500-00	3.0620+00	3.1439+00	3.0773+00	2.1843	1.6996	1.7124
0.2600-00	2.7970+00	2.8482+00	2.7437+00	2.0246	1.6988	1.7178
0.2700-00	2.3980+00	2.4582+00	2.3502+00	2.2136	1.7068	1.7279
0.2800-00	1.9560+00	2.0760+00	1.9836+00	2.1401	1.7198	1.7386
0.3000-00	1.4250+00	1.4834+00	1.4310+00	2.1145	1.7448	1.7496
0.3250-00	1.0220+00	1.0417+01	1.0220+00	2.2847	1.7752	1.7549
0.3500-00	8.0020-01	7.9387-01	7.9029-01	2.2694	1.8155	1.7728
0.3750-00	6.5610-01	6.4519-01	6.4927-01	2.4249	1.8608	1.8042
0.4000-00	5.6240-01	5.4945-01	5.5711-01	2.8432	1.9018	1.8385
0.4250-00	4.6660-01	4.8398-01	4.9312-01	5.1118	1.9338	1.8665
0.4500-00	4.5120-01	4.3693-01	4.4642-01	6.0860	1.9569	1.8833
0.4750-00	4.2480-01	4.0173-01	4.1093-01	5.5462	1.9738	1.8884
0.5000-00	3.8770-01	3.7451-01	3.8303-01	5.0813	1.9875	1.8832
0.5200-00	3.6840-01	3.5684-01	3.6465-01	4.6797	1.9973	1.8737
0.5400-00	3.4890-01	3.4192-01	3.4890-01	4.2591	2.0063	1.8612
0.5700-00	3.3090-01	3.2344-01	3.2905-01	3.5721	2.0162	1.8411
0.6000-00	3.1530-01	3.0846-01	3.1259-01	3.0707	2.0178	1.8246
0.6500-00	2.8670-01	2.8890-01	2.9046-01	3.0035	1.9884	1.8201
0.7000-00	2.7420-01	2.7399-01	2.7291-01	2.8460	1.9237	1.8603
0.7500-00	2.5680-01	2.6221-01	2.5848-01	2.7457	1.9205	1.9546
0.8000-00	2.4630-01	2.5264-01	2.4630-01	2.6171	2.2400	2.1023

Table 4. Covariances (in b^2) for point #1 and #25 for experimental errors and model (RAC, PADE2) least squares fits of the experimental data Lamaze 78 (${}^6\text{Li}(n,t)$ reaction cross-section).

Point #	Point #1			Point #25		
	Experiment	RAC	PADE2	Experiment	RAC	PADE2
1	0.04516	0.00481	0.03427	0.00145	0.00141	0.00140
2	0.00216	0.00383	0.01326	0.00123	0.00121	0.00128
3	0.00187	0.00320	0.00535	0.00111	0.00107	0.00115
4	0.00162	0.00274	0.00220	0.00101	0.00097	0.00104
5	0.00147	0.00243	0.00096	0.00095	0.00090	0.00095
6	0.00141	0.00217	0.00054	0.00083	0.00083	0.00088
7	0.00138	0.00196	0.00047	0.00083	0.00079	0.00082
8	0.00121	0.00179	0.00054	0.00077	0.00075	0.00077
9	0.00101	0.00123	0.00109	0.00061	0.00060	0.00061
10	0.00089	0.00097	0.00116	0.00054	0.00052	0.00054
11	0.00075	0.00083	0.00108	0.00048	0.00048	0.00050
12	0.00071	0.00070	0.00091	0.00045	0.00043	0.00045
13	0.00059	0.00054	0.00058	0.00038	0.00036	0.00038
14	0.00057	0.00050	0.00047	0.00035	0.00033	0.00035
15	0.00055	0.00049	0.00043	0.00033	0.00032	0.00033
16	0.00050	0.00048	0.00043	0.00032	0.00030	0.00032
17	0.00052	0.00049	0.00044	0.00032	0.00030	0.00031
18	0.00051	0.00051	0.00047	0.00032	0.00030	0.00031
19	0.00050	0.00052	0.00049	0.00032	0.00032	0.00031
20	0.00053	0.00057	0.00058	0.00034	0.00042	0.00034
21	0.00066	0.00072	0.00075	0.00041	0.00044	0.00044
22	0.00090	0.00090	0.00092	0.00055	0.00055	0.00059
23	0.00103	0.00102	0.00104	0.00066	0.00066	0.00071
24	0.00123	0.00120	0.00119	0.00078	0.00079	0.00086
25	0.00146	0.00142	0.00140	0.00163	0.00096	0.00104
26	0.00173	0.00172	0.00169	0.00111	0.00115	0.00125
27	0.00211	0.00208	0.00205	0.00135	0.00135	0.00144
28	0.00238	0.00243	0.00240	0.00150	0.00147	0.00156
29	0.00255	0.00262	0.00260	0.00157	0.00149	0.00156
30	0.00252	0.00262	0.00259	0.00155	0.00147	0.00152
31	0.00243	0.00255	0.00250	0.00149	0.00142	0.00146
32	0.00214	0.00228	0.00219	0.00135	0.00121	0.00130
33	0.00190	0.00195	0.00181	0.00117	0.00112	0.00112
34	0.00150	0.00161	0.00148	0.00096	0.00096	0.00096
35	0.00109	0.00113	0.00102	0.00070	0.00071	0.00071
36	0.00086	0.00080	0.00073	0.00050	0.00050	0.00051
37	0.00064	0.00064	0.00059	0.00039	0.00038	0.00039
38	0.00050	0.00054	0.00051	0.00032	0.00031	0.00032
39	0.00044	0.00048	0.00046	0.00027	0.00026	0.00027
40	0.00035	0.00043	0.00043	0.00023	0.00023	0.00024
41	0.00035	0.00039	0.00040	0.00022	0.00020	0.00021
42	0.00035	0.00036	0.00038	0.00021	0.00019	0.00019
43	0.00029	0.00033	0.00035	0.00019	0.00017	0.00018
44	0.00029	0.00031	0.00034	0.00018	0.00017	0.00017
45	0.00029	0.00030	0.00032	0.00017	0.00016	0.00016
46	0.00025	0.00026	0.00030	0.00016	0.00015	0.00015
47	0.00025	0.00025	0.00028	0.00015	0.00014	0.00015
48	0.00022	0.00022	0.00024	0.00014	0.00013	0.00014
49	0.00021	0.00020	0.00021	0.00013	0.00012	0.00013
50	0.00020	0.00020	0.00018	0.00012	0.00012	0.00013
51	0.00019	0.00021	0.00015	0.00012	0.00011	0.00012
Σ (Sum)	0.09522	0.06293	0.09726	0.03314	0.03176	0.03301
$\Sigma / \Sigma(\text{GMA})$	1	0.8233	1.0214	1	0.9583	0.9961

Table 5. Covariances (in b^2) for point #1 and #25 for model (PADE2) least squares fits of the experimental data Lamaze 78 (${}^6\text{Li}(n,t)$ reaction cross-section) processed as independent (I) and correlated (II) measurements.

Point #	Point #1			Point #25		
	PADE2-I	PADE2-II	Absolute ratio (II/I)	PADE2-I	PADE2-II	Absolute ratio (II/I)
1	3.4794-02	3.4270-02	0.98	-1.1490-04	1.4039-03	12.2
2	1.1775-02	1.3260-02	1.13	3.7352-05	1.2763-03	34.2
3	3.4081-03	5.3505-03	1.57	5.2418-05	1.1455-03	21.9
4	2.6961-04	2.1977-03	8.15	3.5400-05	1.0355-03	29.3
5	-8.1301-04	9.6264-04	1.18	1.4678-05	9.4677-04	64.5
6	-1.0545-03	5.4295-04	0.51	-2.2678-06	8.7538-04	386
7	-9.5866-04	4.7280-04	0.49	-1.4171-05	8.1752-04	57.7
8	-7.4393-04	5.4484-04	0.73	-2.1575-05	7.7005-04	35.7
9	2.2615-04	1.0885-03	4.81	-1.9765-05	6.1315-04	31.0
10	4.2149-04	1.1624-03	2.76	-2.3904-06	5.3945-04	226
11	3.7751-04	1.0811-03	2.86	8.6806-06	4.9925-04	57.5
12	2.2738-04	9.0540-04	3.98	1.8020-05	4.5463-04	25.2
13	-5.8690-05	5.7584-04	9.81	1.6902-05	3.8321-04	22.7
14	-1.2815-04	4.7384-04	3.70	8.4473-06	3.5314-04	41.8
15	-1.3767-04	4.3204-04	3.14	-7.4364-07	3.3220-04	447
16	-1.1417-04	4.2677-04	3.74	-8.7313-06	3.1858-04	36.5
17	-7.4445-05	4.4330-04	5.95	-1.4569-05	3.1135-04	21.4
18	-2.8579-05	4.7300-04	16.5	-1.7712-05	3.1016-04	17.5
19	-5.3505-06	4.9118-04	91.8	-1.8138-05	3.1183-04	17.2
20	7.8036-05	5.7876-04	7.42	-1.0772-05	3.3524-04	31.1
21	1.3770-04	7.5254-04	5.47	3.8872-05	4.4007-04	11.3
22	1.0021-04	9.2120-04	9.19	1.1440-04	5.9086-04	5.16
23	4.7829-05	1.0384-03	21.7	1.6994-04	7.0585-04	4.15
24	-2.7733-05	1.1931-03	43.0	2.3594-04	8.5510-04	3.62
25	-1.1490-04	1.4039-03	12.2	3.0229-04	1.0397-03	3.44
26	-1.7953-04	1.6900-03	9.41	3.4281-04	1.2468-03	3.64
27	-1.6480-04	2.0487-03	12.4	3.1529-04	1.4386-03	4.56
28	-3.9566-05	2.4044-03	60.8	1.9453-04	1.5561-03	8.00
29	1.2259-04	2.5956-03	21.2	2.9027-05	1.5576-03	53.
30	1.7385-04	2.5859-03	14.9	-3.8570-05	1.5167-03	39.3
31	1.9090-04	2.5048-03	13.1	-8.3466-05	1.4551-03	17.4
32	1.3676-04	2.1929-03	16.0	-1.0523-04	1.2962-03	12.3
33	3.3804-05	1.8147-03	53.7	-7.3533-05	1.1241-03	15.3
34	-5.2842-05	1.4769-03	27.9	-3.2140-05	9.6406-04	30.0
35	-1.2256-04	1.0175-03	8.30	1.8318-05	7.1253-04	38.9
36	-1.0050-04	7.3005-04	7.26	3.0206-05	5.1328-04	17.0
37	-5.1751-05	5.9079-04	11.4	2.2970-05	3.9439-04	17.2
38	-8.8082-06	5.1375-04	58.3	1.3151-05	3.2002-04	24.3
39	2.2776-05	4.6468-04	20.4	4.9200-06	2.7090-04	55.1
40	4.4003-05	4.2925-04	9.76	-1.1169-06	2.3687-04	212
41	5.6965-05	4.0097-04	7.04	-5.2214-06	2.1233-04	40.7
42	6.3574-05	3.7668-04	5.93	-7.7947-06	1.9404-04	24.9
43	6.5348-05	3.5477-04	5.43	-9.1952-06	1.8003-04	19.6
44	6.4077-05	3.3838-04	5.28	-9.6649-06	1.7105-04	17.7
45	6.0922-05	3.2270-04	5.30	-9.6818-06	1.6356-04	16.9
46	5.3449-05	3.0019-04	5.62	-9.0526-06	1.5446-04	17.1
47	4.3525-05	2.7863-04	6.40	-7.8446-06	1.4728-04	18.8
48	2.3383-05	2.4441-04	10.5	-4.9804-06	1.3825-04	27.8
49	5.9774-07	2.1205-04	355	-1.4870-06	1.3170-04	88.6
50	-2.3414-05	1.8144-04	7.75	2.3159-06	1.2677-04	54.7
51	-4.7751-05	1.5252-04	3.20	6.2313-06	1.2295-04	19.7

Table 6. Comparison of model (RAC, PADE2) and “non-model” (GLUCS, GMA) least squares fits of 5 experimental data sets for the ${}^6\text{Li}(n,t)$ reaction cross-section.

Energy, MeV	GLUCS, b	GMA, b	RAC, b	PADE2, b	$1 - \frac{GMA}{PADE2}, \%$	$1 - \frac{RAC}{PADE2}, \%$
0.2500-02	2.5643+00	2.5679+00	2.6544+00	2.7666+00	7.18	4.06
0.3500-02	2.1340+00	2.1389+00	2.2457+00	2.2997+00	6.99	2.35
0.4500-02	1.8435+00	1.8549+00	1.9831+00	2.0121+00	7.81	1.44
0.5500-02	1.7385+00	1.7392+00	1.7965+00	1.8130+00	4.07	0.91
0.6500-02	1.5777+00	1.5773+00	1.6553+00	1.6647+00	5.25	0.56
0.7500-02	1.4669+00	1.4690+00	1.5437+00	1.5490+00	5.16	0.34
0.8500-02	1.4182+00	1.4138+00	1.4528+00	1.4554+00	2.86	0.18
0.9500-02	1.2888+00	1.2880+00	1.3769+00	1.3778+00	6.52	0.07
0.1500-01	1.0487+00	1.0451+00	1.1091+00	1.1073+00	5.62	-0.16
0.2000-01	9.5192-01	9.5499-01	9.7250-01	9.7200-01	1.75	-0.05
0.2400-01	8.6783-01	8.6615-01	8.9739-01	8.9874-01	3.63	0.15
0.3000-01	7.6349-01	7.6629-01	8.1680-01	8.2134-01	6.70	0.55
0.4500-01	6.6971-01	6.6951-01	7.0144-01	7.1323-01	6.13	1.65
0.5500-01	6.3158-01	6.3043-01	6.5994-01	6.7516-01	6.63	2.25
0.6500-01	6.0471-01	6.0439-01	6.3466-01	6.5208-01	7.31	2.67
0.7500-01	5.7693-01	5.7853-01	6.2129-01	6.3973-01	9.57	2.88
0.8500-01	6.0873-01	6.0811-01	6.1773-01	6.3614-01	4.41	2.89
0.9500-01	5.9780-01	5.9927-01	6.2317-01	6.4055-01	6.44	2.71
0.1000-00	5.9648-01	5.9749-01	6.2925-01	6.4577-01	7.48	2.56
0.1200-00	6.3976-01	6.4001-01	6.7821-01	6.8923-01	7.14	1.60
0.1500-00	7.9289-01	7.9463-01	8.5476-01	8.5307-01	6.85	-0.20
0.1700-00	1.0061+00	1.0051+00	1.0923+00	1.0840+00	7.28	-0.77
0.1800-00	1.2084+00	1.2095+00	1.2708+00	1.2637+00	4.29	-0.56
0.1900-00	1.4454+00	1.4487+00	1.5040+00	1.5049+00	3.73	0.06
0.2000-00	1.7253+00	1.7275+00	1.8017+00	1.8218+00	5.18	1.10
0.2100-00	2.0577+00	2.0604+00	2.1622+00	2.2160+00	7.02	2.43
0.2200-00	2.4852+00	2.4901+00	2.5546+00	2.6513+00	6.08	3.65
0.2300-00	2.8005+00	2.8042+00	2.9001+00	3.0270+00	7.36	4.19
0.2400-00	2.9316+00	2.9417+00	3.0856+00	3.2004+00	8.08	3.59
0.2450-00	2.8906+00	2.8946+00	3.0912+00	3.1819+00	9.03	2.85
0.2500-00	2.8530+00	2.8591+00	3.0368+00	3.0961+00	7.65	1.92
0.2600-00	2.5546+00	2.5568+00	2.7839+00	2.7804+00	8.04	-0.13
0.2700-00	2.3155+00	2.3134+00	2.4296+00	2.3867+00	3.07	-1.80
0.2800-00	1.9120+00	1.9077+00	2.0682+00	2.0126+00	5.21	-2.76
0.3000-00	1.3738+00	1.3790+00	1.4862+00	1.4459+00	4.63	-2.79
0.3250-00	9.8769-01	9.9185-01	1.0394+00	1.0291+00	3.62	-1.00
0.3500-00	7.5831-01	7.5963-01	7.8595-01	7.9506-01	4.46	1.15
0.3750-00	6.2623-01	6.2617-01	6.3395-01	6.5351-01	4.18	2.99
0.4000-00	5.4585-01	5.4581-01	5.3666-01	5.6124-01	2.75	4.38
0.4250-00	4.8323-01	4.8093-01	4.7073-01	4.9715-01	3.26	5.31
0.4500-00	3.8710-01	3.8657-01	4.2388-01	4.5026-01	14.1	5.86
0.4750-00	3.8596-01	3.8682-01	3.8927-01	4.1448-01	6.67	6.08
0.5000-00	3.5704-01	3.5763-01	3.6287-01	3.8620-01	7.40	6.04
0.5200-00	3.4137-01	3.4160-01	3.4597-01	3.6745-01	7.03	5.85
0.5400-00	3.2214-01	3.2279-01	3.3188-01	3.5131-01	8.12	5.53
0.5700-00	3.1541-01	3.1529-01	3.1472-01	3.3082-01	4.69	4.87
0.6000-00	2.9205-01	2.9303-01	3.0111-01	3.1368-01	6.58	4.00
0.6500-00	2.7146-01	2.7221-01	2.8392-01	2.9040-01	6.26	2.23
0.7000-00	2.5607-01	2.5552-01	2.7143-01	2.7170-01	5.96	0.10
0.7500-00	2.3794-01	2.3822-01	2.6213-01	2.5617-01	7.01	-2.33
0.8000-00	2.2406-01	2.2434-01	2.5511-01	2.4294-01	7.66	-5.01

Table 7. Covariances (in b^2) for point #1 and #25 for non-model (GMA) and model (RAC, PADE2) least squares fits of 5 experimental data sets for the ${}^6\text{Li}(n,t)$ reaction cross-section.

Point #	Point #1			Point #25		
	GMA	RAC	PADE2	GMA	RAC	PADE2
1	0.00775	0.00158	0.0074010	0.00047	0.00044	0.0004369
2	0.00076	0.00123	0.0018334	0.00039	0.00038	0.0004151
3	0.00064	0.00102	0.0005340	0.00034	0.00034	0.0003600
4	0.00051	0.00086	0.0002583	0.00031	0.00031	0.0003151
5	0.00050	0.00076	0.0002493	0.00029	0.00029	0.0002825
6	0.00048	0.00067	0.0002998	0.00027	0.00027	0.0002590
7	0.00042	0.00060	0.0003510	0.00025	0.00025	0.0002418
8	0.00038	0.00055	0.0003882	0.00023	0.00024	0.0002288
9	0.00032	0.00036	0.0003974	0.00019	0.00020	0.0001910
10	0.00028	0.00027	0.0003211	0.00017	0.00018	0.0001728
11	0.00025	0.00023	0.0002670	0.00016	0.00016	0.0001616
12	0.00022	0.00019	0.0002100	0.00014	0.00015	0.0001478
13	0.00020	0.00015	0.0001515	0.00012	0.00012	0.0001235
14	0.00018	0.00014	0.0001436	0.00011	0.00011	0.0001133
15	0.00017	0.00014	0.0001449	0.000109	0.000109	0.0001065
16	0.00017	0.00015	0.0001502	0.000106	0.000104	0.0001025
17	0.00016	0.00015	0.0001573	0.000109	0.000103	0.0001010
18	0.00016	0.00016	0.0001652	0.000106	0.000104	0.0001018
19	0.00017	0.00017	0.0001694	0.000108	0.000105	0.0001030
20	0.00018	0.00019	0.0001879	0.00011	0.00012	0.0001140
21	0.00022	0.00024	0.0002281	0.00014	0.00016	0.0001560
22	0.00028	0.00029	0.0002765	0.00018	0.00022	0.0002131
23	0.00033	0.00032	0.0003140	0.00022	0.00026	0.0002554
24	0.00039	0.00038	0.0003657	0.00026	0.00031	0.0003092
25	0.00047	0.00044	0.0004369	0.00072	0.00038	0.0003739
26	0.00056	0.00053	0.0005309	0.00037	0.00045	0.0004436
27	0.00067	0.00064	0.0006422	0.00045	0.00051	0.0005032
28	0.00075	0.00074	0.0007453	0.00050	0.00055	0.0005323
29	0.00075	0.00080	0.0007963	0.00051	0.00054	0.0005218
30	0.00076	0.00082	0.0007920	0.00052	0.00053	0.0005050
31	0.00075	0.00080	0.0007684	0.00051	0.00050	0.0004836
32	0.00065	0.00071	0.0006817	0.00046	0.00045	0.0004348
33	0.00064	0.00061	0.0005776	0.00043	0.00040	0.0003840
34	0.00052	0.00051	0.0004834	0.00035	0.00035	0.0003354
35	0.00038	0.00036	0.0003497	0.00024	0.00026	0.0002537
36	0.00027	0.00026	0.0002575	0.00018	0.00019	0.0001846
37	0.00021	0.00021	0.0002069	0.00014	0.00014	0.0001419
38	0.00017	0.00018	0.0001757	0.00011	0.00012	0.0001147
39	0.00014	0.00015	0.0001544	0.000094	0.000097	0.0000967
40	0.00014	0.00014	0.0001388	0.000089	0.000083	0.0000842
41	0.000098	0.00012	0.0001265	0.000070	0.000073	0.0000752
42	0.000102	0.00012	0.0001164	0.000065	0.000066	0.0000684
43	0.000106	0.000104	0.0001078	0.000065	0.000061	0.0000632
44	0.000100	0.000098	0.0001018	0.000061	0.000059	0.0000599
45	0.000075	0.000092	0.0000963	0.000052	0.000057	0.0000571
46	0.000087	0.000083	0.0000889	0.000058	0.000054	0.0000536
47	0.000079	0.000076	0.0000824	0.000050	0.000052	0.0000509
48	0.000079	0.000068	0.0000728	0.000050	0.000050	0.0000474
49	0.000071	0.000064	0.0000646	0.000047	0.000048	0.0000447
50	0.000065	0.000064	0.0000575	0.000043	0.000045	0.0000426
51	0.000063	0.000067	0.0000512	0.000041	0.000041	0.0000409
Σ (Sum)	0.023875	0.019656	0.023679	0.011163	0.011191	0.011009
$\Sigma / \Sigma(\text{GMA})$	1	0.8233	0.9918	1	1.0025	0.9862

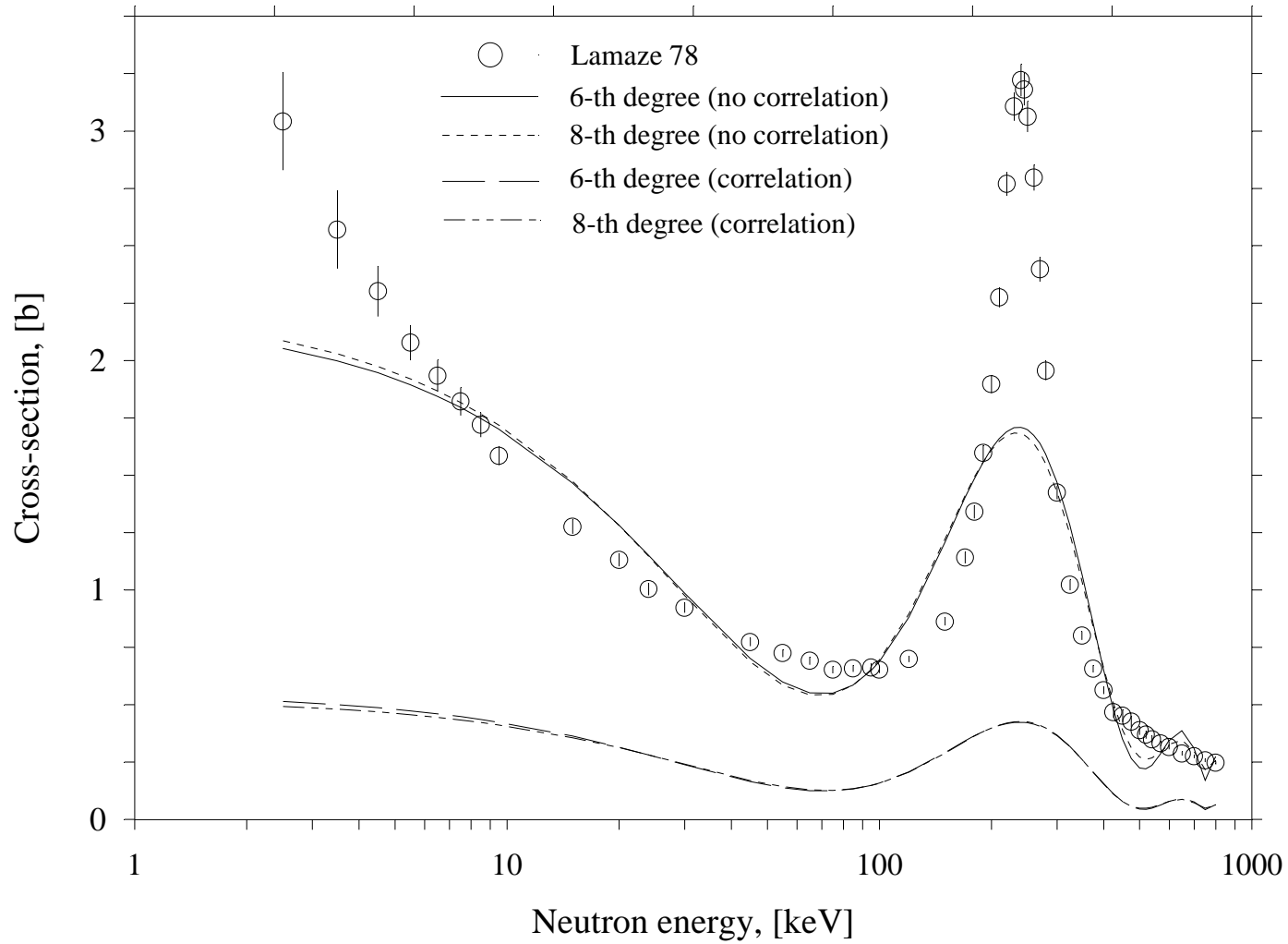


Fig.1 Polynomial approximants of the experimental data Lamaze 78 (${}^6\text{Li}(n,t)$ reaction cross section) calculated with and without taking correlation between experimental errors into account.

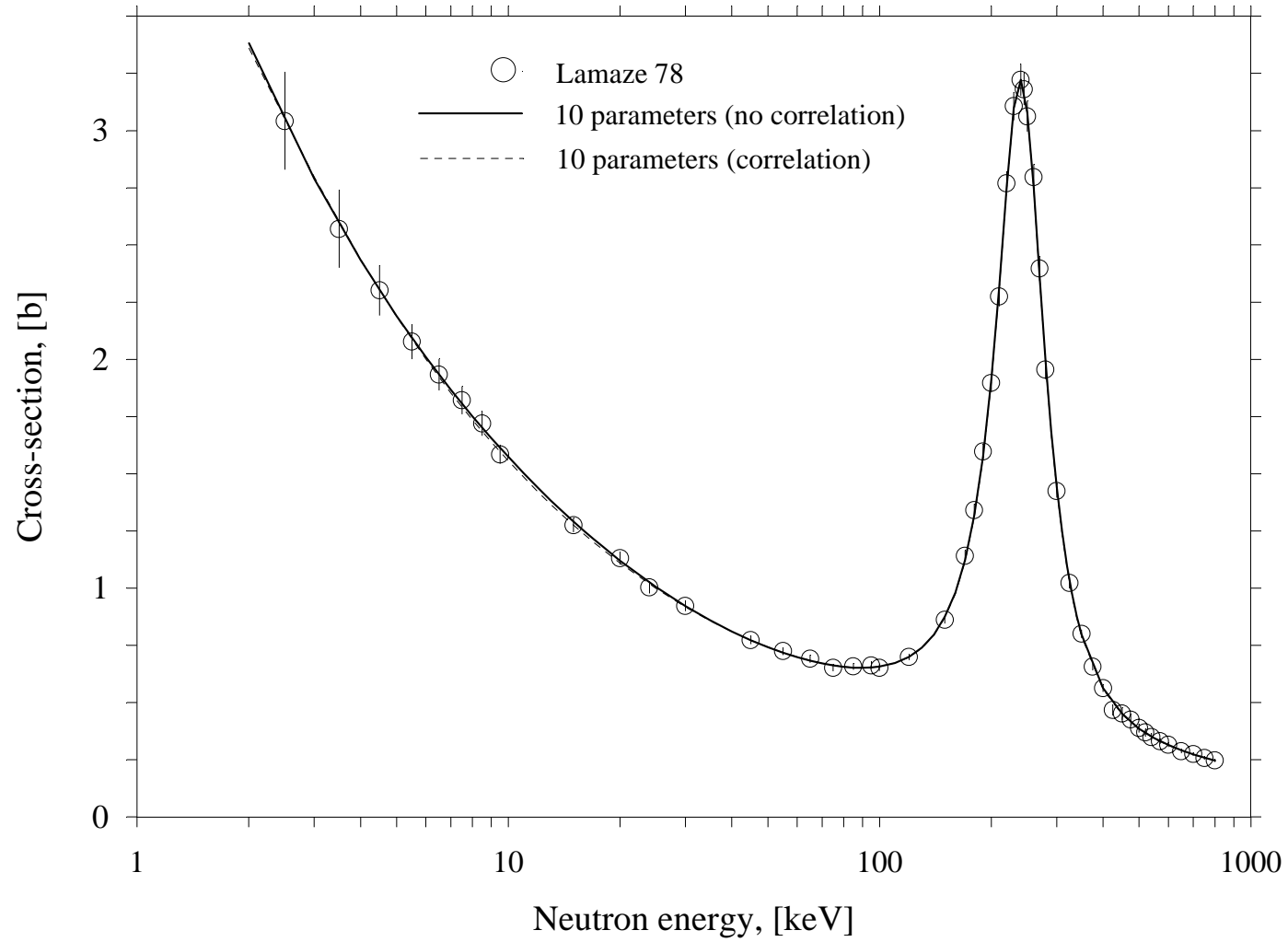


Fig.2 Rational approximants of the experimental data Lamaze 78 (${}^6\text{Li}(n,t)$ reaction cross section) calculated with and without taking correlations between experimental errors into account. Both the approximants almost coincide.

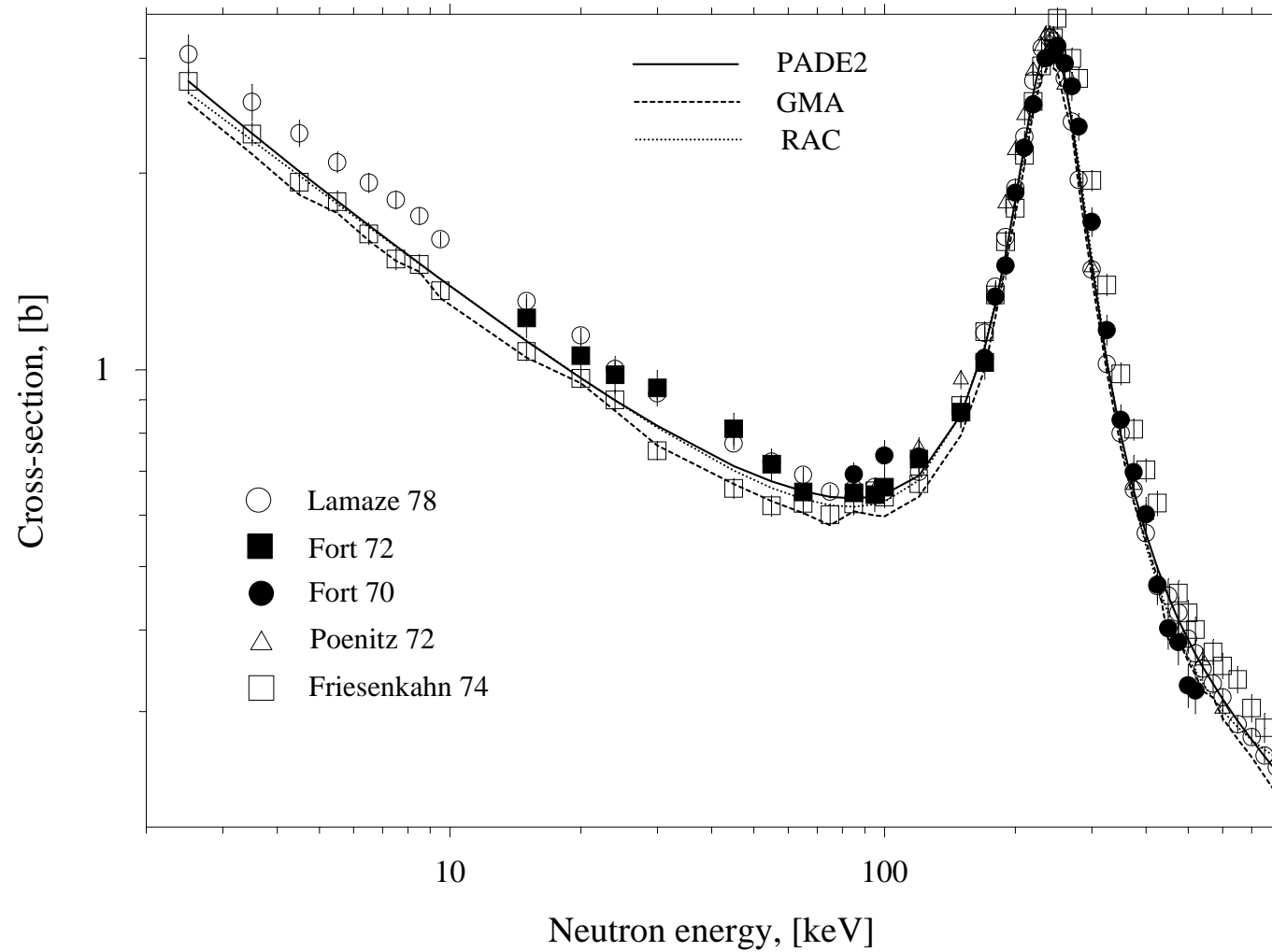


Fig.3 Model (RAC, PADE2) and "non-model" (GMA) least squares fits of the experimental data for the ${}^6\text{Li}(n,t)$ reaction cross-section.



New evaluation of the fission cross section of ^{235}U

F.-J. Hamsch

*Institute for Reference Materials and
Measurements (IRMM)
Geel, Belgium*

<http://www.irmm.jrc.be>
<http://www.jrc.cec.eu.int>



1

Statistical Model

- Below second chance fission the neutron interaction takes place through direct and compound nucleus mechanism. Beside fission the following processes are possible : elastic and inelastic scattering and radiative capture.
- For the direct mechanism the coupled channel method (**ECIS** code) is used and for compound nucleus mechanism a statistical model (**STATIS** code which takes into account sub-barrier effects and the multi-modal fission concept) is used.
- Strong coupling between elastic and other channels.



2

ECIS code provides: $\rightarrow S_t, S_{n,n}^{DI}, S_{n,in}^{DI}, T_{nlj}^{J?}$

Raynal J.

$$S_{n,in}^{DI} = \sum_i^N S_{n,n_i}^{DI}; S^{CN} = S_t - S_{n,n}^{DI} - S_{n,in}^{DI}$$

$N \Rightarrow$ number of coupled levels

STATIS code provides: $\rightarrow S_f, S_{n,?}, S_{n,n}^{CN}, S_{n,in}^{CN}$

Vladuca G., Tudora A.,
Hamsch F.-J., Oberstedt S.,
Nucl.Phys. A707, 32 (2002)

$$S^{CN} = S_f + S_{n,?} + S_{n,n}^{CN} + S_{n,in}^{CN}$$

$$S_{n,n}^{CN} = f(T_{nlj}^{J?}); S_{n,in}^{CN} = f(T_{nlj}^{J?})$$



$$r^{GC}(e, \Pi) = r(e) \cdot r(\Pi)$$

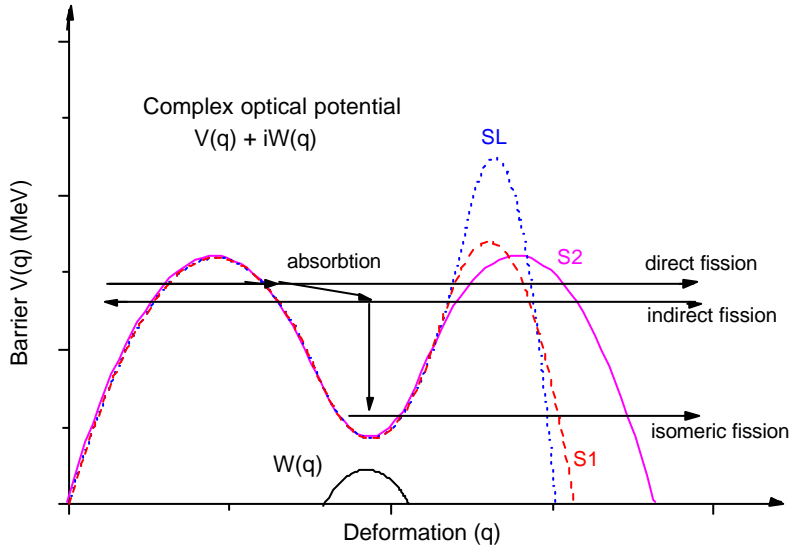
$$r(e) = \begin{cases} r_q(e) = \frac{1}{q} \exp\left(\frac{e - E_0}{q}\right) & e \leq E_r \\ r_{FG}(e) = \frac{\exp(2\sqrt{a(e - \Delta)})}{12\sqrt{2a}^{1/4} (e - \Delta)^{5/4} S} & e \geq E_r \end{cases}; r(\Pi) = \frac{2I + 1}{4S^2} \exp\left(-\frac{(I + 1/2)^2}{2S^2}\right)$$

Table 1. Numerical values of the parameters entering the Gilbert and Cameron level density function.

	TARGET NUCLEUS ^{235}U	COMPOUND NUCLEUS ^{236}U
D_{exp} (eV)	12.00	0.43
B_n (MeV)	5.29784	6.54476
? (MeV)	0.69	1.18
E_r (MeV)	4.42441	4.72746
(MeV ⁻¹)	29.0000	28.7852
E_0 (MeV)	-0.84276	-0.34436
q (MeV)	0.41062	0.41225



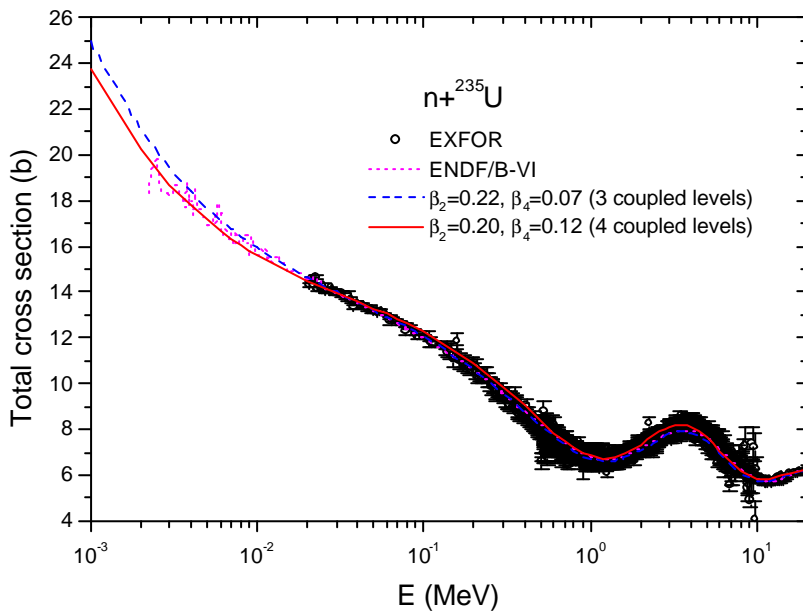
Schematic view of the barrier structure



5



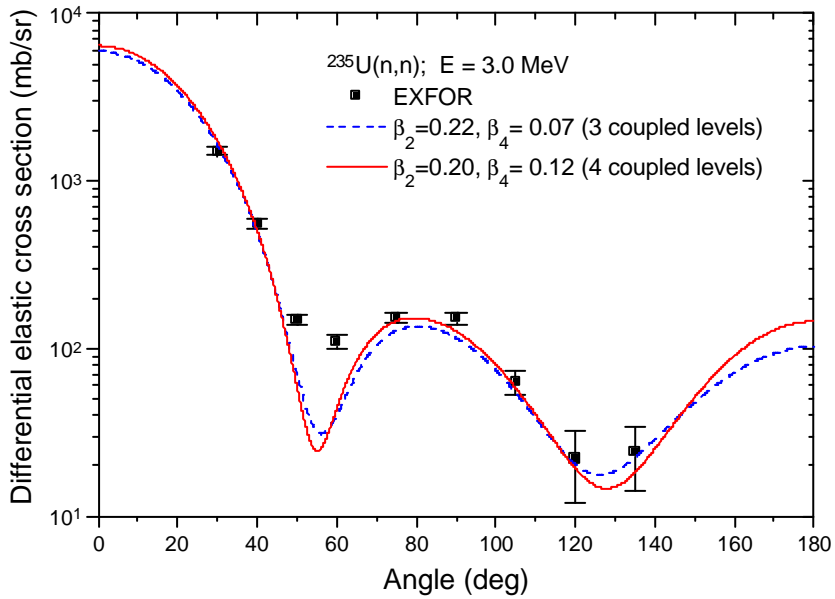
^{235}U Total cross section



6



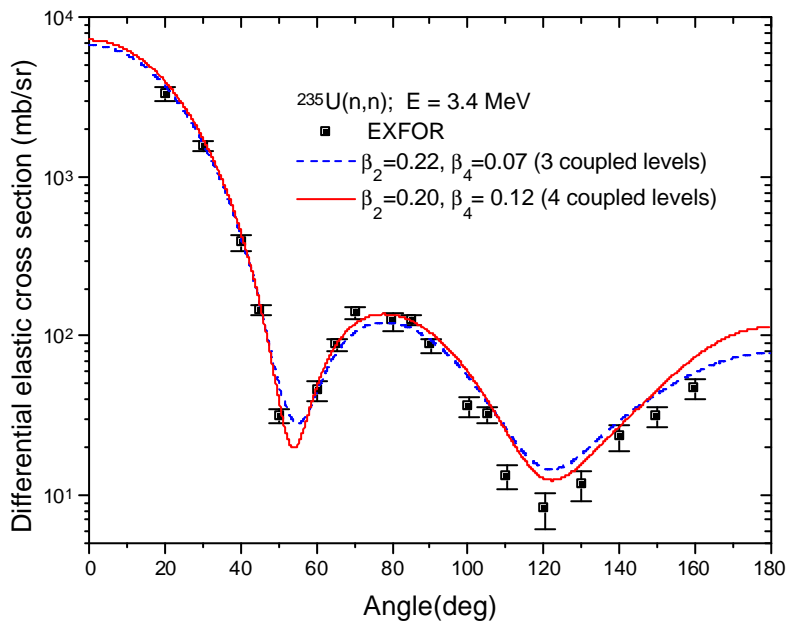
Differential elastic cross section



7



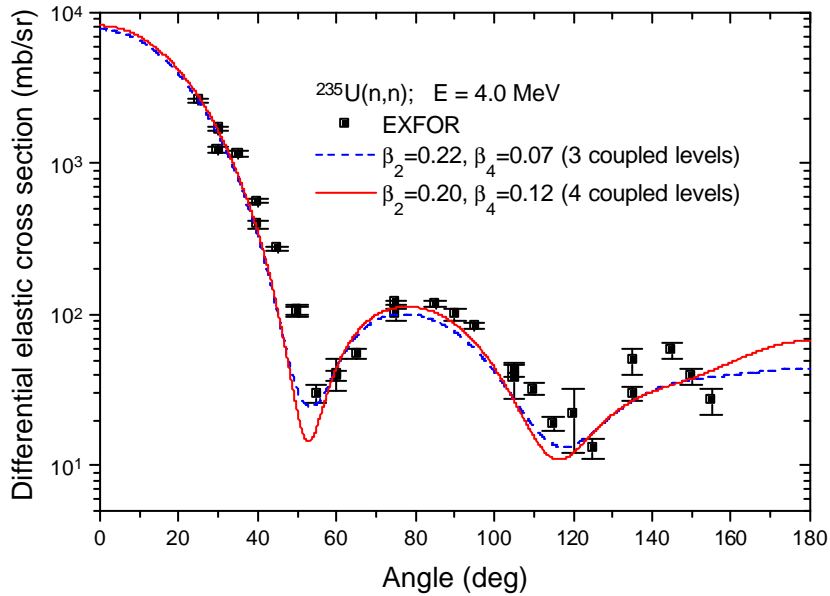
Differential elastic cross section



8



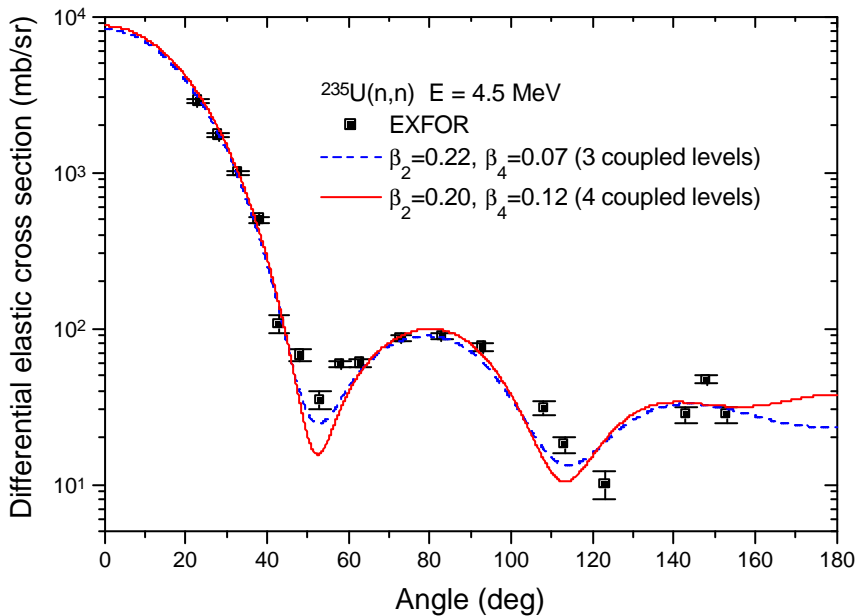
Differential elastic cross section



9



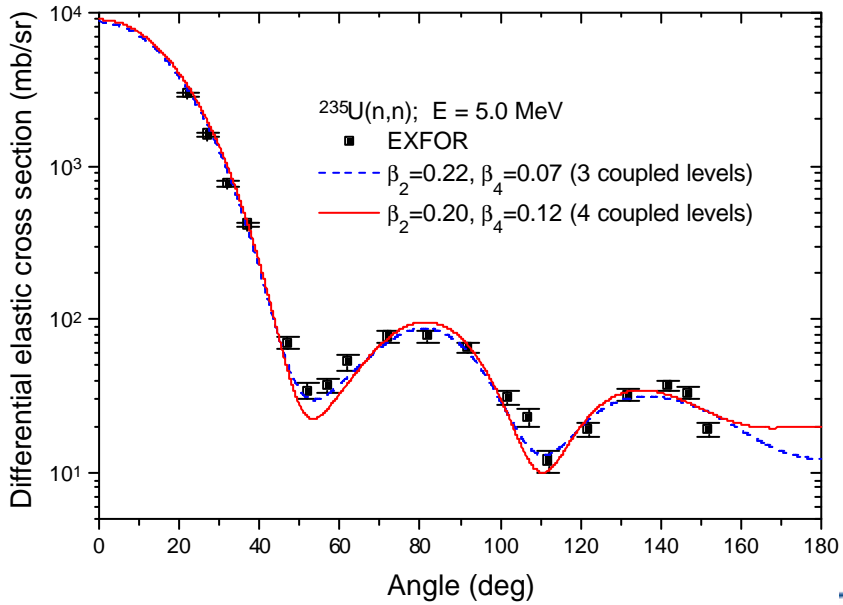
Differential elastic cross section



10



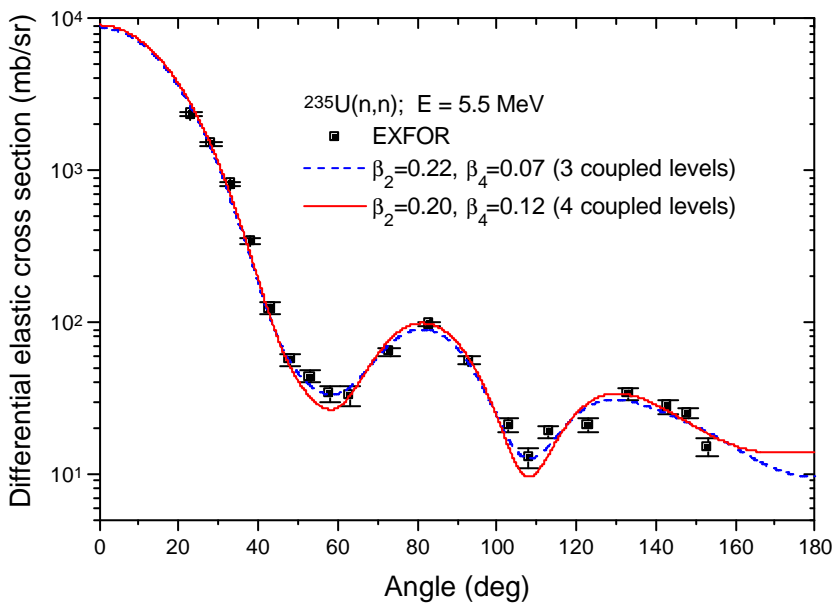
Differential elastic cross section



11



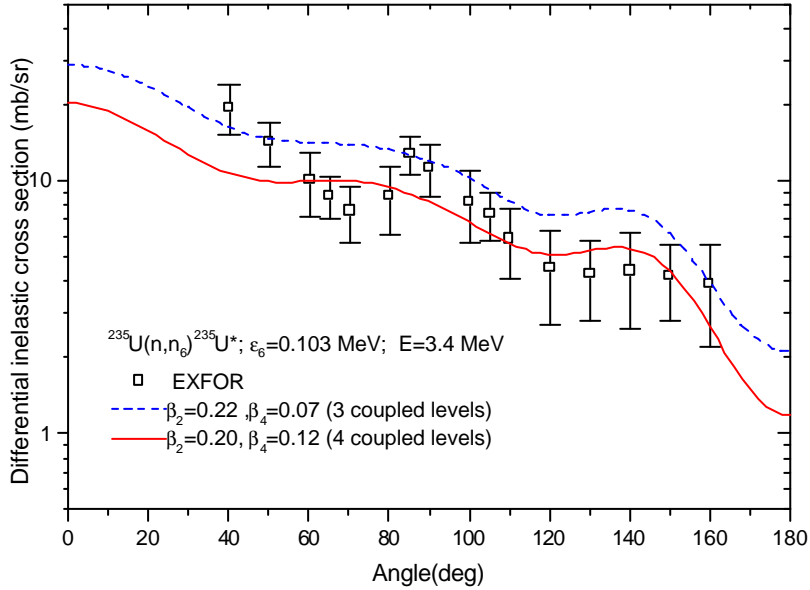
Differential elastic cross section



12



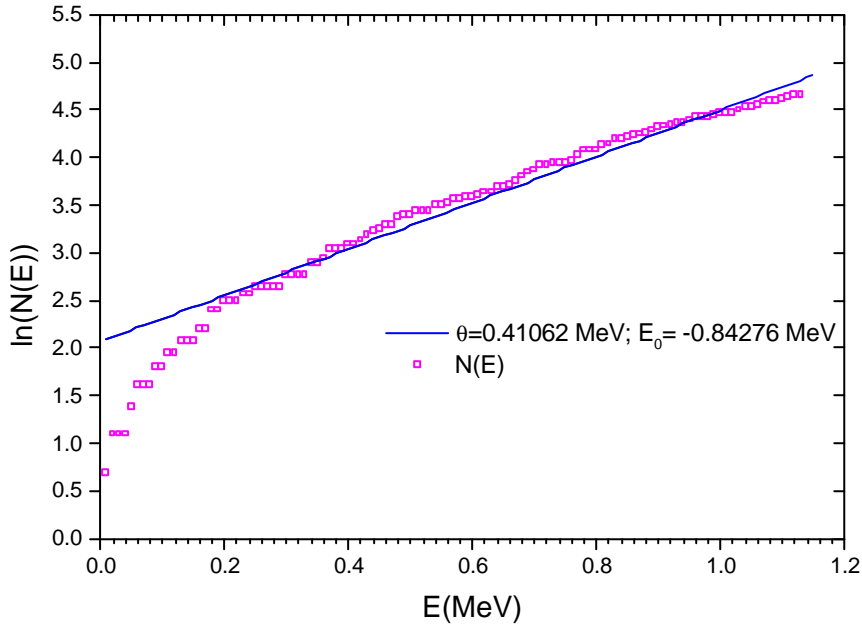
Differential inelastic cross section



13



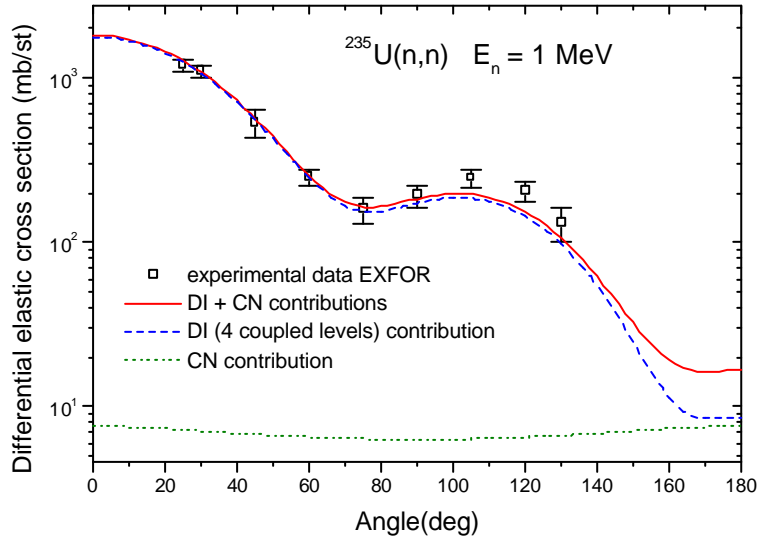
Cumulative number of levels for ^{235}U



14



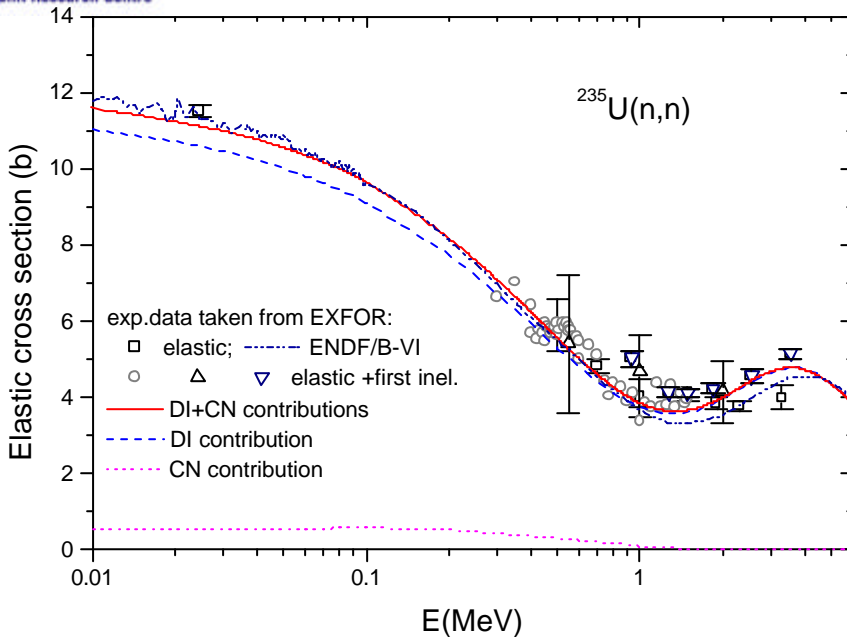
Differential elastic cross section



Separate contribution of direct and compound interaction



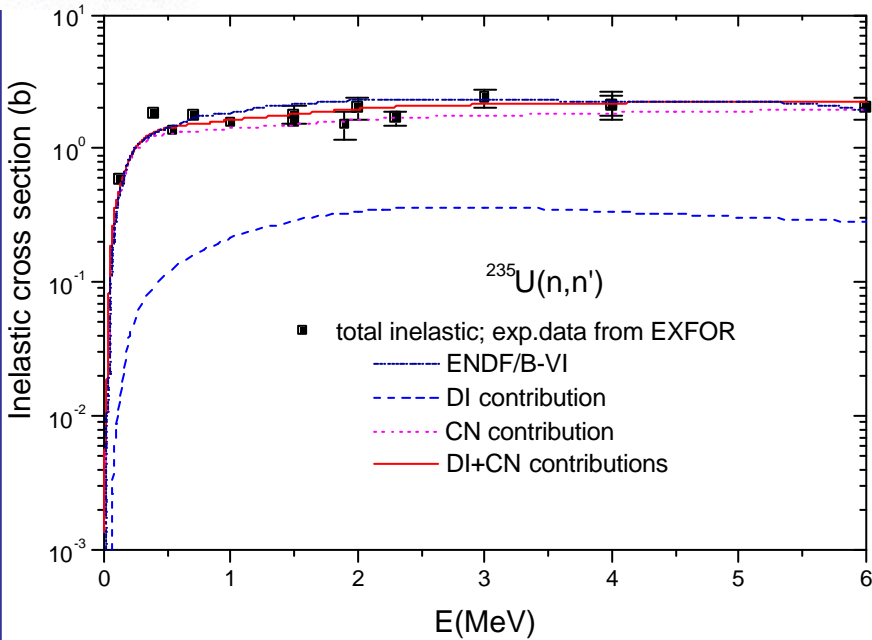
Elastic cross section



Separate contribution of direct and compound interaction



Inelastic cross section

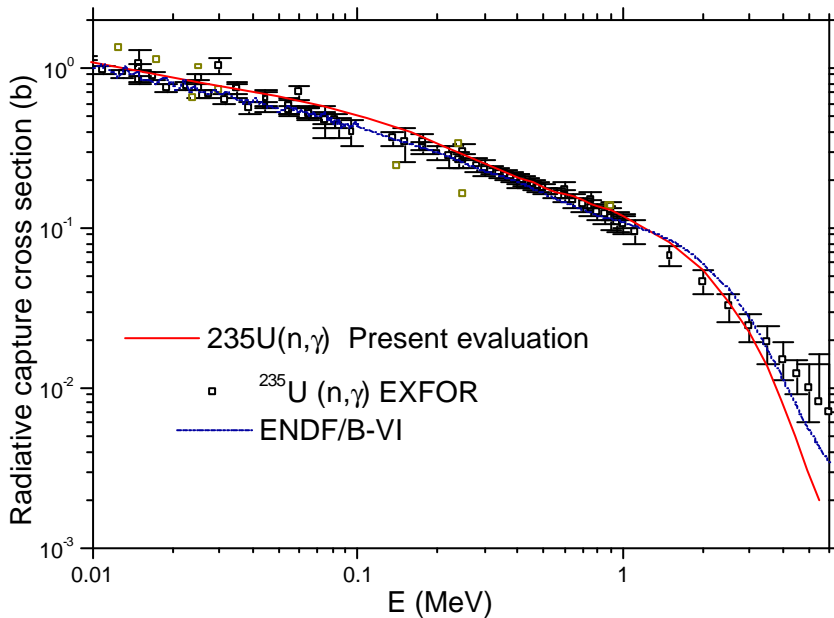


Separate contribution of direct and compound interaction

17



Radiative capture cross section



18

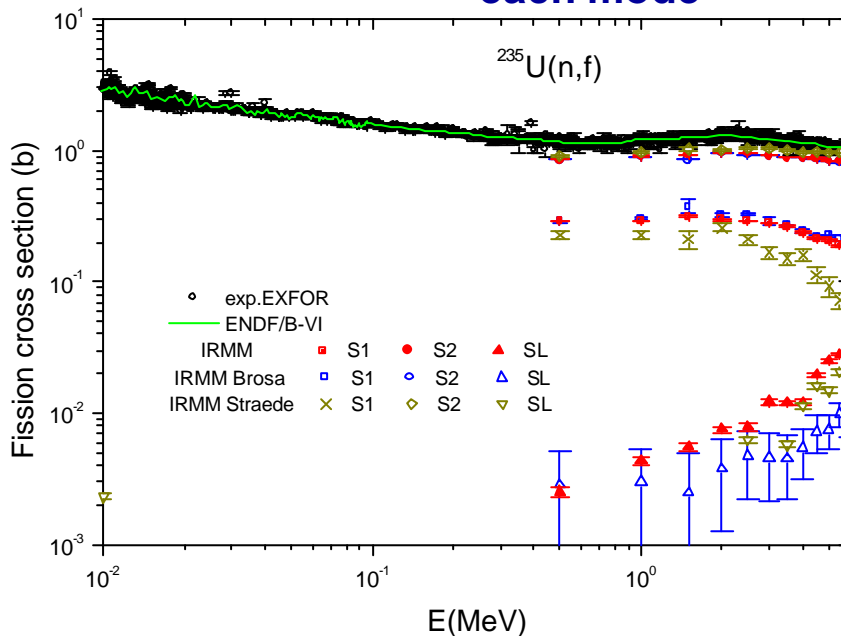


Input parameters in the model

Table 2. Fission barrier parameters for ^{236}U expressed in MeV

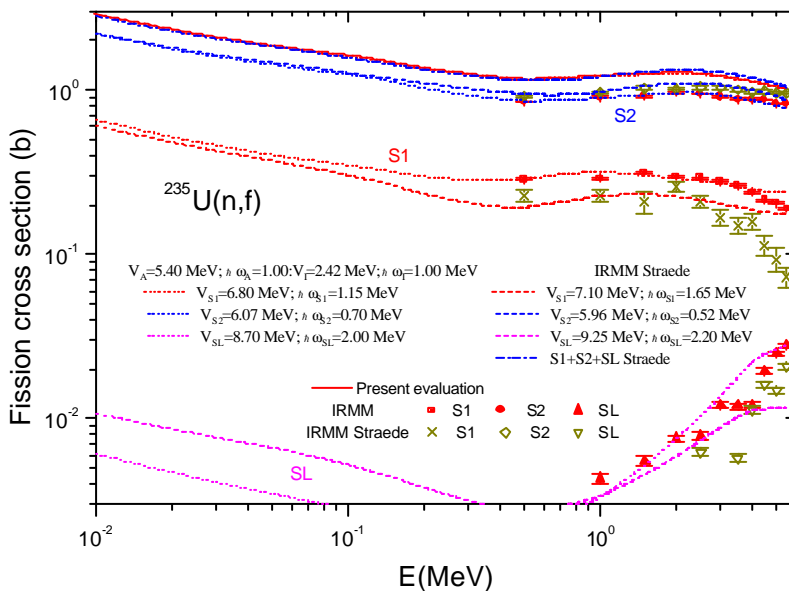
	INNER BARRIER A	ISOMERIC WELL	OUTER BARRIERS		
			S1	S2	SL
V	5.40	2.42	6.80	6.07	8.70
$\hbar\omega$	1.00	1.00	1.15	0.70	2.00
$e(0^+)$	0.00	0.00	0.00	0.00	0.00
$e(2^+)$	0.70	0.40	0.70	0.70	0.40
$e(0^-)$	0.60	0.30	0.15	0.15	0.60
$e(1^-)$	0.65	0.35	0.65	0.65	0.65
$(\hbar^2/2\mathcal{I})$	0.005	0.003	0.002	0.002	0.002

$^{235}\text{U}(n,f)$ experimental cross section of each mode





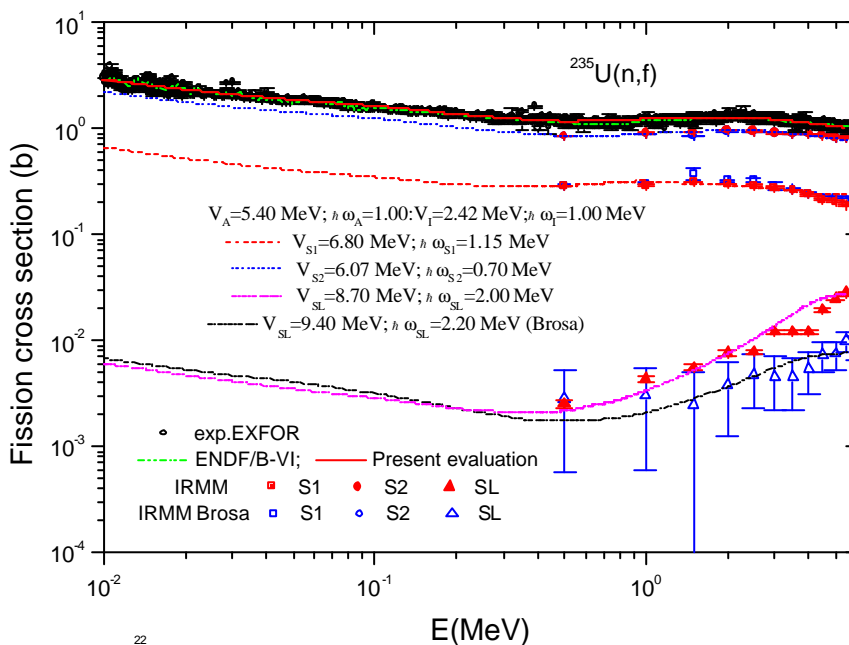
$^{235}\text{U}(n,f)$ cross section of each mode and total



21

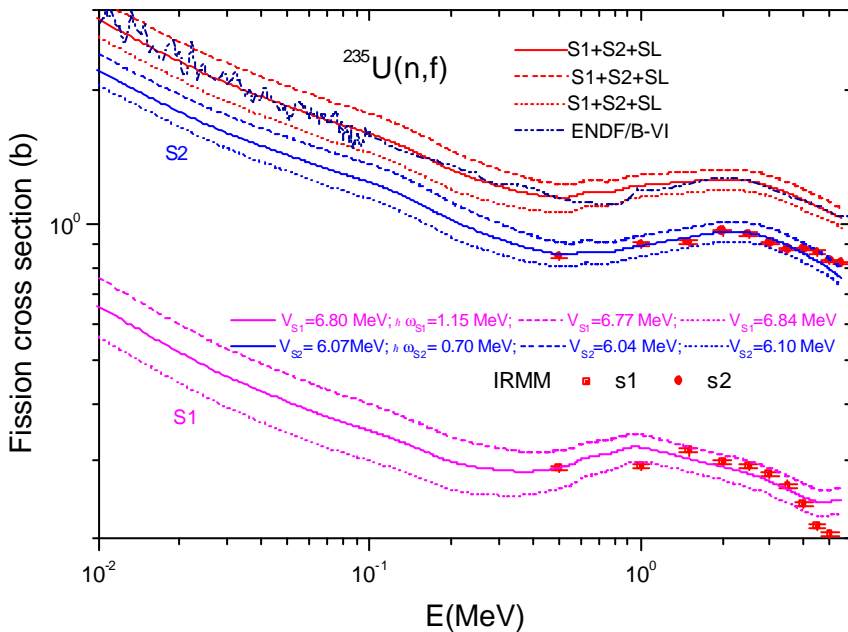
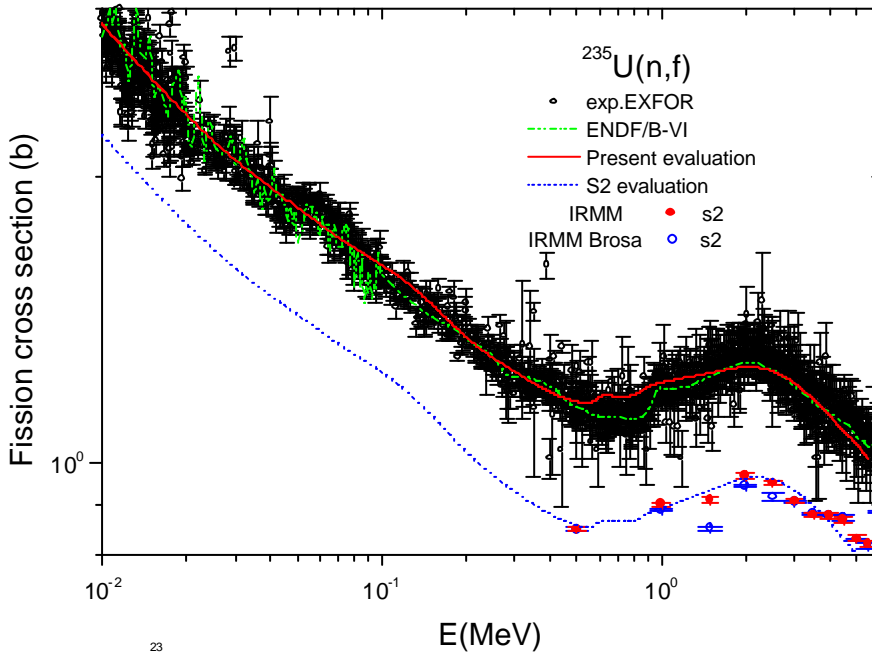


$^{235}\text{U}(n,f)$ cross section of each mode and total

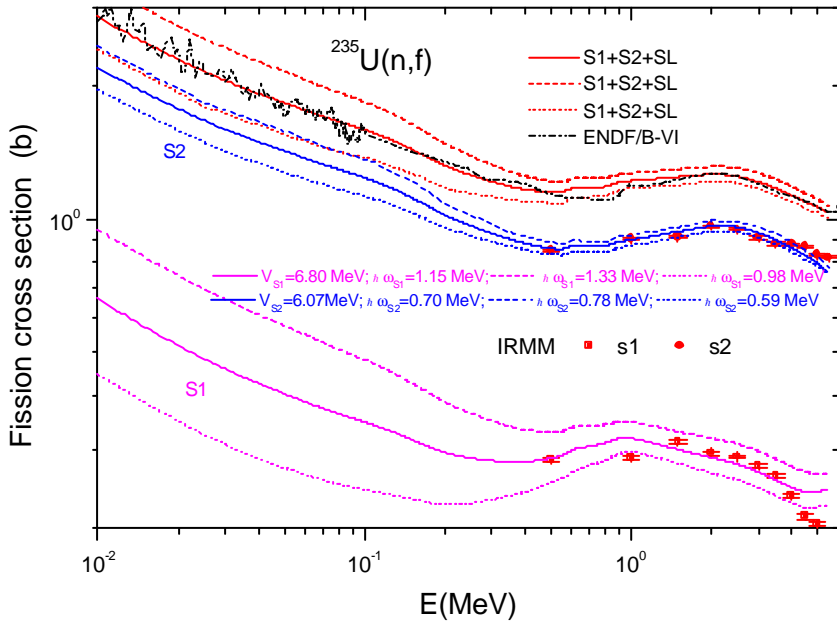


22





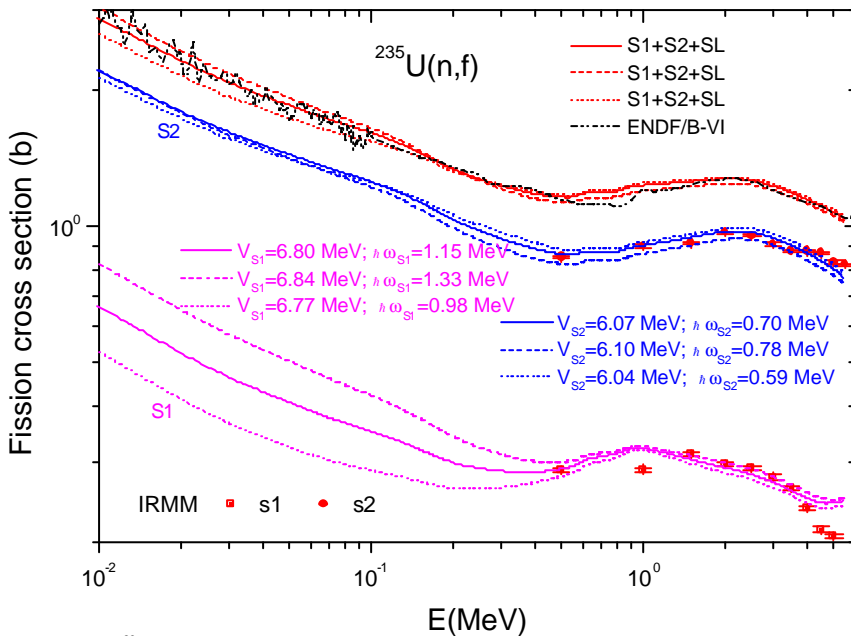
Testing the curvature of the S1 and S2 mode



25



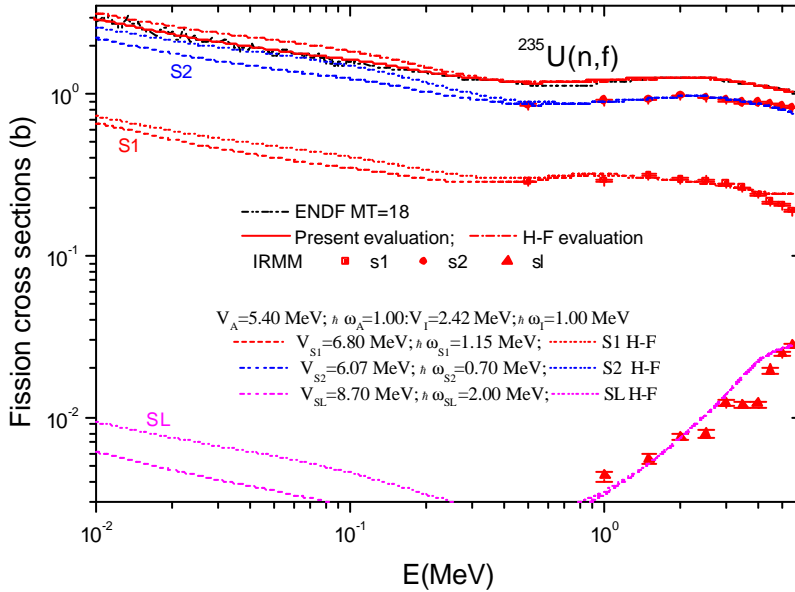
Testing the outer barrier parameters for each mode



26



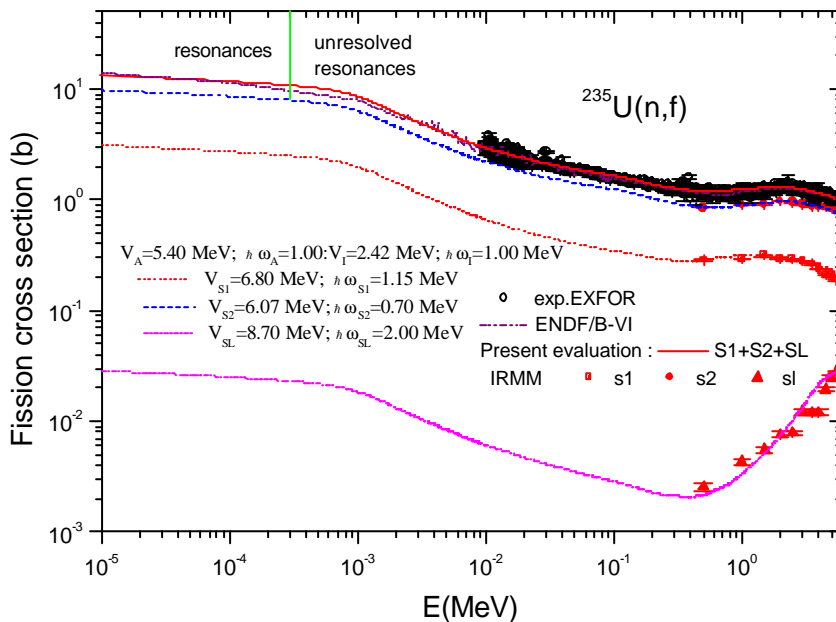
$^{235}\text{U}(n,f)$ cross section of each mode and total in comparison with the Hauser-Feshbach model



Sub barrier effects still important, inner/outer barrier act independently

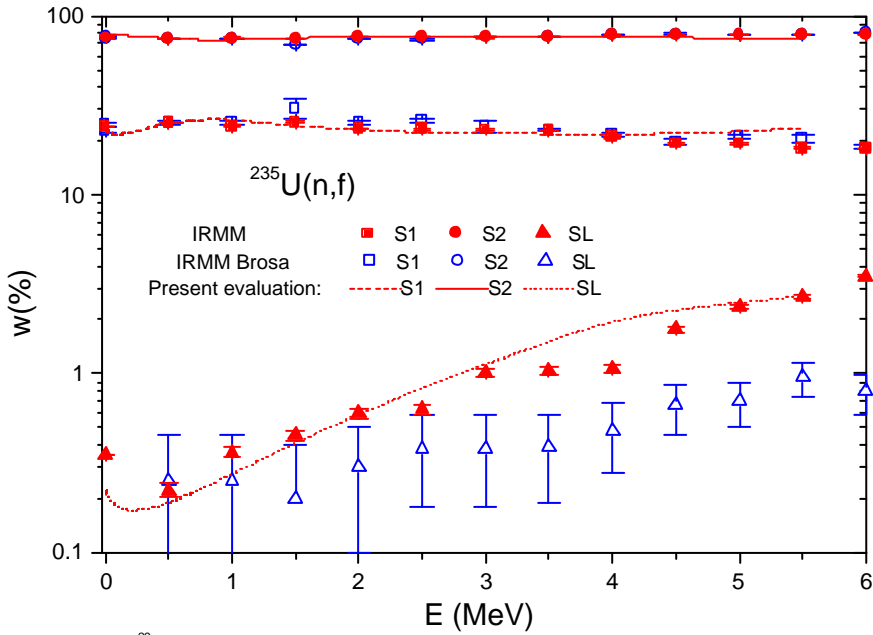


$^{235}\text{U}(n,f)$ cross section of each mode and total



Branching ratios of each mode for ^{235}U

Joint Research Centre

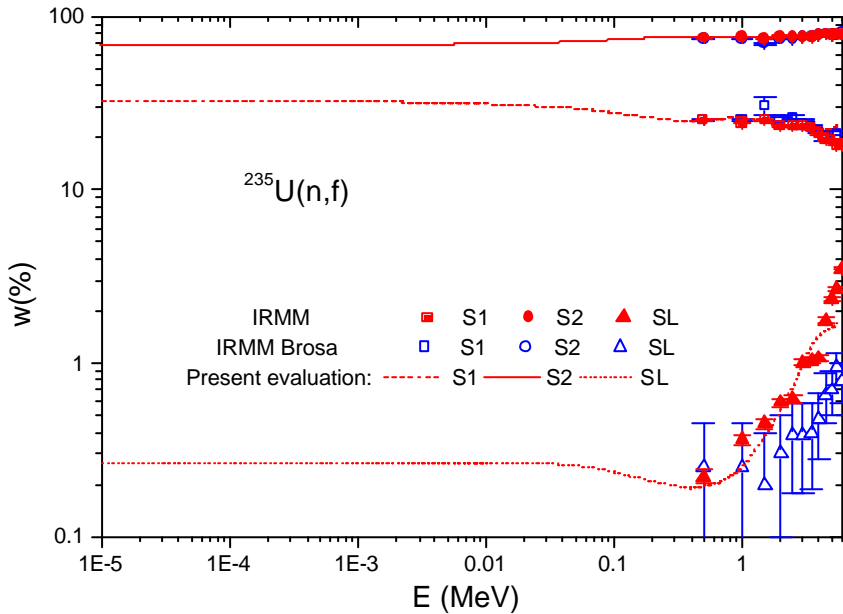


29



Branching ratios of each mode for ^{235}U

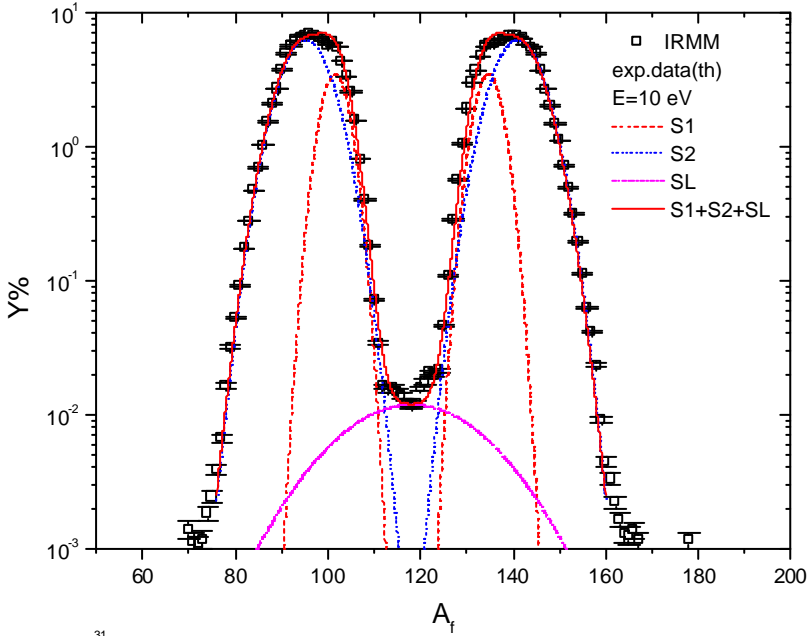
Joint Research Centre



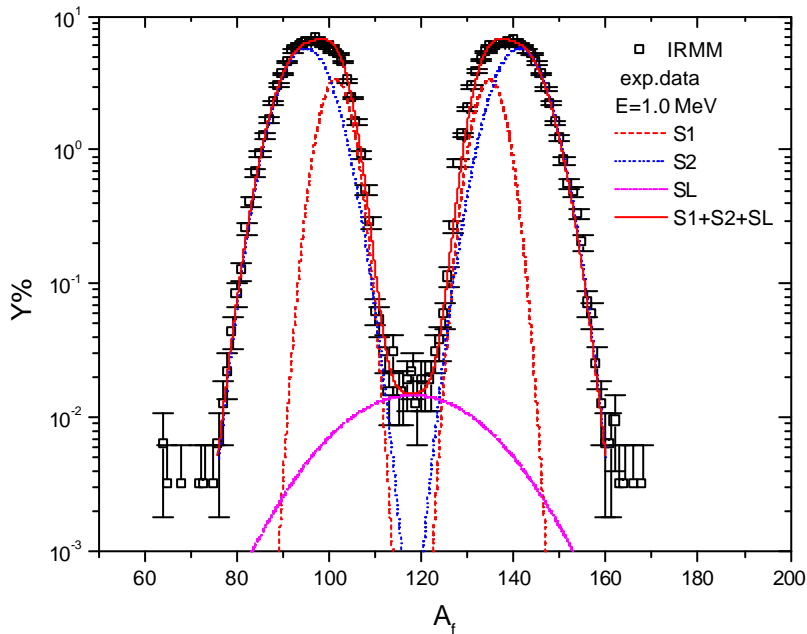
30



Fission fragment mass distribution at $E = 10^{-5}$ MeV

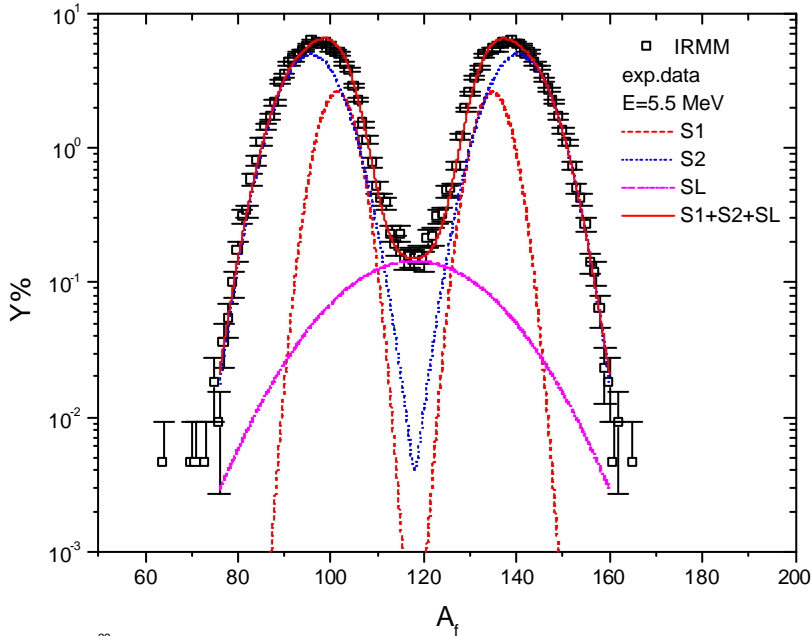


Fission mass fragment distribution at $E = 1.0$ MeV



Fission mass fragment distribution at $E = 5.5 \text{ MeV}$

Joint Research Centre

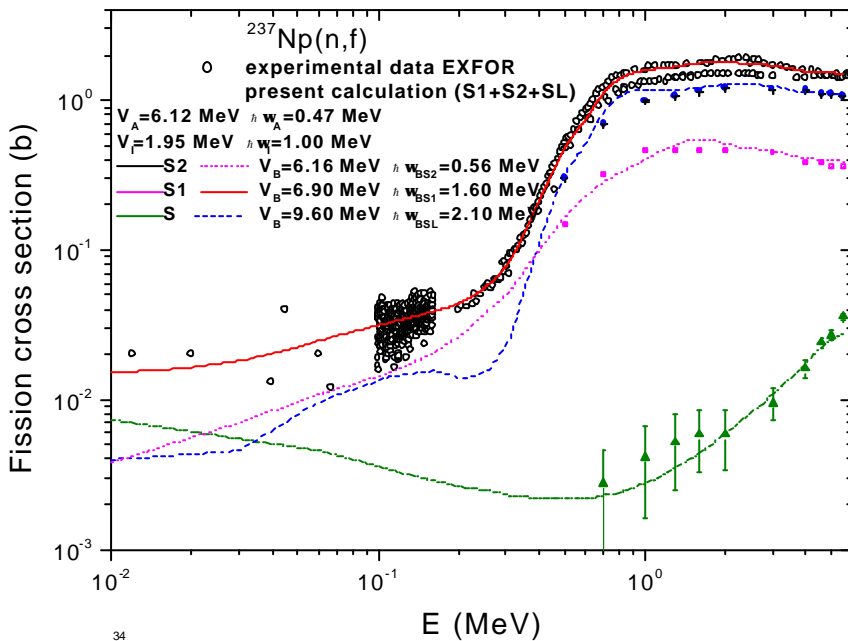


33

irm
m

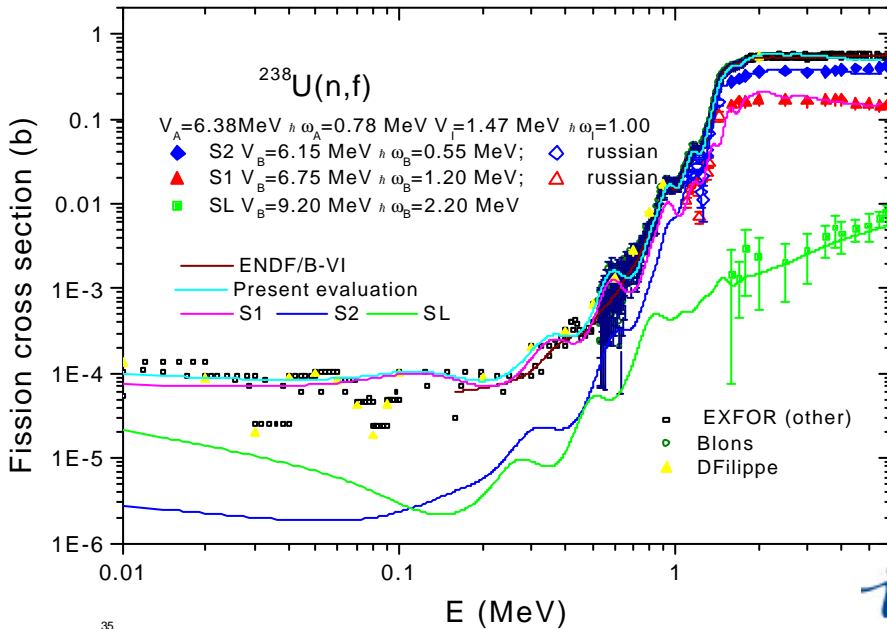
Fission Cross-section for $^{237}\text{Np}(n,f)$

Joint Research Centre



34

irm
m



35



Conclusions

- Incorporation of modality of the fission process based on experimental results.
- Demonstrated ability of the STATIS code to do reaction cross-section calculations.
- Side product are branching ratios of the different modes as a function of incident neutron energy.
- Possibility to predict mass distributions at hitherto unmeasured incident neutron energies.

36



GMA database updating, evaluating procedures and trends in new standards evaluation

(6 October 2003)

V.G. Pronyaev

Nuclear Data Section of the IAEA, Vienna

Introduction

Last evaluation of neutron cross-section standards prepared with the use of EDA R-matrix model and GMA non-model least-square codes was based at experimental data available to 1987[1]. In 1997 the GMA database of experimental data was updated and documented[2]. It contained 397 data sets for different reactions, their combinations and ratios and 23 thermal constants evaluated separately. Test run of GMA done with these data[2] had shown the general trend in small increase of the cross sections.

Database updating

Since last modification of the database the new experimental data have been available and should be included in the database. 26 sets of experimental data shown in the Table 1 were converted, where it was needed in their original form and introduced in the database. Generally there is good consistency between new experimental data shown in Table 1 and posterior evaluation but some discrepancies, eg. between Scherbakov's and Lisowski's data as well as for some data including $^{10}\text{B}(n,a)$ reaction should be reanalyzed.

The energy range for fits of fission cross sections was extended from 20 to 200 MeV with the steps 1 MeV between 20 and 30 MeV, step 2 MeV between 30 and 60 MeV, step 4 MeV between 60 and 120 MeV and step 8 MeV above 120 MeV. The energy nodes were chosen in accordance with the energy points in the presentation of experimental data. Extension of the energy range up to 200 MeV allows to do simultaneous fit of low (below 20 MeV) and high-energy (between 20 and 200 MeV) $^{235}\text{U}(n,f)$ and $^{238}\text{U}(n,f)$ standard cross sections.

Table 1. New data sets introduced in the GMA database.

Reaction	Type of data	Set No.	Reference	Data points	Energy range	Comment; (consistency with a posterior evaluation)
Li6(n,a)/U8(n,f)	Absolute	1010	Guohui Zhang et al. NSE,143,86(2003)	2	1.85, 2.67 MeV	(good)
Li6(n,a)	Absolute	1011	M. Drosz et al. NIM,B94,31(1994)	17	0.5 – 4.1 MeV	Normalized by author (*1.061) (good)
Pu9(n,f)/U5(n,f)	Absolute	1012	O. Shcherbakov et al., JINR-E3-2001-192(2001)	166	0.6 – 196 MeV	Received from Laptev 15-Jul-2003, (good below 64 MeV, discrepancy with Lisowski data should be resolved)

U8(n,f)/U5(n,f)	Absolute	1013	O. Shcherbakov et al., JINR-E3-2001-92 (2001)	142	1.0 – 196 MeV	Received from Laptev 07-2003, (good below 20 MeV, discrepancy with Lisowski data should be resolved)
Pu9(n,f)/U5(n,f)	Absolute	1014	P.Staples, K.Moorley NSE,129,149(1998)	146	0.8 – 62 MeV	(good below 25 MeV, discrepancy with Lisowski data should be resolved)
B(n,a0)/B(n,a1)	Absolute	1015	F.-J.Hambsch, H.Bax NSTS,2(2),1402 (2002)	25	0.04 – 1.0 MeV	(large discrepancies below 400 keV, should be corrected at epithermal neutrons)
Au(n,g)	Absolute	1016	J.Voignier et al., NSE,93,43(1986)	6	0.5 – 3.0 MeV	(good)
U8(n,g)	Absolute	1017	J.Voignier et al., NSE,93,43(1986)	4	0.5 – 1.1 MeV	(good)
Au(n,g)/U5(n,f)	Absolute	1018	A.N.Davlertshin et al., YK,(1),41(1992)	5	0.8 – 2.4 MeV	(good)
Au(n,g)/U5(n,f)	Absolute	1019	A.N.Davlertshin et al., YK,(1),13(1993)	5	0.37 – 1.0 MeV	(good)
Au(n,g)/U5(n,f)	Absolute	1020	V.A.Tolstikov et al., YK,(4),46(1994)	5	0.49 – 0.69 MeV	(good)
Au(n,g)/Li6(n,a)	Absolute	1021	L.E.Kazakov et al., YK,(2),44(1985)	32	0.0035 – 0.105 MeV	(good)
Au(n,g)/B10(n,a1)	Shape	1022	L.E.Kazakov et al., YK,(2),44(1985)	25	0.11 – 0.41 MeV	B10(n,ag)= B10(n,a1), (good)
U5(n,f)/B10(n,a0+a1)	Shape	1023	L.W.Weston, J.H.Todd NSE,111,415(1992)	10	0.15 – 1.5 keV	(satisfactorily)
Pu9(n,f)/B10(n,a0+a1)	Shape	1024	L.W.Weston, J.H.Todd NSE,111,415(1992)	10	0.15 – 15 keV	(satisfactorily)
U5(n,f)	Absolute	1025	R.G.Johnson et al., Priv. Com., A.D.Carlson, (1991)	17	1 – 6 MeV	Data as in X4=12924002, (very good)
U5(n,f)	Absolute	1026	V.A.Kalinin et al., At.En.,71,181(1991)	2	1.88, 2.37 MeV	TUD/KRI collaboration (very good)
U5(n,f)	Absolute	1027	T.Iwasaki et al., C,88Mito,87(1988)	5	13.5 – 14.9 MeV	(very good)
U5(n,f)	Shape	1028	P.W.Lisowski et al., Priv. Com., P.W.Lisowski, 29-Jan-1997	141	3 – 202 MeV	(good)
Pu9(n,f)/U5(n,f)	Absolute	1029	P.W.Lisowski et al., Priv. Com., P.W.Lisowski, 29-Jan-1997	209	0.5 – 257 MeV	(good, discrepancy with Staples and Shcherbakov data above 25 MeV should be resolved)
U8(n,f)/U5(n,f)	Absolute	1030	P.W.Lisowski et al., Priv. Com., P.W.Lisowski, 29-Jan-1997	203	0.8 – 357 MeV	(satisfactorily, discrepancy with Shcherbakov data above 64 MeV should be resolved)

U5(n,f)	Absolute	1031	V.I.Goldanskiy et al., DOK,101,1027 (1955)	2	120, 380 MeV	(bad)
U8(n,f)	Absolute	1032	V.I.Goldanskiy et al., DOK,101,1027 (1955)	2	120, 380 MeV	(bad)
B10(n,a1)	Shape	1033	R.A.Schrack et al., Priv. Com.(2003)	160	0.29 – 13.65 MeV	(satisfactorily for exclusion of end points)
B10(n,a1)	Shape	1034	R.A.Schrack et al., C,Gatlinburg93,43 (1994)	38	5.4 keV – 1.08 MeV	(satisfactorily)
U8(n,f)/U5(n,f)	Absolute	1035	M.Baba et al., JNST,26,11(1989)	4	4.6 – 6.1 MeV	(very good)

The total number of experimental data sets included in the GMA database at present and their distribution by reaction and type is shown in Table 2. Diagonal elements present the cross sections and off-diagonal – the ratio of respective reaction cross sections without account which reaction is in nominator and which is in the denominator of the ratio. The first number in the sum shows the number of data sets with absolute cross sections (or absolute ratios), second number – the number of data sets with shape of cross sections (or shape of ratios of cross sections). Some data sets for reactions induced on ${}^6\text{Li}$ and ${}^{10}\text{B}$ are used in the R-matrix fit, and will be removed from the general least square GMA fit, to avoid the double counting.

Table 2. Number of the experimental data sets in the GMA database (September 2003).

Standard reaction	${}^6\text{Li}(n,t)$								
${}^6\text{Li}(n,t)$	11+8=19	${}^{10}\text{B}(n,\alpha_0)$							
${}^{10}\text{B}(n,\alpha_0)$		5+1=6	${}^{10}\text{B}(n,\alpha_1)$						
${}^{10}\text{B}(n,\alpha_1)$	0+1=1	11+2=13	3+7=10	${}^{10}\text{B}(n,\alpha_0)+$ ${}^{10}\text{B}(n,\alpha_1)$					
${}^{10}\text{B}(n,\alpha_0)+$ ${}^{10}\text{B}(n,\alpha_1)$	1+3=4			3+3=6	${}^{197}\text{Au}(n,\gamma)$				
${}^{197}\text{Au}(n,\gamma)$	3+0=3		0+4=4	4+0=4	23+4=27	${}^{238}\text{U}(n,\gamma)$			
${}^{238}\text{U}(n,\gamma)$	3+0=3		8+2=10	4+0=4	9+1=10	14+4=18	${}^{235}\text{U}(n,f)$		
${}^{235}\text{U}(n,f)$	0+9=9		1+1=2	0+25=25	10+1=11	8+6=14	48+16=64	${}^{239}\text{Pu}(n,f)$	
${}^{239}\text{Pu}(n,f)$	0+7=7			1+17=18		0+1=1	15+5=20	17+2=19	${}^{238}\text{U}(n,f)$
${}^{238}\text{U}(n,f)$	0+1=1						22+5=27	1+0=1	13+5=18

Reactions shown in Table 3 are the constraint reactions. Most of them will be used in the R-matrix but not in the GMA general least square fit. To remove the jumps in the evaluated elastic scattering cross sections in the energy range, where cross section should be constant, strongly correlated shape data sets with a constant cross section were added to the ${}^6\text{Li}(n,n)$ and ${}^{10}\text{B}(n,n)$ reaction cross sections.

Table 3. Number of data sets used as constraint reactions.

Constraint reactions	Number of data sets
${}^6\text{Li}(n,n)$	10
${}^6\text{Li}(n,\text{total}) = {}^6\text{Li}(n,t) + {}^6\text{Li}(n,n)$	12
${}^{10}\text{B}(n,n)$	5
${}^{10}\text{B}(n,\text{total}) = {}^{10}\text{B}(n,\alpha_0) + {}^{10}\text{B}(n,\alpha_1) + {}^{10}\text{B}(n,n)$	12+1=13

Evaluation procedures

GMA code uses a general least square method implemented through the adjustment of some non-informative prior with additive contribution from all correlated experimental data sets. There are two important problems, which require some additional analysis and following correction of data or revision of its covariance matrices of uncertainties. One is a treatment of the discrepant data and other is a possible presence of the Peelle's Pertinent Puzzle (PPP). Both are interconnected and can lead to the biased evaluations when general chi-square per degree of freedom is less than 1 or even when contribution in chi-square from particular experimental data set per degree of freedom is less than one (case of strongly correlated data with a strong local discrepancy in the shape).

Because under PPP we understand the global bias of the evaluation relative the most experimental data and the major reason of PPP appearance is the unphysically strong correlations assigned to the experimental data, the test at PPP presence can be done by comparing the results of evaluations with and without account of correlations in the experimental data. This test done for 1997 GMA database had shown no presence of the PPP although the chi-square value per degree of freedom was close to 3, what points at large discrepancy of the data in the original GMA database.

The discrepancies between experimental data are explained mainly (if no explicit errors in some experiments) by systematical errors, which some data may contain because not all needed corrections are introduced. The consistency is restored usually either correcting the data if corrections are known (can be calculated), or introducing additional components of the uncertainty to the discrepant data. Under discrepant data we will understand here the data having difference above $(1 - 2) \sigma$ relative unbiased posterior evaluation, where σ is the experimental error in some point, or contribution more than 2 per degree of freedom in general chi-square value. The last criteria can be important for the experimental data sets with large correlations but which look consistent if we see only at σ values.

Unfortunately we do not know unbiased posterior evaluation to be used for search of discrepant data before we do the least square fit with consistent data. We can use some good prior approximation to the posterior evaluation and the iterative procedure to get the best evaluation. In particular case of standard cross sections we can use as a best prior approximation to the posterior evaluation: a) arithmetical average of the experimental cross sections (non-weighted average); b) evaluation obtained in the least squares fit with total uncertainties treated as statistical (statistical-weighted average); c) evaluation obtained in the least square fit with covariance matrices of experimental data used as they are given in the GMA database (weighed average); d) previous evaluation of the standards. The drawback of a) is that it assigns too large weight to outliers having usually low uncertainty and strongly overestimates the discrepancy of the high-accuracy data; the b) gives curves which are very non-smoothed; the same is relevant to c) and additionally the presence of PPP can bias the prior and as consequence the posterior evaluation; selection of d) is not the best if new evaluation after least-squares feet moves too far off old evaluation.

Option d) above was used for the procedure of modifying of the uncertainties of the discrepant experimental data. The additional Medium Energy Range Correlation (MERC) component of the uncertainty was added for the experimental data in the points where the difference from old standards was more than 2σ in a single point or more than about 1σ in two or more consecutive points on the energy. After GMA fit with these modified uncertainties, the difference with a new posterior evaluation was obtained and additional MERC component was decreased, removed or increased, introduced according to the difference. There was no need to have more than two iterations for the convergence of the process. Finally, the uncertainties of more than half of all data sets were increased. Most corrections were introduced at begin and/or end points of the data sets, which sometimes are at the limit of the experimental possibilities and have large uncertainty. Due to this procedure, the general chi-square was reduced from about 3 to 0.8. At the same time the evaluated errors have been increased insignificantly (at about 10% but not two times as could be expected from chi-square reduction) because the major contribution in chi-square was from data with large uncertainties. Uncertainties of these data, which practically do not influence the uncertainty of the evaluated data, were increased.

Trends in new standards evaluation

The results of standards evaluation, when all data shown in Tables 2 and 3 were used in GMA fit are shown in Figures given in Attachment 1. The evaluated cross sections and their ratios are compared with the experimental data as they are given in the GMA database. Figures are given for reactions in the order as shown in Table 2 beginning from ${}^6\text{Li}(n,t)$ and ratios of ${}^6\text{Li}(n,t)$ to all other reactions and ending up with ${}^{238}\text{U}(n,f)$. These results can be used only for analysis of the trends in the heavy elements standards evaluation, because the evaluation of light-element standards should be done in the R-matrix model approach and through measured cross section ratios, R-matrix model fit will have influence at the heavy element standards. The Figures show also the “old” standards and latest evaluations JENDL-3.3[3] and LASL[4] made independently using similar least-square method approach but working with different sets of correlated reactions.

More detailed comparison was done for the regions where the cross sections could have some structures and evaluation of the shape of these structures is different in different fits. This was done for fission cross of ${}^{235}\text{U}$ near 1 MeV and ${}^{239}\text{Pu}$ near 1.8 MeV. As seems in all cases the structures obtained in the GMA fit are realistic.

The general trends in new standard evaluations can be characterized by the following:

1. There is a general increase of all standard cross sections at 0.5 – 1.5%. The largest growth is observed for the fission cross sections above 14 MeV.
2. The uncertainty of the evaluated data with inclusion of new experimental data sets and modifying the uncertainty of the discrepant data has not changed much comparing with old standards evaluation and is varying between 0.5% and 2%. Uncertainties close to these are obtained in all least square fits and are determined by the accuracy of the experimental data in the database having the highest precision.

The GMA database can be further improved if the most discrepant data will be reanalyzed, origin of discrepancy will be cleared and either the data will be corrected or their uncertainties will be increased. Good examples of such data are ${}^{10}\text{B}$ reaction cross sections measured with Frish-gridded ionization chambers, which should be corrected at the “particle leaking” effect.

Simple estimations of quality of the ^{235}U thermal neutron induced fission neutron spectrum averaged $^{235}\text{U}(n,f)$ cross section can be done for new standards. The value for new $^{235}\text{U}(n,f)$ standard as calculated with ENDF/B-VI fission spectrum by GMA is equal to 1225.3 mb. W. Mannhart's new evaluation based on integral experiments gives the value[5] 1219 ± 14 mb, which is supported by NIST (I.G. Schroder et al., 1985) measurement for ^{252}Cf spectrum averaged cross section (1234 ± 17) mb. The ^{252}Cf spectrum is harder than the ^{235}U spectrum. Because of the shape of $^{235}\text{U}(n,f)$ cross section, the ^{235}U spectrum averaged cross section will be slightly lower than the ^{252}Cf spectrum averaged cross section.

Combining the R-matrix fit for the light element standard cross sections with GMA fit for heavy element standards

R-matrix code RAC implementing the full version of the error propagation law gives the evaluated uncertainties close to those obtained in the GMA fit, if the same experimental data are used in both cases. The covariance matrices of the uncertainties obtained in the model fit have smaller variances but larger covariances than in the non-model GMA fit. This is due to intrinsic properties of the model function usually introducing large correlations between the neighboring points. But if R-matrix codes use the data for other channels leading to the same compound system (eg. inverse charged particle channels) or additional observables (eg. polarization) for determination of the parameters, the uncertainty of the standard cross sections reconstructed from evaluated R-matrix parameters will be much lower. R-matrix as physical theory introduces also some physical constraints at the cross sections. This is why it is important to use multi-channel R-matrix fit in the practice of the cross sections evaluation.

The combining of the R-matrix model fit for light elements and GMA non-model general least square fit for heavy elements can be done with the GMA code. For this, the evaluated cross sections and covariance matrices of uncertainties reconstructed from the evaluated R-matrix parameters and their covariance matrices of uncertainties can be entered in the GMA database and used as input data in the general least square fit together with other experimental data not used in the R-matrix fit.

This approach was tested by adding the $^{10}\text{B}(n,\alpha_1)$ reaction cross section evaluated with the R-matrix code RAC to the GMA experimental database. Because the purpose of this exercise was to study the possibility of the combining procedure with use of GMA we did not removed from the GMA database the experimental data sets which were used in the RAC R-matrix fit to avoid the double counting. The results of GMA least square fit of $^{10}\text{B}(n,\alpha_1)$ reaction obtained with full GMA database and RAC results of R-matrix fit of the data with all channels of ^{11}B composite system are shown in Figures as ratio to the old standard values. The GMA and RAC fits based on partially different data sets show similar deviation from the old standards demonstrating that either the width of the wide resonance near 300 keV is slightly less than it was evaluated before, or that there are the problems with accounting of experimental resolution. The same trend is seen for $^6\text{Li}(n,t)$ reaction. The combining procedure leads to the solution, which looks physically justified: the resulting cross section is more smoother than GMA fit, although some irregularities at the level of parts of per-cent are clearly seen. There is another problem of the combining procedure, namely the semi-positive definiteness of the covariance matrix of cross sections reconstructed in n points from m evaluated R-matrix parameters (if $n > m$). This is needed in separate discussion.

High-energy fission standard

Updated GMA database has included all available experimental data to 200 MeV and above, which allowed to evaluate simultaneously the standards below 20 MeV and high-energy $^{235}\text{U}(n,f)$, $^{238}\text{U}(n,f)$ standard and $^{239}\text{Pu}(n,f)$ cross section up to 200 MeV neutron incident energies. Unfortunately most high-energy fission data are the shape type and existing absolute cross-section measurement are either old or have low accuracy. The fitting of the high-energy standards together with the low-energy, allows their normalization in the most consistent way. It was mentioned above that two major sets of measurements of ratios of fission cross sections (by Shcherbakov and by Lisowski) are discrepant for energies above 60 MeV. The phenomenological analysis of the fission cross sections induced by high-energy protons[6] as well as a simple physical estimation of possible asymptotical behavior of nuclear fissility at the high energies show that the $^{239}\text{Pu}/^{238}\text{U}$ fission cross section ratio at 200 MeV is probably too large for Shcherbakov's data. At the same time $^{235}\text{U}(n,f)$ cross section measured by Lisowski has some irregularities, which can not be explained by the statistical uncertainty of the data in the energy region where the cross sections should be smooth. These two problems should be resolved before the final evaluation will be produced.

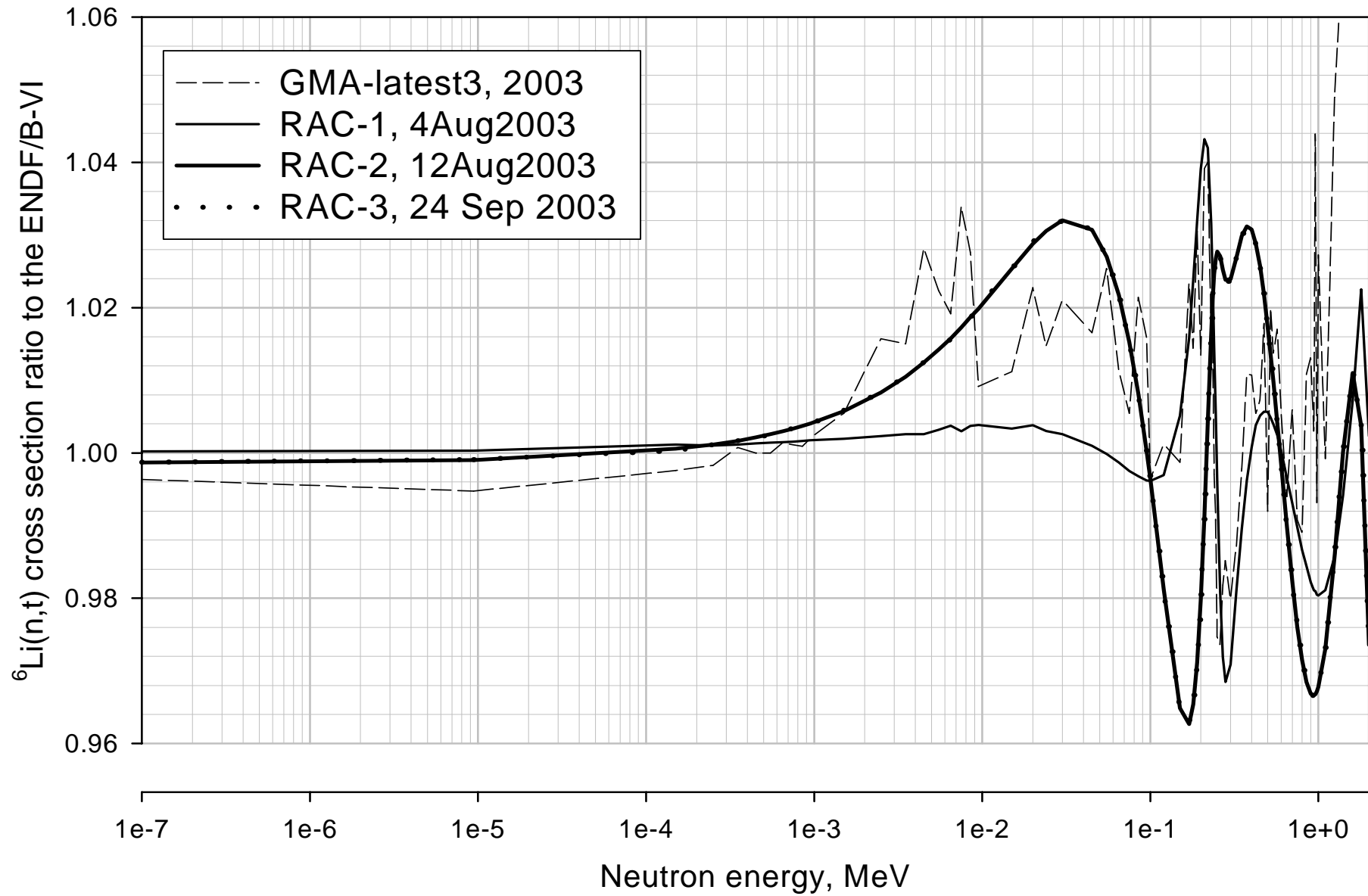
Open problems

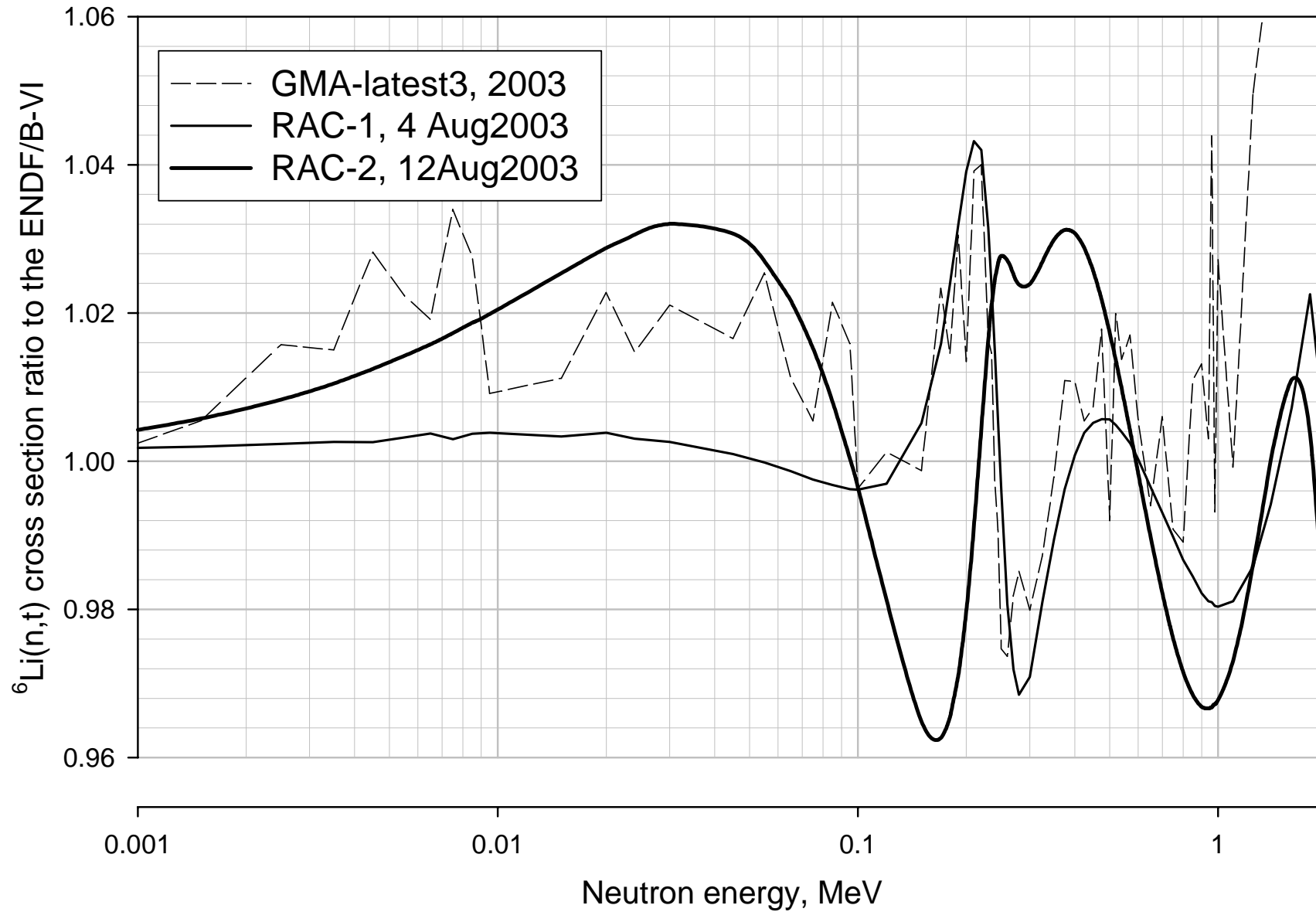
The following problems should be resolved before the final version of the standards will be produced:

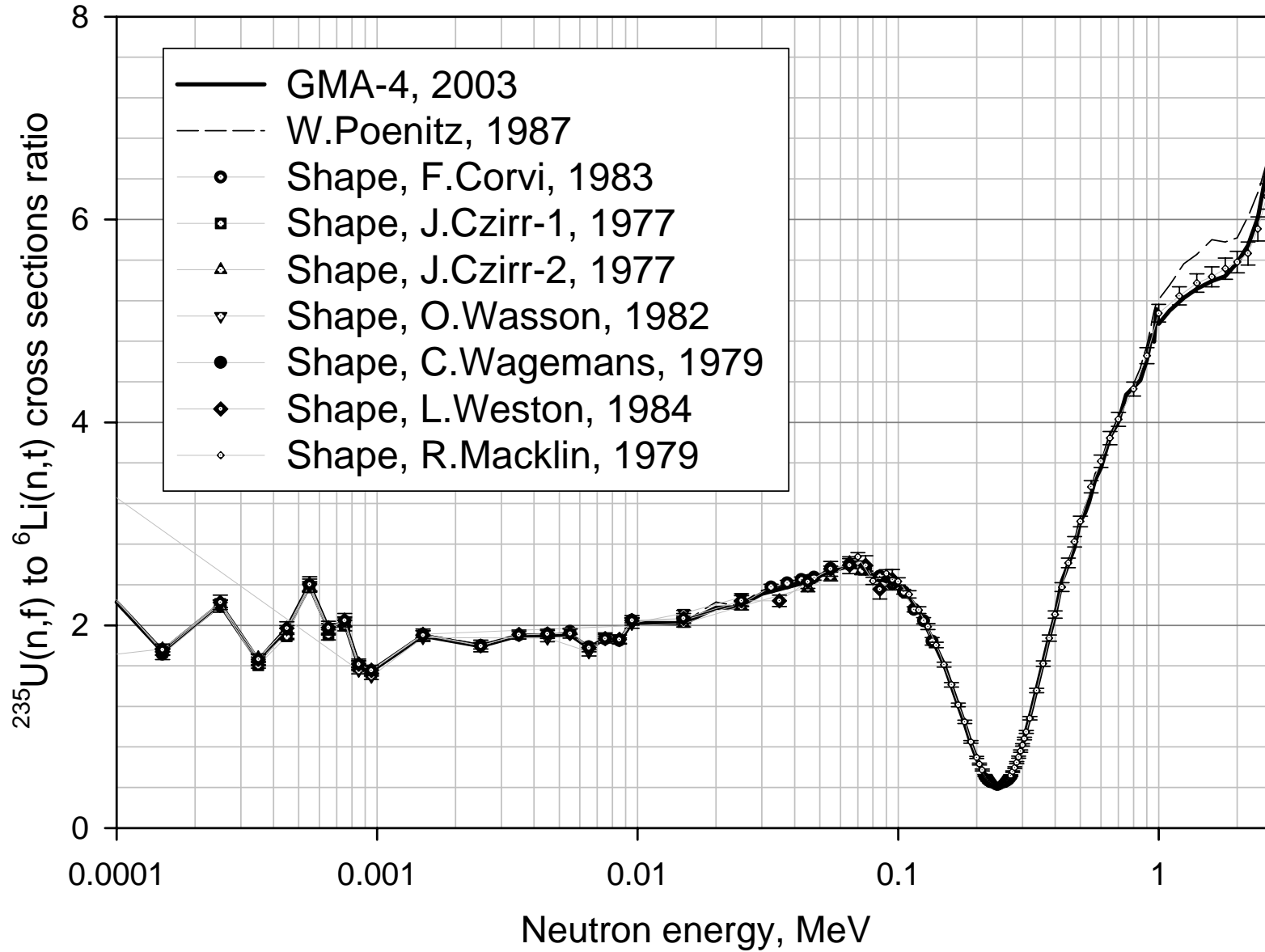
1. It should be shown that the posterior evaluation does not depend much from the procedure used for determining of the outliers and their further treatment.
2. The procedure of the smoothing of the cross sections evaluated in the non-model least-squares fit, which should preserve the physical structure of the cross sections and add to the covariance matrix of the uncertainties the component due to additional smoothing should be developed.
3. The consequences of using the semi-positive definite covariance matrices of uncertainty (dimension n) for cross sections calculated from R-matrix parameter covariance matrix of uncertainty (dimension m , $n>m$) in general combining procedure should be studied.
4. The differences in the resonance widths between GMA and RAC from one side and EDA from other should be studied. The possible reasons could be: the difference in data bases used for R-matrix fit with RAC and EDA or difference in the implementation of error propagation law between GMA, RAC and EDA.
5. The discrepancies of the fission cross sections in the high-energy region should be resolved.

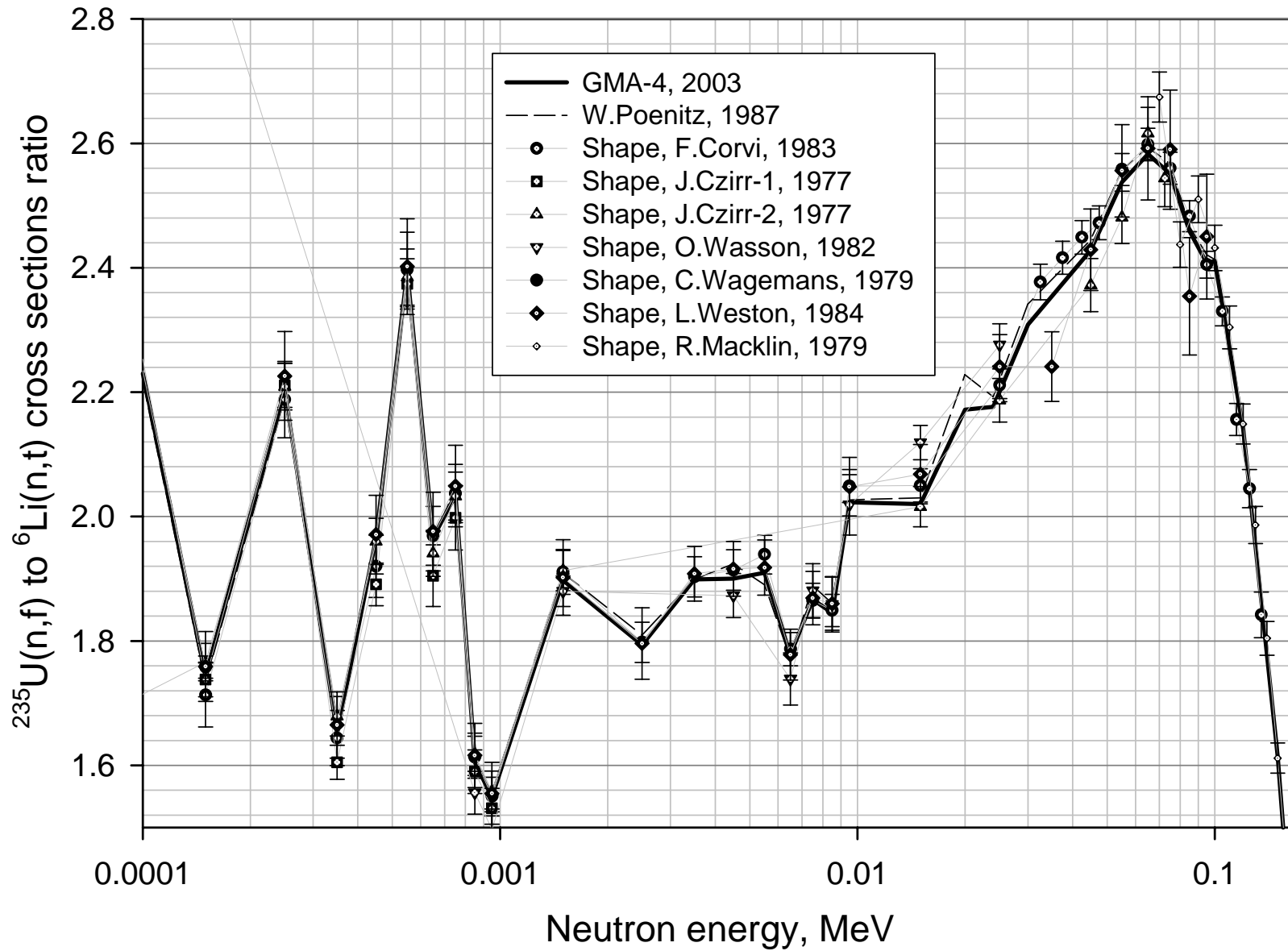
References

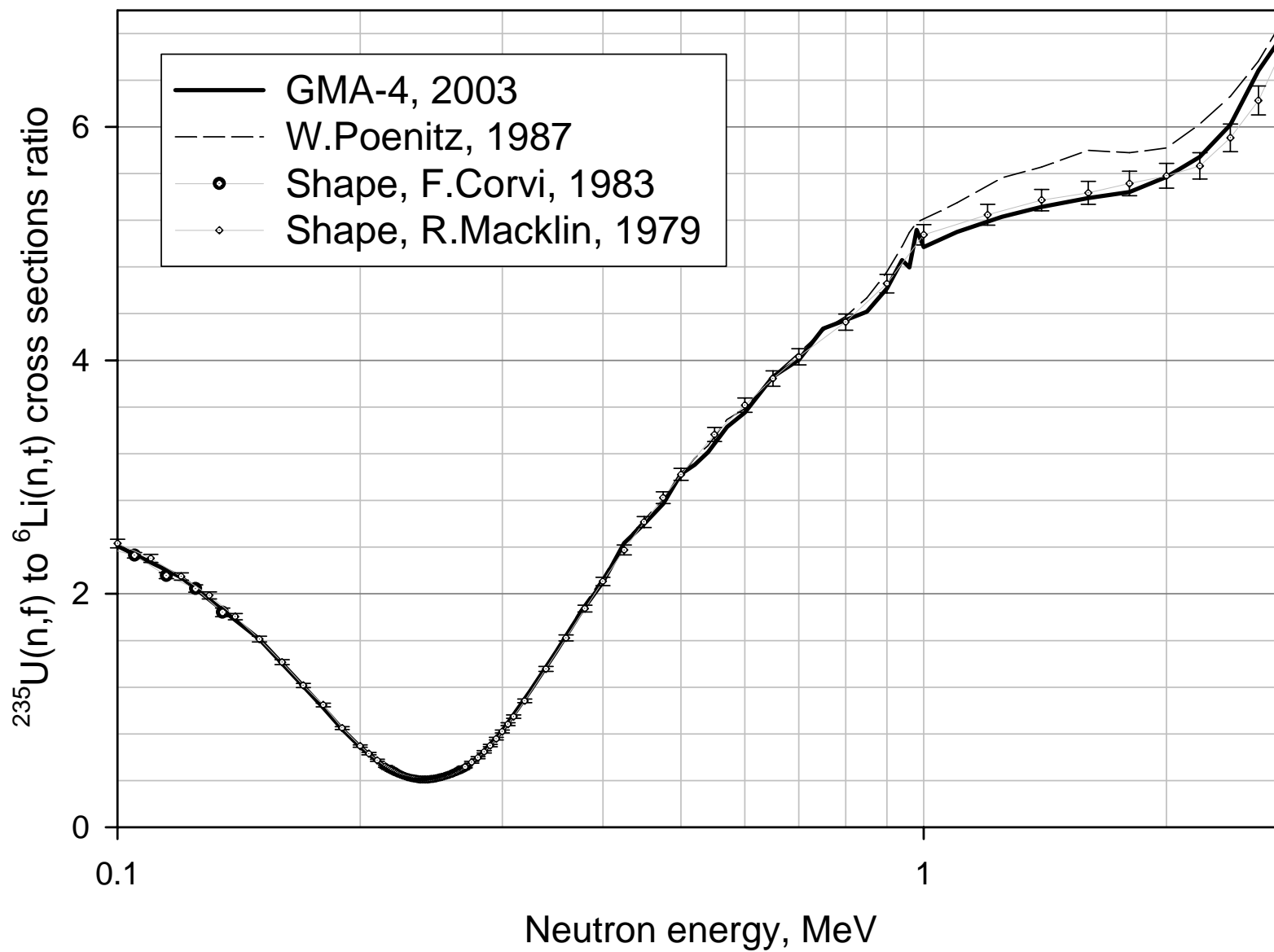
1. H. Conde (ed.), Nuclear Data Standards for Nuclear Measurements, Report NEANDC-311 (1992).
2. W.P. Poenitz and S.E. Aumeier, The Simultaneous Evaluation of the Standards and Other Cross Sections of Importance for Technology, Report ANL/NDM-139 (1997).
3. K. Shibata, T. Kawano et al., Japanese Evaluated Nuclear Data Library Version 3 Revision 3, Journal of Nuclear Science and Technology, 38 (11), p. 1125 (2002).
4. P.G. Young, M.B. Chadwick et al., LANL Revision of NF Cross Section (2003); <http://t2.lanl.gov/data/data/preVII-neutron/> (October 2003).
5. W. Mannhart, Report NEA/NSC/DOC(99)10 (1999).
6. A.V. Prokofiev, Nucl. Instr. and Meth. in Physics Research, A463, p.557 (2001).

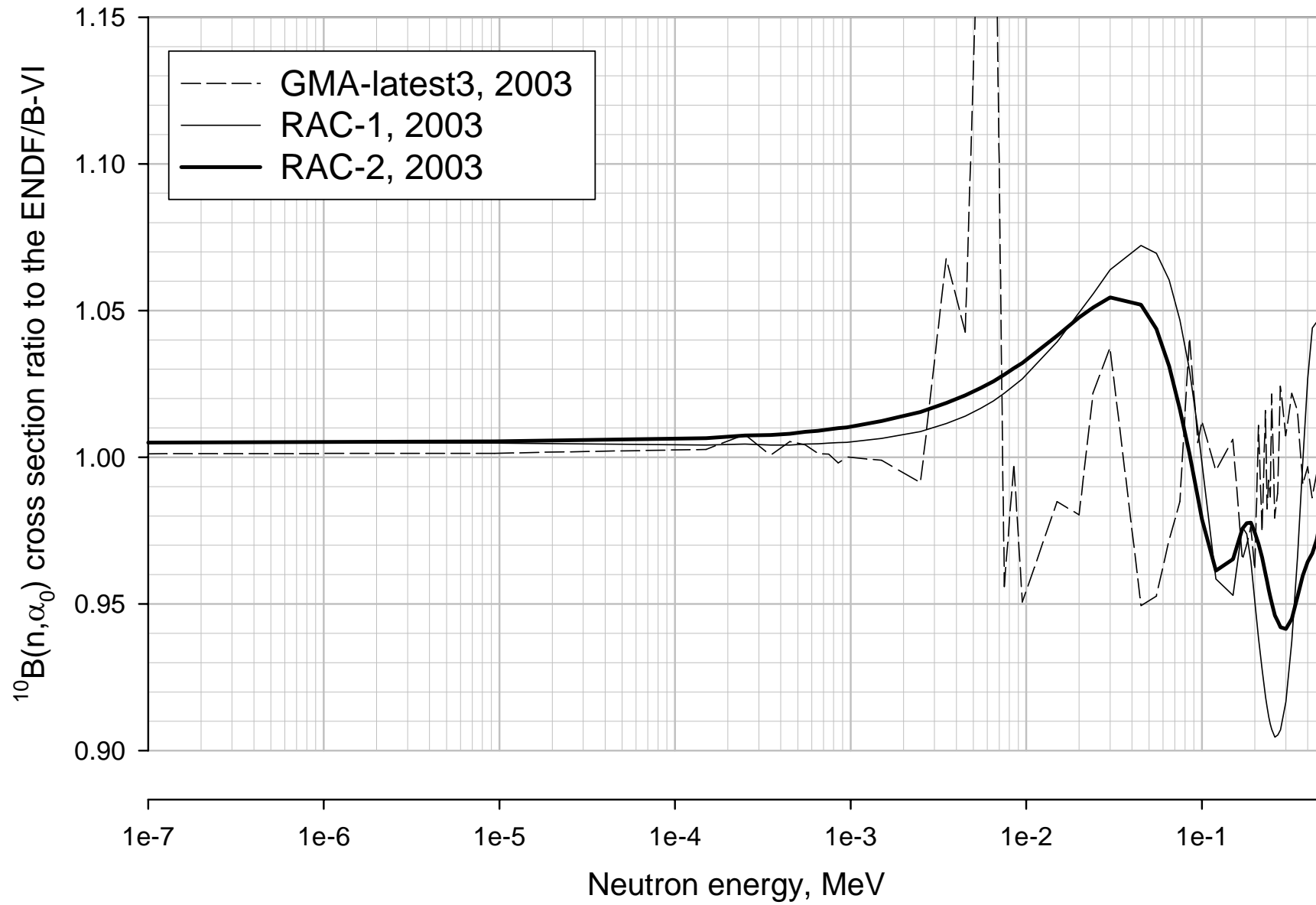


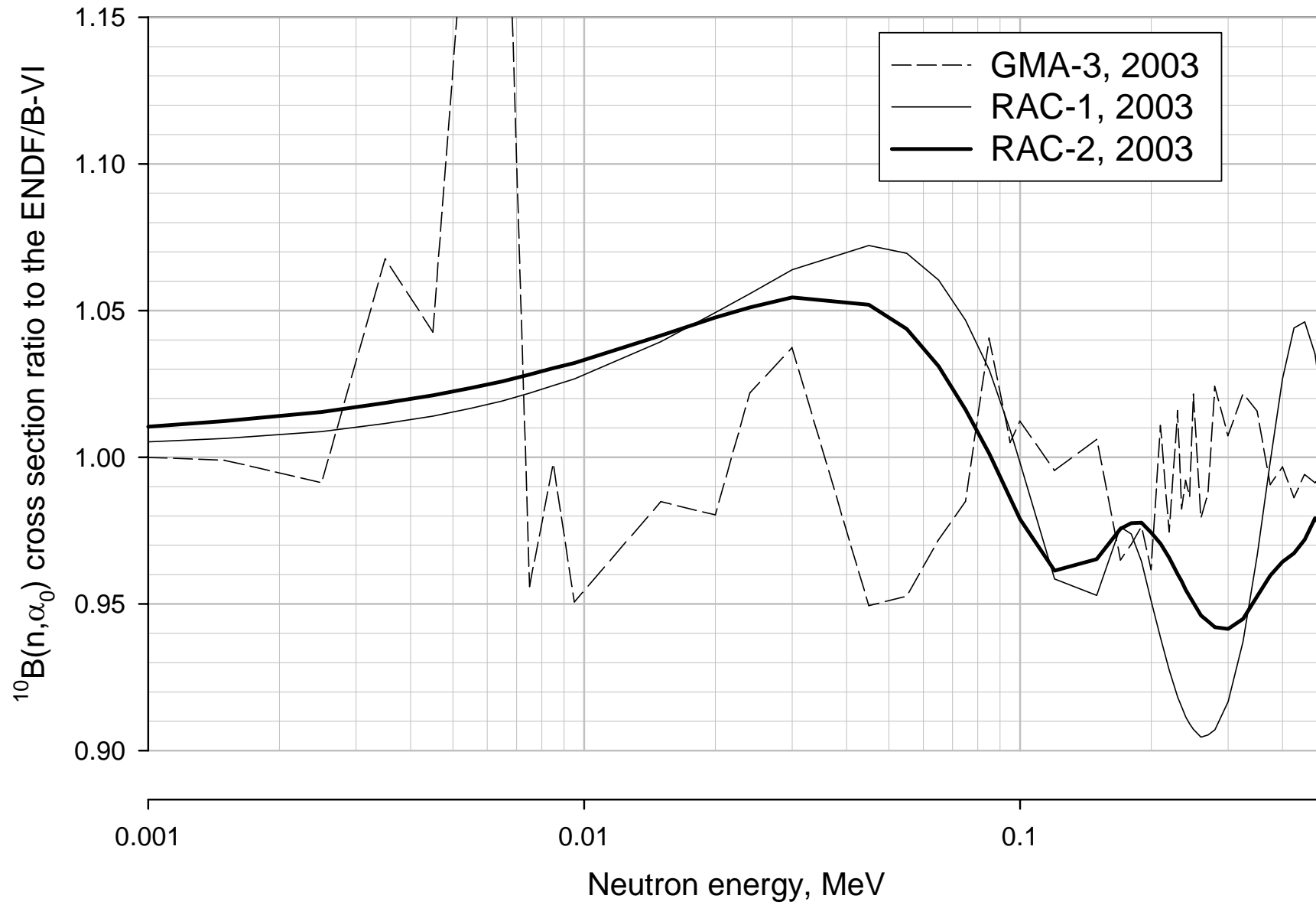


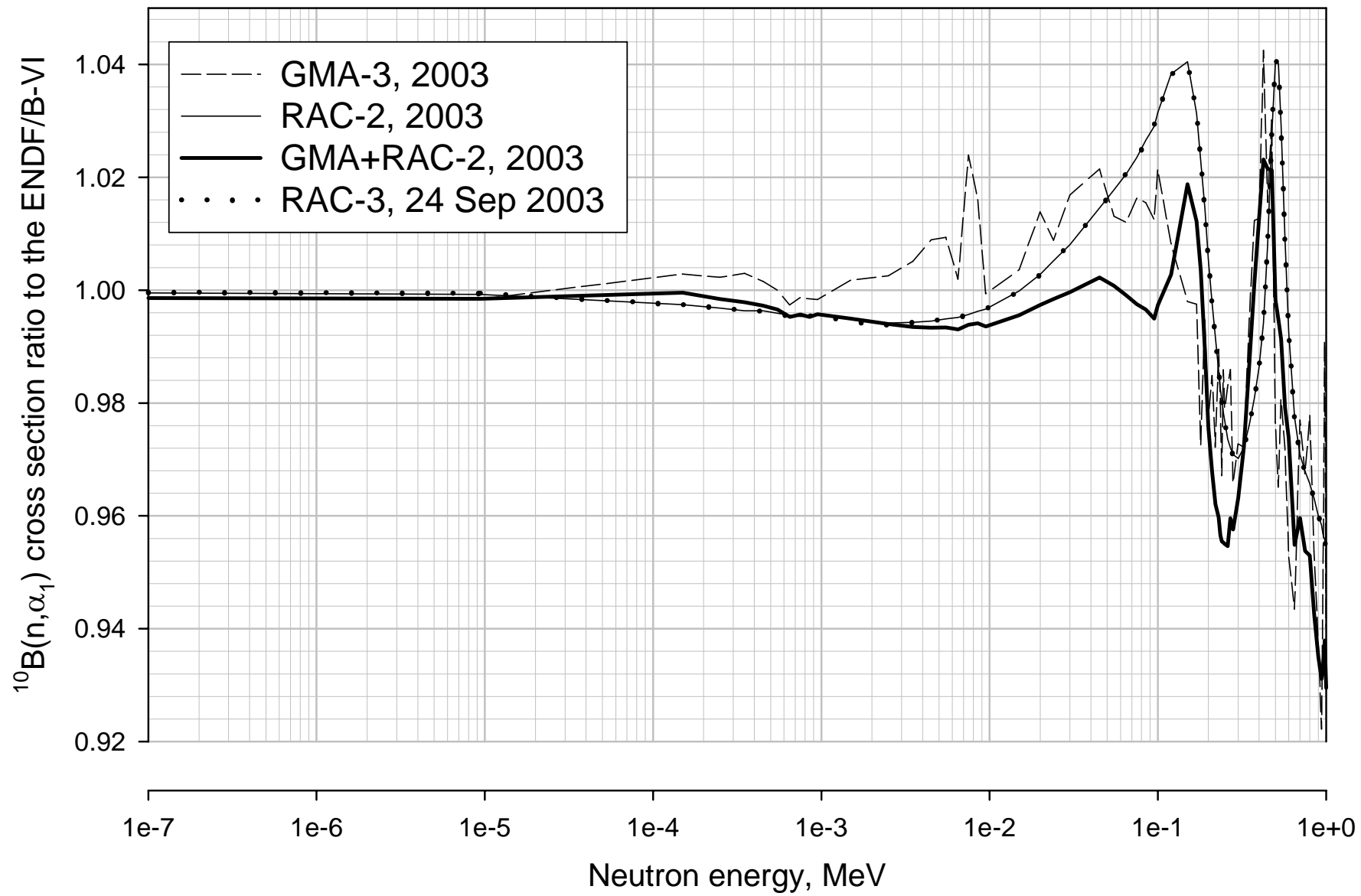


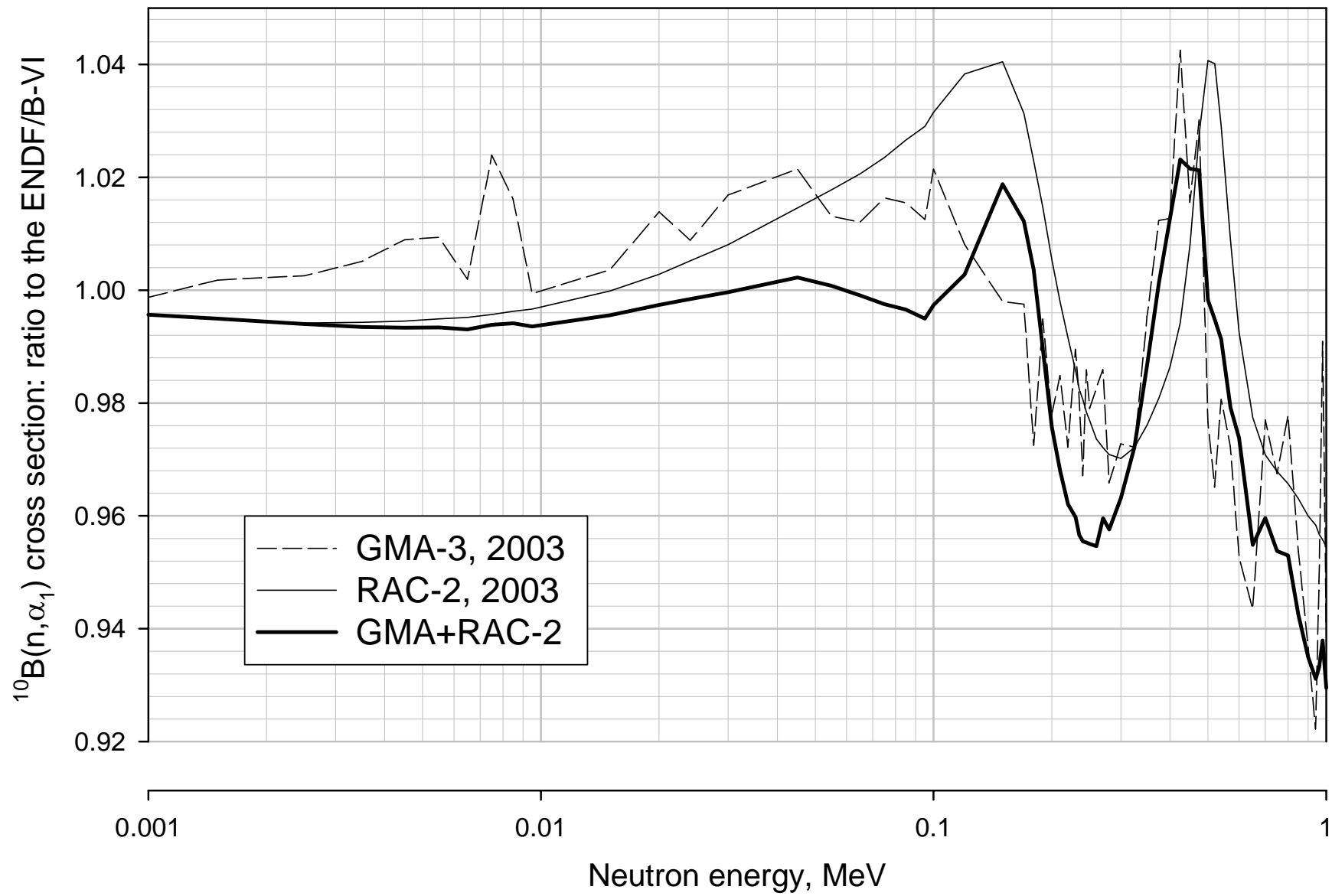


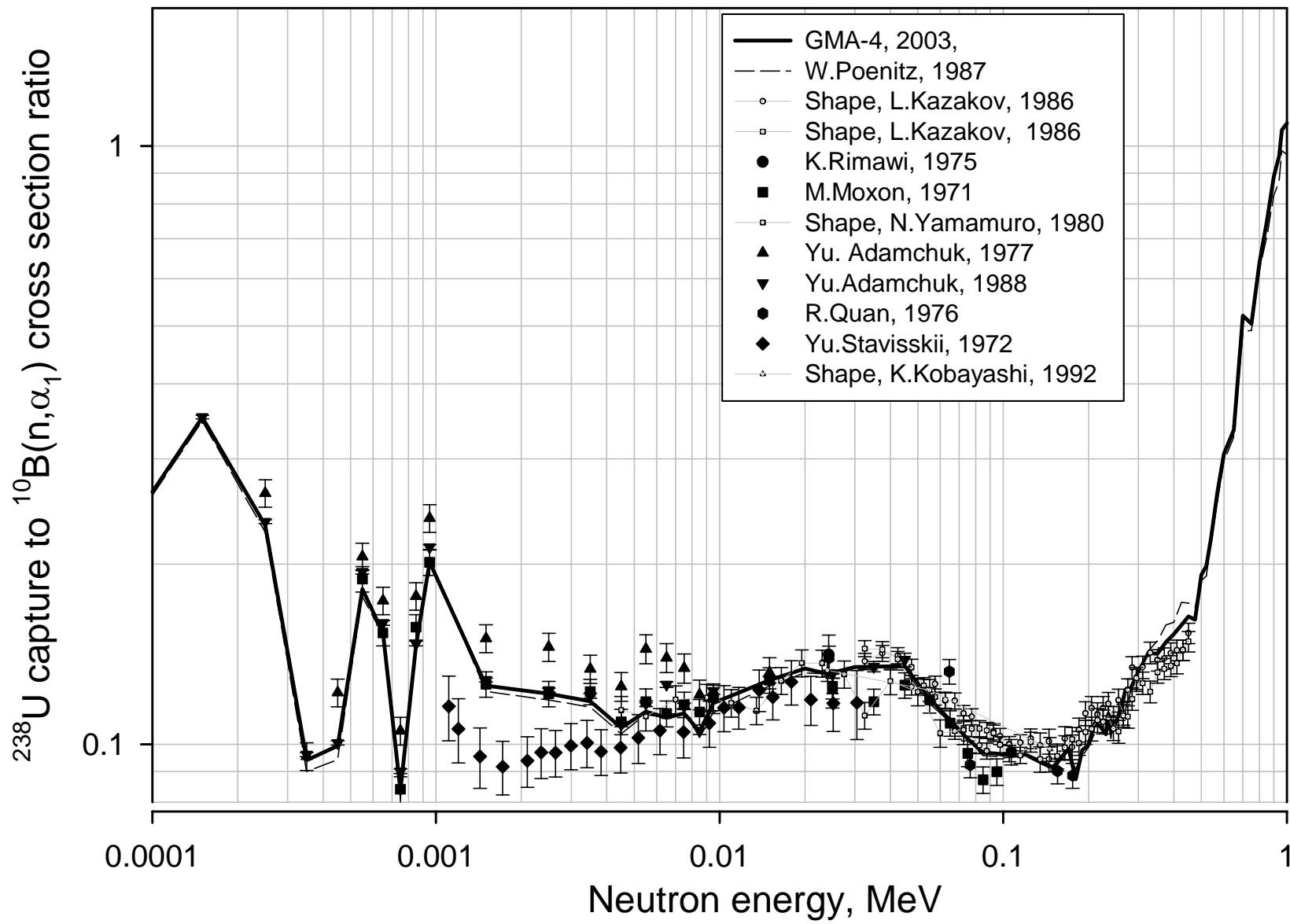


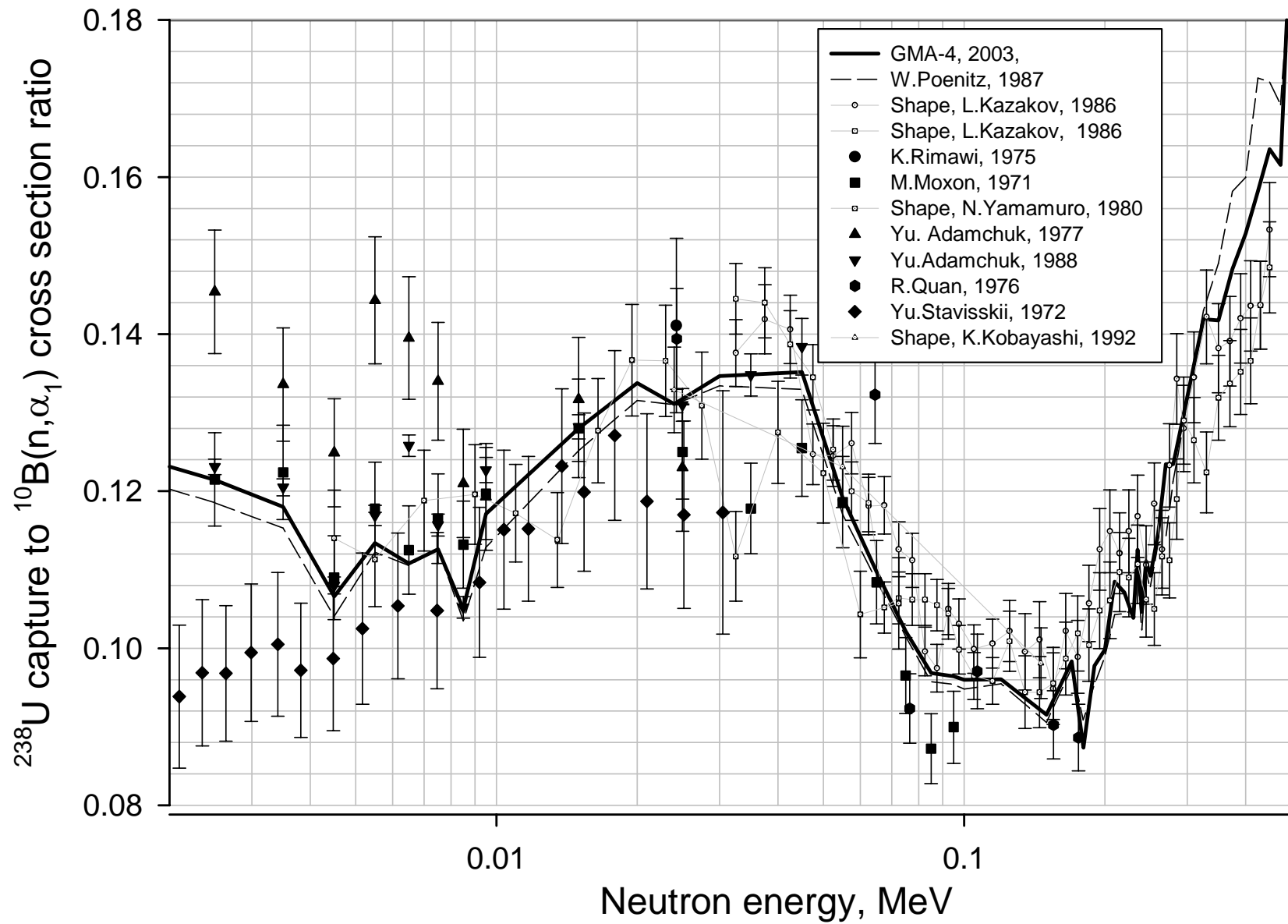


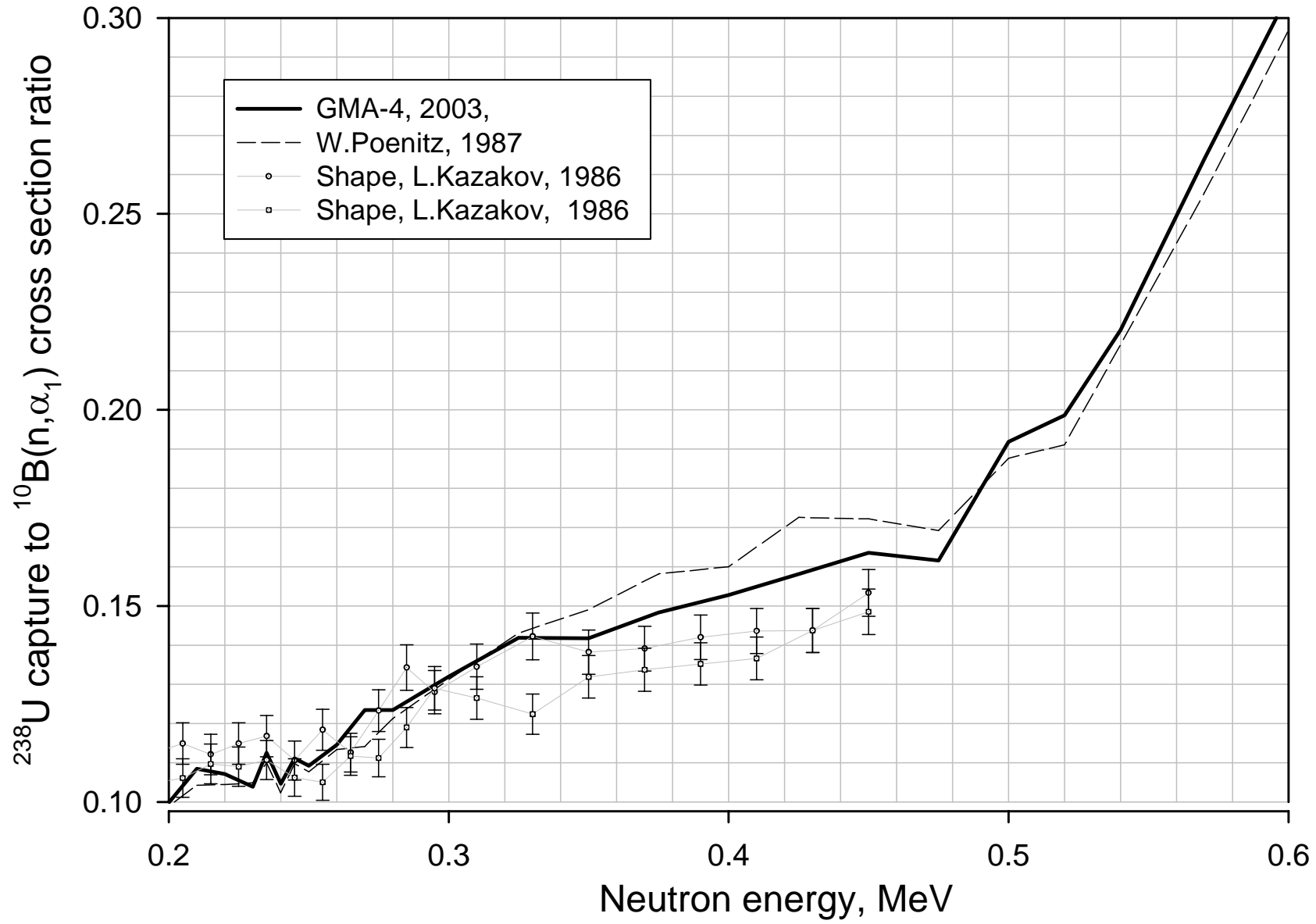


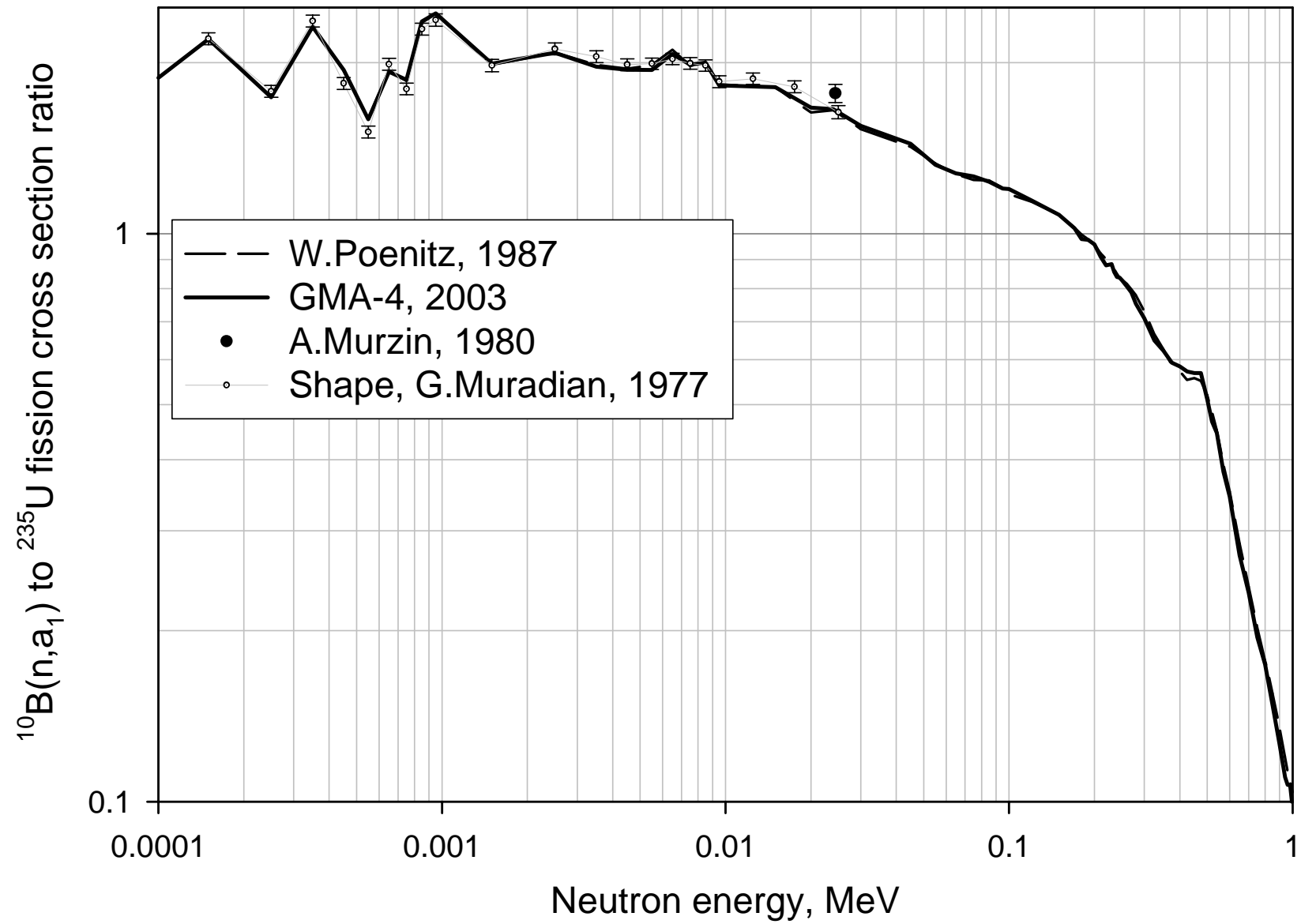


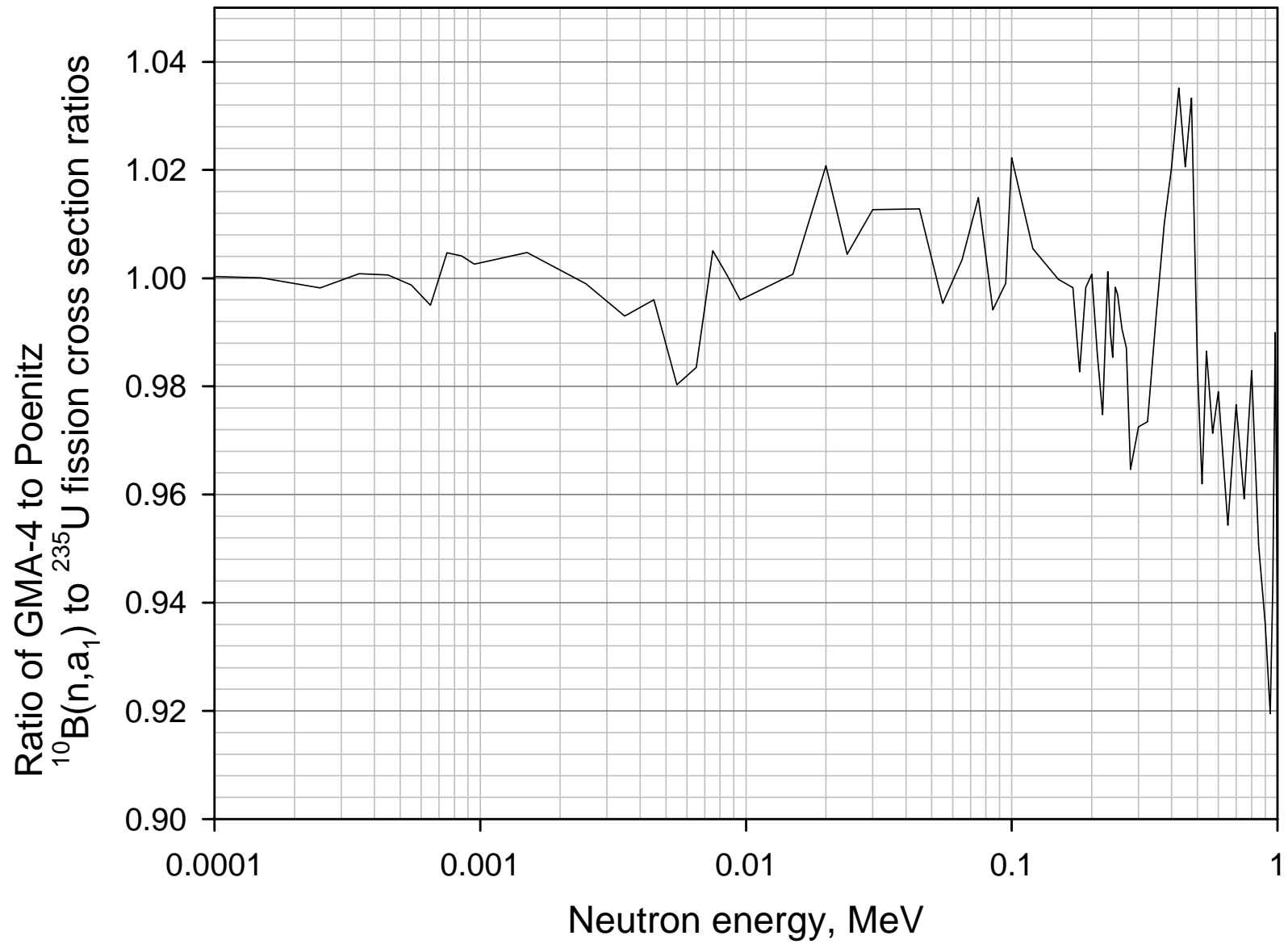


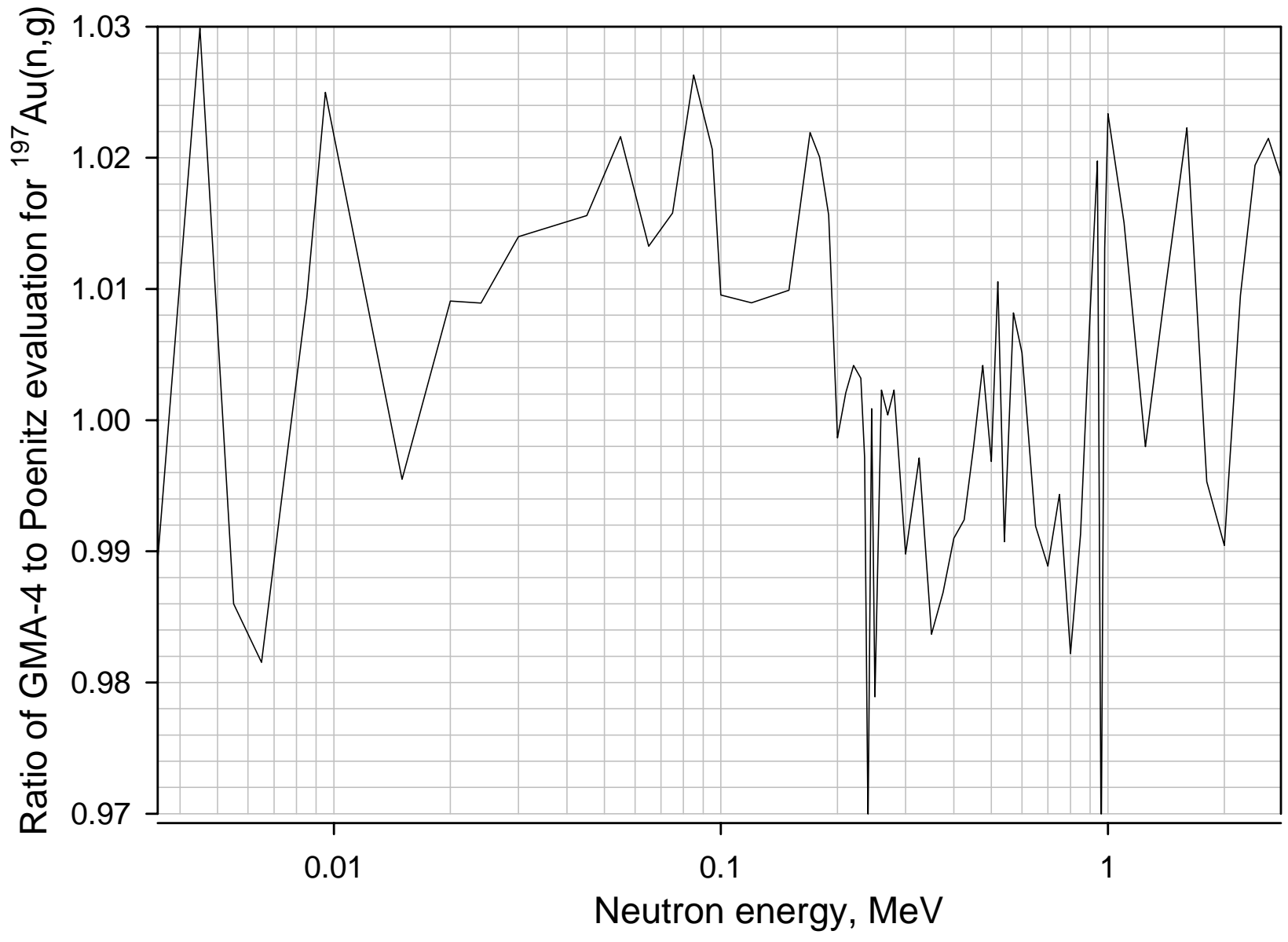


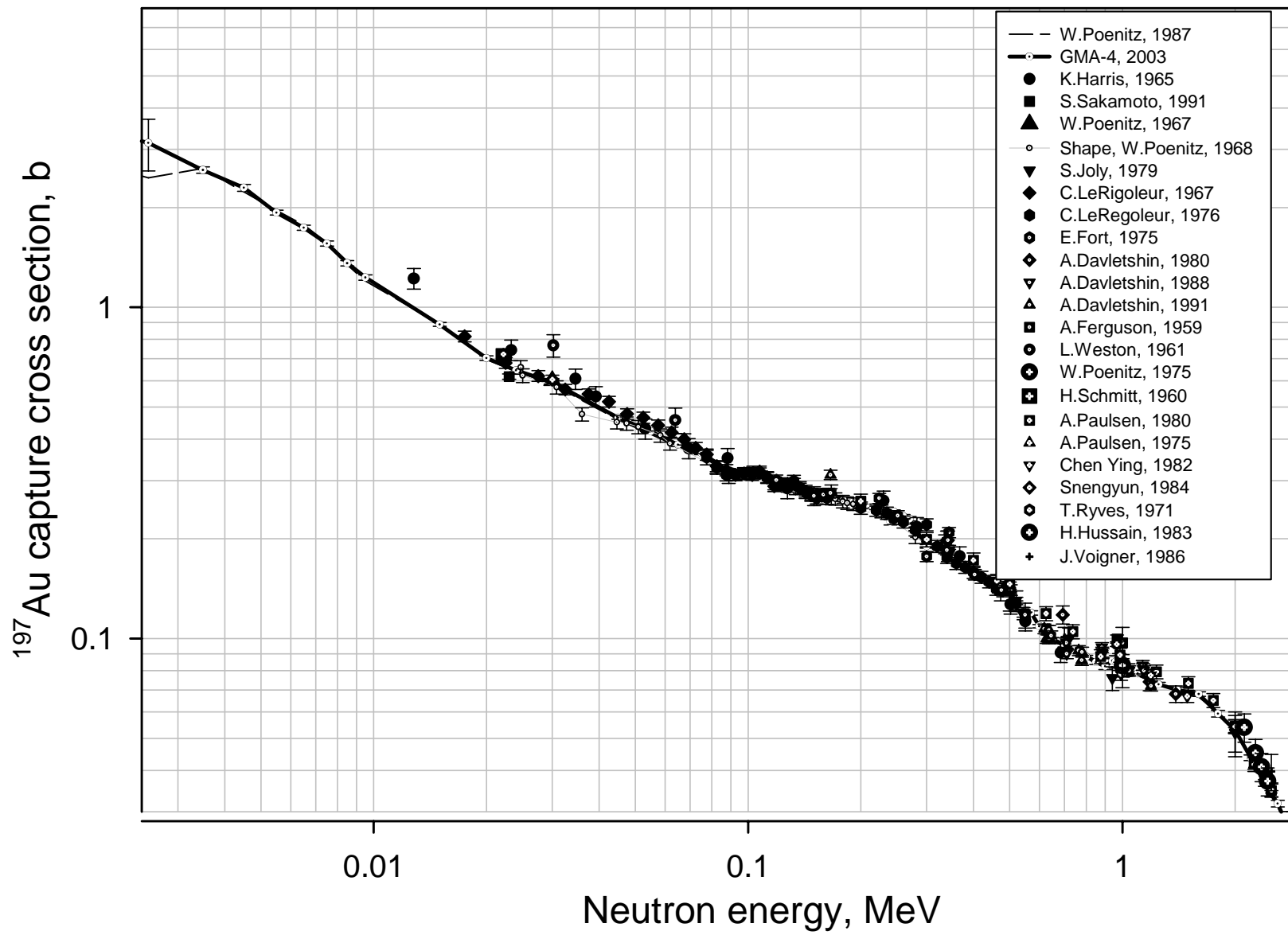


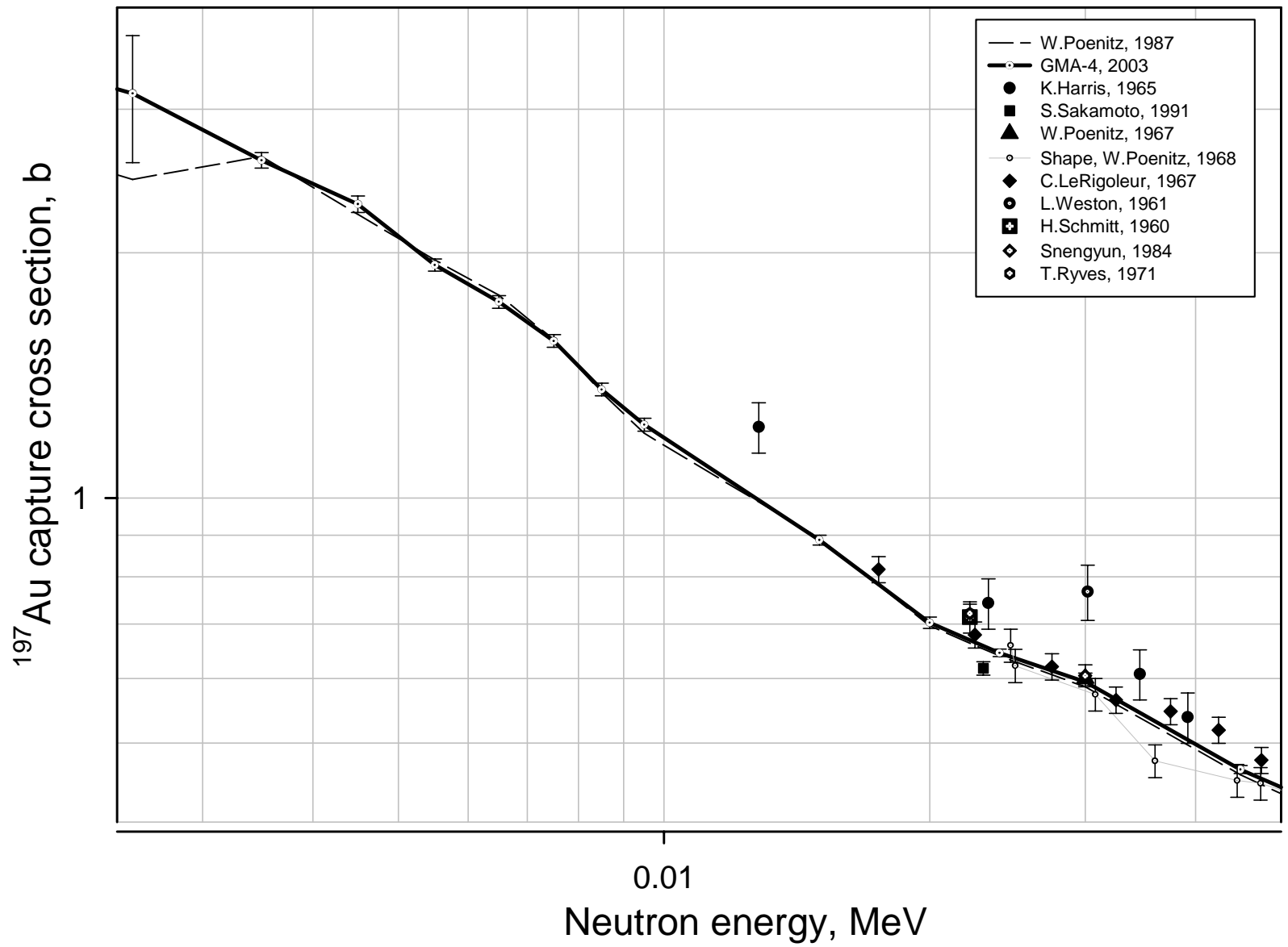


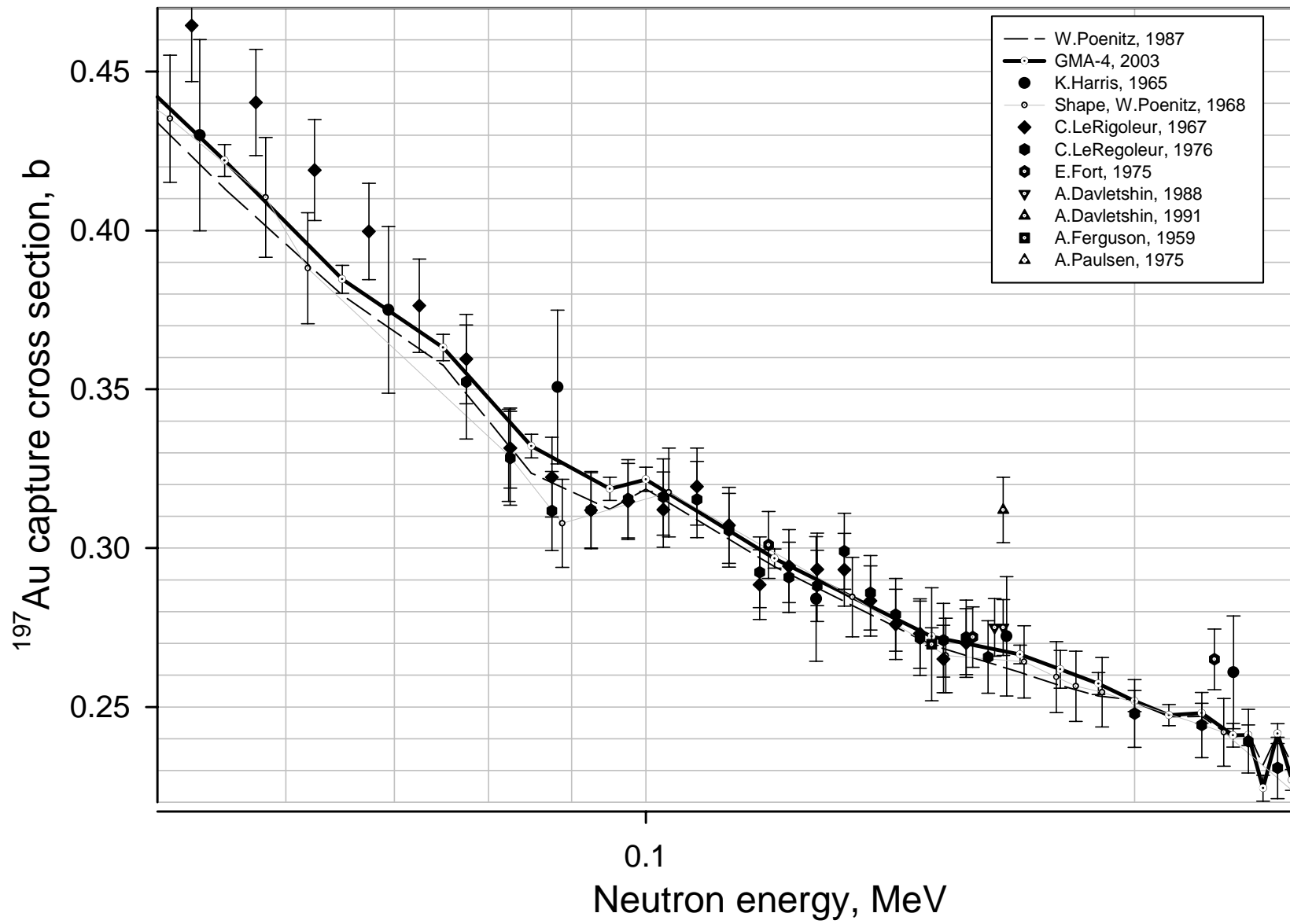


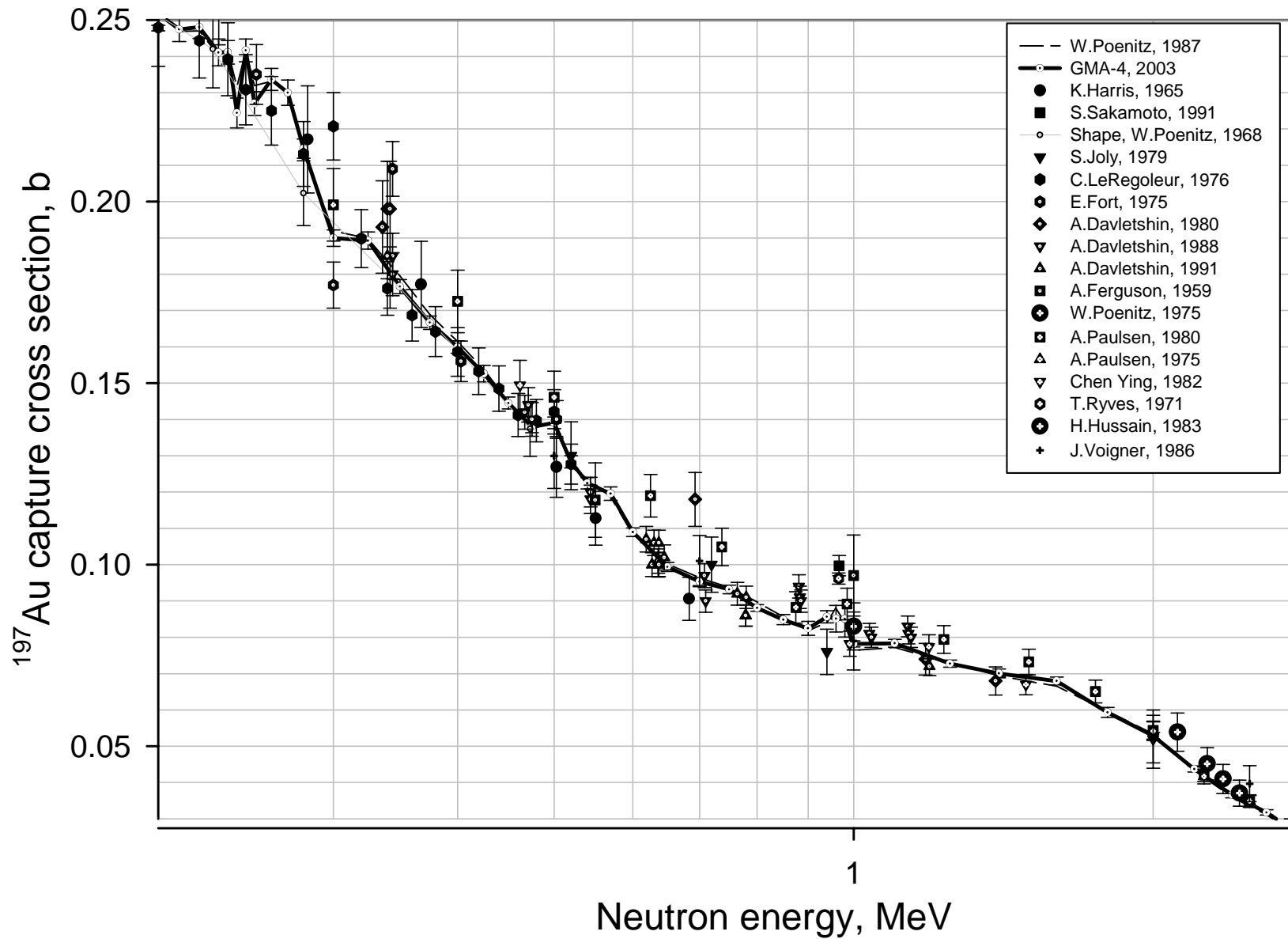


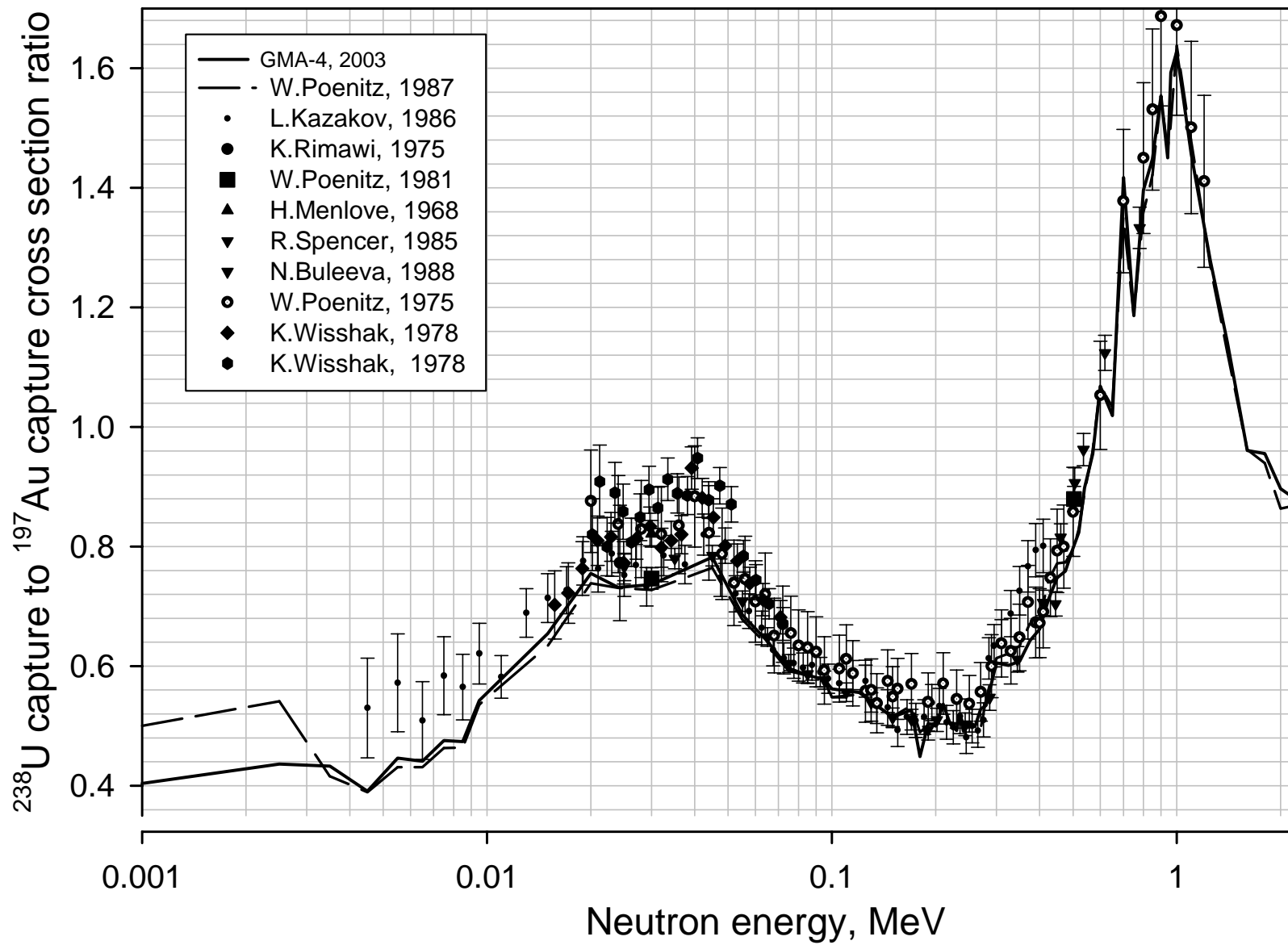


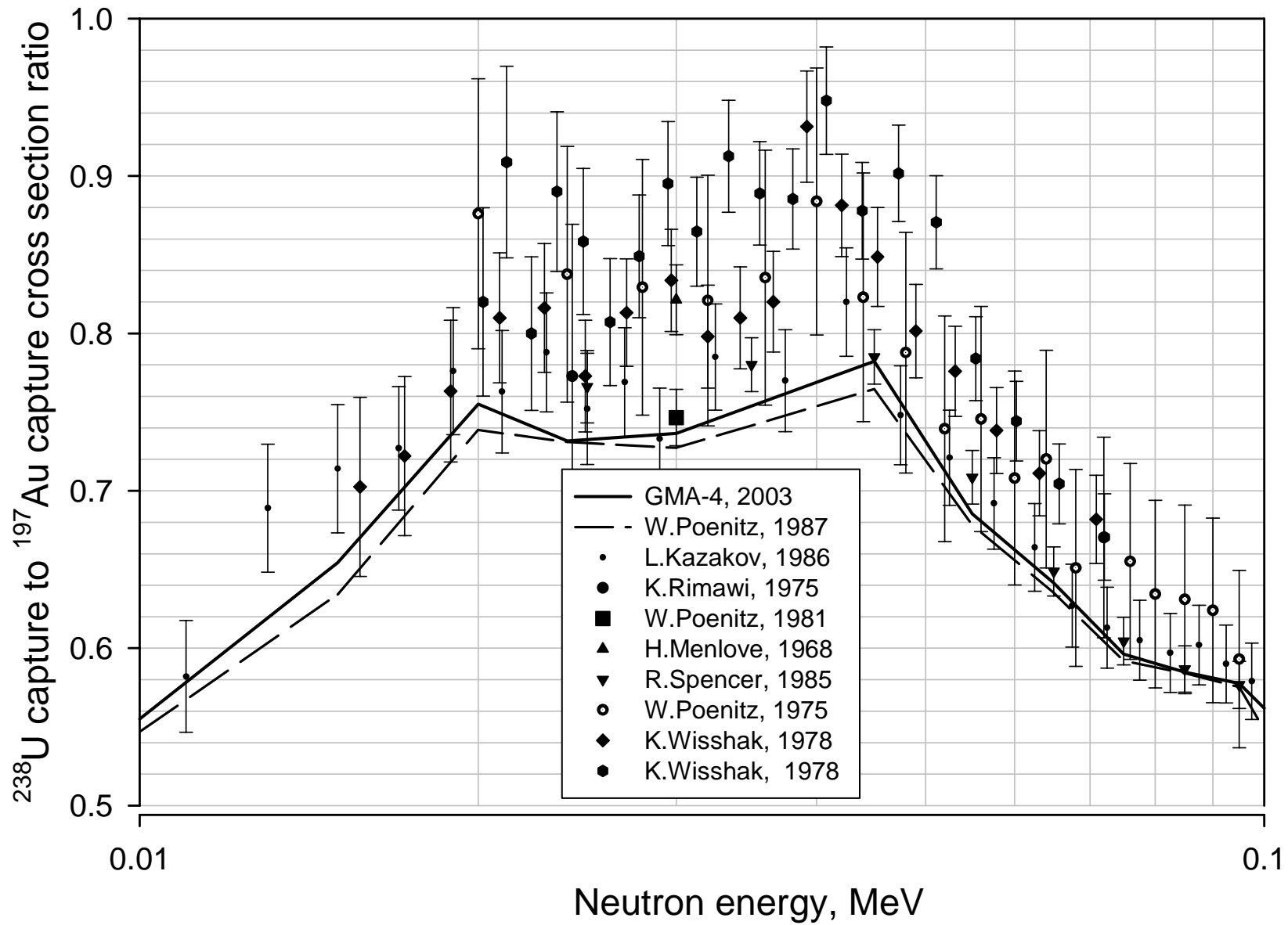


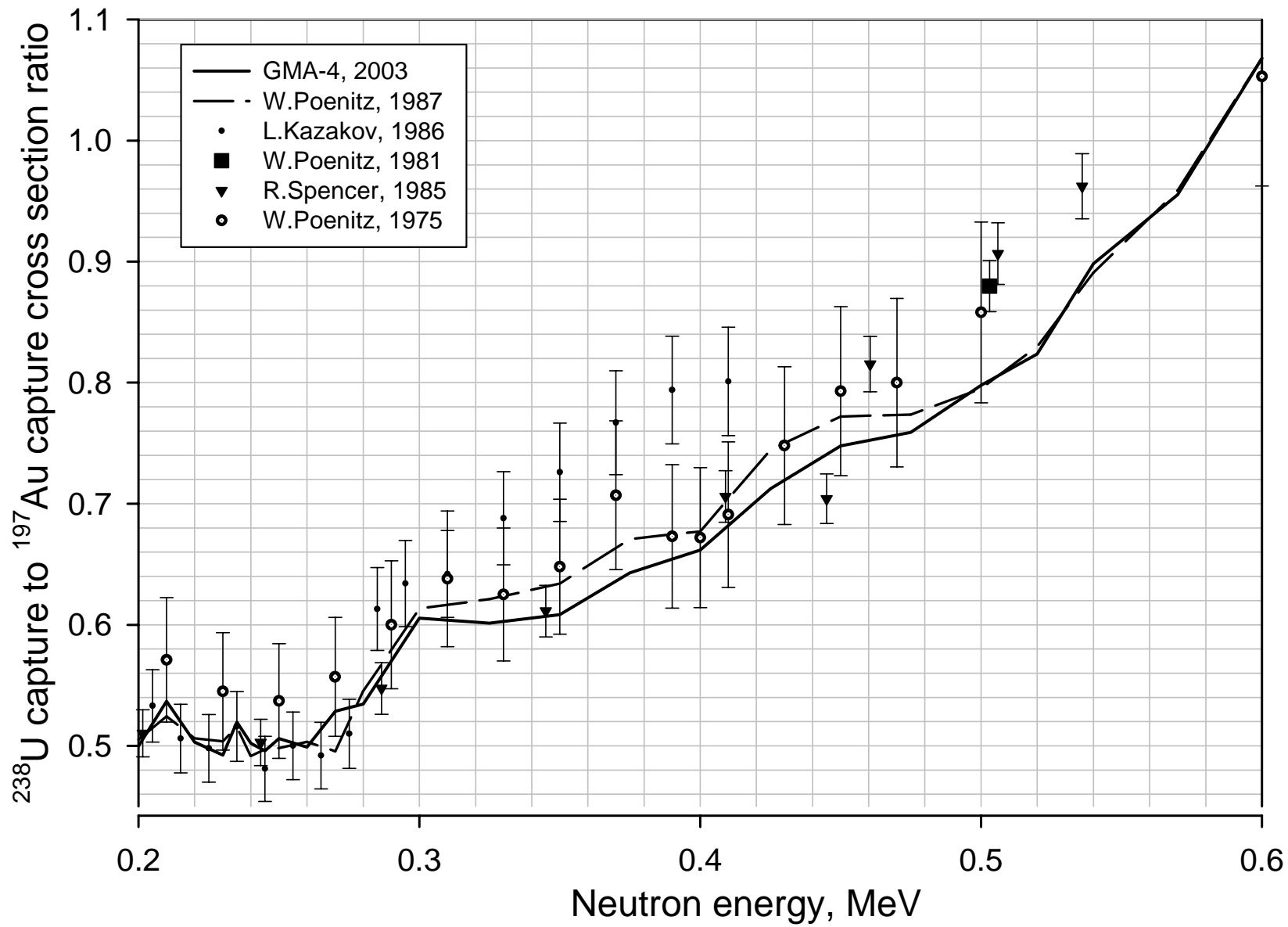


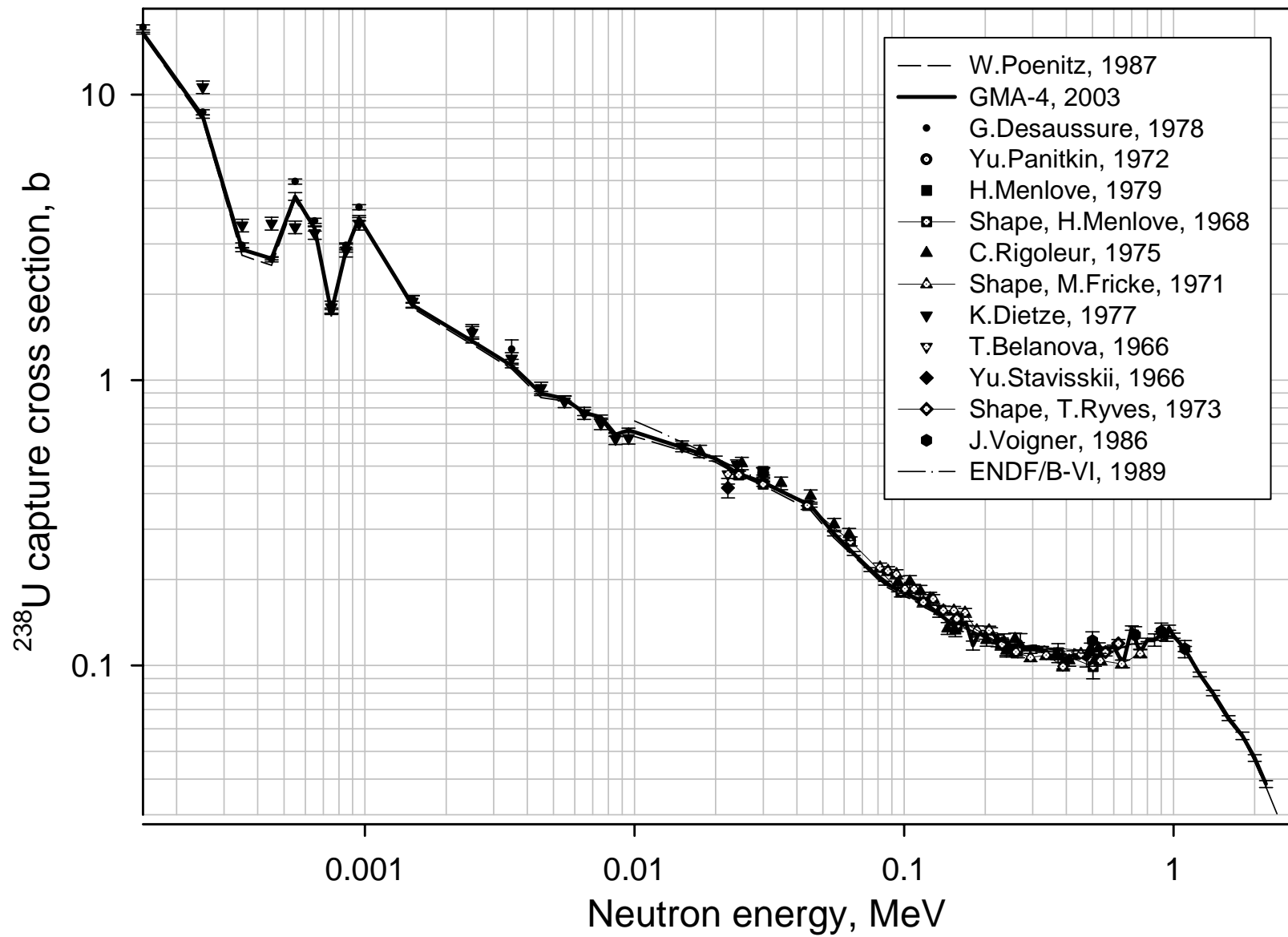


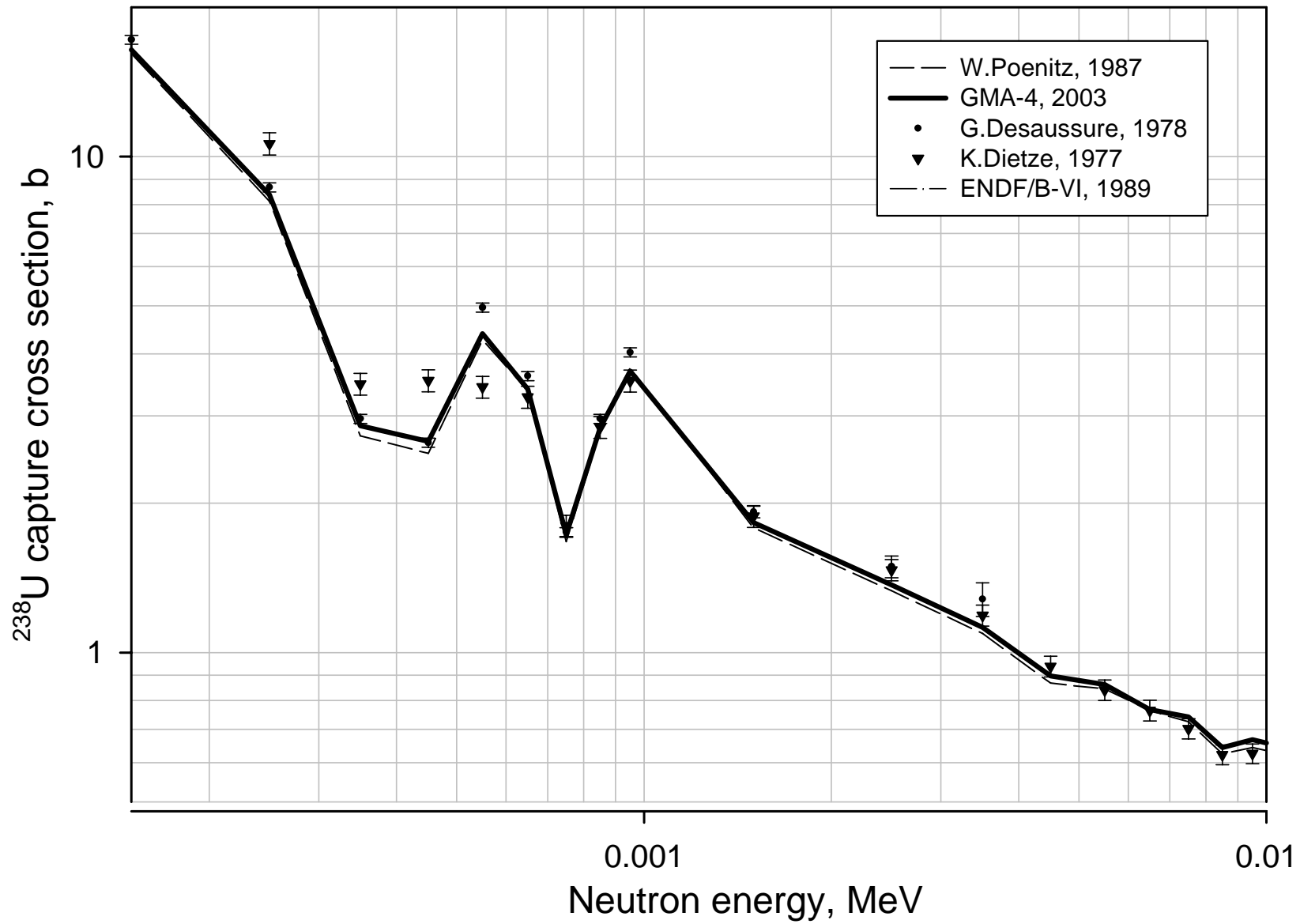


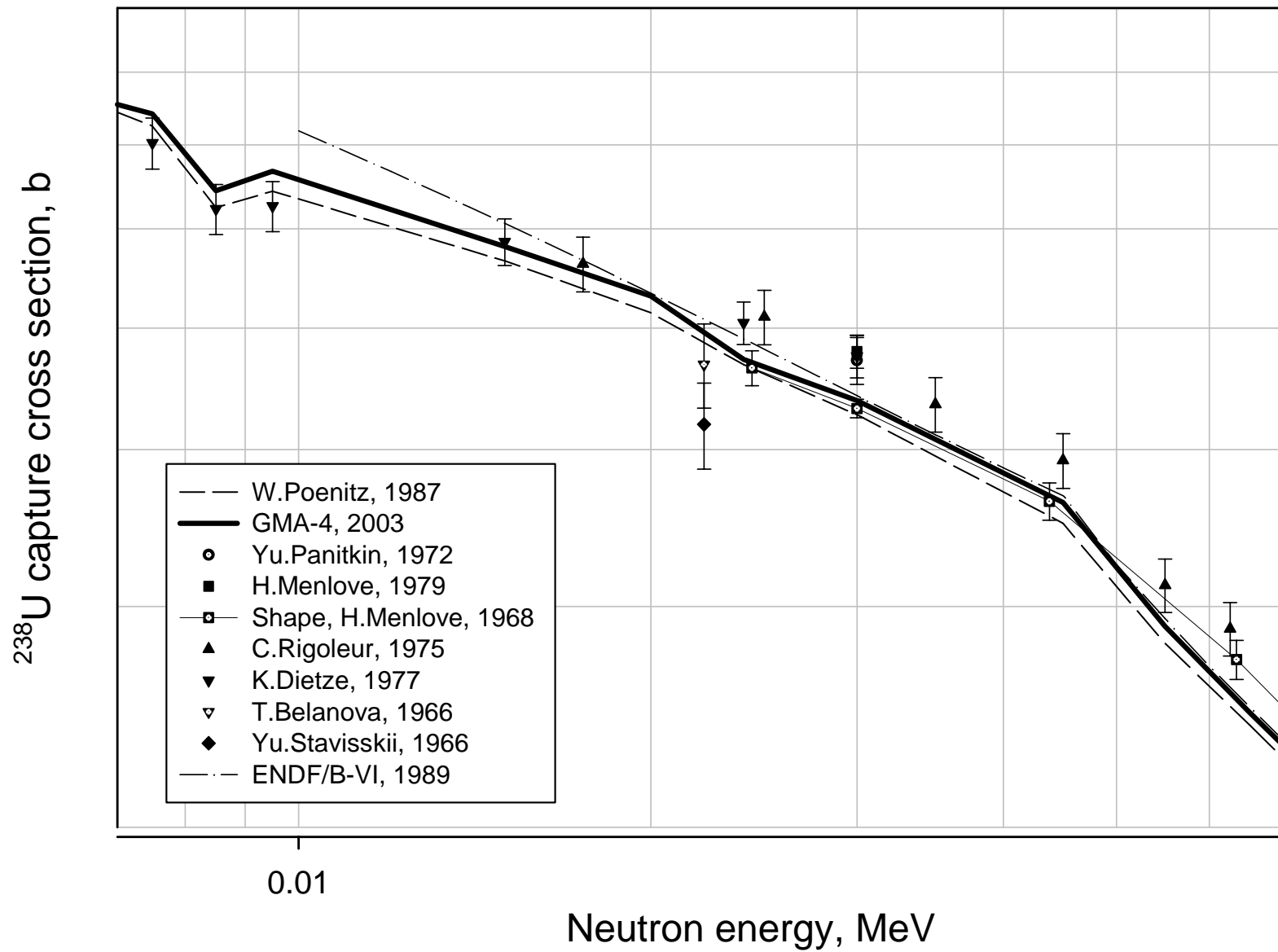


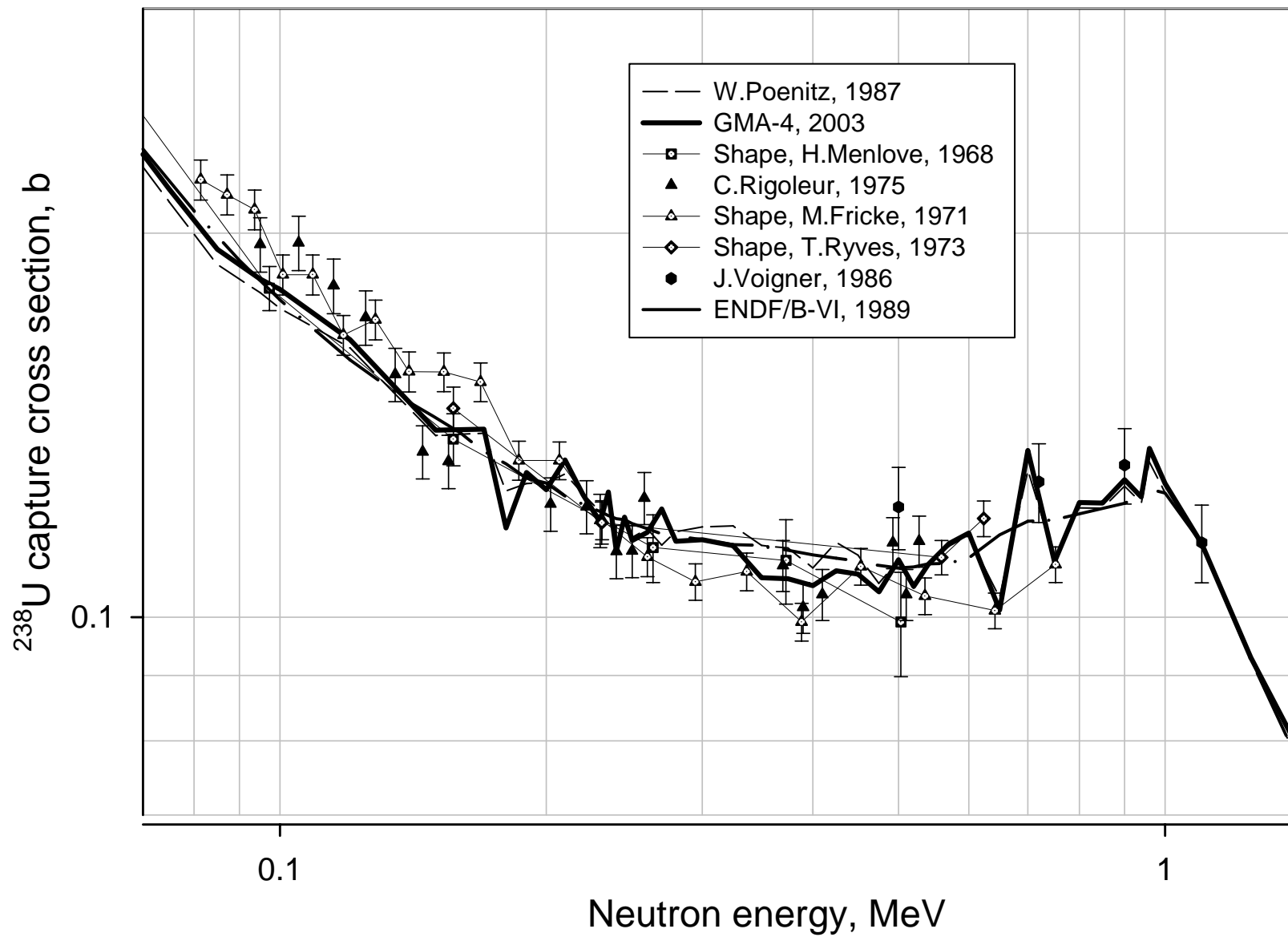


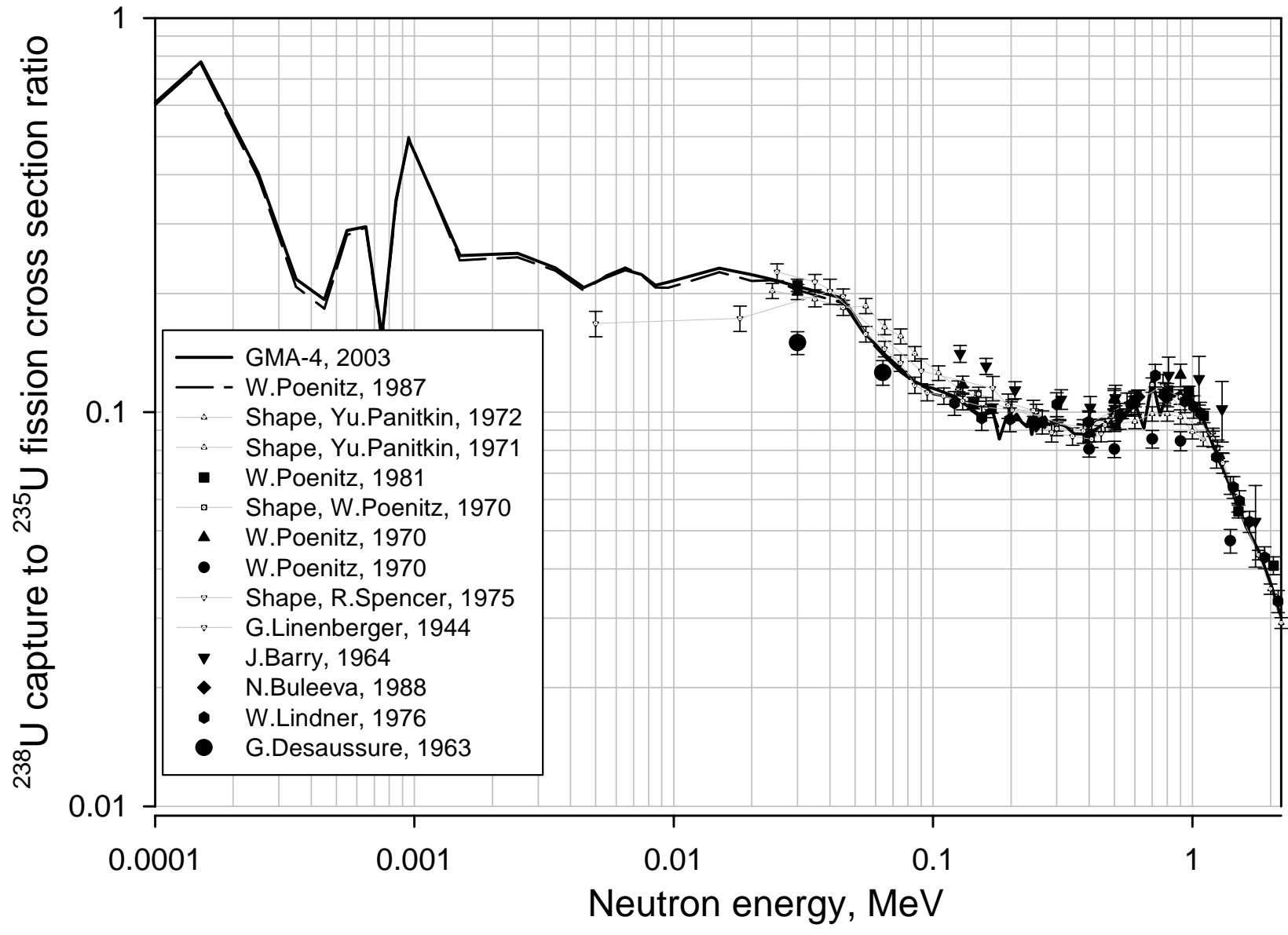


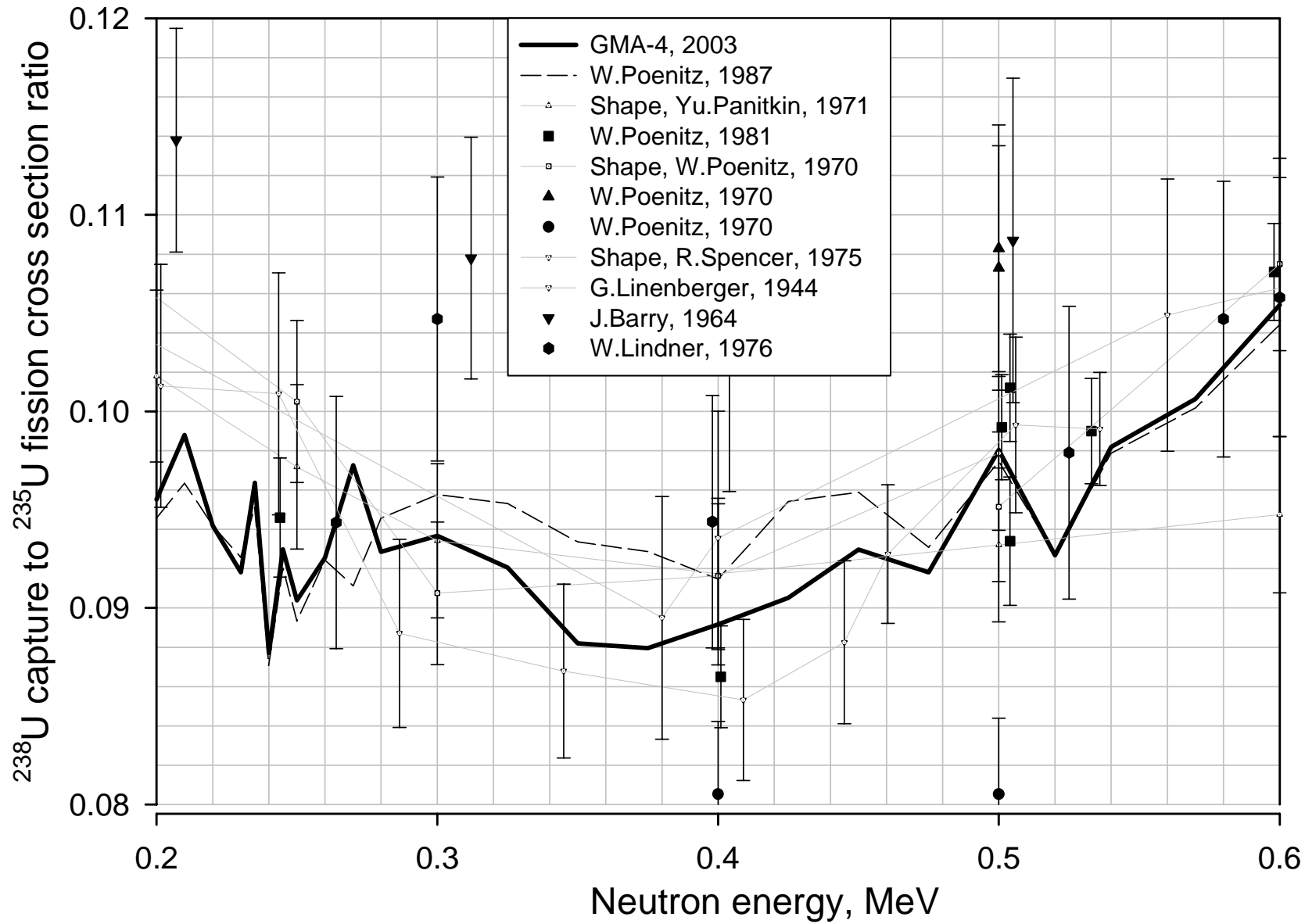


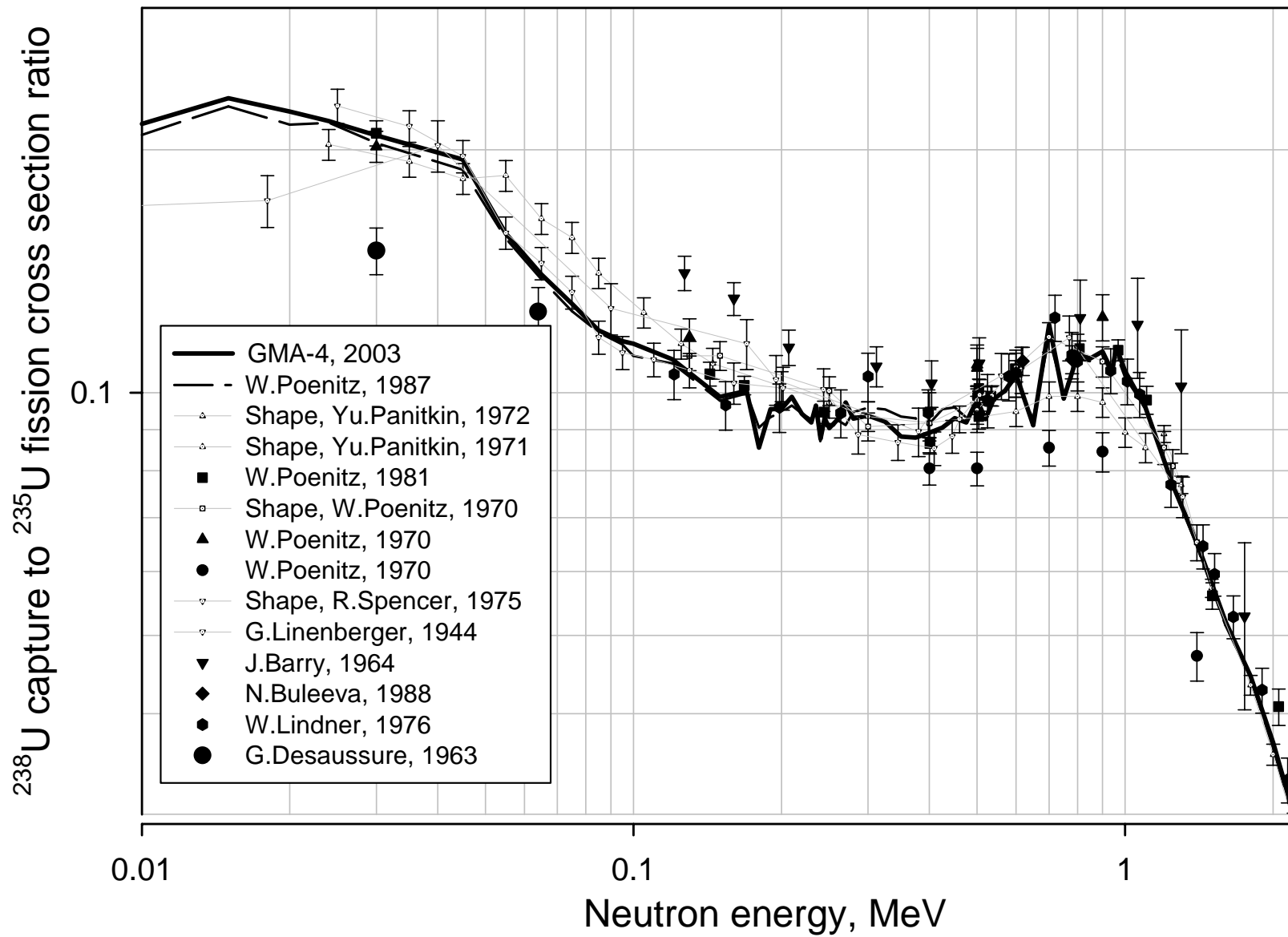


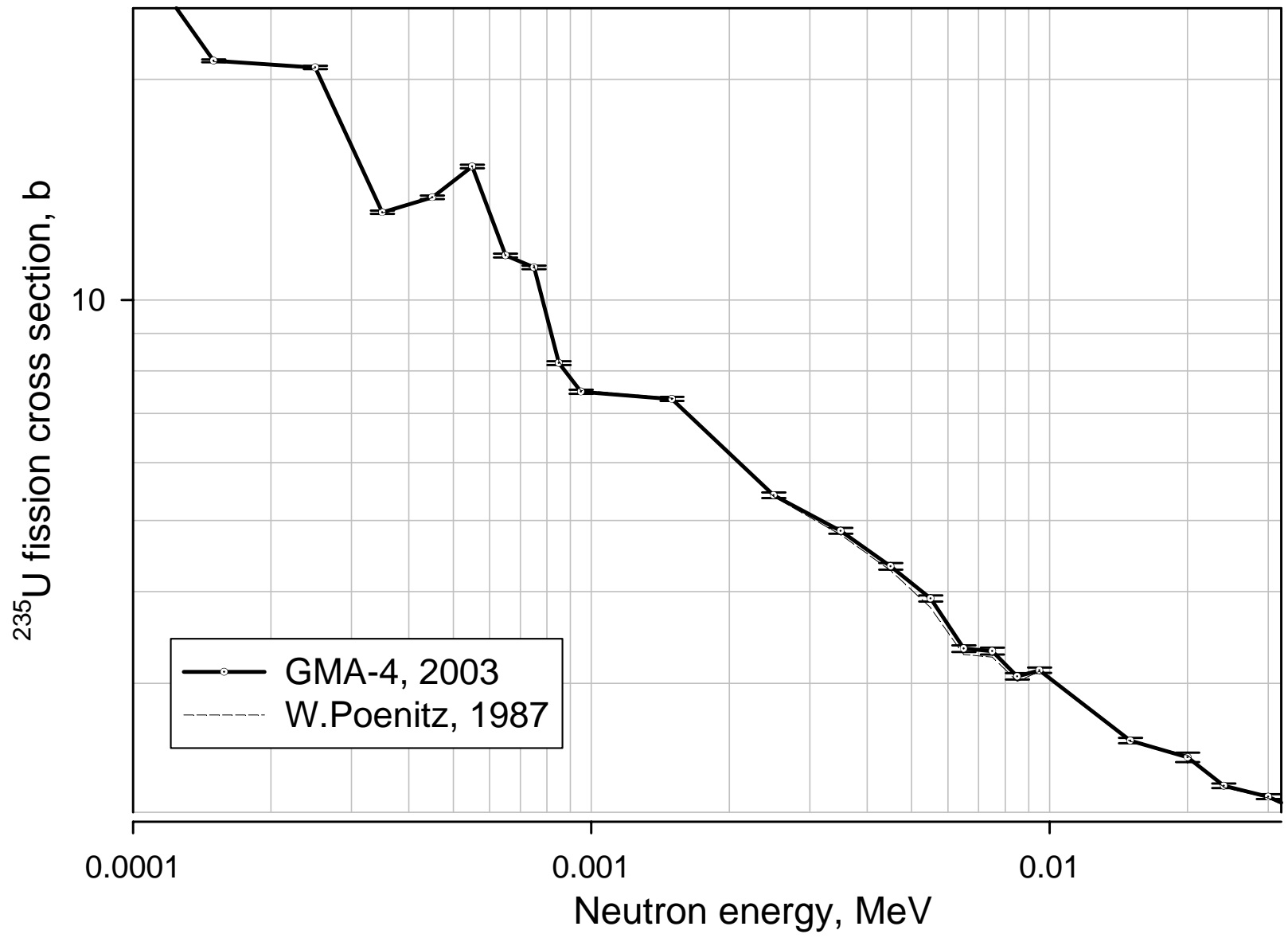


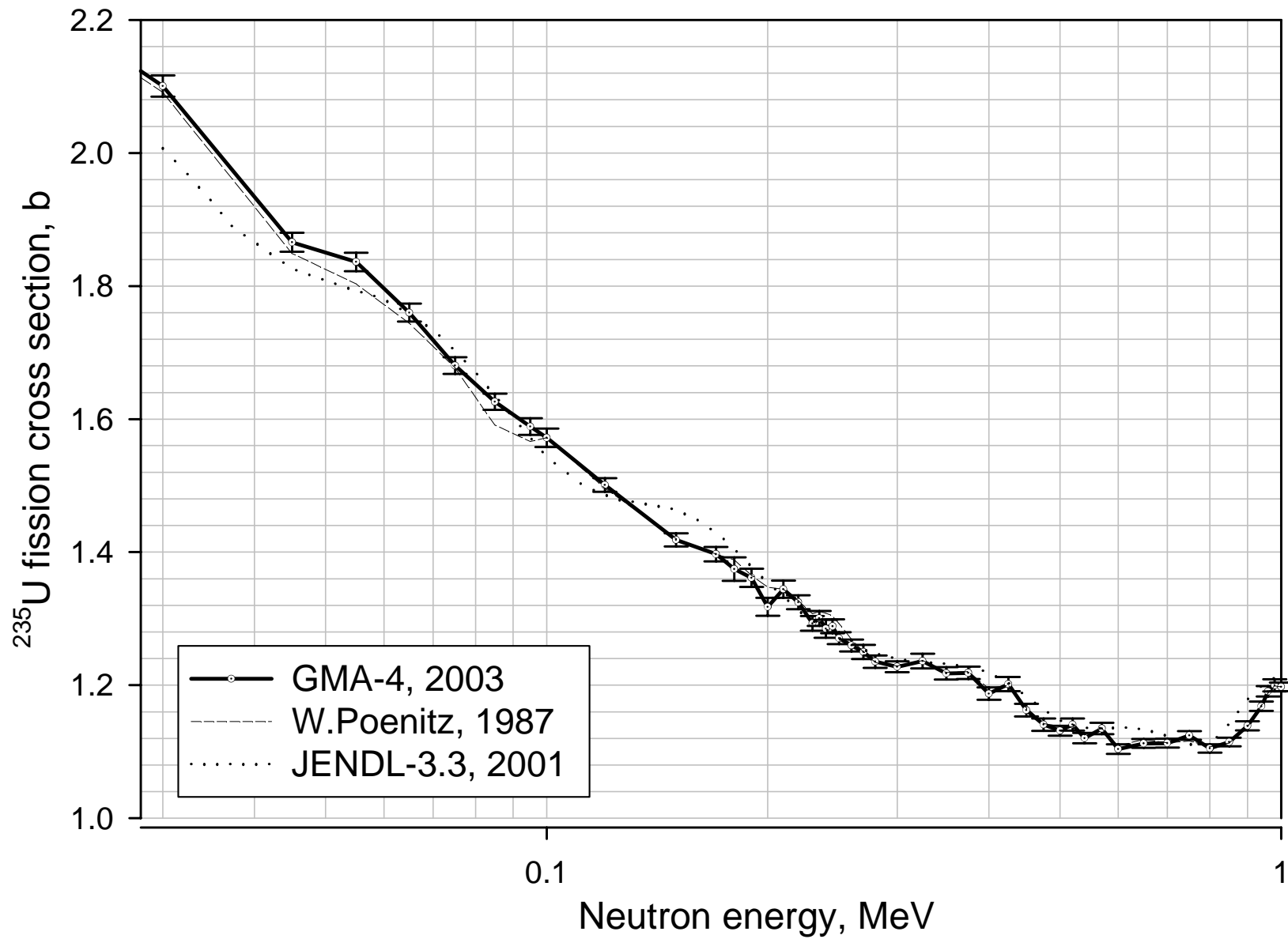


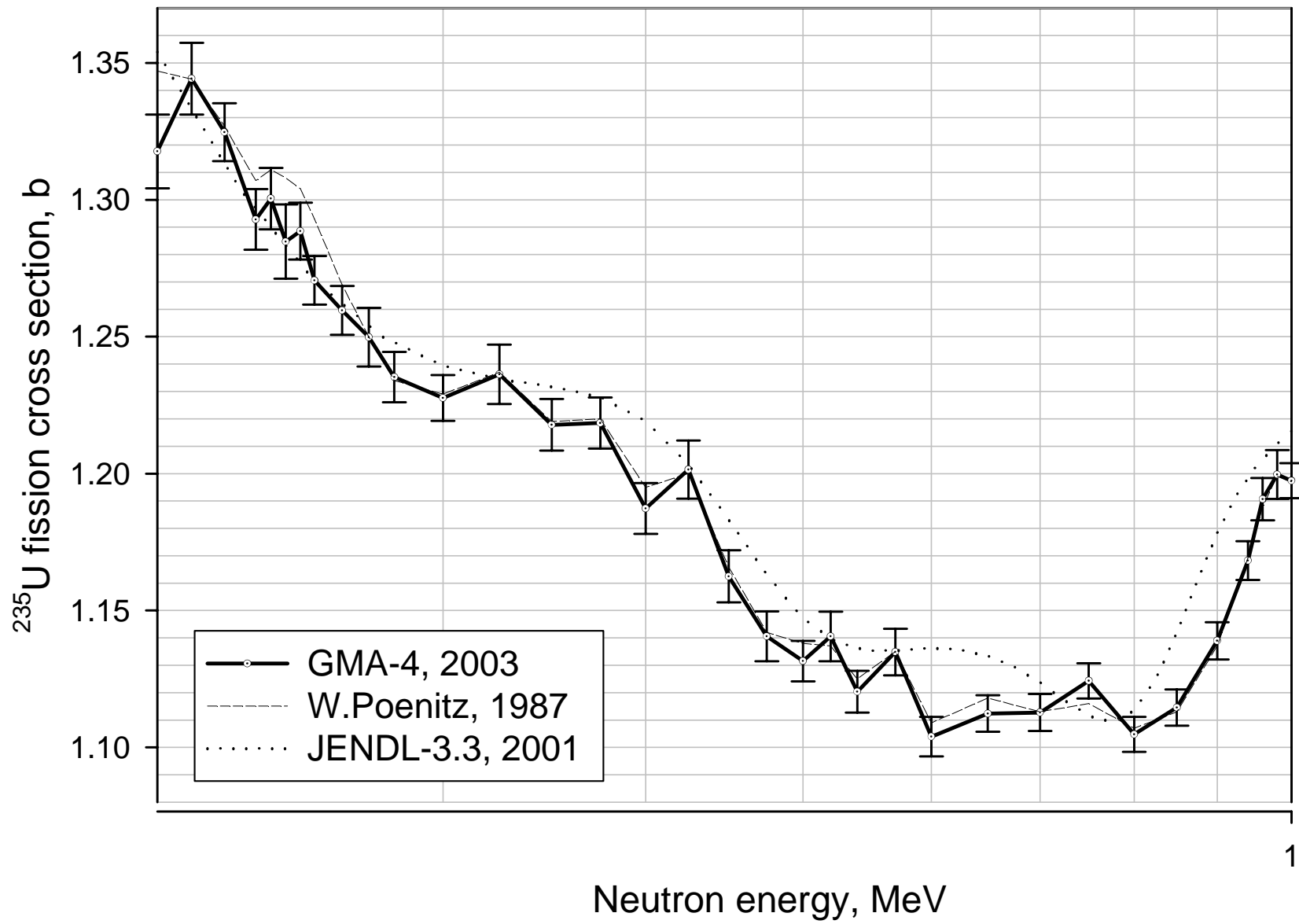


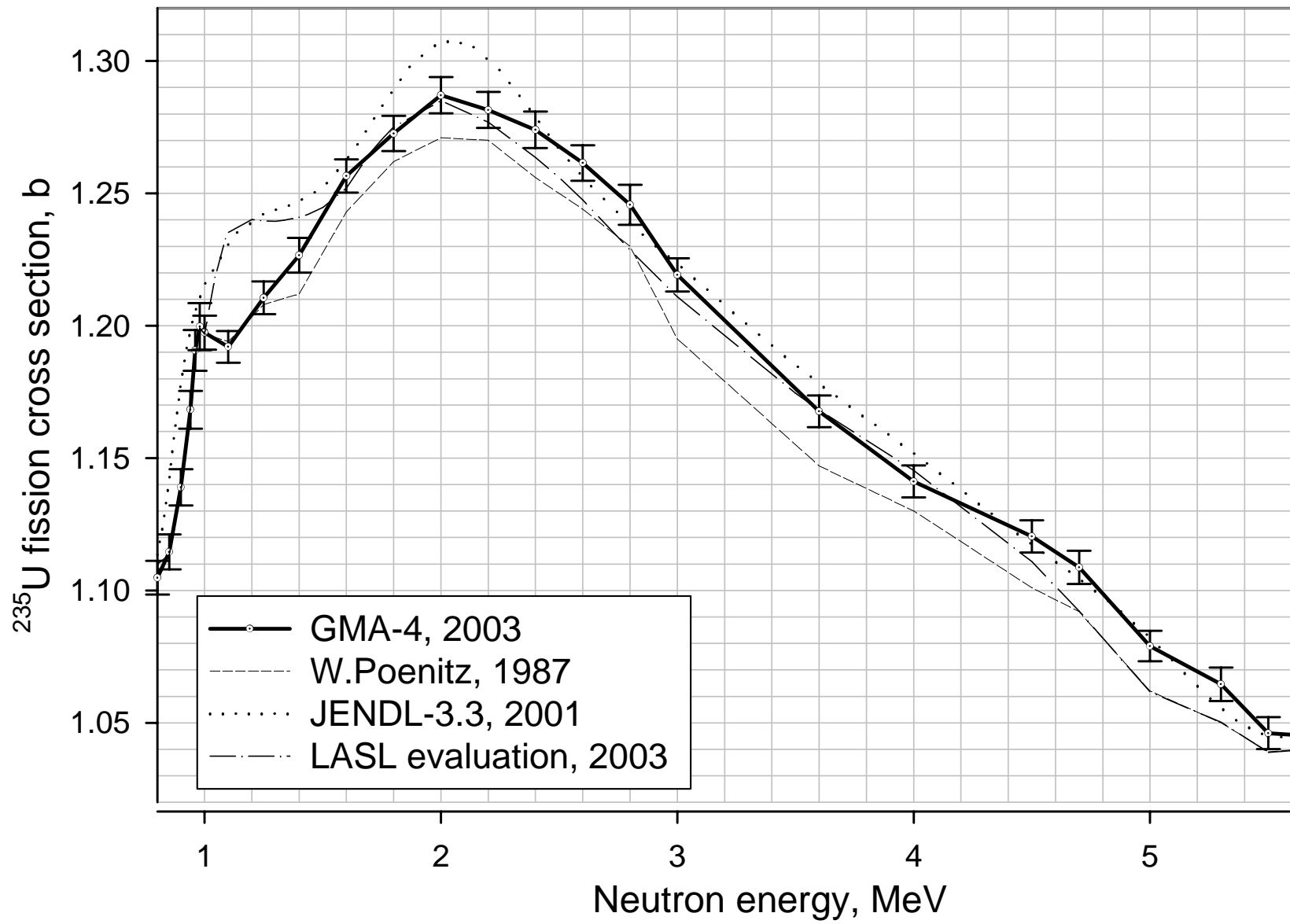


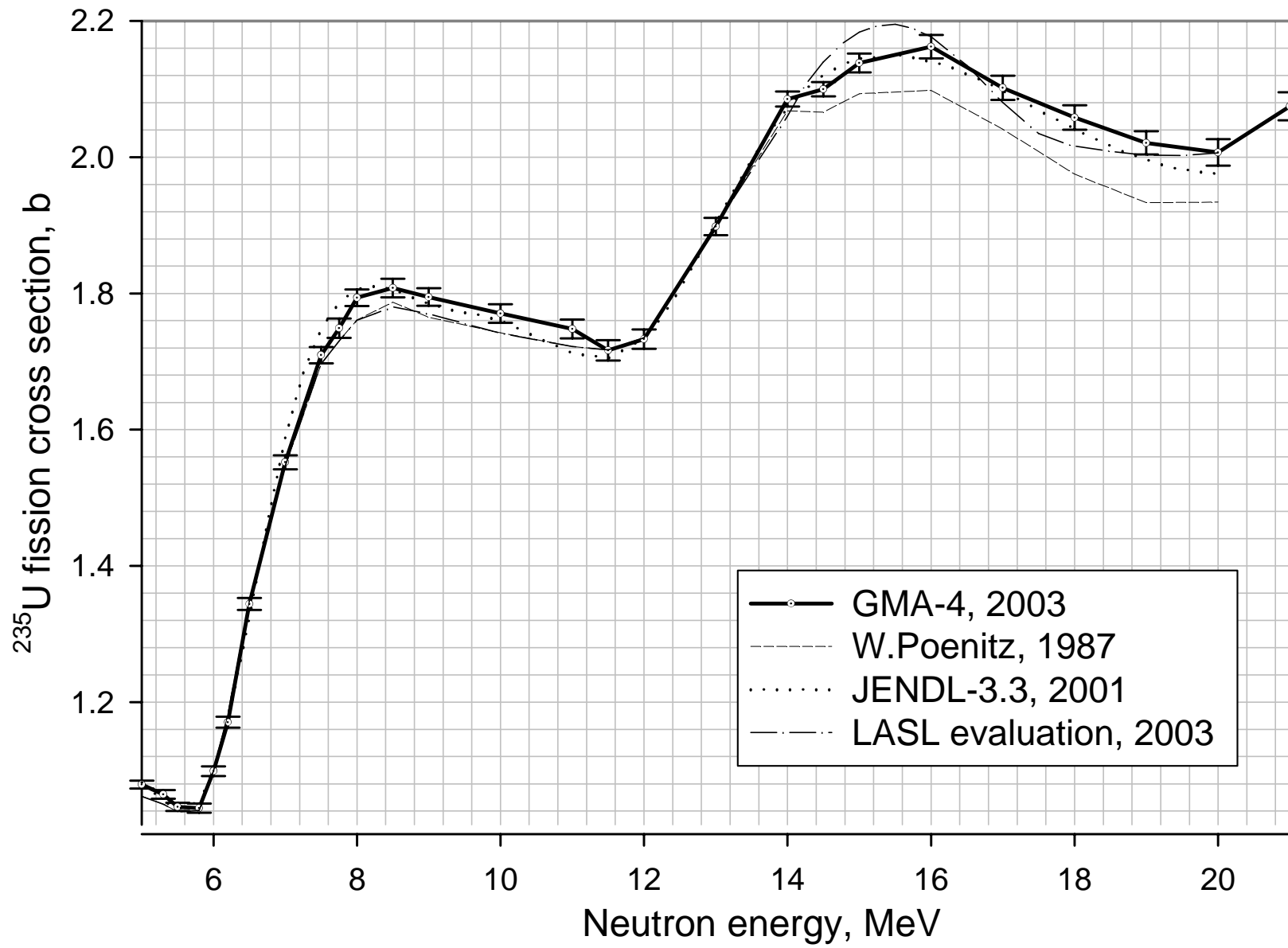


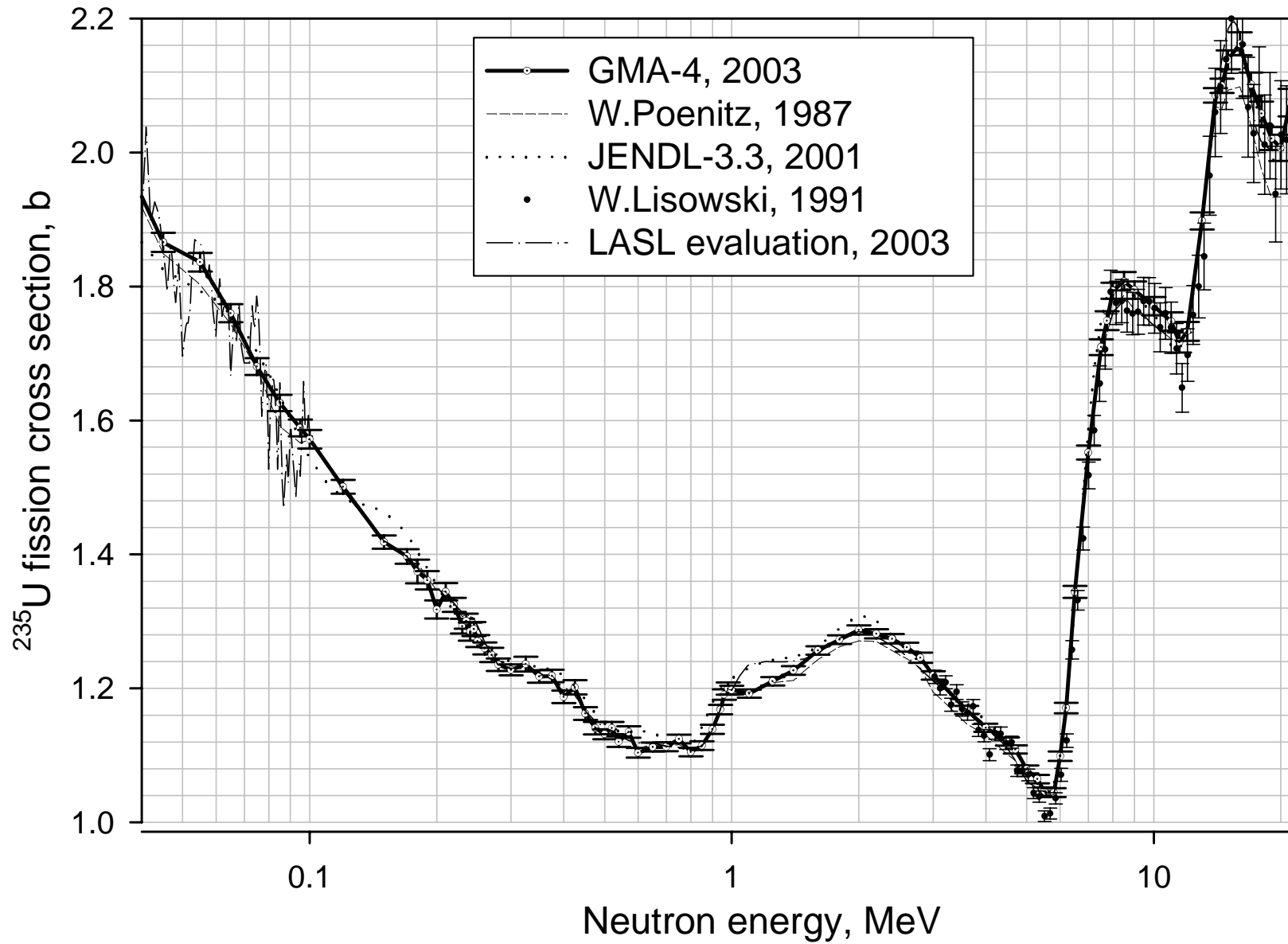


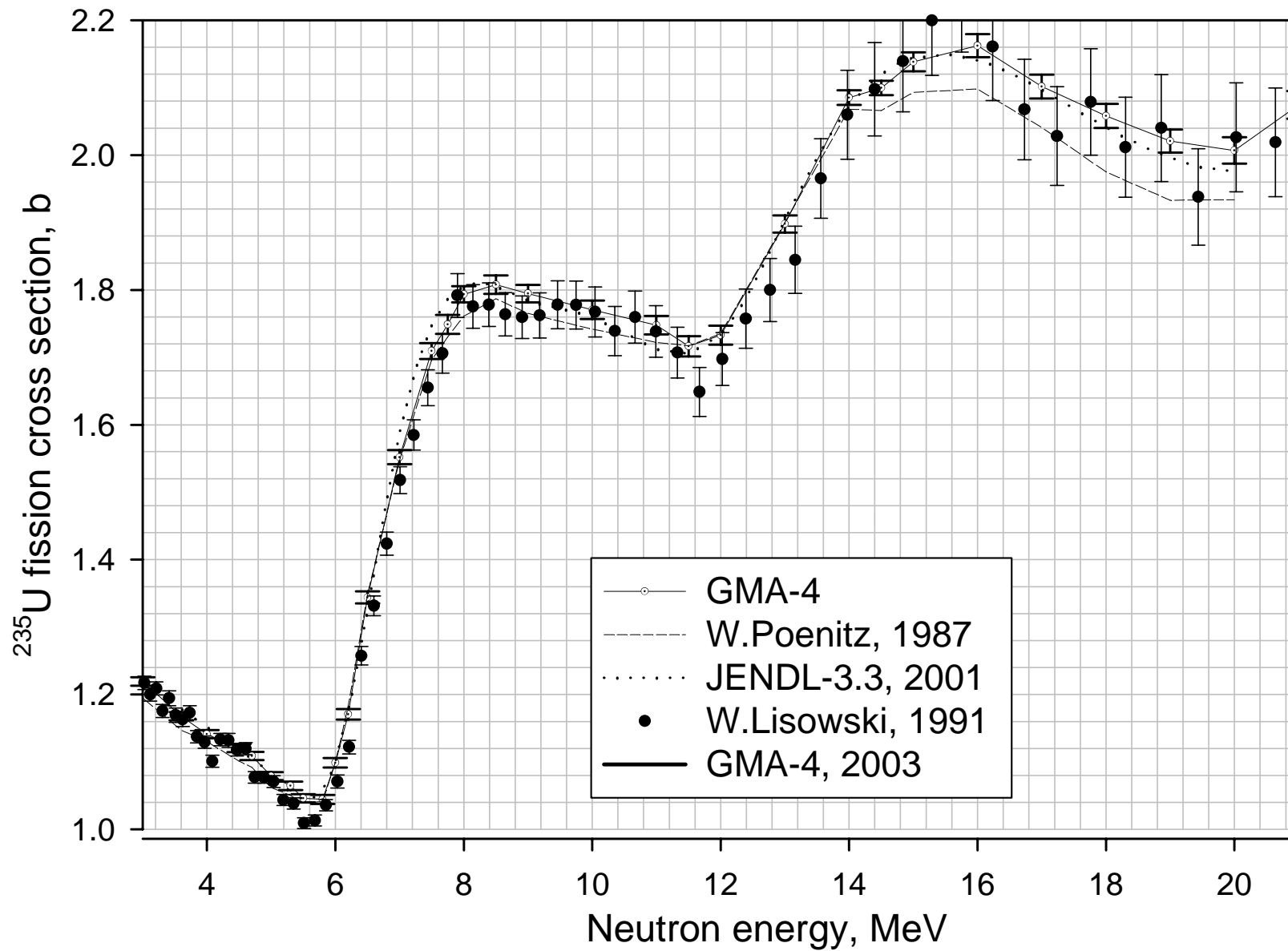


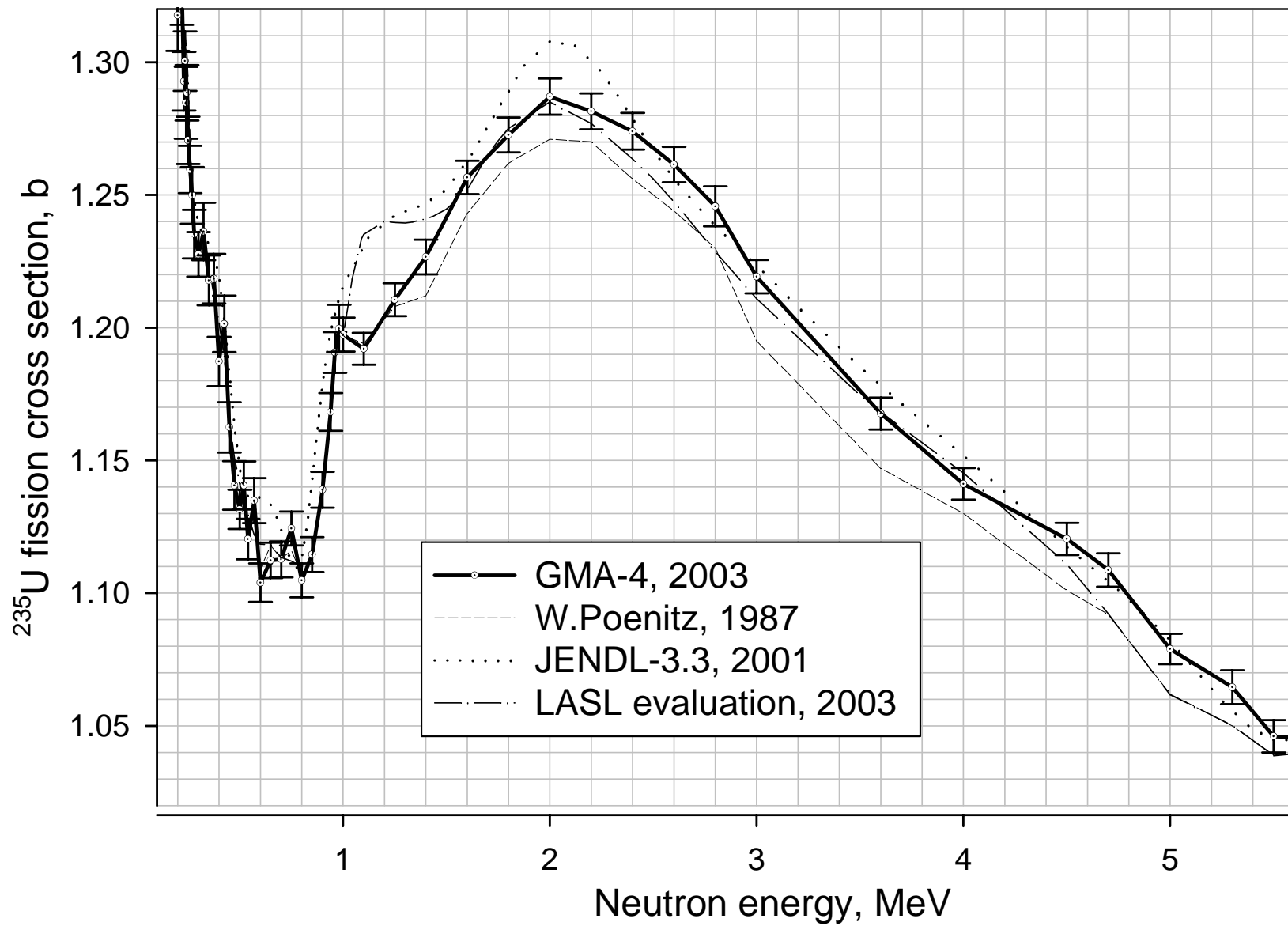


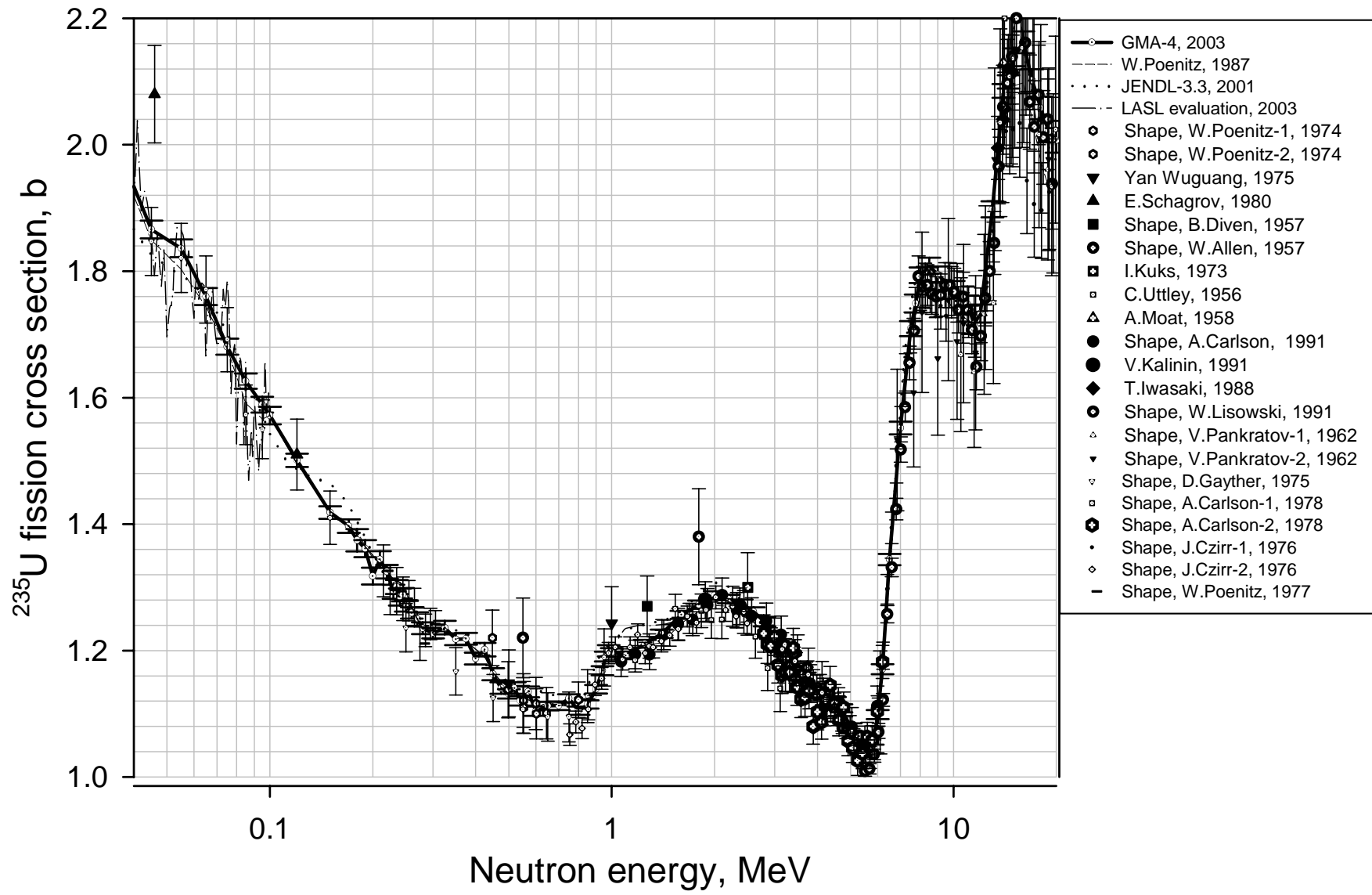


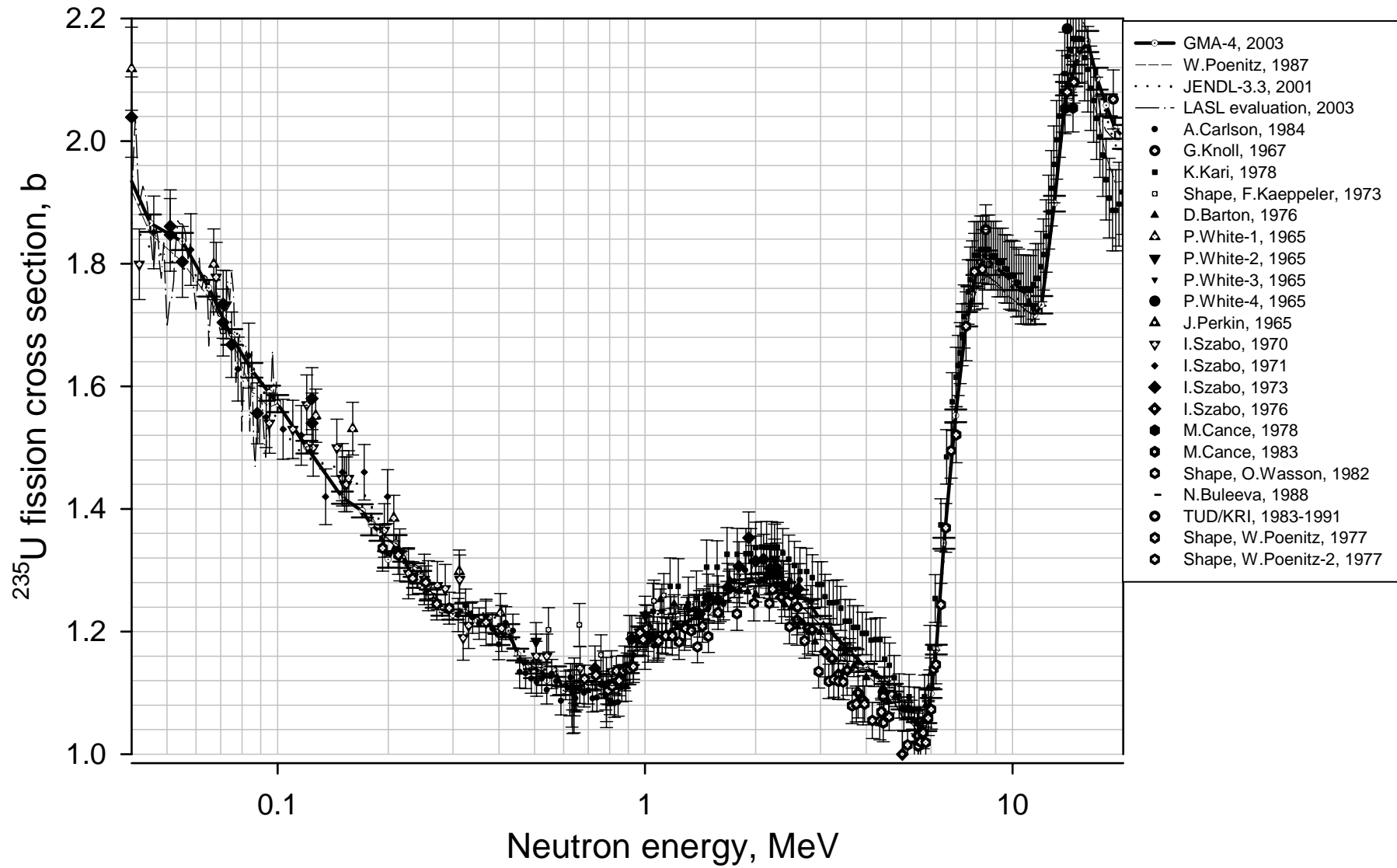


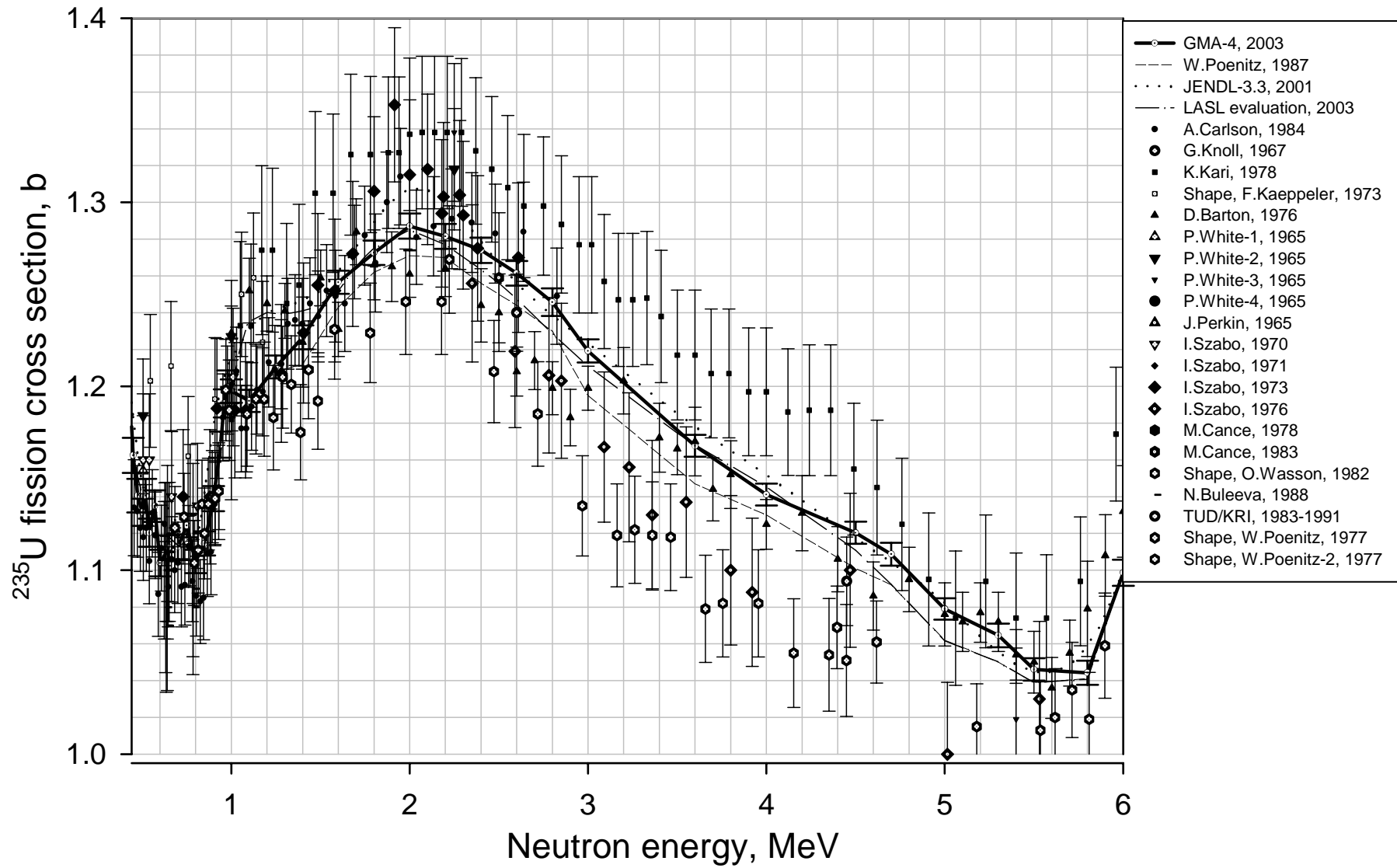


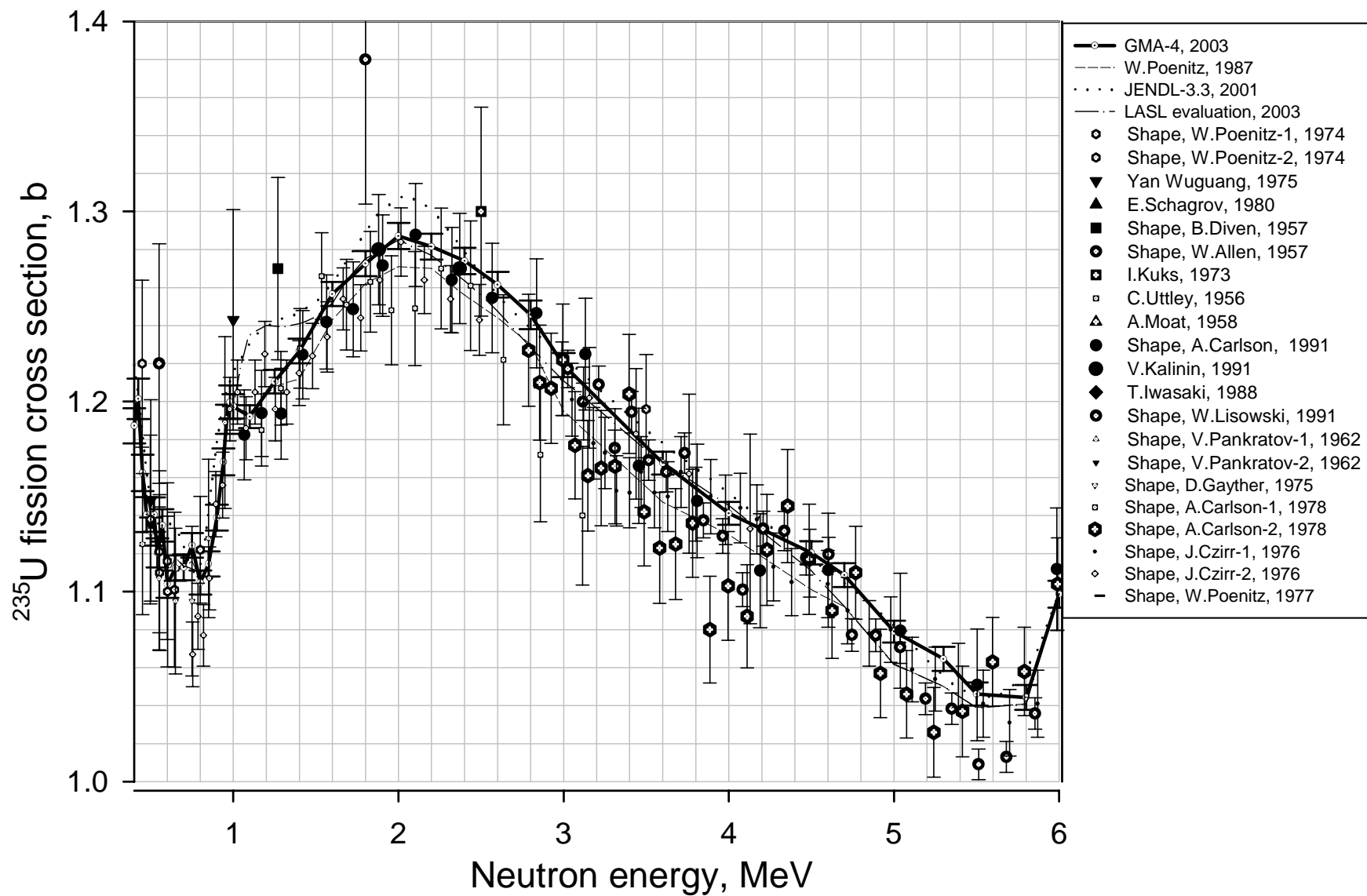


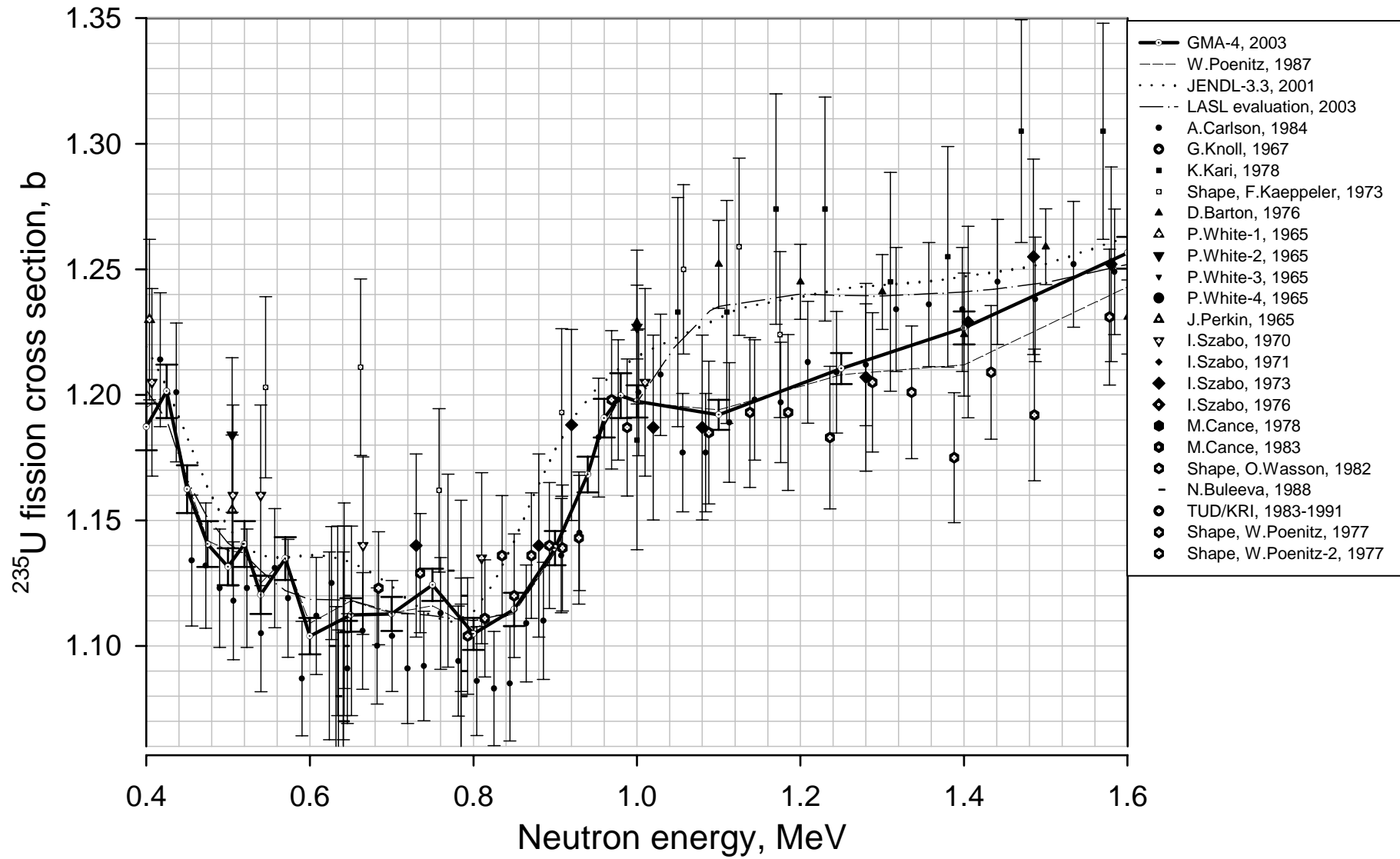


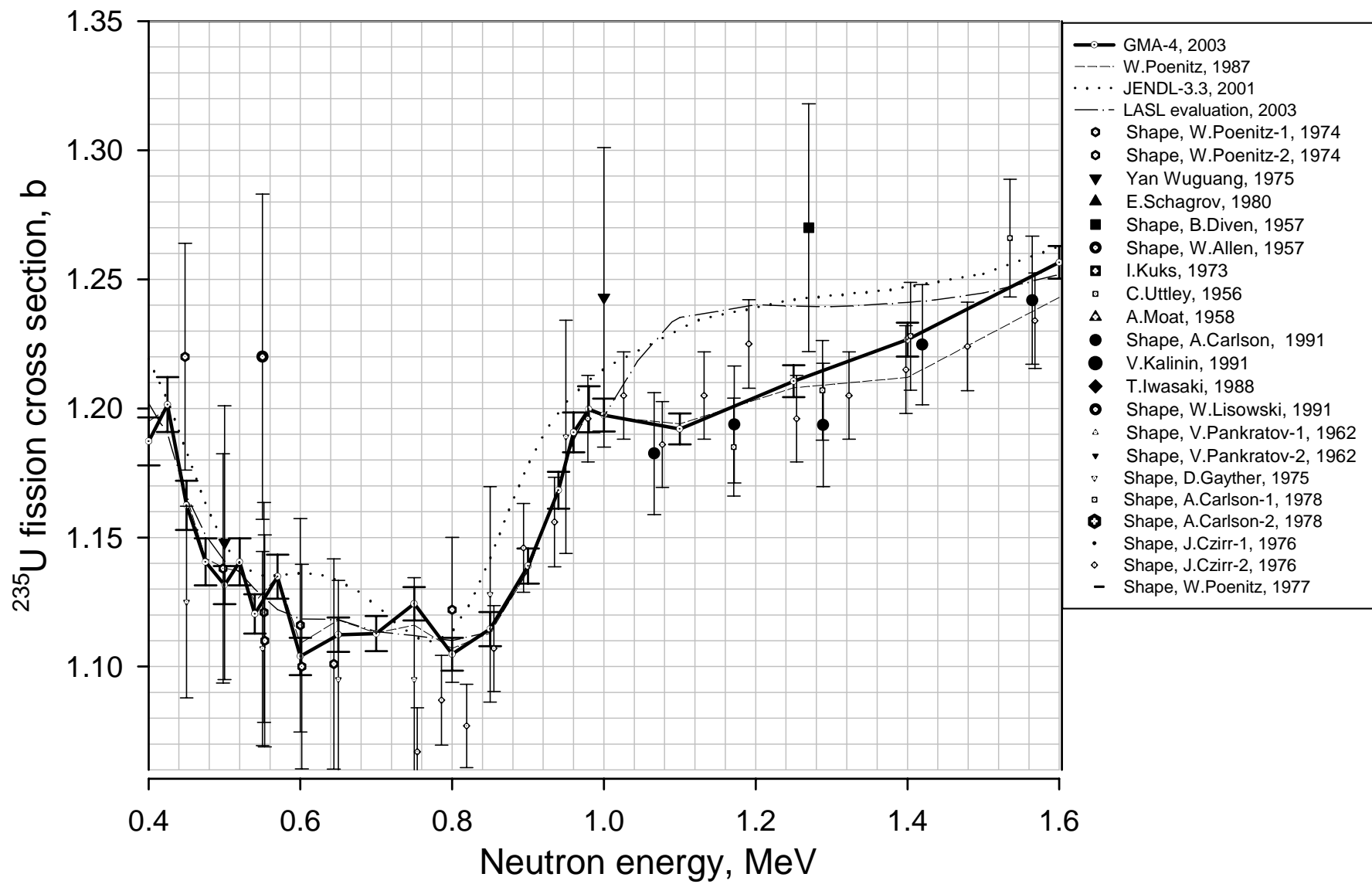


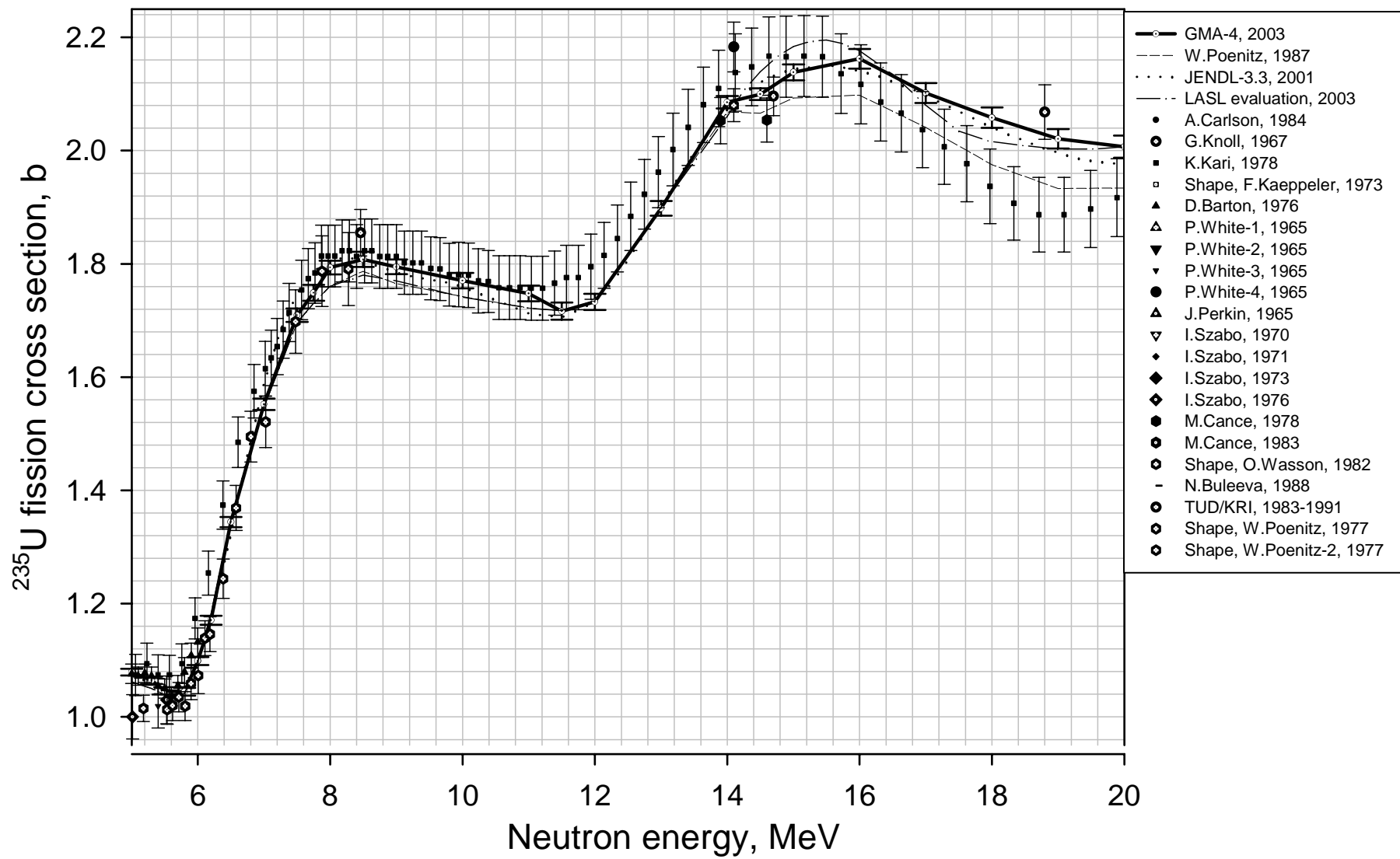


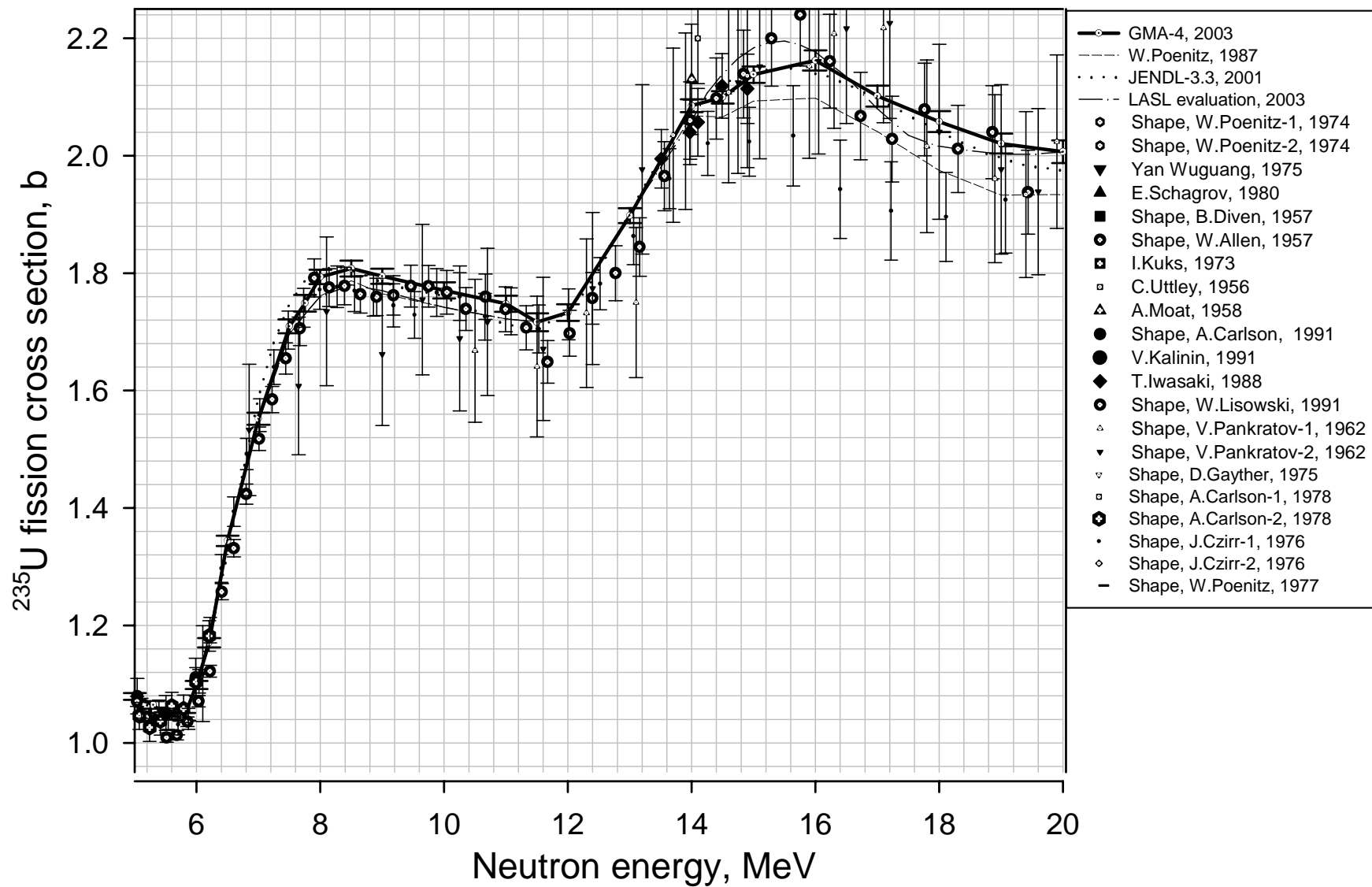


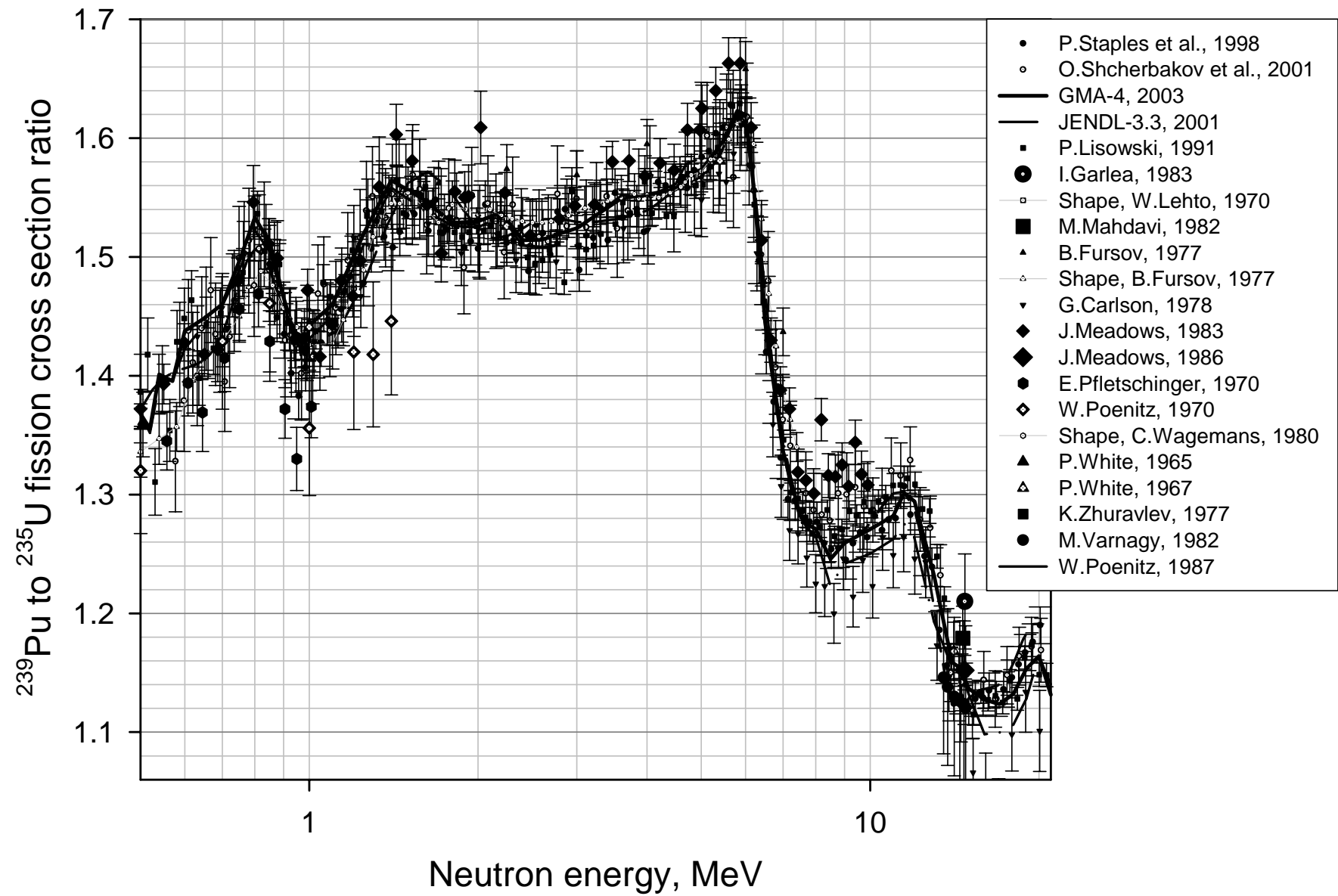


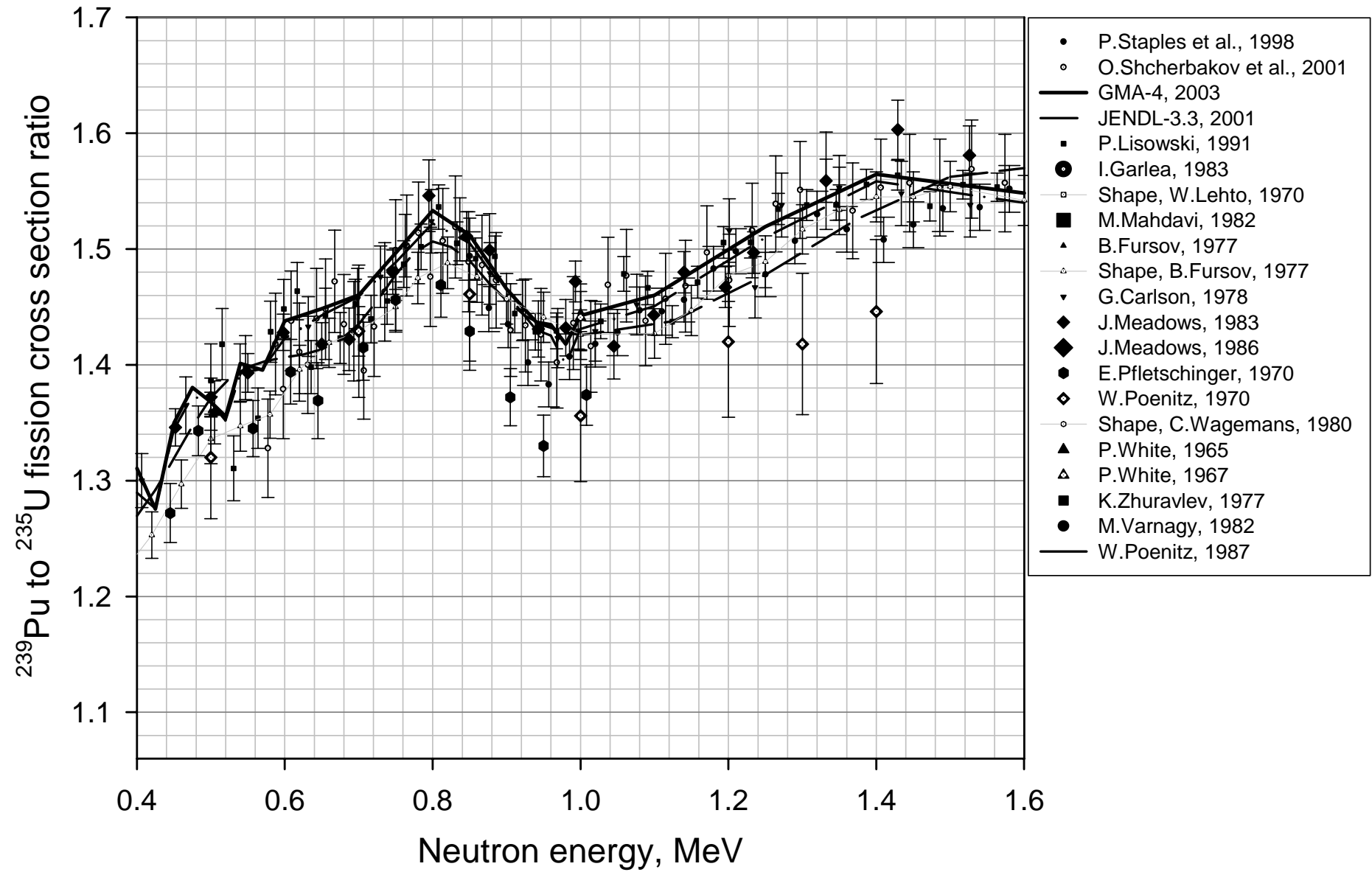


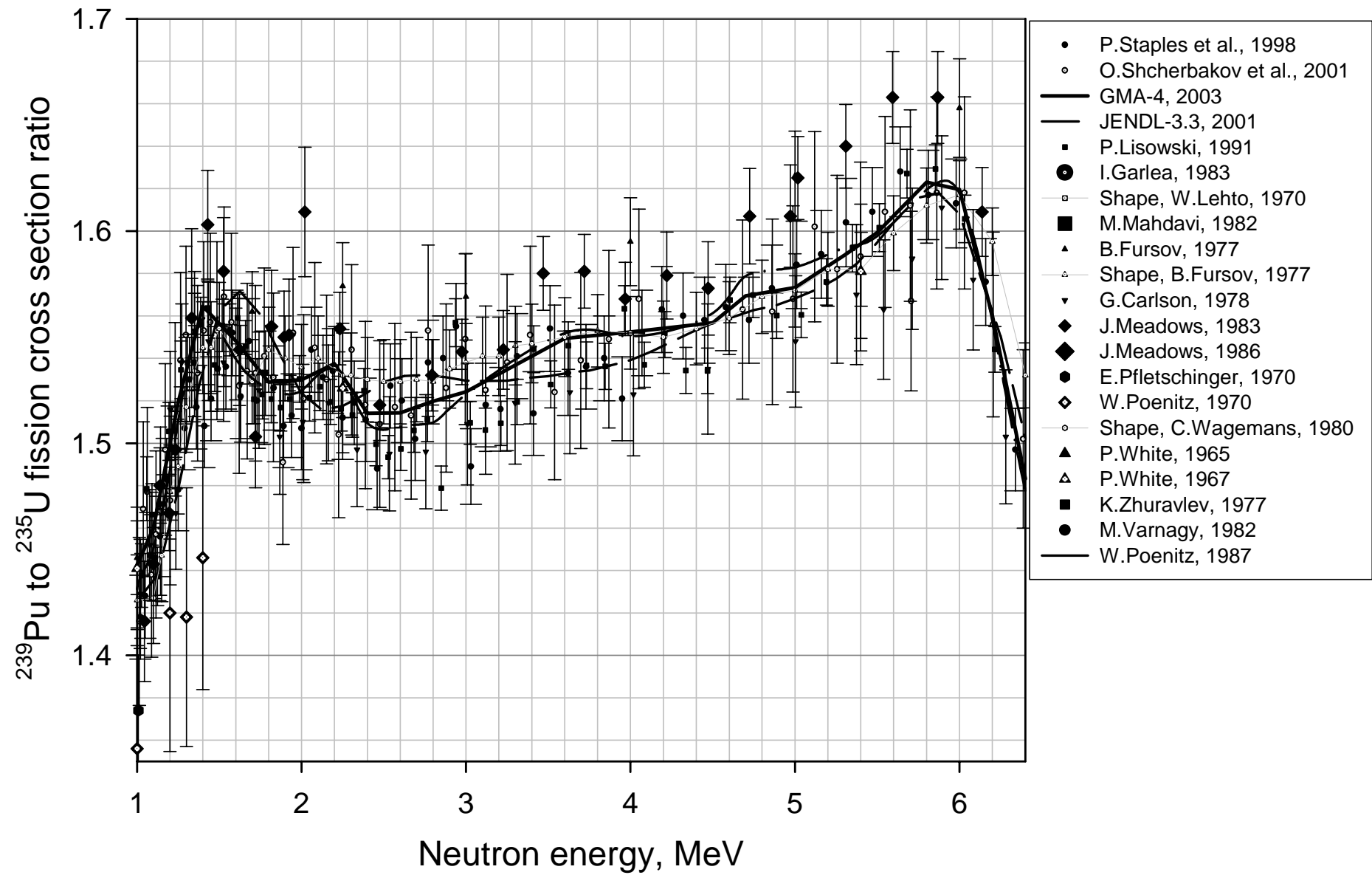


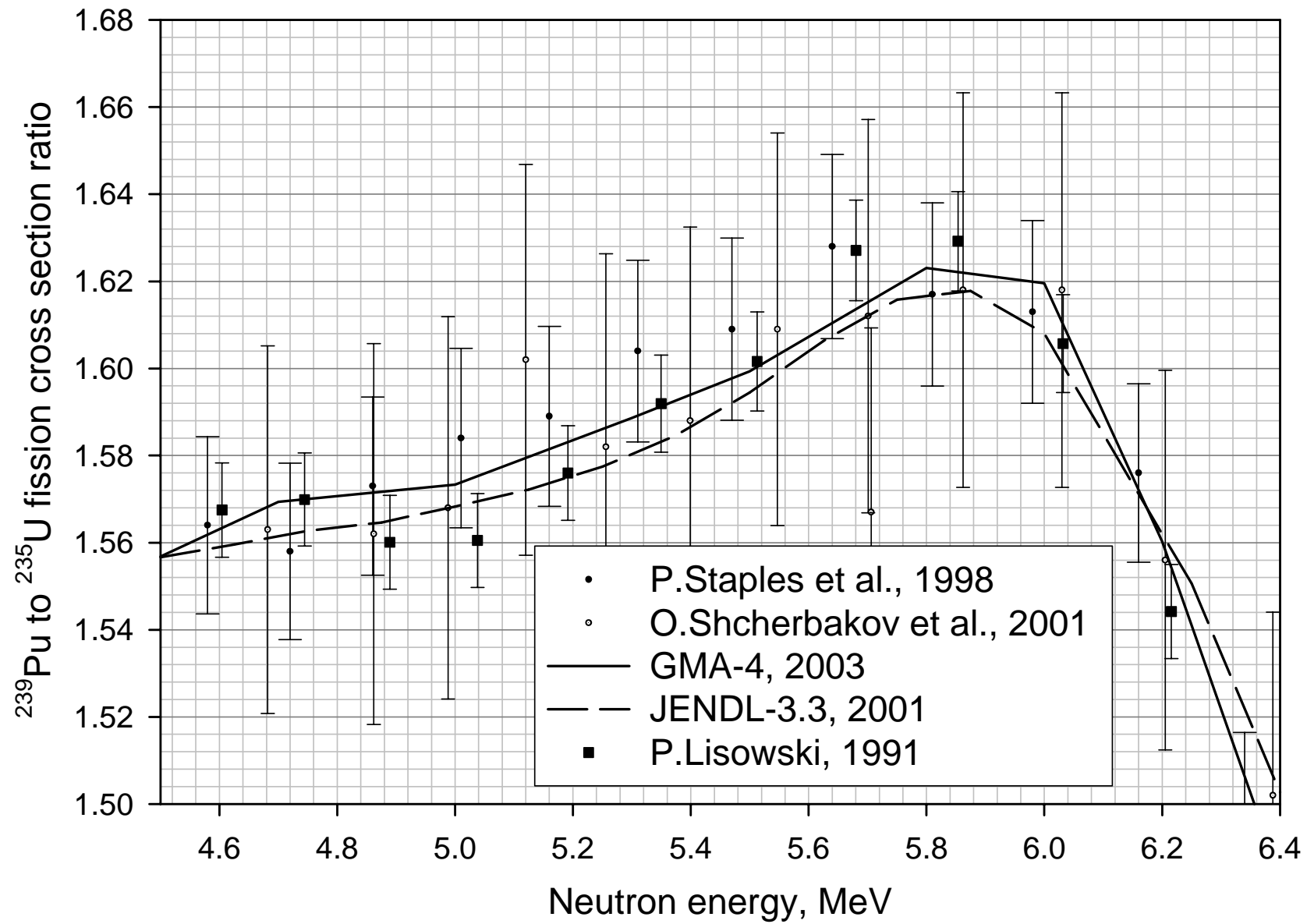


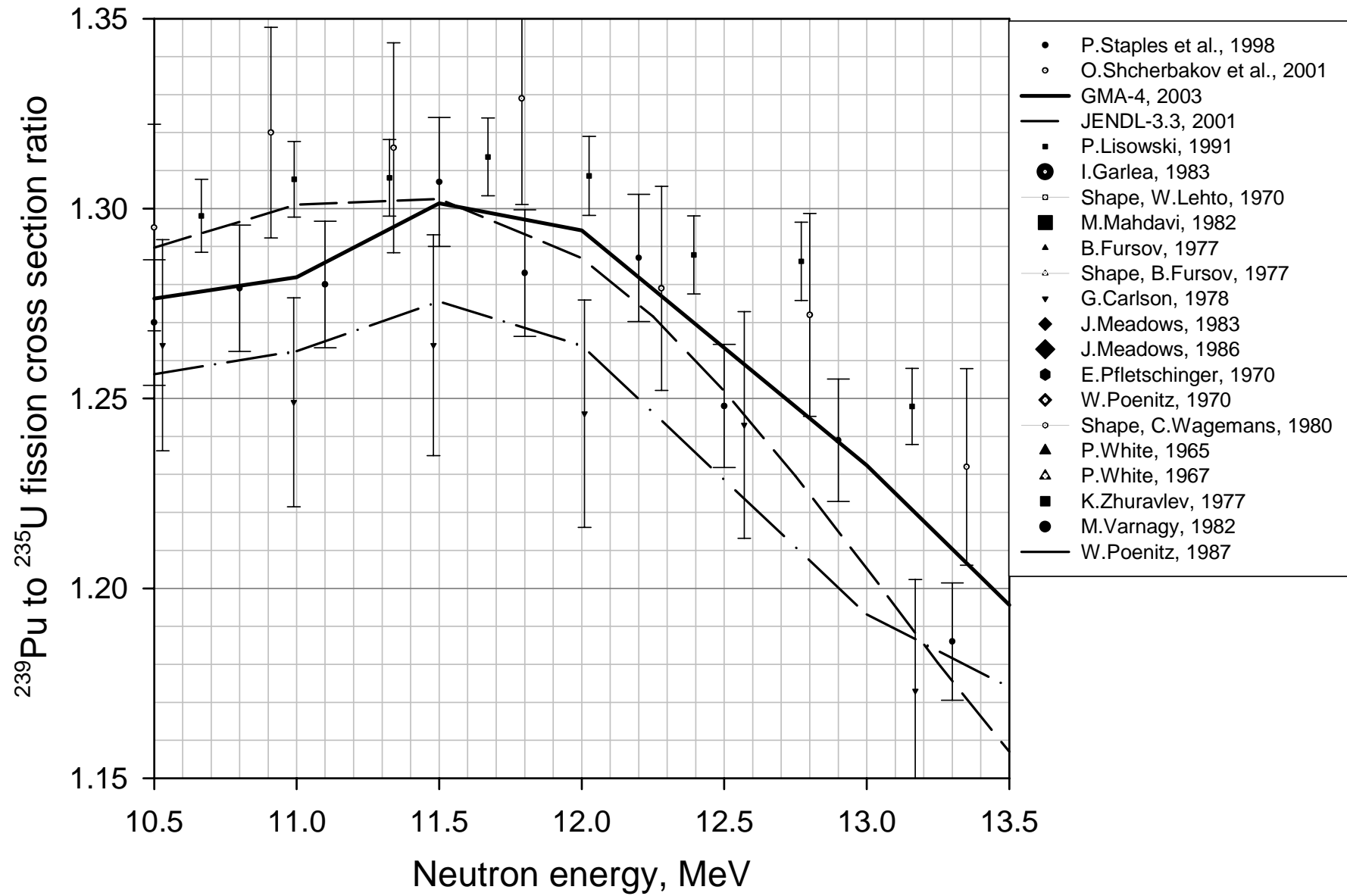


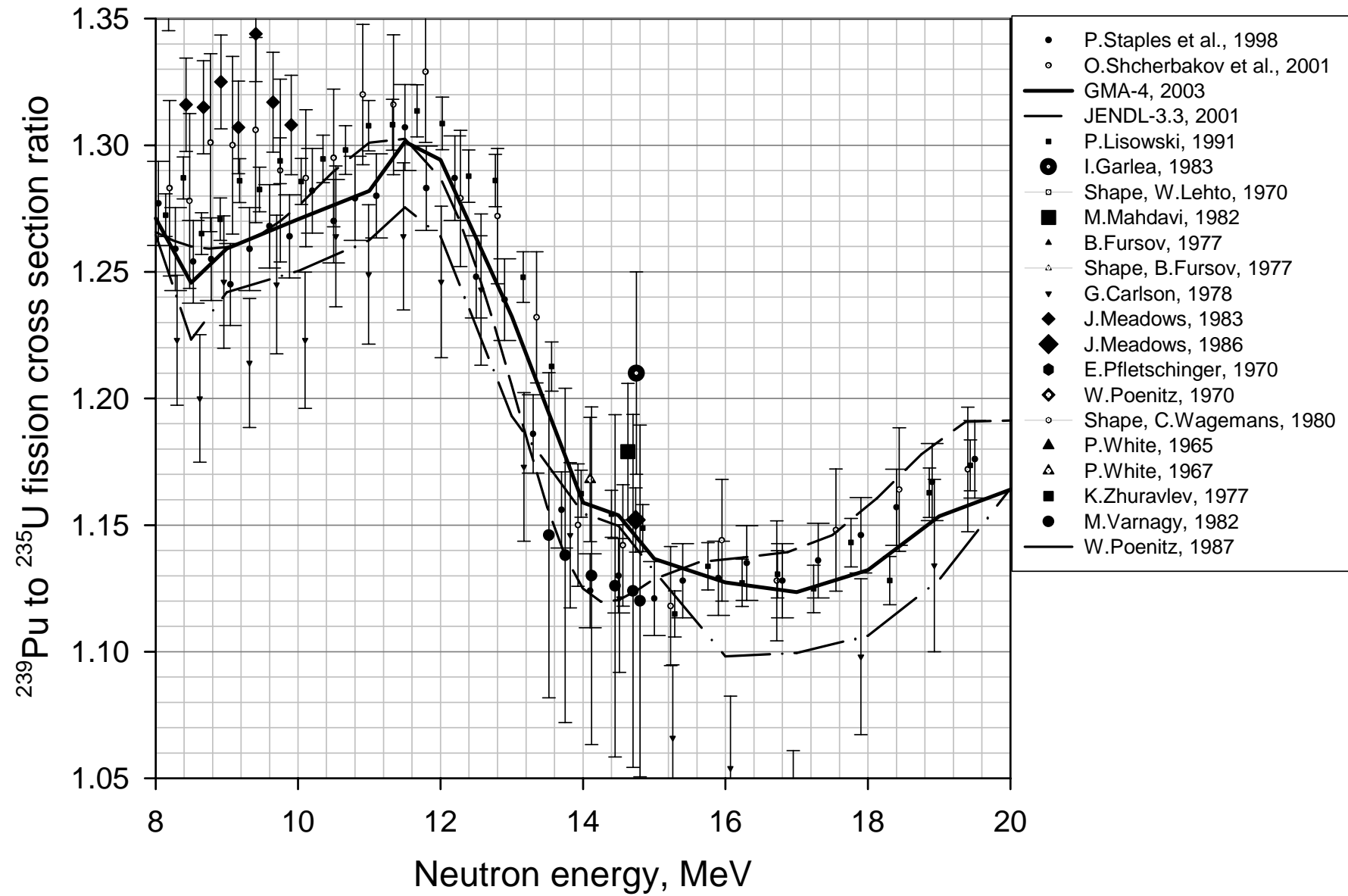


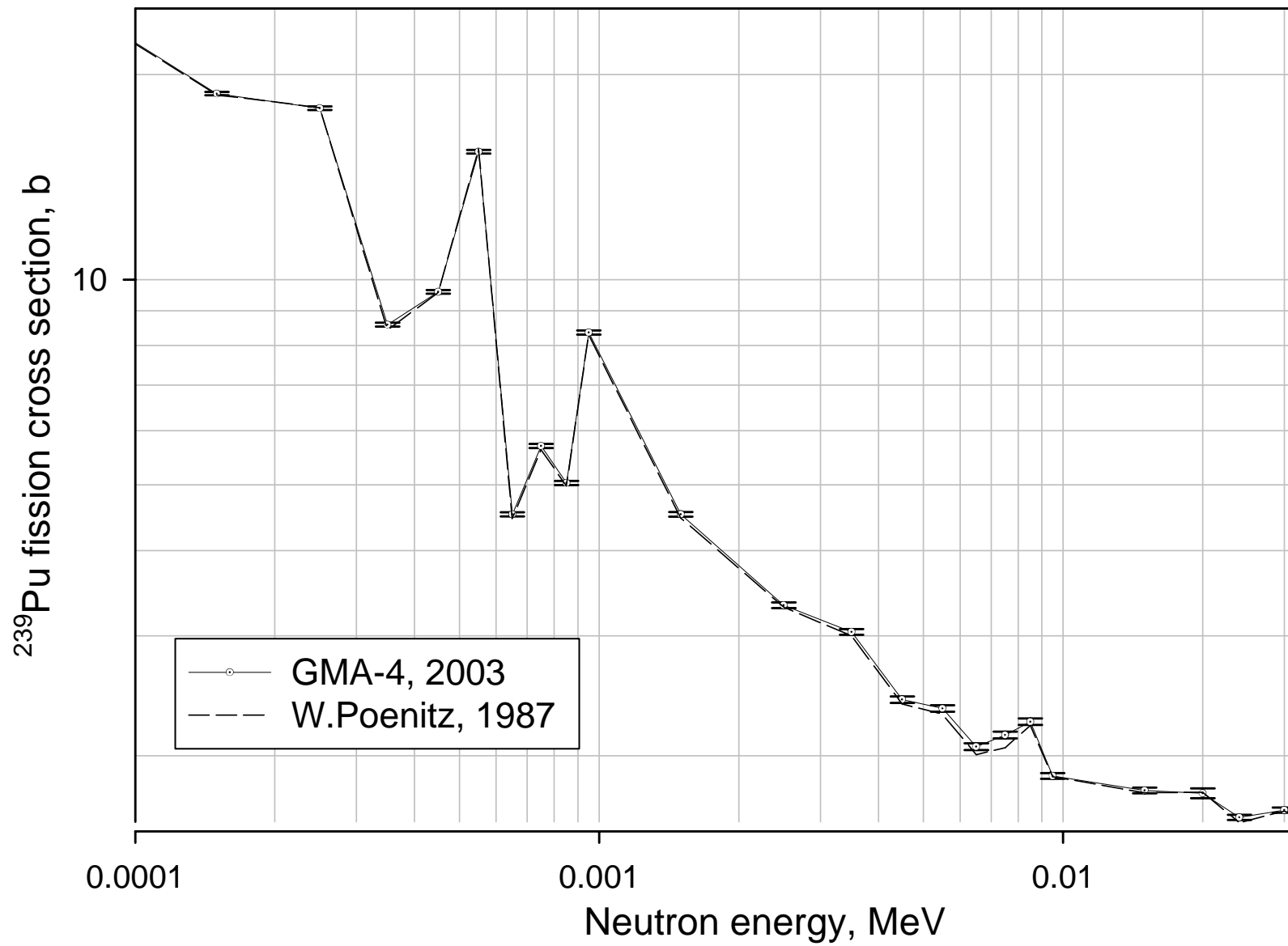


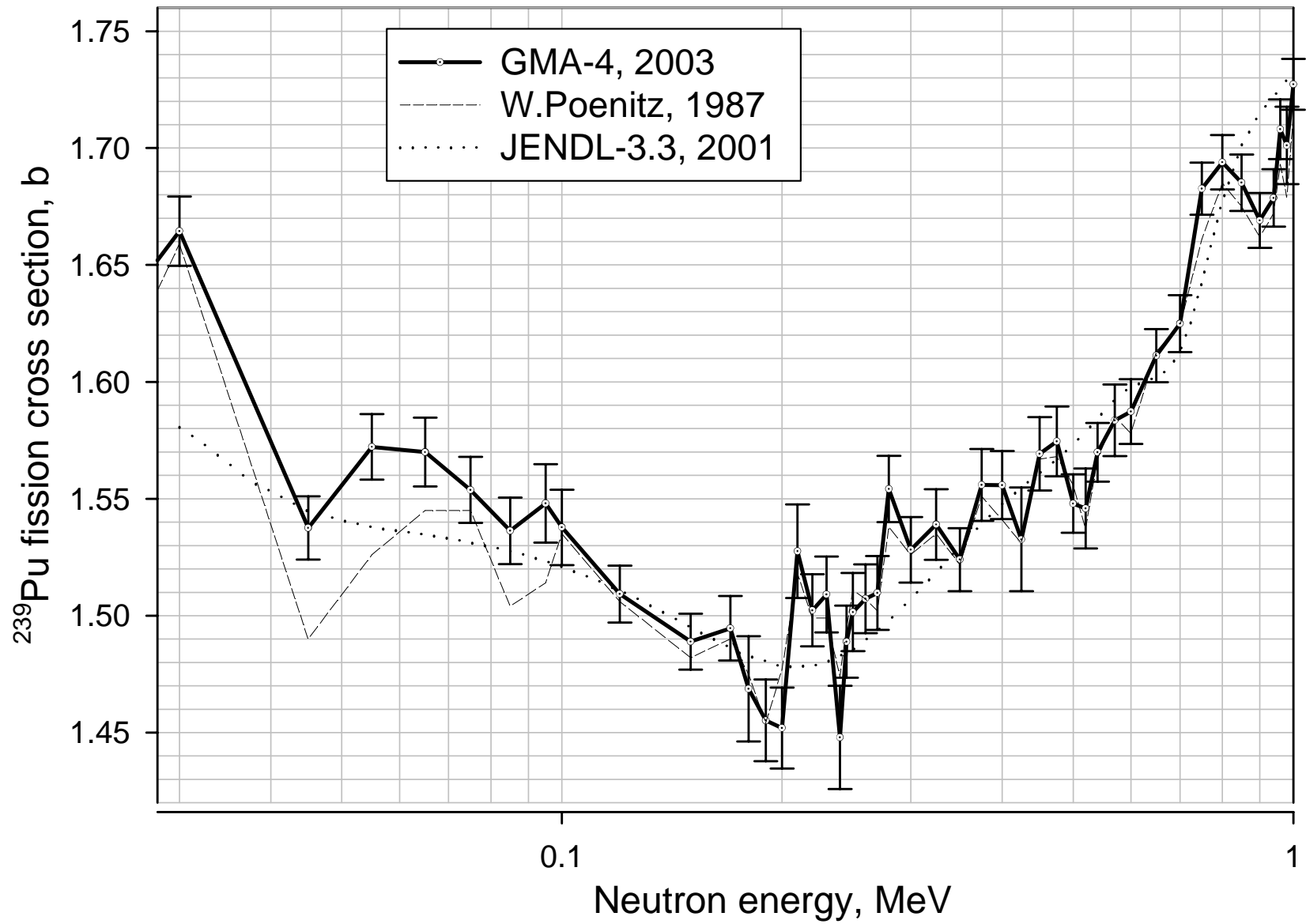


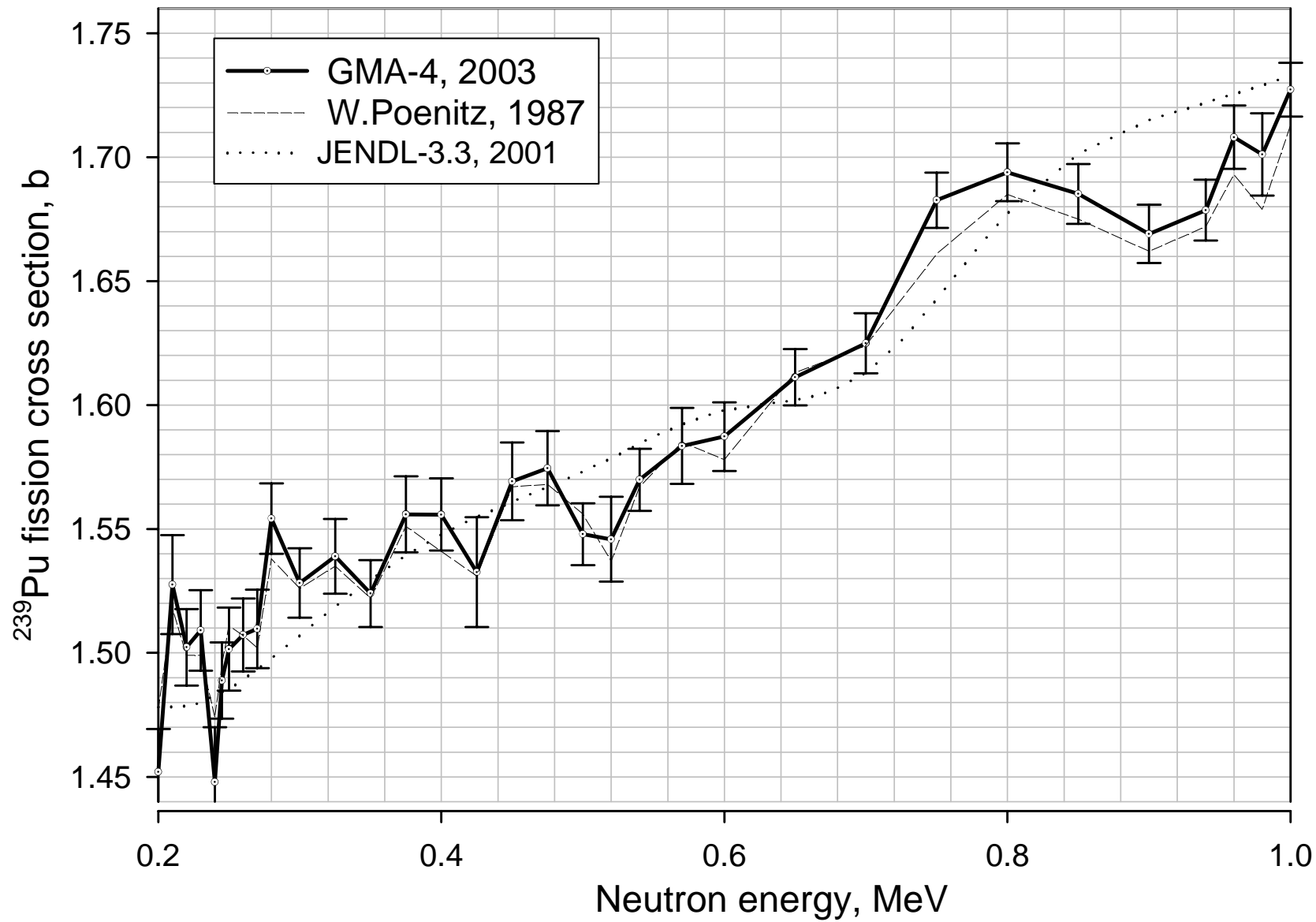


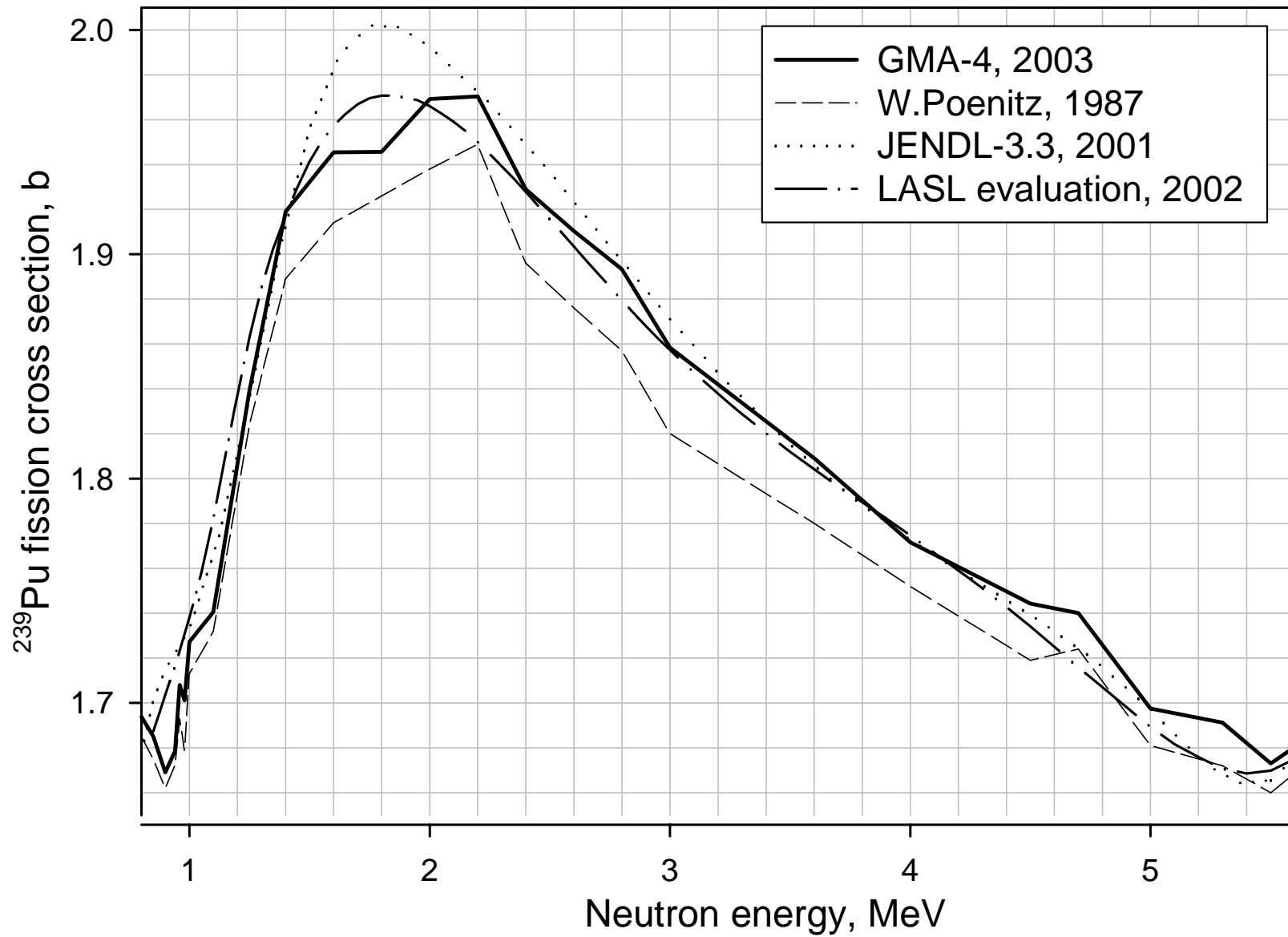


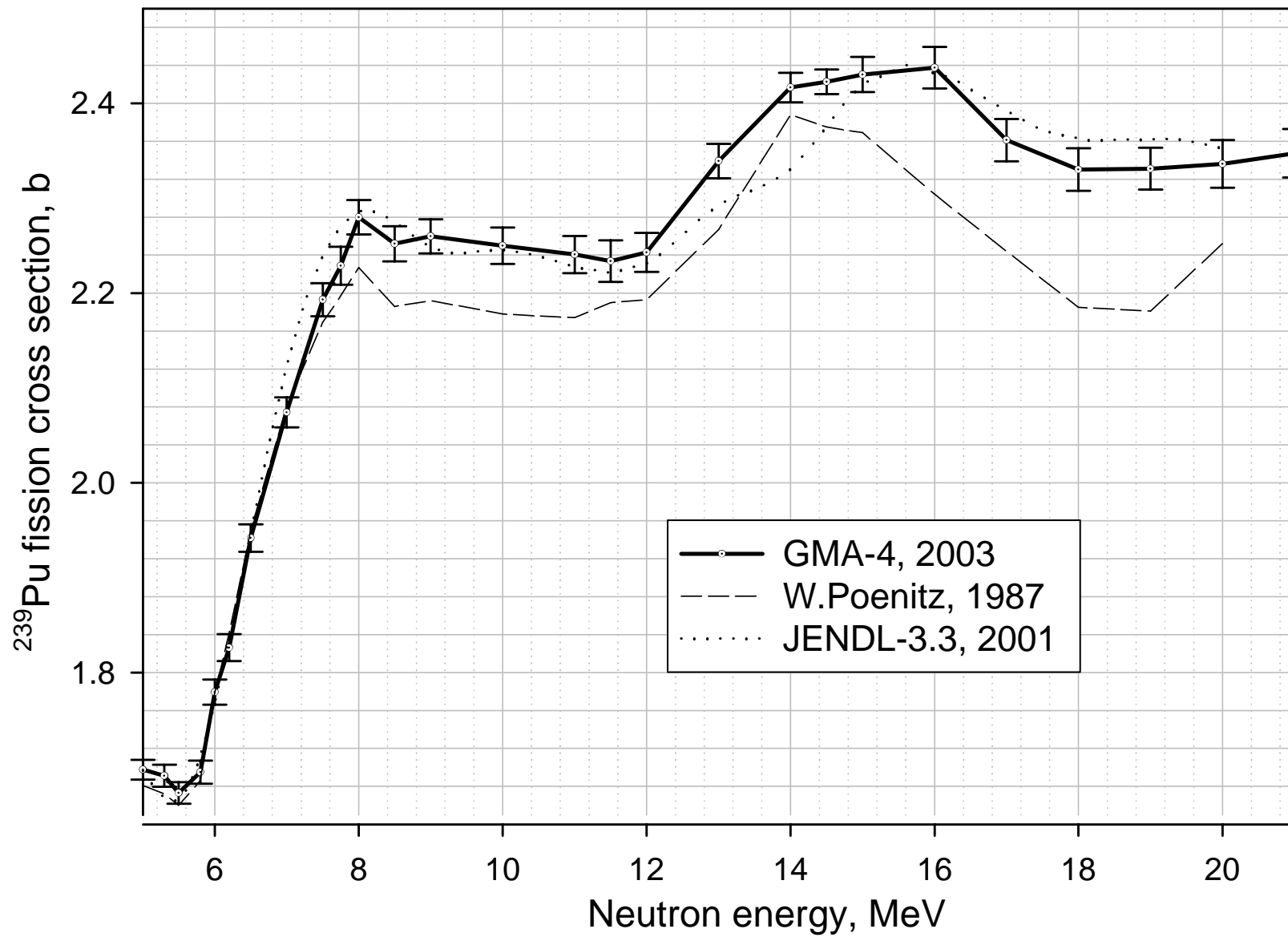


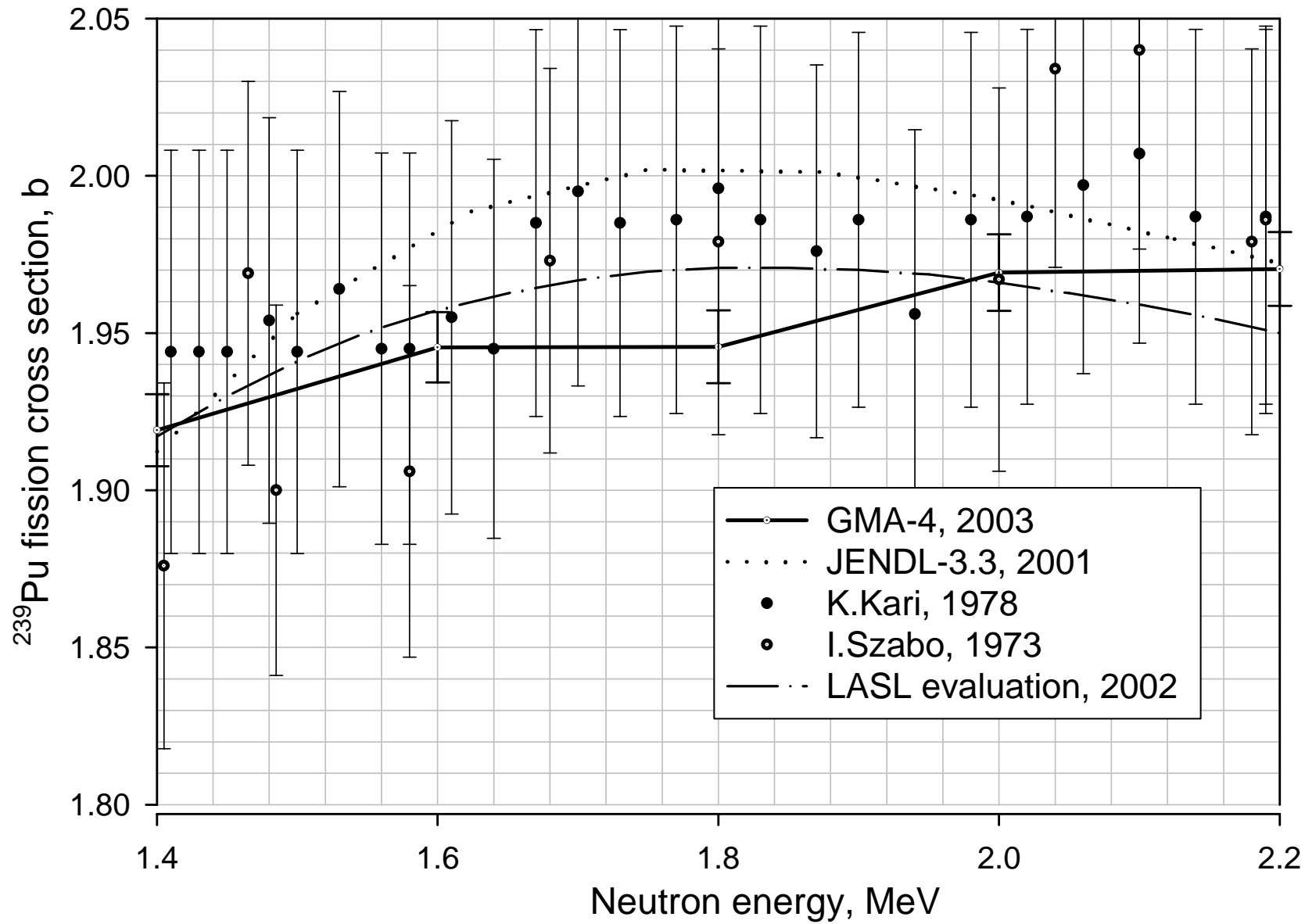


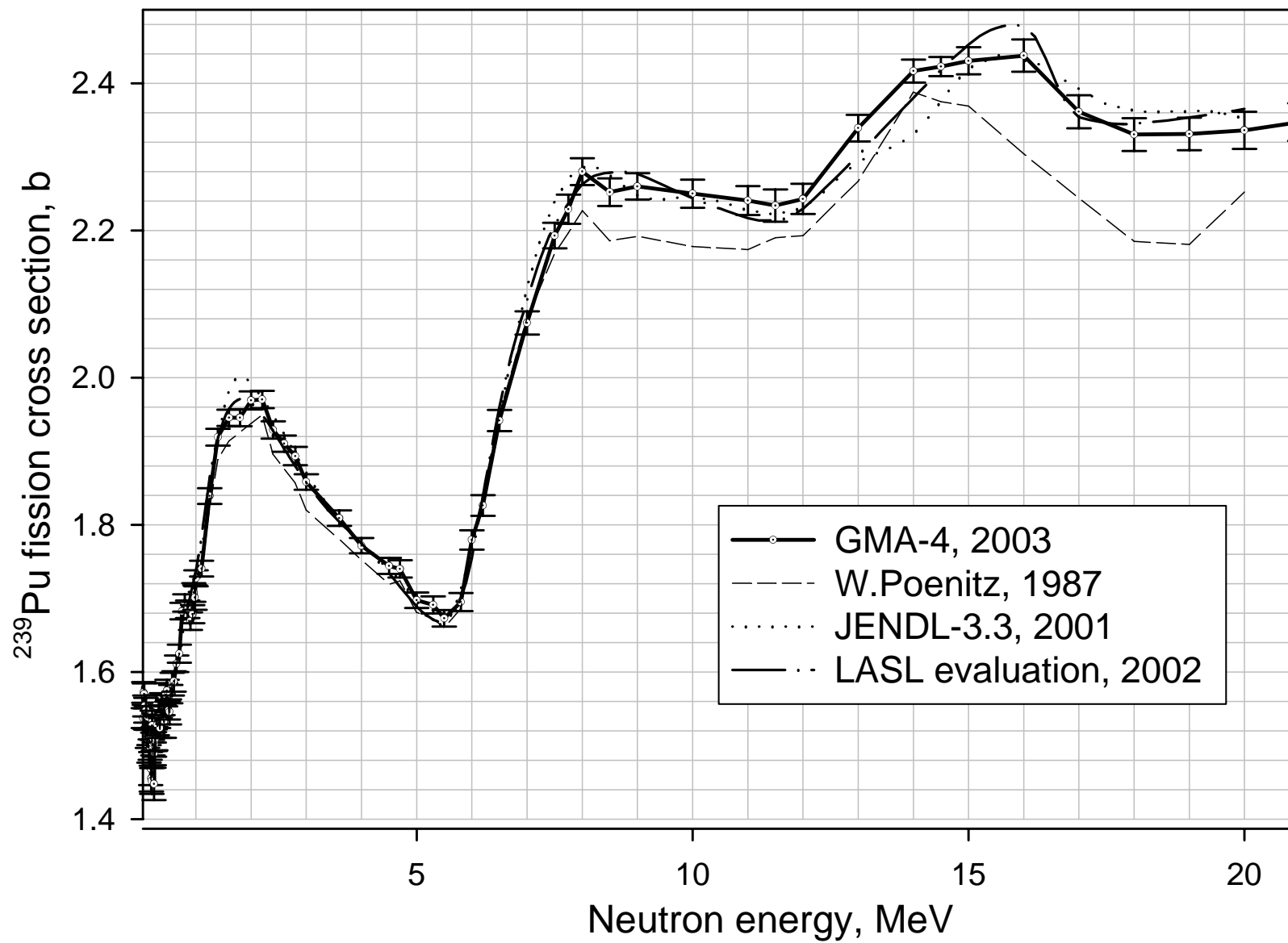


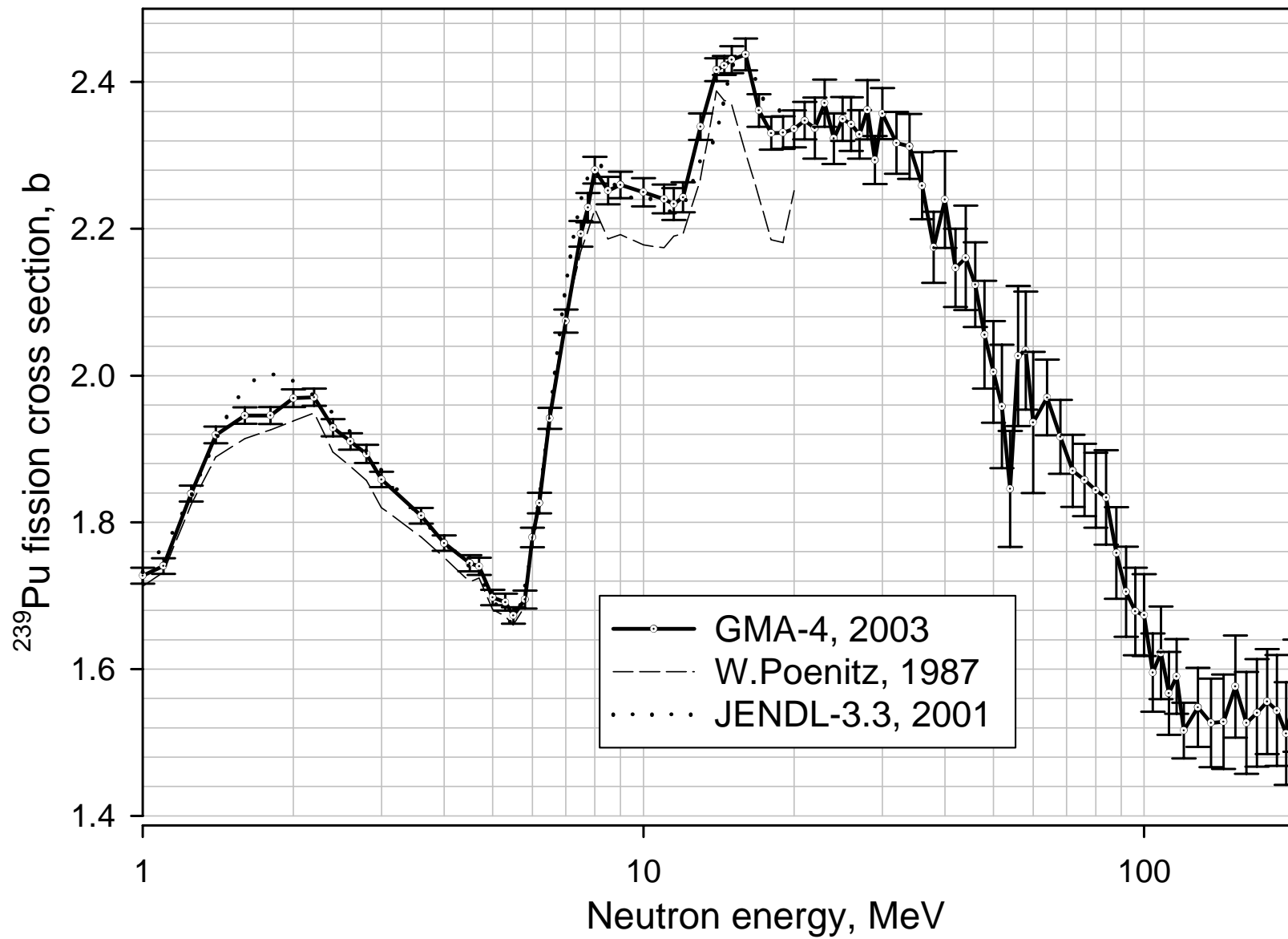


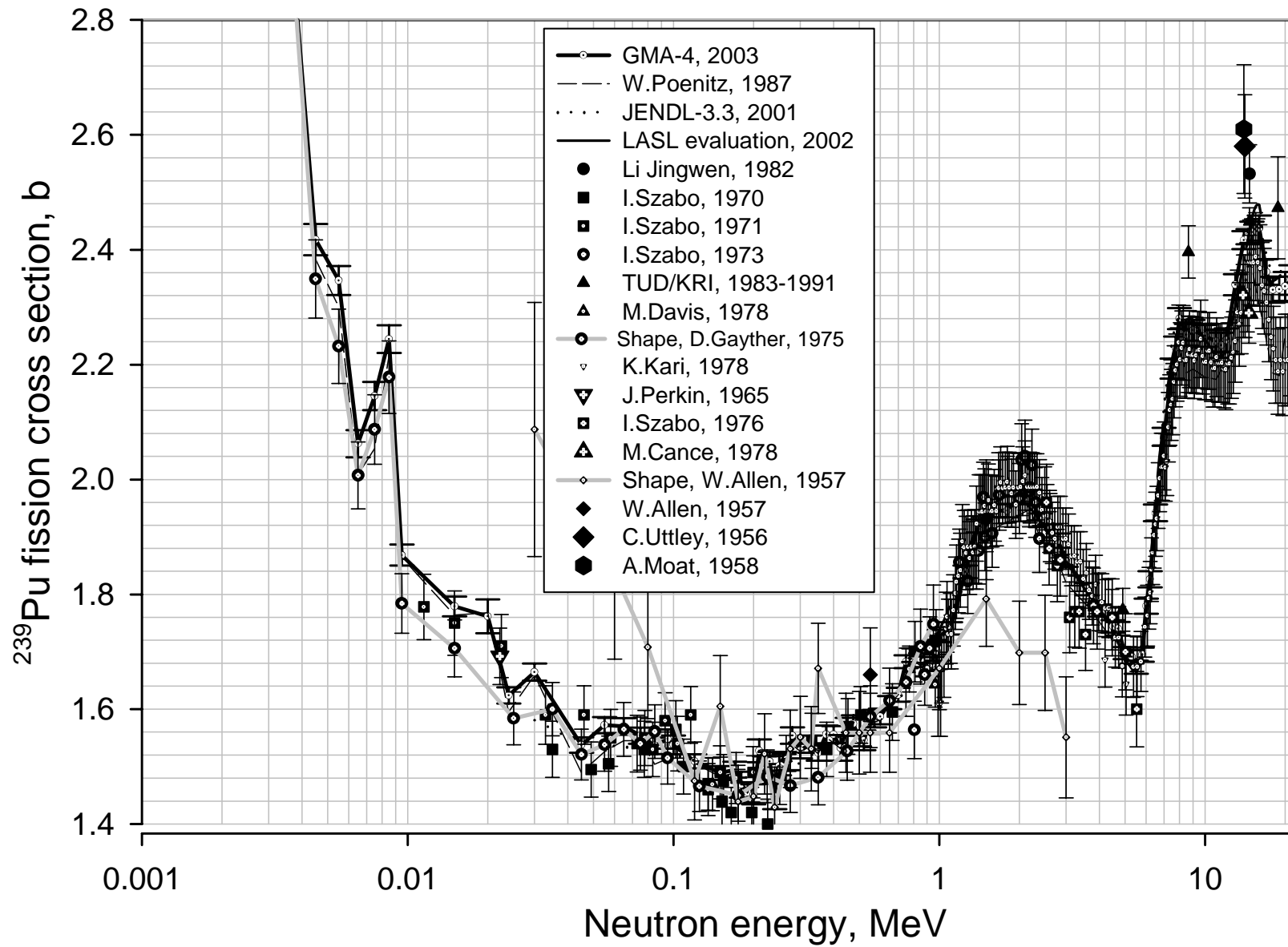


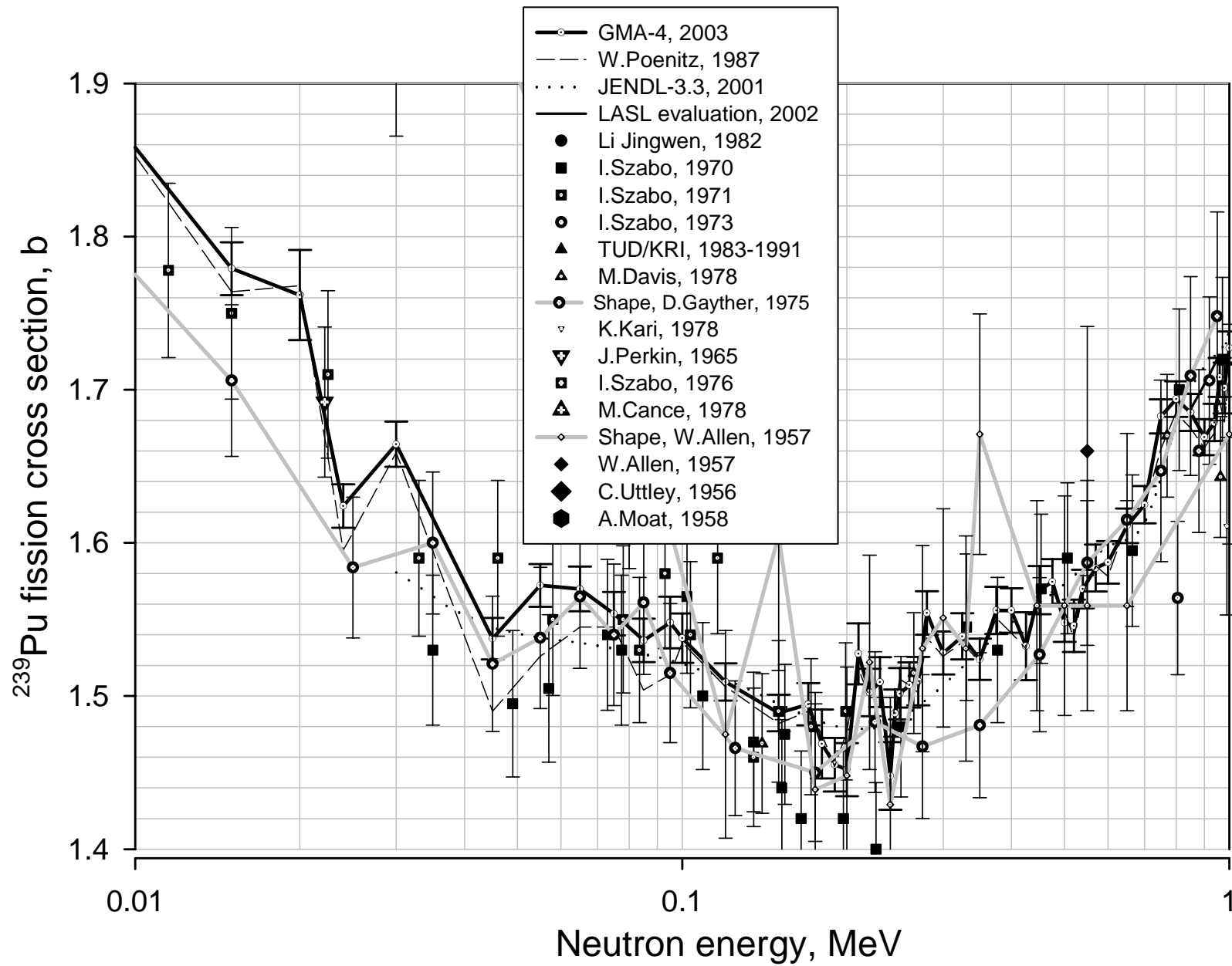


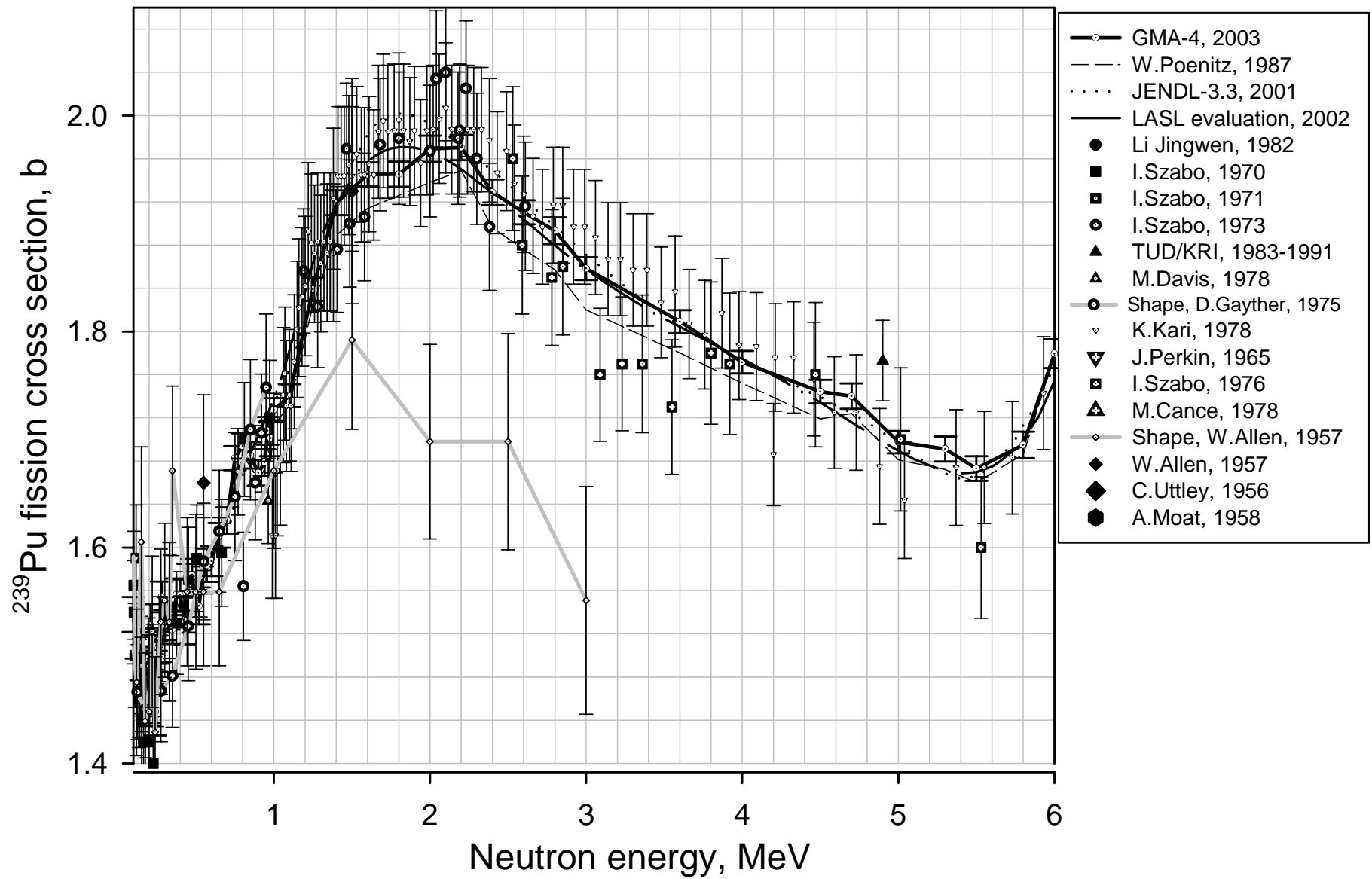


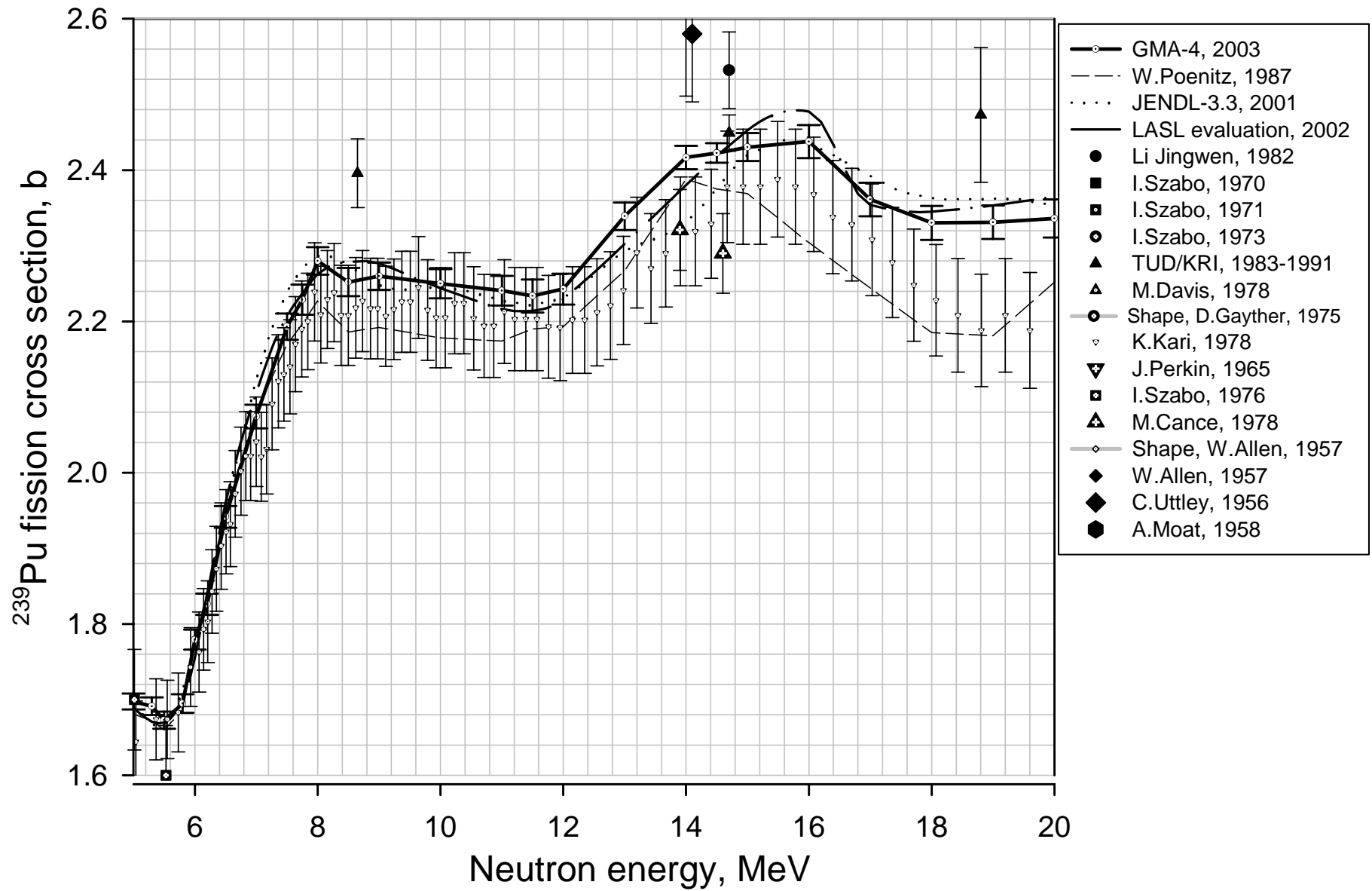


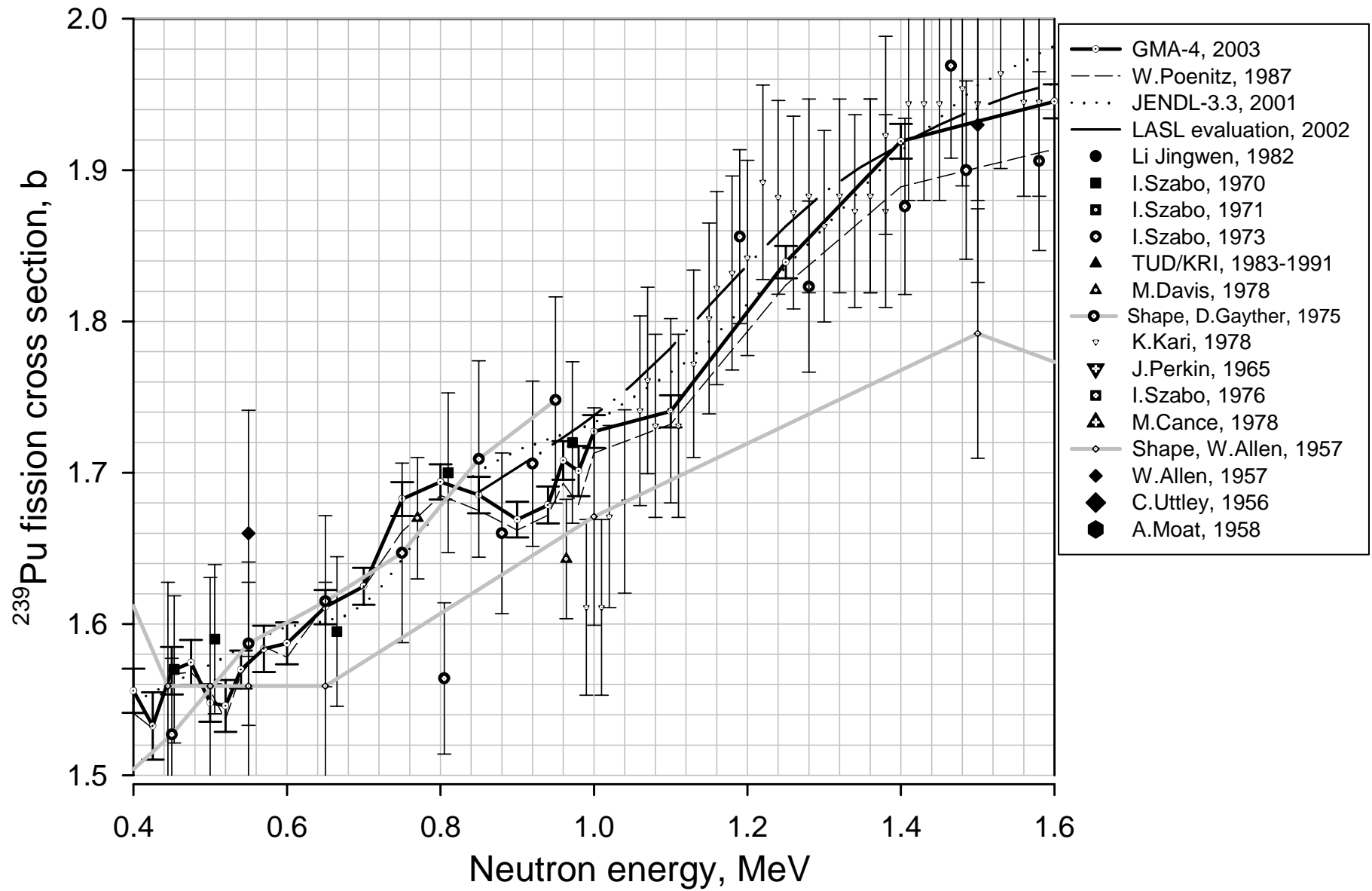


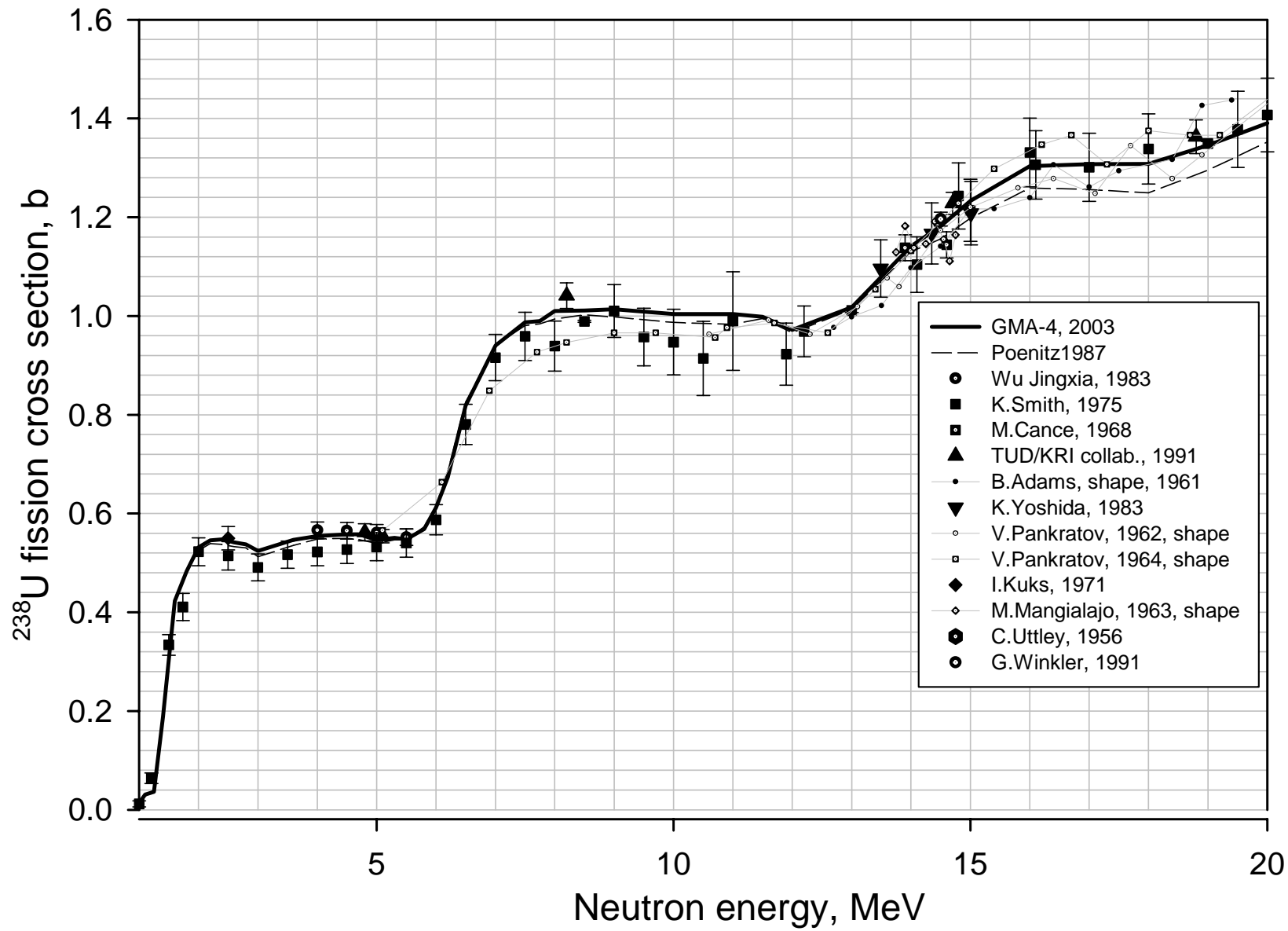


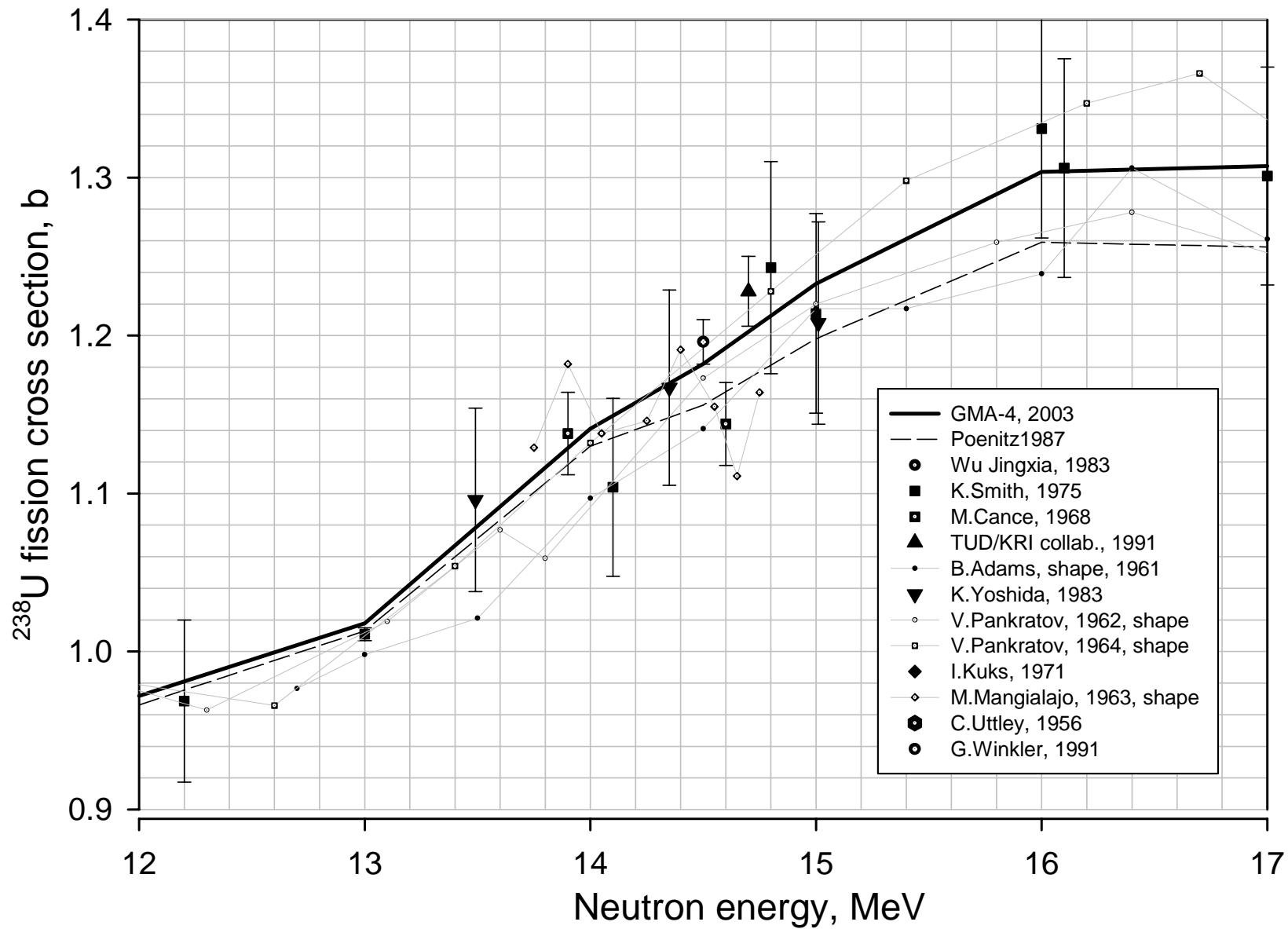


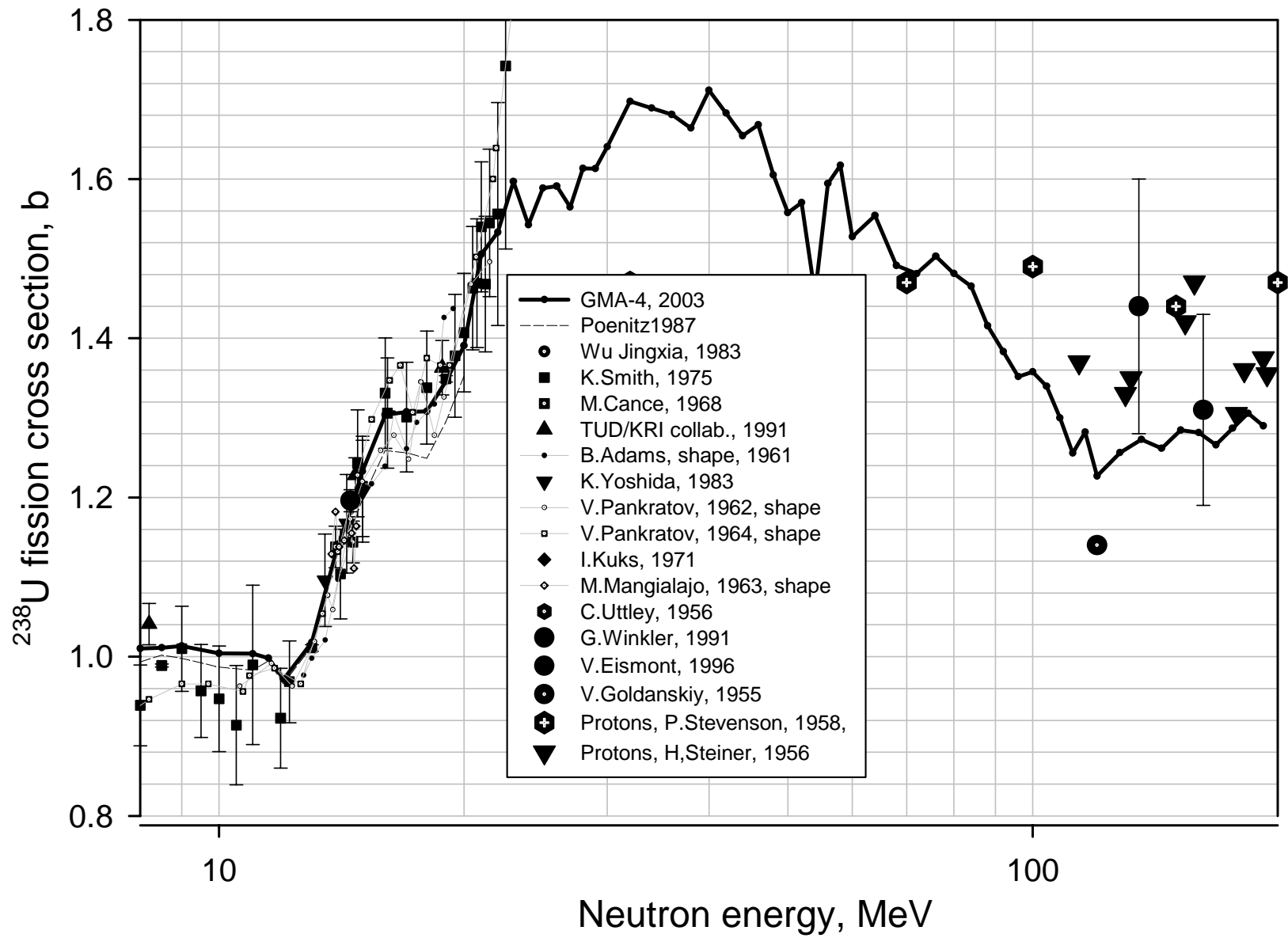


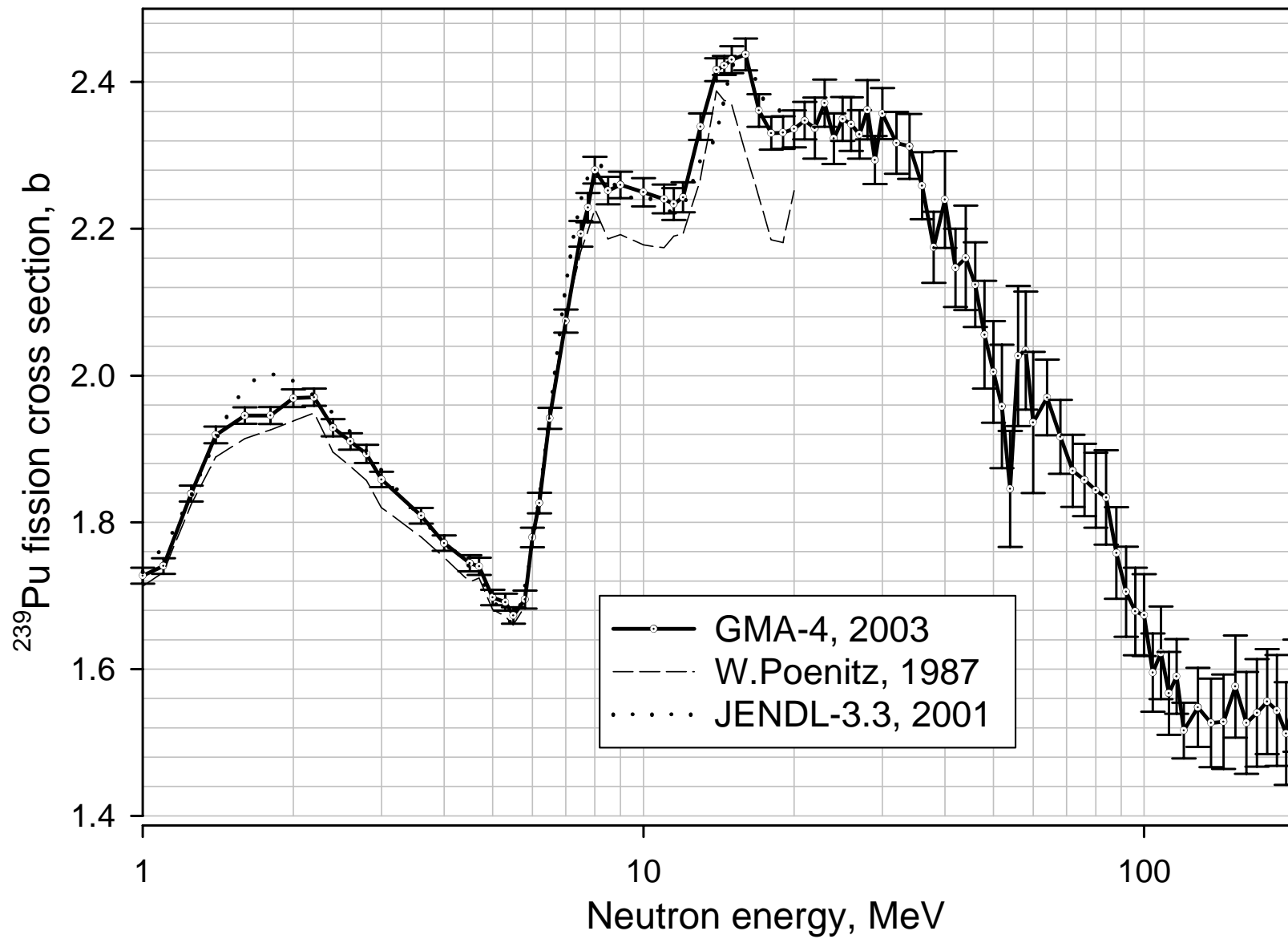


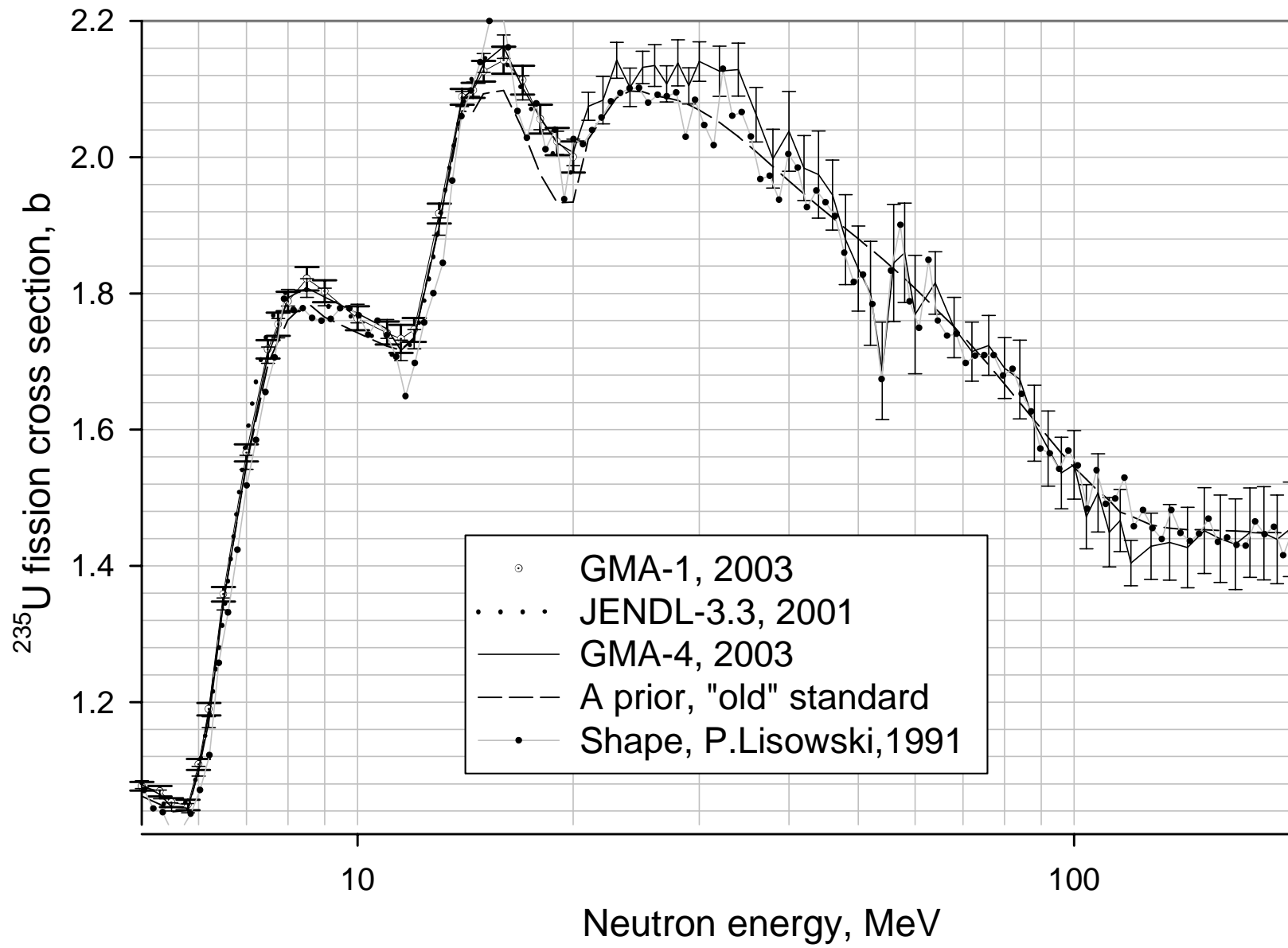


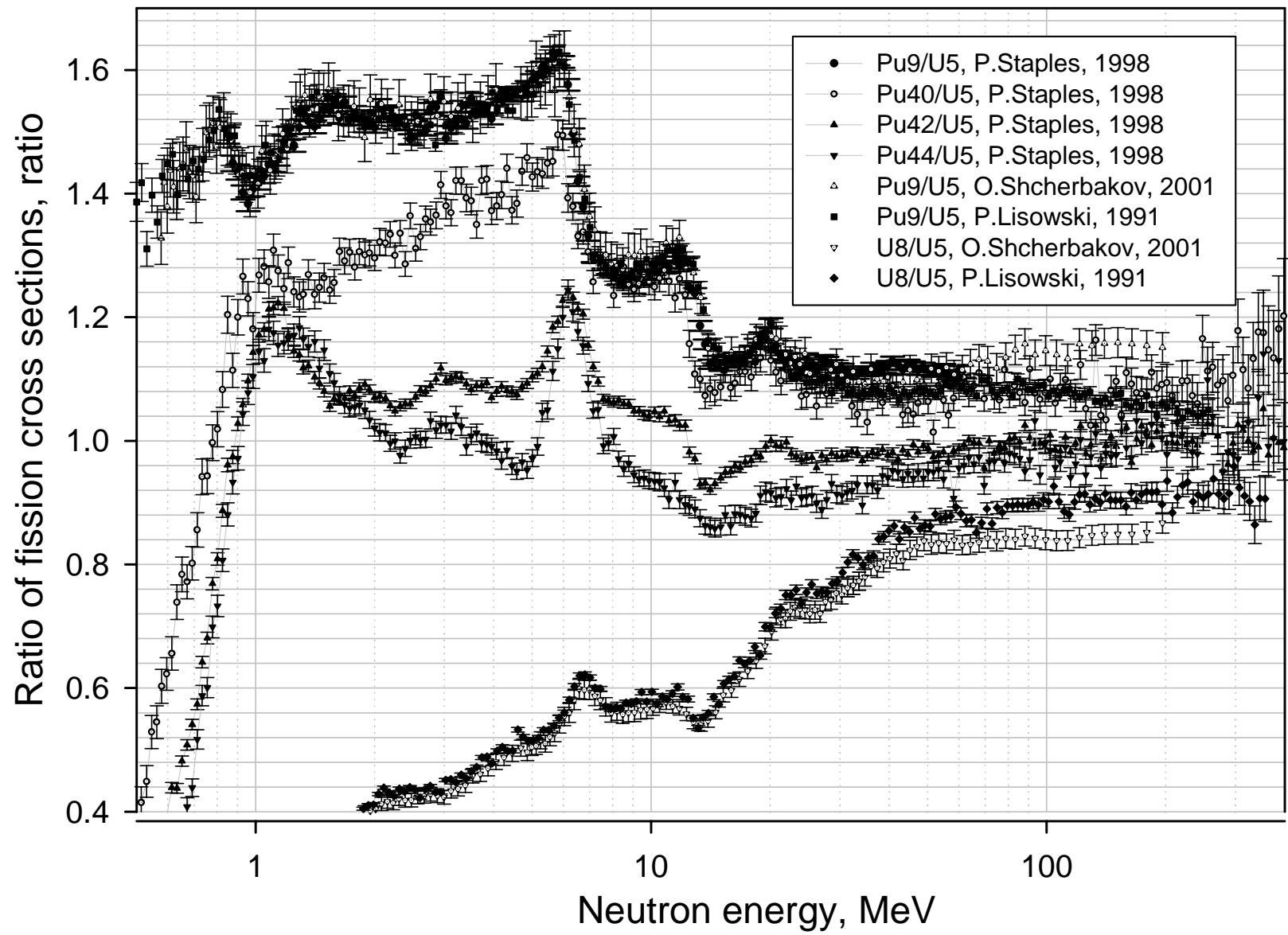


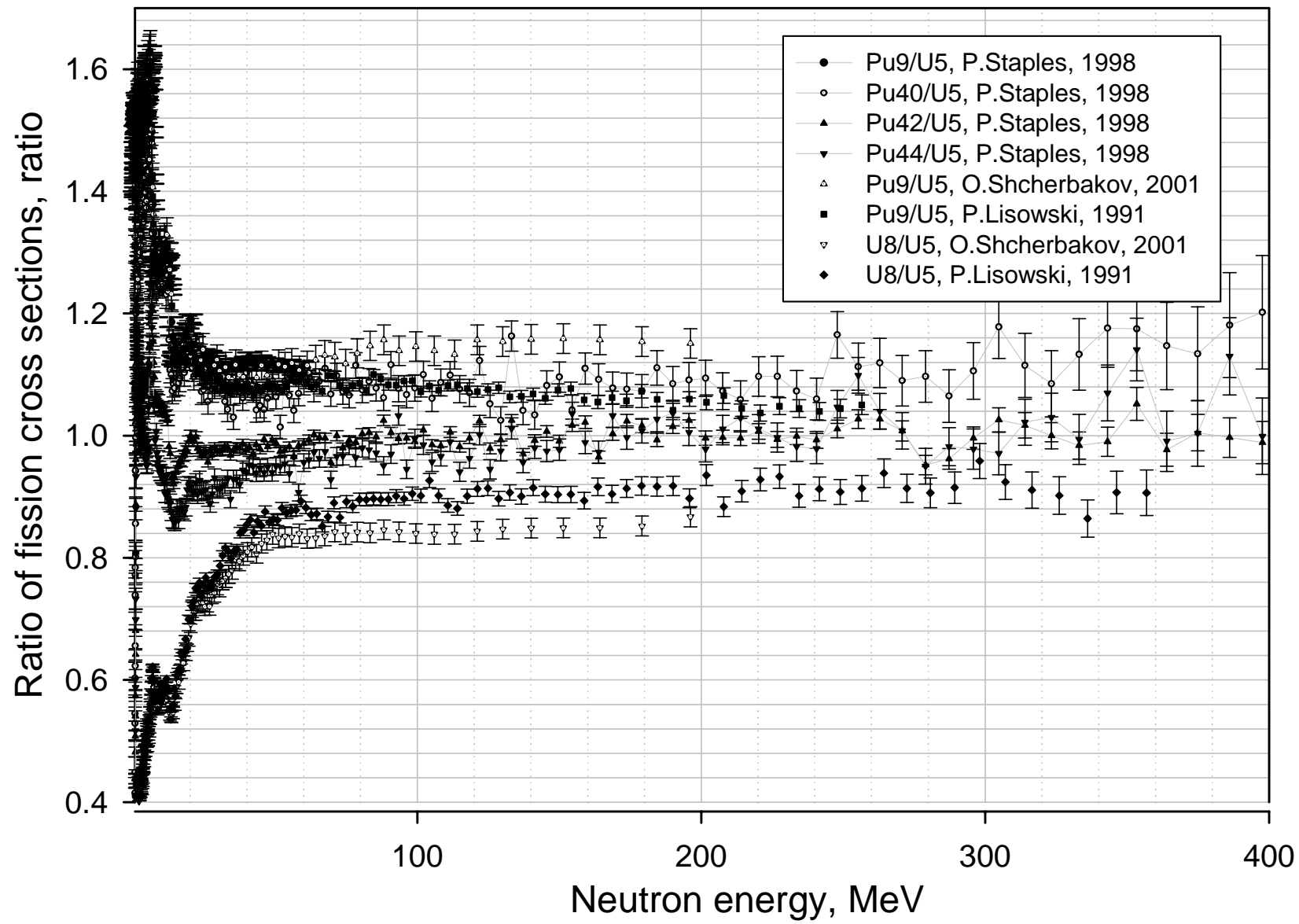


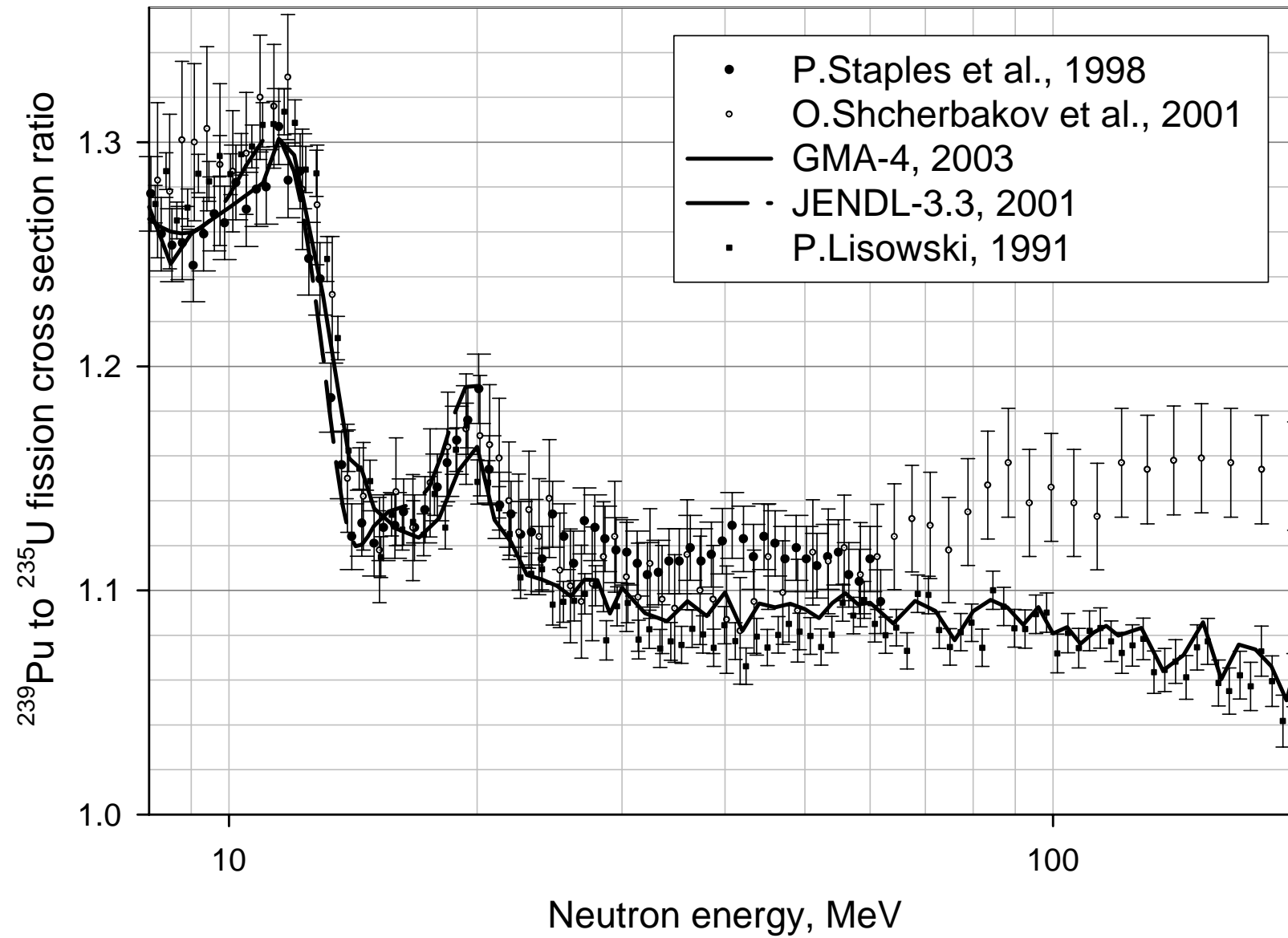


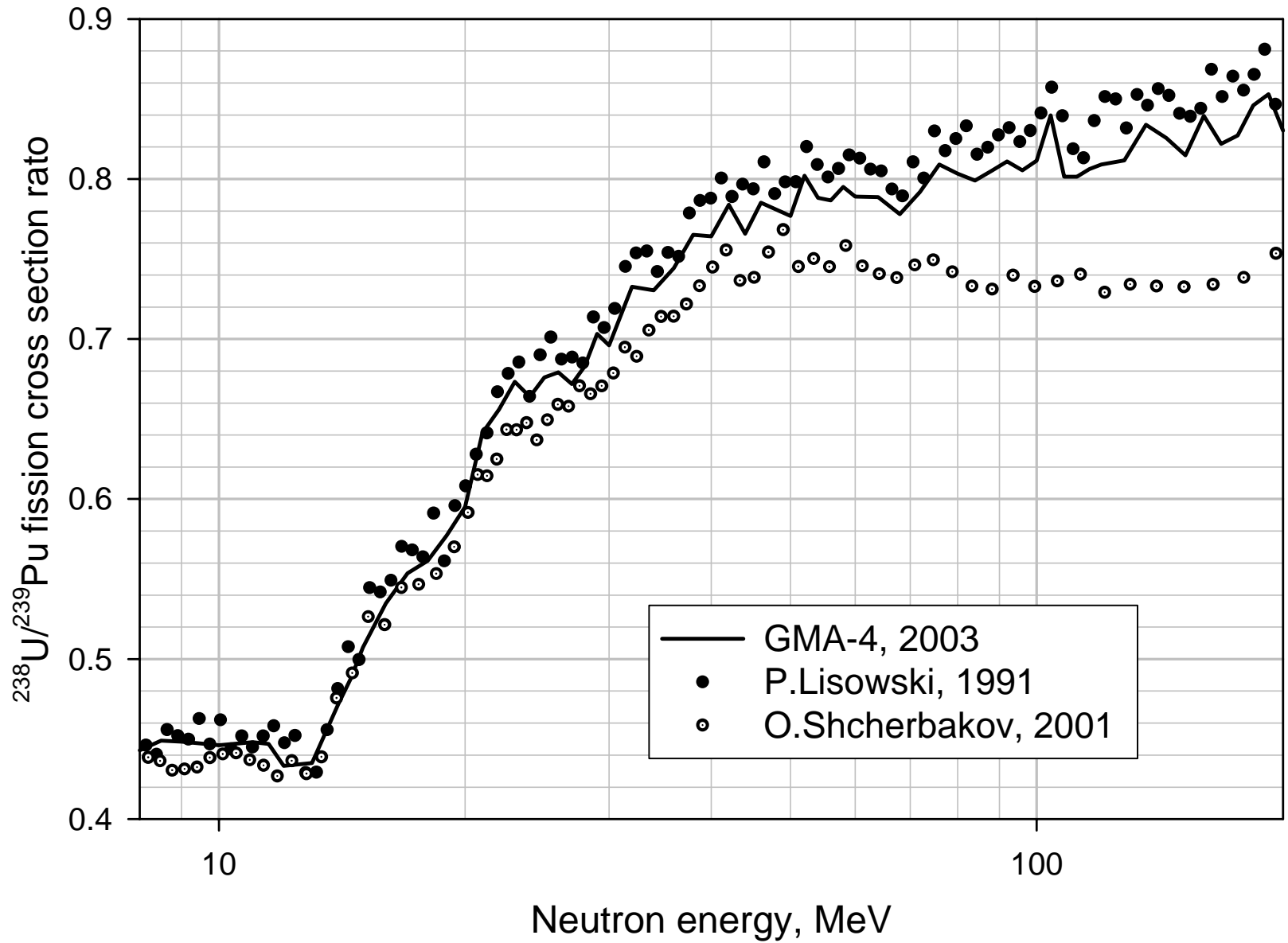


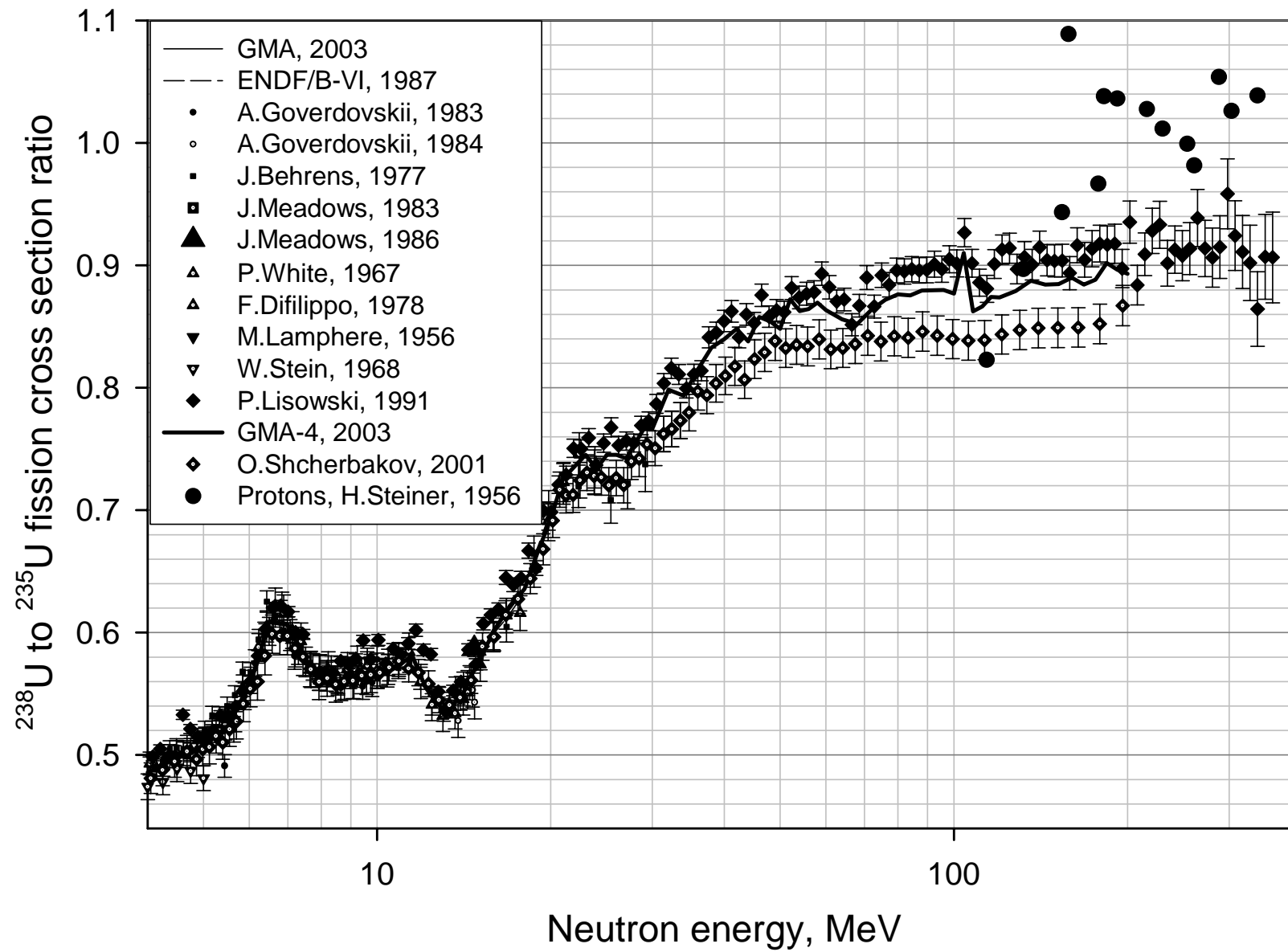


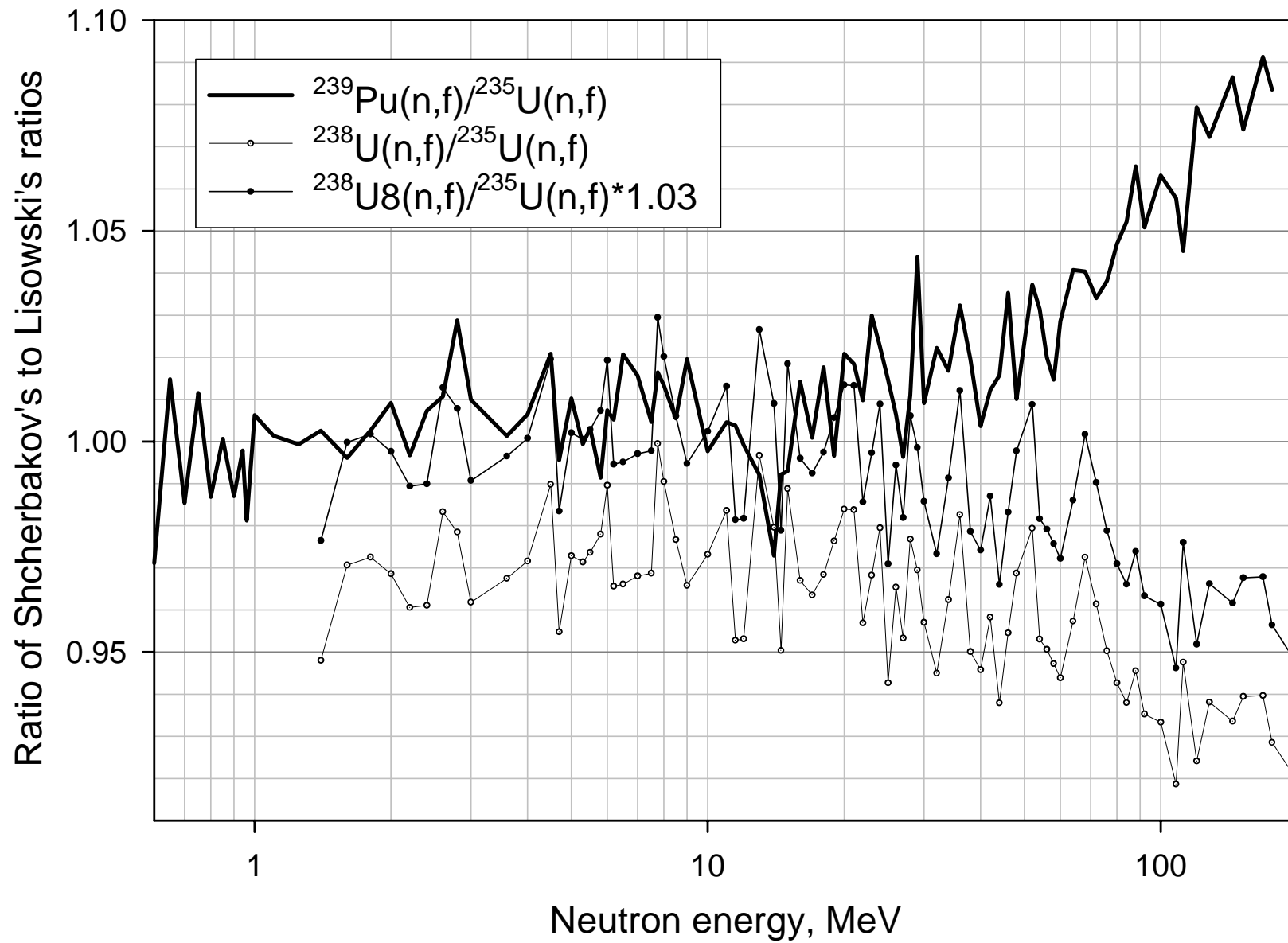


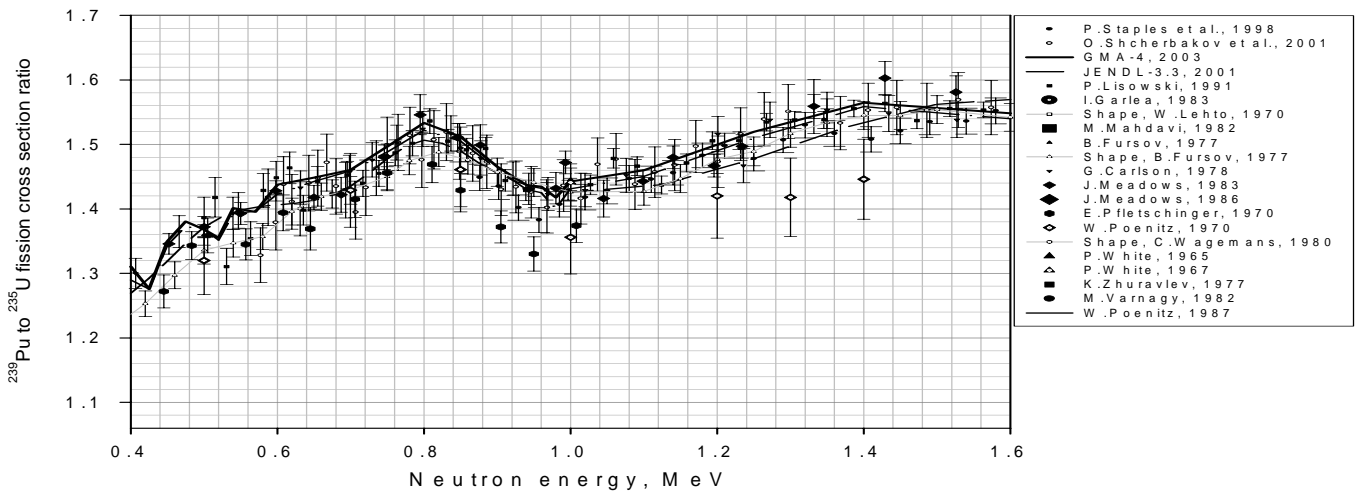
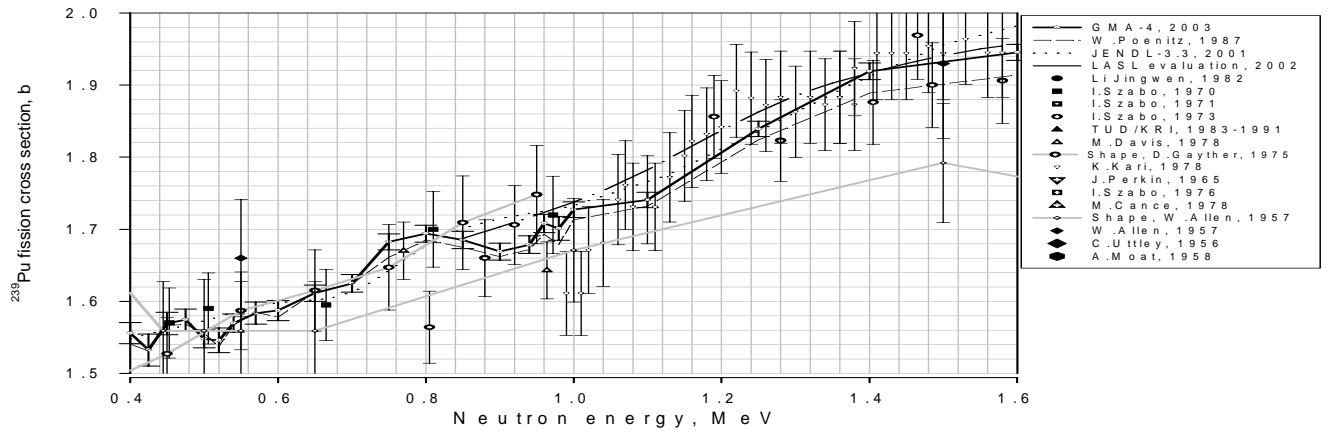
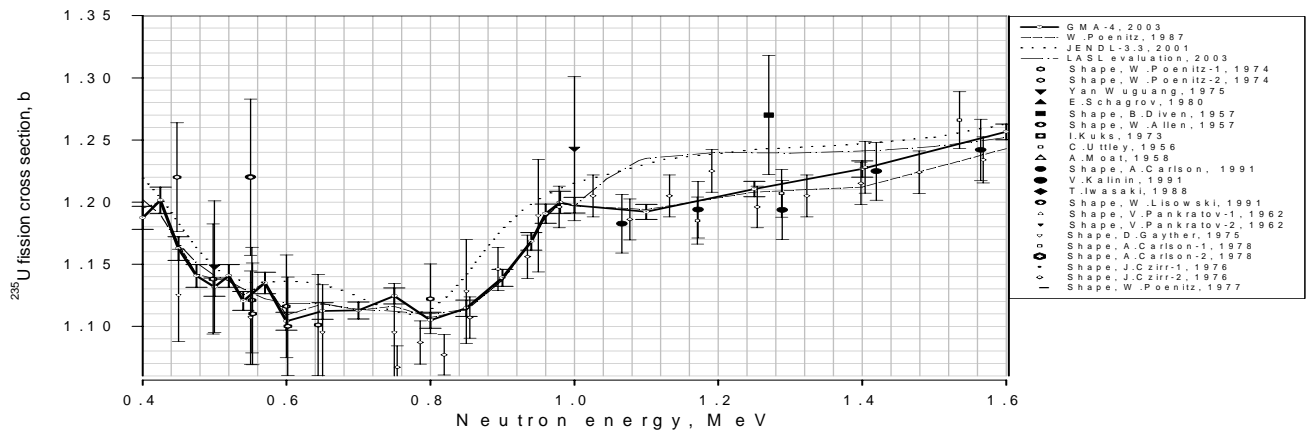
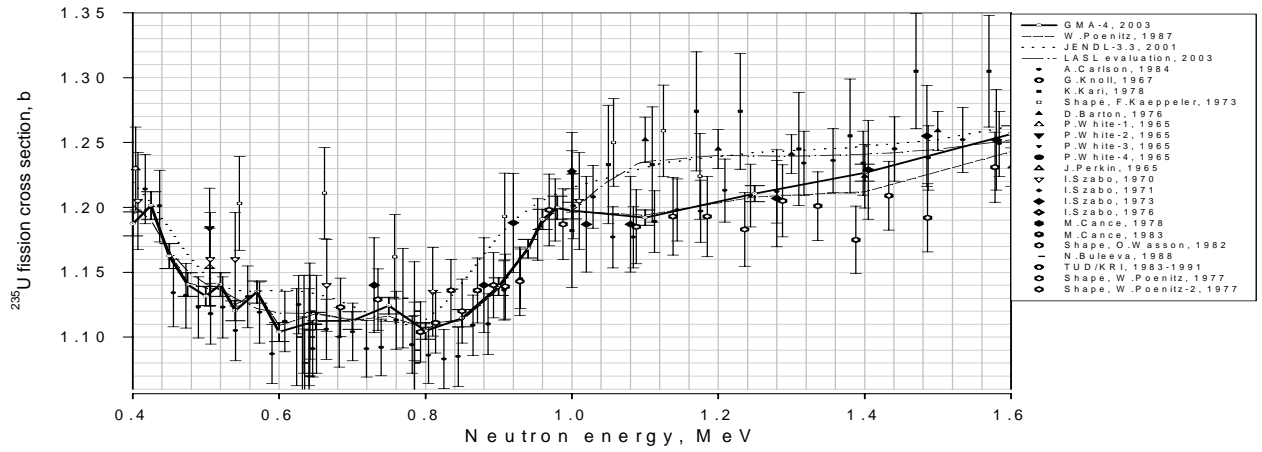


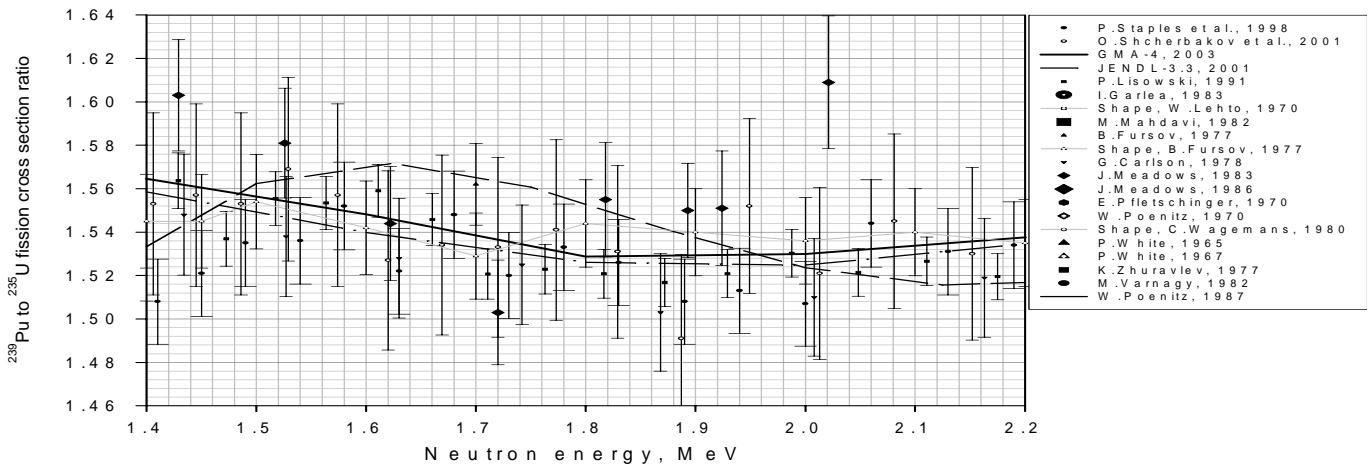
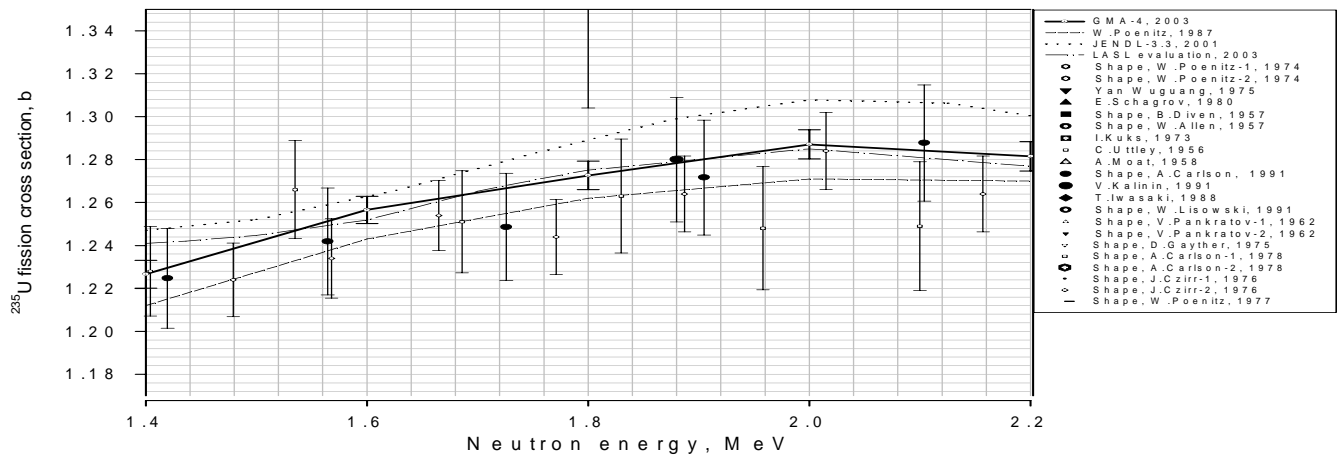
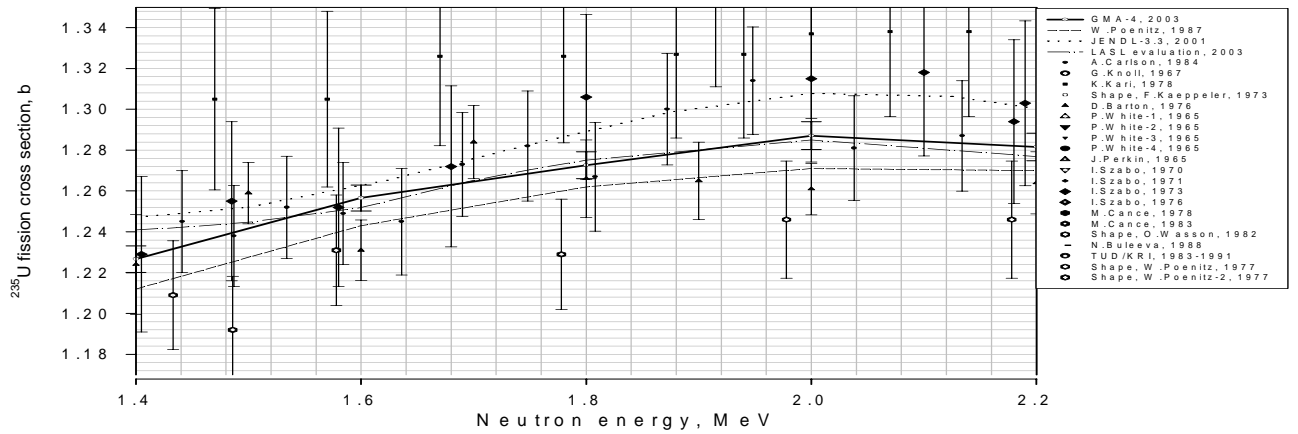
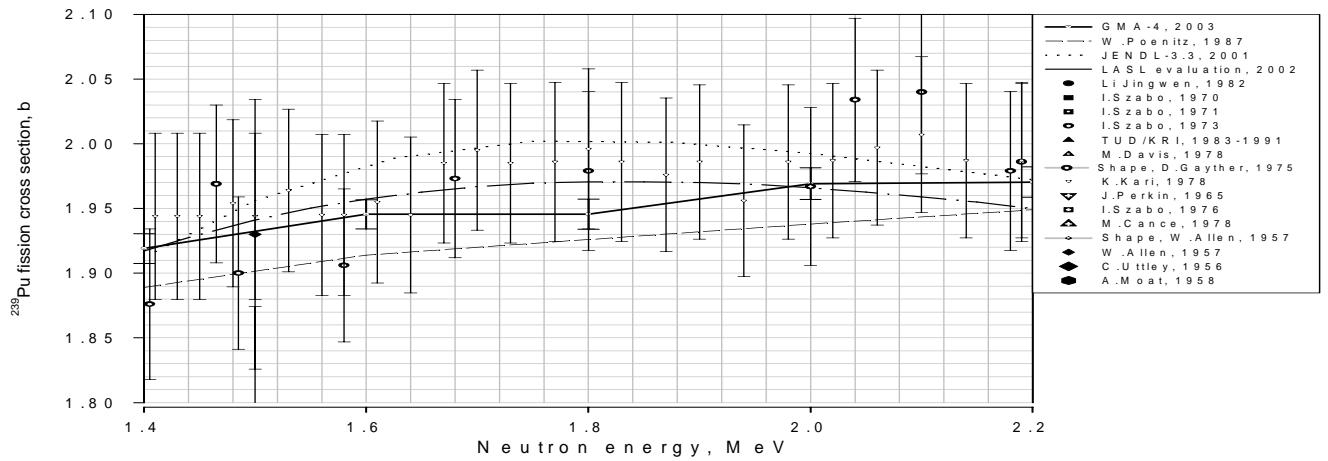












Subjective judgment on measure of data uncertainty

V.G. Pronyaev, A.V. Bychkova*

Nuclear Data Section, IAEA

* cost-free intern, Warwick University, UK

The experts reviewing the results of evaluation of the standard reaction cross sections [1] concluded that the obtained evaluated errors were unrealistically low. This concerns first of all to the R-matrix model least-square fit for light nuclei. But the uncertainties of evaluated data obtained in model or non-model (where parameters of the model are the cross sections themselves) Gauss-Markov-Aitken least-squares formalism are given through rather complex covariance matrices of the uncertainties. The errors, or values of square roots from variances, present only the diagonal elements of covariance matrices. It is known that the variances obtained in the model fits are less than those in the non-model fits of the same data, but the covariances near the matrix diagonal are larger. Thus, the comparison of only errors or variances will give not full picture about the data uncertainty, especially in the cases when correlation matrices are rather different. Direct comparison of covariance matrices also cannot give much because of their complexity and we should look for some integral parameters best characterizing the covariance matrices of uncertainties.

The certain measure of magnitude of the symmetric covariance matrix of uncertainties A with $n \times n$ matrix elements a_{ij} can be characterized by such parameters [2] as $b(A)$ as a bound, $N(A)$ as a norm and $M(A)$ as a maximum.

The bound is the magnitude of the numerically largest element:

$$b(A) = \max |a_{ij}|. \quad (1)$$

The norm is the geometric length defined as:

$$N(A) = (\sum a_{ij}^2)^{1/2}. \quad (2)$$

The maximum is the square root from the largest eigenvalue λ_l of the matrix $B = A^+A$, where A^+ is transpose matrix A :

$$M(A) = (\lambda_l^B)^{1/2}. \quad (3)$$

The norm (2) for symmetric covariance matrix can be also expressed as square root from the sum of the eigenvalues of the matrix $B = A^+A$:

$$N(A) = (\sum \lambda_i^B)^{1/2}. \quad (4)$$

There are the following relations between these quantities:

$$b(A) \leq M(A) \leq N(A), \quad (5)$$

$$N(A) \leq n^{1/2} M(A). \quad (6)$$

Wilks introduced the generalized variance $V(A)$, which is equal numerically to the determinant of the covariance matrix and has a sense of the volume:

$$V(A) = \text{Det}(A). \quad (7)$$

The information entropy $H(A)$ is expressed also through determinant and is equal [3]:

$$H(A) = n/2(1 + \ln(2\pi)) + \ln |\text{Det}(A)|^{1/2}. \quad (8)$$

Wilks' generalized variance and information entropy have physical sense only for positive definite covariance matrices. If covariance matrix is semi-positive definite, the uncertainty of some physical quantities calculated with this covariance matrix can have unphysical zero uncertainty and information entropy is equal to the negative infinity.

The univariate reduced variance $\text{Var}(A)$ can characterize the collapsed univariate uncertainty for the given covariance matrix [3]:

$$\text{Var}(A) = \sum a_{ij} / n^2 \quad (9)$$

The trace of covariance matrix $\text{Tr}(A)$ as a sum of diagonal elements and its ratio $R(A)$ to the sum of all elements can also characterize the correlation properties of the covariance matrix:

$$\text{Tr}(A) = \sum a_{ii}, \quad (10)$$

$$R(A) = \sum a_{ii} / \sum a_{ij} \quad (11)$$

There are some useful properties of covariance matrices, which can be used in calculations and checking of the results:

$$\text{Det}(A) = \prod \lambda_i^A, \quad (12)$$

$$\text{Tr}(A) = \sum \lambda_i^A \quad (13)$$

Let consider the use of these parameters for inter-comparison of complex covariance matrices at the examples of the different fits for rather simple EXAMPLE2 case [4] (4 energy points, 3 data sets) used for study of Peelle's Pertinent Puzzle and for multivariate realistic ${}^6\text{Li}(n,t)$ TEST1 case [5] (51 energy points, 5 data sets).

Parameters of covariance matrices for EXAMPLE2 data in non-model (GMA) and model (linear, quadratic and third order) fits are given in Table 1. Third order fit is equivalent to the GMA fit, because the number of parameters (m) is equal to the number of points (n) in which data are given. The eigenvalues of covariance matrices for different fits are shown in Fig. 1. The covariance matrices for the linear and quadratic fits are semi-positive definite. Linear fit has two ($n-m=2$) and quadratic – one ($n-m=1$) zero eigenvalues.

Table 1. Parameters characterizing the measure of the uncertainty for EXAMPLE2 case fits.

	GMA	Linear	Quadratic	3 rd order
N(A)	0.134	0.104837	0.133275	0.134
M(A)	0.131	0.104	0.131	0.131
b(A)	0.080656	0.041209	0.075076	0.080656
$\Sigma \lambda_i$	0.173	0.120	0.160	0.173
Tr(A)	0.173	0.120	0.160	0.173
λ_1/λ_n (Ratio), $\lambda_1 > \lambda_2 > \dots > \lambda_n$	41.1	∞	∞	41.1
Σa_{ij}	0.469582	0.401793	0.470727	0.469582
Tr(A)/ Σa_{ij}	0.3684	0.2987	0.3399	0.3684
$\Sigma \alpha_{ij}$ (matrices of relative uncertainties)	0.212917	0.223241	0.213918	0.212917
Det(A)	1.28347E-07	0	0	1.28347E-07
H	-2.25850861	$-\infty$	$-\infty$	-2.25850861

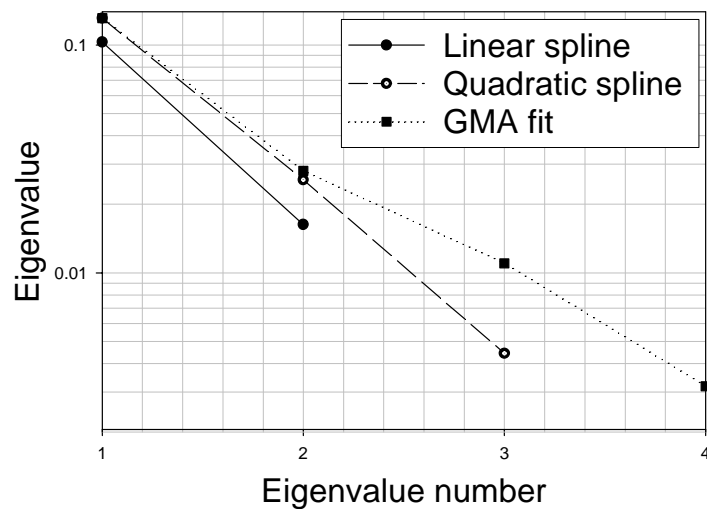


Fig. 1. Non-zero eigenvalues of the covariance matrices for EXAMPLE2 data in different model and non-model least-squares fits.

As seems all parameters given in the Table 1 have a sense for characterizing of the uncertainties given by the covariance matrices. Uncertainty of the data is less if the values of parameters are less (excluding λ_1/λ_n ratio). λ_1/λ_n ratio (if all λ are positive) characterizes how far from semi-positive definiteness is the matrix. Matrix is better positive definite if the ratio λ_1/λ_n is less. There is one parameter Σa_{ij} (or $\text{Var}(A)$), which

may have a global property because practically it does not depend from the type of the least-square fit used (non-model, model and which model). This property can be called as a sum rule for the covariance matrices and formulated as a following statement: *sum of the elements of covariance matrices of the uncertainties of the evaluated data does not depend from which least-squares fit used, namely non-model or (any) model, if the evaluated values obtained in these fits are close.* We cannot give analytical justification of this rule, but numerically it is fulfilled with a rather good accuracy. As we see from Table 1 quadratic and GMA fits (which are rather close) have difference in the sum less than 0.3%, when the difference in some elements is 15% and more. Sums for linear and GMA fits have difference more than 15% and this is because linear model is not fit well the data and has difference 20% and 15% at 2 points relative the GMA evaluated value.

Some parameters of measure of uncertainty calculated for TEST1 case are shown in Table 2 and eigenvalues for 10-parameters model (PADE2) [6] and non-model (GLUCS, GMA) fits are shown in Fig. 2. GLUCS results are close to the GMA and are not presented in the Table 2. Covariance matrix of uncertainty reconstructed in 51 energy points from 10 PADE2 model parameters is initially semi-positive definite. The procedure of conversion it into the positive-definite covariance matrix with a minimal changes of the matrix was used. This is clearly seen from Fig. 2, where the eigenvalues from 1 to 10 are positive and values from 11 to 51 are positive due to subsequent transformation of the matrix. As we see in Table 2 the sum rules is fulfilled with 1% accuracy, although the covariance matrices are rather different with $\text{Tr}(A)$ (or variances) about two times higher in the non-model GMA than in the model PADE2 fit.

Table 1. Parameters characterizing the measure of the uncertainty for TEST1 case fits.

	GMA (51 positive eigenvalues)	PADE (10 positive and 41 zero eigenvalues)
$N(A)$	0.0156	0.0144
$b(A)$	0.00762	0.00740
$\Sigma \lambda_i$	0.0431	0.0233
$\text{Tr}(A)$	0.0431	0.0233
λ_1/λ_n (Ratio), $\lambda_1 > \lambda_2 > \dots > \lambda_n$	543.	∞
Σa_{ij}	0.409	0.405
$\text{Tr}(A)/\Sigma a_{ij}$	0.1053	0.05695
$\text{Det}(A)$	2.117E-185	0.
H	-142.43	$-\infty$

If we consider univariate reduced variance as the measure of the uncertainty (or Σa_{ij}), then we may come to the conclusion that the model (if it does not introduces some physical constraints) reduces substantially the variances but increases simultaneously the covariances by a way that it does not change the measure of the uncertainty. If we consider the trace $\text{Tr}(A)$ as the measure of the uncertainty that we can conclude that the model can substantially reduce the uncertainty, and if we consider the Wilks' determinant or information entropy as the measure then we should say that it is indefinite in the cases when the number of the model parameters is less than the number of points at which the covariance matrix of uncertainty of cross sections is reconstructed.

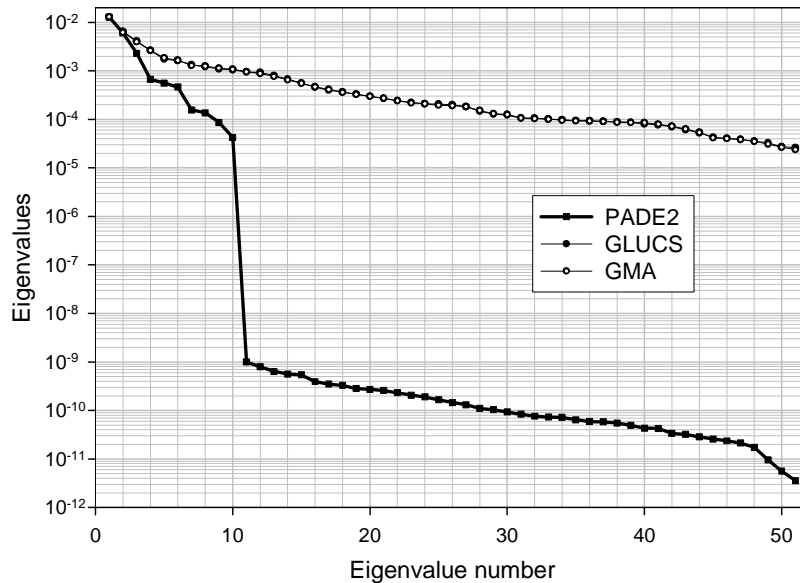


Fig. 2. Eigenvalues of the covariance matrices for TEST1 data in the model (PADE2) and non-model (GLUCS, GMA) least-squares fits.

The physical requirements of the positive definiteness of the covariance matrix of the uncertainties are discussed in [7]. The quadratic form $Q = \sum \sum z_j a_{ij} z_j$, where Q is a scalar, z_i, z_j are the vectors (z_j is transpose of z_i) and a_{ij} is covariance matrix of uncertainty of the data and sums are on i and j , is often used in different nuclear applications for calculation of uncertainty of some integral quantity. In more general form which is also used in applications and follows from the error propagation law it can be written as $Q = \sum \sum \sum m_{ki} a_{ij} m_{jl}^+$, where m_{ki} is some other matrix, m_{jl}^+ - matrix transpose to m_{ki} and sum is on all indexes. If matrix a_{ij} is semi-positive definite, e.g. has one or several zero eigenvalues, then there exists at least one vector z_i for which $Q=0$. It means that the uncertainty of some integral quantity can be equal to 0. This contradicts to our expectations that the error of any physical quantity cannot be equal to zero. But there is no sharp border between unphysical zero error and very small error, which can be obtained in case when we change slightly the covariances of the semi-positive definite matrix that it transforms it in the formally positive definite matrix. This is needed in further clarification.

References

1. H. Conde (ed.), Nuclear Data Standards for Nuclear Measurements, Report NEANDC-311 (1992).
2. A.S. Householder, Principles of numerical analysis, McGraw-Hill, NY (1953).
3. V.G. Pronyaev, Report INDC(NDS)-438, p.172 (2003).
4. Soo-Youl Oh, Report INDC(NDS)-438, p.130 (2003).
5. V.G. Pronyaev, Report INDC(NDS)-438, p.26 (2003).
6. S.A. Badikov, E.V. Gai, Report presented at this RCM.
7. L.P. Geraldo, D.L. Smith, Report ANL/NDM-104 (1988).

Update of GMA Code to Solve the PPP Problem (Technically)

D.L. Smith* and **V.G. Pronyaev**

Nuclear Data Section, IAEA, Vienna

*IAEA consultant

25 November 2003

The GMA code has been updated to introduce the Chiba-Smith option (see report ANL/NDM-121, 1991) to address the problem of PPP. To avoid confusion, we will refer to this code, and results obtained using it, as GMAP. This code revision was accomplished with a minimum of intervention to the original version of GMA in order to avoid introducing coding errors. The Chiba-Smith approach was implemented by means of simple renormalization of the experimental absolute errors (square roots of the variances) after reading them in from the input file. This renormalization was applied to each “experimental” data point and for each class of data, e.g., cross sections, ratios, shape ratios, etc., as $\Delta\sigma'(i) = \Delta\sigma \times (\sigma_p(i)/\sigma)$, where σ represents the experimental data value (whatever it might be) $\Delta\sigma$ is the uncertainty of this experimental data point, $\sigma_p(i)$ is a prior value for this quantity – obtained after i^{th} iteration, and $\Delta\sigma'(i)$ is the renormalized absolute uncertainty of the data after the i^{th} iteration. We use the term “experimental” rather broadly here because it is intended to eventually employ GMAP for merging R-matrix and experimental results, with the R-matrix results introduced as pseudo experimental data. The original GMA code already included an option to iterate the runs with replacement of the prior $\sigma_p(i)$ by the new posterior solution since the prior in GMA is assumed to be ad hoc and non-informative. The convergence to the “true” posterior solution was very fast, usually a few iterations were enough even when first prior was intentionally made discrepant with a bulk of experimental data.

We refer to this option as a “technical” solution to exclude PPP since it is based on the subjective assumption by Chiba and Smith that when experimenters quote absolute total errors these are calculated by multiplying a fractional error (comparable to percent error) by the measured value. Thus, it is supposed that it is the fractional error that actually reflects the accuracy that the experimenter intends to convey to the reader. The PPP problem is a consequence of discrepancies, i.e., the scatter observed for various presumably comparable data obtained by different experimenters that is frequently beyond the quoted errors. Consequently, we believe that the Chiba-Smith approach should be introduced into an evaluation process only after applying the “physical” option, namely, that of identifying the outlying data points (those most discrepant with respect to the main body of evaluated data). Then, where possible, the observed discrepancies should be resolved by applying corrections that were overlooked (or possibly erroneously determined) by the original experimenters, by enhancing quoted errors to compensate for hidden uncertainties not realized by the experimenters, etc. The intent is to reduce the PPP effect as much as possible by objective means before resorting to the above-mentioned “technical” solution. Such an approach is essential to the achievement of a good evaluation since the “corrected” data values are expected to then correspond more closely to the “truth.” However, since the PPP phenomenon does not have a threshold and is continuous in nature (see Appendix), we believe that, after exhausting the possibilities for the abovementioned “physical” option, PPP should

be excluded by applying a technical approach such as that of Chiba-Smith to correct for residual deficiencies in the database and deficiencies of the least-square procedure, even if the PPP effect is small.

While the example given in the Appendix is illustrative of PPP for a simple hypothetical situation, it is more convincing to explore the phenomenon in the “real world” using a realistic data set. The TEST1 data set, which exhibits a large and clearly seen PPP bias, was adopted by the CRP and used to inter-compare different technical options for PPP exclusion. These data were employed in the various fits without any alterations, i.e., they were original data given by the experimenters. No values were adjusted, no errors were enhanced, etc. Those results indicated in Figs. 1 to 3 as “GMAP” were obtained with three computational steps in the framework of the Chiba-Smith approach to exclude the PPP: the first pass using the assumed prior (ENDF/B-VI), GMAP(1) – the result after one iteration, and GMAP(2) – the result after two iterations. GMA presents results without any technical fixes applied to exclude PPP. Therefore, it exhibits the full extent of the PPP bias. GLUCS03 presents results obtained by S. Tagesen and H. Vonach with inclusion of the Chiba-Smith option in the GLUCS code. GMAJ presents results obtained by Soo-Youl Oh (Table 3, p. 153, report INDC(NDS)-438, 2002) with the GMAJ code. GMAJ is a version of the GMA code completely rewritten by Chiba with inclusion of the Chiba-Smith option to exclude PPP. Oh does not mention whether he iterates the solution obtained using GMAJ, so we will assume for present purposes that there is no iteration. Results showing the use of Box-Cox transformation to exclude the PPP effect are also taken from paper by Soo-Youl Oh (Table 3, p. 153, report INDC(NDS)-438, 2002). The PADE-2 model fit (S. Badikov, Private communication) also was performed without any technical fixes to exclude PPP. Two fits obtained using the RAC R-matrix code – without technical options to exclude the PPP effect – are shown in the Figs. 1 and 2. RAC(2002) presents the “old” fit, where selection of the prior parameters was rather free and problems were known to have existed with regard to ambiguity in the determination of parameters. RAC(2003) presents the “new” fit, where parameters determined from the fit of a large number of data in different reaction channels leading to the formation of ${}^7\text{Li}$ system were taken as the set of non-informative prior R-matrix parameters. It may be the case that the RAC(2003) fit corresponds to a particular local minimum of the chi-square function and perhaps should not be compared to results from the other fitting procedures because of the major differences in the employed approaches.

Results from fits obtained by various means are shown in Fig. 1 as ratios to the GMAP(2) fit. The PPP biases observed in the GMA, RAC(2002) and PADE-2 fits are rather large. The RAC(2003) fit (irrespective of the comment in the preceding paragraph), and all other fits that aim to provide technical exclusion of PPP, give results that are relatively close. It is therefore difficult to judge which approach yields the “best” result since we do not know the true values to which these real data should correspond. Figs. 2a and 2b show in more detail the differences between the GMAP results (one and two iterations, respectively) and the various other approaches used to exclude the PPP effect. It is evident that the Box-Cox approach gives slightly higher values than the other methods. The GMAP and GLUCS03 fits are based on the same technical fix to exclude PPP (Chiba-Smith). Nevertheless, they exhibit some differences that can probably be explained in terms of the precision of the numerical solutions of different equations. Because of such issues related to numerical precision, it is seems unreasonable to claim that one approach is better than another when the observed differences are quite small.

We have found that two distinct effects can lead to the presence of PPP in data evaluated by the least-squares method (see Appendix). One effect can be attributed to the different shapes of distinct strongly correlated data sets. We choose to label the PPP effect that results from these strong correlations as maxi-PPP. The second effect arises when there is a spread of data and absolute uncertainties are assigned. Two data points with the same percent uncertainty (same accuracy), but having different values, will then be weighted differently by the least-squares evaluation process. The lowest point will be assigned the heaviest weight since the weighting factor corresponds to the reciprocal square of the absolute error. We will refer to the PPP effect due to an apparent over-weighting of low values as mini-PPP. The contribution of the mini-PPP effect for the standards data is rather small due to the generally small spread encountered for standard-reaction experimental data values. The contribution of these two components for the TEST1 case can be seen in Fig. 3a and 3b. The thick solid line shows the full PPP bias, based on our assumption that the Chiba-Smith approach, as manifested in GMAP calculations with two iterations, gives the best value. The thin solid line shows the effect of mini-PPP for these five TEST1 data sets. For this particular calculation, all non-diagonal elements of the correlation matrices of all experimental data sets were set to 0, i.e., no correlations (nc). So, in this case the difference between the GMA and GMAP results shows the mini-PPP effect explicitly for the rather discrepant TEST1 database. As we see from Figs. 3a and 3b, this effect is not large. However, we believe it still should be addressed and corrected. Since the thin dashed line in Figs. 3a and 3b shows the ratio of the GMA result with no correlations between data to the comparable GMAP result, it is demonstrated that exclusion only of the correlations is not enough to consider a fit to be effectively free from PPP at levels of accuracy consistent with the requirements for the standard cross sections.

Appendix

Mini- and Maxi- PPP for Peelle's Original Problem

An examination of both simple and complex data evaluation problems by the least squares method shows that the phenomenon known as Peelle's Pertinent Puzzle (PPP) inevitably occurs when data scatter and absolute uncertainties are employed in the evaluation. This appears at a more fundamental level to be attributable to the fact that the least-squares formalism is an approximation to the fundamental Bayesian evaluation approach. Robert Peelle of Oak Ridge National Laboratory first demonstrated the PPP phenomenon, at least to the nuclear data community, in an informal memorandum that he distributed in 1987. Since then, PPP has been the subject of numerous debates within the data evaluation and data adjustment communities. Qualitatively speaking, the PPP phenomenon tends (on average) to lead to evaluated results that are intuitively "too low". Quantitatively, the bias known as PPP resulting from applications of the least-squares methodology can range continuously from zero to values that affect the quality of an evaluation significantly.

A closer examination of the PPP phenomenon shows that it is actually comprised of two components. One component – that for the purpose of convenience will be denoted by mini-PPP – tends to have lesser magnitude. It is observed even when no correlations are present in the uncertainties of data to be evaluated, only scatter. A second aspect of PPP, denoted here by maxi-PPP, is manifested when uncertainty correlations are present. Often this component, which can never be separated from the mini-PPP effect, tends to be the larger effect. In the evaluation of real data with uncertainties, scatter (i.e., discrepancies), and error correlations, one encounters total-PPP, or simply PPP as a composite of the mini-PPP and maxi-PPP components.

In this appendix we demonstrate the effect of both mini-PPP and maxi-PPP by considering Peelle's original problem. Two data are averaged. One has a value 1.5 and the other 1.0. Each has a random uncertainty of 10% and they both have a fully correlated error of 20%. These data are obviously discrepant, and blind application of the least-squares method leads to the non-intuitive result 0.88 ± 0.22 for the evaluated solution! Since both values appear to have the same precision, the intuitive best solution would appear to be 1.25. This is the solution obtained using the method proposed by Chiba and Smith (see report ANL/NDM-121, 1991) to eliminate the PPP effect. Peelle's original problem has been examined using both a spreadsheet routine (EXCEL) and the least squares code LSMOD developed by Smith (see report ANL/NDM-128). The first set of calculations, done with EXCEL, involved switching off the error correlation parameter and varying the discrepancy between these data from zero to 40% (40% corresponds to Peelle's original problem since $0.5/1.25$ equals 0.4). The deviation from the Chiba-Smith solution (1.25) varies from zero to about 8% (low) as is seen in the top graph of Fig. A.1. This is the mini-PPP effect. The second set of calculations was performed with LSMOD. The data values 1.5 and 1.0 were retained as originally given, as were the magnitudes of the error components. However, the degree of correlation was varied from zero to 100% (100% corresponds to Peelle's original problem). The results are shown in the bottom graph of Fig. A.1. The correlation strength ranges from 0 to 1.0 (100% correlation). The "mini-PPP effect appears as an 8% reduction for zero correlation strength whereas the full PPP effect at 100% correlation strength is about 30% for this example. The difference is attributed to the maxi-PPP component. Maxi-PPP can be demonstrated only as

an observable difference between the reduction seen for total-PPP and that obtained when correlations are neglected (mini-PPP).

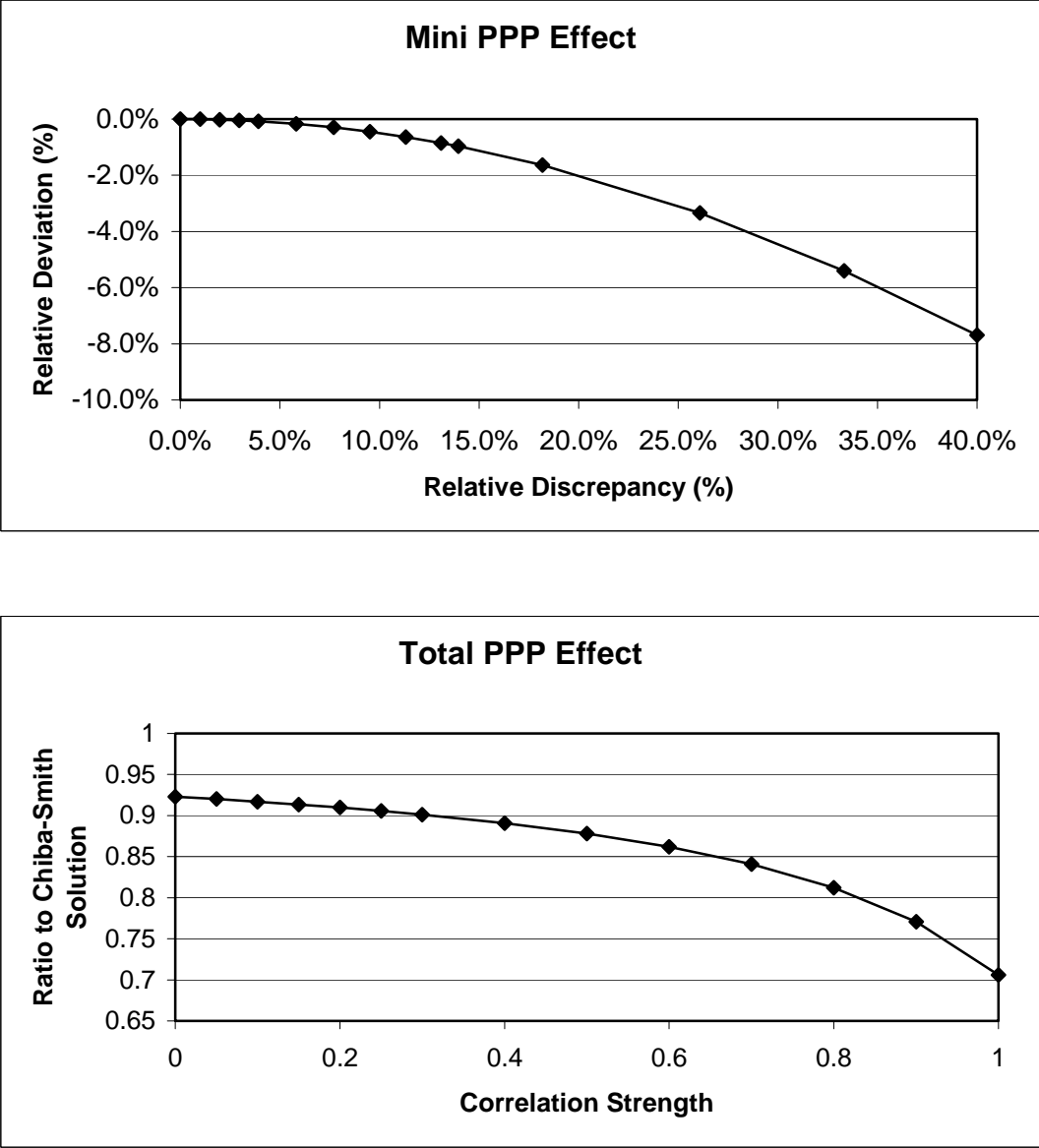


Figure A.1. Demonstration of mini- and maxi-PPP effects

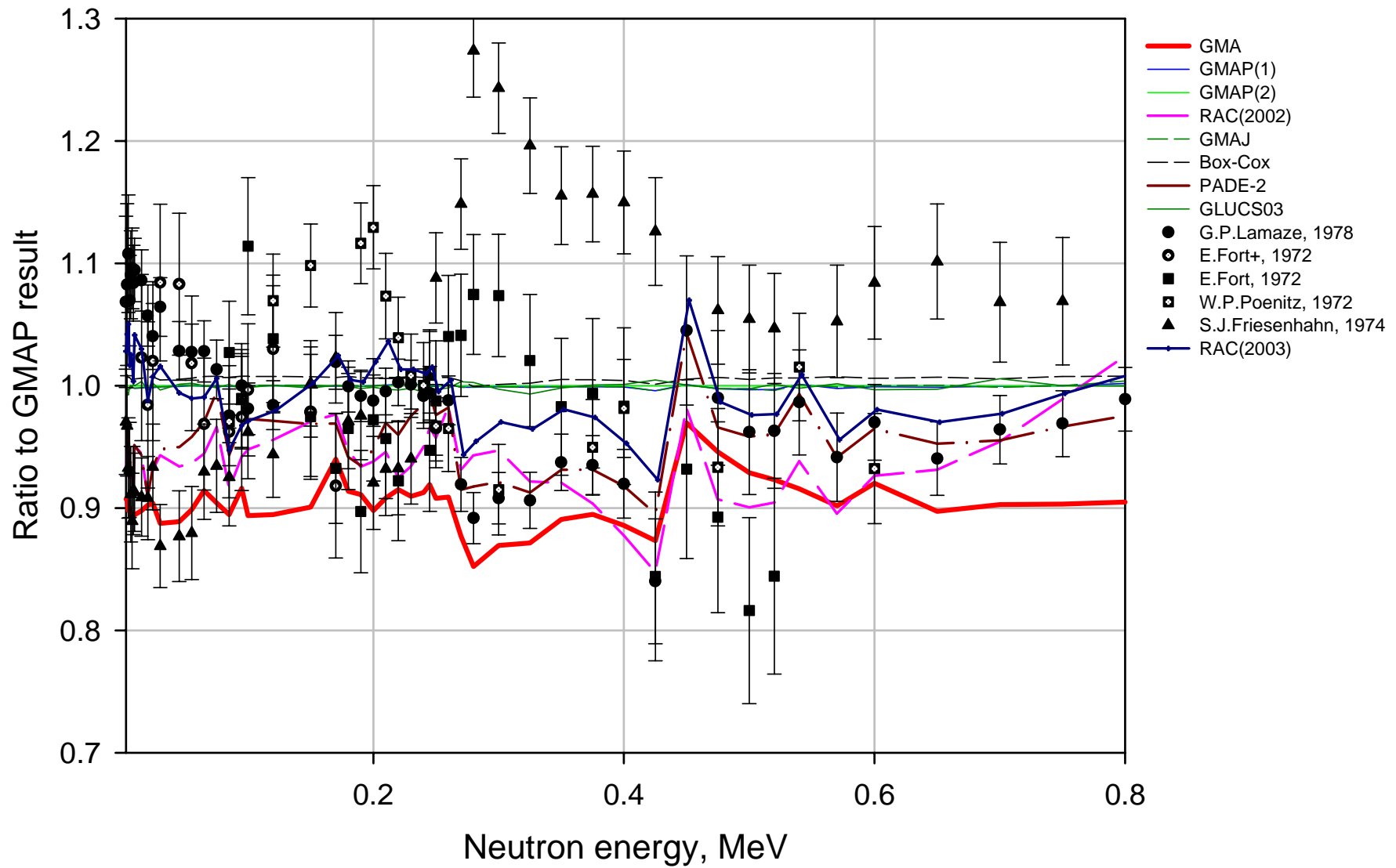


Fig. 1. Ratios of different fits of ${}^6\text{Li}(n,t)$ cross sections to the GMAP(2) iterative fit (Chiba-Smith option).

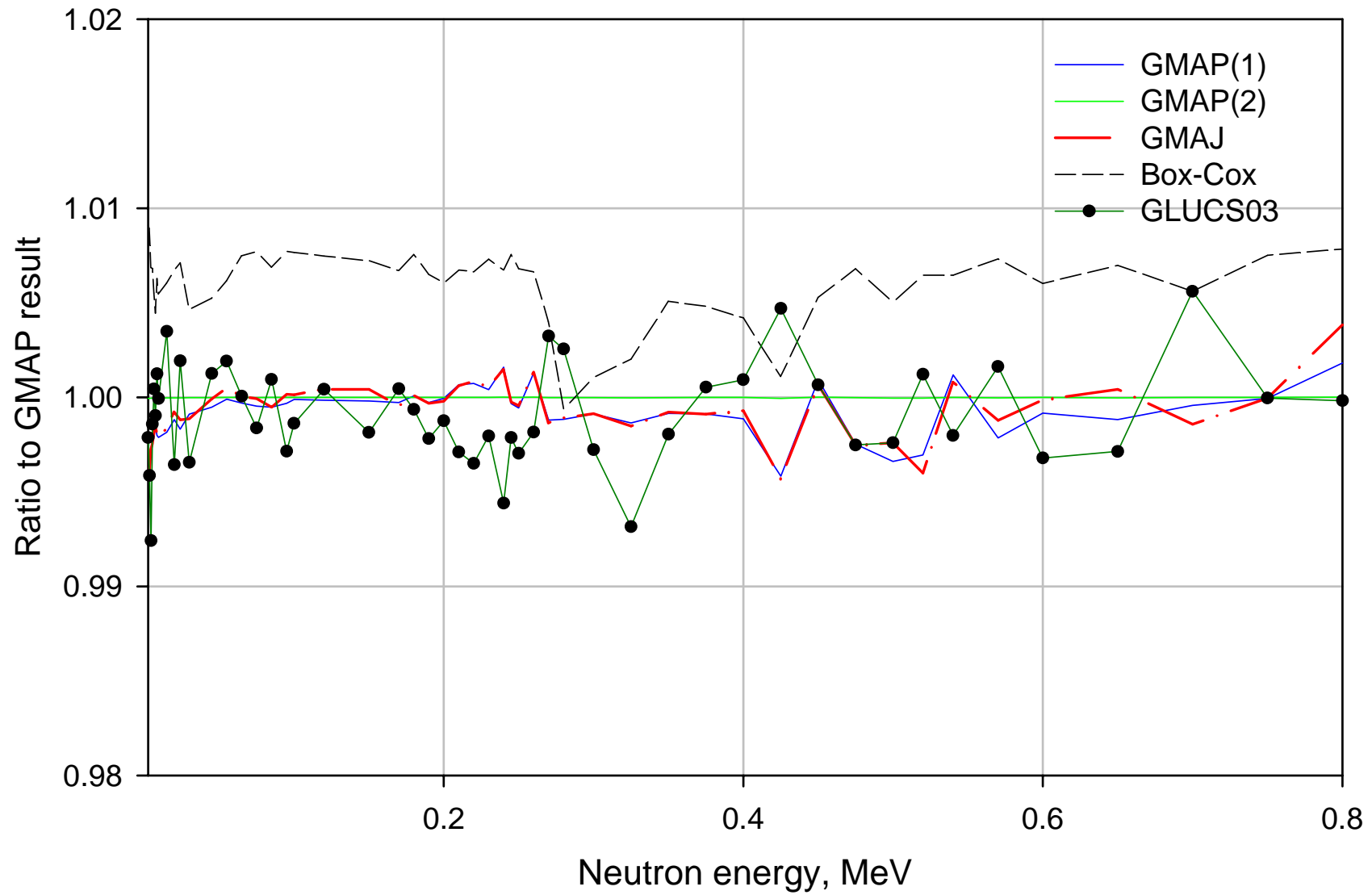


Fig. 2a. Ratios of different fits of ${}^6\text{Li}(n,t)$ cross sections to the GMAP(2) iterative fit (Chiba-Smith option).

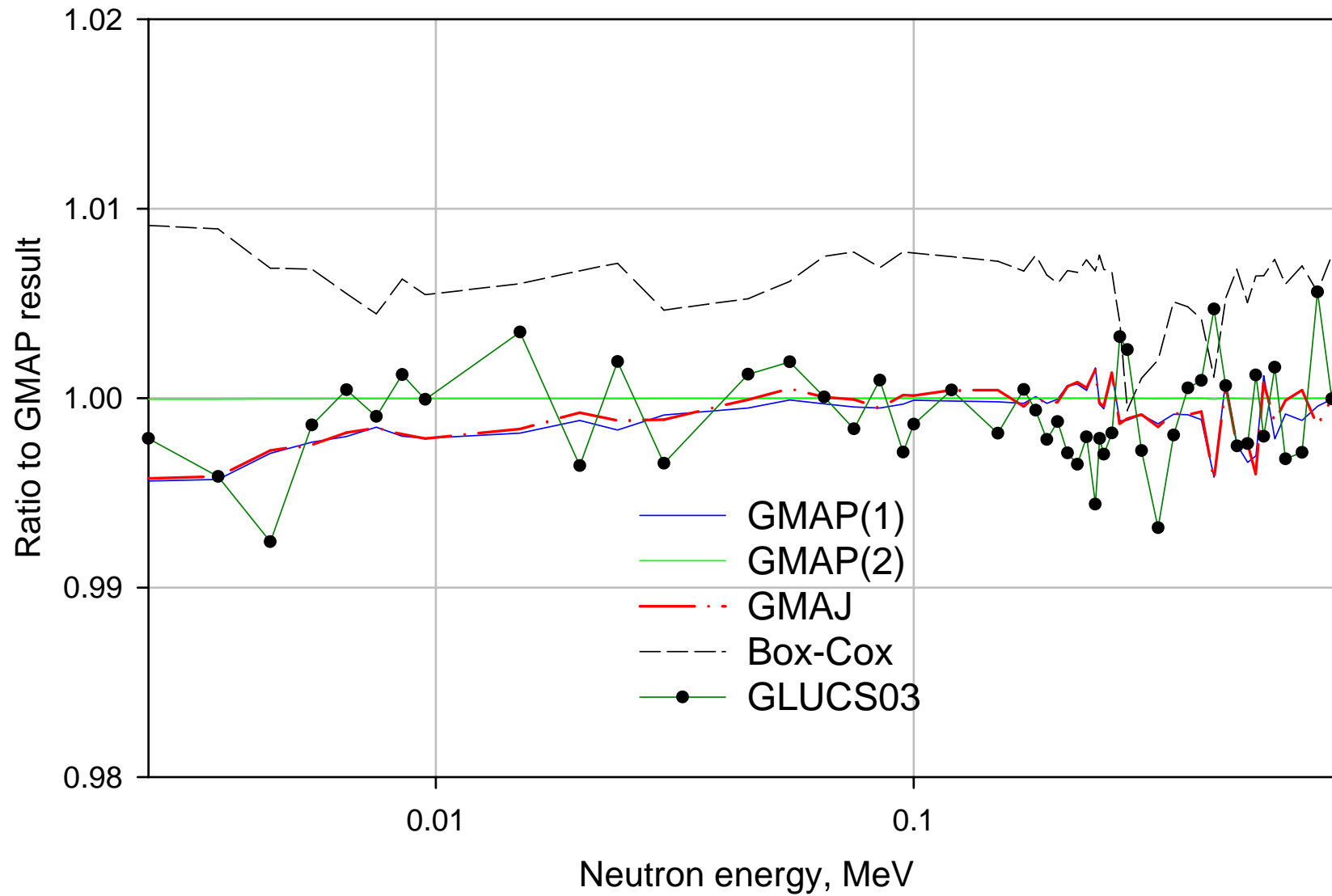


Fig. 2b. Ratios of different fits of ${}^6\text{Li}(n,t)$ cross sections to the GMAP(2) iterative fit (Chiba-Smith option).

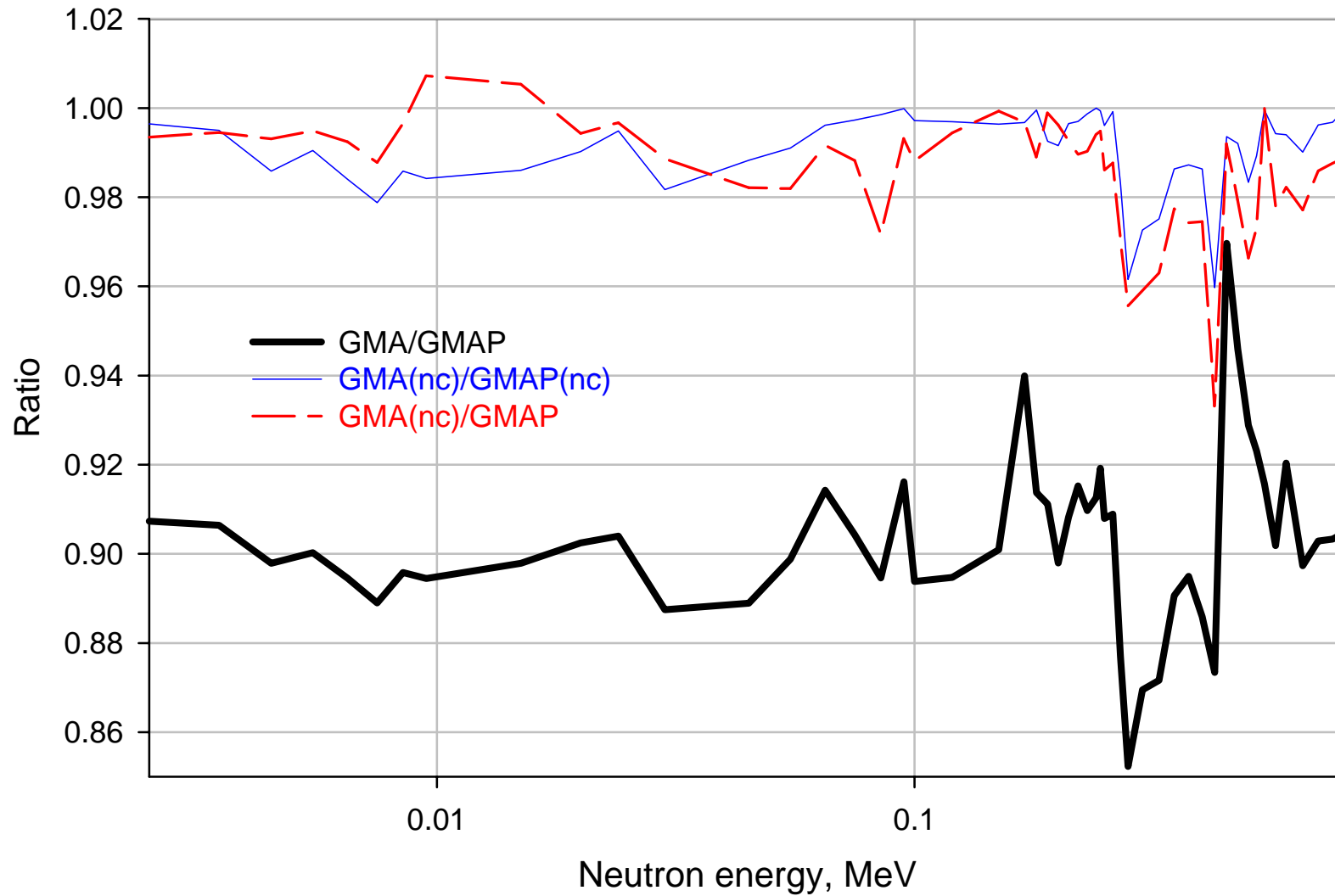


Fig. 3a. Ratios of different fits of ${}^6\text{Li}(n,t)$ cross sections showing the presence of PPP in TEST1 data and the contribution from its components. GMAP result corresponds to two iterations.

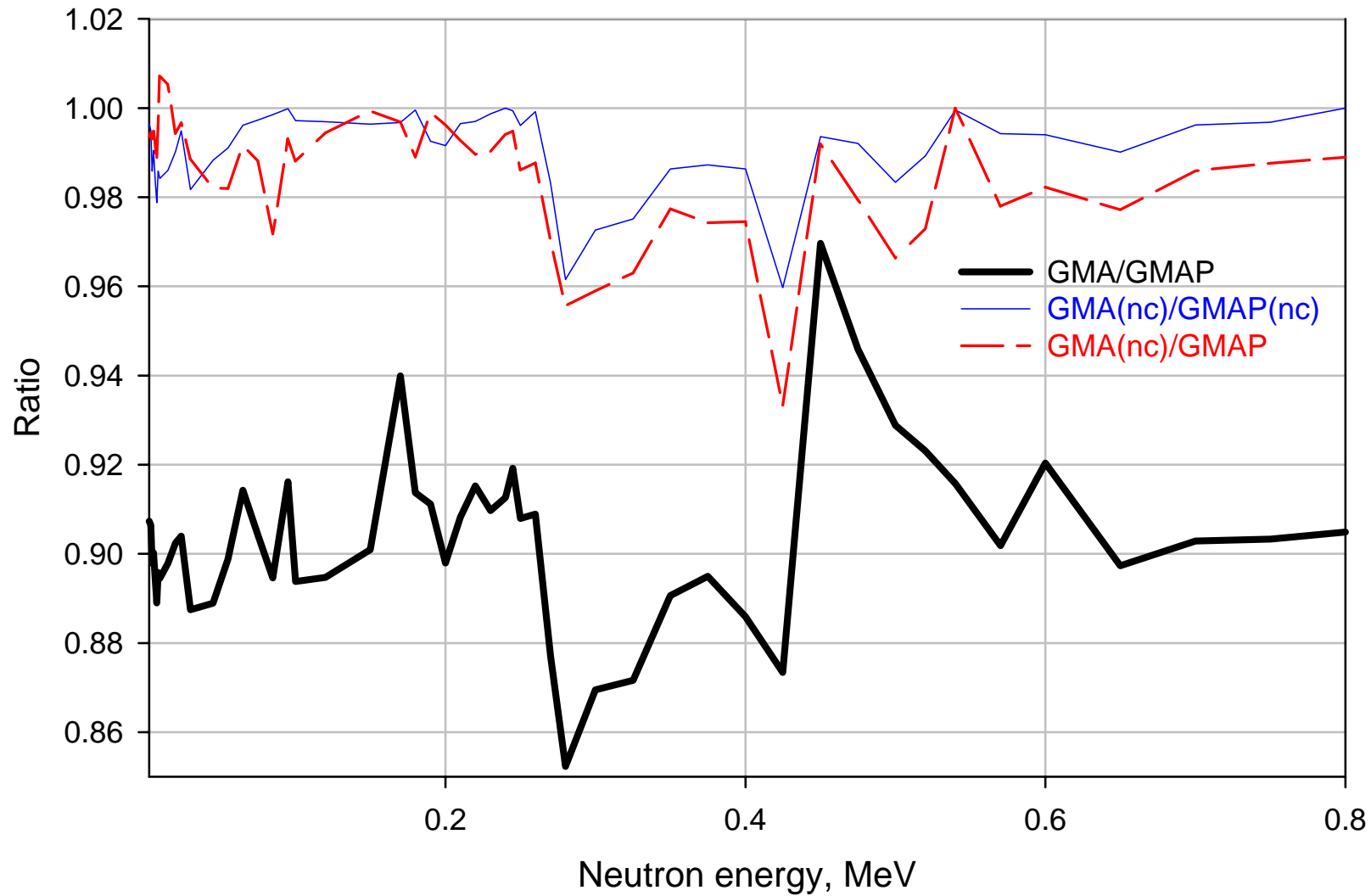


Fig. 3b. Ratios of different fits of ${}^6\text{Li}(n,t)$ cross sections showing the presence of PPP in TEST1 data and the contribution from its components. The GMAP result corresponds to two iterations.

“GMA”-“GMAP” Inter-comparisons for the Full GMA Database Combined with the RAC Result for ${}^6\text{Li}(n,t)$

D.L. Smith*, V.G. Pronyaev

NDS, IAEA

* NDS Consultant

21 November 2003

The results shown in Fig. 1 to 13 were obtained from an inter-comparison of comparable runs using a common database and two distinct operating modes of the GMA code, “GMA” (original mode) and “GMAP” (a technical fix for the PPP effect is applied). Actually, one code, now designated as GMAP, can be operated in either of these two modes by the choice of a single control-switch parameter. The “GMAP” results presented here correspond to ordinary GMA-type runs coupled with the application of the technical solution to the PPP problem proposed by Chiba-Smith that was recently implemented in the code. The ENDF/B-VI evaluations (old standards) were adopted for use as non-informative priors in the runs that employed both the “GMA” mode and the “GMAP” mode. Since this prior is non-informative, some iteration is required for calculations in the “GMAP” mode. It was found that three iterations provided excellent convergence. The choice of the Chiba-Smith approach was based largely on the fact that it was very easy to implement in GMA (effectively just a single line of computational coding plus the addition of a control-switch option). This method gives results which, for the ${}^6\text{Li}(n,t)$ reaction test problem, agree reasonably well with the approaches suggested by Oh (Box-Cox) and Kawano (logarithmic transformation of the data). Since the agreement is quite good between the Chiba-Smith, Oh, and Kawano approaches, the former was used to produce GMAP because of the above-mentioned simplicity in coding this “fix”. Chen has suggested an alternative approach to dealing with PPP whereby the least-squares formalism remains unaltered but an algorithm is used to objectively down-weight highly discrepant data by modifying the original uncertainties. In fact, in the present analysis some modifications were also made to the database to enhance the errors of highly discrepant data. The detailed approach to handling the data is somewhat different to that of Chen but the underlying concept is similar.

The calculations that produced the attached figures were carried out as follows: A set of light-element data for ${}^6\text{Li}(n,t)$ that is essentially uncorrelated to the heavy element data was used separately in a RAC analysis by Chen. This analysis also incorporated certain data not included among the standards database but that correspond to other decay channels of the ${}^7\text{Li}$ compound nuclear system, thereby making use of the capability of the R-matrix formalism to fit such data simultaneously with the corresponding introduction of important physical constraints to the evaluated results for the standard reaction channel. Chen’s analysis produced a set of evaluated values for the ${}^6\text{Li}(n,t)$ reaction along with a covariance matrix. This information was introduced into code GMAP as a single data set along with all the remaining light-element data and heavy element data in the standards database in order to perform a combination by the least-squares method, both with and without the suggested “fix” for PPP. The partitioning of the experimental data used in the RAC R-matrix analysis from the remaining data sets that are essentially uncorrelated to the former avoided “double counting” of data sets by the combination procedure. By this means, the present exercise was designed to conform, as much as is possible at this time, to future runs that ultimately will generate the final intended standards evaluation.

A remaining task to be addressed by this work in the near future is the development of a procedure to introduce $^{10}\text{B}(n,\alpha_0)$ and $^{10}\text{B}(n,\alpha_1)$ cross-correlated information as one single data block in the GMA input. The full covariance/correlation matrix, which will include lower triangles for covariance matrices for $^{10}\text{B}(n,\alpha_0)$ and $^{10}\text{B}(n,\alpha_1)$ plus a rectangular block of cross-covariances/cross-correlations between these two reactions, should be provided by the R-matrix evaluators for use in the combining procedure with code GMAP.

The attached figures all show the difference obtained between the “GMAP” and “GMA” calculations for a common database along with the experimental data and their errors. By this means the degree to which the “GMAP” analysis “corrects” for PPP effects is demonstrated. The trend of the PPP effect, if not corrected, to produce results that are apparently “too low” is evident. In general, the magnitude of the PPP effect tends to become larger at the higher energies, most likely because the discrepancies there are also larger. In those reactions containing a very accurate thermal value included in the data set, the PPP effect is essentially non-existent at very low energies since the thermal value dominates the evaluation.

General conclusion is the following. Effects of PPP in GMA database are rather small, usually in the limits of 30% of uncertainty of the evaluated data. Small $^{235}\text{U}(n,f)$ cross section increase for E_n below 1 MeV will lead even to better agreement with the Godiva benchmark data.

The following specific comments apply to the indicated reactions:

$^6\text{Li}(n,t)$: small, up to 0.2% increase of the cross section is observed in the high energy of the “standard” region. Increase is in the limits of uncertainty of evaluated data.

$^6\text{Li}(n,n)$: no visible bias.

$^{10}\text{B}(n,\alpha_0)$: the presence of PPP is clearly seen for energy above 0.2 MeV.

$^{10}\text{B}(n,\alpha_1)$: the presence of PPP leads to an increase of the cross sections at the level of 30% of uncertainty of evaluated data for E_n below 0.2 MeV.

$^{10}\text{B}(n,n)$: small bias (0.3%) which is negligible compared with the uncertainty of the evaluated data.

$^{197}\text{Au}(n,\gamma)$: large PPP effect (1% bias) is observed.

$^{238}\text{U}(n,\gamma)$: large PPP effect (1 - 1.5% bias) is observed.

$^{235}\text{U}(n,f)$: local PPP effect is observed for E_n below 1 MeV and above 30 MeV. The bias above 30 MeV is 30% from uncertainty of the evaluated data.

$^{239}\text{Pu}(n,f)$: similar behaviour as for $^{235}\text{U}(n,f)$ with slightly larger bias.

$^{238}\text{U}(n,f)$: practically constant 0.2 – 0.3 % bias for E_n below 20 MeV and similar to the $^{235}\text{U}(n,f)$ and $^{239}\text{Pu}(n,f)$ behaviour for E_n above 30 MeV.

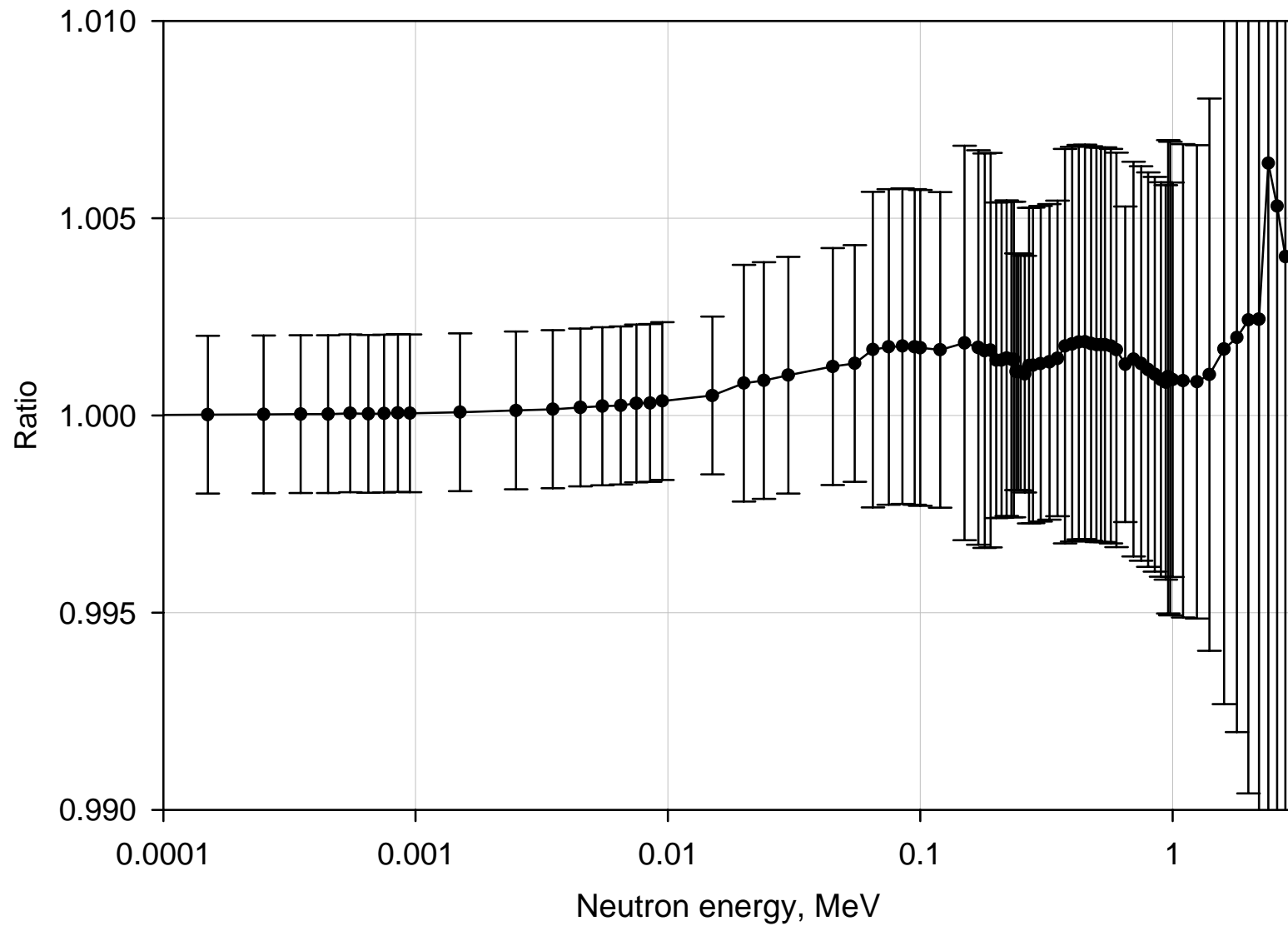
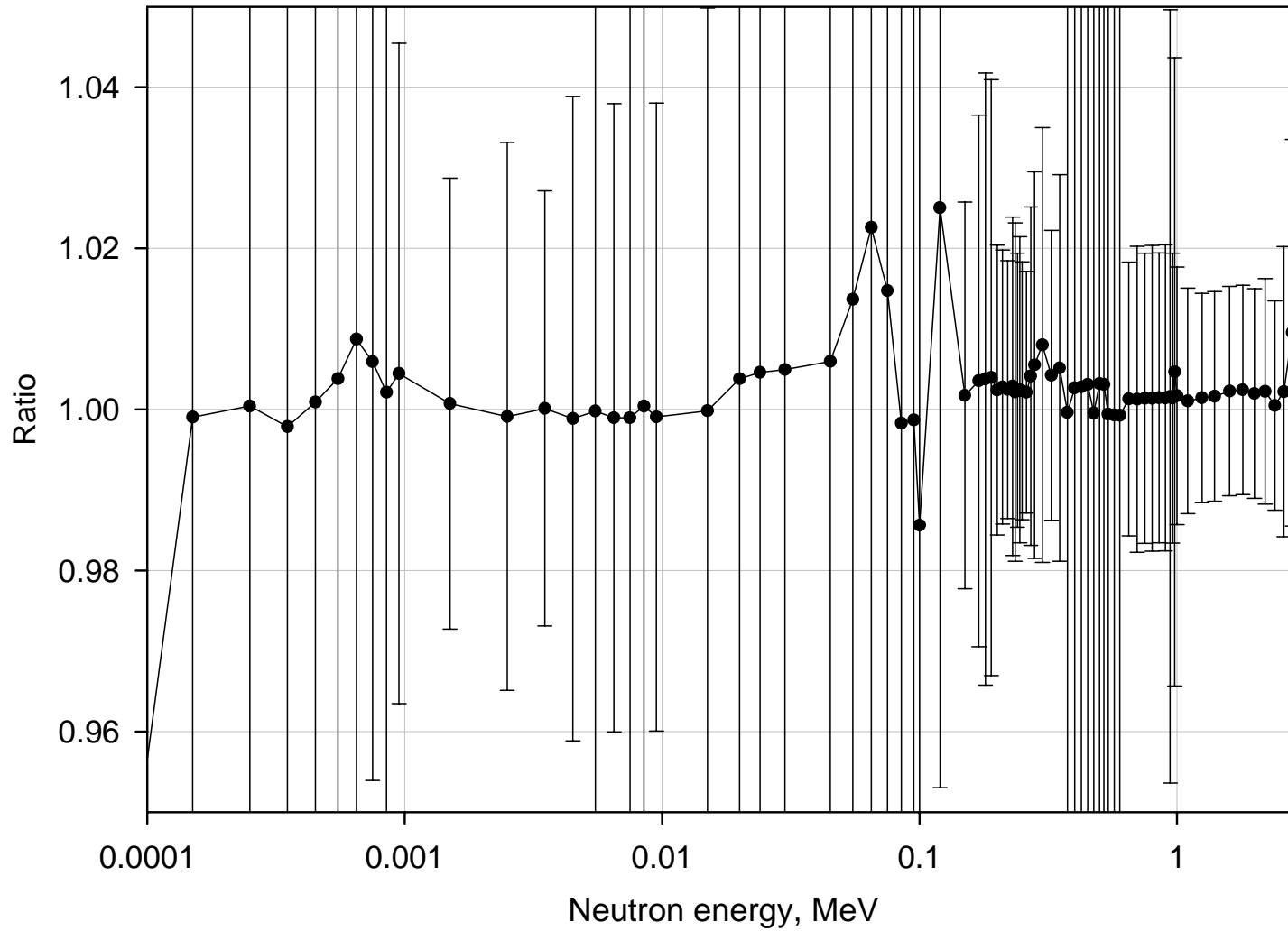


Fig. 1. Ratio of GMAP fit with using of Chiba-Smith option to exclude PPP to the standard GMA fit for ${}^6\text{Li}(n,t)$ reaction.



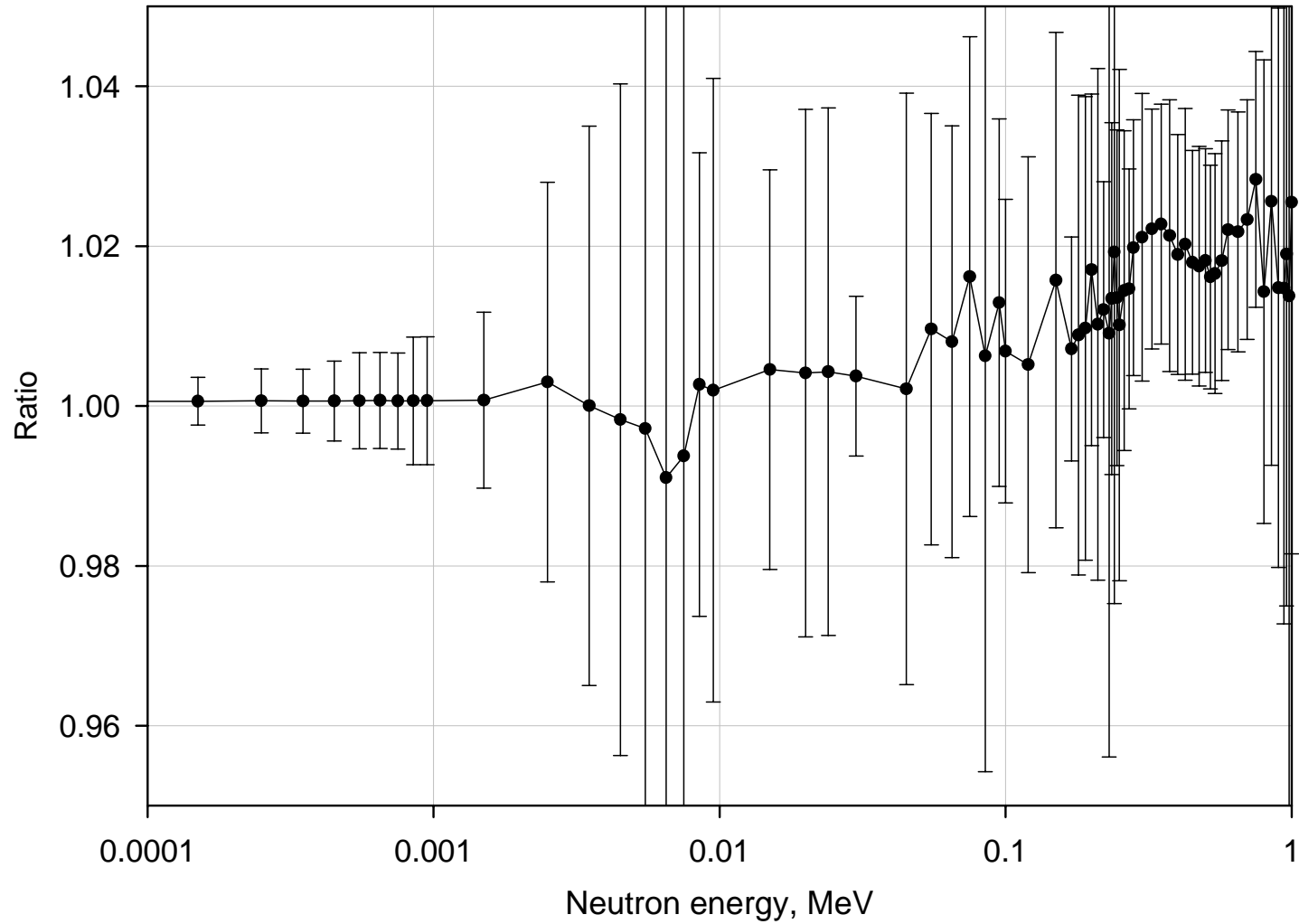


Fig. 3. Ratio of GMAP fit with using of Chiba-Smith option to exclude PPP to the standard GMA fit for $^{10}\text{B}(n,\alpha_0)$ reaction.

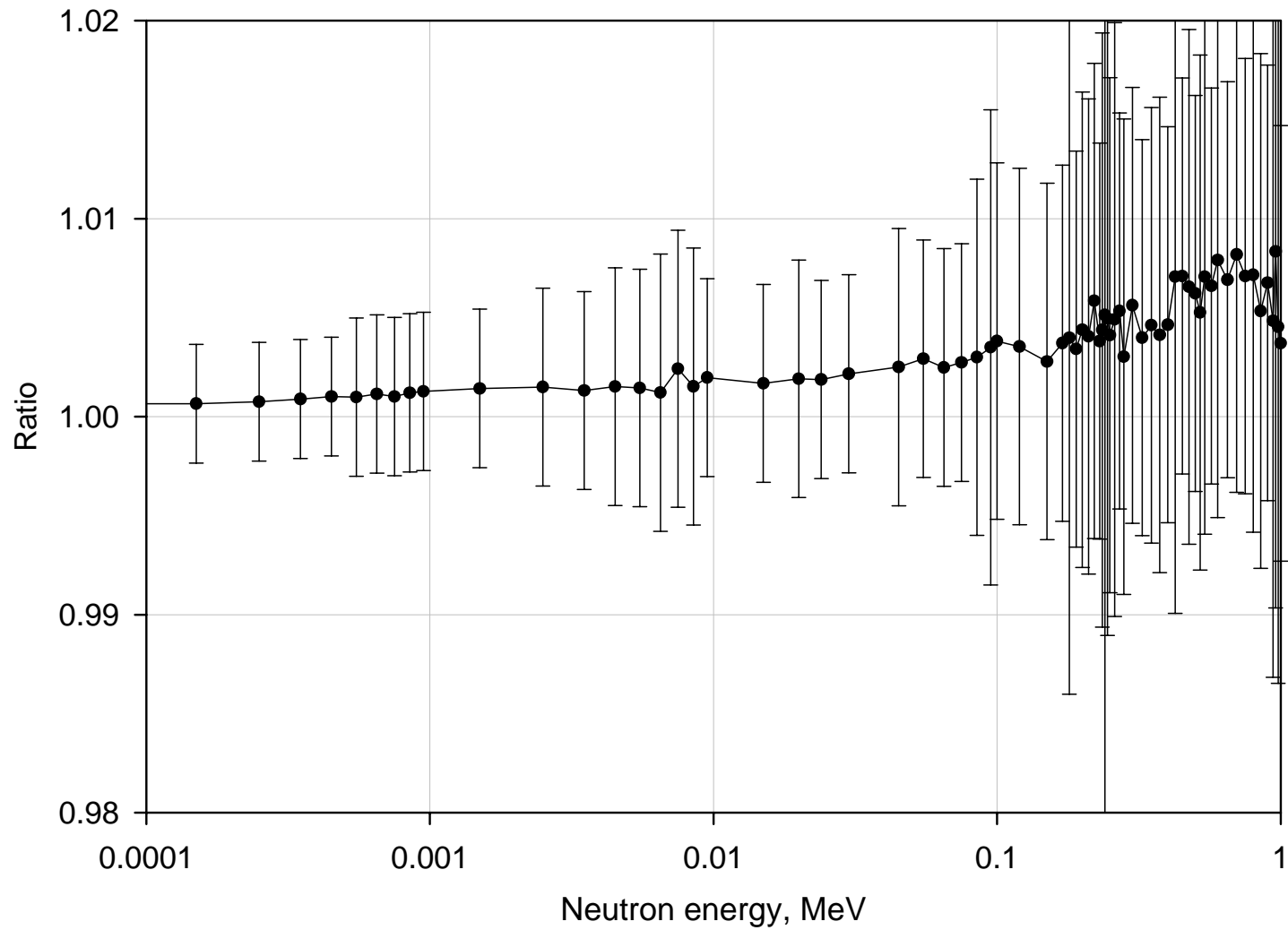


Fig. 4. Ratio of GMAP fit with using of Chiba-Smith option to exclude PPP to the standard GMA fit for $^{10}\text{B}(n,\alpha_1)$ reaction.

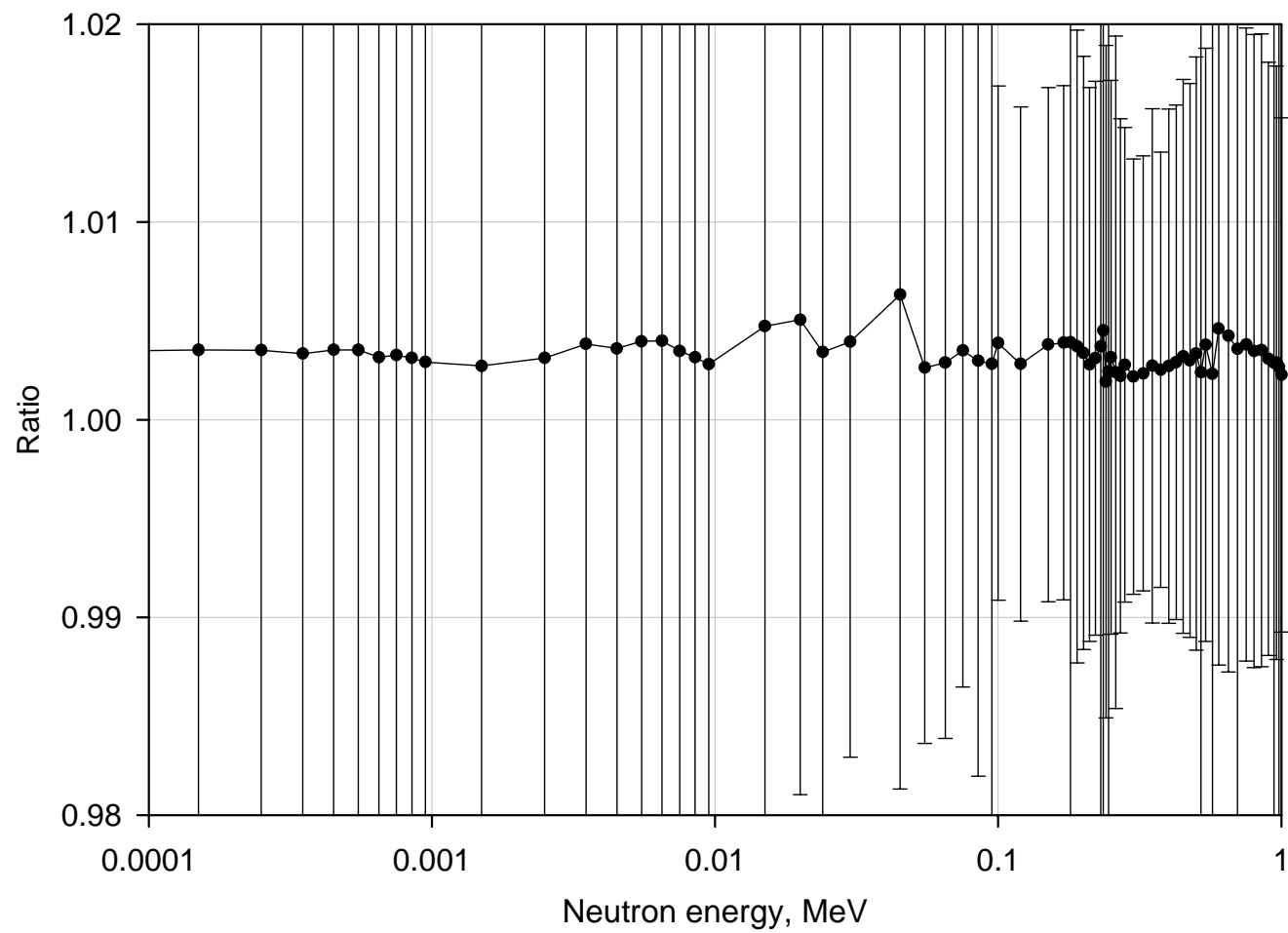


Fig. 5. Ratio of GMAP fit with using of Chiba-Smith option to exclude PPP to the standard GMA fit for $^{10}\text{B}(n,n)$ reaction.

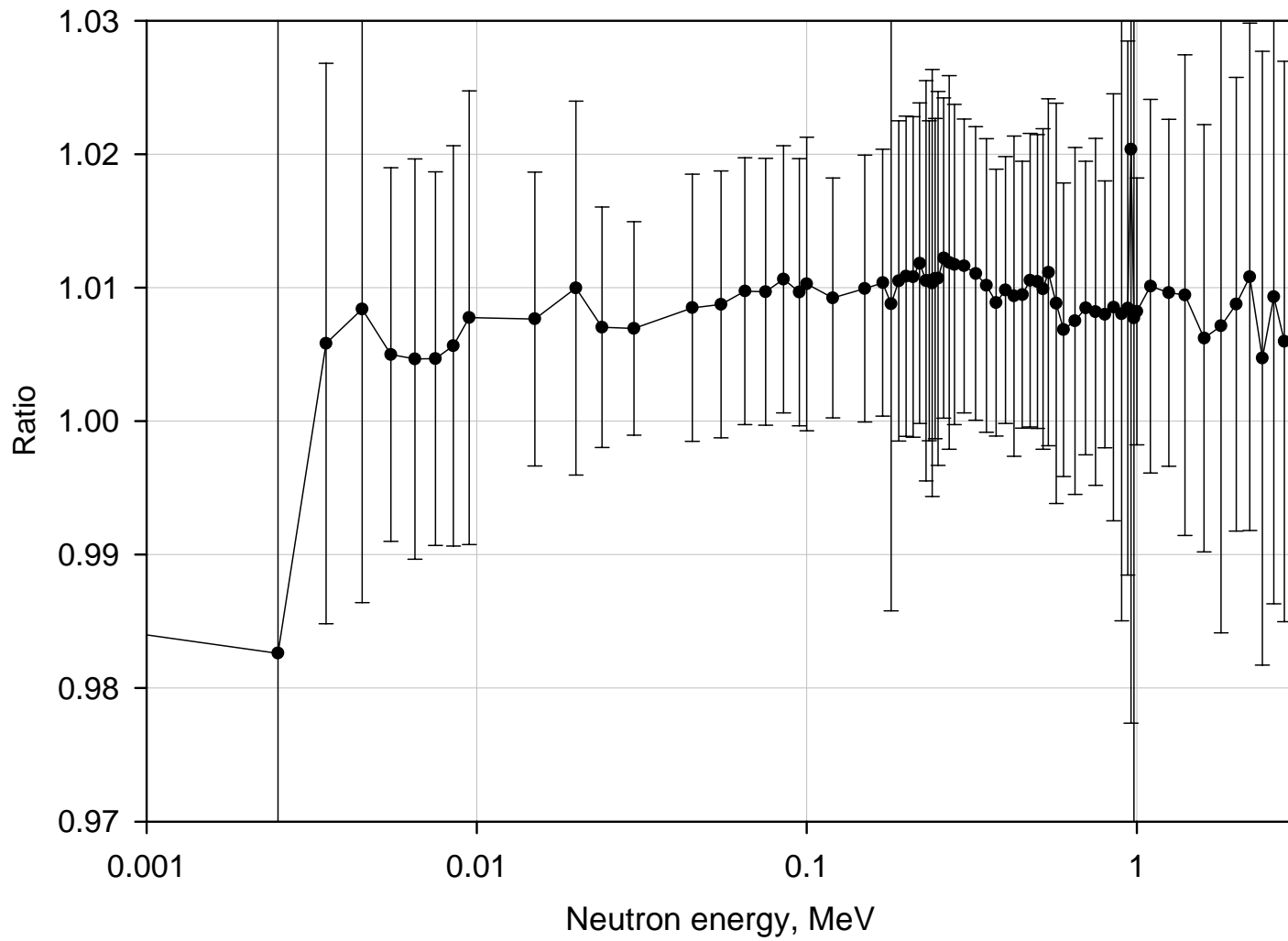


Fig. 6. Ratio of GMAP fit with using of Chiba-Smith option to exclude PPP to the standard GMA fit for $^{197}\text{Au}(n,\gamma)$ reaction.

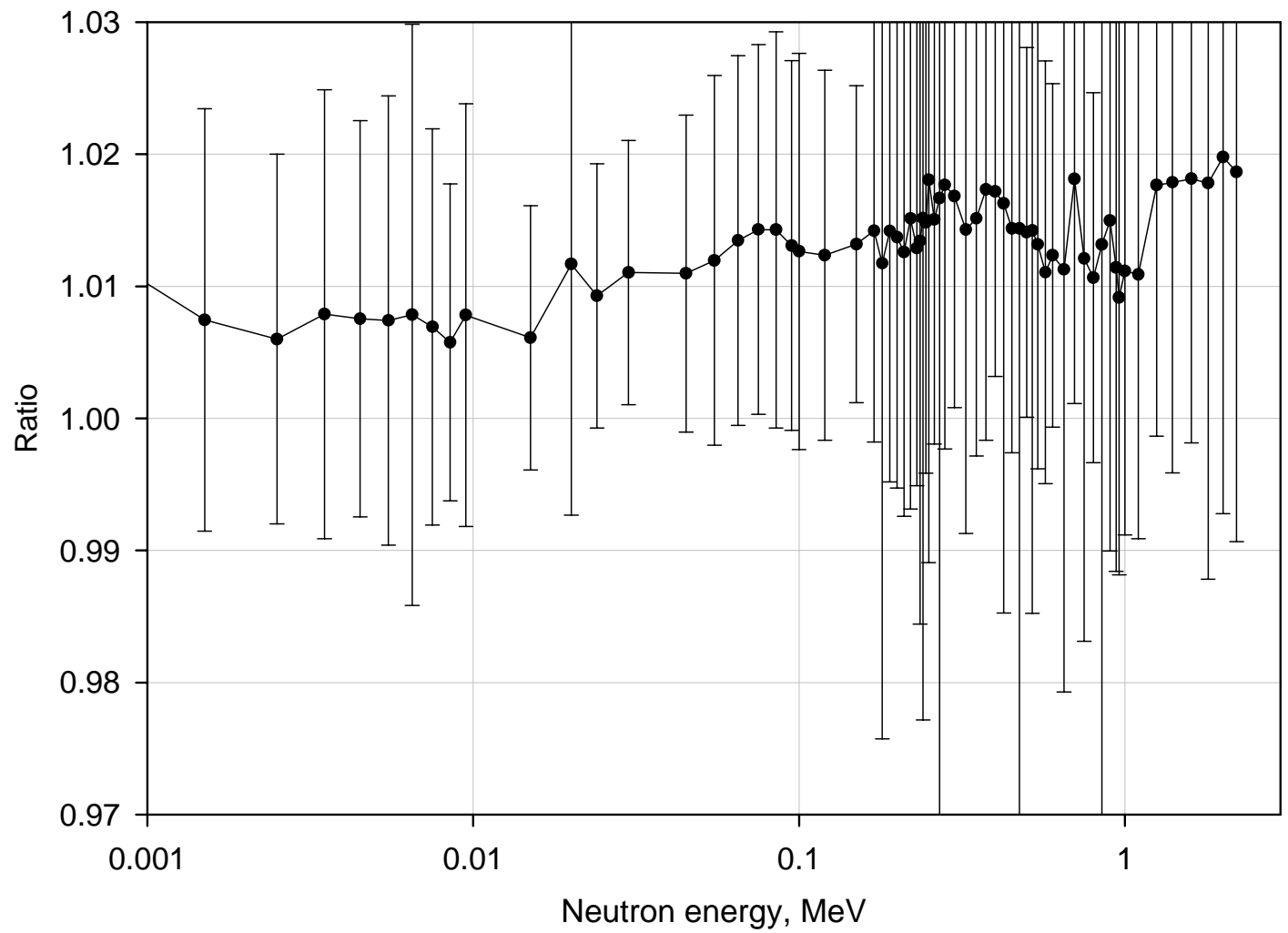


Fig. 7. Ratio of GMAP fit with using of Chiba-Smith option to exclude PPP to the standard GMA fit of $^{238}\text{U}(n,\gamma)$.

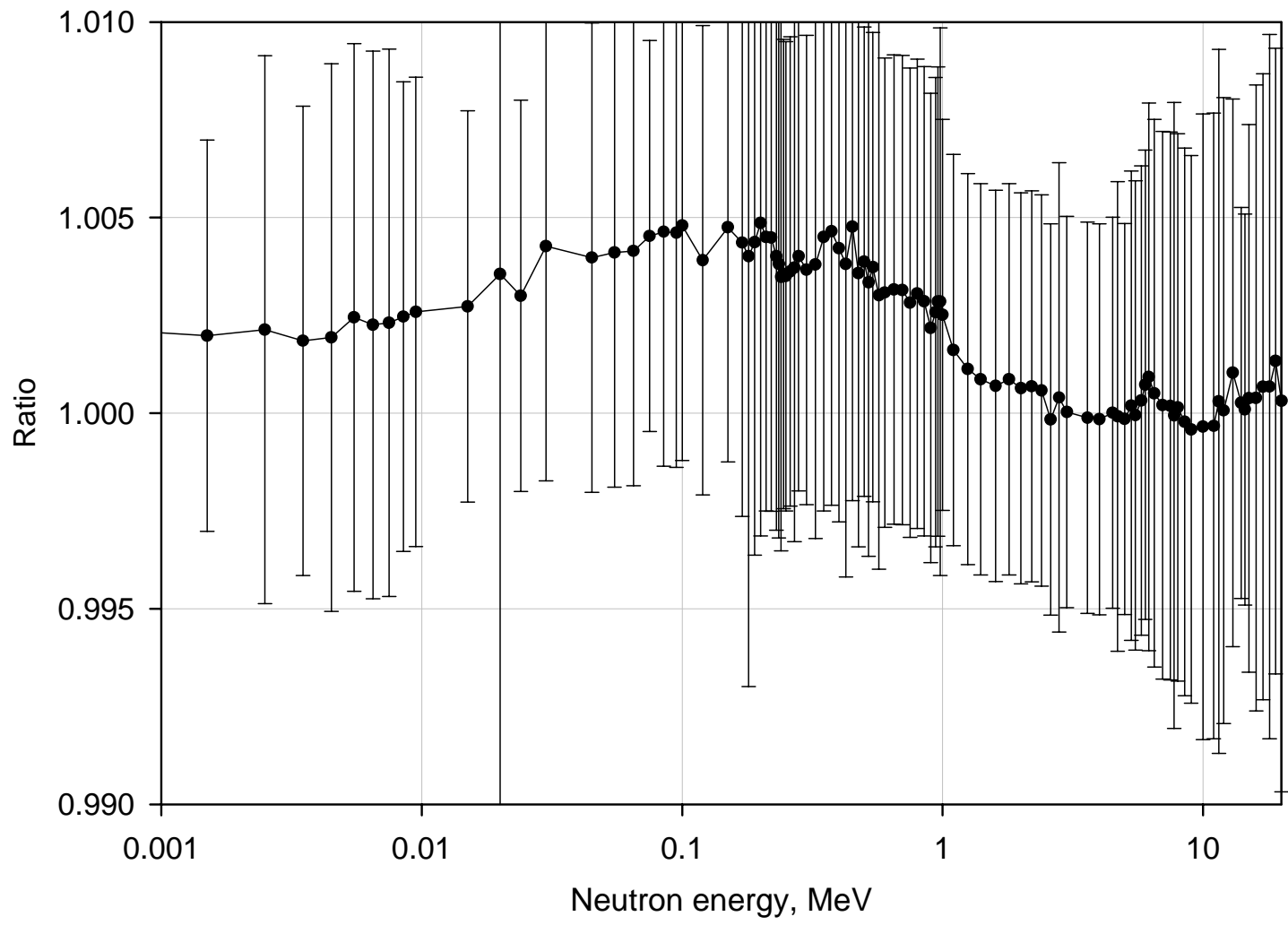


Fig. 8. Ratio of GMAP fit with using of Chiba-Smith option to exclude PPP to the standard GMA fit of $^{235}\text{U}(n,f)$.

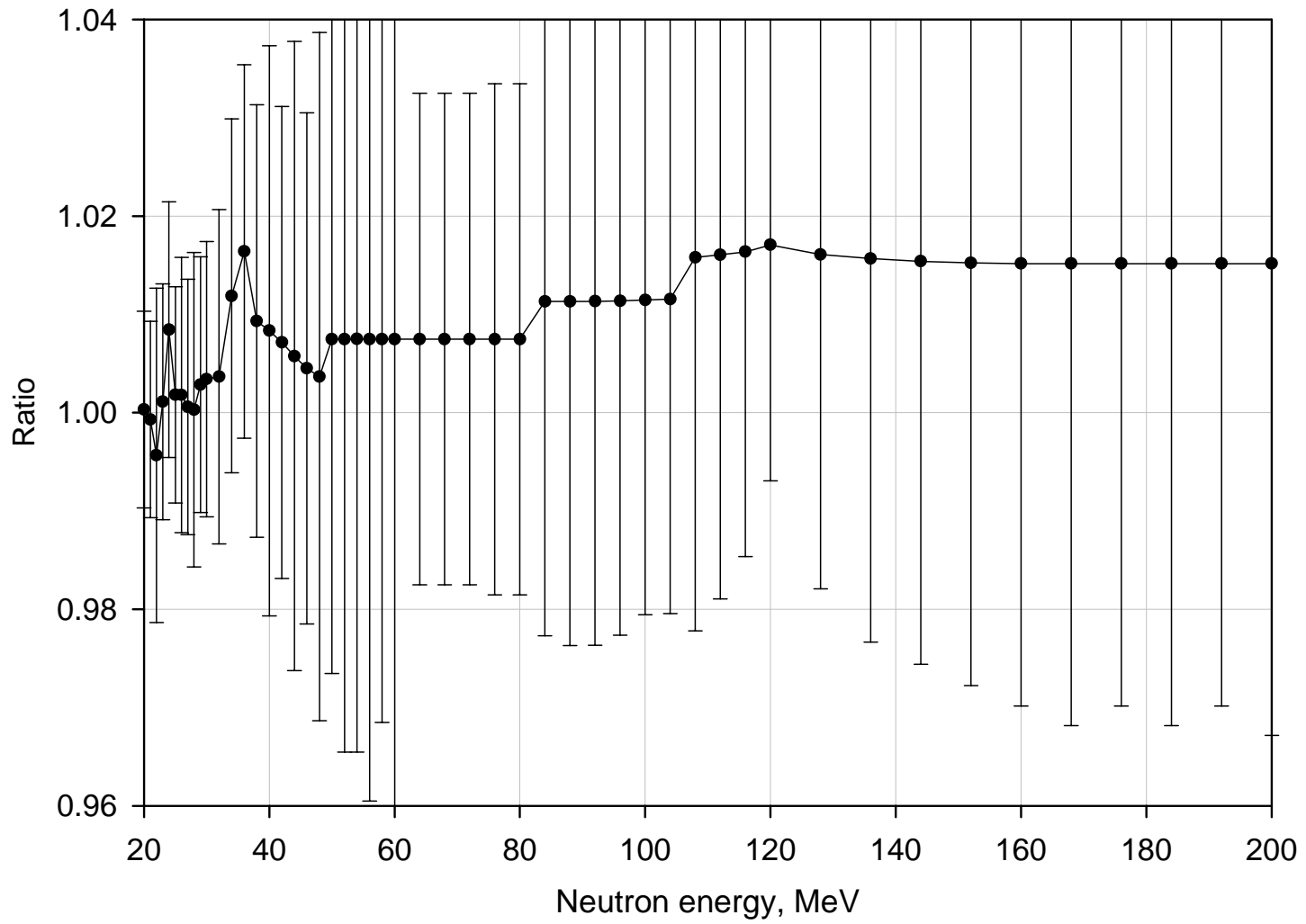


Fig. 9. Ratio of GMAP fit with using of Chiba-Smith option to exclude PPP to the standard GMA fit of $^{235}\text{U}(n,f)$.

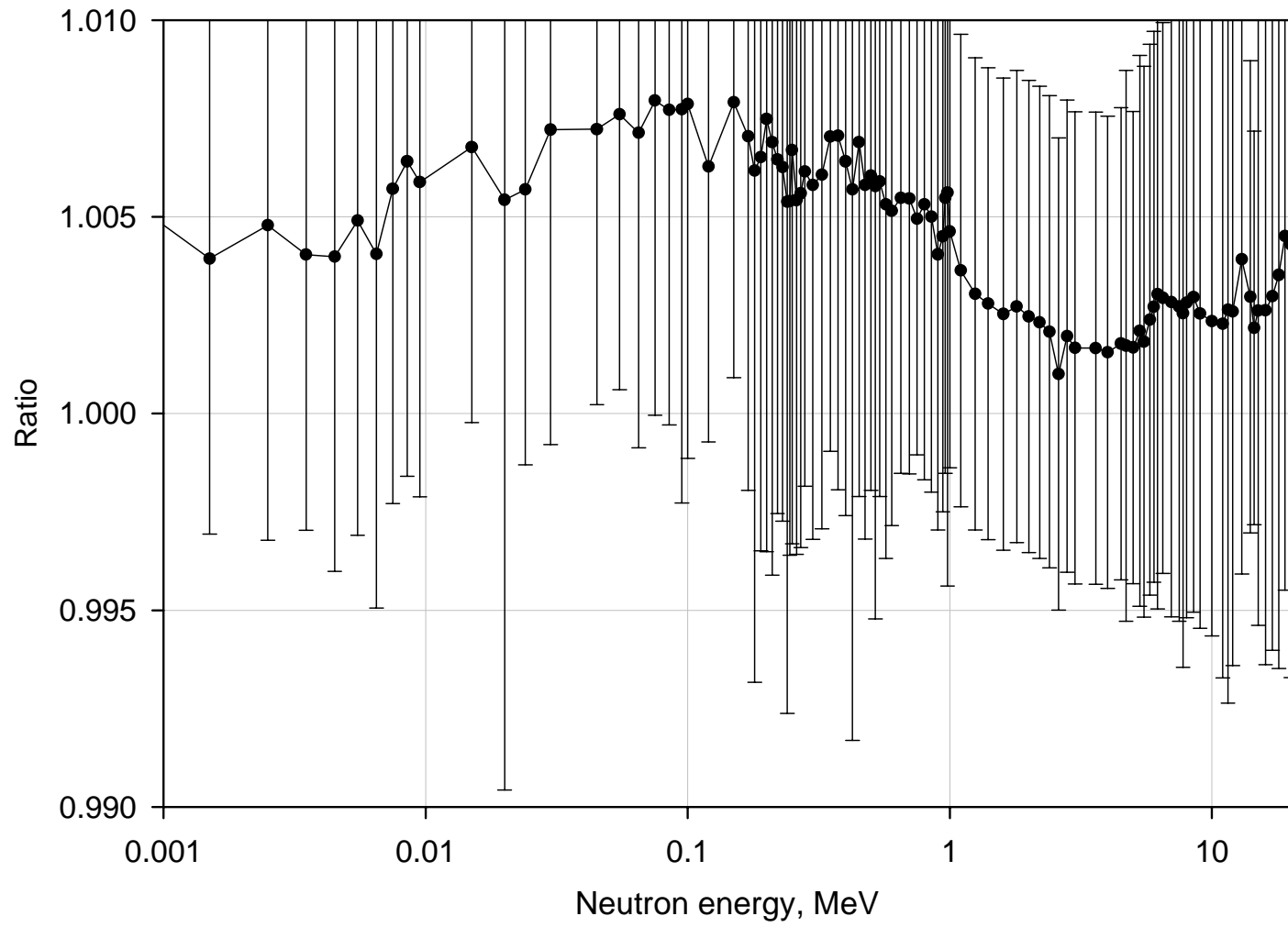


Fig. 10. Ratio of GMAP fit with using of Chiba-Smith option to exclude PPP to the standard GMA fit of $^{239}\text{Pu}(n,f)$.

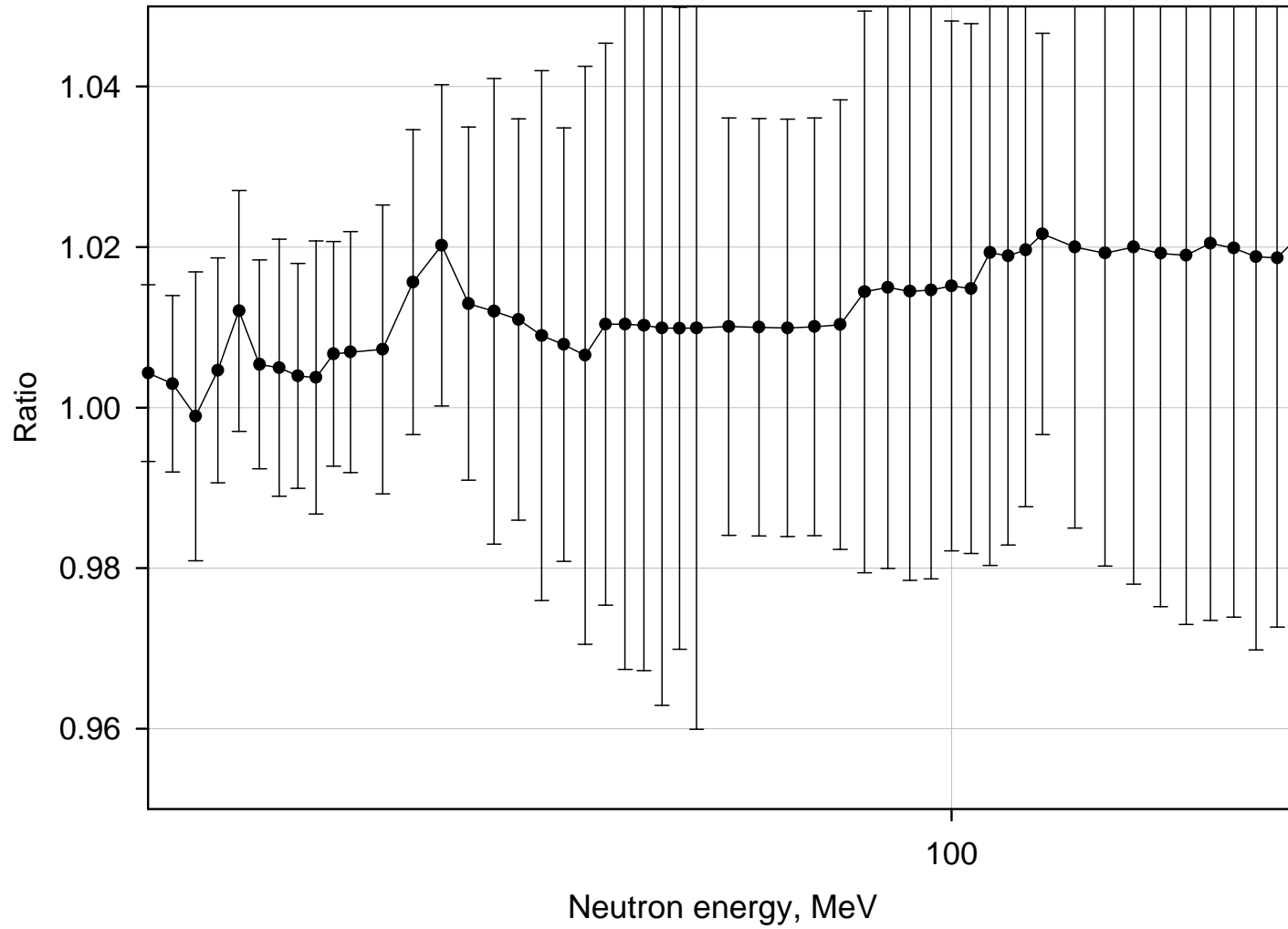


Fig. 11. Ratio of GMAP fit with using of Chiba-Smith option to exclude PPP to the standard GMA fit of $^{239}\text{Pu}(n,f)$.

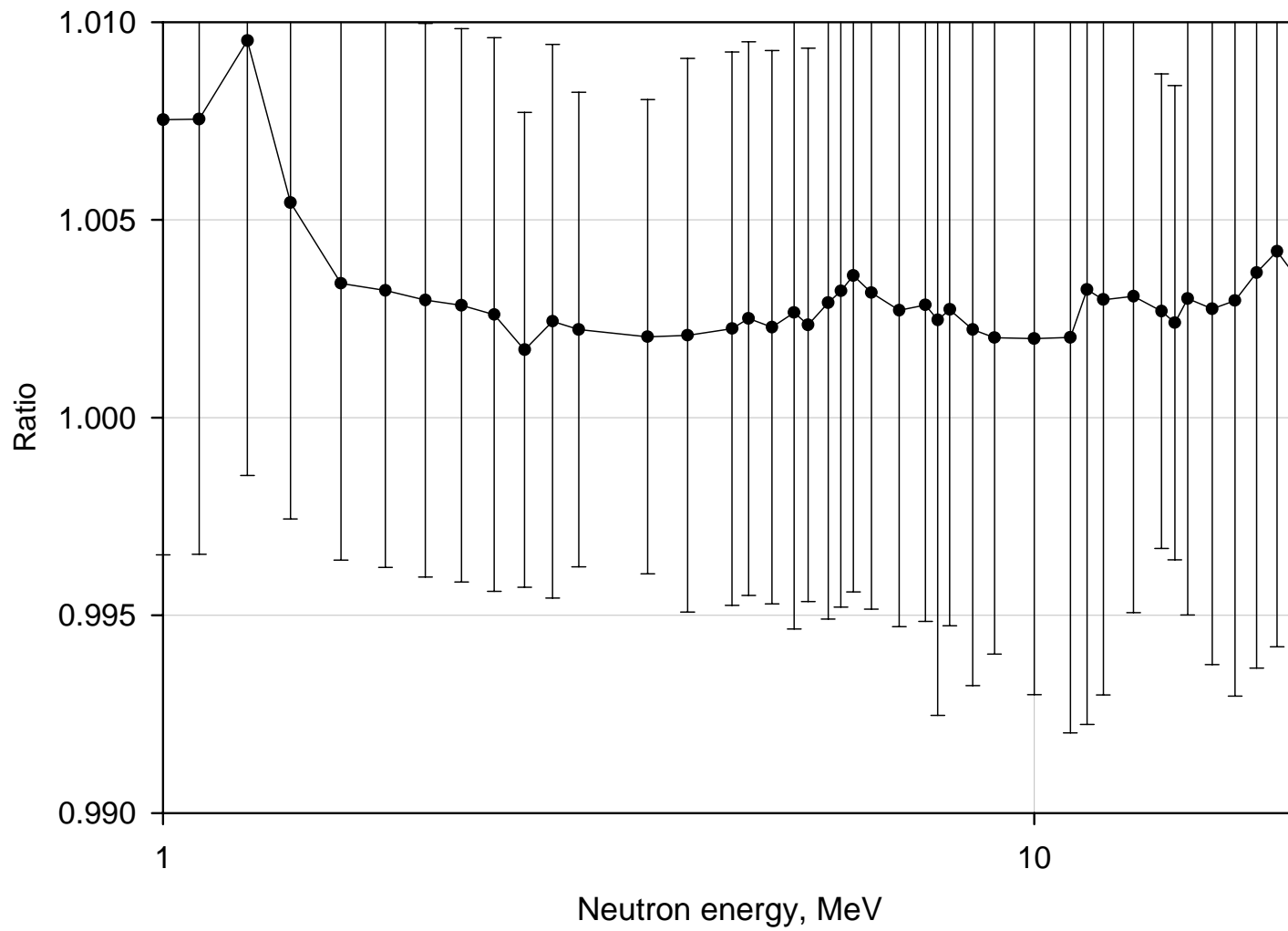


Fig. 12. Ratio of GMAP fit with using of Chiba-Smith option to exclude PPP to the standard GMA fit of $^{238}\text{U}(n,f)$.

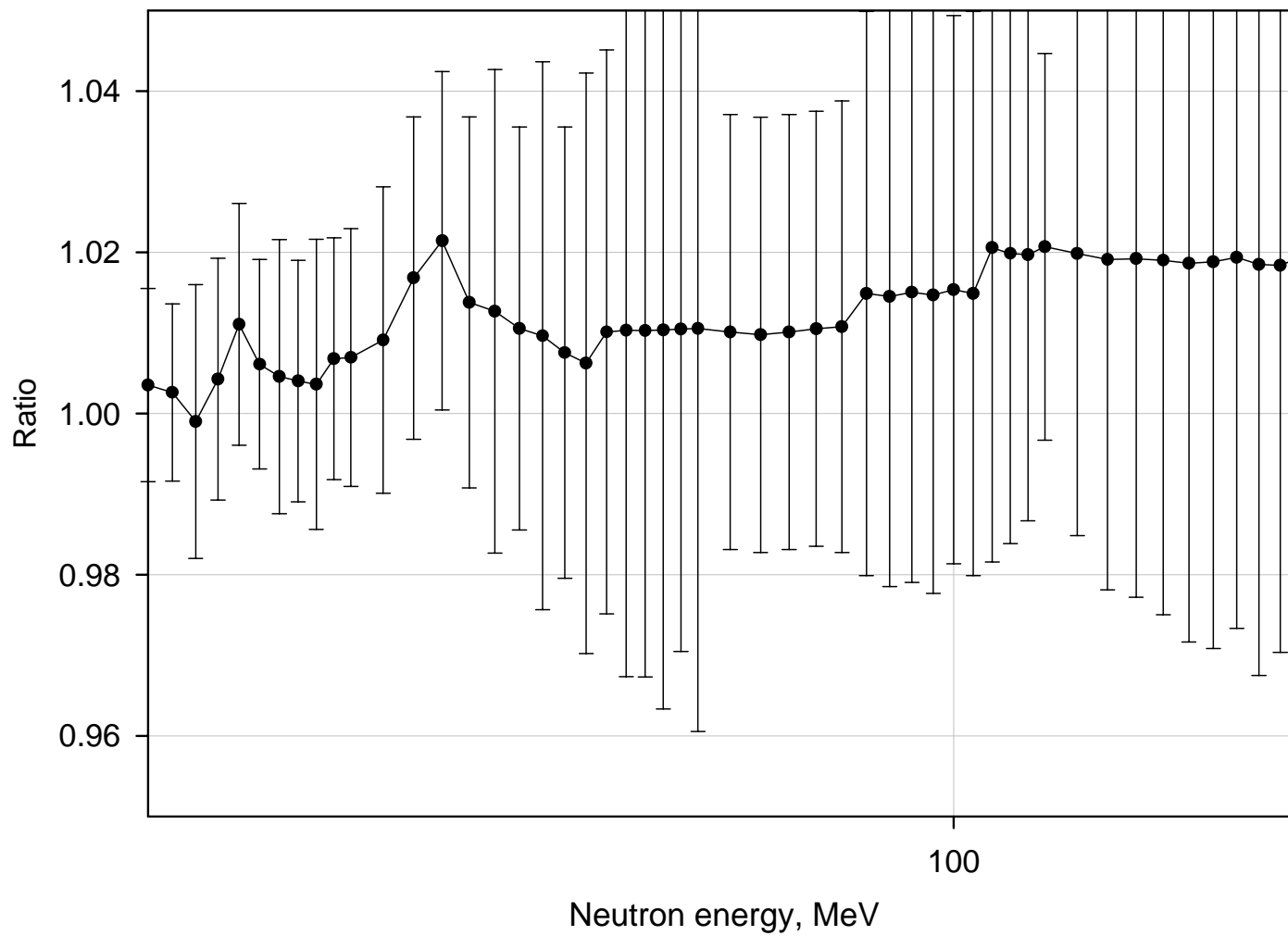


Fig. 13. Ratio of GMAP fit with using of Chiba-Smith option to exclude PPP to the standard GMA fit of $^{238}\text{U}(n,f)$.

The Least Squares Method Formulation with Account of Systematic Errors

E.V.Gai*

Nuclear Data Section, IAEA, Vienna

*IAEA consultant

17 December 2003

Use of the Least Squares Method for simultaneous processing of huge data sets is essentially complicated by two mathematic problems – one arises if regression function is not linear in parameters and second is connected with inversion of "poorly conditioned" covariance matrix of experimental errors in the case when they are correlated. The first problem can be successfully circumvented by method of discrete optimisation of rational approximants [1] and way to circumvent the second is described in this article.

In the case of correlated errors each experimental result can be presented as sum of unknown true value and unknown statistic (random) and systematic errors:

$$Y_i^K = y(x_i^K) + \varepsilon_i^K + \sum_l \lambda_l^K g_l(x_i^K), \quad (1)$$

here Y_i^K - experimental value from set (work) #K corresponding to energy x_i^K , $y(x)$ – true value (unknown, the goal of statistical analyses is estimation of this value), ε_i^K - statistical error of this measurement (unknown to us sample value, not dispersion!), $g_l(x)$ - l-th component of systematic error, λ_l^K - amplitude of this component for set #K (again unknown sample value, not dispersion).

Functional to minimise in Least Squares Method (χ^2 -function) is

$$S = \frac{1}{2} \sum_{i,K_1;m,K_2} \Delta Y_i^{K_1} (\mathbf{R}^{-1})_{i,K_1;m,K_2} \Delta Y_m^{K_2} = \frac{1}{2} \Delta \mathbf{Y} \mathbf{R}^{-1} \Delta \mathbf{Y}^T, \quad (2)$$

where $\Delta Y_i^K = Y_i^K - y(x_i^K)$, $\Delta \mathbf{Y}$ - row vector with length equal to full number of experimental points

$N = \sum_{K=1}^M N_K$ and \mathbf{R} is covariance matrix of experimental errors (rank N),

$$\mathbf{R} = \langle \Delta \mathbf{Y}^T \Delta \mathbf{Y} \rangle = \langle (\boldsymbol{\varepsilon}^T + \mathbf{g}^T \boldsymbol{\lambda}^T)(\boldsymbol{\varepsilon} + \boldsymbol{\lambda} \mathbf{g}) \rangle = \langle \boldsymbol{\varepsilon}^T \boldsymbol{\varepsilon} \rangle + \mathbf{g}^T \langle \boldsymbol{\lambda}^T \boldsymbol{\lambda} \rangle \mathbf{g}, \quad (3)$$

statistical and systematic errors are, by definition, mutually independent. "Poor conditioning" of matrix \mathbf{R} complicates it's inversion.

Covariance matrix of statistic errors is diagonal $N \times N$ matrix with elements $\langle (\varepsilon_i^K)^2 \rangle$, let us denote it by \mathbf{S} . Matrix \mathbf{g} is block matrix of components of systematic errors,

$$\mathbf{g} = \begin{pmatrix} \mathbf{g}_1 & \mathbf{0} & \mathbf{0} & \mathbf{0} \\ \mathbf{0} & \mathbf{g}_2 & \mathbf{0} & \mathbf{0} \\ \mathbf{0} & \mathbf{0} & \mathbf{g}_3 & \mathbf{0} \\ \vdots & \vdots & \vdots & \vdots \end{pmatrix}, \quad (4)$$

block \mathbf{g}_K corresponds to K-th work and has L rows (L - number of components of systematic error) and N_K columns, so \mathbf{g} has $L \times M$ rows and N columns. Row vector

$\boldsymbol{\lambda} = (\lambda_1^1, \lambda_2^1, \dots, \lambda_L^1, \dots, \lambda_1^K, \lambda_2^K, \dots, \lambda_L^K, \dots, \lambda_1^M, \lambda_2^M, \dots, \lambda_L^M, \dots)$ with $L \times M$ elements describes sample values of amplitudes of systematic errors - λ_l^K corresponds to amplitude of l-th component for K-th

work. So $\boldsymbol{\lambda} \mathbf{g}$ is row vector of N systematic errors with elements $\sum_{l=1}^L \lambda_l^K g_l(x_i^K)$. Note that $\mathbf{g}^T \boldsymbol{\lambda}^T \boldsymbol{\lambda} \mathbf{g}$ is, as

\mathbf{R} too, matrix of rank N (full number of experimental points), but matrix $\boldsymbol{\lambda}^T \boldsymbol{\lambda}$ has rank only $L \times M$. Mathematic expectation of $\boldsymbol{\lambda}^T \boldsymbol{\lambda}$ gives us covariance matrix of amplitudes of systematic error components. It is block matrix \mathbf{W} with $M \times M$ blocks, each block is diagonal because different components of systematic error are independent,

$$\mathbf{W}_{K_1 K_2} = \begin{pmatrix} \langle \lambda_1^{K_1} \lambda_1^{K_2} \rangle & 0 & 0 & 0 \\ 0 & \langle \lambda_2^{K_1} \lambda_2^{K_2} \rangle & 0 & 0 \\ 0 & 0 & \dots & 0 \\ 0 & 0 & 0 & \langle \lambda_L^{K_1} \lambda_L^{K_2} \rangle \end{pmatrix} \quad (5)$$

And now we can write functional (2) as

$$S = \frac{1}{2} \Delta \mathbf{Y} \mathbf{R}^{-1} \Delta \mathbf{Y}^T = \frac{1}{2} \Delta \mathbf{Y} (\mathbf{S} + \mathbf{g}^T \mathbf{W} \mathbf{g})^{-1} \Delta \mathbf{Y}^T. \quad (6)$$

In (6) covariance matrix is presented as sum of statistic and systematic parts, but it still needs to be inverted, so it does not give us similar partition of χ^2 -function, because even in simple algebra $(\mathbf{A} + \mathbf{B})^{-1} \neq (\mathbf{A}^{-1} + \mathbf{B}^{-1})$.

Let us examine another LSM functional which is sum of parts, corresponding to statistic and systematic errors:

$$S_1 = \frac{1}{2} \left((\Delta \mathbf{Y} - \boldsymbol{\lambda} \mathbf{g}) \mathbf{S}^{-1} (\Delta \mathbf{Y}^T - \mathbf{g}^T \boldsymbol{\lambda}^T) + \boldsymbol{\lambda} \mathbf{W}^{-1} \boldsymbol{\lambda}^T \right) \quad (7)$$

here $\Delta \mathbf{Y} - \boldsymbol{\lambda} \mathbf{g}$ is row vector with N components $(Y_i^K - y(x_i^K) - \sum_{l=1}^L \lambda_l^K g_l(x_i^K))$ - sample value of statistic error

for i -th point of K -th work. This functional is more simple than S (2) in sense of matrix algebra – now it is necessary to inverse separately diagonal matrix \mathbf{S} and matrix \mathbf{W} with rank equal to $L \times M$, and not a nondiagonal matrix \mathbf{R} with rank N , but now we have $L \times M$ more unknown values of amplitudes of systematic error. Then we shall estimate them in the frames of LSM from system of M linear in λ equations

$$\frac{\partial S_1}{\partial \lambda_i^K} = 0, \quad (8)$$

that gives us

$$\tilde{\boldsymbol{\lambda}} = \Delta \mathbf{Y} \mathbf{S}^{-1} \mathbf{g}^T (\mathbf{g} \mathbf{S}^{-1} \mathbf{g}^T + \mathbf{W}^{-1})^{-1}. \quad (9)$$

Inserting (9) in (7) it is possible to obtain the next expression for LSM functional with estimated systematic errors:

$$\tilde{S}_1 = \frac{1}{2} (\Delta \mathbf{Y} \mathbf{S}^{-1} \Delta \mathbf{Y}^T - \Delta \mathbf{Z} \mathbf{U}^{-1} \Delta \mathbf{Z}^T) \equiv \frac{1}{2} \Delta \mathbf{Y} \mathbf{V}^{-1} \Delta \mathbf{Y}^T \quad (10)$$

where

$$\Delta \mathbf{Z} = \Delta \mathbf{Y} \mathbf{S}^{-1} \mathbf{g}^T \quad (11)$$

and

$$\mathbf{U} = \mathbf{g} \mathbf{S}^{-1} \mathbf{g}^T + \mathbf{W}^{-1} \equiv \mathbf{F} + \mathbf{W}^{-1}$$

$$\mathbf{V}^{-1} = \mathbf{S}^{-1} - \mathbf{S}^{-1} \mathbf{g}^T \mathbf{U}^{-1} \mathbf{g} \mathbf{S}^{-1}. \quad (12)$$

Functional (10) has the same matrix properties as (7) and contains only experimental values, covariance matrixes of statistic and systematic experimental errors and regression function, so it is possible to apply to it LSM without inversion of “poorly conditioned” matrix of rank N !

In (2) we have covariance matrix \mathbf{R} and in (10) we have covariance matrix \mathbf{V} . Let us look at their composition, (\mathbf{E} –unit matrix)

$$\begin{aligned} \mathbf{R}\mathbf{V}^{-1} &= (\mathbf{S} + \mathbf{g}^T\mathbf{W}\mathbf{g})(\mathbf{S}^{-1} - \mathbf{S}^{-1}\mathbf{g}^T\mathbf{U}^{-1}\mathbf{g}\mathbf{S}^{-1}) = \\ \mathbf{E} - \mathbf{g}^T\mathbf{U}^{-1}\mathbf{g}\mathbf{S}^{-1} + \mathbf{g}^T\mathbf{W}\mathbf{g}\mathbf{S}^{-1} - \mathbf{g}^T\mathbf{W}\mathbf{F}\mathbf{U}^{-1}\mathbf{g}\mathbf{S}^{-1} &= \\ \mathbf{E} - \mathbf{g}^T(\mathbf{W} - \mathbf{W}\mathbf{W}^{-1}\mathbf{U}^{-1} - \mathbf{W}\mathbf{F}\mathbf{U}^{-1})\mathbf{g}\mathbf{S}^{-1} &= \mathbf{E} \end{aligned} \quad (13)$$

As it follows from (13), functionals (2), (6) and (10) are equivalent. It is necessary to underline once again that partition of covariance matrix \mathbf{R} on statistic and systematic components does not lead automatically to similar partition of LSM-functional. Partitioned functional (10) consists of two components – one pure statistic $\Delta\mathbf{Y}\mathbf{S}^{-1}\Delta\mathbf{Y}^T$ and another “coupled” component $-\Delta\mathbf{Z}\mathbf{U}^{-1}\Delta\mathbf{Z}^T$, depending both on statistic and systematic covariance matrixes.

Covariance matrix of uncertainties of the regression function parameters is inverse of Fisher’s information matrix [2]:

$$\langle \Delta p_\alpha \Delta p_\beta \rangle = (\mathbf{I}^{-1})_{\alpha\beta} \quad (14)$$

$$I_{\alpha\beta} = \frac{\partial \mathbf{y}}{\partial p_\alpha} \mathbf{S}^{-1} \frac{\partial \mathbf{y}}{\partial p_\beta} - \frac{\partial \mathbf{Z}}{\partial p_\alpha} \mathbf{U}^{-1} \frac{\partial \mathbf{Z}}{\partial p_\beta}. \quad (15)$$

The LSM based on use of discrete optimisation of rational approximants for functional (10) and use of (14)-(15) in covariance matrix of approximant’s errors was practically realised in estimation of cross-sections for some actinides (up to 1800 results from 75 works simultaneously) in approach with only one component of systematic error.

1. Vinogradov V.N., Gai E.V., Rabotnov N.S. Data’s Analytical Approximation in Nuclear and Neutron Physics. Moscow, Energoatomizdat, 1987 (in Russian).
2. Cox D., Hinkley D. Theoretical Statistics.

The Approaches for Processing of the Data Uncertainties in the R-Matrix Fitting

CHEN Zhenpeng *
Nuclear Data Section, IAEA, Vienna
* IAEA consultant
19 December 2003

There are several approaches to process uncertainty of experimental data in data evaluation procedure with R-matrix theory.

The first one is splitting the full uncertainty at statistical uncertainty and normalization uncertainty, it has been used in R-matrix code EDA and SAMMY.

The second one is full implementation of the error propagation law, it has been used in R-matrix code RAC, and the Least-Squares Code GMA.

Other approaches are proposed here to deal with the uncertainty of data. For more clear understanding, simulated data sets for ${}^7\text{Li}$ system are processed with RAC to demonstrate the main ideas of all methods and the differences may occur.

The total relative error of simulation data was assigned according to practical situation. That is 2% for neutron total cross section, 4% for integral cross section, 6% for differential cross section, and 3% for polarization. Another case is that all relative errors were taken as 5%. The systematical error is given with a constant for each data set which is less than the corresponding statistical error; the statistical error is given by using Monto Caro method with normal distribution.

The corresponding examples are shown in Table 1 and Fig. 1 to Fig. 3. The following designations are used in Table 1 and Table 2; 02 to 12 is the method number.

Y_c refers to the calculated value with given R-matrix parameters;
 Y_o refers to the data value in simulated data sets or the data value in real data base;
 St_e refers to the statistical error;
 Sy_e refers to the systematical error ;
 Nof refers to the ratio of Y_o and Y_c , $Y_c = Y_o * Nof$;
 Nnf refers to the new normalization factor evaluated as parameter in the fit;
 Ner refers to the error of Nnf which is considered as parameter in the fit;
 Rmp refers to the given R-matrix parameter for the simulated data base, or optimum R-matrix parameter obtained for the real database fitting;
 $Sens-c$ refers to the sensitivity coefficient used in the calculation of covariance matrix of cross section;

Cov-p1 refers to the maximum value of the evaluated covariance in the region of the resonance(-5/2);

Dat-p1 refers to the evaluated cross section which corresponds to the Cov-p1;

Cov-p2 refers to the maximum value of evaluated covariance of the cross section in the low energy;

Dat-p2 refers to the evaluated cross section which corresponds to the Cov-p2;

MERC refers to medium energy range correlation component of systematical error.

Table 1. Examples for processing a simulation data base

No.	Ste	Sye	Norm. Fac	Rmp	Sens-c	dat-p1	Cov-p1	dat-p2	cov-p2
02	Fix	0	Nof	Fix	Rmp,Nof	3240	53	18400	520
03	Fix	Ner*Y _o	Nnf	Fix	Rmp	3230	110	18200	820
04	Fix	abs(1-Nnf) *Y _o	Nnf	Fix	Rmp	3230	135	18200	1400
11	Fix	Fix	1 or Nof	Fix	Rmp	3235	135	18300	1400
12	Fix	Fix	1 or Nnf	Fix	Rmp ,Nnf				

In all approaches the statistical error (Ste), normalization factor (Nof), R-matrix parameter (Rmp) take the given values.

In all approaches the full error propagation formula is taken to calculate covariance matrix finally.

The difference is only that how to deal with the systematical error (Sye) and the sensitivity coefficient (Sens-c).

In the 02 method, only statistical error is contributed in the covariance matrix of data, the systematical error is not considered, but the given value Nof is taken as normalization factor. In the procedure for calculation of covariance matrix, the sensitivity coefficient (Sens-c) includes both R-matrix parameter (Rmp) and the Nof. **It should be noticed that in this method the systematical error do not be propagated, the contribution for calculated covariance come only from the uncertainty of Nof, that is the uncertainty of evaluated systematical errors.** This uncertainty is mainly depends on the given statistic error. The real systematical errors is eliminated, the calculated covariance will be rather small (see Fig. 1). This method maybe is much close to the method 1 which has been used in EDA.

In the 03 method, only the statistical error is considered to construct the covariance matrix of data, the given systematical error is not considered. But, in the procedure for calculation covariance matrix, the quantity Ner *Y_o is taken as systematical errors, the sensitivity coefficient (Sens-c) will

not include Nof. This method is close to the method 02, the calculated covariance will be smaller than that obtained by using the method 11(See Fig. 2).

In the 04 method, only the statistical error is considered to construct the covariance matrix of data, the given systematical error is not considered. But in the procedure for calculation covariance matrix, the $\text{abs}(1-\text{Nof}) * Y_0$ is taken as systematical errors, the sensitivity coefficient (Sens-c) not includes Nof. For using simulation data base this method is identical to the 11 method; but for dealing with a real date base it is not identical to the method 11, because the Nof will be replaced by the new evaluated value Nnf obtained by the fitting procedure, the evaluated covariance will be medium.

In the 11 method, always both the statistical error and systematical error are considered to construct the covariance matrix of data, for absolute measurement data 1.0 is taken as normalization factor, for relative measurement data the given Nof is taken as normalization factor. The sensitivity coefficient includes just the R-matrix parameter. This method has been used in RAC-2003 evaluation for ${}^7\text{Li}$ and ${}^{11}\text{B}$ systems (RCM2-2003). In this method the propagation of full error is used; if the given errors are correct the calculated covariance should be correct and will be rather large (see Fig.3).

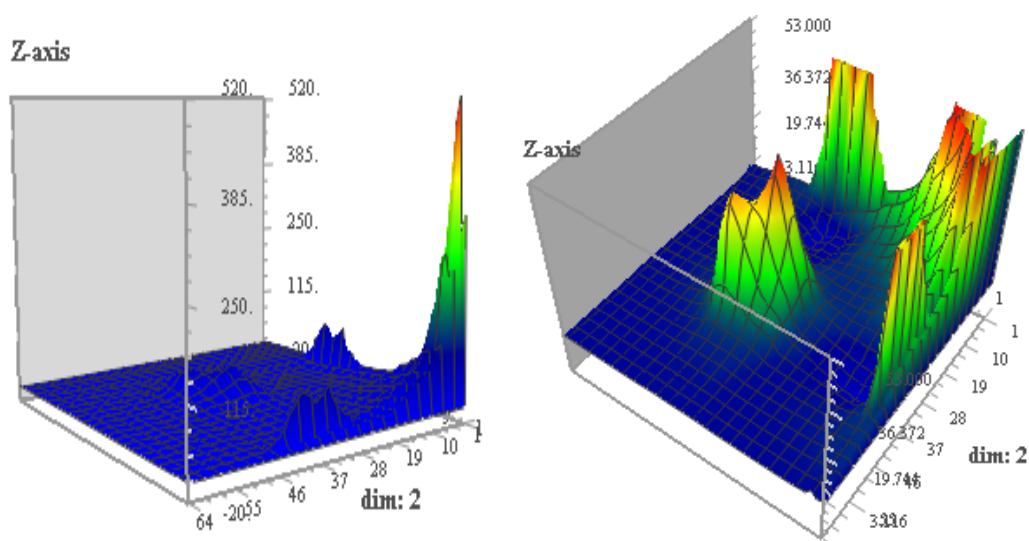


Fig. 1 Calculated covariance matrix of ${}^6\text{Li}(n, t)$ of using the approach 02.

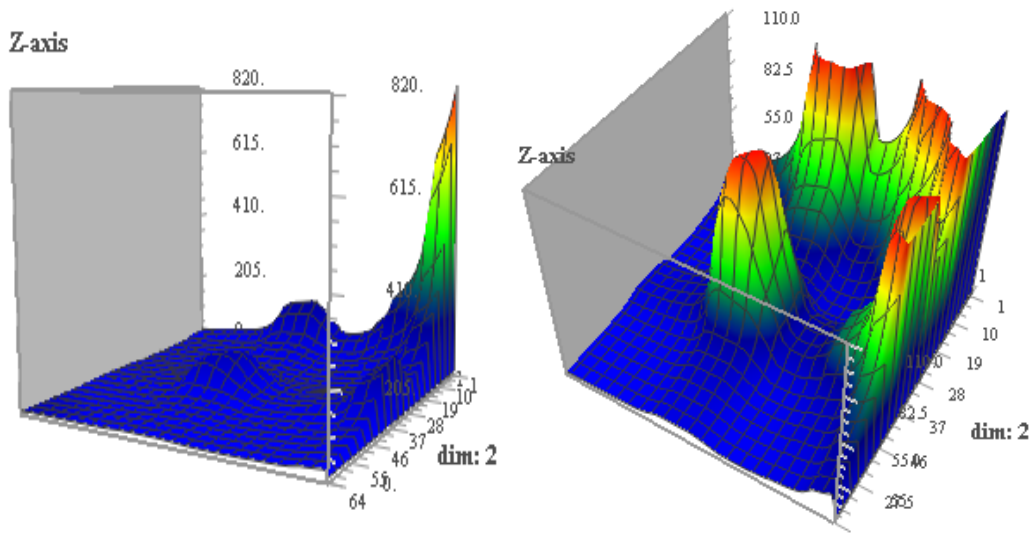


Fig. 2. Calculated covariance matrix of ${}^6\text{Li}(n, t)$ of using the approach 03.

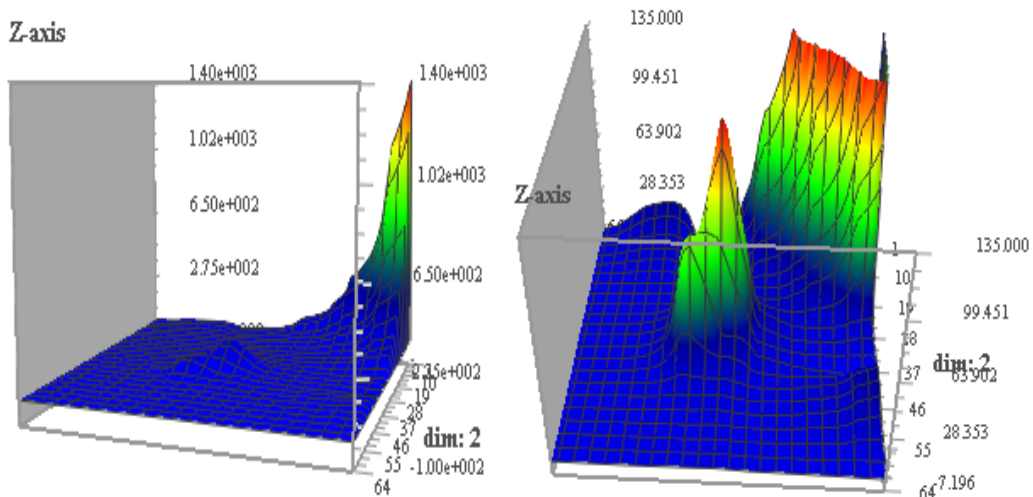


Fig. 3 Calculated covariance matrix of ${}^6\text{Li}(n, t)$ of using the approach 11.

In the 12 method, always both the statistical error and systematical error are considered to construct the covariance matrix of data, for absolute measurement 1.0 is taken as the primary normalization factor, for relative measurement the given Nof is taken as the primary normalization factor. But in fitting procedure the best normalization factor (Nnf) will be obtained by search. The sensitivity coefficient will include both R-matrix parameter and the Nnf. In this method the propagation of full error is used; if the given errors are rather correct the calculated covariance should be correct and will be the most large.

In practical evaluation procedure, the quoted systematical errors or normalization factor of real data base maybe are not good enough. The approach 11 uses the original given systematical errors and normalization factors, the approach 12 uses the new searched systematical errors and normalization factors, the approach 04 uses the systematical errors as given, approaches 02 and 03

use the uncertainty of systematical errors as given; the results of these approaches should be different in some extents.

All covariance are calculated by the error propagation formula as following:

$$\bar{y} - \bar{y}_0 = D(\bar{P} - \bar{P}_0), \quad (1)$$

$$D_{ki} = (\partial y_k / \partial P_i)_0. \quad (2)$$

Here \bar{y} refers to vector of calculated values, D to sensitivity matrix, \bar{P} to vector of R-matrix parameters. Subscript 0 refers to optimized original value, k and i are for fitted data and R-matrix parameter subscript respectively. The covariance matrix of parameter \bar{P} is

$$V_{\bar{p}} = (D^+ V^{-1} D)^{-1}, \quad (3)$$

Here V refers to covariance matrix of the data to be fitted. The covariance matrix of calculated values is

$$V_{\bar{y}} = D V_{\bar{p}} D^+ . \quad (4)$$

For R-matrix parameter, the sensitivity matrix elements D_{ij} were calculated by using finite difference method,

$$D_{ij} = \{T(p+3 \Delta) - T(p-3 \Delta) + 9[T(p-2 \Delta) - T(p+2 \Delta)] + 45[T(p+ \Delta) - T(p- \Delta)]\} / (60 \Delta) \quad (5)$$

(5)

For normalization factor, the method is given as following.

Let Y_o refer to the original experimental value, Y_n refers to the normalized value of Y_o , y refers to the calculated value, P refer to the normalization factor with these relations:

$$Y_n = P * Y_o, \quad (6)$$

$$\partial Y_n = \partial P * Y_o,$$

$$\partial P = \partial Y_n / Y_o \quad (7)$$

$$D_{ij} = \partial y / \partial P = Y_o * \partial y / \partial Y_n = Y_o * \Delta y / \Delta Y_n \quad (8)$$

In RAC fitting procedure, the $\Delta y / \Delta Y_n$ just is the error propagation factor, it is calculated for every datum always.

When the normalization factor is taken as a kind of parameter like as the R-matrix parameter, its uncertainty (Ner) will be calculated, the sensitivity coefficients will include normalization factor too, e. g., in the method 02 and 12; the formula (8) will be used to calculate its sensitivity coefficient. The covariance matrix will be calculated by a iteration procedure.

There are different opinions about how to deal with the uncertainty of data base. In fact it depends from quality of the data and systematical errors or normalization factor assigned to the data. Usually it is considered that the evaluation procedure should be a very objective procedure; the experimenters have credible information to quote the statistical errors, it should not be changed if there are no special evidences. But in really it is hard to quote the systematical errors exactly, especially the medium energy correlation component of systematical errors; the knowledge about systematical errors can be obtained in the procedure of evaluation.

If the data base seems very good, the method 11 should be used.

If the data base seems rather good, but some quoted systematical errors have problems, there are 2 ways to be taken. One is to improve the systematical error at first, and then use the method 11; another is to use the method 12 directly, that is to search both R-matrix parameter and new normalization factor simultaneously in fitting procedure.

If the data base seems not good, there is not quoted systematical errors, or the quoted systematical error is unreasonable, the use of methods 02, 03 or 04 may be considered.

The estimated values of cross sections obtained by using different methods maybe close, but the **covariance obtained with different methods will have rather large differences**. The possibilities are shown in Table 2. In Table 2 y means the corresponding item listed in column 1 is involved, blank means it is not involved.

Table 2. Inter-comparison of calculated covariance with different methods

Involved items	The value of calculated covariance will be				
	maximum	max-med	medium	med-min	minimum
Ste	y	y	y	y	y
Sye	y	y	y	y	
Merc	y	y	y		
Nof	1	y			
Nnf	y		y	y	y
Rmp	y	y	y	y	y

How to do in the future?

The calculated result of R-matrix depends on the data base used. The GMA data base was substantially improved, the MERC component was added to some data sets to eliminate the PPP and decrease the final Chi-square to 0.8~1.0 in GMA fitting. Pronyaev recommends that **all experimental data for ${}^6\text{Li}$ and ${}^{10}\text{B}$ (except the ratio of ${}^6\text{Li}$ to ${}^{10}\text{B}$) and their covariances should be used in RAC fit**, this will make the combining procedure more easy and convenient. The different ideas should be tested by real calculations. It has been planed that **all the approaches for processing of data uncertainty mentioned above will be used in RAC fitting procedure to get several results. The best result will be selected out from the several results and the results of EDA by inter-comparison.**

Nuclear Data Section
International Atomic Energy Agency
P.O. Box 100
A-1400 Vienna
Austria

e-mail: services@iaeand.iaea.org
fax: (43-1) 26007
cable: INATOM VIENNA
telex: 1-12645
telephone: (43-1) 2600-21710

Online: TELNET or FTP: iaeand.iaea.org
username: IAEANDS for interactive Nuclear Data Information System
usernames: ANONYMOUS for FTP file transfer;
FENDL2 for FTP file transfer of FENDL-2.0;
RIPL for FTP file transfer of RIPL;
NDSOVL for FTP access to files saved in "NDIS" Telnet session.

Web: <http://www-nds.iaea.org>
